Immunohistochemical and Genomic Analysis of Ductal Carcinoma in Situ of the Human Breast

Brown, John Peter

Awarding institution:
King's College London

Immunohistochemical and Genomic Analysis of Ductal Carcinoma in Situ of the Human Breast

King's College London
2016

John Peter Brown

PhD

Abstract

Ductal Carcinoma in Situ (DCIS) is a non obligate precursor of invasive breast cancer. Due mainly to improved screening methods the detection of DCIS has risen over the last twenty years. The inability to reliably predict progression to invasive breast cancer results in the possible overtreatment of what can be regarded as a non-life threatening condition. Current treatment options remain controversial with no consensus upon the choice of mastectomy or breast conserving surgery with or without radiotherapy or adjuvant hormone therapies. The natural progression and molecular pathology of DCIS also still remains poorly understood.

Examination of DCIS cases with known clinical outcome has been carried out using traditional pathological criteria, immunohistochemistry and genomic analysis. Tissue microarrays have been constructed and stained with a panel of antibody markers demonstrating the presence of molecular subtypes of DCIS similar to those found in invasive breast disease, although at different frequencies.

Molecular inversion probe arrays have revealed a complex heterogeneity exists in early stages of breast cancer that may be drivers of invasion. Comparison with invasive breast disease and with DCIS associated with invasive breast disease reveals a highly complex system, where progression may rely on genomic changes already established within pure DCIS or those that occur during the DCIS phase of tumourigenesis.

List of Figures and Tables

Tables:

Acknowledgements

There are so many people who have helped me in this endeavour. Firstly I would like to thank Professor Sarah Pinder whom I count as a true friend and also an excellent supervisor. She has been inspirational and also shown great patience in me. I may never be able to thank her enough. Sarah, I said I would submit before Watford FC were in the Premiership again I didn't think it would take quite so long for both to happen.

I would like to sincerely thank the following King's College London colleagues whom, due to their respective expertise, technical abilities and kindness have enabled me to produce this work: Professor Arnie Puroshotham, Professor Andrew Tutt, Dr Cheryl Gillett, Dr Patrycja Gazinska, Vadna Shah, Gursharn Hutchins and Sora Vorapon.

Dr Anita Grigoriadis and Hasan Mirza deserve medals for taking the time to explain to me (in fairly small words) the world of genetics and bioinformatics. Thanks for being so patient with me.

I would like to thank my sponsors Breakthrough Breast Cancer and The Breast Cancer Research Trust whose significant charitable donations have paid for this research. I would like to thank the Guy's and St Thomas's Breast Tissue and Data Bank staff for all their help.

This has been a long pathway and there are too many people to list here, apologies if you are missing but the following people most definitely deserve a mention: Louise Bell, Pierre Lao-Sirieix, Lisa Happerfield, Jill Davis, Ben Onwuegbusi, Mark Pett, Lucy Pett, Paul and Christy Russell & Peter Humphreys. Also I thank Nathan, Andy, Jo, Dan, Chris and Amanda for being such wonderful friends.

It would be remiss of me not to mention both my parents for their support. Thanks to my mother for everything but especially for teaching me the joy that can be found in books. Thanks to my father for showing me the things not found in books; honour, honesty, fishing, sport, pride in work and practicality. I hope I have made you proud. Thanks also to my siblings (especially the good looking one!) for always being there and keeping me sane.

Finally, none of this would be possible or even matter without my wonderful wife Davina. Her love and support over the last twenty five years of marriage, through some hard times, some very painful times but also some very good times, has been the inspiration driving me forward. I can never express the debt of gratitude that I owe her or how much she means to me. Davina, THANK YOU, I love you now and always, your loving husband, John.

Abbreviations and Glossary of Terms

Ab - Antibody

aCGH – array Comparative Genomic Hybridisation

ADH - Atypical ductal hyperplasia

Amplification - An increase in the copies of a gene coding for a specific protein without a proportional increase in other genes

AR - Antigen retrieval

BCS - Breast conserving surgery

BM - Basement membrane

CNA - Copy number aberrations

CCL - Columnar cell lesions

CdLOH – Copy deletion loss of heterozygosity

CK – Cytokerratin

CnLOH – Copy neutral loss of heterozygosity

CNV - Copy number variants

Copy Deletion Loss of Heterozygosity - Complete loss of a gene or gene region.

Copy-neutral LOH (CnLOH) - Also known as uniparental disomy (UPD) or gene conversion. An individual receives two copies of a chromosome, or part of a chromosome, from one parent and no copies from the other parent due to errors in meiosis I or meiosis II. This acquired homozygosity may lead to development of cancer if the individual inherited a non-functional allele of a tumor suppressor gene.

DAB - Diaminobenzidene

DCIS - Ductal Carcinoma in Situ

DFS - Disease free survival

Duplication - The repeating of an extra segment of DNA resulting in redundant copies of a part of a gene, a whole gene or sequence of genes

EGFR – Epidermal growth factor receptor

ER – Oestrogen receptor

FEA - Flat epithelial hyperplasia

FNA - Fine needle aspirate

FNAC - Fine needle aspiration cytology

H&E - Haematoxylin and eosin

HUT - Hyperplasia of usual type

IHC - Immunohistochemistry

IMF - Immunofluorescence

LCIS – Lobular carcinoma in situ

LOH –Loss of heterozygosity

MCM - Minichromosome maintainence

MIP – Molecular inversion probe

MRI - Magnetic resonance imaging

NHS - National Health Service

OR - Overall risk

PCR - Polymerase chain reaction

PR – Progesterone receptor

RT - Radiotherapy

Sc gains – Gain of a single copy of a gene.

SNP - Single nucleotide polymorphism

Total Loss - An entire gene sequence coding for a protein is missing from the genome

UEH - Usual epithelial hyperplasia

UPD - Unipartietal disomy

Chapter 1. Introduction

5.6 The Normal Breast and Ductal Carcinoma in Situ

The normal human female breast consists of six to ten major duct systems which, along with the lobules, comprise the parenchymal tissue of the breast. Ducts converge via multiple central ducts to the nipple; however each system exhibits little symmetry in shape and size. The ductal system is embedded in stromal connective tissue composed of varying amounts of fat and collagen-rich fibrous tissue. The large ducts and the interspersed smaller terminal ducts terminate in lobular acini. The acini consist of a lumen surrounded by columnar or cuboidal epithelial cells above a single myoepithelial cell layer, which sits upon a basement membrane. The stromal connective tissue around the ducts also contains lymphoid and plasma cells in small quantities. Epithelial cells of the lobular and ductal system are not quiescent, having a high degree of proliferative activity particularly during the secretory phase of the menstrual cycle. Proliferation also increases during pregnancy and lactation and slows down with age and the onset of the menopause.

Ductal carcinoma in situ (DCIS) is defined as a pre-invasive proliferation of cells confined to the breast parenchyma showing no invasion into surrounding tissues, or metastasis (1). The ducts become populated with a clonal expansion of epithelial cells that line, or fill, the breast duct. Cells exhibit the cytological features of malignancy but do not invade across the basement membrane. DCIS is believed to originate in the terminal duct lobular units and not specifically in the larger ducts (1).

1.2 Epidemiology of Ductal Carcinoma in Situ

1.2.1 Incidence of ductal carcinoma in situ (DCIS)

The incidence of DCIS has risen from 1- 5% of lesions detected prior to mammographic screening to approximately 20 - 25 % of all screen detected lesions in the UK (1-3). DCIS may be described as intraductal carcinoma or non-invasive tumour but regardless of terminology it now has the highest increase in frequency of all breast cancers (4). The reason for this seeming rise in incidence is almost entirely down to breast screening mammography, where, in some series, almost 50% of detected lesions are DCIS (5). In some screening populations DCIS is associated with age, where a younger screening population has a higher incidence of the disease than older women (3).

Breast cancer worldwide accounted for 22.9% of all female cancers (1,384,155 cases) and 13.7% (458,503 cases) of all cancer deaths according to the World Health Organisation's figures for 2008. Currently there are no worldwide statistics available on the incidence on DCIS. Countries in the developed world utilising breast screening programs would, by default, register a higher incidence than developing and third world countries, thus making direct comparison difficult. Statistics released by the National Health Screening Breast Screening Program (NHSBSP) for 2010/11 provides data for the incidence of breast cancer and DCIS in the screening population (women aged 47-97 years) for the United Kingdom (6); 2,188,608 women were screened with 17,258 cancers detected. Of these, 3522 were non-invasive or microinvasive carcinoma, accounting for approximately 20.4% of screen detected lesions. In the UK, for all ages, 2,221,975 women underwent breast screening with 14,177 (0.8%) breast cancers detected, with 3613 (25%) of these being classed as non-invasive cancers. There is currently no data available for the type of non-invasive disease, i.e. either DCIS or lobular carcinoma in situ (LCIS), but it is likely that the majority of these will be DCIS, due to its tendency to present with microcalcification

(see below) whereas LCIS is often identified co-incidentally within a biopsy. Cancer Research UK gives figures of 5,765 women and 26 men diagnosed with in situ breast carcinoma in 2010 (7).

In the USA, the incidence of DCIS increased sevenfold from the 1970's to the 1990's. The National Institutes of Health (NIH) Consensus and State of the Science Statement on the Diagnosis and Management of DCIS gave an estimation of approximately half a million women living with DCIS in 2005 (8). The prevalence is higher in Caucasians compared to other ethnicities. A Surveillance, Incidence and End Results (SEER) publication for the USA gives an incidence for in situ cancer of the female breast from 1973 to 2007 for all ages of 21.19 cases per 100,000 (9). This figure rises to 53.42 per 100,000 in the over fifty age group. The incidence of in situ disease in black women and white women is essentially similar in those aged over 50, at 53.41 and 53.35 per 100,000 respectively, but is reportedly higher for white females below 50 years, at 9.03 compared to 7.29 per 100,000. Of note, the NIH advises caution interpreting these data as trends in pathological reporting and definitions have changed over time; as an example, one relevant element may be the absence of data on atypical ductal hyperplasia, which may have been previously reported as benign. However, another review of the SEER data from 1973 to 2000 by Joslyn (10) also identified that women between the ages of 35-44 have a higher incidence of DCIS than older groups. Differences between ethnics groups were also apparent with Asian women more likely to be diagnosed with DCIS followed by black women, white women and finally native Alaskan or American Indians. Thus the NIH data and SEER data are contradictory when comparing the incidence between black and white women but the relative times frames, changes in mammographic breast screening and diagnosis patterns are also possible causes of this discrepancy and highlight the difficulty in analysis of DCIS incidence.

1.2.2 Ductal Carcinoma in Situ and Gender.

Breast cancers are significantly more common in women than men with only 1% of breast cancers being found in males (11). Of this 1% of male lesions it is estimated that approximately 5% are DCIS. The lower incidence can be almost entirely attributed to the increased detection of DCIS in asymptomatic women due to breast screening programs and the absence of screening in the male population.

1.2.3 Risk Factors of Ductal Carcinoma in Situ

Risk factors for DCIS are difficult to quantify due to the absence of data prior to breast screening programmes and the difficulty in defining the asymptomatic incidence in the general population. Risk factors for DCIS are understandably believed to be similar to those known for invasive breast cancer. BRCA mutations are a known risk factor for invasive breast cancer with the cumulative risk by age 70 being 65% for BRCA1 and 45% for BRCA2 mutation carriers (12). Smith et al (12) found that patients carrying the BRCA1 mutation had a lower incidence of DCIS than found in sporadic cases. This may indicate that DCIS has a shorter or 'not observed' phase in BRCA1 mutation carriers. Conversely, Hwang et al (13) found that DCIS was equally prevalent in BRCA mutation carriers as in non-carriers although the onset of DCIS was at an earlier age in the former.

Comparison studies of risk factors for DCIS and invasive breast carcinoma have shown similarities in overall risk (OR). A family history of breast cancer and early menarche showed an increase OR (14). Late childbirth and nullparity however only showed an increased OR in older patients (>50 years) for both DCIS and invasive breast cancer (14). Invasive breast cancer risk is strongly associated with increased age, whereas DCIS is associated comparatively with younger age (14). This would fit with the hypothesis that DCIS is a precursor lesion of invasive disease.

Kerlikowske et al (14) found that increased body mass index (>25kg/m2) resulted in reduced OR in younger females (<45 years) for DCIS with a "trend bordering on

significance". They hypothesise that this is due to composition of breast tissue; women with lower body mass indices tend to have mammographically dense breasts and a two-threefold increased risk of invasive breast cancer compared to those with less dense, fatty tissue found in breasts (as seen in women with a higher body mass index). No increase in risk was found for DCIS in association with alcohol intake, smoking or previous smoking, hormone replacement therapy or oral contraception in individual studies (15-19).

1.2.4 Risk of Ductal Carcinoma in Situ Progressing to Invasive Disease.

The natural history of DCIS remains unclear. When DCIS has been detected subsequent treatment is generally aimed at complete excision of the lesion. Studies focussed upon misdiagnosed DCIS as a benign lesion that could be used to look at the natural history are rare, as are series where the patient has declined surgical excision after definitive diagnosis of DCIS.

The Nurses' Health Study is the largest epidemiological study of women in the USA. It consists of two cohorts funded by the USA's National Institutes of Health, the first started in 1976 by Dr F Speizer (20) and the second in 1989 by Dr W Willett (20), with data on over 120,000 registered nurses. The study provides data on risk indicators for cancer, as well as other diseases. Collins et al (21) reviewed this cohort looking for the incidence of untreated DCIS finding only thirteen cases, thus highlighting the rarity of such incidences. Observations of the natural progression of these untreated DCIS found that ten women developed either a subsequent ipsilateral invasive or an in-situ lesion (2-5 years post original biopsy). The original DCIS lesions included lesions of low, intermediate and high nuclear grade. Although the number of cases studied is small the incidence of 'recurrences' is highly indicative of DCIS presenting a high risk of presenting with a subsequent cancer. In 1978 Betsill et al (22) reviewed intraductal carcinomas treated by biopsy alone and reported that an invasive recurrence occurred in 39% (range 25%-75%) of cases reported in the literature,

however, some recurrences were quoted at ten months and could arguably represent disease that was present at the time of initial DCIS diagnosis.

1.3 Detection of Ductal Carcinoma in Situ

1.2.1 Mammography

The primary screening tool for the detection of DCIS is mammography. Other techniques such as magnetic resonance imaging (MRI), ultrasound and scintimammography are generally regarded as insufficiently sensitive, in the absence of invasive disease (23). Mammograms are radiographic images of the breast that utilise low energy x-rays to identify the contrasting difference between normal breast parenchymal tissue, adipose tissue and breast tumours (1). Radiographic images are usually taken through two aspects, the cranio-caudal and medial-lateral oblique views, to determine the exact location of any lesion. Calcification seen by mammography can be, but is not exclusively predictive of, an indicator of malignant change (see Figure 1).

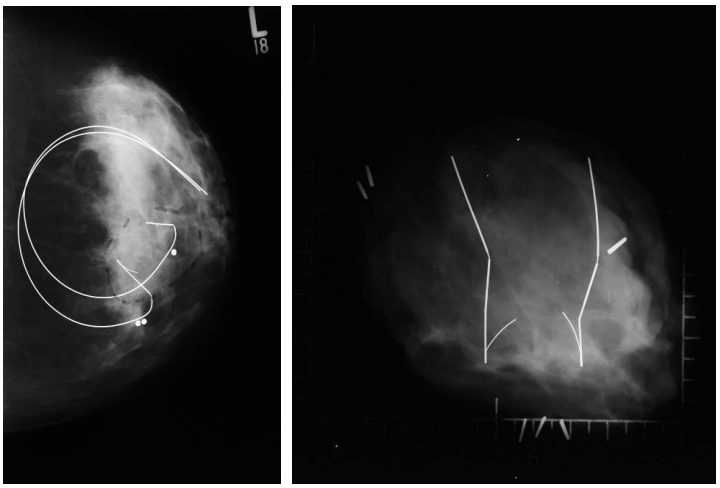

Figure 1: Cranio-caudal and medio-lateral oblique mammographic views of a case with two needle-localisation wires in place to mark an area of abnormality.

The most common mammographic feature of DCIS is microcalcification, seen in 80-90% of cases radiographically (24). Mammographic detection of DCIS thus typically relies upon the identification of calcification deposits that either result from a breakdown product of cells, seen as comedo-type necrosis, or from secretions in the luminal spaces. The clinical presentation of symptomatic cases is variable and may appear as a palpable mass, nipple discharge or as Paget's disease of the nipple (23). Radiographic abnormalities are also often seen in the presence of symptomatic disease with up to 50% of Paget's disease also showing some form of radiological abnormality (23).

Mammographic calcifications (and histological microcalcifications) are not specific for DCIS and occur in many other processes, including normal breast tissue and both benign and malignant lesions, such as involutional changes, duct ectasia and fibrocystic change. It is not possible to accurately grade DCIS on mammography alone and even high grade DCIS lesions can be missed if the area is small.

1.2.2 Ultrasound

Ultrasound is a useful imaging tool for women who present with symptomatic breast disease and can be used to differentiate between a benign and malignant mass in some cases, for example by assessment of the regularity of the margin of the lesion. Its use for identification of DCIS is limited due to a low sensitivity for this disease (1). Nevertheless, ultrasound may be of use in the detection of DCIS where calcification is not present (approximately 16% of cases) which are undetected using mammography. A small study, of 22 cases, has shown that high definition ultrasound can improve upon mammographic screening where calcification is not present (25). Practically, however, it would be difficult to implement ultrasound screening for every patient who attends for breast screening who does not exhibit calcification in the breast on mammography.

1.2.3 Magnetic Resonance Imaging (MRI)

Magnetic resonance imaging (MRI) is a highly sensitive method for detection of invasive breast carcinoma. Historically, the sensitivity for benign lesions and for DCIS has been shown to be less reliable than other techniques (1, 2, 26) but more recent studies have indicated that it is more sensitive than mammography (1, 27). MRI does not visualise calcification but uses a contrast agent to detect neovascularisation. Identification of soft tissue changes in DCIS has been reported in 27% of cases using analogue mammography and 60% using digital mammography (27). The cost and time consuming nature of MRI coupled with the claustrophobic nature of the process, however, also inhibits its acceptance as a population screening technique for those not at high risk of developing cancer.

1.3 Histology of Ductal Carcinoma in Situ

1.3.1 Histological Diagnosis of Ductal Carcinoma in Situ

Once a breast lesion has been identified and sampled it requires histological diagnosis and classification. Specimens are placed in a fixative or snap frozen before undergoing microtomy followed by haematoxylin and eosin staining (H&E) of cut sections. H&E staining provides morphological and nuclear detail of cellular structures and is a reliable stain for a diagnosis of a particular disease state.

The biological events in the transition from a normal to a malignant state in breast tissues are difficult to assign into predefined groups. There is a spectrum of breast lesions with variable, but low, risk of developing invasive disease. Hyperplastic and atypical changes, such as usual epithelial hyperplasia (UEH), columnar cell lesions (CCLs) including flat epithelial atypia (FEA), and atypical ductal hyperplasia (ADH), represent a disparate group of entities that may exhibit some of the features of, but fall short of, DCIS. These entities are included here to highlight possible diagnostic pitfalls and to demonstrate the morphological and molecular similarities with DCIS.

1.3.2 Usual Epithelial Hyperplasia

Usual epithelial hyperplasia (Figure 2) is defined as a proliferation of cells above the basement membrane (BM) that have only mild or no abnormal architectural and/or cytological features. In the normal breast there is a two cell layer above the BM, that of a single layer of myoepithelial cells and a layer of epithelial cells. Where the intraluminal proliferation is confined to four layers or less then the term mild usual epithelial hyperplasia is used. Where five or more cells are present above the BM the term used is moderate epithelial hyperplasia. Where cells have undergone significant proliferation and crossed the ductal spaces enlarging the ducts then the term florid may be used. Clinically there is no increased risk of developing breast cancer where mild epithelial hyperplasia is present and the risk due to moderate or florid usual epithelial hyperplasia is low. Features that distinguish usual epithelial hyperplasia from more serious lesions such as atypical ductal hyperplasia (ADH) or DCIS as set out by the NHSBSP guidelines for 2005 are:

1. The presence of a mixed cell population
2. A syncytial growth pattern
3. Irregular lumen often with a slit-like shape
4. Peripheral lumina
5. Streaming epithelial bridges
6. No abnormal mitoses and few normal ones

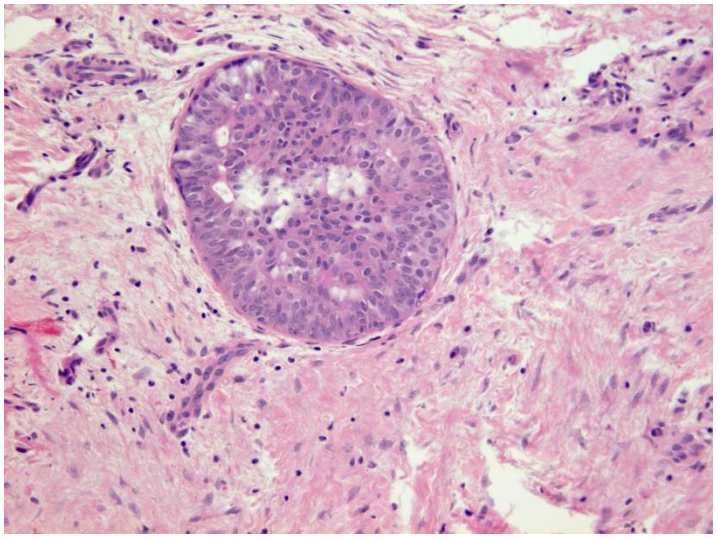

Figure 2: Usual epithelial hyperplasia

1.3.3 Columnar Cell Lesions (CCLs) including Flat Epithelial Atypia (FEA)

Columnar cell lesions (CCLs) are formed from enlarged terminal duct lobular units typically with dilated acini lined by columnar shaped epithelial cells. These lesions are increasingly seen in image guided needle biopsies targeting mammographic microcalcification, which is typically present within secretions in the luminal spaces. In 2003 Schnitt and Vincent–Salomon (28) proposed a classification system consisting of four categories: columnar cell change, columnar cell hyperplasia, columnar cell change with atypia and columnar cell hyperplasia with atypia. The latter two categories were combined to a single entity of flat epithelial atypia (FEA) in 2003 by the World Health Organisation (WHO) Working Group on the Pathology and Genetics of Breast Tumours. Columnar cell change and columnar cell hyperplasia are not considered to increase a risk of breast cancer development. FEA lesions are being detected with increased frequency due to breast screening programs where they may present with mammographic microcalificatons (29). The natural history of these lesions is poorly understood but possible progression to ADH, low grade DCIS and invasive carcinoma cannot be ruled out (29). This necessitates the distinction of FEA (Fig 3) from non-atypical CCLs for future patient management and surveillance.

Molecular evidence indicates that FEA may be the earliest morphological identification of neoplastic change in the breast (30), as FEA lesions have a loss of heterozygosity (LOH) matched by those seen in adjacent concurrent DCIS or invasive cancers. In addition, common chromosomal alterations have been identified on 16q, 11q and 13q, which are not observed in UEH but are frequently seen ADH and DCIS (30, 31).

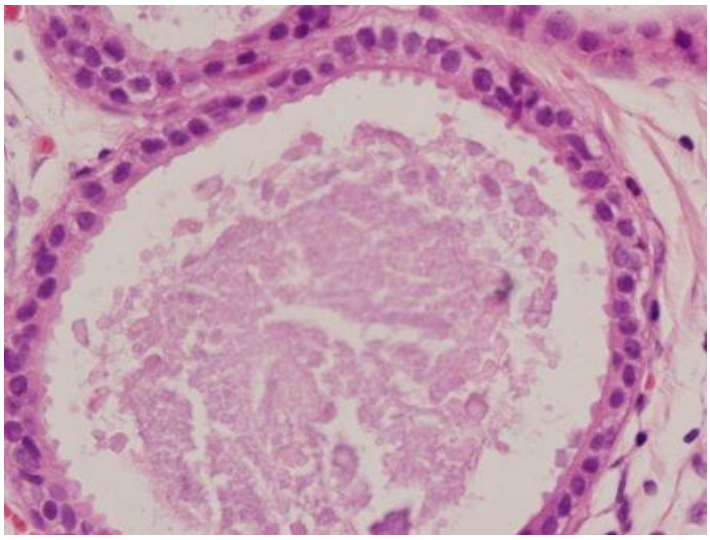

Figure 3: Flat epithelial atypia

1.3.4 Atypical Ductal Hyperplasia (ADH)

The morphology and cytological features of ADH are similar to low grade DCIS but this is a microfocal lesion that is generally confined to a single lobular unit. Specifically, ADH does not involve two complete membrane-bound spaces. The nuclei in ADH are uniform, small, regular and evenly-spaced. As well as the uniformity of cells, ADH forms rigid cellular bars and secondary spaces, which are not seen in FEA (Figure 4). There are presently no immunohistochemical markers available to distinguish ADH from low grade DCIS.

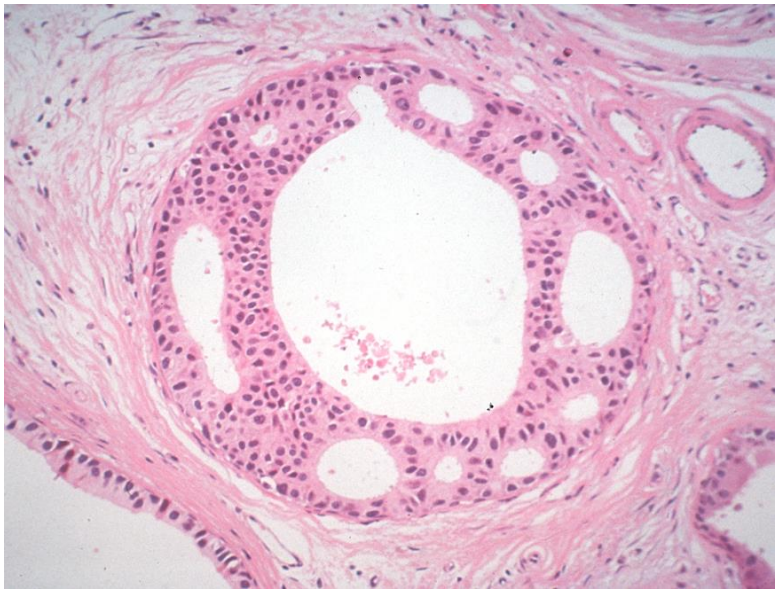

Figure 4: Atypical Ductal Hyperplasia

1.3.5 Lobular Carcinoma In Situ, Atypical Lobular Hyperplasia, Lobular Neoplasia

Atypical lobular hyperplasia and lobular carcinoma in situ have identical cytological features and are distinguished from each other by the extent of involved spaces (1). As such, the term lobular neoplasia was coined to describe both lesions. Cells lack cellular adherence, exhibit eccentric nuclei and often have intracytoplasmic mucinous vacuoles (Figure 5) (1). Lobular carcinoma in situ is considered a separate morphological non-obligate precursor to DCIS, conferring less risk of progression over a longer latent phase.

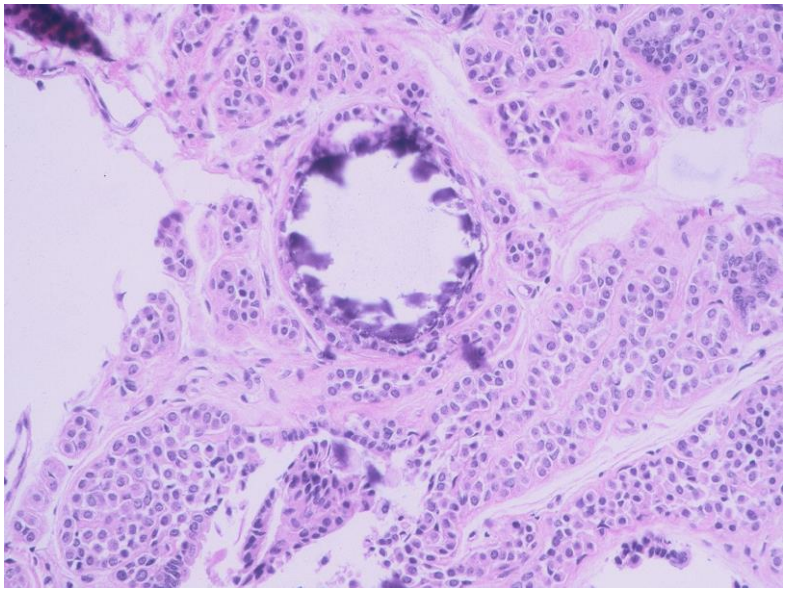

Figure 5. Lobular carcinoma in-situ

1.3.6 Microinvasive Carcinoma

Where a DCIS lesion exists and one or more foci of invasion are present but none measure more than 1mm in diameter the classification of microinvasion is given. This is most commonly seen in association with high grade DCIS but is uncommon in DCIS of any grade. Microinvasion may be misdiagnosed when DCIS spreads into lobules, a term known as ‘cancerisation’ of lobules. Correct classification can often be given by examination of further tissue sections (‘levels’) and/or immunohistochemistry with myoepithelial and basement marker examination. Cancerisation remains within the breast parenchymal structures and does not extend through the myoepithelial layer and basement membrane (Figure 6).

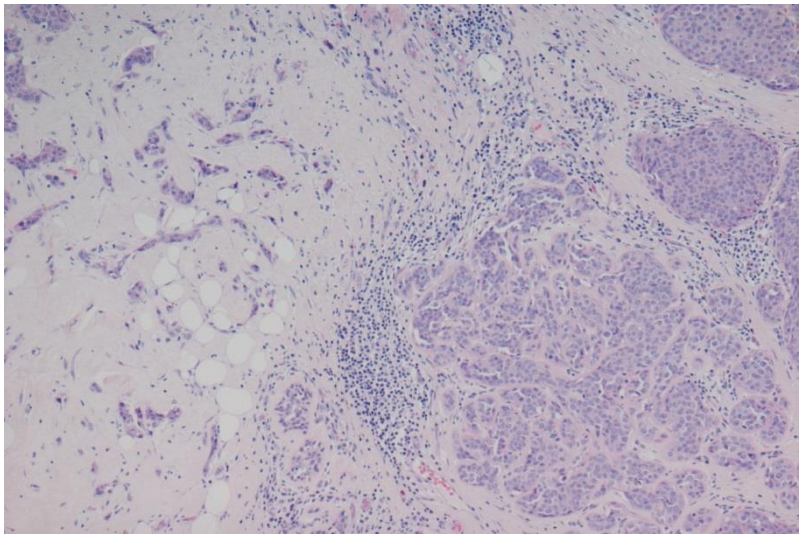

Figure 6: DCIS (top right) with microinvasion (left).

1.3.7 Histological Variants of Ductal Carcinoma in Situ.

Histologically DCIS was classified by the architectural pattern of the proliferating epithelial cells. Both the cytology and architecture of DCIS are complex and giving credence to DCIS as a group of heterogeneous lesions. In the United Kingdom the NHS Breast Screening Programme has issued a “Pathology Reporting of Breast Disease Guideline” (32) outlining criteria for the classification and reporting of all breast disease, including DCIS. A brief description and microphotograph of each entity is given below (1, 5, 32).

Comedo pattern DCIS (Figure 7), also historically known as comedo carcinoma, is characterised by sheets of high grade malignant cells with an area of central necrosis typically surrounded by apoptotic cells. The necrotic area often contains microcalcifications identified mammographically. “Comedo” describes the central necrosis, rather than a specific cell type or grade and is therefore not now regarded as a true architectural type of DCIS.

Solid DCIS (Figure 8) is characterised by sheets of malignant cells completely filling the duct space. Cells may be small with few mitoses or, more commonly, large and pleomorphic. Solid DCIS can be confused with lobular carcinoma in situ (LCIS), however the cells of solid DCIS have cell-cell adhesion, seen as distinct cell

boundaries, and may bear microacini with cells showing polarisation around small luminal spaces.

Papillary DCIS/papillary carcinoma in situ (Figure 9) presents architecturally as finger-like projections into the ductal lumen. These are composed of fine fibrovascular fronds surrounded by columnar carcinoma cells. Duct spaces can be expanded/dilated. Myoepithelial cells are not observed between the epithelial cells and the fibrovascular cores, but are present around the external aspect of the duct space in true in situ disease. Where the projections are composed of epithelial cells alone and lack a fibrovascular core the term micropapillary is used. Micropapillary DCIS often also forms complex intraductal bridges and maybe admixed with cribriform patterns.

Cribriform DCIS (Figure 10) has intraepithelial luminal spaces that are classically evenly-distributed and regular in shape. The central area of the lumen is usually present and may or may not contain areas of microcalcification and necrotic material.

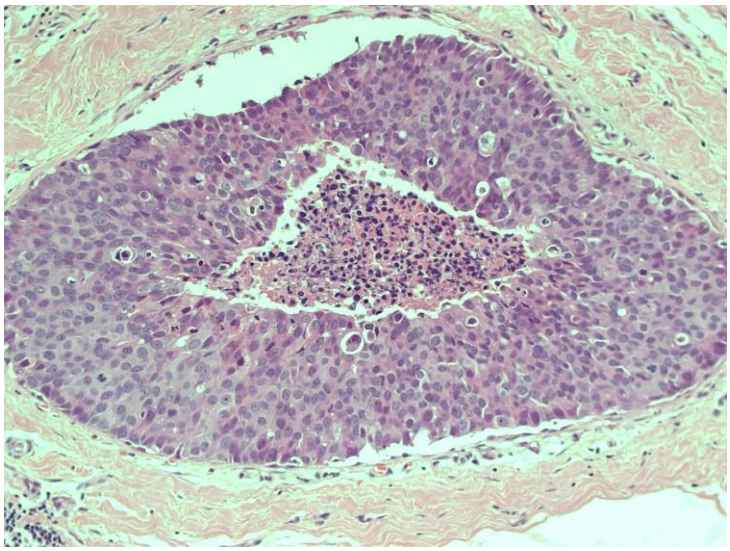

Figure 7: Central comedo necrosis within DCIS

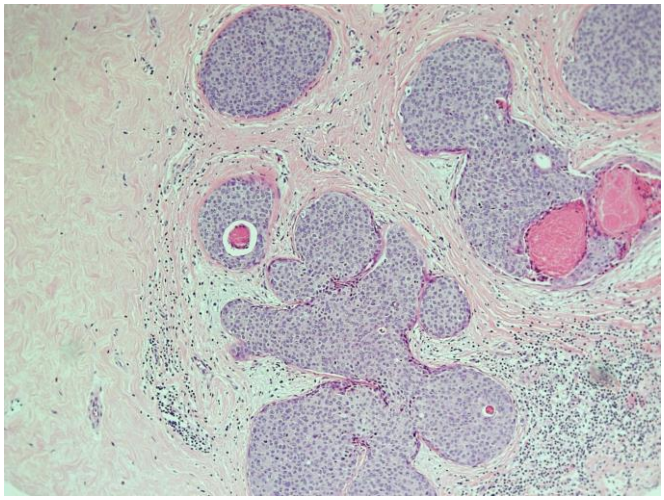

Figure 8: Solid architecture DCIS

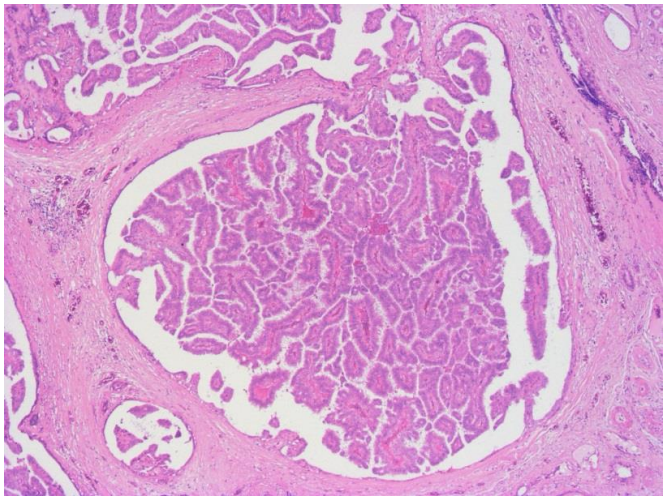

Figure 9: Papillary DCIS/papillary carcinoma in situ

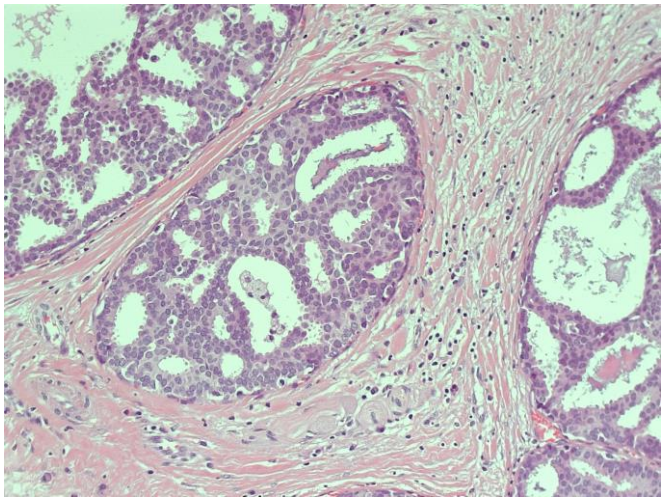

Figure 10: Cribriform DCIS

1.3.8 Rare Histological Forms of Ductal Carcinoma in Situ.

Several rarer morphological variants of DCIS exist, some of which exhibit features that have potential for causing errors in histological diagnosis. The clinical significance of the histological features and genetic mutations present in such lesions remains poorly researched and are not understood.

Clear cell DCIS is formed of cells with distinct margins and clear cytoplasm. Both cribriform and solid structures may be present with central necrosis. Poorly fixed tissues can take on the appearance of clear cell lesions (1).

In apocrine DCIS the cells have the features of apocrine cells with abundant, granular eosinophilic cytoplasm, large nuclei and prominent nucleoli. Severe cytological atypia is often present, as is central necrosis (1).

Neuroendocrine DCIS has polygonal or spindle shaped cells that usually have granular cytoplasm. A pseudo-rosette architecture and papillary areas may be seen. Often positive for oestrogen receptor and neuroendocrine markers this lesion should not be confused with epithelial hyperplasia which has a similar “streaming” architecture (1).

Flat high grade DCIS is possibly a variant of micropapillary DCIS. The features are similar to a variety of columnar cell changes seen in both benign and malignant breast disease which makes identification and classification difficult (1).

Cystic hypersecretory DCIS is also a variant of micropapillary DCIS but produces eosinophilic or mucinous secretions, which expand the ducts to give a cystic appearance. Microcalcifications are common (1).

One of the challenges encountered with classification based on architectural features lies with the presence of more than one of the morphological subtypes coexisting in the same lesion. Descriptive histology terms such as comedo, cribriform, micropapillary, solid, papillary or even “clinging” provide some indication of extent and likely behaviour of disease but are often present in combination, making

categorisation difficult for the pathologist. Quinn et al (33) found that heterogeneity or a mixed architecture was present in up to 62% of cases.

1.4 Classification Systems for Ductal Carcinoma in Situ

1.4.1 Growth Patterns for Ductal Carcinoma in Situ

DCIS usually presents in a single duct system and rarely exhibits a multifocal distribution (34). Several studies have been carried out looking at growth patterns in DCIS (35-37). All postulate that where apparently multicentric disease (i.e. more than one cancer separated by normal breast tissue) is present it is due to large lesion size with extended growth along the ductal system. Micropapillary DCIS, however, has been shown to have a greater incidence of multiple foci when compared to other histological subtypes (37).

1.4.2 High Grade, Intermediate Grade and Low Grade Ductal Carcinoma in Situ

There are several grading systems (38-43) classifying DCIS largely utilising cytonuclear features, into high grade, intermediate grade or low grade categories. It should be noted that whichever grading system is used that there is a degree of interobserver variability between pathologists, particularly with regard to intermediate grade DCIS. The current UK grading system for is based upon guidelines set by the NHSBSP (6).

High Grade DCIS is characterised by large pleomorphic cells with variation in size shape and polarity. Coarse chromatin and prominent nucleoli are abundant and mitotic cells are frequently seen. Nuclear outlines have irregular contours and may appear crenelated with the enlarged nuclei being greater than three times the size of erythrocytes. High grade DCIS is usually associated with a central necrosis and

calcification deposits within this area. This calcified necrotic debris is identified on mammographic screening.

Low grade DCIS comprises more evenly-spaced uniform cells that are generally smaller than other forms of the disease. The cells have regular, round nuclei located centrally and are normally one to two times the size of erythrocytes. Cells are arranged in well-ordered patterns showing polarity. Mitotic figures are sparse. A solid sheet architecture is rare but cribriform and micropapillary patterns are common, often with both present in the same lesion. When both are seen the cribriform pattern tends to dominate.

Intermediate grade DCIS cells exhibit moderate pleomorphism and lack the uniformity of a low grade lesion. Nuclear size is greater than that seen in low grade DCIS being two to three times the size of erythrocytes and occasional nucleoli are present. Lesions can have a cribriform, solid or micropapillary pattern with some polarisation of cells.

Although rare, sometimes a DCIS lesion will exhibit a range of nuclear features; when this occurs the classification is according to the highest nuclear grade present.

1.4.3 The Van Nuys Grading System for DCIS and the Van Nuys Prognostic Index (VNPI)

The Van Nuys grading system (38) applies a combination of cytonuclear features (as above), combined with the presence of comedo-type necrosis to classify DCIS. High grade lesions are classified according to the cytonuclear grade, regardless of the presence of necrosis, whilst non-high grade lesions are classified as non-high grade with necrosis or non-high grade without necrosis. This classification divides DCIS into three groups with differing risk of recurrence.

The grading system was further enhanced into a prognostic index for DCIS by adding tumour size and margin width (distance of tumour cells from excision margin) to the pathological classification. This classification was named the Van Nuy's Prognostic

Index (VNPI) (39). The VNPI takes into account these three parameters associated with local tumour recurrence in patients with DCIS. Tumour size, margin width and pathological classification are all assigned a score of 1-3; 1 relating to best prognosis. A sum of the scores, of 3-9, was determined and a cut-off point relating to treatment failure, i.e. recurrence, was calculated. The original classification study was carried out on 333 patients and determined that a VNPI score of 3 or 4 showed no additional benefit for disease free survival from radiation treatment compared to scores of 6 or 7 who did receive benefit. Those patients with scores of 8 and 9 had a high recurrence rate regardless of treatment. The VNPI was updated by Silverstein et al as the University of California/ VNPI in 2003 with the addition of age as a factor in determining treatment (44).

1.4.4 The Tavassoli Grading/Classification System

The Tavassoli system (40) splits high grade, intermediate and low grade DCIS into ductal intraepithelial neoplasia groups (DIN). The designation removes ‘carcinoma’ from the terminology, similar to neoplasia grading in cervical screening. DIN3 represents high grade DCIS with, or without, marked intraluminal necrosis and severely atypical nuclei. DIN2 is characterised by cribriform or micropapillary type lesions with mild to moderate nuclear atypia, with or without necrosis. The classification of DIN1 requires the absence of necrosis and mild atypia with uniform nuclei and includes hyperplasia of usual type (HUT) and atypical hyperplasia (see above).

1.4.5 R Holland and the European Pathologists Working Group Classification System

This grading system, first proposed by Holland et al (41), uses nuclear pleomorphism combined with cell polarity to define high grade, intermediate grade and low grade DCIS. Polarisation of cells is the orientation in relationship to luminal spaces, where

loss of polarisation indicates a higher risk of local recurrence. The European Breast Screening Working Group adopted a similar system (42), relying on nuclear grade but ignoring polarisation on the grounds of difficult reproducibility amongst pathologists. This is the system currently recommended in the NHSBSP guidelines (32).

1.4.6 Summary of Classification of DCIS

There are at least ten grading systems described for reporting of DCIS. All have their merits and disadvantages. Shoker and Sloane (45) reviewed the available classifications in 1999 and determined that nuclear grade was the best predictor of risk of recurrence. Pinder et al (46) reviewed over 1600 cases of DCIS for the UK Coordinating Committee on Cancer Research (UKCCCR) trial. A full pathological assessment of all cases was undertaken and compared the Van Nuy's, Nottingham and Holland classifications. There results found that all grading systems of DCIS showed a significant association with recurrence of ipsilateral DCIS or invasive disease. However, they identified an additional subgroup, which had a particularly poor recurrence rate. This group was defined by over 50% of ducts showing central comedo type necrosis, a high cytonuclear grade and over 50% of ducts showing a solid architecture pattern. Pinder et al proposed a new three group system to define DCIS. The categories are: 1) low and intermediate cytonuclear grade DCIS, (2) high cytonuclear grade DCIS with non-solid architecture and < 50% of ducts with necrosis (3) high cytonuclear grade DCIS with a predominantly solid architecture and >50% of ducts bearing central comedo necrosis.

All of the classification systems rely upon traditional pathological evaluation of H&E stained tissue sections. Whilst they all have been shown to have a predictive element and be related to risk of disease recurrence, none are currently definitive in the assessment of a possible relapse; thus even patient's with low grade (low risk) DCIS may develop recurrent disease as in situ or invasive breast cancer. This may be due

in some part to the subjective nature of pathology reporting and interpretation of morphological definitions.

1.5 Treatment of Ductal Carcinoma in Situ

1.5.1 Surgical Procedures and Options for Ductal Carcinoma in Situ

Treatment options for DCIS are similar to those for invasive carcinoma being mastectomy, or breast conserving surgery (BCS) with or without radiotherapy (RT) (47). The American College of Radiology (ACR) issued appropriateness criteria in 2011 which reflect both the heterogeneity of DCIS and the patient-driven choice (47). The recommendations state that BCS with whole breast radiotherapy for localised DCIS is acceptable, as opposed to mastectomy. Older patients with fully excised low grade DCIS may undergo observation alone. In cases where microinvasion is present with DCIS (mDCIS) then a sentinel lymph node biopsy is advised.

1.5.2 Radiotherapy for Ductal Carcinoma in Situ

Radiotherapeutic treatment for DCIS is primarily recommended after breast conserving surgery and seldom performed after a mastectomy for DCIS. There remains some controversy as to the clinical need and effectiveness compared to breast conserving surgery alone. In 2013 Donker et al (48) reviewed the treatment of DCIS with and without radiotherapy (RT) after local excision of lesions. They studied survival rates over a period of fifteen years for both groups from a European Organisation for Research and Treatment of Cancer (EORTC) randomized phase III trial (number EORTC10853). They found that 30% of women who underwent local excision for DCIS without radiotherapy had a local recurrence (LR) with 50% of these being invasive. In the group in receipt of both local excision and RT, only 17% had a recurrence, with 56% of these having an invasive recurrence. In both groups the risk of recurrence in the first five years was greater than ten or fifteen years. From these data radiotherapy is shown to decrease the risk of local recurrence. However, a

difference in local recurrence between the two groups was not translated into any change in breast cancer specific survival. All subgroups of DCIS had a reduced recurrence rate with RT with clinging/micropapillary DCIS showing the least additional benefit (no RT = 12.5% recurrence, with RT = 5%).

Other clinical trials have similarly demonstrated a reduction in local recurrence with the use of RT (49-52). In a Swedish study, Holmberg et al (49) found that RT substantially reduced the risk of recurrence but was more beneficial in older women compared to younger women. Confounding factors in the treatment of DCIS with RT such as DCIS grade, age, RT dose, length of dosage time and the use of boost (a higher final dose aimed at the tumour bed) and the effect of adjuvant intervention (such as hormone therapy) make definitive conclusions difficult to make over such long survival periods. The Loris trial (53) is an ongoing a phase III trial addressing possible overtreatment of low grade DCIS by using active monitoring as opposed surgical treatment for screen detected or asymptomatic low grade DCIS.

Cuzick et al (50) looked at the effect of Tamoxifen and RT in DCIS patients. 1701 women were randomly assigned to treatment groups: RT and Tamoxifen, RT alone, Tamoxifen alone, or to no adjuvant treatment. Their findings also showed a benefit in reducing either DCIS or invasive ipsilateral recurrence with RT. They also found that RT had no benefit for overall survival (OR). They reported that Tamoxifen had an increased benefit in prevention of development of cancer in the contralateral breast.

1.5.3 Hormone Therapy for Ductal Carcinoma in Situ

DCIS may be treated with anti-oestrogens such as Tamoxifen or aromatase inhibitors (AI) if a lesion is positive for oestrogen receptors. Staley et al (54) reviewed the Cochrane Central Register of Controlled Trials (CENTRAL, *The Cochrane Library*), the Cochrane Breast Cancer Group's Specialised Registry, and the World Health Organization's International Clinical Trials Registry Platform (WHO ICTRP) in 2011 looking at randomised clinical trials using Tamoxifen with or without radiotherapy.

They conclude that, in a similar fashion to RT, Tamoxifen reduces the recurrence rate but has no effect on OS. The NASBP-24 trial (55) found that Tamoxifen reduced recurrence in ER positive DCIS but not in ER negative DCIS.

1.5.4 Chemotherapy for Ductal Carcinoma in Situ

Chemotherapy as a treatment is not usually given or recommended for DCIS. As pure DCIS is a non-invasive lesion, which has not metastasized, systemic treatment is regarded as having little or no benefit for patients.

1.6 Techniques for the Diagnosis and Investigation of Prognosis in DCIS and Invasive Breast Cancer

1.6.1 Sampling Techniques.

Once a suspected lesion is identified, either through screening or symptomatic presentation, a confirmed histological diagnosis is required. In order to achieve this there are several possible sampling techniques the clinician may choose. These are discussed below with relation to suitability for a diagnosis of DCIS.

Fine needle aspirate (FNA) or fine needle aspiration cytology (FNAC) is a percutaneous process of using a small needle attached to a syringe to extract cells. Cells are directly drawn from the site of interest and smeared onto glass slides where the cells are stained and interpreted. This procedure is suitable for the identification of cancerous cells but has severe limitations in its ability to distinguish in-situ lesions from invasive carcinoma, due to the lack of relevant architecture/morphology. The NHS Breast Screening Programme specifically does not recommend FNAC for the diagnosis of microcalcifications.

A core biopsy is the removal of a solid core of tissue by the use of a hollow needle. The needles can be of various sizes or gauges. The choice of biopsy size for palpable lesions is often a matter of clinical preference, although there are studies that indicate that a 14 gauge is superior to either a 16 or 18 gauge needle (56, 57). The use of

ultrasound guidance and/or a stereotactic needle biopsy (where 3 dimensional coordinates are used to locate the area to be sampled on x-ray) are required for non-palpable lesions. There is evidence that ultrasound guidance reduces the false negative rate in identifying breast carcinoma using core biopsies (58, 59). Core needle biopsies are suitable for the identification of DCIS, however some caution is advised when giving a definitive diagnosis based on core biopsy alone (60); studies of the underestimation of invasive disease where a core needle biopsy shows DCIS range from 8% to 41% (58, 61). Chan et al found that lesion size and the number of cores taken were predictive factors in cases where a diagnosis of DCIS was made but there was adjacent invasive disease present compared to core sampling alone (62).

Vacuum-assisted biopsies utilise a larger gauge needle and have the advantage that multiple tissue samples can be obtained from one insertion. Vacuum-assisted biopsies are normally performed under image guidance, in the form of x-rays or ultrasound, to assist the sampling of breast abnormalities. Studies comparing vacuum-assisted biopsies against non-vacuum stereotactic biopsies have shown that the need for repeat biopsies is reduced, although not eliminated (63, 64).

In some instance definitive diagnosis with FNAC or core biopsy pre-surgery may not be possible. If there is a high suspicion of malignancy then an open biopsy may be performed by surgical excision.

1.6.2 Fixation and Processing of Biopsies

Once a tissue sample has been removed, it requires preparation for light microscopy. The standard practise in most UK laboratories is to fix tissues in a formaldehyde fixative, or one of its derivatives, and process to paraffin wax blocks. Fixation stops putrefaction and autolysis whilst processing to paraffin wax has a twofold aim. This is the removal of water, which assists fixation, and the hardening of tissue so that it can be suspended in a suitable medium (paraffin wax). This enables slicing thin enough

for light to pass through thus enabling light microscopy. Processing is achieved by passing tissues through a variety of graded alcohols and organic solvents followed by impregnation with molten wax. Thin sections of wax embedded tissue are cut, usually 3-4μm thick, and stained with haematoxylin and eosin stain (H&E) to demonstrate the nuclear and cytological components of cells. A diagnosis is generally made on the H&E stains, although a panel of immunohistochemistry (IHC) antibodies may also be used as ancillary tests to aid in a definitive diagnosis. In invasive breast cancer additional IHC is then performed to establish the expression of hormonal markers such as oestrogen and progesterone receptors and growth factors such as HER2 in order to determine subsequent optimum clinical treatment.

Immunohistochemistry (IHC) is a technique for identifying tissue components (antigens) by means of an antibody-antigen reaction. Antibodies specific to a known epitope, or epitopes, can be produced by injecting a host species (usually a mouse or rabbit) with the antigen. The host then produces an immune response in the form of antibodies. These antibodies (known as the primary antibody) can be harvested and applied to histological sections where they will bind to their target antigen if it is present. In fluorescence microscopy a fluorophore is usually bound to the primary antibody to give a fluorescent image. In chromogenic or light microscopy the primary antibody signal is usually amplified by the application of secondary antibodies. These secondary antibodies are links binding to the primary antibody and an enzyme, either with the use of a polymer chain or an avidin biotin complex. The substrate for the enzyme forms an insoluble coloured end product when applied and can be viewed using light microscopy. The most common enzyme substrate reaction used in IHC is currently horseradish peroxidase (HRP) combined with a diaminobenzidine (DAB) substrate, which produces a brown coloured end product. The use of IHC to identify proteins or antigens in tissues has significant advantages over other protein assays, as the target protein can be identified in its morphological setting. This enables identification of proteins in tumours or normal tissues.

IHC as a technique does however have some inherent problems. In the UK, the majority of tissues for examination are fixed in formaldehyde or one of its derivatives. Whilst an excellent fixative, formalin produces cross links in the form of hydroxymethyl and methylene bridges, which may effectively mask the antigen of interest (65), and prevents primary antibody binding. In order to overcome this, antigen retrieval (AR) techniques utilising heat and salt solutions have been incorporated in many IHC protocols. Unfortunately there is little standardisation of the use of fixatives with regard to type and length of fixation, resulting in the need for optimisation of individual antibodies with known positive controls in each different laboratory. The lack of standardisation in laboratories may affect interpretation of IHC markers and is one of the contributory factors that make IHC scoring somewhat subjective in nature. However, despite these limitations, IHC has proven to be a valuable tool in both diagnosis and in prediction of response to therapy in breast cancer diagnosis.

1.6.3 Immunohistochemistry in Assessment and Prognosis of Ductal Carcinoma in Situ

Immunohistochemistry is commonly used to assess DCIS. The demonstration of an intact basement membrane (BM) or myoepithelial cell layer is integral to a diagnosis of DCIS as opposed to an invasive lesion. Antibodies raised against the BM include collagen IV and laminin whilst myoepithelial markers such as smooth muscle myosin heavy chain (SMMHC), p63 and smooth muscle actin (SMA) are all used in diagnostic laboratories to confirm that the lesion is in-situ. Other IHC markers may be used to help in the differential diagnosis of a lesion, for example E-cadherin is typically positive in DCIS but absent or reduced in LCIS, and ER and basal cytokeratins, such as cytokeratin 5 and cytokeratin 14, typically show homogenous staining patterns in DCIS and can be used to aid in a differential diagnosis between UEH and DCIS (1). There are currently no IHC markers to distinguish ADH from DCIS.

The demonstration of hormonal markers, HER2 or other IHC markers are not routinely used to classify DCIS or predict the possibility of invasion. ER expression in DCIS remains difficult to assess mainly due to the lack of clinical data defining positive and negative thresholds. The various scoring techniques employed e.g. Histoscore, Allred and percentage score also prevent systematic comparison. Expression of ER is lower in high grade DCIS than low grade DCIS and the percentage of DCIS ER positive cases is approximately 70%, which is similar to that found in invasive series (1). The expression of HER2 in DCIS has been shown to be higher in high grade DCIS than in grade 3 invasive tumours, with expression in 50-60% cases compared to approximately 20%, cases respectively. For example, Park et al (66) found that pure DCIS expressed HER2 at a greater frequency than invasive breast disease. Borgquist et el used tissue microarrays to determine Her2 expression in primary DCIS. In their cohort of 458 patients over 30% had Her2 positive DCIS (n=132). They found the risk of developing an invasive breast cancer recurrence was “statistically significantly lower subsequent to a HER2 positive DCIS compared to a HER2 negative DCIS(67)”,

1.6.4 Tissue Microarrays (TMAs)

Tissue microarrays (TMAs) were first described in their current format by Kononen as a tool for gene expression and copy number analyses (68). Subsequently, the technique was recognised, and has been widely used, as an efficient method for assessing biological markers on large numbers of cases economically. Biomarker validation using TMAs with immunohistochemistry (IHC) and in situ hybridisation (ISH) is valuable for evaluation of putative diagnostic and prognostic markers and also drug targets when applied to large series and especially to randomised clinical trial samples. Tissue microarrays (TMAs) have become an established research tool over the last ten years enabling rapid assessment of significant numbers of test tissues using tinctorial staining, IHC or ISH. The premise of the procedure is to sample pre-existing blocks of histologically processed tissue for further evaluation by

removing individual cores from each test case and amalgamating these into one block from which multiple tissue sections can be taken for analysis. The procedure allows simultaneous testing of multiple cores, giving reduced costs and improved standardisation of experiments. The vast majority of TMAs are constructed from formalin fixed paraffin wax embedded tissues using 0.6mm, 1.0mm or 1.5mm cores taken from a donor block using a hollow tube (stylet) to biopsy the original tissue which are then are placed into a recipient wax block (Figure 11) into which up to a hundred or more cores can be placed. Once the blocks have been constructed the cores are annealed to the recipient block by a process of gentle heating and cooling. Once this has been achieved, sections are cut in the normal manner on a microtome and subsequent slides can undergo IHC or ISH testing.

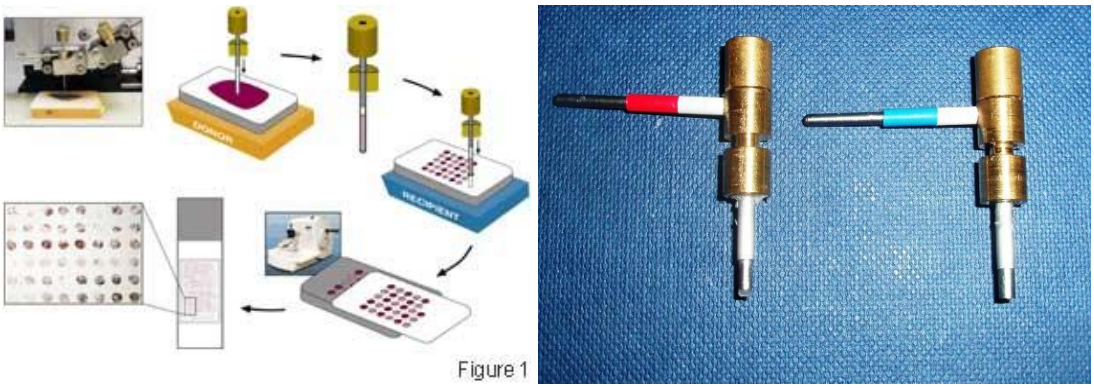

Figure 11: TMA manufacture and stylets

(TMA image courtesy of Yale University, Department of Pathology, Connecticut USA.)

1.6.5 Genetic Aberrations & Molecular Inversion Probe Arrays for Genomic Profiling

Profiling of the human genome is increasing our understanding of the disease process and is seen as a potential tool to identify new biomarker targets for interventional therapy. However, the human genome contains more than ten million nucleotide

positions that have >1% or “common” variations between individuals. Identification of these differences and subsequent comparison of the genomic changes found in progression from normal to a tumour state in breast and other, cancers requires reliable and robust sequencing methodologies. The field of genomics has made significant advances since the publication of the human genome sequence simultaneously by Lander et al (69) and Ventner et al (70).

An individual has two copies of the genome, one from each parent. Where a single base differs in the genome between these two inherited copies a single nucleotide polymorphism (SNP) is present giving rise to heterozygosity in the individual’s genome. Chromosomal arrangement in humans is paired, allowing for heterozygosity. However, loss of a genomic region from one parent can occur giving only one region, which by default cannot be heterozygous at a SNP location; this is termed as loss of heterozygosity (LOH). LOH of a tumour suppressor gene results in only one copy of the suppressing gene. A point mutation (replacement of a single base) can lead to inactivation of the tumour suppressing gene given rise to potential tumourigenesis. However, LOH is not restricted to a loss of a genomic region; copy neutral LOH can occur where no overall net loss of chromosomes or copy number is apparent. Also known as unipartietal disomy (UPD) (71), errors during meiosis may result in two copies, or partial copies, of a genomic region which are inherited from one parent and not the other parent. This can cause inherited homozygosity and, if a non-functional tumour suppressor gene is present, may also result in tumorigenesis. It is estimated that up to 50-75% of human cancers demonstrate LOH (71, 72).

In addition to LOH, and copy neutral LOH, deletions of chromosomal regions and amplifications can also lead to cancer development. Copy number variations (CNVs) are abnormal variants in one or more regions of the genome. They usually correspond to large regions ranging from one kilobase to several megabases and can be either deletions or amplifications. They differ from SNPs in that the copy number variation can be repeated along the length of DNA, e.g. a section that has repeat elements with

GGATCC may be replaced with GGGATCC (duplication) or GGATC (deletion). CNVs have been estimated to account for approximately 13% of human genomic DNA (73). Various platforms have been developed to improve the speed, accuracy and quality of genomic profiling (74). The goal of personalised whole genome association studies requires the ability to identify aberrant genomically regions from very little tissue or DNA with minimal cross reaction; as may seen with PCR amplification where carryover of PCR products to subsequent amplification reactions can occur, in a cheap and reproducible system (75). Molecular Inversion Probe (MIP) arrays are a technology for analysis of SNPs, copy number alterations, somatic mutations and loss of heterozygosity (LOH) (including copy-neutral LOH). The probes consist of primers of approximately 20 nucleotides separated by a linker region (usually an endoribonuclease) and sequences of single stranded DNA that are complimentary to regions adjacent to a SNP in the target DNA sequence of a sample. The technique works on the principle of a SNP-genotype reaction being placed directly upon the genomic DNA target prior to any amplification and then subsequently using a PCR step to only increase the amplification of detected target molecules. This alleviates problems of multiplex PCR where undesired reactions such as “primer dimers” are caused by unwanted binding of complimentary bases instead of the intended DNA amplicons. Each MIP has two sequences that are complementary to the target DNA at the 3 primed (3’) and 5 primed (5’) ends of the DNA strand (Figure 12). Each sequence hybridizes to the target, becoming “inverted” and forming a circle with the 3’ and 5’ ends adjacent to each other with the restriction endoribonuclease forming a free hanging loop.

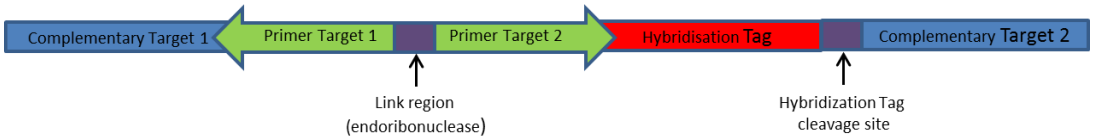

Figure 12: MIP Array Probe:

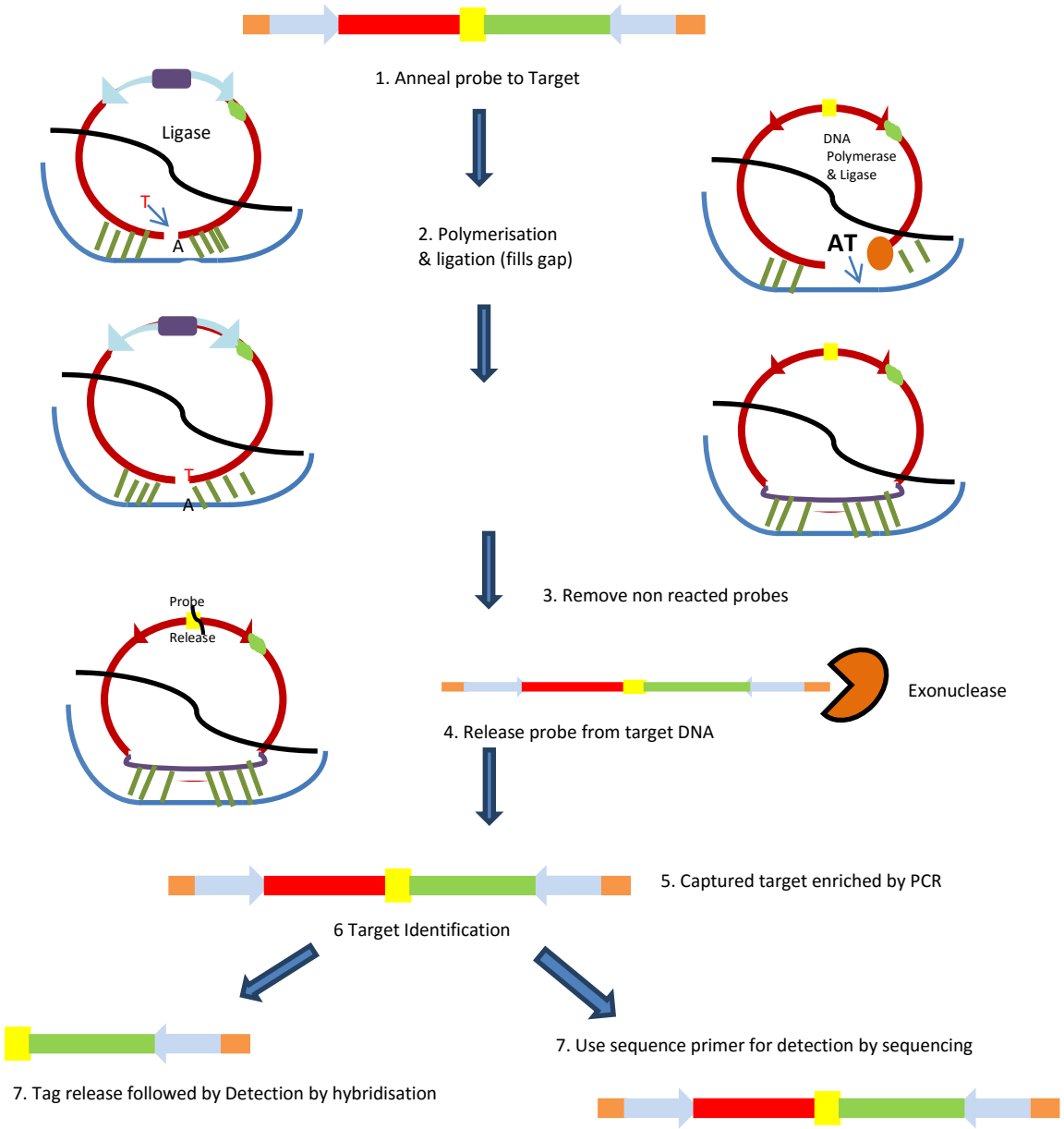

Figure 13: MIP array process for genomic profiling

(Adapted from http://en.wikipedia.org/wiki/File:MIP_technique_timothy.png#filelinks copyright permission licensed under the GFDL see: Appendix 1)

MIP array technology has been further developed by the commercial company, Affymetrix (California, USA), to be used in archival formalin fixed paraffin wax embedded material (FFPE). The company cites the advantages of MIP array as the ability to identify genomic regions of interest in partially degraded samples such as FFPE tissue allowing as little as 40bp per genomic region of interest and being able

to identify difference in copy number states in as little as 60bp with a high discrimination between “signal” and “noise” ratio in degraded samples. One additional advantage of MIP array technology is the multiplexing ability where thousands of loci can be simultaneously analysed; the Affymetrix system offers over 300,000 markers.

1.7 Molecular Portraits of Breast Cancer

1.7.1 Genetic Subgroups of Invasive Breast Cancer

The morphological and molecular heterogeneity of breast tumours makes the classification of lesions challenging. Perou (76) and Sorlie (77) have shown that invasive breast cancers can be classified into distinct genetic subgroups that correlate with overall survival (OS) and disease free survival (DFS) and have potentially important clinical implications. Their findings have been corroborated in other studies (76, 78, 79). The sub-groups of invasive breast carcinoma, designated as luminal A, luminal B, ERBB2-positive, basal-like and “normal” demonstrate that the phenotypic variety seen histologically is, unsurprisingly, present at the molecular level. The molecular phenotypes correlate well with certain immunohistochemical profiles. Approaches have confirmed the existence of some subclasses, such as the basal-like groups of tumours which had been previously described in some IHC series (78, 80-83) but which, until genomic expression profiling, had not been truly regarded as a distinct subgroup of invasive breast cancer.

Perou’s experiments examined breast cancer profiles using known gene clusters for 65 tissue tumour samples along with cultured cell lines of known genomic sequences to ascertain a molecular signature of the breast cancers studied. In developing a system for classifying tumours based upon the gene expression, a second subset of genes (known as the intrinsic subset) to further classify tumours was examined/proposed. Using the rationale that any samples taken from the same tumour should demonstrate a similar profile and that separate tumours should vary in

their expression, twenty paired samples were analysed and gave rise to identification of 496 genes with significant variation between tumours compared to the paired samples. As Perou points out there, is a great multidimensional variation in gene expression in that the patterns are mainly independent. However, there are distinct molecular portraits that relate to both similarities and differences of tumours. These include a proliferation cluster as the largest group, which correlated with the histological mitotic index and the immunohistochemical markers of proliferation, Ki67 and PCNA. As the hierarchical cluster is further broken down, two dendogram branches reveal oestrogen receptor (ER) positive and ER negative tumours separated by clusters of genes expressed by luminal cells of the breast. The ER positive, luminal grouping was also correlated with immunohistochemical expression of cytokeratins 8 and 18. Further evaluation by Sorlie et al, elucidated that these luminal groups could be further subdivided into groups luminal A, B and “normal” like. Six tumour samples from the original Perou experiments clustered in a group associated with genes characterised in basal or myoepithelial cells of the breast. This group had a protein expression of cytokeratins 5/6 and 17. The basal-like subgroup has particular clinical implications as the vast majority of these tumours exhibit negative IHC staining profiles for ER, progesterone receptor (PR) and HER2. These tumours are unlikely, therefore, to respond to Tamoxifen or aromatase inhibitors as they lack expression of hormone receptors. Similarly, the lack of HER2 expression means that tailored anti-HER2 therapy, such as with trastuzumab, is also likely to be of little value. The lack of expression of these three markers which is frequently seen in these basal-like lesions has resulted in the ‘triple negative’ term being erroneously used synonymously to such “basal–like” tumours. Rakha (84) reviewed the expression profiles of basal-like lesions and addressed some of the confusion surrounding the definition of basal-like tumours. Rakha points out that there is a large subset of the basal-like group that is triple negative in immunophenotype but that the absence of these three markers does not automatically indicate a basal-like

phenotype. Conversely, tumours within other molecular sub-groups may also exhibit a triple negative profile. It should also be noted that the expression of one single "basal" IHC marker does not necessarily detect a basal tumour. Rakha advocates the use of a panel (CK5/6, CK14, CK17, EGFR), with positive expression of these, as well as ER and HER2 negativity required for the identification of a basal-like tumour. The majority of invasive breast cancers arising in BRCA1 carriers also fall into the basal group, but this also is not exclusive. The definition of basal-like tumours cannot therefore be defined by either a triple negative phenotype or a BRCA1 carrier group, once again demonstrating the heterogeneity of invasive breast tumours. The basal-like immunophenotype has also been identified in forms of DCIS (85-87).

The next subdivision postulated by Perou et al is the HER2 expressing group. This cluster contained not only the Erb-B2 locus, but also several other genes located in the same region on chromosome 17. This subset also showed lower levels of ER positivity.

The "normal like" subgroup was identified and named based on similarities in gene expression patterns to those of normal epithelial cells, adipose tissue and other non-epithelial cell type. Norum describes these tumours in 2014 as "clearly carcinomas that have gene expression features common to both basal-like and luminal subtypes, showing no expression of proliferation-associated genes" There is an acknowledgement that these samples may have a low tumour cell percentage within the samples(88).

The molecular profiling of invasive breast tumours, and subsequent subdivision of tumours into groups, may have wide-ranging clinical implications. Currently, the pathological assessment of tumours and patient's prognosis and subsequent clinical management is based upon descriptive histological factors such as lymph node stage, pathological measurement of carcinoma size and histological grade, the latter incorporating a proliferative assessment, and morphological (architectural and cytological) subtypes. These factors are routine coupled with the IHC expression of

several markers, notably ER, PR and HER2, which are used as predictive markers and on which likelihood of response to hormone therapy and trastuzumab is based. Other antibodies can help with the identification of morphological tumour type but have a limited prognostic value; for example, it is well recognised that invasive lobular carcinoma typically shows a loss of E-cadherin immunohistochemically. In addition, many novel markers, although demonstrating some potential as prognostic markers, for example c-kit (86, 87), Aurora A (89, 90) and BCL2 (91-93) are not widely accepted as independent predictive markers of significance compared to existing pathological criteria.

The molecular expression profiles demonstrate that morphologically similar tumours may be subdivided into groups which appear to have different genetic origins, leading to questions regarding current histological classification, particularly the “histological special types” (94, 95). Such findings also raise questions as to the validity of current practice. However, it should be noted that studies of genetic molecular profiling of invasive breast tumours have been carried out on relatively small numbers. Validation of these classification criteria using microarray based systems on thousands of samples is cost prohibitive and any novel genetic taxonomy would require detailed correlation with existing clinical practice.

1.7.2 IHC as a Surrogate to Genomic Profiling.

The use of tissue microarrays and IHC can facilitate the examination of the robustness of the genetic subdivisions. Several studies have focussed upon this method, with promising results (82, 86, 96). Abd El-Rehim (96) et al analysed over 1000 breast tumours with a large immunohistochemical panel of 25 antibodies. These included antibodies for the luminal phenotype based upon the expression of cytokeratins 7/8, 18 & 19 and the basal phenotype with cytokeratins 5/6 and 14. In addition to this hormonal markers ER, PR, androgen receptor (AR), tumour suppressor genes (p53, BRCA1, Anti-FHIT), cell adhesion molecules (E-cadherin, P-

cadherin), mucins (Muc-1, Muc-1 core, Muc-2), apocrine differentiation (Anti-GCDFP-15), and neuroendocrine differentiation (chromogranin A, synaptophysin) were evaluated. Using an agglomerative clustering approach, Abd El-Rehim et al classified tumours into six groups, with nine of the twenty five antibodies being key discriminatory markers (AR, c-erbB-2, CK18, MUC1, CK5/6, p53, nuclear BRCA1, ER and E-cadherin). Interestingly, the results broadly correlate with the genomic arrays of Perou and Sorlie and defined six classes of breast cancer. Two were hormonal positive luminal groups having similar immunohistochemical profiles to luminal A and B sub-groups but having differing overall disease free survival, a third group had c-erbB2 (HER2) positivity with strong Muc1 expression, altered E-cadherin and weak hormonal marker expression. The fifth group showed elevated p53 and basal marker expression and lower hormone receptor expression, group six consisted of HER2 and E-cadherin positive tumours that had weak or no hormone receptor status and MUC1. Group four only consisted of four tumours so it is difficult to draw conclusions for this division.

These authors similarly showed, like Perou et al, that the IHC identification of sub-groups was of prognostic value in invasive breast cancer. The grouping determined in this series was defined by a panel of antibodies reflecting the various genetic pathways that may be responsible for tumour growth. Other workers, such as Nielsen (82) and Rakha (84), have also demonstrated that the basal subgroup can be identified using IHC markers.

In 2011, the St Gallen International Expert Consensus on the Primary Therapy of Early Breast Cancer agreed to define subgroups for invasive breast cancer based on clinicopathological criteria, including immunohistochemistry for ER, PR, HER2 and Ki67, as opposed to a gene expression array criterion. Their reasoning was that systemic therapy approximately matches the subtype classification (97). They proposed the following subgroups: luminal A (ER and/or PR positive, HER2 negative and Ki67 <14%), luminal B/HER2- (ER and/or PR positive, HER2 negative and Ki67

≥14%), luminal B/HER2+ (ER and/or PR positive, HER2 positive), HER2+/ER- (non luminal) (ER and PR negative and HER2 positive) and triple negative (ductal), (ER, PR and HER2 negative). To date only one study (98) has used this specific criteria to assess DCIS, finding no link between the subgrouping and risk of recurrence, as either invasive carcinoma or DCIS, over a ten year period.

1.8 Conclusion

DCIS still represents a clinical dilemma for patient management. The inability to reliably predict possible progression to invasive breast cancer results in the possible overtreatment of what can be regarded as a non-life threatening condition. Current treatment options remain controversial with no consensus upon the choice of mastectomy, or breast conserving surgery with or without radiotherapy, or indeed adjuvant hormone treatments.

The natural progression and molecular pathology of DCIS also still remains poorly understood. This thesis aims to address some of these problems by analysing a series of DCIS cases with known clinical outcome. This includes DCIS lesions that have not progressed (pure DCIS), DCIS lesion that have had a DCIS recurrence and DCIS lesions that have an invasive recurrence with or without associated DCIS. A further series of cases of pure DCIS and DCIS admixed with invasive disease contemporaneously allows comparison of biomarker and genomic changes in the different disease states. Analysis of genomic changes using Molecular Inversion Probe arrays (MIPs) and immunohistochemical (IHC) profiles in these cases will hopefully identify possible biomarkers of interest and genetic abnormalities that confer greater or lesser risk of progression from DCIS to invasive disease and allow comparison of groups of lesions with regard to genetic changes and biology.

1.9 Hypothesis

An immunohistochemical and genomic assessment of “pure” DCIS and of DCIS associated with invasive breast cancer will identify differences in biomarkers and gene expression between individual cases. Within immunophenotypic sub-groups variations in biomarkers and gene patterns may identify cases with increased risk of recurrence and/or progression.

Summary of Aims:

1. To determine the expression of a range of immunohistochemical markers in DCIS lesions and determine if these markers can identify molecular subtypes similar to those found in invasive breast cancer.
2. To create a database of significant size providing information on DCIS samples with genomic, immunohistochemical and demographic data. This database will provide a resource for further research beyond the scope of this thesis.
3. To undertake an analysis of archival DCIS samples to identify genomic variation, abnormalities and changes between different pure DCIS lesions and DCIS lesions associated with invasion
4. To identify any protein and/or genomic changes in all DCIS (pure and that associated with invasion) compared to invasive breast disease to determine potential biomarkers responsible for progression to an invasive state.

Chapter 2. Construction of Tissue Microarrays (TMAs) for Immunohistochemical Evaluation of Ductal Carcinoma in Situ

2.1 Introduction

In this study, the evaluation of multiple immunohistochemical markers is used to determine if DCIS can be classified and sub-typed in a similar fashion to invasive breast carcinoma on an immunohistochemical level. In order to assess multiple markers on significant numbers of DCIS cases, TMAs have been used. The nature of DCIS, including size and distribution of lesions and intralesional heterogeneity, introduces some challenges in TMA construction. The design and manufacture of TMAs had to address several criteria specific to DCIS, as well as some general principles not often cited in the literature. These include core size, number of cores, core placement, tissue selection criteria, heterogeneity of tissue and subsequent TMA analysis. These issues are discussed below.

2.2 Materials and Methods

A search was carried out for DCIS specimens within the King's Health Partners Tissue Bank (KHPB), formerly the Guy's and St Thomas's Breast Tissue and Data bank (BTBD), yielding a list of 579 cases for evaluation. The specimens were defined as containing a "pure" DCIS component not associated with invasive carcinoma, or DCIS as a recurrence. All tissue had been uniformly fixed in 10% neutral buffered formalin within 60 minutes of surgery. The haematoxylin and eosin (H&E) stained slides for cases were retrieved from the archive and screened by a consultant breast histopathologist (SEP) to reclassify each lesion using the current classification and

terminology. Each case was then assessed for suitability for coring for tissue microarray. Cases where core biopsy material alone was available were discounted due to lack of tissue.

Once the slides had been reviewed, the matching formalin fixed paraffin wax embedded (FFPE) blocks corresponding to the marked slides were retrieved from the archive. The blocks were assessed for amount of remaining tissue and any deemed insufficient were excluded from the study. It was noted that for some of the cases the tissue in the FFPE blocks did not match the shape of the tissue sections due to taking of multiple sections for other, previous, studies. All the blocks were subsequently re-embedded and a single section cut and H&E stained for marking using an optical marker (Nikon-Melville, New York U.S.A.) attached to a microscope (Figure 14).

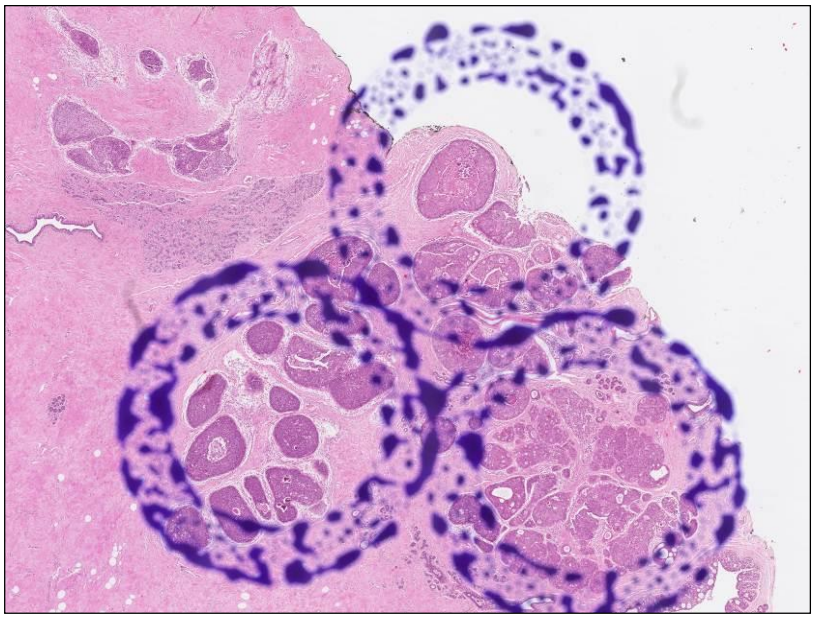

Figure 14. Optical marking of disease on an H&E section.

Once areas of interest had been marked, TMAs were constructed. As described in Chapter 1, the basic principle is to take an empty paraffin wax block (recipient block) with which a small hole is drilled using a first stylet. Then a second, slightly larger, stylet is used to sample the paraffin wax block containing the tissue of interest (donor block). This core of tissue is then inserted into the small hole in the recipient block.

Once all the desired cores have been transferred from the donor to the recipient block then the newly constructed TMA undergoes an annealing process. This process involves heating and cooling the newly constructed TMA block to just below the melting temperature of the wax to enable the cores to meld to the wax of the recipient block. Various temperatures and times are used dependent upon core size and tissue type. For this study, trial and error demonstrated that placing the new TMA blocks in a pre-warmed oven at 56ºC for ten minutes followed by 30 minutes cooling repeated thrice produced TMAs with suitable annealing to prevent core loss.

Each case of DCIS had three 2mm cores taken, with each of these cores placed into a separate block labelled A, B and C respectively. The standard size for TMA cores in studies of invasive carcinoma is 0.6-1.0 mm (99). A larger core size (2mm) has been used in this study to be certain of obtaining representative morphology from ducts bearing in-situ carcinoma. This results in a larger tissue surface area to demonstrate IHC expression and to assess the presence of staining heterogeneity. Each TMA block consisted of twenty DCIS test cases, and five control tissue cores of either kidney or liver tissue, to enable easy orientation of cores when examining the sections under light microscopy (Figure 15).

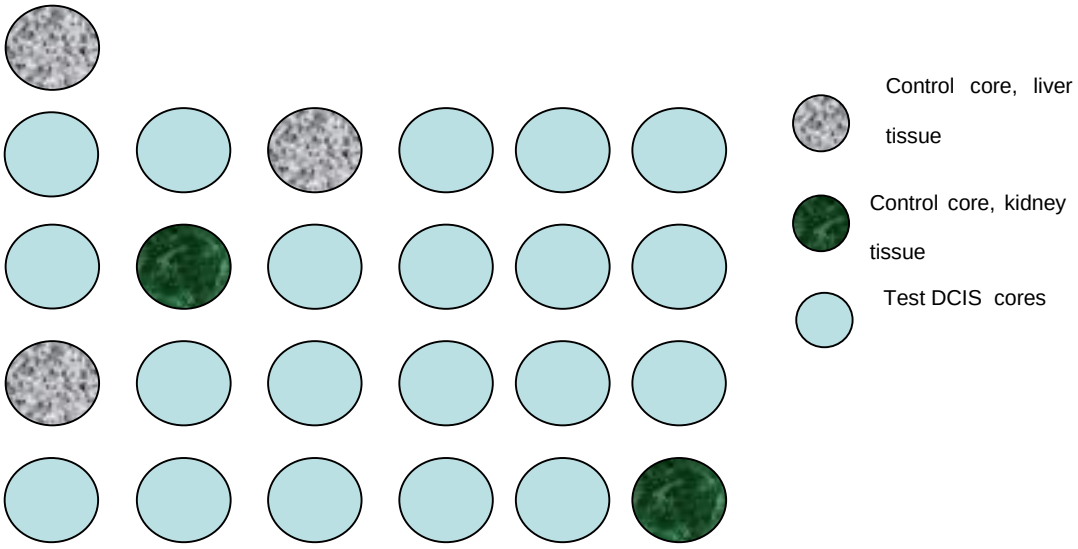

Figure 15. Template for TMA composed of 2.0mm cores

Once constructed, a peripheral surface section was cut from the TMAs and an H&E stained slide produced in order to assess the accuracy of the coring and confirm the presence of DCIS. Examples of sample 2.0mm cores with DCIS present are shown in Figure 16 with an example of a whole TMA section in Figure 17.

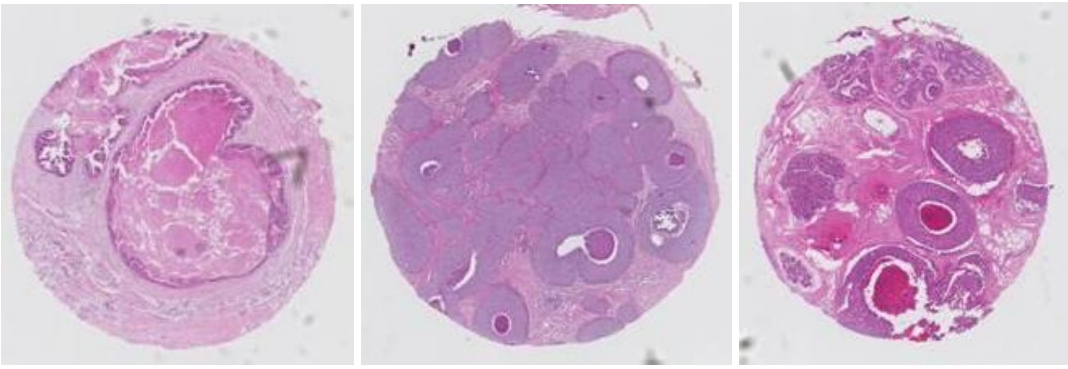

Figure 16: DCIS in 2.0mm cores

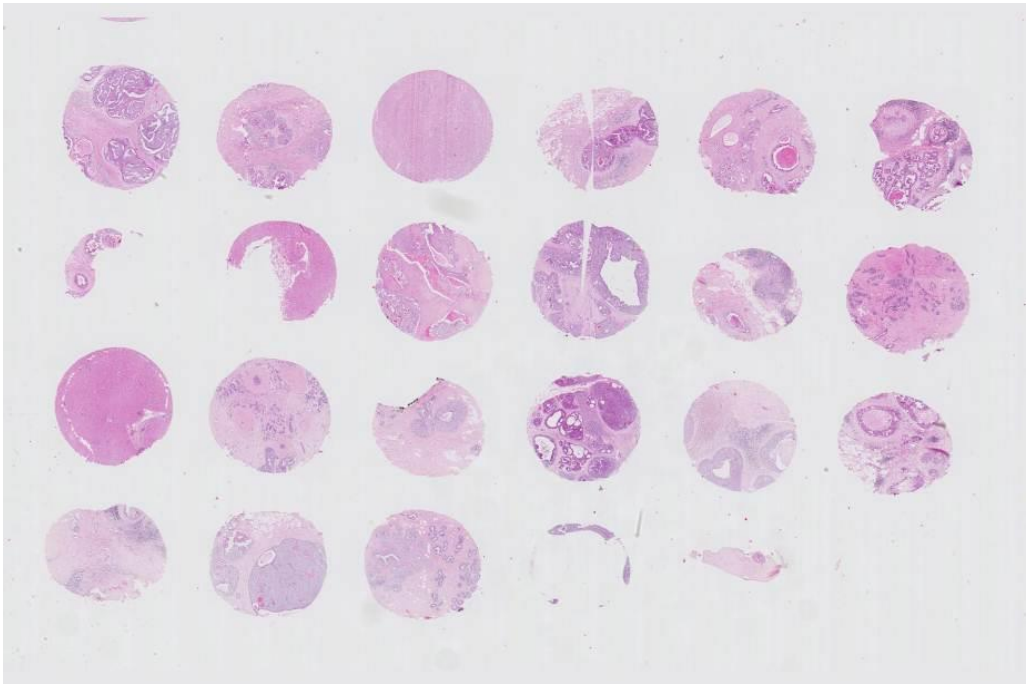

Figure 17: TMA construct

Use of tissues and data (see 3.2.1) was approved under NHS REC agreement (07/H0874/131) with Biobank Access Committee approval.

2.3 Results

2.3.1 TMA Constructs

The 579 cases of DCIS in the initial database yielded a total of 280 cases of pure DCIS suitable for TMA construction. These were made into 14 tissue microarray blocks in triplicate giving a total of 740 cores for IHC staining.

2.3.2 Scanning

All TMAs had a 4μm section cut and stained with H&E to verify the presence of DCIS within cores. A total of 42 H&E sections were taken and scanned using a "Nanzoomer" digital scanner (Hamamatsu, Welwyn Garden City, UK) to provide digital images for analysis. Loss of DCIS due to either missing cores, incorrect coring from donor block or lack of viable cells was evident in 15-20% of cases.

2.4 Discussion

2.4.1 Tissue Selection Criteria

The selection of good quality tissue for inclusion in any TMA is paramount. However, the vast majority of TMAs are drawn from archival diagnostic stores with very few having tissue prospectively acquired. A major problem with the use of archival tissue is that fixation and processing is typically poorly documented, and often highly variable even within a single institution. The archive based at Guy's and Thomas' Tissue and Data bank has specimens dating back to the early 1970's available for research. The archive also includes accurate records of time to fixation and duration in fixative; the breast tissue used in this study were expertly sliced and placed in

formalin within 30 minutes of surgery. The maximum duration of fixation was 48 hours. The quality of the archive owes much to the foresight of the individuals who established the tissue bank, and who recognised the importance of adequate fixation and detailed record keeping before the advent of modern immunohistochemistry and molecular techniques.

2.4.2 TMA cores size, number and distribution within a TMA block

There is variation in the literature as to what is considered “representative” when selecting the number, size and distribution of cores within a TMA. Core diameter and number ranging from a single 1.0 mm core to six 0.6 mm cores have been suggested as suitable. Some authors have reported that a single core, regardless of size (1.0mm to 0.6mm), correlated with whole section mounts when assessed for ER, PR, HER2 and Ki67 (100-102). However, others have advocated the use of multiple cores to provide more accurate concordance; Graham et al suggested that a minimum of four assessable cores from six sampled areas were required for accurate evaluation of HER2 status of invasive breast cancer (103). Bharghava showed that between two to four cores had a high (99%) concordance with whole sections for HER2 status by fluorescent in-situ hybridisation (FISH), again in invasive disease (104). Sapino et al recommended that at least 4 cores are required and that where a negative hormonal marker such as ER or PR is found then the IHC should be repeated on a whole section (105). Thus there is little agreement, for even standard biomarkers, on the number of TMA cores that should be assessed, let alone the number of cells required.

Table 1 compares the surface areas of the most common cores sizes: 0.6mm, 1.0mm, 1.5mm and 2.0mm and the total surface area obtained when multiple cores are examined. Taking one 1.0mm core is roughly equivalent to three 0.6mm cores. This excludes demonstration of regional heterogeneity within a cancer, but for markers with uniform expression significant time and cost savings could be made by use of a larger core size. Where multiple cores are taken from lesions of known heterogeneity,

increasing the core size from 0.6mm to 1.0 mm will give a threefold increase in tissue area for analysis.

Core Diameter (mm)	Core Radius (mm)	Core Circumference (mm)	Core Area (mm^2)
0.60	0.30	1.885	0.283
1.00	0.50	3.142	0.785
1.50	0.75	4.712	1.767
2.00	1.00	6.283	3.142

Table 1: Surface areas of different TMA core sizes.

There is an inevitable loss of cores when cutting TMA sections and performing subsequent tests such as IHC. Such loss can be due to tissue type, fixation, poor region selection, poor annealing of cores in the donor block, core size, section thickness, section drying and overuse of organic solvents. Technical expertise can minimise some of these, although the use of archival material that is poorly processed will have an influence on core preservation. Heating of sections for processes such as antigen retrieval in IHC and denaturation of DNA in ISH are a particular cause of core loss and a percentage will be lost in such processes, even when performed by expert technicians.

Histopathological sections of diseased tissue are, by their very nature, a small representation of an entire tumour or disease state. Rarely is a tumour sampled in its entirety with every section of tissue cut and examined for tumour heterogeneity with repeated antibody testing. Large tumours are excised and the pathologist selects representative pieces which, in general, have only one H&E section taken and examined from the block. TMAs have, since their inception, have been dogged with the criticism that they are not representative of the entire tumour and cannot capture

the heterogeneity seen in whole sections. Camp et al (99) point out that the general consensus is that in most cases two 0.6mm cores are representative of a whole section but that some antibodies, such as those involved in hypoxia, that show heterogeneous expression may require more cores. In this study, selection was based on the diagnosis of DCIS. Larger cores were chosen as they allowed entire duct spaces, with their surrounding myoepithelial layer and basement membrane to be visualised within the TMA core. This would also address issues of potential staining heterogeneity (by manufacturing triplicate blocks) and included a sufficient quantity of tissue to be considered representative of a lesion when compared to the guidelines quoted in the literature. Indeed the actual sampling in this thesis exceeds the vast majority of current studies. It is anticipated that this would give a true reflection of IHC staining patterns in the tissues examined.

Chapter 3. Immunohistochemical Studies on Ductal Carcinoma in Situ

3.1 Introduction

The expression of key proteins, or biomarkers, is of prognostic and/or predictive importance in invasive breast cancer. Panels of proteins have been proposed that can divide breast cancer into clinically important subtypes with differing survival outcomes. However, there is currently a lack of information as to whether these tumour subtypes are represented at the in situ stage, and their prognostic significance in DCIS. Immunohistochemical experiments looking at a number of proteins of known importance in invasive breast cancer were carried out for this thesis to investigate their expression within DCIS. Sections 3.3 to 3.9 refer to specific types of antibody with regard to their target antigen and the rationale for inclusion into a prospective panel. The procedure for staining for all antibodies was similar and is summarised below with details of any variations given.

3.2 Material and Methods

3.2.1 Correlation of Immunohistochemical Results to Patient Data and Outcome

See Appendices 2, 3 & 4

In order to evaluate the effect of any IHC biomarker upon the likelihood of recurrence, whether invasive, in situ or not present, it was necessary to determine the patient outcome in our cohort. Patient demographics including age, treatment, details of local, ipsilateral and contralateral recurrence, if any, were retrieved from the King's Health Partner's Breast Cancer Biobank records.

Samples of pure DCIS tissues from this cohort of patients were taken between the years 1974 and 2005. Patient details in some instances were incomplete and not

suitable for further analysis. Reasons for these losses included patient relocation, loss of records or conflicting data. This reduced the total number of TMA cases available for correlation with patient demographics. For these cases TMA core loss also occurred in a small percentage of cases giving a slight variance in numbers available for each antibody assessed.

The data in the bank is prospectively populated with follow up data from clinical visits by patients and from cause of death registration. Patients were diagnosed with DCIS between 1974 and 2005.

Table 2 summarises patient demographics. Records for 180 patients were available. Mean patient age at diagnosis was 72 (range 22-90).

Records list 112 patients with an excision biopsy as first form of surgery, 11 had microductectomy, 2 had a needle localisation excision biopsy, 5 had a wide local excision and 12 had a simple mastectomy. Data on type of first surgery was unavailable for 20 patients. The majority of patients underwent further treatment (n=131), of these patients 41 had a simple mastectomy, 50 has a wide local excision, 7 were listed as both wide local excision and simple mastectomy, 14 had a modified radical mastectomy, 2 had an excision biopsy, one biopsy and one microdochectomy. There was no data on the type of subsequent surgery for two patients.

Twenty three patients had a known recurrence more than 3 months (range 108-4363 days) after original diagnosis and surgery.

3.2.2 Histological Assessment of Necrosis and Inflammatory Response.

.

Histological re-assessment of samples (Chapter 2) provided details of the degree of comedo-type necrosis and of inflammatory response as well as cytonuclear grade and architecture of the DCIS. The histological data frequencies are shown in Table 2. The presence of necrosis was scored as “mild”, “moderate” or “marked” where 10% or less of the ducts bearing comedo-type necrosis were defined as a mild degree,

moderate corresponded to approximately 10-50% and marked to 50% or more of ducts exhibiting necrosis (46). Assessment of the presence of inflammation was based on 'routine' categorisation of the degree of chronic inflammatory cell infiltrate adjacent to and/or surrounding the duct spaces bearing DCIS. Previous work in classifying inflammation in DCIS has shown good reproducibility between consultant pathologists in (RM and SEP unpublished data).

Table 2: Patient Demographics and Histological Details.

		Number of patients	% (of 180 in TMA series)
Mean patient age at diagnosis (range)	72 (range 22-90)	166	92
Size of DCIS (mm)	Average 14.9 Median 14.9 Range 1.0 - 31.0	168	93
Dominant architecture n (%)	Solid 74 (43) Cribriform 69 (40) Micropapillary 18 (10) Papillary 13 (7)	174	97
Side n (%)	Left 92 (58) Right 68 (42)	160	89
Cytonuclear grade n (%)	High 103 (60) Intermediate 57 (33) Low 13 (7)	173	96
Invasive Recurrence n (%)	Yes 18 (13) No 140 (87)	161	91
Invasive Recurrence Site n (%)	Ipsilateral 9 (50) Bilateral 1 (6) Unknown side 8 (44)	18	10
Invasive Recurrence Grade n (%)	High 8 (77) Intermediate 3 (23) Low 0 (0)	11	7
DCIS Recurrence	2 (100)	2	1
DCIS Recurrence Site	Ipsilateral 1 (50) Unknown side 1 (50)	2	0.5 0.5

DCIS Recurrence Grade	High	2 (100)	2	1
New Lesion (contralateral)		3	3	2

3.2.3 Immunohistochemical Experiments

Tissue sections from the manufactured in-house TMAs (Chapter 2) were cut at 4μm and dried overnight at 37 ºC before being baked at 57 ºC for two hours prior to IHC staining. Immunohistochemical staining, using antibodies raised against oestrogen receptor (ER) clone 6F11 (Leica, Newcastle, UK), progesterone receptor (PR) clone 636 (Dako, Ely, UK), HER2 (Oracle kit, Leica, Newcastle, UK) cytokeratin 5/6 (CK5/6) clone D5/16 B4 (Dako, Ely, UK), cytokeratin 5 (CK5) clone XM26 (Leica, Newcastle, UK) , cytokeratin 14 (CK14) clone NCL-CK14 (Leica, Newcastle, UK), Ki67 (clone MIB1) (Dako, Ely, UK), MCM2 –clone NCL-MCM2 (Leica, Newcastle ,UK) and epidermal growth factor receptor (EGFR) clone 384 (Leica, Newcastle, UK), was performed. All TMAs were stained in triplicate to reduce the loss of data due to core loss and ensure sufficient cells were available for assessment. Sections were stained using a two-step compact polymer chain biotin free IHC protocol using a 3-3'diaminobenzindine chromogen on the BondMax™ Leica automated staining system. HER2 tests were carried out on the same system using the HER2 Oracle kit (Leica, Newcastle, UK). All slides underwent blocking for endogenous peroxidase and a haematoxylin counterstain prior to coverslipping in an organic medium. Antigen retrieval was undertaken for each antibody according to manufacturer's recommendations. All slides were stained alongside appropriate known positive control sections for quality control purposes. ER and PR status was previously recorded for some of the cases in this study, however due to changes in IHC methodology and improvements in antibody clones it was determined that repeat would be undertaken for all. Appendix 4 lists reagents and protocols for immunohistochemical staining.

3.3 Hormone Receptors

3.3.1 Oestrogen Receptor Structure and Function

Oestrogens are steroidal sex hormones involved in a large number of physiological processes (106). They have a major effect on the female reproductive system, including ovulation, pregnancy, childbirth and lactation (106). They are also involved in the cardiovascular system, immune response, central nervous system and bone growth (106). Many of the physiological actions of oestrogen are mediated via binding to the oestrogen receptor (ER) (106-108).

ER is a ligand-activated intracellular transcription factor responsible for the biological effects of oestrogen via gene regulatory pathways (109-111). ER belongs to a groups of proteins known as the nuclear hormone receptor (NHR) superfamily which includes progesterone (PR), testosterone and vitamins A and D (111). There are two identified isoforms, ERα and ERβ, coded for by the genes ESR1 (located 6q24-q27) and ESR2 (located 14q21-q22). These isoforms have 95% amino acid homology (110). ER protein structure (Figure 18) consists of a variable N terminal domain containing an activation domain, AF1, followed by a DNA binding domain (DBD). The DBD is linked to a variable hinged region connected to a ligand binding domain (LBD). The LBD contains a second activation domain AF2. The activation domains regulate the transcriptional activity of ER (110, 112). The DBD allows the ER to bind to specific DNA loci within the nucleus, known as oestrogen response elements (EREs), due to the presence of two highly conserved zinc fingers distinct to the NHR superfamily. The variable hinged region of ER is a flexible region of the protein and acts as a

nuclear localisation signal connecting the DBD and LBD (110). The LBD acts as a "molecular switch" which, upon binding the hormone oestrogen, becomes transcriptionally active (112, 113). ERα and ERβ binding of 17β estradiol (E2) via the EREs and the transcriptional activation has been designated the classic pathway of oestrogen action (114). The binding of E2 to the receptor results in conformational changes leading to dimerisation with coactivator or corepressor molecules which regulate downstream physiological responses (115).

Figure 18: Structure and Functional Domains of ER

3.3.2 Oestrogen Receptor and Breast Cancer

Unlike most of the NHR superfamily, oestrogen receptor (ER) (and androgen receptor (AR)) have the ability to stimulate cellular proliferation and are essential for the normal development of the female breast during puberty and pregnancy (116). However, it is this very ability that, when aberrations occur, can lead to tumourigenesis and uncontrolled proliferation. The exact mechanism of how the ER/E2 complex initiates cellular proliferation remains elusive.

IHC expression of ER status is a weak prognostic marker of independent clinical outcome but a strong predictive marker of response to therapy in invasive breast cancer (117). Approximately 60-70% of breast cancers in women under 50 years and 80% of breast cancers in women over 50 are ER positive (118). Unlike many IHC markers, ER is used clinically to help determine the likelihood of response to endocrine therapy for patients with invasive breast cancer, which can be in the form of antagonists that directly block the receptor pathway (Tamoxifen) or indirect blocking such as the aromatase inhibitors which prevent conversion of androgens to oestrogen (119).

3.3.3 The Oestrogen Receptor and Ductal Carcinoma in Situ

The expression of oestrogen receptor in DCIS may have important implications for the treatment of precursor lesions, with some studies showing ER, PR and HER2 predict an increased risk of local recurrence (120, 121). Up to 80% of DCIS lesions are ER positive. (122). However, treatment of DCIS with anti-oestrogen therapy such as Tamoxifen has not shown an overall decrease in mortality (54). Randomised trials by the National Surgical Adjuvant Breast and Bowel Project (NSABP) have demonstrated a reduction of incidence of both invasive breast cancer and DCIS with Tamoxifen treatment for women aged over 35 recognised to be at increased risk of developing breast cancer (123).

3.3.4 Progesterone Receptor

Progesterone receptor (PR) is another member of the steroid receptor superfamily important for growth and development in the breast and female genital tract. PR expression is induced by oestrogen, and is thought to be an indicator of an intact ER pathway. Thus, PR positivity may be an adjunct to prediction of response to oestrogen related therapies (118). PR is also often advocated as an IHC marker where a possible false negative ER result is suspected (118). It has been shown that some ER+ PR- invasive breast tumours have a reduced response to tamoxifen compared to ER+ PR+ tumours, however the exact mechanism as to how both oestrogen and progesterone interact is not known (118, 119, 124). Tamoxifen therapy induces a greater drop in PR than ER levels, with some lesions losing PR expression completely; this may be one mechanism in the development of acquired tamoxifen resistance and a poorer overall survival (OS) in patients with invasive breast cancer (124). The ATAC trial (125) studied the response of ER positive breast disease treated with tamoxifen or anastrozole (arimidex) alone or in combination. Results from this study showed that patients treated with anastrozole had prolonged disease free survival, time to recurrence, distant metastases and contralateral breast cancers after

five years compared to tamoxifen (125) . These findings were also reported in a long term follow up of the ATC trial after 10 years (126).

3.4 Epidermal Growth Factor Receptors

3.4.1 Epidermal Growth Factor Receptor Structure and Function.

The epidermal growth factor receptor (EGFR) or ErbB family of tyrosine kinases (phosphorylation enzymes) comprises four related transmembrane proteins (HER1 to HER4) that can form oligomers, usually in the form of a homo-dimers or hetero-dimers (127). The HER family of proteins acts as conduits for the activation of intracellular signalling pathways from extracellular signals (128). All four of the HER proteins are characterised by an extracellular ligand binding domain, a transmembrane domain and an intracellular tyrosine kinase domain (128). Crystollographic studies by Burgess et al (129) defined the structure and ligand induced dimerization, however the exact kinetic mechanisms remained elusive. Zhang et al (130) elucidated, through further crystallographic & mutational analysis, that the allosteric mechanism was similar to CDK2/cyclin A activation, where the C-terminal lobe of one kinase interacts with the N terminal of the adjacent kinase. The Erb family of proteins plays key roles in mediating the cellular proliferation of cells, differentiation, metabolism and motility (131).

The *HER2* gene was first identified in human breast cancer by King et al in 1985. Also known as ErbB2 (referring to both human and rodent gene), "*HER2*" refers to the human gene and protein and not the rodent (128). Unlike HER1, HER3 and HER4, HER2 does not bind specific ligands but relies on hetero-dimerisation, with one of the other ligand-bound HER proteins (132) (Figure 19).

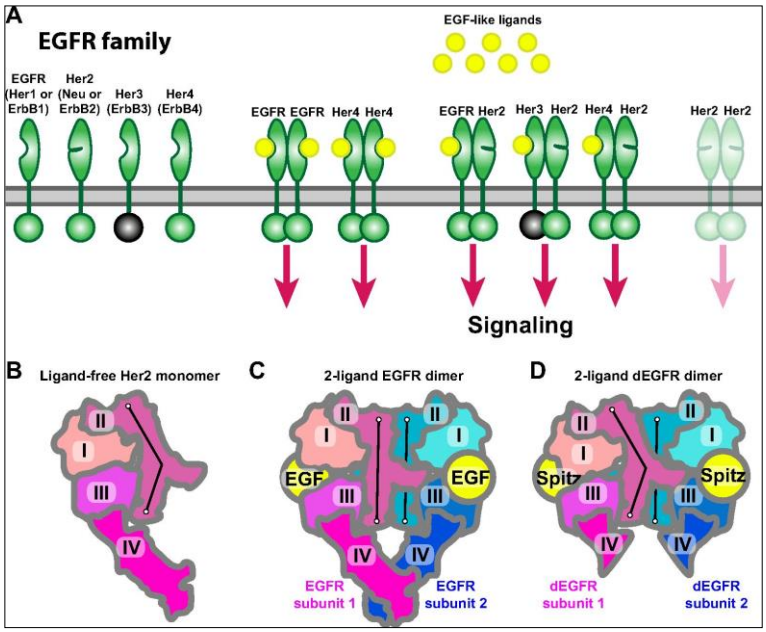

Figure 19: EGFR Structure. DOI: http://dx.doi.org/10.7554/eLife.00708.003 reproduced through Creative Commons Attribution license: original image from reference (132)

The overexpression of both HER1 (EGFR) and HER2 (C-erbB2) has been implicated in many solid tumours, including bladder, breast, colon and lung cancers (127, 133, 134).

EGFR (HER1) has been shown to be expressed in the basal-like invasive breast tumours and in some DCIS (127, 134) and is one of the targets currently under investigation for monoclonal antibody therapy with drugs such as erlotinib, cetuximab, and lapatanib in invasive breast cancer (135, 136). There are a several antibodies commercially available for the immunohistochemical assessment of EGFR. Although membrane reactivity is regarded as ‘positive’ for EGFR, significant staining variation between antibodies exists (unpublished data) and there is yet to be a defined pathological scoring system such as the HER2 scoring system for this antibody.

In breast cancer HER2 overexpression is present in between 15-25% of invasive lesions. Although associated with a poorer prognosis overall, targeted therapy, for

example with the drug trastuzumab (Herceptin), is available (137) and widely recommended and effective for patients with HER2 positive invasive breast cancer.

3.5 Proliferation Markers

3.5.1 Introduction

Deregulated proliferation is one of the hallmarks of the cancerous state (138). In order for a tumour to grow and infiltrate surrounding tissues, the ability for a neoplastic cell to replicate is essential for the progression of a lesion. Several IHC markers have been established as indicators of proliferation, and have found use in both the research and diagnostic laboratory setting. In this study, Ki67and the minichromosome maintenance protein 2 (MCM2) have been selected as suitable indicators of proliferation.

3.5.2 Ki-67

Ki-67 is an established marker for the assessment of cellular proliferation (139). First used to show proliferative activity in frozen or freeze-dried sections of human lung tissue (140) it is one of the most utilised biomarkers in cancer research. A Pubmed enquiry in 2015 using the search criteria “Ki-67 & cancer” yields over 15,000 articles, a search for Ki-67 alone yields over 19,000. The large number of articles belies the fact that the exact function of this protein is still not fully understood and there is a relative paucity of papers looking at Ki-67 structure and function (139). However, it is almost universally accepted that Ki-67 protein expression is essential for the cell cycle (139). Removal of phosphorylated Ki67 from cells using antisense nucleotides prevents cell cycling (141). Loss or inhibition of Ki67 results in ribosomal RNA synthesis inhibition (142). Ki67 is expressed during all stages of the cell cycle, G1, G2, S and mitosis, however, it is not expressed in G0 (143).

3.5.2.1 Ki-67 nomenclature

The Ki-67 antigen is known to be a large protein and is referred to as Ki67 protein, as opposed to the original antibody, raised against the protein which is referred to as the Ki67 antibody. This antibody was the prototype for other Ki67 antibodies raised to different epitopes on this large molecule and was produced by immunizing mice with nuclei from a Hodgkin lymphoma cell line (L428) (139, 141). These include the clone MIB1 (Molecular Immunology Borstel), MIB5 and TEC-3. The name Ki-67 originates from the city of discovery (Kiel) and the position in a 96 well plate of the original clone (139).

3.5.2.2 The Structure and Function of Ki-67

Ki-67 has 2 prominent forms detectable at the protein level (Figure 20), a 395kDa and a 320kDa protein encoded by nearly 30,00 base pairs (141). Schulter et al (144) published the cDNA sequence encoding for the *Ki-67* protein in 1993 identifying 2 spliced isoforms of mRNA (modifications of the RNA transcript by removing introns and introducing exons) which differed by the absence in one region encoded by exon 7. They also describe a series of 366 base pair “Ki67 repeat” elements in a 6,845 base pair exon located centrally within the antigen. This exon (138) is one of the largest mammalian exons known. They concluded that Ki-67 has no known homology with other known amino acid sequences and it is a short-lived category of cell cycle associated nuclear non-histone protein. Further studies by Hofmann and Butcher identified a forkhead associated domain (FHA) in Ki67 as well as other unrelated proteins found in yeast, bacteria and mammals but all believed to be involved in DNA repair, synthesis or cell cycle regulation (145). The Ki-67 protein contains 143 protein kinase C, 89 casein kinase II and 2 tyrosine kinases (protein kinases phosphorylate serine, threonine, tyrosine, or histidine residues to modify a protein function) (139). Analysis of the amino acid sequence has led to the prediction of ten nuclear targeting

signals, which may explain why Ki-67 is only found in the nuclei during interphase (139, 146-148).

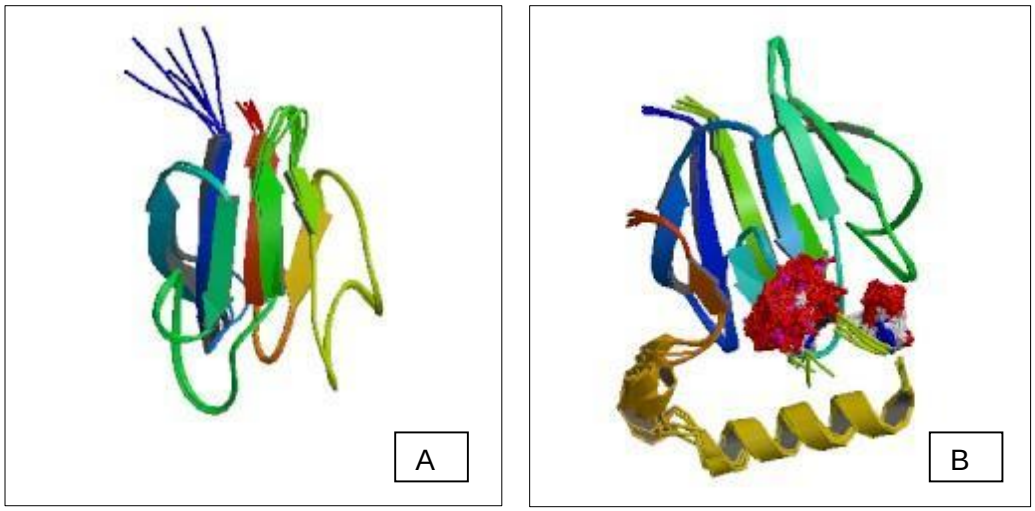

Figure 20: Ki-67: Protein structure 1R-21-1-120 (human) A & 2AFF-1-120 (human) B. Images courtesy of RCSB PDB rendering based on 1r21.en.wikipedia.org

Despite the fact that Ki-67 has been described, and used in immunohistochemical studies, for over thirty years the exact function remains elusive as do its possible interactions with other cell cycle markers. There are several possible explanations why Ki67 function is difficult to elucidate. Scholzen et al suggest that its large size and susceptibility to proteolytic cleavage make biochemical assays difficult. Secondly, they cite the lack of similarity to other proteins makes study of this molecule with standard methods difficult. To date there is no definitive explanation of Ki-67 function. Although believed to be expressed solely in the active proliferative phases of cell cycling (G_1, G_2, S and mitoses) there is some evidence that Ki67 can be detected in quiescent cells (G_0) and has a possible role in RNA transcription (149) and RNA synthesis (142).

3.5.2.3 Ki-67 as a Biological Marker in Cancer

There have been many studies showing that Ki67 assessment has prognostic value in invasive cancer. Brown and Gatter's review in 2002 showed a total of 23 papers

examining Ki67 in breast cancer alone as having an independent prognostic value (141). A Pubmed search on the 26th April 2015 for “Ki-67, breast cancer and independent prognostic factor” yielded over 160 journal articles citing Ki67 alone, or in combination with other markers, having potential value as a prognostic marker. More recently, the focus has been on the use of Ki67 as a predictive factor (i.e. in selection of response to therapy) with Darb-Esfahani al reporting that Ki67 can be utilised as an independent predictor of response to anthracycline/taxane-based neoadjuvant chemotherapy regardless of invasive tumour type (150) although Jones et al found no association with Ki67 and clinical response (151). Other studies have reported that changes in Ki67 level are a valuable predictor of response to hormone therapy. Finally, groups, such as Cheang et al, have used a Ki67 Index in association HER2 and ER to define/classify the luminal B subgroup of invasive breast cancer using immunohistochemistry (152).

3.5.2.4 Ki67 and Ductal Carcinoma in Situ

In DCIS, Ki67 expression in conjunction with COX-2 and p16 expression, has been suggested to be an important factor and associated with an increased risk of developing subsequent invasive disease (120). Altinas et al examined a range of biological markers, including Ki67, as possible predictors of local recurrence and no found evidence that Ki67 alone or in conjunction with other markers was significant (153).

However, much of the data on Ki67 and definition of sub-groups for comparison with outcome has been undertaken on invasive disease. Zhou et al used Ki67 with a cut-off of >14% to distinguish positive cases to assign subgroups in invasive disease. Those with >14% were defined luminal A and those with <14% were defined as luminal B/HER2 negative (as defined by the St Gallen International Expert Consensus from Cheang’s publication (145), although they found no significant prognostic value in their cohort (97). Ruiz et al (154) compared three molecular classification

subgroups, finding that only the classification including Ki67 as a marker improved prediction of overall survival in invasive disease.

3.5.3 Mini Chromosome Maintenance Proteins

3.5.3.1 The Structure and Function of Mini Chromosome Maintenance Proteins

Unlike Ki67, the structure and function of the Mini Chromosome Maintenance (MCM) proteins are well understood. A review by Bochman & Schwacha in 2009 (155) references 280 articles on MCM structure and function in both archaeal and eukaryotic forms. For the purpose of this thesis, information on eukaryotic MCM function is given.

MCM proteins are essential components of DNA replication in the cell cycle (156). Several gene variants exist encoding for the proteins MCM2 to MCM7, which are required to establish a pre-replication complex prior to cellular division. MCM2, MCM3 and MCM5 were first discovered in the yeast Schizosaccharomyces cerevisiae (157), followed by the discovery of MCM4, MCM7 and cell division mutations (155). MCM6 was discovered in Schizosaccharomyces pombe in 1994 (158). Further studies on Xenopus Laevis (African clawed frog) identified that all six proteins (MCM2 to MCM7) were required to couple to DNA for replication to occur (155, 159). In eukaryotic cells, all six cell cycle related MCMs have a similar 250 amino acid region encoding for ATPases. ATPases, also known as AAA proteins, are a diverse group of proteins with a wide range of functions acting as DNA helicases and proteases (155).

MCM proteins form ring-like structures to incorporate ATP binding and enable hydrolysis to alter DNA within the central circle or channel of the ring-like structure and perform helicase activity, unwinding the DNA and forming replication forks (160). The MCM2 to MCM7 helicase structure is essential for initiation and elongation of double stranded DNA (155).

The activation of MCMs from an inactive form to an enzymatic helicase requires the recruitment of several protein cofactors. This includes, but may not be exclusive of, proteins Cdt1, Cdc6, MCM10, geminin and the kinase Cdc7-Dbf4 (161). During G_1 inactive MCM proteins are transported by Cdt1 protein to the origin of replication site where cells undergo ”licensing” for replication by a group of six polypeptides, known as the origin recognition complex1-6 (ORC1-6)(162). ORC1-6 is a heterohexameric protein complex which binds proteins Cdt1 and Cdc6 (162, 163) followed by the binding of MCMs thus forming a heterohexamer pre-replication complex (Figure 22). The binding of MCMs requires the presence of ORC1-6 and Cdc6, which provide ATP hydrolysis and thus the energy for this active process (155, 164). Once the MCMs are bound to DNA ORC1-6 and Cdc6 are disassociated from the complex. In S phase of the cell cycle, cyclin dependent kinases (CDKS) promote the formation of DNA replication forks and possibly the initiation of MCM function (155). MCMs demonstrate a helicase activity responsible for the unwinding of the DNA helix prior to replication (165). Once the pre-replication complex has loaded, DNA polymerases are recruited and DNA replication ensues. Sanchez-Berrondo et al (166) demonstrated in Bacillus cereus MCMs bind DNA and not only act as a helicase but also function as a primase and a polymerase.

Once replication has occurred, MCMs are inactivated by phosphorylation, leading to their dissociation from the pre-replicative complex thus limiting replication to once per cell cycle (Figure 22).

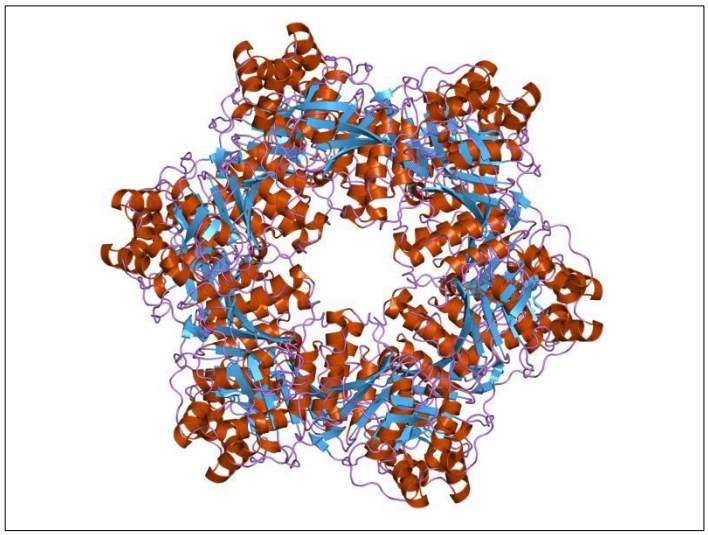

Figure 21: Examples of a Hexameric Helicase Protein Structure for DNA replication.

(Image courtesy of *http://www.ebi.ac.uk/)*

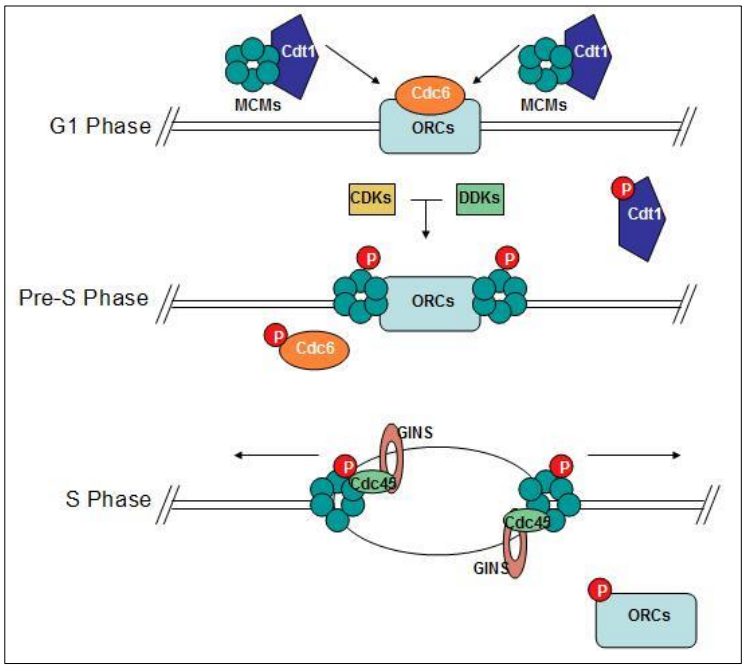

Figure 22: MCM Proteins in the Cell Cycle

(Creative Commons Attribution-Share Alike 3.0 Unported license, author: Azackta1 2013)

3.5.3.2 Minichromosome Maintenance Proteins and Cancer

Previous studies examining MCM2 and MCM5 have shown them as potential alternatives to Ki67 for assessment of proliferation in invasive cancer (167-170). Some have shown MCMs to be independent prognostic markers in invasive breast cancer (171, 172) although MCM expression correlates with Ki67 expression and histological grade (173). The deregulation of MCMs 2-7 has been shown to be an early event in tumourigenesis, both in actively cycling cells and, unlike Ki67, non-proliferating cells that have the potential to enter the cell cycle (167, 170, 174-178). To date, there are only two studies examining the relationship between precursors of invasive breast cancer and MCM2 (179, 180). Reena et al (179) advocate MCM2 as a reliable proliferation marker in DCIS, whilst Nasir et el (180) included MCM2 in a panel alongside TOP2A and BUB1B as “potential molecular biomarkers of malignancy in histologically normal and benign breast tissues”.

3.6 Basal Markers

3.6.1 Cytokeratins 5, 6 and 14

Basal epithelial cells were traditionally described as cells adjacent to the basement membrane (181). However, since Moll’s work on cytokeratins (182), the term has become synonymous with those cells expressing the high molecular weight cytokeratins, 5 and 14 and 17 (CK5, CK14, CK17). The term ‘basal cell’ is often incorrectly applied to myoepithelial cells although the expression of these cytokeratins is not solely confined to myoepithelial cells (183). This has led to a dual meaning for the term basal, which can now refer to either myoepithelial cells or cells expressing “basal” cytokeratins, and is further complicated by the term basal-like breast cancer, which is a molecular phenotype. Basal-like breast tumours are often triple negative (i.e. tumours negative for ER, PR and HER2) and a significant proportion of the triple

negative carcinomas express CK5, 14 or 17. However, the two terms are not synonymous, with some triple negative tumours lacking basal marker expression and occasional basal like tumours being positive for hormone receptors or HER2. Triple negative invasive tumours have a poorer prognosis that many other types of breast carcinoma, with no targeted therapy currently available (86, 184). Thus accurate identification of the premalignant stage could be beneficial in the early identification of these difficult to manage lesions, without the need for adjuvant systemic treatments. In the context of this study, the immunohistochemical expression of one or more of CK5, 5/6 and 14 and / or EGFR is used to define basal breast carcinoma (BBC) as a pathological entity.

3.7 Scoring of Antibody Markers in Immunohistochemical Studies

5.7 TMA slides with immunohistochemical stains were independently scored by a consultant breast pathologist (SEP) and the author (JPB). Original Excel TMA maps and scores are given in Appendix 2: Excel TMA Maps and IHC Scores

TMA block number	DCIS TMA location	ER Average	PR	HER2	EGFR	CK5/6	CK14	KI67	MCM2
DCIS 15A	A1	0	0	0	0	0	1	1	0

DCIS 15A	A2	0	0	0	0	0	0	x	0
DCIS 15A	A4	2	0	0	0	x	10	1	0
DCIS 15A	A5	0	0	1	3	0	5	40	10
DCIS 15A	B1	x	x	x	0	x	x	x	x
DCIS 15A	B3	0	0	0	3	0	0	10	40
DCIS 15A	B4	0	0	0	0	0	0	30	x
DCIS 15A	B5	2	0	0	1	0	0	15	30
DCIS 15A	C2	5	0	0	0	0	0	5	5
DCIS 15A	C3	1	0	1	2	0	0	5	5
DCIS 15A	C4	5	7	2	0	0	0	1	1
DCIS 15A	C5	8	8	0	0	0	0	0	2
DCIS 15A	D1	x	x	x	x	x	x	x	x
DCIS 15A	D2	x	x	x	x	x	x	x	x
DCIS 15A	D3	0	x	x	x	x	x	x	x
DCIS 15A	D4	x	x	x	x	x	x	x	x
DCIS 15A	E1	2	x	x	x	x	x	x	x
DCIS 15A	E2	0	0	0	0	0	x	0	5
DCIS 15A	E3	5	x	x	x	x	x	x	x
DCIS 15A	E4	8	x	0	0	0	0	1	1
DCIS 16A	A1	0	x	x	x	x	x	x	x
TMA block number	INVASIVE TUMOUR location	ER (Allred)	PR (Allred)	HER2 (HER2)	EGFR (HER2)	CK5/6 (%)	CK14 (%)	KI67 (%)	MCM
DCIS 16A	A2	8	5	x	0	0	0	1	3
DCIS 16A	A4	7	0	3	0	0	0	1	5

DCIS 16A	A5	2	4	2	0	0	0	0	0
DCIS 16A	B1	3	x	x	x	x	x	x	x
DCIS 16A	B3	5	8	2	0	0	0	2	5
DCIS 16A	B4	1	x	x	x	0	0	x	x
DCIS 16A	B5	4	0	0	x	0	0	20	45
DCIS 16A	C2	5	8	2	x	0	0	10	25
DCIS 16A	C3	4	0	1	3	0	0	25	30
DCIS 16A	C4	2	0	0	1	0	0	10	25
DCIS 16A	C5	4	0	3	1	0	0	5	35
DCIS 16A	D1	0	0	0	0	0	0	15	40
DCIS 16A	D2	3	x	x	x	x	x	x	x
DCIS 16A	D3	5	x	x	x	x	x	x	x
DCIS 16A	D4	5	8	0	0	0	0	x	x
DCIS 16A	E1	5	0	x	x	0	0	10	10
DCIS 16A	E2	1	x	3	0	0	0	x	x
DCIS 16A	E3	4	0	3	0	0	0	10	30
DCIS 16A	E4	2	0	2	1	1	0	2	10
DCIS 16A	E5	x	0	x	2	0	0	3	35
INV T 15	A1	0	0	0	3	15	0	8	8
INV T 15	A2	0	0	0	3	0	0	5	2
INV T 15	A4	0	0	0	3	60	95	4	53
INV T 15	A5	0	0	1	3	0	0	50	17
TMA block number	INVASIVE TUMOUR location	ER (Allred)	PR (Allred)	HER2 (HER2)	EGFR (HER2)	CK5/6 (%)	CK14 (%)	KI67 (%)	MCM

INV T 15	A6	0	0	2	3	0	20	30	17
INV T 15	A7	0	0	0	3	0	100	10	37
INV T 15	B1	0	0	0	0	0	0	50	17
INV T 15	B3	4	0	x	2	0	25	20	15
INV T 15	B4	6	0	1	2	0	0	20	7
INV T 15	B5	8	6	0	0	0	0	3	1
INV T 15	B6	8	7	2	0	0	0	15	5
INV T 15	B7	8	8	0	0	0	0	0	0
INV T 15	C2	8	7	1	0	0	0	15	5
INV T 15	C3	8	8	1	0	0	0	4	1
INV T 15	C4	3	0	0	1	0	0	x	x
INV T 15	C5	8	0	3	1	0	0	5	2
INV T 15	C6	4	0	0	3	0	0	20	7
INV T 15	C7	6	0	0	3	0	0	5	2
INV T 15	D1	8	8	3	0	0	0	8	3
INV T 15	D2	8	7	0	0	0	0	5	2
INV T 15	D3	7	8	2	1	0	0	4	1
INV T 15	D4	8	6	0	1	0	0	3	1
INV T 15	D6	8	6	1	1	0	0	4	1
INV T 15	D7	8	0	3	0	0	0	4	1
INV T 15	E1	8	7	0	0	0	0	0	0
INV T 15	E2	8	8	0	0	0	0	4	1
INV T 15	E3	7	0	3	0	0	0	5	x
INV T 15	E4	6	0	0	1	0	80	30	37

TMA block number	INVASIVE TUMOUR location	ER (Allred)	PR (Allred)	HER2 (HER2)	EGFR (HER2)	CK5/6 (%)	CK14 (%)	KI67 (%)	MCM
INV T 15	E5	8	8	0	1	0	0	5	2
INV T 15	E6	4	0	0	2	0	0	35	12
INV T 15	E7	0	0	0	2	0	0	20	7
INV T 15	F1	3	0	3	0	0	0	x	x
INV T 15	F2	0	3	0	2	5	4	20	10
INV T 15	F3	8	8	3	0	0	0	8	3
INV T 15	F4	8	8	0	0	0	0	5	2
INV T 15	F5	8	4	0	1	0	0	4	1
INV T 15	F7	8	0	0	0	0	0	5	2
INV T 15	G1	4	0	3	1	0	0	15	5
INV T 15	G2	8	0	3	0	0	0	x	x
INV T 15	G3	3	0	0	2	20	0	25	15
INV T 15	G4	0	0	0	2	10	0	40	17
INV T 15	G6	8	0	2	0	0	0	5	2
INV T 15	G7	4	0	0	3	0	0	12	4

2. ER and PR stained sections were scored according to the Allred method based upon the proportion and staining intensity of tumour nuclei. A score between 0 and 3 is given for intensity of staining and a score of 0-5 for % of cells stained. These two scores are combined to give a score out of eight. At the current time, an Allred score of three or more is regarded as positive in invasive breast carcinoma, with patients with ER positive invasive breast cancers eligible for anti-oestrogen therapy (32).

HER2 and EGFR were scored using the HerceptTest™ (DAKO, Ely, UK) scoring method, based upon tumour cell membrane staining. The membranous staining of tumour cells is assigned a value of 0-3 with zero being completely negative for staining, one having less than 10% of complete tumour cell membrane staining with faint or barely perceptible staining intensity. A value of two relates to greater than 10% of cells staining with moderate, complete, membrane reactivity and a score of three is assigned when greater than 10% of cells show complete tumour cell membrane staining with strong intensity. Normal breast ducts should be negative and thus act as an internal control to ensure no over-staining has occurred. Where a score 2+ for HER2 is found the result is deemed to be equivocal. For this study chromogenic in-situ hybridisation (CISH) was selected to test those cases of DCIS with HER2 scores of 2+ for genomic amplification of the HER2 gene. Fluorescence in-situ hybridisation (FISH) is a regarded by some authors as being more consistent for identifying HER2 gene amplifications in FFPE tissues (185). However, concordance has been demonstrated between chromogenic in-situ hybridisation (CISH) and FISH (186) and the former does not require a fluorescence microscope or specialist filters. In this Study the “INFORM HER2 Dual ISH DNA Probe Cocktail Assay” (Ventana, Tuscan, USA) was assessed on all cases scoring 2+ using IHC. HER2 gene status is determined by enumeration of the ratio of the HER2 gene to Chromosome 17 with a ratio of HER2 to chromosome 17 of more than 2.00 or copy number of 6 or more indicating gene amplification/HER2 positivity.

Cytokeratins were deemed as staining positively where cytoplasmic and/or membranous staining was present in tumour cells and a semi-quantitative percentage score recorded for the number of tumour cells stained.

Ki67 (MIB1) staining was scored semi-quantitatively as a percentage of positive tumour cell nuclei.

Fourteen TMAs containing 20 cases of DCIS each were stained in triplicate giving a total of 840 cores for assessment for each antibody. The use of large 2.0mm cores gives a greater area than generally deemed representative in the literature, as described above. For this reason for scoring purposes only one core was required to meet the criteria of adequate for inclusion in analysis. Where two or three cores were available either an average or the maximum/highest score was recorded dependent upon the protein under evaluation (see below).

3.7.1 Analysis of differing IHC Scores.

Each antibody had a potential of three TMA cores requiring a score. This could, depending upon tissue heterogeneity, result in different scores for each TMA core per case. This posed a dilemma for analysis. As previously stated, the consensus in the literature indicates that a single core in this study would be regarded as representative but three separate scores in a single case would question this assumption. If variation between cores existed in a single lesion as scored by an individual observer then how should the final score be assigned? Should the highest or an average score of cores available be taken for each antibody?

There are guidelines for ER, PR and HER2 scoring of invasive tumours, with clinical cut-off values relating to suitability for targeted therapy. For ER and PR, the Allred method of scoring was chosen, as it is the recommended scoring system from the UK NHS Breast Screening Program for invasive breast cancer (NHSBSP guidelines

2005) for invasive cancer. For these antibodies the same rationale for scoring was applied to DCIS (Table 3).

The Allred of scoring was chosen, as it is the recommended scoring system from the UK NHS Breast Screening Program for invasive breast cancer (NHSBSP guidelines 2005) for invasive cancer. For these antibodies the same rationale for scoring was applied to DCIS).

Similarly, as the scoring for EGFR mirrored HER2 in terms of pattern, the same cut-off principles were applied. Cut-off values for the basal cytokeratins and Ki67 were harder to determine, with significant variation in the literature (see discussion). For these an average score of all representative cores was taken.

Currently there are limited data on the value of TMAs for setting quantitative relationships or cut-off values to clinical samples and this invariably plays a role in comparison of different series. The International Ki67 in Breast Cancer working group (187) suggest that TMAs should not be used to predict cut-offs, however, the use of 2mm cores as opposed to 0.6mm may somewhat ameliorate any discrepancy between whole sections and TMAs. In this series the median value was chosen as a cut-off due to the lack on consensus for a clinical cut-off value for Ki67 in cases of DCIS.

3.7.2 Inter Observer Variability in Scoring Immunohistochemistry

All cores were independently scored by the two reviewers. Comparison of results between the two reviewers was performed to determine reproducibility. The degree of variance allowed and the best scoring method needed to be defined prior to

screening to eliminate any possible bias; the allowances for inter observer variation are given in 4. Scores that differed between individuals greater than the accepted variance underwent joint review by both scorers with a consensus being reached.

Score for proportion	Score for intensity
0 = no staining	0 = no staining
1 = <1% nuclei staining	1 = weak staining
2 = 1-10% nuclei staining	2 = moderate staining
3 = 11-33% nuclei staining	3 = strong staining
4 = 34-66% nuclei staining	
5 = 67-100% nuclei staining	

Table 3: Allred Scoring Method

3.8 Statistical Analysis of Immunohistochemical Scoring

Statistical analyses were performed using the software pakage StatView (SAS Institute Inc. San Francisco, CA). Frequency distrubutions and non parametric univariate analysis was undertaken to compare the expression the biomarkers with each other and with the pathological criteria utilising the Chi-square (χ^2) and Fisher's exact tests as appropriate. Fisher's exact test is suitable for defining a p value where two categorical variables have small values (usually less than 5). Chi- square is used to test for associations between larger values. Frequency distributions and univariate analyses tables are listed in Appendix 5.

3.9 Immunohistochemistry Results

3.9.1 Immunohistochemical Scoring

Immunohistochemical results for staining of DCIS are given below (Table 5) with the number of positive and negative stained cases according to the scoring criteria above. Staining frequencies for each antibody are listed in Table 5. Representative images for IHC staining of pure DCIS & CISH for HER2 are seen in Figure 23 to Figure 29 (section 3.9.2) Sections 3.9.3 to 3.9.9 give representative examples of paired univariate analysis for IHC markers and observed frequencies. Appendix 5 lists all other sets.

Antibodies	Scoring Method, recorded score	Allowed variance between observers
ER and PR	Allred (0-8). The average of all cores is taken.	Scores must be within 1 of each other i.e. a score of 7 on one core and 6 or 8 on the others is acceptable.
HER2 and EGFR	HER2 score, 0-3. Highest value is regarded as definitive.	No variance accepted
CKs (5, 5/6, 14)	%, an average of scores from the cores is regarded as final result.	Variance of 5% is acceptable
Ki67	%, an average of scores from the cores is regarded as final score.	Variance of 5% is acceptable

Table 4: IHC methods of scoring, of handling differing scores from cores and defined acceptable variation for DCIS immunostaining.

Antibody	Total Number of Cases Stained	Number of Positive Cases (%)	Number of Negative Cases (%)
ER	224	165 (74)	59 (26)
PR	236	113 (48)	123 (52)
HER2	248	57 (23)	191 (77)
EGFR	227	11 (5)	213 (95)
CK5	227	32 (14)	195 (86)
CK5/6	220	69 (31)	151(69)
CK14	231	38 (16)	193 (84)
Ki67	237	136 (57)	101 (43)
MCM2	237	130 (55)	107 (45)

Table 5: Staining frequencies for immunohistochemical antibody staining.

3.9.2 Immunohistochemical Images

Figure 23: ER staining of DCIS in 2mm TMA core (X40, X200)

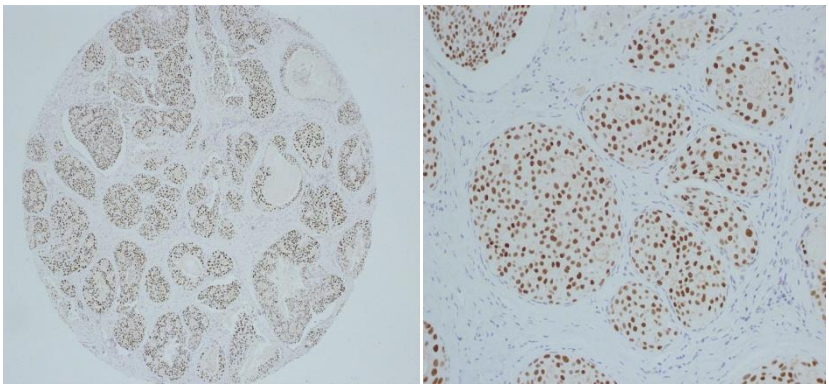

Figure 24: PR staining of DCIS in 2mm TMA core (X40, X200)

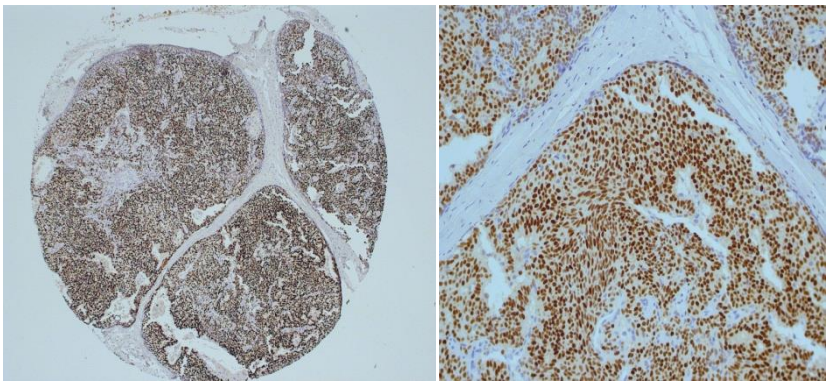

Figure 25: HER2 staining of DCIS in 2mm TMA core (X100, X200)

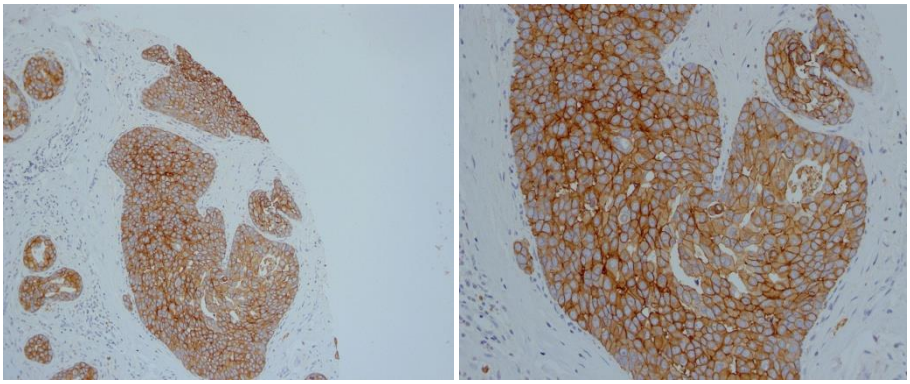

Figure 26: EGFR staining of DCIS in 2mmm TMA core (X40, X100, X200)

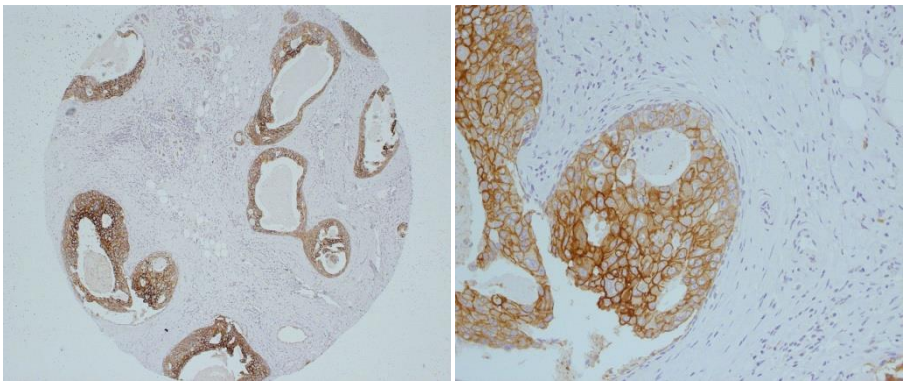

Figure 27: CK14 staining of DCIS in 2mm TMA core (X40, X200).

[Peripheral myoepithelial cell staining was not included in assessment of the DCIS]

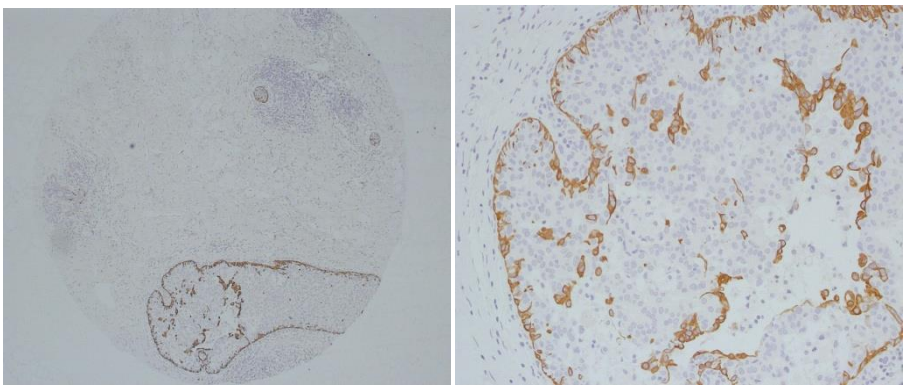

Figure 28: Ki67 staining of DCIS in 2mm TMA core (X40, X200)

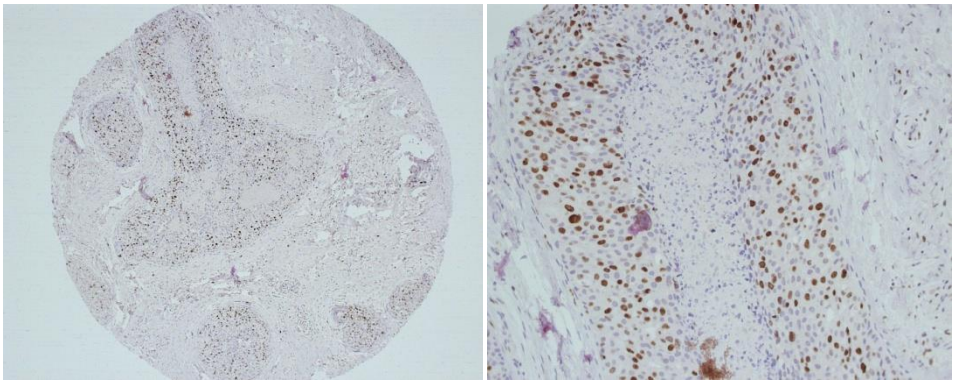

Figure 29: CISH for HER2 showing amplification of the *HER2* Gene in DCIS, 2mm Core (x40, X200)

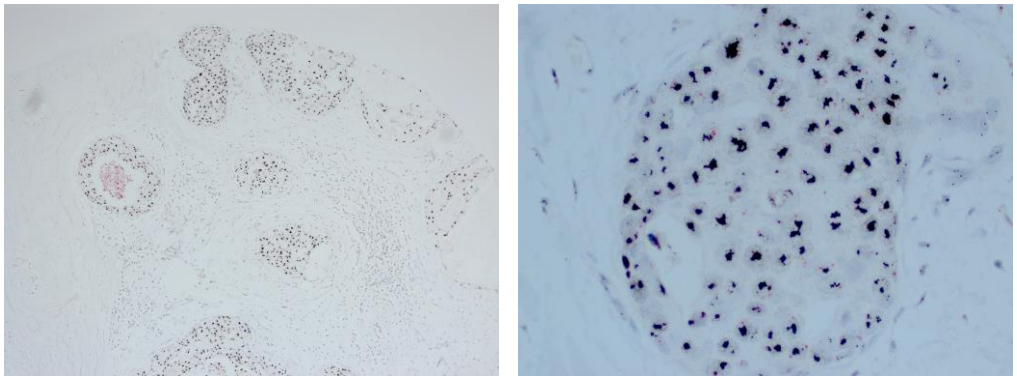

3.9.3 Non Parametric Tests- Univariate Paired analysis:

Positive univariate paired analyses tables and p-values for ER, PR, HER2, EGFR, Ki67, MCM2, CK5, CK5/6, CK14 and histological parameters are given below (Table 6).

Antibody	HER2	ER	PR	Ki67	Grade	Inflam-mation	Nec-rosis	MCM2	Archit-ecture	CK5/6	CK14	CK5	EGFR
HER2													
ER	<0.0001												
PR	<0.0001	<0.0001											
Ki67	<0.0001	<0.0001	<0.0001										
Grade	0.0001	<0.0001	0.0006	0.0009									
Inflammation	<0.0001	<0.0001	<0.0001	<0.0001	<0.0001								
Necrosis	<0.0001	<0.0001	0.0013	<0.0001	<0.0001	<0.0001							
MCM2	<0.0001	0.0032	0.0033	<0.0001	<0.0001	0.0003	<0.0001						
Architecture	0.0003	<0.0001	0.0011	0.0073	<0.0001	0.0025	0.0008	0.0098					
CK5/6	0.0041	0.0298	0.0542	0.2279	0.1044	0.0025	0.0515	0.3772	0.0066				
CK14	0.0037	0.0018	0.2791	0.29	0.115	0.2056	0.042	0.215	0.1355	<0.0001			
CK5	0.0443	0.0033	0.2385	0.3305	0.1364	0.0422	0.804	0.4392	0.2011	<0.0001	0.0003		
EGFR	0.7324	<0.0001	0.0008	0.0294	0.0865	0.0126	0.0816	0.0254	0.1527	>0.9999	>0.9999	0.2139	
Ipsilateral Recurrence	>0.9999	0.2912	0.3666	0.0812	0.3851	0.6047	0.4063	>0.9999	0.4834	>0.9999	0.7327	0.6594	>0.9999
All Recurrence	0.1952	0.784	>0.9999	0.4856	0.8452	0.8269	0.8352	0.4938	0.9266	>0.9999	0.4113	>0.9999	>0.9999

Table 6: Univariate analysis p-values for immunohistochemical and histological parameters.

3.9.4 Univariate Analysis of Hormone Receptor Immunohistochemistry

Summary Table for FINAL ER STATUS, FINAL HER2 STATUS
Row exclusion: DCIS STATVIEW DATASET

Num. Missing	52
DF	1
Chi Square	57.061
Chi Square P-Value	<.0001
G-Squared	52.622
G-Squared P-Value	<.0001
Contingency Coef.	.451
Phi	.506
Cty. Cor. Chi Square	54.443
Cty. Cor. P-Value	<.0001
Fisher's Exact P-Value	<.0001

Observed Frequencies for FINAL ER STATUS, FINAL HER2 STATUS
Row exclusion: DCIS STATVIEW DATASET

	0	1	Totals
0	23	36	59
1	145	19	164
Totals	168	55	223

Summary Table for FINAL EGFR STATUS, FINAL ER STATUS
Row exclusion: DCIS STATVIEW DATASET

Num. Missing	60
DF	1
Chi Square	25.989
Chi Square P-Value	<.0001
G-Squared	22.528
G-Squared P-Value	<.0001
Contingency Coef.	.328
Phi	.348
Cty. Cor. Chi Square	22.514
Cty. Cor. P-Value	<.0001
Fisher's Exact P-Value	<.0001

Observed Frequencies for FINAL EGFR STATUS, FINAL ER STATUS
Row exclusion: DCIS STATVIEW DATASET

	0	1	Totals
0	45	159	204
1	10	1	11
Totals	55	160	215

Table 7: Univariate paired analysis for oestrogen receptor immnunohistochemistry

Summary Table for FINAL PR STATUS, FINAL HER2 STATUS
Row exclusion: DCIS STATVIEW DATASET

Num. Missing	45
DF	1
Chi Square	40.858
Chi Square P-Value	<.0001
G-Squared	45.748
G-Squared P-Value	<.0001
Contingency Coef.	.388
Phi	.421
Cty. Cor. Chi Square	38.915
Cty. Cor. P-Value	<.0001
Fisher's Exact P-Value	<.0001

Observed Frequencies for FINAL PR STATUS, FINAL HER2 STATUS
Row exclusion: DCIS STATVIEW DATASET

	0	1	Totals
0	70	50	120
1	104	6	110
Totals	174	56	230

Summary Table for FINAL EGFR STATUS, FINAL PR STATUS
Row exclusion: DCIS STATVIEW DATASET

Num. Missing	57
DF	1
Chi Square	10.764
Chi Square P-Value	.0010
G-Squared	•
G-Squared P-Value	•
Contingency Coef.	.217
Phi	.222
Cty. Cor. Chi Square	8.829
Cty. Cor. P-Value	.0030
Fisher's Exact P-Value	.0008

Observed Frequencies for FINAL EGFR STATUS, FINAL PR STATUS
Row exclusion: DCIS STATVIEW DATASET

	0	1	Totals
0	102	105	207
1	11	0	11
Totals	113	105	218

Table 8: Univariate paired analysis for progesterone receptor immunohistochemistry.

The majority of DCIS cases were positive for hormone receptors (ER n=165, PR n=144- Table 7Table 8). For ER status there was an inverse correlation (p=0.001) with both EGFR and HER2 (Table 9); ER positive DCIS was associated with a negative EGFR and/or HER2 status. All PR positive cases were also ER positive

(n=102 Table 10) There was an inverse correlation for CK5 and CK14 and ER with 90% (n=147) and 88% (n=142) of ER positive cases being CK5 and CK14 negative respectively (Table 12). Few cases were negative for both ER and proliferation markers (ER-ve + Ki67-ve n=8 Table 13 and ER-ve MCM –ve n=15

Table 14) All low grade DCIS (n=9) was ER positive (6% of all graded cases) and 82% (n=46) of intermediate grade DCIS (n=50) was ER positive (34% of all graded cases; Table 15). High grade DCIS (n=90) made up 60% of cases and 61% (n=55) of these lesions were ER positive (p<0.0001). ER positive cases were more likely to have cribriform (n=55) or solid (n=38) architecture (Table 16). ER status did not predict the likelihood of recurrence of either DCIS or invasive disease (p=0.784; Table 20).

	ER -ve	ER +ve	Total
HER2 -ve	23	145	168
HER2 +ve	36	19	55
Total	59	164	223

Table 9: Univariate analyses for ER and HER2 IHC: Fishers exact test p value < 0.0001

	ER -ve	ER +ve	Total
PR -ve	56	55	111
PR +ve	0	102	102
Total	56	157	213

Table 10: Univariate analysis for ER and PR IHC; Fishers exact test p value <0.0001

	ER -ve	ER +ve	Total
CK5 -ve	41	147	188
CK5 +ve	15	16	31
Total	56	163	219

Table 11: Univariate analyses for ER and CK5 IHC; Fishers exact test p value = 0.0033.

	ER -ve	ER +ve	Total
CK14 -ve	40	142	182
CK14 +ve	18	19	37
Total	58	161	219

Table 12: Univariate analyses for ER and CK14 IHC; Fishers exact test p value = 0.0018.

	ER -ve	ER +ve	Total
Ki67 -ve	8	78	86
Ki67+ve	51	79	130
Total	59	157	216

Table 13: Univariate analyses for ER and Ki67 (>5%) IHC; Fishers exact test p value <0.0001

	ER -ve	ER +ve	Total
MCM2 -ve	15	77	92
MCM2+ve	44	83	127
Total	59	160	219

Table 14: Univariate analysis for ER and MCM2; (>5%) IHC Fishers exact test p value = 0.0032

	ER -ve	ER +ve	Total
HG	35	55	90
IG	4	46	50
LG	0	9	9
Total	39	110	149

Table 15: Univariate analyses for ER and Histological Grade; ER; Chi Square p value <0.0001

	ER -ve	ER +ve	Total
Crib	5	55	60
Micropap	7	6	13
Pap	1	11	12
Solid	26	38	64
Total	39	110	149

Table 16: Univariate analyses for ER IHC and Histological Architecture; Chi square p Value < 0.0001

3.9.5 Univariate Analysis for HER2 Immunohistochemistry

Summary Table for FINAL HER2 STATUS, FINAL EGFR STATUS
Row exclusion: DCIS STATVIEW DATASET

Num. Missing	50
DF	1
Chi Square	.050
Chi Square P-Value	.8229
G-Squared	.049
G-Squared P-Value	.8249
Contingency Coef.	.015
Phi	.015
Cty. Cor. Chi Square	0.000
Cty. Cor. P-Value	>.9999
Fisher's Exact P-Value	.7324

Observed Frequencies for FINAL HER2 STATUS, FINAL EGFR STATUS
Row exclusion: DCIS STATVIEW DATASET

	0	1	Totals
0	162	8	170
1	52	3	55
Totals	214	11	225

Summary Table for FINAL HER2 STATUS, FINAL ER STATUS
Row exclusion: DCIS STATVIEW DATASET

Num. Missing	52
DF	1
Chi Square	57.061
Chi Square P-Value	<.0001
G-Squared	52.622
G-Squared P-Value	<.0001
Contingency Coef.	.451
Phi	.506
Cty. Cor. Chi Square	54.443
Cty. Cor. P-Value	<.0001
Fisher's Exact P-Value	<.0001

Observed Frequencies for FINAL HER2 STATUS, FINAL ER STATUS
Row exclusion: DCIS STATVIEW DATASET

	0	1	Totals
0	23	145	168
1	36	19	55
Totals	59	164	223

Table 17: Univariate paired analysis for HER2 immunohistochmistry.

A total of 248 cases had HER2 IHC results (Table 17), of these 23% (n=57) were HER2 positive. This included 5% (n=13) of the 2+ cases on IHC (n=47) which were subsequently shown to show *HER2* gene amplification by CISH. Of the HER2 positive cases 9% (n=19) were also ER positive. 24% (n=39) of patients for whom clinical data was available (n=161) had HER2 positive DCIS. Of these HER2 positive cases 28% (n=11) were also ER positive ($p<0.0001$) 13% (n=5) was of intermediate grade ($p=0.0001$). Of note, 4 of the 5 cases of intermediate grade DCIS which were HER2 positive were also ER positive (80%). There were no low grade HER2 positive DCIS cases. A significant p value was given between HER2 positivity and architectural pattern ($p=0.0003$), the presence of necrosis ($p=0.0001$) and chronic inflammation ($p<0.001$). None of the 11 HER2/ER positive cases had an invasive recurrence, 45% (n=5) underwent mastectomy as a result of the DCIS diagnosis and 3 had recurrent DCIS in the same year. Three cases of DCIS were both HER2 and EGFR positive 7%, all had a simple mastectomy.

3.9.6 Univariate Analysis for Proliferation Marker Immunohistochemistry

Summary Table for FINAL KI67 (AT MEDIAN, 5%), FINAL HER2 STATUS
Row exclusion: DCIS STATVIEW DATASET

Num. Missing	43
DF	1
Chi Square	15.451
Chi Square P-Value	<.0001
G-Squared	16.560
G-Squared P-Value	<.0001
Contingency Coef.	.250
Phi	.258
Cty. Cor. Chi Square	14.255
Cty. Cor. P-Value	.0002
Fisher's Exact P-Value	<.0001

Observed Frequencies for FINAL KI67 (AT MEDIAN, 5%), FINAL HER2 STATUS
Row exclusion: DCIS STATVIEW DATASET

	0	1	Totals
0	87	11	98
1	89	45	134
Totals	176	56	232

Summary Table for FINAL EGFR STATUS, FINAL KI67 (AT MEDIAN, 5%)
Row exclusion: DCIS STATVIEW DATASET

Num. Missing	53
DF	1
Chi Square	4.869
Chi Square P-Value	.0273
G-Squared	5.872
G-Squared P-Value	.0154
Contingency Coef.	.146
Phi	.148
Cty. Cor. Chi Square	3.580
Cty. Cor. P-Value	.0585
Fisher's Exact P-Value	.0294

Observed Frequencies for FINAL EGFR STATUS, FINAL KI67 (AT MEDIAN, 5%)
Row exclusion: DCIS STATVIEW DATASET

	0	1	Totals
0	90	121	211
1	1	10	11
Totals	91	131	222

Summary Table for FINAL MCM2 (AT MEDIAN, 27.5%), FINAL HER2 STATUS
Row exclusion: DCIS STATVIEW DATASET

Num. Missing	39
DF	1
Chi Square	19.314
Chi Square P-Value	<.0001
G-Squared	20.682
G-Squared P-Value	<.0001
Contingency Coef.	.275
Phi	.286
Cty. Cor. Chi Square	17.992
Cty. Cor. P-Value	<.0001
Fisher's Exact P-Value	<.0001

Observed Frequencies for FINAL MCM2 (AT MEDIAN, 27.5%), FINAL HER2 STATUS
Row exclusion: DCIS STATVIEW DATASET

	0	1	Totals
0	94	11	105
1	85	46	131
Totals	179	57	236

Summary Table for FINAL EGFR STATUS, FINAL MCM2 (AT MEDIAN, 27.5%)
Row exclusion: DCIS STATVIEW DATASET

Num. Missing	50
DF	1
Chi Square	5.588
Chi Square P-Value	.0181
G-Squared	6.671
G-Squared P-Value	.0098
Contingency Coef.	.156
Phi	.158
Cty. Cor. Chi Square	4.217
Cty. Cor. P-Value	.0400
Fisher's Exact P-Value	.0254

Observed Frequencies for FINAL EGFR STATUS, FINAL MCM2 (AT MEDIAN, 27.5%)
Row exclusion: DCIS STATVIEW DATASET

	0	1	Totals
0	97	117	214
1	1	10	11
Totals	98	127	225

Table 18: Univariate Analysis of Proliferation Marker Immunohistochemistry.

The proliferation markers examined (Table 18), Ki67 and MCM2, were both scored as positive when >5% of DCIS cells showed nuclear positivity, which corresponded to the median value for Ki67. 91% (n=78) of Ki67 negative cases were positive for ER. Only 4% (n=8) of cases were negative for both Ki67 and ER (p=<0.0001).

The association between PR and Ki67 was similar to ER and Ki67; 16% (n=36) cases were negative for both PR and Ki67 (p<0.0001). If one of these markers was positive the other was most likely to be negative. MCM2 and ER showed a similar profile to Ki67 and ER, with 7% (n=15) of cases negative for both markers and 75% (n=44) of ER negative cases being MCM2 positive (p=0.0032). Similar to Ki67 and PR, 18% (n=42) of DCIS cases were negative for both PR and MCM2, whilst cases tended to be positive for one of these markers and negative for the other (p=0.0033)

3.9.7 Univariate Analysis for Cytokeratin Immunohistochemistry

Summary Table for FINAL CK5 (AT 1%), FINAL HER2 STATUS
Row exclusion: DCIS STATVIEW DATASET

Num. Missing	49
DF	1
Chi Square	5.022
Chi Square P-Value	.0250
G-Squared	4.594
G-Squared P-Value	.0321
Contingency Coef.	.147
Phi	.149
Cty. Cor. Chi Square	4.081
Cty. Cor. P-Value	.0434
Fisher's Exact P-Value	.0443

Observed Frequencies for FINAL CK5 (AT 1%), FINAL HER2 STATUS
Row exclusion: DCIS STATVIEW DATASET

	0	1	Totals
0	151	43	194
1	19	13	32
Totals	170	56	226

Summary Table for FINAL EGFR STATUS, FINAL CK5 (AT 1%)
Row exclusion: DCIS STATVIEW DATASET

Num. Missing	60
DF	1
Chi Square	1.405
Chi Square P-Value	.2360
G-Squared	1.190
G-Squared P-Value	.2754
Contingency Coef.	.081
Phi	.081
Cty. Cor. Chi Square	.566
Cty. Cor. P-Value	.4518
Fisher's Exact P-Value	.2139

Observed Frequencies for FINAL EGFR STATUS, FINAL CK5 (AT 1%)
Row exclusion: DCIS STATVIEW DATASET

	0	1	Totals
0	175	29	204
1	8	3	11
Totals	183	32	215

Summary Table for FINAL CK5/6 (AT 1%), FINAL HER2 STATUS
Row exclusion: DCIS STATVIEW DATASET

Num. Missing	58
DF	1
Chi Square	8.863
Chi Square P-Value	.0029
G-Squared	8.507
G-Squared P-Value	.0035
Contingency Coef.	.198
Phi	.202
Cty. Cor. Chi Square	7.892
Cty. Cor. P-Value	.0050
Fisher's Exact P-Value	.0041

Observed Frequencies for FINAL CK5/6 (AT 1%), FINAL HER2 STATUS
Row exclusion: DCIS STATVIEW DATASET

	0	1	Totals
0	120	28	148
1	43	26	69
Totals	163	54	217

Summary Table for FINAL EGFR STATUS, FINAL CK5/6 (AT 1%)
Row exclusion: DCIS STATVIEW DATASET

Num. Missing	62
DF	1
Chi Square	.139
Chi Square P-Value	.7094
G-Squared	.143
G-Squared P-Value	.7053
Contingency Coef.	.026
Phi	.026
Cty. Cor. Chi Square	.002
Cty. Cor. P-Value	.9653
Fisher's Exact P-Value	>.9999

Observed Frequencies for FINAL EGFR STATUS, FINAL CK5/6 (AT 1%)
Row exclusion: DCIS STATVIEW DATASET

	0	1	Totals
0	136	66	202
1	8	3	11
Totals	144	69	213

Summary Table for FINAL CK14 (AT 1%), FINAL HER2 STATUS
Row exclusion: DCIS STATVIEW DATASET

Num. Missing	47
DF	1
Chi Square	9.474
Chi Square P-Value	.0021
G-Squared	8.599
G-Squared P-Value	.0034
Contingency Coef.	.200
Phi	.204
Cty. Cor. Chi Square	8.253
Cty. Cor. P-Value	.0041
Fisher's Exact P-Value	.0037

Observed Frequencies for FINAL CK14 (AT 1%), FINAL HER2 STATUS
Row exclusion: DCIS STATVIEW DATASET

	0	1	Totals
0	150	40	190
1	21	17	38
Totals	171	57	228

Summary Table for FINAL EGFR STATUS, FINAL CK14 (AT 1%)
Row exclusion: DCIS STATVIEW DATASET

Num. Missing	55
DF	1
Chi Square	.007
Chi Square P-Value	.9348
G-Squared	.007
G-Squared P-Value	.9352
Contingency Coef.	.006
Phi	.006
Cty. Cor. Chi Square	0.000
Cty. Cor. P-Value	>.9999
Fisher's Exact P-Value	>.9999

Observed Frequencies for FINAL EGFR STATUS, FINAL CK14 (AT 1%)
Row exclusion: DCIS STATVIEW DATASET

	0	1	Totals
0	173	36	209
1	9	2	11
Totals	182	38	220

Table 19: Paired univariate analysis for CK immunohistochemistry.

The frequency of expression of CK5 and CK5/6 was distinctly different; 31% of cases were positive for CK5/6 (n=69) compared to only 14% for CK5 (n=32)(Table 19). Few cases showed EGFR positivity (n=11, 5%); 3 EGFR positive cases were also either CK5/6 or CK5 positive and 2 cases exhibited both CK14 and EGFR positivity.

Of the basal cytokeratin markers, CK14 (p=0.0018) and CK5 (p=0.0033) demonstrated an inverse relationship with ER but no significant association between CK5/6 (p=0.298) and ER was seen. Over 90% of EGFR positive cases were ER negative and over 99% of ER positive cases were EGFR negative (p<0.0001). All but one case of EGFR positive DCIS was positive for both proliferation markers Ki67 (p=0.0294) and MCM2 (p=0.0254) EGFR positive DCIS was of higher cytonuclear grade and was more likely to have solid architecture with comedo-type necrosis and associated chronic inflammation present.

3.9.8 Univariate Analysis and Recurrence of DCIS and/or Invasive Breast Disease

Univariate paired analyses were carried out for all antibodies to determine any significant correlation with recurrence (Table 20).

Summary Table for REC Y/N, FINAL HER2 STATUS
Row exclusion: DCIS STATVIEW DATASET

Num. Missing	121
DF	1
Chi Square	2.156
Chi Square P-Value	.1420
G-Squared	2.426
G-Squared P-Value	.1194
Contingency Coef.	.118
Phi	.118
Cty. Cor. Chi Square	1.461
Cty. Cor. P-Value	.2268
Fisher's Exact P-Value	.1952

Observed Frequencies for REC Y/N, FINAL HER2 STATUS
Row exclusion: DCIS STATVIEW DATASET

	0	1	Totals
N	95	36	131
Y	20	3	23
Totals	115	39	154

Summary Table for FINAL EGFR STATUS, REC Y/N
Row exclusion: DCIS STATVIEW DATASET

Num. Missing	130
DF	1
Chi Square	.084
Chi Square P-Value	.7723
G-Squared	.080
G-Squared P-Value	.7773
Contingency Coef.	.024
Phi	.024
Cty. Cor. Chi Square	0.000
Cty. Cor. P-Value	>.9999
Fisher's Exact P-Value	.6738

Observed Frequencies for FINAL EGFR STATUS, REC Y/N
Row exclusion: DCIS STATVIEW DATASET

	N	Y	Totals
0	114	20	134
1	9	2	11
Totals	123	22	145

Summary Table for FINAL ER STATUS, REC Y/N
Row exclusion: DCIS STATVIEW DATASET

Num. Missing	135
DF	1
Chi Square	.152
Chi Square P-Value	.6971
G-Squared	.148
G-Squared P-Value	.7002
Contingency Coef.	.033
Phi	.033
Cty. Cor. Chi Square	.013
Cty. Cor. P-Value	.9092
Fisher's Exact P-Value	.7840

Observed Frequencies for FINAL ER STATUS, REC Y/N
Row exclusion: DCIS STATVIEW DATASET

	N	Y	Totals
0	33	6	39
1	88	13	101
Totals	121	19	140

Summary Table for FINAL PR STATUS, REC Y/N
Row exclusion: DCIS STATVIEW DATASET

Num. Missing	125
DF	1
Chi Square	.004
Chi Square P-Value	.9489
G-Squared	.004
G-Squared P-Value	.9489
Contingency Coef.	.005
Phi	.005
Cty. Cor. Chi Square	0.000
Cty. Cor. P-Value	>.9999
Fisher's Exact P-Value	>.9999

Observed Frequencies for FINAL PR STATUS, REC Y/N
Row exclusion: DCIS STATVIEW DATASET

	N	Y	Totals
0	64	10	74
1	66	10	76
Totals	130	20	150

Summary Table for FINAL CK5 (AT 1%), REC Y/N
Row exclusion: DCIS STATVIEW DATASET

Num. Missing	130
DF	1
Chi Square	.005
Chi Square P-Value	.9436
G-Squared	.005
G-Squared P-Value	.9438
Contingency Coef.	.006
Phi	.006
Cty. Cor. Chi Square	0.000
Cty. Cor. P-Value	>.9999
Fisher's Exact P-Value	>.9999

Observed Frequencies for FINAL CK5 (AT 1%), REC Y/N
Row exclusion: DCIS STATVIEW DATASET

	N	Y	Totals
0	107	17	124
1	18	3	21
Totals	125	20	145

Summary Table for FINAL CK5/6 (AT 1%), REC Y/N
Row exclusion: DCIS STATVIEW DATASET

Num. Missing	133
DF	1
Chi Square	.061
Chi Square P-Value	.8050
G-Squared	.062
G-Squared P-Value	.8039
Contingency Coef.	.021
Phi	.021
Cty. Cor. Chi Square	0.000
Cty. Cor. P-Value	>.9999
Fisher's Exact P-Value	>.9999

Observed Frequencies for FINAL CK5/6 (AT 1%), REC Y/N
Row exclusion: DCIS STATVIEW DATASET

	N	Y	Totals
0	82	14	96
1	40	6	46
Totals	122	20	142

Summary Table for FINAL CK14 (AT 1%), REC Y/N
Row exclusion: DCIS STATVIEW DATASET

Num. Missing	126
DF	1
Chi Square	.941
Chi Square P-Value	.3321
G-Squared	1.028
G-Squared P-Value	.3106
Contingency Coef.	.079
Phi	.079
Cty. Cor. Chi Square	.477
Cty. Cor. P-Value	.4898
Fisher's Exact P-Value	.4113

Observed Frequencies for FINAL CK14 (AT 1%), REC Y/N
Row exclusion: DCIS STATVIEW DATASET

	N	Y	Totals
0	98	19	117
1	29	3	32
Totals	127	22	149

Summary Table for FINAL KI67 (AT MEDIAN, 5%), REC Y/N
Row exclusion: DCIS STATVIEW DATASET

Num. Missing	128
DF	1
Chi Square	.632
Chi Square P-Value	.4267
G-Squared	.646
G-Squared P-Value	.4214
Contingency Coef.	.065
Phi	.066
Cty. Cor. Chi Square	.314
Cty. Cor. P-Value	.5755
Fisher's Exact P-Value	.4856

Observed Frequencies for FINAL KI67 (AT MEDIAN, 5%), REC Y/N
Row exclusion: DCIS STATVIEW DATASET

	N	Y	Totals
0	51	7	58
1	74	15	89
Totals	125	22	147

Summary Table for FINAL MCM2 (AT MEDIAN, 27.5%), REC Y/N
Row exclusion: DCIS STATVIEW DATASET

Num. Missing	124
DF	1
Chi Square	.508
Chi Square P-Value	.4761
G-Squared	.504
G-Squared P-Value	.4778
Contingency Coef.	.058
Phi	.058
Cty. Cor. Chi Square	.232
Cty. Cor. P-Value	.6303
Fisher's Exact P-Value	.4938

Observed Frequencies for FINAL MCM2 (AT MEDIAN, 27.5%), REC Y/N
Row exclusion: DCIS STATVIEW DATASET

	N	Y	Totals
0	54	11	65
1	75	11	86
Totals	129	22	151

Summary Table for GRADE, REC Y/N
Row exclusion: DCIS STATVIEW DATASET

Num. Missing	118
DF	2
Chi Square	.336
Chi Square P-Value	.8452
G-Squared	.370
G-Squared P-Value	.8310
Contingency Coef.	.046
Cramer's V	.046

Observed Frequencies for GRADE, REC Y/N
Row exclusion: DCIS STATVIEW DATASET

	N	Y	Totals
HG	78	13	91
IG	47	7	54
LG	11	1	12
Totals	136	21	157

Summary Table for ARCH, REC Y/N
Row exclusion: DCIS STATVIEW DATASET

Num. Missing	118
DF	3
Chi Square	.465
Chi Square P-Value	.9266
G-Squared	.439
G-Squared P-Value	.9322
Contingency Coef.	.054
Cramer's V	.054

Observed Frequencies for ARCH, REC Y/N
Row exclusion: DCIS STATVIEW DATASET

	N	Y	Totals
CRIB	56	8	64
MICROPAP	14	3	17
PAP	10	2	12
SOLID	56	8	64
Totals	136	21	157

Summary Table for NECROSIS, REC Y/N
Row exclusion: DCIS STATVIEW DATASET

Num. Missing	118
DF	3
Chi Square	.860
Chi Square P-Value	.8352
G-Squared	.914
G-Squared P-Value	.8219
Contingency Coef.	.074
Cramer's V	.074

Observed Frequencies for NECROSIS, REC Y/N
Row exclusion: DCIS STATVIEW DATASET

	N	Y	Totals
MARKED	35	6	41
MILD	39	4	43
MOD	29	5	34
NONE	33	6	39
Totals	136	21	157

Summary Table for CI, REC Y/N
Row exclusion: DCIS STATVIEW DATASET

Num. Missing	120
DF	3
Chi Square	.894
Chi Square P-Value	.8269
G-Squared	.947
G-Squared P-Value	.8142
Contingency Coef.	.076
Cramer's V	.076

Observed Frequencies for CI, REC Y/N
Row exclusion: DCIS STATVIEW DATASET

	N	Y	Totals
MARKED	32	3	35
MILD	47	7	54
MOD	29	5	34
NONE	27	5	32
Totals	135	20	155

Summary Table for REC Y/N, SIZE RECODED AT MEDIAN (15)
Row exclusion: DCIS STATVIEW DATASET

Num. Missing	125
DF	1
Chi Square	.853
Chi Square P-Value	.3556
G-Squared	.854
G-Squared P-Value	.3553
Contingency Coef.	.075
Phi	.075
Cty. Cor. Chi Square	.460
Cty. Cor. P-Value	.4977
Fisher's Exact P-Value	.4625

Observed Frequencies for REC Y/N, SIZE RECODED AT MEDIAN (15)
Row exclusion: DCIS STATVIEW DATASET

	LESS THAN MEDIAN	MEDIAN (15) OR MORE	Totals
N	61	70	131
Y	11	8	19
Totals	72	78	150

Summary Table for AGE RECODED AT 50, REC Y/N
Row exclusion: DCIS STATVIEW DATASET

Num. Missing	121
DF	1
Chi Square	.414
Chi Square P-Value	.5201
G-Squared	.402
G-Squared P-Value	.5261
Contingency Coef.	.052
Phi	.052
Cty. Cor. Chi Square	.156
Cty. Cor. P-Value	.6924
Fisher's Exact P-Value	.6208

Observed Frequencies for AGE RECODED AT 50, REC Y/N
Row exclusion: DCIS STATVIEW DATASET

	N	Y	Totals
AGE 50 OR LESS	35	8	43
MORE THAN 50	95	16	111
Totals	130	24	154

Summary Table for LUMINAL A, REC Y/N
Row exclusion: DCIS STATVIEW DATASET

Num. Missing	138
DF	1
Chi Square	.052
Chi Square P-Value	.8204
G-Squared	.052
G-Squared P-Value	.8204
Contingency Coef.	.019
Phi	.019
Cty. Cor. Chi Square	0.000
Cty. Cor. P-Value	>.9999
Fisher's Exact P-Value	>.9999

Observed Frequencies for LUMINAL A, REC Y/N
Row exclusion: DCIS STATVIEW DATASET

	N	Y	Totals
0	60	8	68
1	60	9	69
Totals	120	17	137

Summary Table for LUMINAL B, REC Y/N
Row exclusion: DCIS STATVIEW DATASET

Num. Missing	131
DF	1
Chi Square	1.042
Chi Square P-Value	.3073
G-Squared	1.177
G-Squared P-Value	.2780
Contingency Coef.	.085
Phi	.085
Cty. Cor. Chi Square	.500
Cty. Cor. P-Value	.4797
Fisher's Exact P-Value	.5290

Observed Frequencies for LUMINAL B, REC Y/N
Row exclusion: DCIS STATVIEW DATASET

	N	Y	Totals
0	99	16	115
1	27	2	29
Totals	126	18	144

Summary Table for HER2 GROUP, REC Y/N
Row exclusion: DCIS STATVIEW DATASET

Num. Missing	135
DF	1
Chi Square	.173
Chi Square P-Value	.6778
G-Squared	.180
G-Squared P-Value	.6713
Contingency Coef.	.035
Phi	.035
Cty. Cor. Chi Square	.011
Cty. Cor. P-Value	.9182
Fisher's Exact P-Value	>.9999

Observed Frequencies for HER2 GROUP, REC Y/N
Row exclusion: DCIS STATVIEW DATASET

	N	Y	Totals
0	97	16	113
1	24	3	27
Totals	121	19	140

Summary Table for LUMINAL-HER2, REC Y/N
Row exclusion: DCIS STATVIEW DATASET

Num. Missing	135
DF	1
Chi Square	1.875
Chi Square P-Value	.1710
G-Squared	•
G-Squared P-Value	•
Contingency Coef.	.115
Phi	.116
Cty. Cor. Chi Square	.829
Cty. Cor. P-Value	.3625
Fisher's Exact P-Value	.3605

Observed Frequencies for LUMINAL-HER2, REC Y/N
Row exclusion: DCIS STATVIEW DATASET

	N	Y	Totals
0	110	19	129
1	11	0	11
Totals	121	19	140

Summary Table for BASAL-LIKE GROUP, REC Y/N
Row exclusion: DCIS STATVIEW DATASET

Num. Missing	136
DF	1
Chi Square	.181
Chi Square P-Value	.6709
G-Squared	.187
G-Squared P-Value	.6658
Contingency Coef.	.036
Phi	.036
Cty. Cor. Chi Square	.020
Cty. Cor. P-Value	.8863
Fisher's Exact P-Value	.7830

Observed Frequencies for BASAL-LIKE GROUP, REC Y/N
Row exclusion: DCIS STATVIEW DATASET

	N	Y	Totals
0	90	16	106
1	29	4	33
Totals	119	20	139

Summary Table for LUMINAL B1, REC Y/N
Row exclusion: DCIS STATVIEW DATASET

Num. Missing	141
DF	1
Chi Square	.085
Chi Square P-Value	.7705
G-Squared	.084
G-Squared P-Value	.7716
Contingency Coef.	.025
Phi	.025
Cty. Cor. Chi Square	.001
Cty. Cor. P-Value	.9780
Fisher's Exact P-Value	.7955

Observed Frequencies for LUMINAL B1, REC Y/N
Row exclusion: DCIS STATVIEW DATASET

	N	Y	Totals
0	75	11	86
1	41	7	48
Totals	116	18	134

Summary Table for LUMINAL A1, REC Y/N
Row exclusion: DCIS STATVIEW DATASET

Num. Missing	141
DF	1
Chi Square	.486
Chi Square P-Value	.4856
G-Squared	.502
G-Squared P-Value	.4787
Contingency Coef.	.060
Phi	.060
Cty. Cor. Chi Square	.186
Cty. Cor. P-Value	.6659
Fisher's Exact P-Value	.6004

Observed Frequencies for LUMINAL A1, REC Y/N
Row exclusion: DCIS STATVIEW DATASET

	N	Y	Totals
0	74	13	87
1	42	5	47
Totals	116	18	134

Table 20: Recurrence data for IHC Markers and Luminal Groups

3.9.9 Histological Grade in DCIS

Immunohistochemical expression of all markers in this study was compared to histological grade to determine any correlation between grade and specific markers. Table 21 gives the number of positive and negative cases expressing IHC markers in relation to cytonuclear grade.

	High Grade (n)	High Grade (% of total)	Intermediate Grade (n)	Intermediate Grade (% of total)	Low Grade (n)	Low Grade (% of total)	Total (n)
ER -ve	35	90	4	10	0	0	39
ER +ve	55	50	46	42	9	8	110
Total	90		50		9		149
PR -ve	54	70	23	30	0	0	77
PR +ve	37	46	33	41	10	13	80
Total	91		56		10		157
EGFR -ve	81	57	53	37	8	6	142
EGFR +ve	10	91	1	9	0	0	11
Total	91		54		8		153
HER2 -ve	60	49	51	41	12	10	123
HER2 +ve	33	87	5	13	0	0	38
Total	93		56		12		161
Ki67 low	26	42	28	45	8	13	62
Ki67 high	65	71	24	26	3	3	92
Total	91		52		11		154
MCM2 low	28	39	36	51	7	10	71
MCM2 high	66	76	17	20	4	5	87
Total	94		53		11		158
CK5 -ve	73	57	46	36	10	8	129
CK5 +ve	17	77	5	23	0	0	22
Total	90		51		10		151
CK5/6 -ve	56	54	42	41	5	5	103
CK5/6 +ve	34	72	11	23	2	4	47
Total	90		53		7		150
CK14 -ve	69	55	49	39	7	6	125
CK14 +ve	23	74	6	19	2	6	31
Total	92		55		9		156

Table 21: Biomarker expression by cytonuclear grade of DCIS.

Paired univariate analysis between the immunohistochemical markers and histological parameters such as cytonuclear grade, comedo type necrosis, chronic inflammation was undertaken to determine any correlations (Table 22).

Summary Table for GRADE, FINAL HER2 STATUS
Row exclusion: DCIS STATVIEW DATASET

Num. Missing	114
DF	2
Chi Square	17.675
Chi Square P-Value	.0001
G-Squared	•
G-Squared P-Value	•
Contingency Coef.	.315
Cramer's V	.331

Observed Frequencies for GRADE, FINAL HER2 STATUS
Row exclusion: DCIS STATVIEW DATASET

	0	1	Totals
HG	60	33	93
IG	51	5	56
LG	12	0	12
Totals	123	38	161

Summary Table for FINAL EGFR STATUS, GRADE
Row exclusion: DCIS STATVIEW DATASET

Num. Missing	122
DF	2
Chi Square	4.894
Chi Square P-Value	.0865
G-Squared	•
G-Squared P-Value	•
Contingency Coef.	.176
Cramer's V	.179

Observed Frequencies for FINAL EGFR STATUS, GRADE
Row exclusion: DCIS STATVIEW DATASET

	HG	IG	LG	Totals
0	81	53	8	142
1	10	1	0	11
Totals	91	54	8	153

Summary Table for FINAL ER STATUS, GRADE
Row exclusion: DCIS STATVIEW DATASET

Num. Missing	126
DF	2
Chi Square	19.267
Chi Square P-Value	<.0001
G-Squared	•
G-Squared P-Value	•
Contingency Coef.	.338
Cramer's V	.360

Observed Frequencies for FINAL ER STATUS, GRADE
Row exclusion: DCIS STATVIEW DATASET

	HG	IG	LG	Totals
0	35	4	0	39
1	55	46	9	110
Totals	90	50	9	149

Summary Table for FINAL PR STATUS, GRADE
Row exclusion: DCIS STATVIEW DATASET

Num. Missing	118
DF	2
Chi Square	14.910
Chi Square P-Value	.0006
G-Squared	•
G-Squared P-Value	•
Contingency Coef.	.294
Cramer's V	.308

Observed Frequencies for FINAL PR STATUS, GRADE
Row exclusion: DCIS STATVIEW DATASET

	HG	IG	LG	Totals
0	54	23	0	77
1	37	33	10	80
Totals	91	56	10	157

Summary Table for FINAL CK5 (AT 1%), GRADE
Row exclusion: DCIS STATVIEW DATASET

Num. Missing	124
DF	2
Chi Square	3.985
Chi Square P-Value	.1364
G-Squared	•
G-Squared P-Value	•
Contingency Coef.	.160
Cramer's V	.162

Observed Frequencies for FINAL CK5 (AT 1%), GRADE
Row exclusion: DCIS STATVIEW DATASET

	HG	IG	LG	Totals
0	73	46	10	129
1	17	5	0	22
Totals	90	51	10	151

Summary Table for FINAL CK5/6 (AT 1%), GRADE
Row exclusion: DCIS STATVIEW DATASET

Num. Missing	125
DF	2
Chi Square	4.519
Chi Square P-Value	.1044
G-Squared	4.680
G-Squared P-Value	.0963
Contingency Coef.	.171
Cramer's V	.174

Observed Frequencies for FINAL CK5/6 (AT 1%), GRADE
Row exclusion: DCIS STATVIEW DATASET

	HG	IG	LG	Totals
0	56	42	5	103
1	34	11	2	47
Totals	90	53	7	150

Summary Table for FINAL CK14 (AT 1%), GRADE
Row exclusion: DCIS STATVIEW DATASET

Num. Missing	119
DF	2
Chi Square	4.325
Chi Square P-Value	.1150
G-Squared	4.658
G-Squared P-Value	.0974
Contingency Coef.	.164
Cramer's V	.167

Observed Frequencies for FINAL CK14 (AT 1%), GRADE
Row exclusion: DCIS STATVIEW DATASET

	HG	IG	LG	Totals
0	69	49	7	125
1	23	6	2	31
Totals	92	55	9	156

Summary Table for FINAL KI67 (AT MEDIAN, 5%), GRADE
Row exclusion: DCIS STATVIEW DATASET

Num. Missing	121
DF	2
Chi Square	13.981
Chi Square P-Value	.0009
G-Squared	14.052
G-Squared P-Value	.0009
Contingency Coef.	.288
Cramer's V	.301

Observed Frequencies for FINAL KI67 (AT MEDIAN, 5%), GRADE
Row exclusion: DCIS STATVIEW DATASET

	HG	IG	LG	Totals
0	26	28	8	62
1	65	24	3	92
Totals	91	52	11	154

Summary Table for FINAL MCM2 (AT MEDIAN, 27.5%), GRADE
Row exclusion: DCIS STATVIEW DATASET

Num. Missing	117
DF	2
Chi Square	21.592
Chi Square P-Value	<.0001
G-Squared	21.981
G-Squared P-Value	<.0001
Contingency Coef.	.347
Cramer's V	.370

Observed Frequencies for FINAL MCM2 (AT MEDIAN, 27.5%), GRADE
Row exclusion: DCIS STATVIEW DATASET

	HG	IG	LG	Totals
0	28	36	7	71
1	66	17	4	87
Totals	94	53	11	158

Summary Table for ARCH, GRADE
Row exclusion: DCIS STATVIEW DATASET

Num. Missing	106
DF	6
Chi Square	47.715
Chi Square P-Value	<.0001
G-Squared	•
G-Squared P-Value	•
Contingency Coef.	.469
Cramer's V	.376

Observed Frequencies for ARCH, GRADE
Row exclusion: DCIS STATVIEW DATASET

	HG	IG	LG	Totals
CRIB	25	33	10	68
MICROPAP	11	4	3	18
PAP	3	10	0	13
SOLID	59	11	0	70
Totals	98	58	13	169

Summary Table for NECROSIS, GRADE
Row exclusion: DCIS STATVIEW DATASET

Num. Missing	106
DF	6
Chi Square	69.559
Chi Square P-Value	<.0001
G-Squared	•
G-Squared P-Value	•
Contingency Coef.	.540
Cramer's V	.454

Observed Frequencies for NECROSIS, GRADE
Row exclusion: DCIS STATVIEW DATASET

	HG	IG	LG	Totals
MARKED	39	3	0	42
MILD	22	24	1	47
MOD	28	10	0	38
NONE	9	21	12	42
Totals	98	58	13	169

Summary Table for CI, GRADE
Row exclusion: DCIS STATVIEW DATASET

Num. Missing	108
DF	6
Chi Square	50.846
Chi Square P-Value	<.0001
G-Squared	•
G-Squared P-Value	•
Contingency Coef.	.483
Cramer's V	.390

Observed Frequencies for CI, GRADE
Row exclusion: DCIS STATVIEW DATASET

	HG	IG	LG	Totals
MARKED	37	0	0	37
MILD	27	28	4	59
MOD	24	11	1	36
NONE	10	17	8	35
Totals	98	56	13	167

Table 22: Paired Univariate Analysis for Histological Grade.

3.9.10 Assignation of Molecular Subtypes to DCIS

3.9.10.1 Molecular Subgrouping of DCIS

Surrogate molecular subgroups (76) were assigned to the pure DCIS cohort using the criteria in Table 23. These groups broadly correlate to the five molecular subtypes proposed by Perou et al. A subgroup which was both HER2 and ER positive was also identified within the series and categorised as luminal/HER2.

DCIS subgroup	IHC Expression Pattern	Number of Cases	% of Cases
Luminal A	ER + PR+ HER2 -	103	38
Luminal B	ER + PR- HER2 -	55	20
HER2	ER – HER2 +	47	17
Basal-like	EGFR+ and/or CK5, CK5/6, CK14+	50	18
Luminal HER2	ER + HER2 +	20	7

Table 23: Definitions for Surrogate Molecular Subgroups for DCIS:

Additionally, the expression of Ki67 was examined in the ER positive and HER2 negative DCIS cases in order to define luminal A and luminal B according to proliferation rate (Table 24). Subgroups of luminal A1 and luminal B1 were defined as ER positive, Ki67 low and ER positive, Ki67 high respectively, in addition to the alternative method of defining cases according to ER and PR status, i.e. ER positive,

PR positive as luminal A and ER positive, PR negative as luminal B. Table 24 gives details of numbers of ER positive cases as assigned by high or low Ki67 expression.

Group	Definition	No. Cases (TMA total n = 280, relevant (ER+) cases n= 158)	% of assessable Cases
Luminal A1	ER+ Ki67 low (<5% tumour cells)	78	49
Luminal B1	ER + Ki67 high (>5% tumour cells)	80	51

Table 24: Subgrouping of ER positive DCIS with Ki67 expression; cut-off defined at median, 5%.

3.10 Immunophenotypic Subtypes of DCIS and Recurrence

Three HER2 positive (HER2 group) cases recurred (n=47; 6.4%) and three of the basal-like group (n=50; 6%) had a recurrence (Table 20). In this cohort of pure DCIS the luminal A group (n=103), as defined above, showed no association with recurrence; nine of the recurrent cases belonged to the luminal A group. Only one of the recurrent cases was found in the luminal B group (n=55).

For ER positive cases (n=95), 51% (n=48) had high Ki67 expression. High Ki67 status resulted in a 19% (n=18) shift from the luminal A (ER positive but low proliferation, defined as A1) to the luminal B1 (ER positive but high proliferation, defined as B1) group. In this series, seven of the luminal B1 group and four of the luminal A1 had a

recurrence. Overall, cases of DCIS that were ER and PR positive had a higher incidence of recurrence than cases which were ER positive with high Ki67 expression. In our series 74% of DCIS are ER positive. Approximately 70-80% of invasive ductal carcinomas of no special type (NOS) are ER positive according to the literature (188). This is related to cytonuclear grade of DCIS in the present series (p value < 0.001); 61% of high grade cases (HG) are ER positive (n=90), 92% of intermediate grade (IG) (n=50) and 100% of low grade (LG) DCIS are ER positive n=9). Previous studies have demonstrated variation in ER expression in high grade DCIS, ranging from 31.8% (189), 69% (190) to 72% (191).

3.11 Discussion

The genomic profiling of invasive breast cancers has revealed subtypes of invasive breast cancer, namely luminal A, luminal B, HER2, basal, normal and (subsequently) null. A search of the literature (Pubmed in 2014: search criteria; DCIS + molecular subtype, DCIS + IHC, DCIS + basal, DCIS + luminal, DCIS + phenotype) has yielded a small number of studies that examine the possibility of using IHC as a surrogate for genetic profiling to classify DCIS in a similar manner. To date only a few (82, 192) of these have taken a comparative approach by assigning the genetic molecular profile to samples then assessing the corresponding IHC as opposed to simply assigning groups by IHC expression alone.

In this series immunohistochemistry (IHC) on “pure” DCIS was performed to ascertain if any potential marker or markers could be identified as a biological indicator of known progression to either a recurrence of DCIS or invasive disease. However, no association or predictor has been found for recurrence of DCIS with any of ER, PR, HER2, EGFR or the basal cytokeratins 5, 5/6 or 14, high or low expression of proliferative markers in univariate analysis. Unsurprisingly, a correlation is seen

between cytonuclear grade increased expression of proliferative markers (Ki67 and MCM2), which largely mirrors findings in invasive breast carcinoma.

None of the IHC biomarkers evaluated in this cohort were significantly associated with recurrence of disease, although this may be due to the small numbers of patients in this series who suffered with recurrence. Additionally, the cohort for this study was based upon patients diagnosed with DCIS between 1995 and 2006 with 50% (n=71) of patients undergoing a mastectomy within 65 days of original histology report. Thomas et al (193) examined data from the Sloane Project, currently the largest prospective audit on DCIS. Examination of over 8000 cases indicates that mastectomy rates dropped to 26% between April 2003 and March 2012 with more women undergoing breast conserving surgery (BCS). They also highlight the significant degree of practice variation between institutions affecting patient outcome. These differences in practice should be considered when looking at data sets from an individual institution.

Molecular profiling of *invasive* breast carcinomas gives subgroup frequencies of luminal A - 40%, luminal B - 20%, HER2 - 10-15% and basal-like - 15-20%. (76, 82, 194, 195). In this series of DCIS the subgroup frequencies for DCIS as determined by IHC profiling were luminal A - 37%, luminal B - 20%, HER2 - 17%, luminal/HER2 - 7% and basal-like - 18%, indicating an essentially similar frequency between the invasive carcinoma immunosub-types and that seen in DCIS.

There is, however, no consensus agreement on assigning sub-type based on IHC panels for invasive disease, and this has not been satisfactorily addressed for DCIS. Whilst there is a increase in the frequency of HER2 positive DCIS compared to invasive breast carcinoma, 7% of these would be assigned to the luminal A group based on the surrogate panels suggested by some authors (82, 196, 197). In this cohort these patients are designated to a small group that is positive for both HER2 and ER as thus as luminal/HER2.

Other studies have looked at the possibility of using IHC as a method of classifying DCIS, either to define potential molecular subtypes (86, 196-199) or specifically to identify a sub-set of basal-like DCIS, or to predict outcome or recurrence. Tamimi et al (200) identified subgroups in both invasive breast carcinomas (n=2897) and DCIS (n=272) noting that the luminal A group was more prevalent in the invasive cohort, whilst the HER2 and luminal B groups had a higher incidence in DCIS. Zhou et al (198) identified a basal–like subtype of DCIS with an increased risk of recurrence of disease. They constructed TMAs from 485 cases of primary DCIS found in Swedish women between 1986 and 2004. Using IHC markers (ER, PR, HER2, CK5/6 and EGFR) as surrogates for genomic profiling they defined groups as triple negative, non-triple negative and basal-like. Results for 392 women were available. Basal-like DCIS in their series (n=32) had a higher risk of local recurrence with hazard ratio (HR) of 1.8 (Confidence interval (CI) 95% 0.8 – 4.2) and also invasive risk recurrence of 1.9 (CI 0.7 – 5.1) but these results were not statistically significant. They found no significantly increased risk of recurrence of disease for patients with triple negative DCIS.

Meijenen et al (196) evaluated 16 IHC markers identifying six (ER, PR, androgen receptor, Bcl2, HER2 and p53) which they suggested were suitable for defining DCIS into two major groups, luminal and non-luminal, and 5 subgroups. They also noted that intermediate grade DCIS had more IHC similarities to well differentiated than poorly differentiated disease. Clark et al (197) also classified DCIS into molecular subgroups with IHC, suggesting a role for BCL2 as a possible identifier for good prognosis. Overall, therefore the present, and other, studies show that it is possible to identify differences between cases of DCIS using panels of IHC markers. Such markers show correlations with each other and with features of known clinico-pathological relevance and can be combined into sub-groups equivalent to those in invasive breast cancer. However, no individual marker, or combination, shows a

strong association with recurrence of disease and thus to be of significant clinical value at this time.

Few studies have looked directly at genomic and IHC parameters in the same lesions, either invasive or in situ. Nielsen et al (82) studied *invasive* breast carcinoma with both IHC and genomic profiling and identified a concordant set of basal-like tumours using four IHC markers (HER2, EGFR, CK5/6 and ER). In the present series we have defined a basal-like group by utilising three basal cytokeratin antibodies (CK14, CK5 and CK5/6) in addition to EGFR, ER, PR and HER2, but we note that the frequencies of expression of CK5/6 and CK5 showed distinct disparity. This highlights one of the concerns in the definition of molecular subtypes using IHC; the variability of clones and the interpretation of scoring are parameters that currently have no defined values. What constitutes a positive CK score varies in the literature, with some researchers advocating any staining as positive (196, 200) and some using a threshold of ≥ 10% (197, 199). Indeed, one of the issues that requires addressing before a molecular taxonomy equivalent to genomic profiling, for either invasive or DCIS, can be adopted by application of IHC is the precise and globally acceptable definitions using specific antibodies, and possibly even clones. Robust scoring criteria and a need for standardisation of collection, fixation, processing and reporting are also fundamental to accurate assignation of molecular subtypes. Tang et al (201) reviewed the IHC classification of invasive breast cancers and advocated a molecular classification, which could be similarly used for DCIS. They suggest for invasive breast cancer subgrouping as luminal A (ER positive, HER2 negative), luminal B (ER positive, HER2 positive), HER2 group (ER negative, HER2 positive), basal subgroup (ER negative, HER2 negative, CK5/6 and/ EGFR positive) and an unclassified group (ER negative, HER2 negative, CK5/6 negative, EGFR negative).

The present study aimed to identify the possibility of using IHC as a genomic surrogate to identify subgroups of DCIS and to investigate associations with patient outcome. We have found that molecular subgroups can be identified using an IHC approach. However, further work is required to evaluate the usefulness of such a system in DCIS, particularly with regard to prediction of recurrence. Retrospective studies will probably lack the statistical power or accuracy required to give reliable data, given the variation in clinical management in historical series, including the proportion of cases treatment by breast conserving surgery, differences in the definiton of a tumour-free margin of excision, as well as the use of radiotherapy and hormone treatments.

Chapter 4. DCIS Associated with Invasive Breast Carcinoma

4.1 Introduction

The molecular profiling and immunohistochemical studies described in Chapter 3 focused upon the IHC marker expression and the propensity for “pure” DCIS to become invasive or recur as further DCIS. However, DCIS may also be expressed alongside an invasive breast lesion. Previous genomic studies have demonstrated that similar genetic profiles exist between DCIS and synchronously expressed invasive breast disease (202-204). Conversely, there is some evidence of intra-tumour heterogeneity between some DCIS and the respective invasive breast lesion given rise to the possibility of divergent clonal pathways within an individual tumour (202). This may indicate that, in synchronous DCIS and invasive breast disease at least, that DCIS is already at an advanced stage committed to invasive progression. We aimed therefore to explore the possibility of different IHC profiles or frequencies in a subset of DCIS with associated invasive carcinoma and to determine whether any potential difference existed between pure DCIS and DCIS lesions associated with invasive breast tumours. These would be stained with the same antibody panel as the pure DCIS in Chapter 3. This subset would also provide part of the cohort for further genomic studies (see Chapter 5).

4.2 Materials and Methods

DCIS and associated invasive tissue were provided by King’s Health Partners Tissue Bank (KHPB) with tissue microarrays constructed in the same manner as described in section 2.2. Similarly, TMA sections were stained with the same antibodies using

the similar conditions as set out in section 3.2. However, in this instance cores were taken from a minimum of two defined processes, namely DCIS and invasive components. For DCIS regions three 2mm cores were taken and for the invasive component three 0.6mm cores were taken. The DCIS component was identified by the presence of a complete basement membrane and myoepithelial layer surrounding the malignant epithelial cell islands by the author and consultant breast pathologist (SEP). In lesions where there was a doubt regarding the presence of an intact membrane, IHC for the marker smooth muscle myosin heavy chain (SMMHC) was used to identify DCIS by demonstration of the surrounding myoepithelial cell layer (Figure 30).

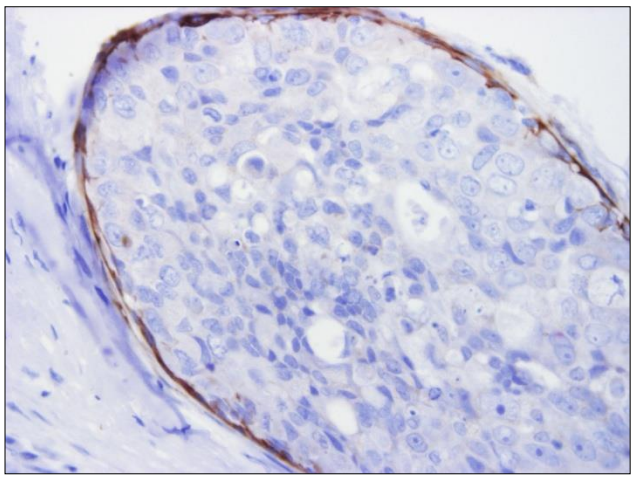

Figure 30: SMMHC IHC showing intact myoepithelial cell layer around DCIS.

A total of 41 cases dating between 1989 and 2004 with synchronous invasive breast disease and DCIS lesions was identified and stained with ER, PR, HER2, EGFR, CK5/6, CK14, MCM2 and Ki67. IHC scoring was carried out as per section 3.7.

Molecular subgroups were assigned as defined by Perou et al using the following criteria: ER positive, PR positive, HER2 negative = luminal A; ER positive, PR negative, HER2 negative = luminal B; HER2 positive, ER negative = HER2 group; ER

negative, PR negative, HER2 negative with any/or EGFR, CK5/6, CK14 = basal–like; no expression of any of ER, PR, HER2, basal CKs or EGFR = null. A subgroup of disease which was HER2 positive and ER positive was also noted within our series and designated luminal HER2. Additionally, the expression of proliferative markers was examined in ER positive cases to determine any association with prognosis and recurrence. Subgroups luminal A1 and luminal B1 were defined as ER positive, Ki67 low and ER positive, Ki67 high respectively as opposed to ER positive, PR positive (luminal A) and ER positive PR negative (luminal B) within the HER2 negative sub-set.

4.3 Results

4.3.1 Individual IHC Antibody Staining Concordance between Invasive Tumour and DCIS in the Same Case:

The TMAs constructed and stained with IHC markers had scores generated for both the DCIS and invasive carcinoma components within each case. The DCIS and invasive component scores with each antibody were compared. Table 25 shows the association between DCIS and invasive IHC scores.

Antibody IHC scoring method and cut-off value)	Positive in DCIS and invasive carcinoma	Positive in invasive only	Positive in DCIS only	Negative for both	DCIS loss of core	Invasive loss of core	Total
ER (Allred >3)	23	3	2	2	11	0	41
PR (Allred >3)	9	1	3	8	20	0	41
HER2 (HER2 score 3+)	8	0	7	13	13	0	41
EGFR (HER2-like score 3+)	5	6	2	4	24	0	41
CK5/6 (>2% tumour cells stained)	1	4	0	32	4	0	41
CK14 (>2% tumour cells stained)	1	4	2	30	4	0	41
Ki67 (>5% tumour cells stained)	9	16	1	10	3	2	41
MCM2 (>5% tumour cells stained)	9	1	6	2	20	3	41

Table 25: Comparison of IHC scores between cases of admixed DCIS and invasive carcinoma

4.3.2 Assignation of Molecular Subgroups

Molecular subgroups were assigned according to both the invasive carcinoma IHC scores and DCIS IHC scores. Tables 26 and 27 give details of numbers and sub-groups and concordance. Table 26 shows the number of cases assigned to each group according to DCIS or Invasive component. Table 27 shows the distribution according to proliferative (Ki67) and hormonal status.

	Invasive Carcinoma	DCIS	Paired Cases (Invasive carcinoma and DCIS match in same case)	Unpaired cases (Invasive carcinoma and DCIS do not match in the same case)
Luminal A (ER positive, PR positive, HER2 negative)	14	6	4	2
Luminal B (ER positive, PR negative, HER2 negative)	3	4	3	0
HER2 (HER2 positive, ER negative)	0	4	1	3
Basal-like (ER negative, PR negative, HER2 negative, EGFR /CK5/ CK5/6 and/or CK14)	12	9	4	5
Luminal/ HER2 (ER positive, HER2 positive)	7	11	7	0
Null (All negative)	1	1	0	1
Total	37	35	18	12

Table 26: IHC Molecular Subgroups for Invasive Carcinomas and Associated DCIS

	Invasive Carcinoma	DCIS	Paired Cases (Invasive carcinoma and DCIS match in same case)	Unpaired cases (Invasive carcinoma and DCIS do Not match in the same case)
Luminal A1 ER positive, Ki67 high expression	10	9	6	3
Luminal B1 ER positive, Ki67 low expression	10	16	6	4
Total	*20	25	12	7
	*3 cases no Ki67 Score			

Table 27: IHC Molecular Subgroups for Invasive Carcinomas and Associated DCIS

for ER Positive and Ki67 Expression

4.4 Discussion

In this series of DCIS associated with invasive breast carcinoma several observations can be made. For ER positive DCIS and invasive breast disease there is a high degree of concordance with 83% (n=25/30) of cases showing a similar ER status. Analysis of the Allred scores also shows that cores have a similar degree of ER expression. A similar pattern is seen with PR, with 81% (n=17/21) having concordant scores.

HER2 expression with IHC showed 75% concordance (n=21/28); although 25% of the DCIS was HER2 IHC positive whereas the invasive breast disease was negative, even in this small series.

For EGFR there was no distinct pattern of correlation between DCIS and invasive breast disease; 3 cases were EGFR positive in both the invasive breast cancer and the DCIS, 3 cases showed positivity in the invasive disease only and 2 cases positivity in the DCIS only.

Interestingly, there was also little similarity between invasive breast disease and DCIS with regard to basal cytokeratin expression; in 5 cases positive CK5/6 expression was seen in the invasive carcinoma whilst the DCIS was CK5/6 negative. Similarly, CK14 positive invasive breast disease (n=4) was negative in the associated DCIS in 3 cases. Conversely, DCIS was positive for CK14 in 3 cases and negative in the associated invasive cancer in two. One DCIS case was CK5/6 positive but negative in the invasive breast disease.

Ki67 showed concordance (scores within 5% of each other) for 63% of admixed DCIS and invasive breast disease (n=22). Of note, the 37% (n=13) of discordant cases had elevated Ki67 in the invasive breast disease in all cases (range = 7-32% mean = 10%). MCM2 expression was concordant in the DCIS and the invasive disease in 37% of cases (n=7/19), 52% (n=10/19) of cases showed elevated MCM2 expression

(range = 7-73% mean = 38%) in the invasive tumour compared to the DCIS and 11% (n= 2/19) showing elevated MCM2 in the DCIS lesion (range= 12-49% mean =30%). Unlike the pure DCIS cohort, HER2 expression was associated with ER positivity in the DCIS component with 73% (n=11/15) showing positive staining for both. In the invasive component, unexpectedly, 100% of the HER2 positive disease was ER positive (n=7/7). Although there are many studies on ER positive HER2 negative breast cancer there are few articles addressing ER positive HER2 positive lesions. Ryden et al (205) describe HER2+ and ER+ breast cancer as a separate subgroup of tumours with poor prognosis in premenopausal breast cancer. Alqaisi et al (206) found co-expression of ER-positive HER2 positive disease was found in younger age, had higher grade and increased visceral involvement in de novo metastasis.

Unfortunately, in the DCIS TMA there was a marked loss of cores for ER, PR, EGFR, HER2 and MCM2 during the antigen retrieval step. The reason for this remains unclear as all TMAs were constructed with the same guidelines as other TMAs, including the invasive TMA from the same tissue samples, which retained tissue during antigen retrieval steps. The same cases for each antibody had tissue loss possibly indicating a fixation or necrotic tissue problem. It was possible therefore to assign only 35 cases to molecular subgroup for both the invasive and the in situ elements..

Intriguingly, however, in this cohort such molecular subgrouping does not show perfect concordance between the DCIS and the associated invasive tumour for most groups. Only the luminal/HER2 group has complete concordance with all available samples being ER positive and HER2 positive in both the DCIS and HER2. 66% of luminal A, 0% of luminal B, 44% of basal-like and 0% of null had concurrent IHC staining in this series. This could be due to several factors:

1. Tumour heterogeneity and, in particular, clonal expansion of particular cell types once invasion has occurred;

2. Synchronous development of unrelated tumour and DCIS within the same patient (highly unlikely);
3. Down- or up-regulation of proteins once invasion has begun.

The limitations of this experiment must be fully acknowledged before such conclusions can be drawn. The substantial loss of cores in the DCIS TMA during IHC staining has compromised the ability to group samples by more than one marker and have reduced the cohort size significantly.

Chapter 5. Genomic Studies on DCIS

5.1 Introduction

Understanding the genomic basis of DCIS and how it relates to invasive breast carcinoma may help elucidate the underlying mechanisms of progression to invasive disease or demonstrate that DCIS in certain instances may already represent a commitment to an invasive phenotype. The progression of DCIS to an invasive phenotype has been previously studied using gene expression profile analysis (203, 207) and array comparative genomic hybridisation (aCGH) in small numbers of studies and cases (208-210). These studies have demonstrated that DCIS lesions of the same grade have similar genetic profiles to the concurrent invasive tumour, although qualitative differences such as prevalence are reported in matched series (211).

Copy number variations (CNVs) are genomic variations of greater than one kilobase affecting the number of copies of genes possessed by an individual compared to a reference sample. First reported by Charles Lee in 2002 (212) CNVs represent deletions, insertions or duplications of DNA. Shlien et al (213) described the importance of CNVs succinctly:

"DNA copy number variations (CNVs) are an important component of genetic variation, affecting a greater fraction of the genome than single nucleotide polymorphisms (SNPs). The advent of high-resolution SNP arrays has made it possible to identify CNVs. Characterization of widespread constitutional (germline) CNVs has provided insight into their role in susceptibility to a wide spectrum of disease, and somatic CNVs can be used to identify regions of the genome involved

in disease phenotypes. The role of CNVs as risk factors for cancer is currently underappreciated."

Identification of CNVs in DCIS may provide clues to progression and help improve targeted treatment for both those with low and high risk invasive potential.

5.2 Genetic Aberrations of DCIS and Invasive Breast Disease – Literature Review

Changes in DNA copy numbers may be inherited or due to somatic mutations. Copy number variants (CNVs) usually refer to inherited variation whilst copy number aberrations (CNAs) refer to somatic mutation (214). Whilst beyond the scope of the thesis to identify every potential copy number gain or loss found in invasive breast disease in the literature, due to the vast array of data, commonly found copy number aberrations (CNAs) have been identified (215-219). These include gains on 1q, 6p, 8q, 11q, 16p, 17q, 19, 20q and losses on 5q, 6q, 7p, 13q, 16q, 17p and 22q. In DCIS, several studies have identified a variety of CNAs (202, 207, 210, 220, 221). Copy number gains on 1q, 5q, 8q, 16p, 19q, 20 and losses on 1p, 3q, 6q, 8p, 9p, 11q, 13q,16q, 17p and 17q are reported. These include known loci for *HER2* (17q12), ER (6q25.1), EGFR (7p11) and p53 (17p1).

In addition to the known CNAs there are many novel potential candidate genes identified in both DCIS and invasive breast disease that could be biomarkers for therapeutic intervention. Hanneman et al (192) identified 35 genes which differed between DCIS and invasive breast disease and 43 genes that differed between low grade and high grade DCIS in 2006. Since then a few studies (210, 222-224) have identified genes that may be implicated in transformation of DCIS into an invasive phenotype.

5.3 Materials and Methods

Several criteria were used for selections of MIP array samples. Due to the cost, it was deemed unfeasible to perform analysis on the whole cohort from the DCIS TMA set. Additionally, although only a comparatively small amount of tissue was required from the DCIS samples there was an issue of tissue availability. In general DCIS is not markedly cellular, TMAs had already been manufactured from the cases, and clearly one has a commitment not to exhaust a resource that must legally be retained as part of the patients' diagnostic record. Subsets for genomic analyses were therefore chosen to represent two groups, namely pure DCIS and DCIS associated with Invasive component. To further represent the larger cohort, DCIS lesions were chosen with the following IHC profiles: ER positive, HER2 positive and triple negative. Where a DCIS lesion was matched to invasive tissue samples were taken from both components and if possible a sample of adjacent normal tissue. Table 28 gives the number and type of sample selected for MIP array analysis.

Specimen type	Number of Cases
Triple negative pure DCIS	12
Triple negative DCIS associated with invasive breast disease* and	10
Triple negative invasive breast disease associated with DCIS*	10
ER positive pure DCIS	10
ER positive DCIS associated with invasive breast disease^ and	9
ER positive invasive breast disease associated with DCIS^	9
HER2 positive pure DCIS	8
Matched normal from ER positive DCIS and invasive breast disease^	7
Matched normal from triple negative DCIS and invasive breast disease*	8
Total number of samples	83

Table 28: Sample Selection and Case Numbers for MIP Array Analysis.

[* and ^ represent different microdissected components of the same cases]

5.4 Hypothesis for MIP Arrays Studies in DCIS and Invasive Breast Carcinoma

Genomic analysis of tissue samples may provide additional knowledge in our understanding of breast cancer progression and help define treatments in the future. Whilst not exhaustive in sample size this does represent one of the largest studies on DCIS using MIP array to date. A comparison of the various groups may shed light on genomic differences found within the different disease states i.e. precursor versus invasive breast cancer. This could be used to determine if the expression the immunohistochemical markers used in Chapter 3 are present at the genomic level (as expected), for example, is there HER2 amplification in the HER2 positive IHC cases? It also creates a database of genomic data with to study alongside the immunohistochemical and demographic data. This database will provide a resource for further research beyond the scope of this thesis. The analysis will also provide insights into variations between genomic changes seen in DCIS and invasive breast cancers and may present novel genes not currently identified in the literature. Identification of genes that represent an underlying commitment to invasive potential established before the expression of a molecular subtype may also be found. To address these issues comparisons of different comparative analysis of the following groups was carried out to help elucidate possible genetic aberrations, for all cases of DCIS, both pure and that associated with invasive disease:

1. ER+ DCIS compared to non ER+ DCIS
2. ER+ pure DCIS compared to ER+ DCIS associated with invasive disease
3. ER+ pure DCIS compared to ER+ invasive breast disease
4. All ER+ DCIS (pure and matched) compared to all ER+ invasive disease
5. Triple negative pure DCIS compared to triple negative invasive breast disease
6. All triple negative DCIS compared to all non-triple negative DCIS

7. Triple negative pure DCIS compared to triple negative DCIS associated with invasive disease
8. All triple negative DCIS compared to triple negative invasive disease
9. HER2+ pure DCIS compared to non-HER2+ DCIS

5.4.1 DNA Extraction

DNA was extracted using a modified technique incorporating elements from the QIAGEN FFPE DNA kit (QIAGEN Ltd. Manchester UK) and protocols provided by Dr Jorge Reis-Filho (Cheaty Beatty Laboratories, London, UK). 4µm sections were cut from blocks already identified from the TMA cohorts, and H&E stained to ascertain the amount of available tissue. Where a suitable quantity of DCIS and/or invasive tumour/normal tissues was present, up to 20 sections were cut at 8µm and dried overnight at 37ºC. Sections were dewaxed in xylene then stained with nuclear fast red dye. Sections were viewed through a dissecting microscope and any areas of tissue not required for DNA analysis were scraped away using a fine aspirate needle (gauge 10). This included any stroma, lipid or connective tissue. Sections were immersed in sodium thiocyanate overnight to remove formalin fixation crosslinks. Slides were then rinsed in changes of ultra-pure H_2O and sections examined under the dissecting microscope where components such as DCIS, invasive tumour and normal tissues were scraped into individual 1.5ml eppendorf tubes using individual aspirate needles for each component. Samples were immersed in proteinase K for 48 hours at 40ºC to aid proteolysis, followed by DNA extraction using the QIAamp DSP DNA FFPE Tissue Kit (Qiagen, Manchester UK). DNA quality was initially assessed by taking a spectrophotometer reading (Nanodrop, Thermo Scientific Wilmington, Delaware, USA) to determine DNA presence. DNA absorbs light at 260nm, a spectrophotometer can detect the amount of light absorbed in a sample, thus the more DNA the greater the absorbance of light. However, contaminants such

as proteins and RNA may also absorb light at 260nm so errors are possible. Once the presence of DNA was confirmed by this approach, samples were then assessed using a fluorimeter (Qubit- Life Sciences, Paisley, UK). The Qubit system uses fluorescent dyes that bind to target molecules (e.g. DNA); these dyes have a minimal fluorescent signature which becomes greatly enhanced upon target binding. When compared to a standard sample of known concentration an accurate DNA concentration can be given. Protocols for DNA extraction are listed in Appendix 6.

5.4.2 MIP Array

DNA samples were shipped to AffyMetrix MIP laboratory (California, USA). Samples were allocated an anonymised number and all identifying data removed to ensure sample blinding, including the matched normal tissues. Using the OncoScan™ FFPE Express Service samples underwent MIP array assays.

Data quality was assessed using the sample 2-point relative standard error. The majority (95%) of FFPE tumours samples applied to the MIP arrays passed the 2p-RSE threshold (GSE31424).

5.4.3 Statistical methods

Tumour Aberration Prediction Suite (TAPS), a bioinformatics tool for the identification of allele-specific copy numbers in tumour samples using data from Affymetrix SNP arrays, was run on all samples to obtain allele specific absolute copy numbers at genomic segment level. Raw output tables from TAPS output are seen on the attached disc. Gene centric versions of these tables i.e. each row represents a gene and its respective CN and other parameters are directly copied from TAPS raw tables are also provided (attached disc). This shows gene level copy numbers for each sample. Using these gene centric tables, intra-group gene centric count/percentage tables were created according to the IHC groups (ER+, triple negative and HER2+) (also

see attached disc). These tables show counts/percentage for each gene and each CN type, as well as the respective sample IDs.

To compare groups, Fisher's exact tests were performed between two groups for each copy number type. For example, frequencies were calculated for "gains" for each segment among the two groups into a contingency table which was used to run Fisher's test, resulting in a p-value for each segment for that copy number type. Files are stored on the attached disc and give Fisher tests output for all segments for each comparison respectively. Genome frequency plots for these tables are also provided (see attached disc). Significantly different segments between 2 groups i.e. based on p-values cut-off of <=0.05, are also presented on the attached disc, along with tables and genomic frequency plots for segments based on the above mentioned threshold.

5.4.4 Analyses of Raw Data Tables

The raw data (TAPS tables) produced a significant amount of data, which is too large for a single thesis to adequately analyse. Mining of the data to elicit possible key genes was determined to be a suitable way forward; this approach has been used by others previously (221).

Data was compiled into groups for comparison e.g. ER positive pure DCIS compared to pure non ER positive DCIS (similarly all triple negative, HER2 etc.).

Genomic regions were sorted into those with significant p-values for the various genomic states: amplification, deletion, copy neutral loss of heterozygosity (cnLOH), copy deletion loss of heterozygosity (cdLOH) and total loss.

Of the samples with significant p values, genomic bands with the greatest difference between the number of samples (and the greatest percentage difference) were selected, e.g. in ER positive pure DCIS there is genomic band (region) where 5 samples had amplification within this region compared to no amplification in any of the pure non ER positive samples.

In many instances there were multiple genetic aberrations listed in a general locus of a particular chromosome or arm. In others there were only one or two genetic aberrations identified. A rationale that the occurrence of the same genetic aberrations found in multiple samples are more likely to be key players than genetic aberrations found in any one individual sample representing heterogeneity or genetic plasticity in tumourigenesis was adopted. Although this concept may be potentially flawed, analysis of multiple genes on the same locus also produces very complex and varied biological processes when analysed by PANTHER (see 5.2.2).

In addition to the above method, a literature search of genes associated with DCIS and invasive progression previously identified as potential drivers by other researchers was carried out.

5.5.5 Analysis of MIP array Data Using "PANTHER" Classification System

The large amount of genomic data generated, and subsequently analysed by the Breakthrough Breast Cancer/Research Oncology, King's College London bioinformatics team, based upon the MIP array results requires further analysis in order to identify similarities and differences between groups. There are many gene analysis software packages available online (e.g. GeneOntology, Webgestalt, GeneGo, Pubgene, TopGeneSuite). It is beyond the scope of this thesis to determine the pros and cons of each individual package. Under advice from the Breakthrough Breast Cancer/Research Oncology, King's College London bioinformatics team, and based upon the type of analysis required, the "protein annotation through evolutionary relationships" or PANTHER protein and gene analysis software was selected. In 2013 Mi et al (225) described the analysis software thus: "PANTHER (protein annotation through evolutionary relationship) classification system (http://www.pantherdb.org/) is a comprehensive system that combines gene function, ontology, pathways and

statistical analysis tools that enable biologists to analyse large-scale, genome-wide data from sequencing, proteomics or gene expression experiments."

5.5.6 Analysis of DCIS and Invasive Breast Disease Subgroups.

Groups were compared using the 7 copy number types (excluding undefined segments) shown below. Generalized copy number types of "gains" and "losses" were also included (Table 29).

Cn	mCn	New CN Type	Combined CN Type
NA	NA	Undefined	Undefined
0	0	Total Loss	Total loss
2	NA	Normal with unknown allele specificity	Normal
2	1	Allele specific normal	
1	NA/0	Copy deletion LoH	Copy deletion LoH
2	0	Copy neutral LoH	Copy neutral LoH
3	NA	Single copy gain with unknown allele specificity	Single copy gain
3	0	Copy neutral single copy gain	

Table 29: Copy number analysis types for MIP arrays.

5.8 Results

5.8.1 DNA Extraction for MIP Arrays

For each of the 82 samples undergoing MIP array DNA quantities and Qubit fluorescence readings can be found in appendix 7.

5.8.2 MIP Array Maps

All MIP array data was analysed by the Bioinformatics Unit of King's College London, Breakthrough Breast Cancer. MIP array data was analysed by three Independent researchers (AG, HM & SR). A total of 73 cases (Table 30) were provided for analysis separated into the different phenotypic groups. These phenotypic groups were then compared with each other (Table 31).

All MIP array chromosomal maps can be found in appendix 8 & 9. Representative figures are given below for ER positive pure DCIS (Figure 31), HER2 positive pure DCIS (Figure 32) and triple negative pure DCIS (Figure 33). Additionally, representative figures showing comparisons of normal breast tissue, DCIS and invasive breast disease for ER positive (Figure 34) and triple negative cases (Figure 34) are given below.

Specimen type	Number of Cases
ER positive pure DCIS	8/10
ER positive DCIS associated with invasive disease	9/9
ER positive invasive breast disease associated with DCIS	9/9
Triple negative pure DCIS	9/12
Triple negative DCIS associated with invasive breast disease	10/10
Triple negative invasive disease associated with DCIS	7/10
HER2 positive pure DCIS	7/8

Table 30: MIP array cases with chromosomal maps

Title	Group1	Group2
ER+ DCIS compared to non ER+ DCIS	ER Pure DCIS, ER DCIS with invasive disease (n=17)	TN pure DCIS, TN DCIS with invasive disease, HER2 positive pure DCIS (n=26)
ER+ DCIS associated with invasive breast disease compared to ER+ pure DCIS	ER+ DCIS with invasive disease (n=9)	ER+ pure DCIS (n=8)
ER+ invasive breast disease compared to all ER+ DCIS	ER+ invasive breast disease (n=9)	ER+ pure DCIS, ER DCIS with invasive disease (n=17)
ER+ pure DCIS compared to ER+ invasive breast disease	ER+ pure DCIS (n=8)	ER+ invasive breast disease (n=9)
Triple negative invasive breast disease compared to all triple negative DCIS	TN invasive breast disease (n=7)	TN Pure DCIS, TN DCIS with invasive disease (n=19)
Triple negative DCIS associated with invasive breast disease compared to triple negative pure DCIS	TN DCIS with invasive disease (n=10)	TN pure DCIS (n=9)
Triple negative pure DCIS compared to triple negative invasive breast disease	TN pure DCIS (n=9)	TN invasive breast disease (n=7)
HER2+ pure DCIS compared to ER+ pure DCIS	HER2 positive pure DCIS (n=7)	ER+ pure DCIS (n=8)
HER2+ pure DCIS compared to TN pure DCIS and ER+ pure DCIS	HER2 positive pure DCIS (n=7)	TN pure DCIS, ER+ pure DCIS (n=17)

Table 31: MIP Array Comparison Groups

[TN = triple negative; ER+ = oestrogen receptor positive]

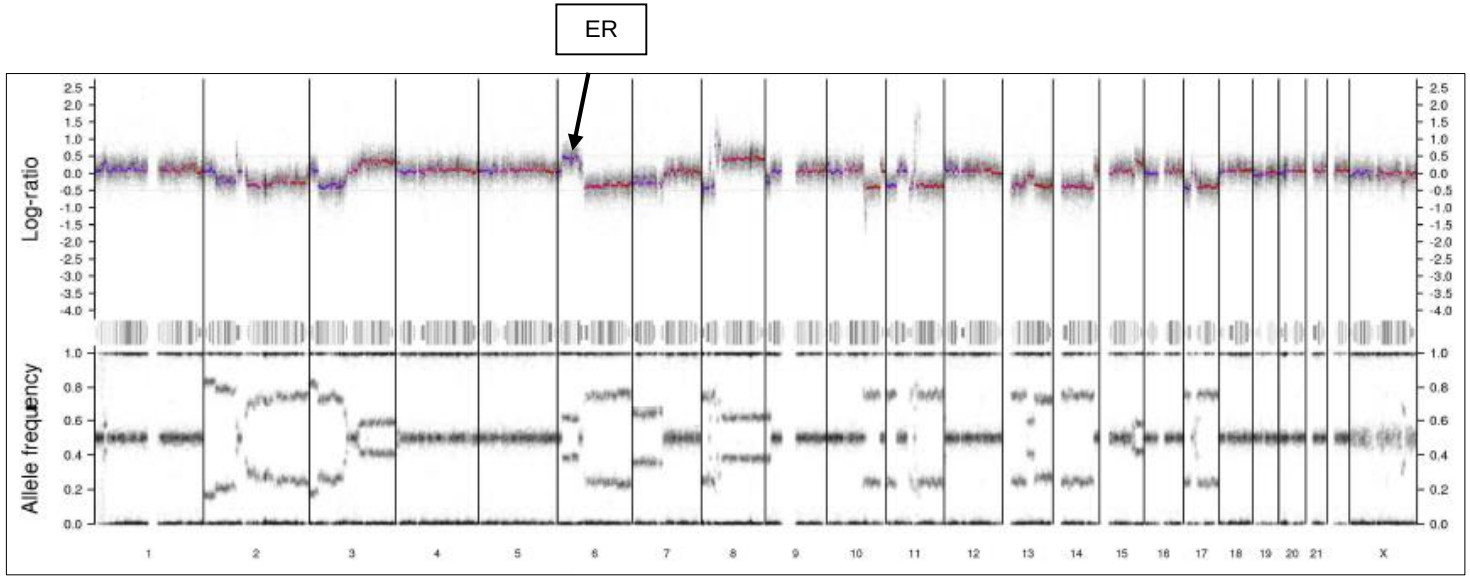

Figure 31: Chromosomal map for a ER Positive pure DCIS Case (DCISJPB10K 066).

The X axis in the diagram refers to chromosome number (1-21 and X) and the Y axis is split into two sections. The upper section shows log of ratio of signal of the same probe from the tumour and normal samples. The lower section of the plot shows allelic-ratio. Usually, this represents the ratio of B-allele as compared to A-allele. The value always lies between 0 and 1. e.g. if there is one copy each of both allele then allele ratio would be 1 / 2 = 0.5 which represent the normal allele pairing. Each probe represents the number of copies for a genomic region. The probe signal from the normal sample is subtracted from the tumour samples and a log ratio (usually base 2)

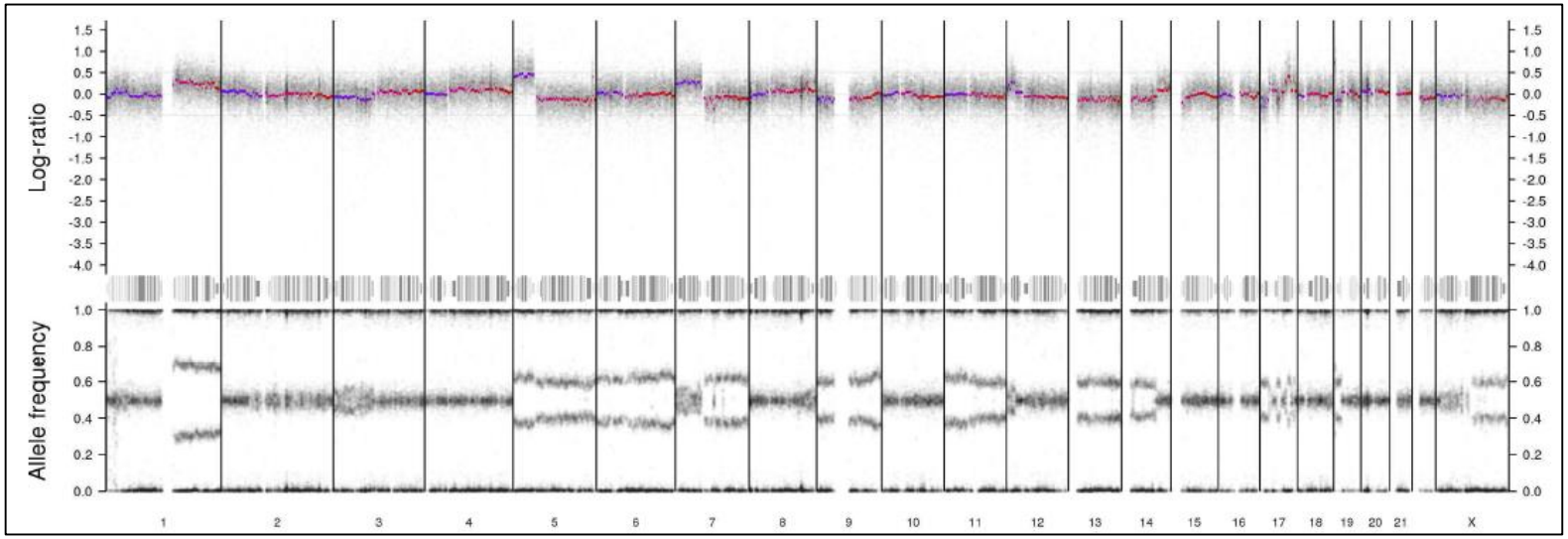

Figure

Figure 32: Chromosomal Map for a Pure DCIS Triple Negative Case (DCISJPB10K001)

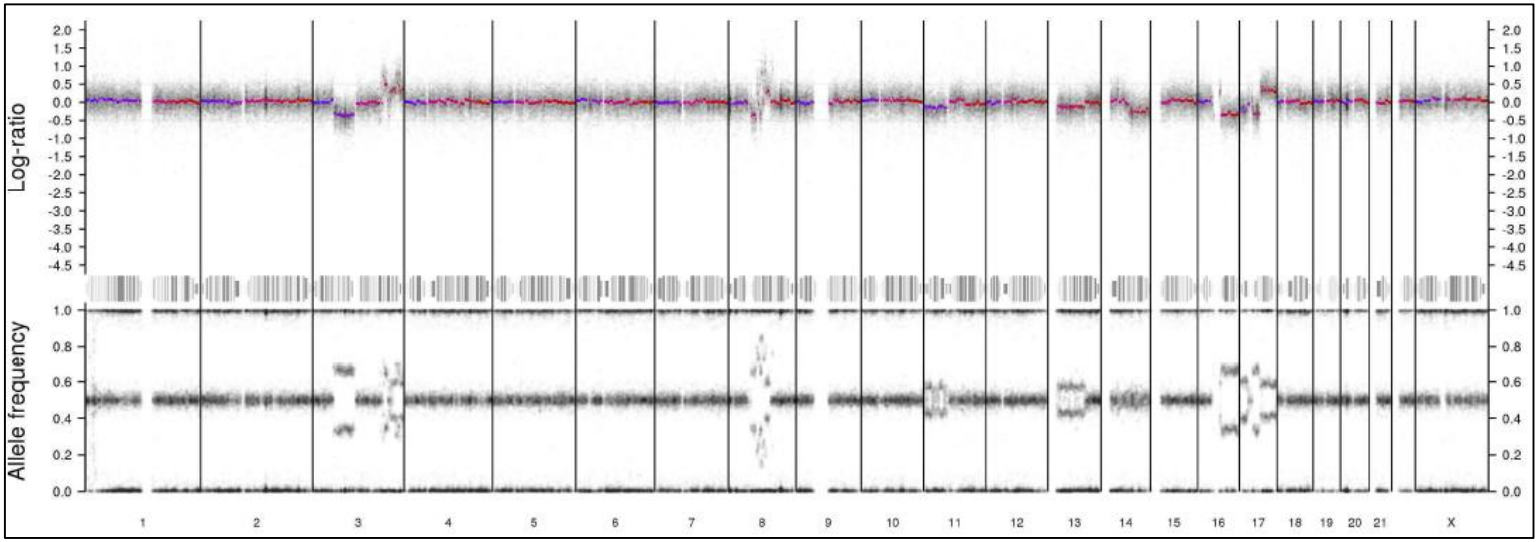

Figure 33: Chromosomal Map for a Pure HER2 Positive Case (DCISJPB10K070); note chromosome 17 allelic amplification.

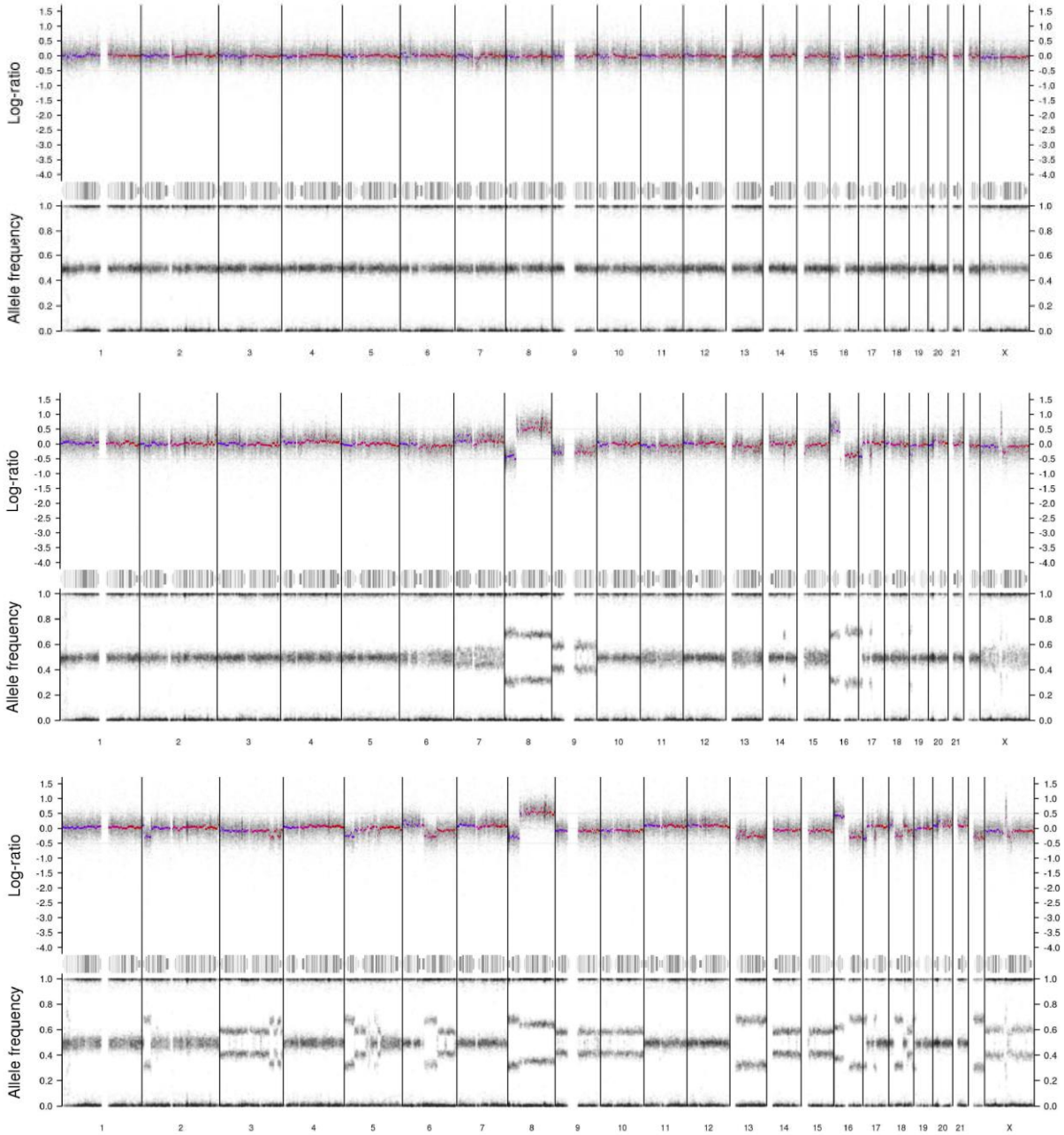

Figure 34: Chromosomal map for normal, DCIS and invasive samples from an ER positive lesion.

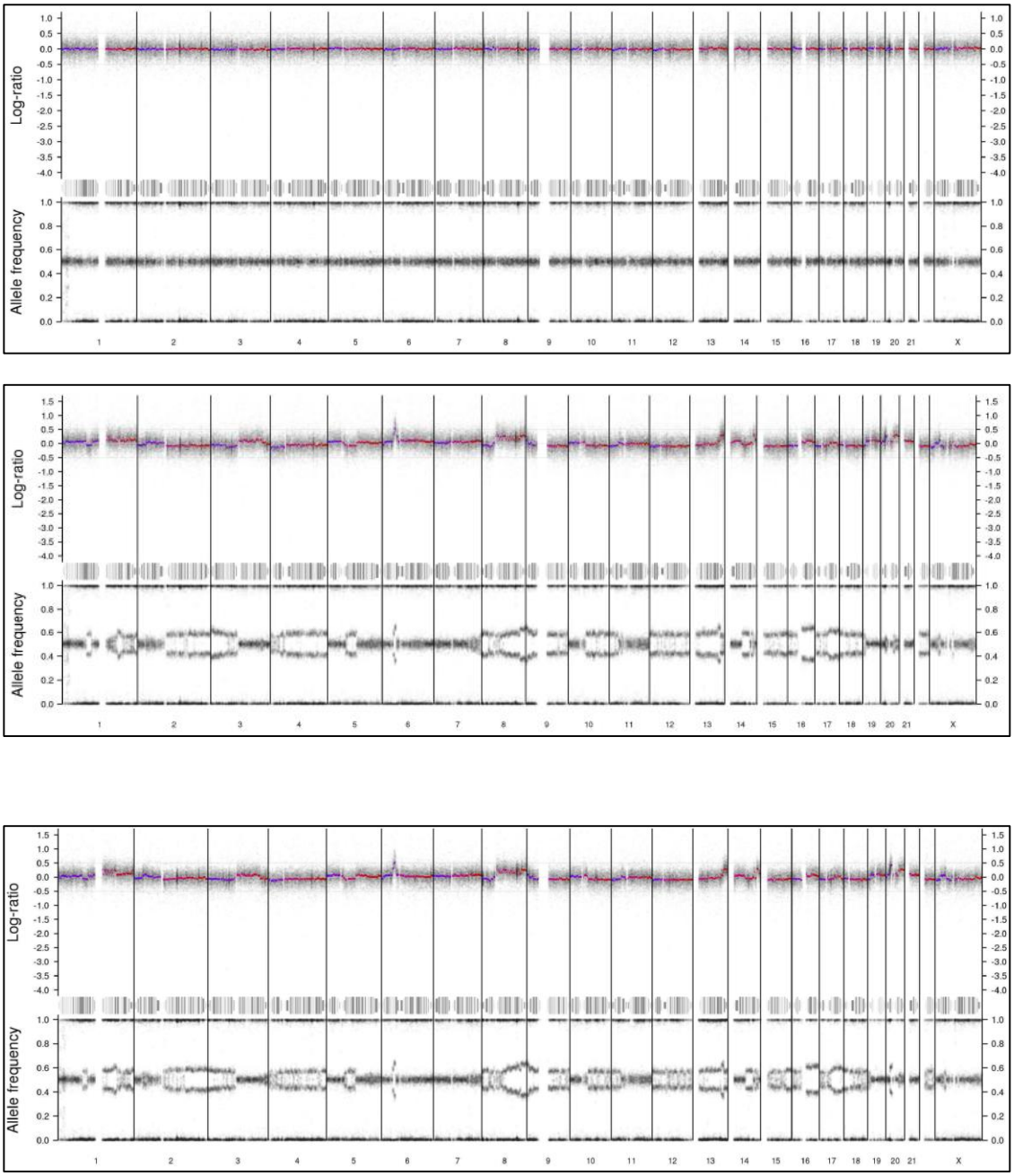

Figure 35: Chromosomal Map for normal, DCIS and invasive samples from a triple negative case.

5.8.3 Copy Number Aberrations for Oestrogen Receptor Positive DCIS Compared to Non Oestrogen Receptor DCIS

These series examines the difference between oestrogen receptor positive DCIS and non oestrogen receptor positive DCIS.

Frequency plots showing copy number aberrations between Oestrogen receptor positive DCIS and oestrogen receptor negative DCIS were provided by Breakthrough Breast Cancer/Research Oncology, King's College London Bioinformatics Department (Figure 37).

Figure 36: Frequency plots showing copy number aberrations between oestrogen receptor positive DCIS and non oestrogen positive DCIS (pages 165-167).

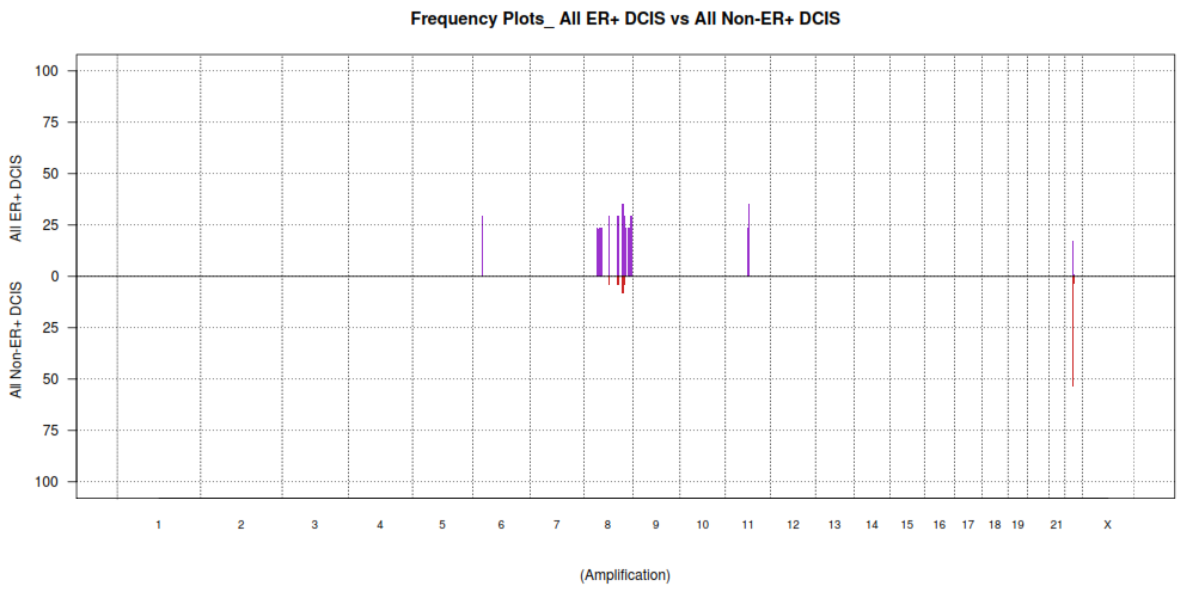
Frequency Plots_ All ER+ DCIS vs All Non-ER+ DCIS
All ER+ DCIS
All Non-ER+ DCIS
100
75
50
25
0
25
50
75
100
1
2
3
4
5
6
7
8
9
10
11
12
13
14
15
16
17
18
19
21
X
(Amplification)

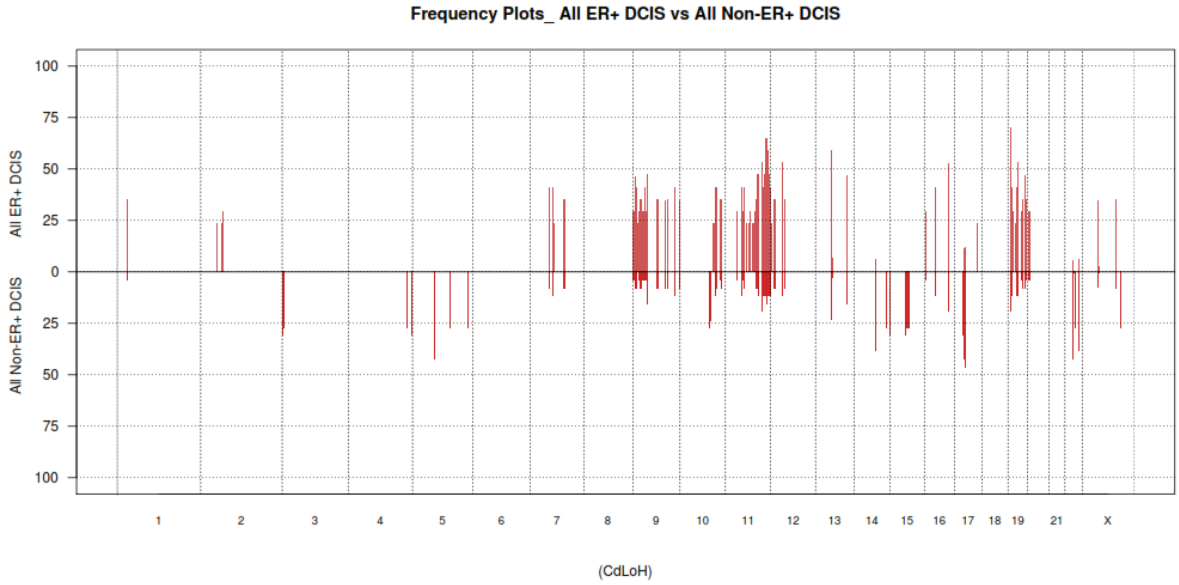
Frequency Plots_ All ER+ DCIS vs All Non-ER+ DCIS
All ER+ DCIS
All Non-ER+ DCIS
100
75
50
25
0
25
50
75
100
1
2
3
4
5
6
7
8
9
10
11
12
13
14
15
16
17
18
19
21
X
(CdLoH)

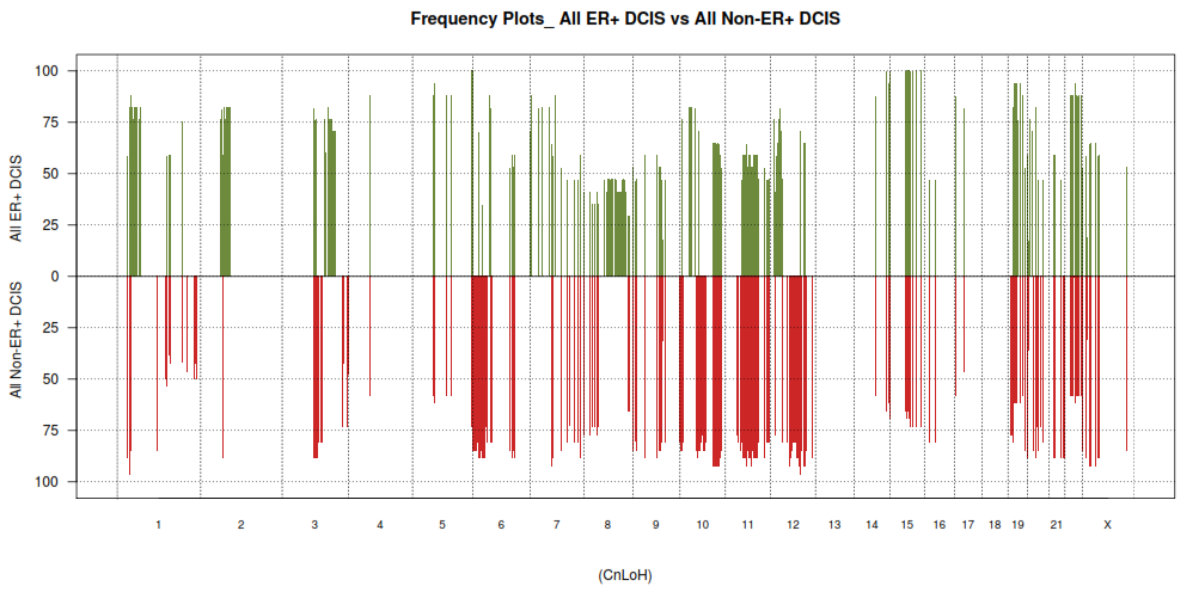
Frequency Plots_ All ER+ DCIS vs All Non-ER+ DCIS
All ER+ DCIS
All Non-ER+ DCIS
100
75
50
25
0
25
50
75
100
1
2
3
4
5
6
7
8
9
10
11
12
13
14
15
16
17
18
19
21
X
(CnLoH)

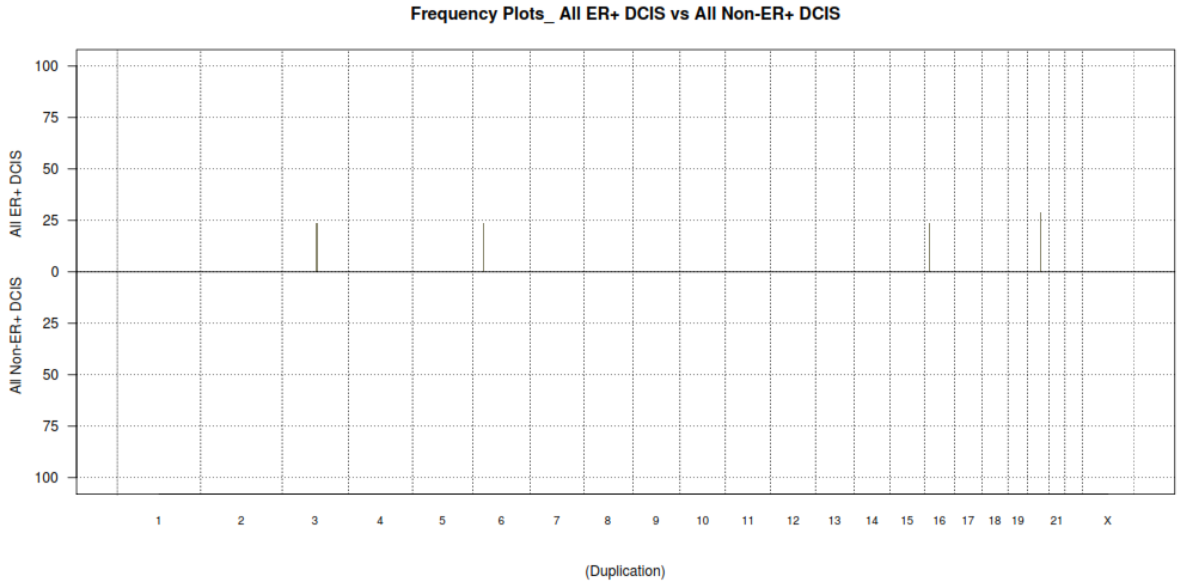
Frequency Plots_ All ER+ DCIS vs All Non-ER+ DCIS
All ER+ DCIS
All Non-ER+ DCIS
100
75
50
25
0
25
50
75
100
1
2
3
4
5
6
7
8
9
10
11
12
13
14
15
16
17
18
19
21
X
(Duplication)

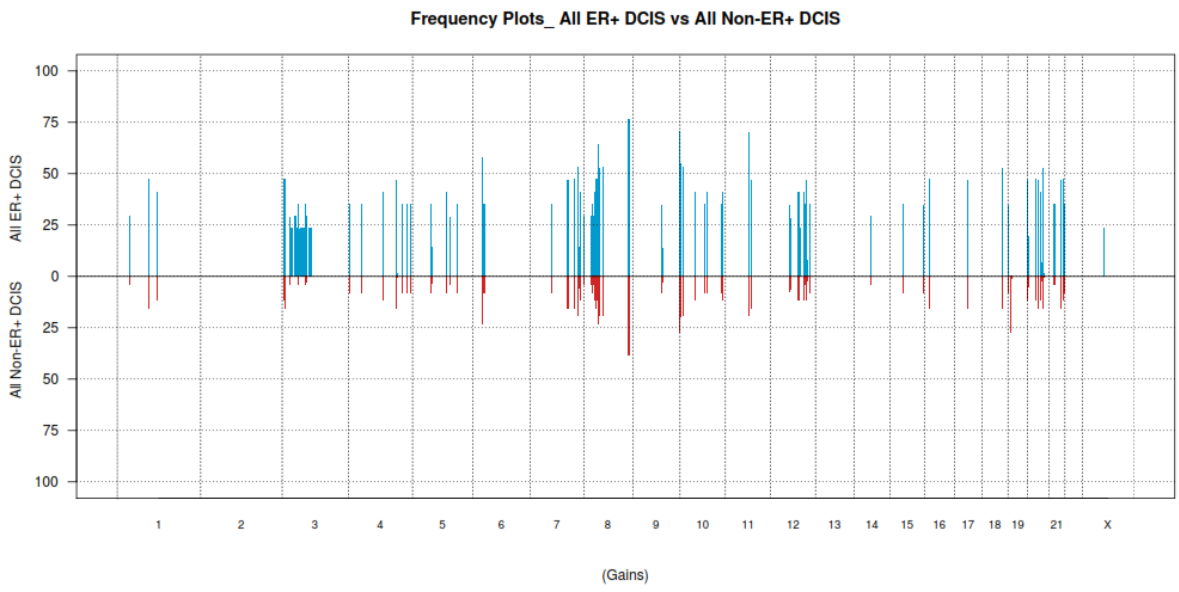
Frequency Plots_ All ER+ DCIS vs All Non-ER+ DCIS
All ER+ DCIS
All Non-ER+ DCIS
100
75
50
25
0
25
50
75
100
1
2
3
4
5
6
7
8
9
10
11
12
13
14
15
16
17
18
19
21
X
(Gains)

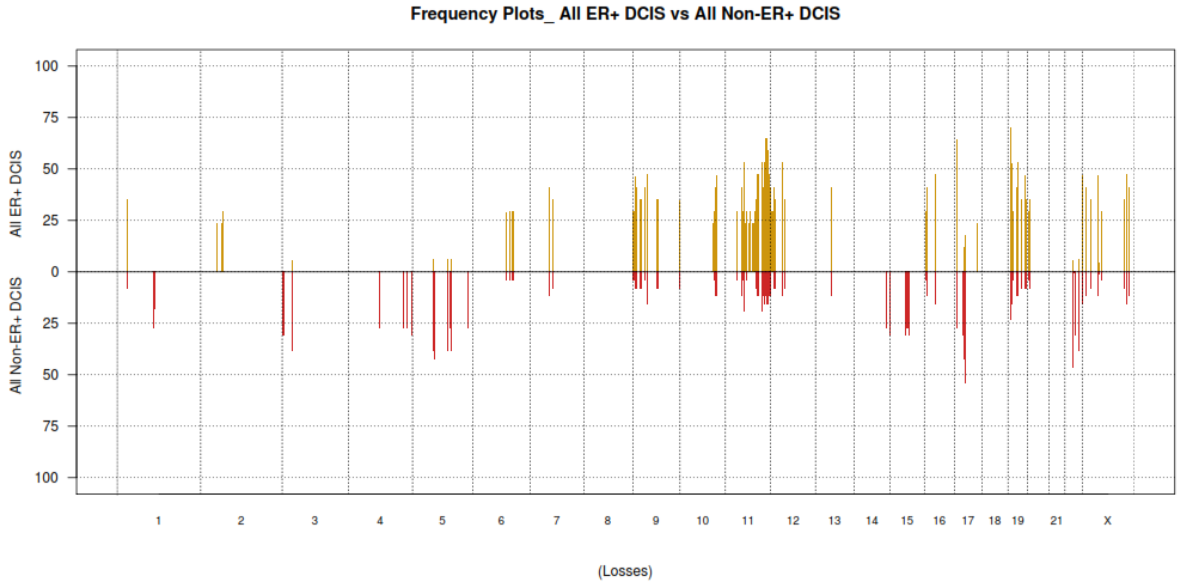
Frequency Plots_ All ER+ DCIS vs All Non-ER+ DCIS
All ER+ DCIS
All Non-ER+ DCIS
100
75
50
25
0
25
50
75
100
1
2
3
4
5
6
7
8
9
10
11
12
13
14
15
16
17
18
19
21
X
(Losses)

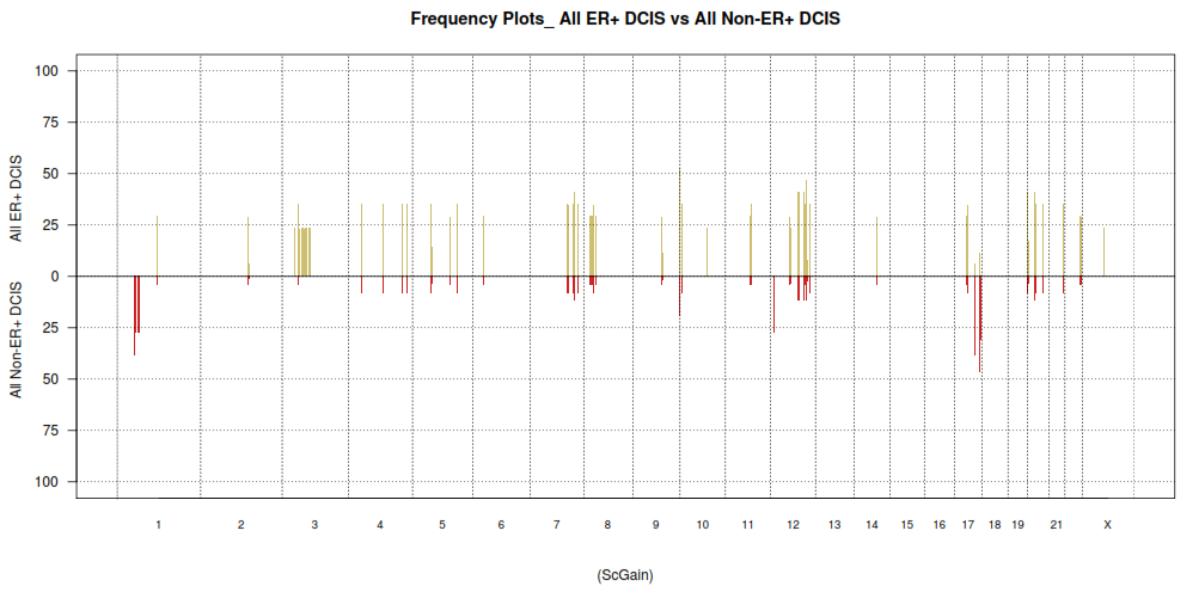

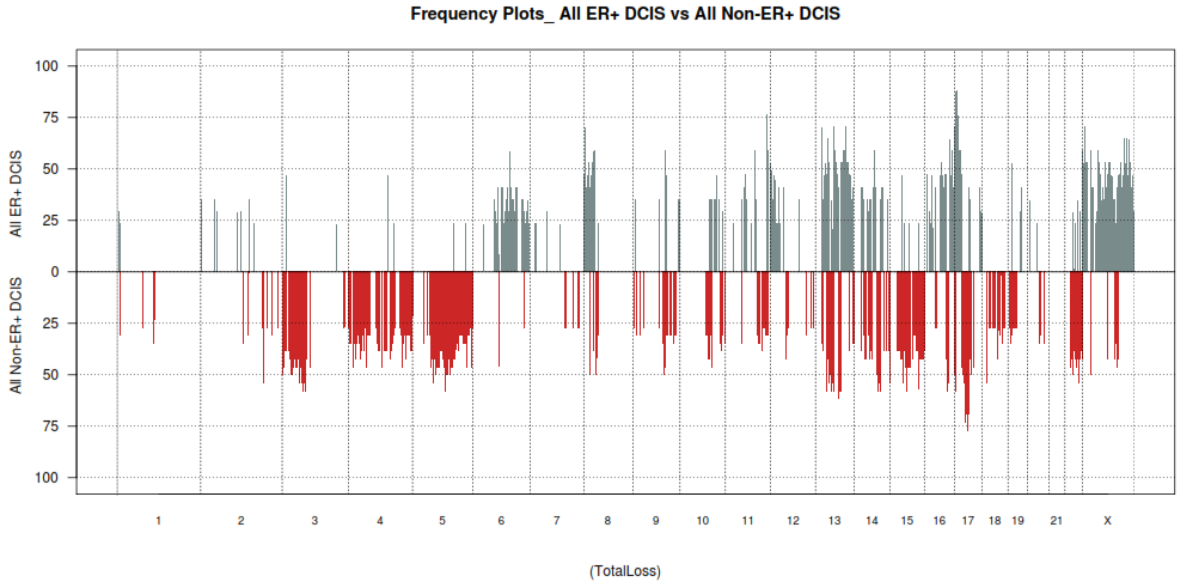

5.8.3.1 Amplification in Oestrogen Receptor (ER) Positive DCIS and Oestrogen Receptor Negative DCIS

There are amplifications found in ER positive DCIS (n=5/17) not observed in the majority of non ER DCIS (n=2/26).

1. p-values < 0.05;
2. A gene list is mapped from 16 genomic regions found on chromosomes 8, 11;
3. These regions encompass 118 genes altered in ER positive DCIS;

Genes:

5S_rRNA AC011626.1 AC021636.1 AC027238.1 AC090821.2 AC090821.3 AC090821.4 AC090821.5 AC103706.1 AC103764.1 AC103863.1 AC107374.1 AC115836.1 AF130342.1 AF178030.2 AF186191.1 AF230666.2 AL031777.1 ANKRD46 AP003385.1 AP003716.2 AP003716.4 AP003716.5 CCND1 CEBPD CHRAC1 CSMD3 CTC-458A3.1 CTD-2182N23.1 DENND3 DEPDC6 EIF2C2 FGF19 FGF3 FGF4 GDAP1 HFE HIST1H1C HIST1H1D HIST1H1E HIST1H1PS1 HIST1H1T HIST1H2AB HIST1H2AC HIST1H2AD HIST1H2AE HIST1H2APS3 HIST1H2APS4 HIST1H2BB HIST1H2BC HIST1H2BD HIST1H2BE HIST1H2BF HIST1H2BG HIST1H2BH HIST1H2BI HIST1H3A HIST1H3B HIST1H3C HIST1H3D HIST1H3E HIST1H3F HIST1H3G HIST1H4A HIST1H4B HIST1H4C HIST1H4D HIST1H4E HIST1H4F HIST1H4G hsa-mir-151 hsa-mir-30b hsa-mir-30d IKBKB KB-1615E4.1 KCNK9 KIAA0146 KIAA0196 MYEOV NCALD NDRG1 NSMCE2 ORAOV1 PHF20L1 POLB PRKDC PTK2 PXDNL RAD21 RNF19A RP11-1023P17.1 RP11-231D20.1 RP11-697N18.1 RP11-709P2.1 RP1-221C16.7 RPS10P1 RRM2B SLA SLC45A4 SNORA40 SNORA7 SPAG1 SQLE ST18 ST3GAL1 TG TMEM71 TRAPPC9 TRPS1 U6 U7 U91328.2 UNC93B5 WISP1 Y_RNA ZFAT ZFATAS ZMAT4

PANTHER analysis: 56 mapped ids are found, 62 mapped ids are not found.

There are amplifications found in non ER DCIS (n=2/26) that are also present in some ER positive DCIS (n=6/17).

1. p=values <0.05;
2. A gene list is mapped from 13 genomic regions on chromosome 8;
3. These regions encompass 49 genes altered in non ER DCIS;

Genes:

AC021636.1 AC090821.2 AC090821.3 AC090821.4 AC090821.5 AC103706.1 AC103764.1 AC107374.1 AC115836.1 AF186191.1 AF230666.2 CEBPD CSMD3 CTC-458A3.1 CTD-2182N23.1 DENND3 DEPDC6 hsa-mir-30b hsa-mir-30d IKBKB KCNK9 KIAA0146 KIAA0196 NDRG1 NSMCE2 PHF20L1 POLB PRKDC PTK2 PXDNL RP11-1023P17.1 RP11-231D20.1 RP11-697N18.1 RP11-709P2.1 SLA SLC45A4 SNORA40 SNORA7 SQLE ST18 ST3GAL1 TG TMEM71 TRAPPC9 U6 WISP1 ZFAT ZFATAS ZMAT4

PANTHER analysis: 25 mapped ids are found, 24 mapped ids are not found.

5.8.3.2 Duplication in Oestrogen Receptor Positive DCIS and Oestrogen Receptor Negative DCIS

There are no duplications in ER negative DCIS (check the status of the HER2 positives) in this series.

There are duplications in ER positive DCIS (n=4/17) not observed in non ER positive DCIS (n=0/26)

1. p-values < 0.05;
2. A gene list is mapped from 4 genomic regions found on chromosomes 3, 6, 16;
3. These regions encompass 27 genes altered in ER positive DCIS;

Genes:

AC136443.1 AC138932.2 AL645941.2 AL669918.1 BFAR HLA-DMB HLA-DOB HLA-DQA2 HLA-DQB2 HLA-DQB3 HLA-Z hsa-mir-1972 NIT2 NOMO1 NPIP PDXDC1 PLA2G10 PPP1R2P1 PSMB8 PSMB9 TAP1 TAP2 TBC1D23 XXbac-BPG181M17.5 XXbac-BPG246D15.8 XXbac-BPG246D15.9 Y_RNA

PANTHER analysis: 15 mapped ids are found, 12 mapped ids are not found.

5.8.3.3 Genomic Gains in Oestrogen Receptor Positive DCIS and Non Oestrogen Receptor Positive DCIS

There are genomic gains in ER positive DCIS (n=6/17) not observed in non ER positive DCIS (n=0/26).

1. p-values < 0.05;
2. A gene list is mapped from 10 genomic regions on chromosome 3;
3. These regions encompass 75 genes altered in ER positive DCIS;

Genes:

5S_rRNA AC096971.2 AC097359.1 AC097359.2 AC097359.3 AC099668.5 AC104186.1 AC104448.1 AC121252.1 AC121252.2 AC126118.1 AC126118.2 AC141002.1 AMIGO3 APEH ATRIP C3orf35 C3orf54 CAMP CCDC51 CCDC72 CDC25A CDH29 CELSR3 COL7A1 CTD-3211M3.1 FBXW12 FOXP1 GMPPB GOLGA4 hsa-mir-2115 hsa-mir-711 IP6K1 IP6K2 LRRFIP2 MLH1 MST1 NCKIPSD NDUFB1P1 NME6 PFKFB4 PLXNB1 PRKAR2A RNF123 RP11-20O23.1 RP11-24C3.2 RP11-391M1.3 RP11-430J3.1 RP11-430J3.2 RP11-502L5.2 RP11-520A21.1 RP11-528N21.1 RP11-528N21.2 RP11-528N21.3 RP11-905F6.1 RP13-1056D16.2 RP13-480C15.1 RPL14 SHISA5 SLC26A6 snoU13 SPINK8 TMEM89 TREX1 U5 U6 U7 UBA7 UCN2 UQCRC1 Y_RNA ZNF589 ZNF619 ZNF620 ZNF621

PANTHER analysis: 36 mapped ids are found, 39 mapped ids are not found.

There were gains present in non ER DCIS (n=10/17) which are also present in ER positive DCIS (n=13/10).

1. p-values < 0.05;
2. A gene list is mapped from 16 genomic regions found on chromosomes 6, 8, 10, 19;

3. These regions encompass 30 genes altered in both non ER DCIS and ER DCIS;

Genes:

5S_rRNA AC008734.2 AC090821.2 AC090821.3 AC090821.4 AC090821.5 AC103706.1 AF186191.1 AF216667.1 AF230666.2 AL713922.2
CTC-458A3.1 CTD-2182N23.1 DIP2C IKBKB IL9RP2 LRRC6 MUC16 NDRG1
PHF20L1 RP11-631M21.1 RP11-631M21.2 RP11-631M21.6 SLA SNORA40 ST3GAL1 TG
TMEM71 WISP1 ZMYND11

PANTHER analysis: 12 mapped ids are found, 18 mapped ids are not found.

5.8.3.4 Genomic Sc Gains in Oestrogen Receptor Positive DCIS and Non Oestrogen Positive Receptor DCIS

There are some overlaps in Sc gains found in ER positive DCIS (n=9/17) and non ER positive DCIS (n=4/26).

1. p-values < 0.05;
2. A gene list is mapped from 49 genomic regions found on chromosomes 3, 4, 5, 7, 8, 10, 11, 12, 17, 20, 21;
3. These regions encompass 180 genes altered in for ER positive DCIS and some non ER positive DCIS;

Genes:

5S_rRNA ABCG1 ABHD12 AC004001.1 AC005355.1 AC008038.1 AC008264.4 AC008937.2 AC009365.4 AC009518.8 AC013434.1
AC016831.7 AC018642.1 AC058791.1 AC058791.2 AC079595.1 AC079595.2 AC080112.3 AC087071.1 AC087071.2 AC092214.10
AC097534.1 AC097534.2 AC105285.1 AC105285.2 AC121247.2 AC121252.2 AC135506.1 AC137630.1 AF213884.1 AL031666.1
AL034548.1 AL034548.2 AL034548.3 AL109954.2 AL121894.1 AL157718.1 AL365356.1 AL713922.2 AL732437.1 ANKS1B
AP002827.1 ARIH2 ARL1 ASB13 C10orf18 C12orf23 C20orf26 C21orf121 C21orf128 C2CD2 C3orf62
C3orf71 C5orf15 CALML3 CALML5 CCDC25 CCDC36 CCDC71 CDC6 CDKL3 CDKN2AIPNL
CHCHD3 CRNKL1 CRY1 CST11 CST3 CST8 CST9 CST9L CSTL1 CTD-2410N18.1
DALRD3 DIP2C DOCK4 EIF4E2P1 ENTPD6 EPHA1 GALNT7 GDPD4 GPX1 GZF1
HMGB2 hsa-mir-191 hsa-mir-425 hsa-mir-620 IL9RP2 IMPDH2 KLHDC10 KLHDC8B LAMB2 MAP3K1
MED13L MKLN1 MTERFD3 NAPB NAT5 NDUFAF3 NET1 NFKB1 NRSN2 NXT1
P4HTM PAK1 PODXL PPIAP2 PPP2CA PRKAR2A PYGB QARS QRICH1 RALGAPA2 RARA
RHOA RHOH RIN2 RP11-10K16.1 RP11-135F9.1 RP11-215P8.1 RP11-215P8.2
RP11-215P8.3 RP11-215P8.4 RP11-218C14.2 RP11-218C14.6 RP11-218C14.7 RP11-23O13.1
RP11-306G20.1 RP11-312A15.2 RP11-312A15.3 RP11-316M24.1 RP11-336A10.4
RP11-336A10.5 RP11-336A10.7 RP11-395I6.2 RP11-3B7.1 RP11-3B7.6 RP1-148H17.1
RP11-631M21.1 RP11-631M21.2 RP11-631M21.6 RP11-694I15.6 RP11-775D22.2 RP11-798M19.3
RP13-131K19.1 RP13-131K19.2 RP13-463N16.6 RP3-322G13.5 RP3-333B15.2 RP4-569M23.2
RP5-1002M8.4 RP5-1103G7.4 RPS27P23 SAP30 SKP1 SLC24A3 SLC25A20 snoU13 SOX12 SPIC

TCF7 TMTC2 TOP2A TRIB3 U5 U6 UBE2B UBE2H UMODL1 USP19 USP4
UTP20 VDAC1 WDR6 Y_RNA ZC3HC1 ZCCHC3 ZMYND11 ZMYND8 ZNF295

PANTHER analysis: 87 mapped ids are found, 92 mapped ids are not found.

There are some overlaps in Sc gains for non ER positive DCIS (n=12/26) and ER positive DCIS (n=9/17).

1. p-values < 0.05;
2. A gene list is mapped from 25 genomic regions found on chromosomes 1, 7, 10, 12, 17.
3. These regions encompass 83 genes altered in non ER positive DCIS and ER positive DCIS.

Genes:

5S_rRNA AC013434.1 AC016182.1 AC018628.1 AC018628.3 AC058791.2 AC079595.1 AC079595.2 AC096947.1 AGBL4
AL713922.2 ANKS1B ARMC7 BRIP1 C12orf23 C1orf123 C1orf185 C20orf26 CDKN2C
CFLP2 CPT2CRNKL1 CRY1 CSDA CYTH1 DIP2C DMRTA2 DNAH17 FAF1 HN1
IL9RP2 INTS2 LRP8 MAGOH MED13 MKLN1 MTERFD3 NAT5 NFIA
NT5C PRH1 PRH2 PRR4 RIN2 ROR1 RP11-117D22.1 RP11-183G22.2
RP11-183G22.3 RP11-24J23.2 RP11-323N12.1 RP11-323N12.2 RP11-631M21.1
RP11-631M21.2 RP11-631M21.6 RP4-784A16.1 RP4-784A16.2 RP4-784A16.3 RP4-
784A16.4 RP4-784A16.5 RP5-1002M8.4 RP5-1024G6.2 RP5-1024G6.5 RP5-833A20.1
RP5-850O15.3 RP5-926E3.1 SLC16A5 TAS2R10 TAS2R13 TAS2R14 TAS2R19
TAS2R20 TAS2R31 TAS2R50 TAS2R7 TAS2R8 TAS2R9 TIMP2 TMTC2 U6 USP36
Y_RNA ZMYND11 ZNF859P

PANTHER analysis: 46 mapped ids are found, 47 mapped ids are not found.

5.8.3.5 Losses in Oestrogen Receptor Positive DCIS and Non Oestrogen Receptor Positive DCIS

There are genomic losses found in ER positive DCIS (n=8/17) not observed in non ER positive DCIS (n=0/26).

1. p-values < 0.05;
2. A gene list is mapped from 25 genomic regions found on chromosomes 2, 7, 9, 10, 11, 1;
3. These regions encompass 79 genes altered in ER positive DCIS;

Genes:

AC006432.1 AC007403.1 AC007403.2 AC007537.1 AC007537.2 AC009474.1 AC009474.2 AC022882.1 AC036111.1 AC068339.1 AC079920.1 ACSM4 AP000720.1 AP001482.1 AP002826.1 AP003065.3 AP006437.1 APLNR ARAP1 ARHGEF17 BCL2L14 CACNA1C CD163L1 ETV6 FAM168A GRM5 LRP6 LRRC55 MANSC1 OR10AG1 OR5AK3P OR5AK4P OR5AQ1P OR5AS1 OR5BE1P OR5D13 OR5D14 OR5D16 OR5D18 OR5F1 OR5G3P OR5G5P OR5I1 OR5J1P OR5J2 OR5L1 OR5L2 OR5T1 OR5T2 OR5T3 OR5W1P OR5W2 OR7E5P OR8H1 OR8H2 OR8H3 OR8I2 OR8J3 OR8K5 OR8V1P OR9M1P P2RX3 PRG2 PRG3 PTPRD RELT RP11-267J23.1 RP11-31L22.2 SBDS SLC22A8 SLC43A3 snoU13 SPRYD5 SSRP1 TNKS1BP1 TYR TYW1 U2 U6

PANTHER analysis: 46 mapped ids are found, 33 mapped ids are not found.

There are genomic losses found in non ER positive DCIS (n=11/26) not observed in ER positive DCIS (n=0/17).

1. p-values < 0.05;
2. A gene list is mapped from 17 genomic regions found on chromosomes 3, 4, 5, 14, 15, 17, 22;
3. These regions encompass 35 genes altered in non ER positive DCIS;

Genes:

AB019437.56 AC008772.1 AC008872.1 AC026202.1 AC026202.5 AC026214.2 AC092373.1 C22orf30 CD180 CNTN6 FAT1 IGHV1-67 IGHV1-68 IGHV1-69 IGHV2-70 IGHV3-66 IGHV3-71 IGHV3-72 IGHV3-73 IGHV3-74 IGHVII-67-1 IGHVIII-67-2 MAST4 PISD RAB27A RP11-173M1.1 RP11-287J9.1 RP11-287J9.2 RP11-308K2.1 RP11-5P22.1 RP11-5P22.2 RP11-5P22.3 RP5-858B16.5 SFRS12 snoU13

PANTHER analysis: 6 mapped ids are found, 29 mapped ids are not found.

5.8.3.6 Total Losses in Oestrogen Receptor Positive DCIS and Non Oestrogen Receptor Positive DCIS

There were total losses present in ER positive DCIS (n=13/17) not observed in non ER positive DCIS (n=0/26).

1. p-values < 0.05;
2. A gene list is mapped from 11 genomic regions found on chromosomes 8, 11, 13, 17;
3. These regions encompass 88 genes altered in ER positive DCIS;

Genes:

5S_rRNA AC005696.2 AC005696.3 AC006435.1 AC015799.1 AC015799.2 AC027763.1 AC027763.2 AC032044.1 AC055839.2 AC087742.1
AC087742.2 AC090617.1 AC091153.4 AC116914.1 AC118754.2 AC118754.4 AC127521.1 AC130689.5 AIPL1 AL450226.1
AL450226.2 ALOX12 ALOX15 AP001970.1 ARRB2 ASGR1 ASGR2 ATP2A3 BCL6B BHLHA9
C17orf100 C17orf49 C17orf85 CAMKK1 CLEC10A CRKCSMD1 CTD-2545G14.1 DLG4 DPH1 FAM64A
FBXO39 GAS7 GGT6 GSG2 HIC1 hsa-mir-132 hsa-mir-195 hsa-mir-212 hsa-mir-497 ITGAE
KIAA0664 KIAA0753 MED31 METT10D MNT MYBBP1A OVCA2 P2RX1 PAFAH1B1 PELP1 PITPNM3
RNASEK RP11-314A20.1 RP11-314A20.2 RP11-609D21.1 RP11-76K19.5 SGSM2
SLC13A5 SLC16A11 SLC16A13 SMG6 SMTNL2 SNORD91 snoU13 SPNS2 SPNS3 SRR TEKT1
TSR1 TUSC5 TXNDC17 U6 U8 UBE2G1 XAF1 YWHAE

PANTHER analysis: 51 mapped ids are found, 37 mapped ids are not found.

There were total losses present in non ER positive DCIS (n= 20/26) not observed in ER positive DCIS (n=0/17).

1. p-values < 0.05;
2. A gene list is mapped from 21 genomic regions from chromosome 17;
3. These regions encompass 182 genes altered in non ER positive DCIS;

Genes:

5S_rRNA ABHD5 AC008734.2 AC011816.4 AC020626.1 AC025029.1 AC092038.1 AC092798.2 AC092798.3 AC093416.3
AC098477.1 AC098477.2 AC098647.1 AC099539.1 AC099544.1 AC099544.2 AC099557.1 AC099778.3 AC104163.1 AC104184.1
AC104307.1 AC104434.1 AC104434.2 AC104434.3 AC104445.1 AC105935.1 AC112512.1 AC115283.1 AC121251.1 AC121252.2
AC124914.3 AC133141.1 AC133680.1 AC135966.1 ANO10 C3orf35 C3orf39 CACNA1D CADM2 CAMKV
CDC25A CDCP1 CELSR3 CLEC3B CSPG5 CTNNB1 DHX30 EIF1B EIF4BP9 ENTPD3 EXOSC7
FAM116A FAM198A FOXP1 FYCO1 GBE1 hsa-mir-1226 hsa-mir-564 ITGA9 KIF15 LARS2
LIMD1 LRIG1 MAP4 MITF MLH1 MUC16 MYRIP NCKIPSD NGLY1 NKIRAS1
NR1D2 OXSM PRICKLE2 RARB RP11-1029M24.1 RP11-1029M24.2 RP11-107O13.1 RP11-129B22.1
RP11-129B22.2 RP11-129B22.4 RP11-129B22.5 RP11-136C24.1 RP11-136C24.2 RP11-141M3.2
RP11-142L1.2 RP11-142L1.3 RP11-148G20.1 RP11-188P20.2 RP11-260O18.1 RP11-26G10.1
RP11-272D20.2 RP11-30M20.1 RP11-341J3.1 RP11-353H3.1 RP11-372H2.1
RP11-391M1.2 RP11-391M1.3 RP11-395P16.1 RP11-420K5.1 RP11-564P9.1 RP11-681O4.1
RP11-697K23.1 RP11-755B10.3 RP11-814M22.1 RP11-88B8.2 RPL15 SACM1L
SLC6A20 SLMAP SMARCC1 SNORA64 SNORD5 SNRK TGM4 TMEM42 TOP2B TRAIP U2
U3 U5 U6 U7 UBE2E1 UBE2E2 ULK4 Y_RNA ZDHHC3

PANTHER analysis: 50 mapped ids are found, 78 mapped ids are not found.

5.8.3.7 CdLOH in Oestrogen Receptor Positive DCIS and Non Oestrogen Receptor Positive DCIS

There is CdLOH present in ER positive DCIS (n=8/17) not observed in non ER positive DCIS (n= 0/26).

1. p-values < 0.05;
2. A gene list is mapped from 13 genomic regions found on chromosomes 9, 11;
3. These regions encompass 30 genes altered in ER positive DCIS;

Genes:

AC022882.1	AC036111.1	AP000866.1	AP000866.2	AP006437.1	C11orf61	ESAM	NRGN	OR5D13	OR5D14	OR5D16
OR5D18	OR5G3P	OR5G5P	OR5L1	OR5L2	OR5T1	OR5T2	OR5T3	OR8H1	OR8V1P	
P2RX3	PRG2	PRG3	PTPRD	snoU13	SSRP1	TNKS1BP1	U2	VSIG2		

PANTHER analysis: 19 mapped ids are found, 11 mapped ids are not found.

There is CdLOH in non ER positive DCIS (n=11/26) not observed in ER positive DCIS (n=0/17).

1. P-values < 0.05;
2. A gene list is mapped from 13 genomic regions found on chromosomes 8, 9, 10, 11;
3. These regions encompass 27 genes altered in non ER positive DCIS;

Genes:

AB019437.56	AC008772.1	AC026214.2	AC092373.1	CNTN6	FAT1	IGHV1-67	IGHV1-68	IGHV1-69	IGHV2-70
IGHV3-66	IGHV3-71	IGHV3-72	IGHV3-73	IGHV3-74	IGHVII-67-1	IGHVIII-67-2	MAST4	RP11-173M1.1	
RP11-287J9.1	RP11-287J9.2	RP11-308K2.1	RP11-5P22.1	RP11-5P22.2					
RP11-5P22.3	SFRS12	snoU13							

PANTHER analysis: 3 mapped ids are found, 24 mapped ids are not found.

5.8.3.8 CnLOH in Oestrogen Receptor Positive DCIS and Non Oestrogen Receptor Positive DCIS

There is CnLOH in ER positive DCIS (n=15/17) not observed in non ER positive DCIS (n=0/26).

1. p-values < 0.05;

2. A gene list is mapped from 40 genomic regions found on chromosomes 1, 2, 3, 6, 7, 10, 12 19, 20;
3. These regions encompass 200 genes altered in ER positive DCIS;

Genes:

5S_rRNA 7SK AC004906.3 AC007040.5 AC008686.2 AC010733.4 AC012671.2 AC022021.2 AC062029.1 AC074389.1 AC074389.6 AC074389.7 AC074389.9 AC078841.5 AC083864.3 AC083864.4 AC104134.2 AC104170.1 AC110781.3 AC110781.5 ACOT11 AKIRIN1 AL031289.1 AL031985.1 AL139244.1 AL160287.2 AL161740.1 AL161932.2 AL929472.1 AL929472.3 APBB1IP ARHGAP12 BAZ1B C10orf50 C1orf122 C1orf168 C1orf175 C1orf191 C1orf228 C2orf51 C8A C8B CARD11 CDCP2 CITED4 CST1 CST4 CSTP2 CTPS CYB5RL DAB1 DEM1 DEPDC1 EDN2 EEPD1 EGFR EIF2AK3 ELFN1 EPHA10 EPS15 FAM151A FHL3 FOXI3 FOXO6 GLIS1 GLUDP5 GRIK3 HEYL HIVEP3 HPCAL4 hsa-mir-23a hsa-mir-24-2 hsa-mir-27a hsa-mir-30c-1 hsa-mir-30e IL20RB INPP5B KCNQ4 KIF2C KIF5B MAD1L1 MANEAL MPP7 MRPL37 MTF1 NCK1 NDUFS5 NFYC NRP1 NT5C1A OMA1 OSBPL3 OSBPL9 OVCH1 PABPC4 PARS2 PDSS1 PPAP2B PPIE PRKAA2 RET RIMS3 RNF220 RP11-109P14.1 RP11-109P14.10 RP11-109P14.2 RP11-109P14.8 RP11-109P14.9 RP11-128B16.3 RP11-15J6.1 RP11-167O6.2 RP11-191G24.1 RP11-191G24.2 RP11-213P13.1 RP11-240D10.2 RP11-240D10.4 RP11-241I20.1 RP11-241I20.3 RP11-241I20.4 RP11-241I20.5 RP11-253A20.1 RP11-269F19.2 RP11-275F13.1 RP11-275F13.3 RP11-342D11.2 RP11-348A7.1 RP11-348A7.2 RP11-351M16.1 RP11-351M16.2 RP11-351M16.3 RP11-377K22.2 RP11-377K22.3 RP11-378I13.1 RP11-399E6.1 RP11-399E6.4 RP1-144F13.3 RP11-472N13.3 RP11-486B10.3 RP11-486B10.4 RP11-524K22.1 RP11-575C1.1 RP11-656D10.3 RP11-656D10.5 RP11-656D10.6 RP11-781D11.1 RP11-85F14.1 RP11-85F14.6 RP1-28O17.1 RP13-16H11.1 RP13-16H11.2 RP13-16H11.5 RP13-16H11.6 RP13-16H11.7 RP1-63P18.2 RP4-614N24.1 RP4-678E16.4 RP4-694A7.2 RP4-694A7.3 RP4-694A7.4 RP4-705F19.1 RP4-705F19.2 RP4-710M16.2 RP4-739H11.1 RP4-739H11.3 RP4-783C10.3 RP5-1033K19.2 RP5-1066H13.4 RP5-1103B4.3 RP5-866L20.1 RP5-866L20.2 RP5-866L20.3 RP5-997D24.3 RP5-997D24.5 RP6-239D12.1 RPE65 RPIA SDK1 SF3A3 SNORA63 SNORD112 snoU13 SSBP3 TCEB1P18 TMEM53 TMTC1 TTC39A TTC4 U3 U5 U6 U7 UTP11L VAX2 WAC Y_RNA YRDC ZNF642 ZNF643 ZNF684 ZSWIM4

PANTHER analysis: 77 mapped ids are found, 123 mapped ids are not found.

There is CnLOH present in non ER positive DCIS (n=24/26) not observed in ER positive DCIS (n=0/17).

1. p-values < 0.05;
2. A gene list is mapped from 38 genomic regions found on chromosomes 1, 3, 6, 10, 12, 21;
3. These regions encompass 126 genes altered in non ER positive DCIS;

Genes:

5S_rRNA 7SK AACS ABI3BP AC078811.1 AC083805.1 AC083805.2 AC106728.2 AC108739.1 AC117377.1
ADPRHL2 AF015262.1 AF015262.2 AL008732.1 AL034372.1 AL136180.1 AL136230.1 AL138724.3 AL138889.1 AL139044.1
AL139286.1 AL590403.1 AL773603.1 AL844908.5 ANKS1B AP000304.12 AP000313.1 AP000313.2 AP000318.2 AP000320.6
AP000322.53 AP000322.54 AP000569.2 AP000569.8 AP001630.1 AP001630.5 AP001631.9 ARHGAP9 ATP5O
C21orf51 C21orf67 C21orf70 C6orf125 CAP2 CBS CLDND1 CLIC6 COL8A2 CPOX CTD-2021J15.1
CTD-2021J15.2 DCBLD2 DCTN2 EIF2C1 EIF2C3 EIF2C4 FAM8A1 GNL1 GPR15 GRM4 hsa-mir-1275 hsa-mir-548a-1 IFNGR2 IMPG2 IP6K3 ITGB2 ITPR3 ITSN1 KCNE1 KCNE2 KIF13A KIF5A
LEMD2 MARS MGAT4C MIP MLN MRPL51P2 NCRNA00160 NDUFV3 NUP153 OR5K2 PKNOX1
PRKG1 PRR3 PTTG1IP RCAN1 RNF144B RP11-14H3.3 RP11-204E9.1 RP11-227H4.1
RP11-227H4.4 RP11-227H4.5 RP11-254A17.1 RP11-301G23.1 RP11-319J24.1 RP11-319J24.3
RP11-377N20.1 RP11-40M23.1 RP11-524C21.1 RP11-569H14.1 RP11-663C11.1 RP11-686D16.1
RP11-686D16.2 RP1-273P12.3 RP1-67M12.1 RP3-322L4.2 RP3-468B3.2 RP4-665N4.4
RP4-665N4.5 RUNX1 SNORA11 snoU13 SOX4 ST3GAL6 SYT1 TEKT2 TIMELESS
TMEM50B TMTC2 TRIM38 U2AF1 U6 U7 Y_RNA

PANTHER analysis: 56 mapped ids are found, 70 mapped ids are not found.

5.8.4 Copy Number Aberrations for Oestrogen Receptor Positive Pure DCIS Compared to Oestrogen Receptor Positive DCIS Associated with Invasive Breast Disease

These series examines the difference between oestrogen receptor positive pure DCIS and oestrogen receptor positive DCIS associated with invasive breast disease i.e. the DCIS component and not the invasive breast disease.

Frequency plots showing copy number aberrations between oestrogen receptor positive pure DCIS and oestrogen receptor positive DCIS associated with invasive breast disease were provided by Breakthrough Breast Cancer/Research Oncology, King's College London Bioinformatics Department (Figure 37).

Figure 37: Frequency plots showing copy number aberrations between oestrogen positive pure DCIS and oestrogen positive DCIS associated with tumour (amplifications, duplications, gains, Sc gains, losses, total losses CdLOH and CnLOH,) (pages 177-180).

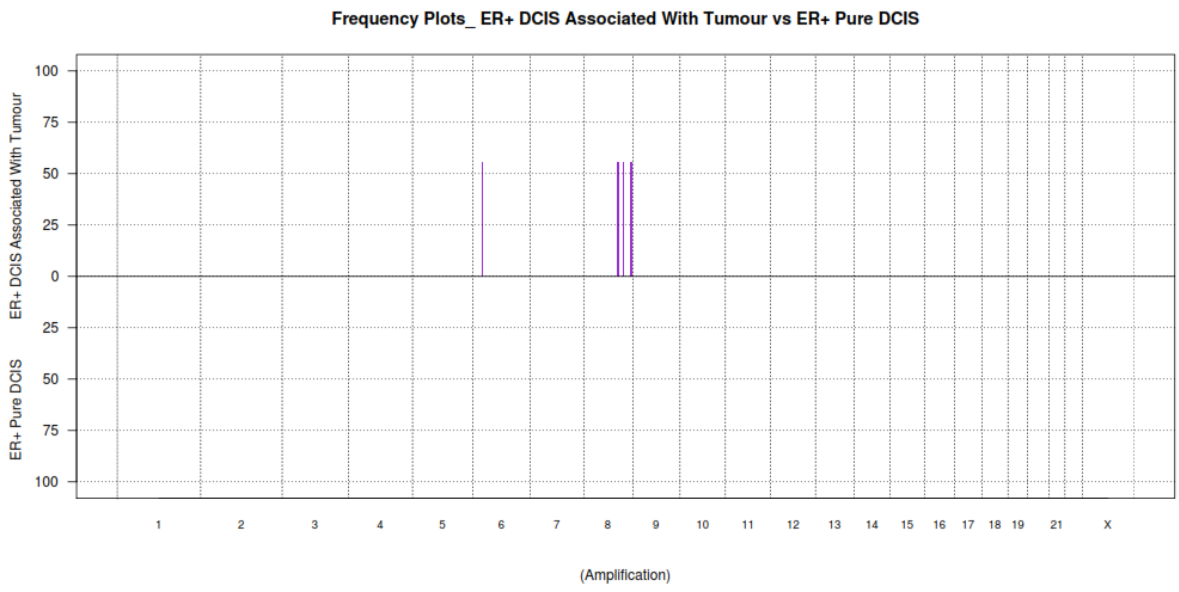
Frequency Plots_ ER+ DCIS Associated With Tumour vs ER+ Pure DCIS
ER+ DCIS Associated With Tumour
ER+ Pure DCIS
100
75
50
25
0
25
50
75
100
1
2
3
4
5
6
7
8
9
10
11
12
13
14
15
16
17
18
19
21
X
(Amplification)

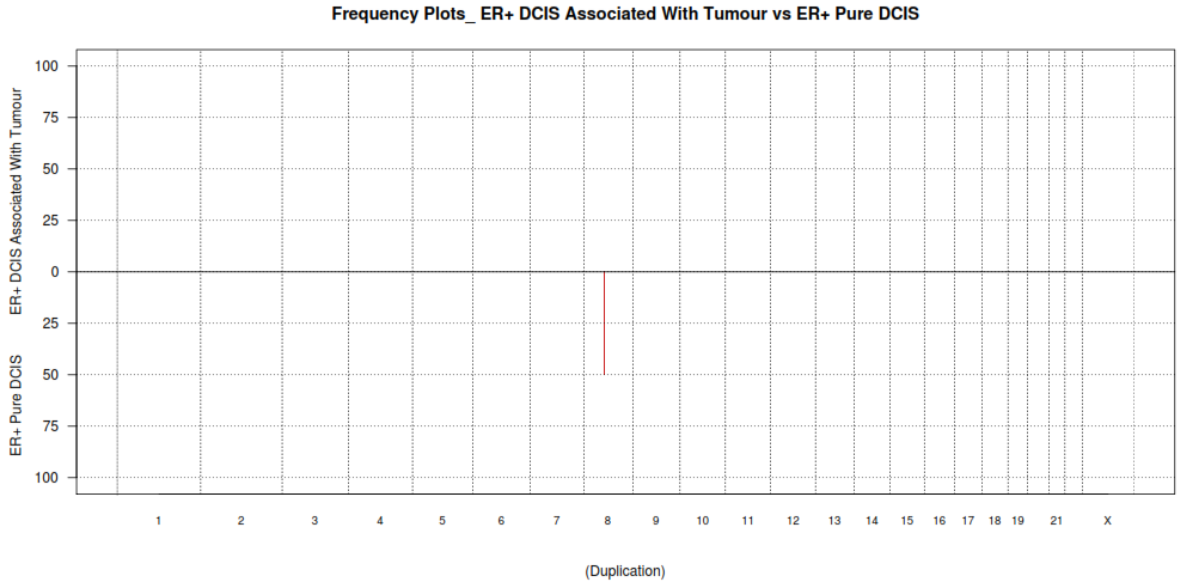
Frequency Plots_ ER+ DCIS Associated With Tumour vs ER+ Pure DCIS
ER+ DCIS Associated With Tumour
ER+ Pure DCIS
100
75
50
25
0
25
50
75
100
1
2
3
4
5
6
7
8
9
10
11
12
13
14
15
16
17
18
19
21
X
(Duplication)

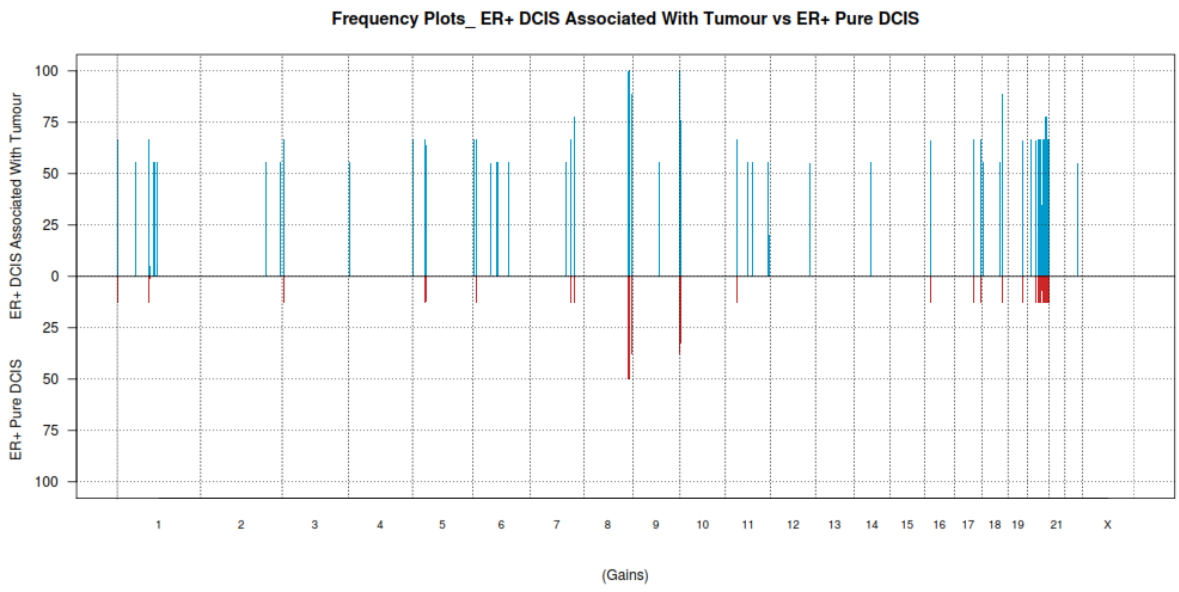
Frequency Plots_ ER+ DCIS Associated With Tumour vs ER+ Pure DCIS
ER+ DCIS Associated With Tumour
ER+ Pure DCIS
100
75
50
25
0
25
50
75
100
1
2
3
4
5
6
7
8
9
10
11
12
13
14
15
16
17
18
19
21
X
(Gains)

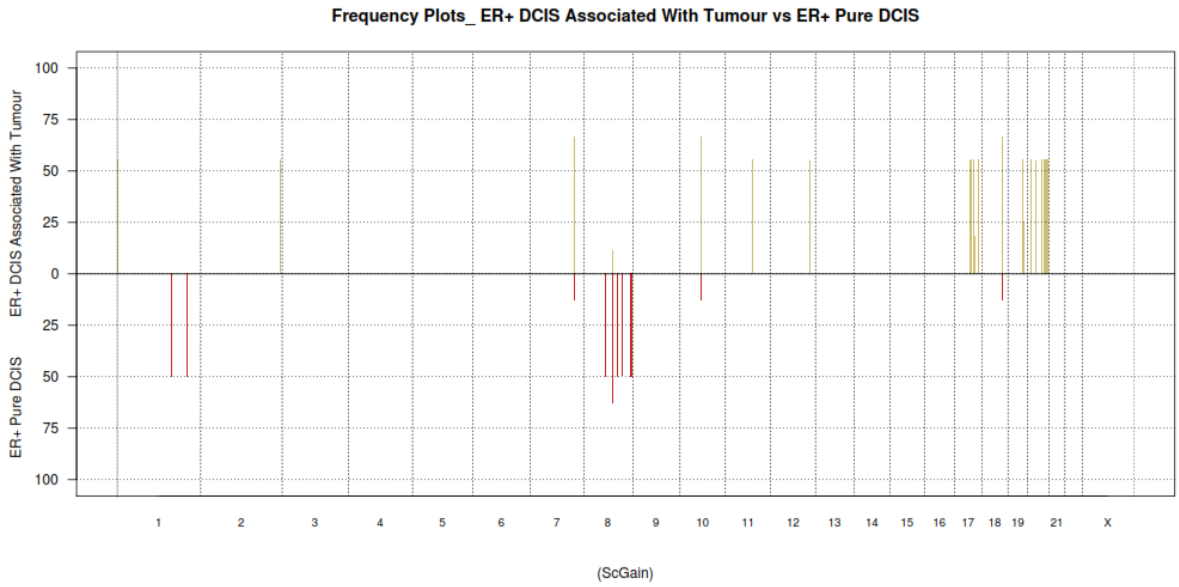
Frequency Plots_ ER+ DCIS Associated With Tumour vs ER+ Pure DCIS
ER+ DCIS Associated With Tumour
ER+ Pure DCIS
100
75
50
25
0
25
50
75
100
1
2
3
4
5
6
7
8
9
10
11
12
13
14
15
16
17
18
19
21
X
(ScGain)

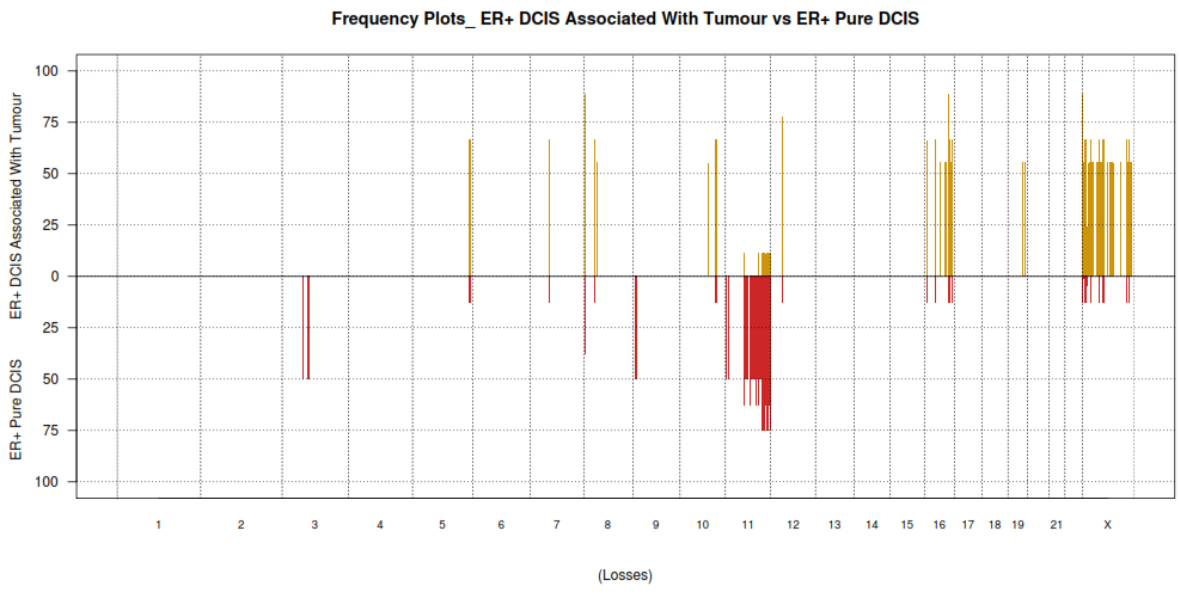
Frequency Plots_ ER+ DCIS Associated With Tumour vs ER+ Pure DCIS
ER+ DCIS Associated With Tumour
ER+ Pure DCIS
100
75
50
25
0
25
50
75
100
1
2
3
4
5
6
7
8
9
10
11
12
13
14
15
16
17
18
19
21
X
(Losses)

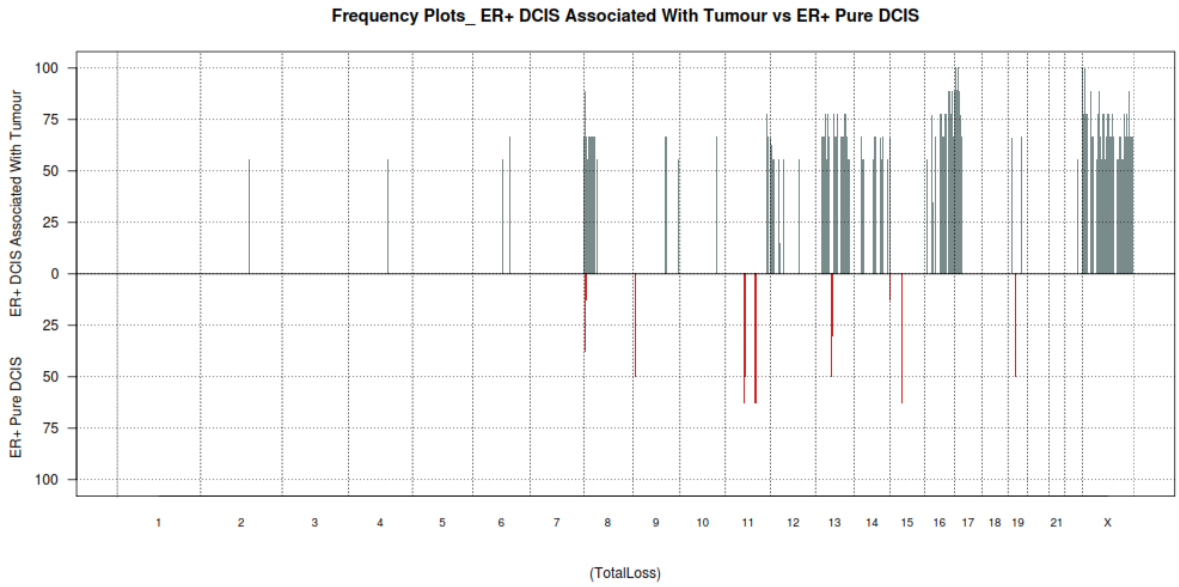
Frequency Plots_ ER+ DCIS Associated With Tumour vs ER+ Pure DCIS
ER+ DCIS Associated With Tumour
ER+ Pure DCIS
100
75
50
25
0
25
50
75
100
1
2
3
4
5
6
7
8
9
10
11
12
13
14
15
16
17
18
19
21
X
(TotalLoss)

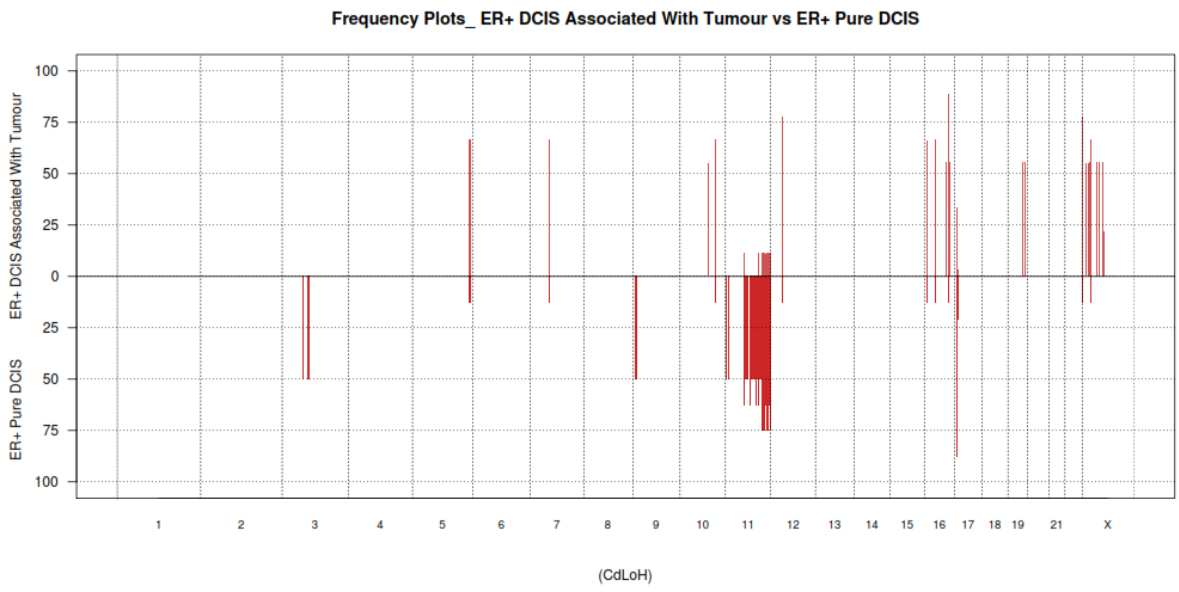

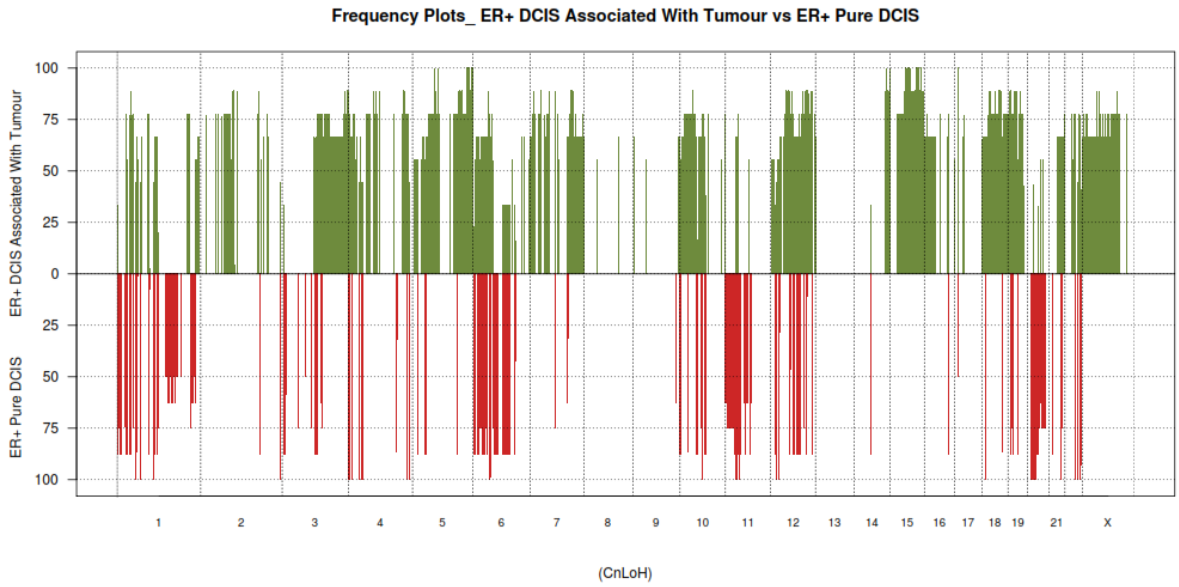

5.8.4.1 Amplification in Oestrogen Receptor Positive Pure DCIS Compared to Oestrogen Receptor Positive DCIS Associated with Invasive Breast Disease

There were no amplifications in ER positive pure DCIS (n=0/8) in this series. However, there were amplifications present in cases of ER positive DCIS associated with invasive breast disease (n=5/9).

1. p-values < 0.05;
2. A gene list is mapped from 7 genomic regions found on chromosomes 6, 8.

3. These regions encompass 69 genes altered in ER positive DCIS associated with invasive breast disease;

Genes:

5S_rRNA AC025647.3 AC103863.1 AF130342.1 AL031777.1 ANKRD46 AP001207.1 AP001208.1 AP001208.2 AP002852.1 AP002907.1 CHRAC1 DENND3 EIF2C2 FBXO43 GRHL2 HFE HIST1H1C HIST1H1D HIST1H1E HIST1H1PS1 HIST1H1T HIST1H2AB HIST1H2AC HIST1H2AD HIST1H2AE HIST1H2APS3 HIST1H2APS4 HIST1H2BB HIST1H2BC HIST1H2BD HIST1H2BE HIST1H2BF HIST1H2BG HIST1H2BH HIST1H2BI HIST1H3A HIST1H3B HIST1H3C HIST1H3D HIST1H3E HIST1H3F HIST1H3G HIST1H4A HIST1H4B HIST1H4C HIST1H4D HIST1H4E HIST1H4F HIST1H4G hsa-mir-1273 hsa-mir-151 KB-1615E4.1 NCALD PTK2 RGS22 RNF19A RP1-221C16.7 RPS10P1 RRM2B SNORD77 snoU13 SPAG1 TRAPPC9 U6atac U7 U91328.2 UBR5 Y_RNA

PANTHER analysis: 29 mapped ids are found, 40 mapped ids are not found.

5.8.4.2 Duplication in Oestrogen Receptor Positive Pure DCIS Compared to Oestrogen Receptor Positive DCIS Associated with Invasive Breast Disease

There were no duplications present in ER positive DCIS associated with invasive breast disease in this series. However, there were duplications identified in ER positive pure DCIS (n=4/8).

1. p-values < 0.05;
2. A gene list is mapped from 1 genomic region and chromosome 8;
3. These regions encompass 2 genes altered in ER positive pure DCIS;

Gene: ASPH 7SK

PANTHER analysis: 1 mapped id is found.

Gene ID:	ENSG00000198363
Protein ID:	Q12797
Gene Name:	Aspartyl/asparaginyl beta-hydroxylase
Gene Symbol(s):	ASPH

5.8.4.3 Genomic Gains in Oestrogen Receptor Positive Pure DCIS Compared to Oestrogen Receptor Positive DCIS Associated with Invasive Breast Disease

There were gains associated with both ER positive pure DCIS (n=4/8) and ER positive DCIS associated with invasive breast disease (n=9/9).

1. p-values < 0.05;
2. A gene list is mapped from 43 genomic regions found on chromosomes 1, 3, 5, 6, 7, 10, 11, 16, 17, 18, 19, 20;
3. These regions encompass 283 genes altered in both ER positive pure DCIS and ER positive DCIS associated with invasive breast disease;

Genes:

5S_rRNA 7SK AC005220.3 AC006076.1 AC006486.1 AC007431.1 AC007431.2 AC009362.2 AC013434.1 AC016831.7 AC018642.1 AC018816.3 AC058791.1 AC058791.2 AC090625.1 AC090821.2 AC090821.3 AC090821.4 AC090821.5 AC090955.3 AC103706.1 ACAP3 ADIG AGRN AL021394.1 AL021578.1 AL096828.1 AL109823.2 AL109840.1 AL118506.1 AL118506.3 AL121673.1 AL121673.2 AL121827.1 AL133330.1 AL136532.1 AL139348.1 AL162505.1 AL365229.1 AL390719.1 AL669831.3 AL713922.2 ARF4P2 ARFGAP1 ARFRP1 ARL6IP1 ATP5E AURKAIP1 B3GALT6 BCAS1 BCAS4 BCL2 BCL2L1 BHLHE23 BIRC7 C1orf159 C1orf170 C20orf11 C20orf135 C20orf166 C20orf181 C20orf195 C20orf20 C20orf200 C20orf83 C20orf90 CANT1 CBFA2T2 CD44 CDH4 CHRNA4 CIC COL20A1 COL9A3 COX4I2 CPSF3L CST3 CTD-3184A7.4 CTSZ DBNDD2 DENND3 DIDO1 DIP2C DNAJC5 DPH3B DVL1 EDN3 EEF1A2 EGOT ERF F3 FAM132A FAM41C FAM65C GATA5 GLTPD1 GMEB2 GNAS GNASAS GPR20 GSK3A HAR1A HAR1B HAR1F HES4 HM13 hsa-mir-1-1 hsa-mir-124-3 hsa-mir-133a-2 hsa-mir-1914 hsa-mir-200a hsa-mir-200b hsa-mir-296 hsa-mir-298 hsa-mir-429 hsa-mir-647 hsa-mir-941-1 hsa-mir-941-3 hsa-mir-941-4 ID1 IL9RP2 ISG15 ITPR1 KCND2 KCNQ2 KDSR KIAA0406 KLHL17 LGALS3BP LIME1 MKLN1 MRPS16P MSI2 MXRA8 NCOA3 NCRNA00029 NKAIN4 NOC2L NTSR1 NXT1 OGFR OSMR PAFAH1B3 PARD6B PDHX PHACTR3 PIGT PLEKHN1 PPDPF PRPF6 PTK6 PUSL1 RALGAPB RBPJL RICTOR RP11-164D18.2 RP11-206L10.13 RP11-243J16.7 RP11-261N11.8 RP11-305P22.5 RP11-358D14.2 RP11-429E11.2 RP11-429E11.3 RP11-465B22.3 RP11-465B22.5 RP11-465B22.6 RP11-54O7.1 RP11-54O7.10 RP11-54O7.11 RP11-54O7.14 RP11-54O7.2 RP11-54O7.3 RP11-631M21.1 RP11-631M21.2 RP11-631M21.6 RP11-86H7.6 RP11-93B14.4 RP11-93B14.5 RP11-93B14.6 RP1-1J6.2 RP1-290I10.2 RP1-290I10.3 RP1-290I10.6 RP1-290I10.7 RP1-290I10.8 RP1-309F20.2 RP1-309F20.3 RP13-30A9.1 RP13-30A9.2 RP3-322G13.7 RP3-324O17.2 RP3-324O17.4 RP3-324O17.5 RP3-453C12.8 RP3-461P17.10 RP4-530I15.6 RP4-543J19.8 RP4-564F22.2 RP4-564F22.5 RP4-583P15.10 RP4-583P15.11 RP4-614C15.2 RP4-614C15.3 RP4-697K14.12 RP4-697K14.3 RP4-697K14.7 RP4-719C8.1 RP4-724E16.2 RP4-797C5.2 RP4-806M20.2 RP5-1049G16.4 RP5-1100H13.3 RP5-827L5.1 RP5-827L5.2 RP5-885L7.10 RP5-885L7.11 RP5-890O3.3 RP5-890O3.9 RP5-902P8.10 RP5-963E22.4 RPL7P3 RPRD1B RPS3P2 RTEL1 SAMD10 SAMD11 SCNN1D SDC4 SDF4 SFRS1 SLC17A9 SLC1A2 SLC2A4RG SLC45A4 SLCO4A1 SLMO2 SMG1 SNHG11 SNORA40 SNORA71 SNORA71A SNORA71B snoU13 SNTA1 SRMS ST3GAL1 STMN3 SULF2 SUMO1P1 SYCP2 SYS1 TAF4 TAS1R3 TCFL5 TFAP2A TGM2 TH1L TMSL6 TNFRSF18 TNFRSF4

TNFRSF6B TOP1 TP53TG5 TPD52L2 TPX2 TSPAN12 TTLL10 TUBB1 U1 U6 U7
UBE2J2 UCKL1 VSTM2L WFDC2 Y_RNA YTHDF1 ZBTB46 ZGPAT ZMYND11 ZNF217
ZNF512B ZNF831

PANTHER analysis: 131 mapped ids are found, 152 mapped ids are not found.

There were gains present in ER positive DCIS associated with invasive breast disease (n=5/9) not observed in ER positive pure DCIS (n=0/8).

1. p-values < 0.05
2. A gene list is mapped from 35 genomic regions found on chromosomes 1, 2, 4, 5, 6, 7, 9, 11, 12, 14, 18, 19, 20, 22;
3. These regions encompass 147 genes altered in ER positive DCIS associated with invasive breast disease;

Genes:

5S_rRNA 7SK AC000032.1 AC010442.1 AC012305.1 AC022724.2 AC026740.1 AC027097.1 AC064834.2 AC064834.3
AC064834.4 AC091609.1 AGAP1 AHRR AIM1 AL031963.1 AL031963.2 AL031963.3 AL031963.5 AL109754.1
AL117692.1 AL117692.2 AL133351.1 AL136164.1 AL139092.1 AL161626.1 AL356735.1 AMIGO1 AMPD2 ANKRD5
AP000769.1 AP000944.1 AP002478.2 AP002478.4 ATG5 ATP5F1 ATP8B1 ATXN7L2 BPHL C14orf182
C14orf183 C5orf55 C6orf155 C6orf195 CCDC127 CELSR2 CEP72 CTD-2083E4.4 CTD-2083E4.5
CTD-2083E4.6 CTD-2228K2.1 CTD-2228K2.2 CTD-2228K2.5 CTD-2231H16.1
CTD-2589H19.4 CYB561D1 DLGAP1 ETS1 EXOC3 FAM136B FRMD8 GCNT1 GNAI3
GNAT2 GPR61 GSK3A GSTM2 GSTM3 GSTM4 GSTM5 hsa-mir-197 hsa-mir-30a hsa-mir-30c-2
hsa-mir-612 KDSR LRRC14B MYBPHL MYLK4 NQO2 OGFRL1 OVGP1 PDCD6 PLEKHG4B
PRDM1 PRUNE2 PSMA5 PSRC1 RIPK1 RP11-101C11.1 RP11-109I2.3 RP11-145H9.3
RP11-154D6.1 RP11-214N16.2 RP11-218C14.5 RP11-310P5.1 RP11-310P5.2
RP11-404H14.1 RP11-416N4.1 RP11-416N4.4 RP11-420G6.3 RP11-420G6.4
RP11-422N19.3 RP11-552M11.2 RP11-552M11.4 RP11-58E21.1 RP11-66C24.1
RP11-811I15.1 RP11-94F13.1 RP1-40E16.11 RP1-40E16.2 RP1-40E16.3 RP1-40E16.4 RP1-40E16.8 RP1-40E16.9 RP1-90J20.10 RP1-90J20.2 RP1-90J20.7 RP1-90J20.8 RP3-331H24.4 RP4-630J13.1 RP4-735C1.4 RP5-1160K1.1 RP5-1160K1.3 RP5-1160K1.6
RP5-839B4.7 RP5-839B4.8 RSL24D1P11 SDHA SERPINB1 SERPINB6 SERPINB9
SLC39A10 SLC9A3 SNAP25 SORT1 SYPL2 TPPP TUBB2A U6 USP24 WDR77 WI2-80423F1.1 WRNIP1 Y_RNA ZDHHC11 ZDHHC11B ZFYVE28

5.8.4.4 Genomic Sc Gains in Oestrogen Receptor Positive Pure DCIS Compared to Oestrogen Receptor Positive DCIS Associated with Invasive Breast Disease

There were Sc gains present in ER positive pure DCIS (n=4/8) not observed in any ER positive DCIS associated with invasive breast disease (n=0/9) in this series.

1. p-values < 0.05;
2. A gene list is mapped from 6 genomic regions found on chromosomes 1, 8;
3. These regions encompass 16 genes altered in ER positive pure DCIS;

Genes:

AC018442.1 AC023933.1 AL590138.1 CD244 CSMD3 F11R hsa-mir-151 ITLN1 ITLN2 PLXNA2 PTK2 RP11-312J18.5 RP11-312J18.6 RP11-312J18.7 RP11-544M22.1 VPS13B

PANTHER analysis: 8 mapped ids are found, 8 mapped ids are not found.

There were Sc gains present in ER positive DCIS associated with invasive breast disease (n=6/9) not observed in ER positive pure DCIS (n=0/8).

1. p-values < 0.05;
2. A gene list is mapped from 23 genomic regions found on chromosomes 1, 2, 11, 12, 17, 19, 20;
3. These regions encompass 143 genes altered in ER positive DCIS associated with invasive breast disease;

Genes:

ABCC3 AC005220.3 AC007431.1 AC012305.1 AC091062.2 AC092066.6 ACAP3 AGAP1 AGRN AL049736.1 AL109754.1 AL109840.1 AL136532.1 AL139348.1 AL365229.1 AL390719.1 AL669831.3 ANKRD5 ATP5E AURKAIP1 B3GALT6 BCAS1 BCAS4 BCL3 C17orf73 C1orf159 C1orf170 C20orf177 C20orf83 CBLC CDH26 CDH4 CPSF3L CTB-22K21.2 CTSZ CYP24A1 DOK5 DVL1 FAM132A FAM41C FAM65C GLTPD1 GNAS HES4 HOXB3 HOXB4 HOXB5 hsa-mir-10a hsa-mir-200a hsa-mir-200b hsa-mir-429 ISG15 KLHL17 LUC7L3 MRPS16P MSI2 MXRA8 NOC2L NXT1 PARD6B PFDN4 PHACTR3 PLEKHN1 PPP1R3D PTPRT PUSL1 RNFT1 RP11-164D18.2 RP11-206L10.13 RP11-294J22.5 RP11-357H14.7 RP11-416N4.1 RP11-416N4.4 RP11-429E11.2 RP11-429E11.3 RP11-465B22.3 RP11-465B22.5 RP11-465B22.6 RP11-506D12.1 RP11-506D12.3 RP11-54O7.1 RP11-54O7.10 RP11-54O7.11 RP11-54O7.14 RP11-54O7.2 RP11-54O7.3 RP11-700H6.1 RP11-700H6.2 RP1-232N11.2 RP1-309F20.2 RP1-309F20.3 RP3-322G13.7 RP4-530I15.6 RP4-543J19.8 RP4-583K8.1 RP4-614C15.2 RP4-614C15.3 RP4-715N11.2 RP4-719C8.1 RP4-723E3.1 RP4-724E16.2 RP4-730D4.1 RP5-1022J11.1 RP5-1022J11.2 RP5-1030M6.2 RP5-1073F15.1 RP5-827L5.1 RP5-827L5.2 RP5-839B4.7 RP5-839B4.8

RP5-890O3.3 RP5-890O3.9 RP5-902P8.10 RPL12P4 RPS6KB1 SAMD11 SCNN1D
SDF4 SLC39A11 SLMO2 SNAP25 SNORA70 snoZ6 SYCP2 TAS1R3 TH1L TMSL6
TNFRSF18 TNFRSF4 TOB1 TTLL10 TUBB1 U4atac U6 U7 UBE2J2 WFIKKN2
Y_RNA ZFP64 ZNF217 ZNF831

PANTHER analysis: 62 mapped ids are found, 79 mapped ids are not found.

5.8.4.5 Losses in Oestrogen Receptor Positive Pure DCIS Compared to Oestrogen Receptor Positive DCIS Associated with Invasive Breast Disease

There is some overlap in the losses found in ER positive pure DCIS (n=5/8) compared to ER positive DCIS associated with invasive breast disease (n=1/9). DCIS.

1. p-values < 0.05;
2. A gene list is mapped from 35 genomic regions found on chromosomes 3, 9, 11;
3. These regions encompass 510 genes altered in ER positive pure DCIS;

Genes:

5S_rRNA 7SK ABCG4 AC015689.1 AC019227.1 AC019227.2 AC025029.1 AC087441.1 AC090587.2 AC090587.4
AC090587.5 AC090804.1 AC108448.2 AC108448.3 AC109309.4 AC132217.4 ACA59 ACAD8 ADAMTS15 ADAMTS8
AMICA1 AMOTL1 ANKK1 ANKRD42 ANKRD49 AP000560.1 AP000619.1 AP000620.1 AP000620.2 AP000642.1
AP000654.1 AP000654.2 AP000757.1 AP000767.1 AP000769.1 AP000787.1 AP000797.1 AP000797.2 AP000843.2 AP000844.1
AP000866.1 AP000866.2 AP000873.1 AP000880.1 AP000892.4 AP000907.1 AP000907.2 AP000907.3 AP000908.1 AP000911.1
AP000925.2 AP000936.1 AP000936.3 AP000936.4 AP000936.5 AP000944.1 AP001007.1 AP001007.3 AP001122.1 AP001267.1
AP001267.2 AP001528.1 AP001582.1 AP001767.1 AP001781.1 AP001830.1 AP001891.1 AP001922.1 AP001972.1 AP001979.1
AP001992.2 AP001999.1 AP002364.1 AP002364.2 AP002380.1 AP002380.2 AP002451.1 AP002754.1 AP002783.1 AP002783.2
AP002783.3 AP002783.4 AP002783.5 AP002783.6 AP002802.1 AP002884.4 AP002886.2 AP002956.4 AP002962.1 AP002986.1
AP002991.1 AP003025.2 AP003039.3 AP003039.4 AP003041.1 AP003070.1 AP003072.1 AP003122.1 AP003175.1 AP003304.2
AP003392.1 AP003392.3 AP003402.1 AP003402.2 AP003461.1 AP003461.10 AP003461.11 AP003461.2
AP003461.3 AP003461.4 AP003461.5 AP003461.6 AP003461.7 AP003461.8 AP003461.9 AP003499.3 AP003500.1 AP003774.4
AP003774.5 AP003774.7 AP003780.2 AP003781.1 AP003971.1 AP004242.1 AP004242.2 AP004248.4 AP004372.1 AP004607.1
AP004607.2 AP004607.3 AP004609.2 AP004609.4 AP005273.1 AP005435.1 AP005597.1 AP005638.1 AP005638.3 AP005718.1
AP005814.1 AP006216.10 AP006216.11 AP006216.12 AP006216.5 AP006288.1 APLP2 APOA1
APOA4 APOA5 APOC3 ARCN1 ARHGAP32 ARHGAP42 ARHGEF12 ARHGEF17 ARRB1 ATM
ATP5L B3GAT1 BACE1 BARX2 BCL9L BCO2 BEST1 BIRC2 BIRC3 BTG4 BUD13
C11orf1 C11orf10 C11orf2 C11orf30 C11orf36 C11orf45 C11orf52 C11orf53 C11orf54 C11orf57
C11orf61 C11orf63 C11orf65 C11orf66 C11orf71 C11orf75 C11orf82 C11orf84 C11orf88 C11orf9
C11orf90 C11orf92 C11orf93 CADM1 CAPN1 CARS CBL CCDC15 CCDC153 CCDC67
CCDC82 CCDC83 CCDC84 CCDC89 CCDC90B CD3D CD3E CD3G CDC42EP2 CEP164 CEP57
CHEK1 CHORDC1 CHRM1 CLDN25 CNTN5 CREBZF CRTAM CRYAB CTSC CUL5 CWC15
CXCR5 DAGLA DCUN1D5 DDI1 DDX25 DDX6 DGAT2 DIXDC1 DLAT DLG2
DPF2 DRD2 DSCAML1 DYNC2H1 EI24 EIF3F ENDOD1 ESAM ETS1 EXPH5
FADS1 FADS2 FADS3 FAM168A FAM181B FAM55A FAM55B FAM55D FAM76B FAU
FCHSD2 FDX1 FDXACB1 FEN1 FLI1 FOLH1B FOLR4 FOXR1 FRMD8 FTH1 FUT4

FXYD2 FXYD6 FZD4 GBE1 GLB1L2 GLB1L3 GPR83 GUCY1A2 HEPACAM HEPN1
HRASLS5 hsa-mir-1304 hsa-mir-1908 hsa-mir-34b hsa-mir-34c hsa-mir-483 hsa-mir-548l hsa-mir-611 hsa-mir-612 HSPB2 HTR3A
HTR3B HYLS1 IFT46 IGF2 IGF2AS IGSF9B IL10RA IL18 INS JAM3 JRKL
KCNJ1 KCNJ5 KDELC2 KDM4D KDM4DL KIAA1731 LAYN LRRC10B MALAT1 MAML2
MAP6 MARK2 ME3 MED17 MLL MMP1 MMP10 MMP12 MMP13 MMP20 MMP27
MMP3 MMP7 MMP8 MOGAT2 MPZL2 MPZL3 MRE11A MRGPRE MRGPRG MRPL49
MTMR2 MYLKP1 NAALAD2 NCAM1 NCAPD3 NCRNA00167 NEU3 NFRKB NLRX1 NNMT
NOX4 NPAT NRGN NUP98 OPCML OR10V1 OR2AT2P OR2AT4 OR4A15 OR4A16
OR55B1P OR8A1 OR8B12 OR8B9P OSBP OSBPL5 P2RY2 P2RY6 PAFAH1B2 PANX3 PATL1
PCF11 PCSK7 PDGFD PDZD3 PGAP2 PGR PHLDB1 PICALM PIH1D2 PIWIL4
PKNOX2 POLA2 POU2AF1 PPIHP1 PPP2R1B PRCP PRDM10 PTPRD PUS3 RAB30
RAB38 RAB39 RAB3IL1 RBM7 RDX RELT REXO2 RHOG RNF169 RNF214
ROBO3 ROBO4 RP11-142L1.1 RP11-142L1.2 RP11-142L1.3 RP11-147I3.1 RP11-160H12.1
RP11-237N19.1 RP11-358N4.2 RP11-359D24.1 RP11-399J13.1 RP11-438N5.1
RP11-447G14.1 RP11-567M21.1 RP11-657K20.1 RP11-659G9.1 RP11-667M19.1
RP11-690D19.1 RP11-727A23.1 RP11-742N3.1 RP11-810P12.1 RP11-832N8.1
RP11-861M13.1 RP11-864G5.1 RP11-959F10.1 RPL23AP64 RPL37AP8 RPLP0P2 RRM1
SCARNA11 SCN2B SCN4B SDHD SESN3 SFRS2B SIAE SIDT2 SIK2 SIK3 SLC22A10
SLC22A20 SLC22A24 SLC22A25 SLC22A9 SLC25A45 SLC35F2 SLC36A4 SLC37A2 SLCO2B1 SNORA1
SNORA18 SNORA25 SNORA32 SNORA40 SNORA7 SNORA70 SNORA8 SNORD112 SNORD5 SNORD56
snoU13 snoU2_19 snoU2-30 snoZ40 SORL1 SPA17 SPATA19 SPCS2 SPDYC ST14 STIM1
STT3A SYT7 SYTL2 SYVN1 TAF1D TAGLN TBRG1 TEX12 THYN1 TIGD3
TIMM8B TM7SF2 TMEM123 TMEM126A TMEM126B TMEM135 TMEM136 TMEM218 TMEM25 TMEM45B
TMPRSS13 TMPRSS4 TMPRSS5 TP53AIP1 TREH TRIM48 TRIM49 TRIM49L TRIM53 TRIM53B
TRIM64 TRIM64B TRIM77 TTC12 TTC36 U2 U6 U7 UBASH3B UBE4A UBTFL2
UBTFL3 UPK2 USP28 UVRAG VPS26B VSIG2 XRRA1 Y_RNA ZBTB16 ZBTB44
ZC3H12C ZNF259 ZNHIT2 ZW10

PANTHER analysis: 286 mapped ids are found, 224 mapped ids are not found.

There were losses present in ER positive DCIS associated with invasive breast disease (n=6/9) not observed in ER positive pure DCIS (n=0/8).

1. p-values < 0.05;
2. A gene list is mapped from 56 genomic regions found on chromosomes 5, 8, 10, 16, 19, X;
3. These regions encompass 149 genes altered in ER positive DCIS associated with invasive breast disease;

Genes: 5S_rRNA AC002366.3 AC003666.1 AC009055.1 AC009110.1 AC009120.1 AC009161.1 AC010546.1 AC018558.1 AC022164.1
AC023824.2 AC025287.1 AC025287.2 AC025287.3 AC025287.4 AC069278.1 AC073493.1 AC073493.2 AC073493.3 AC135776.1
ADAM3A ADAM5P AGTR2 AKR1B1P8 AL035443.1 AL133512.1 AL353698.1 AL591398.1 AMELX ANKRD26P1
ARHGAP6 ARHGEF9 ASPDH BMP15 BX119964.1 BX119964.2 BX119964.3 BX119964.4 C5orf50 CCNYL3 CDH11
CDH8 CLCN4 CTD-2503H21.1 CXorf29 DHRSX DMD EFHC2 EIF2S3 FAAH2 FAM48B2 FDPSL5

FMR1 FMR1NB FRMPD4 GPR112 GPR64 GS1-256O22.1 GS1-256O22.5 GS1-466O4.2 GS1-466O4.3 GS1-466O4.5 GS1-541M1.2 JOSD2 KLF8 L29074.1 L29074.2 L29074.3 L29074.5 LRRC4B MAGEB18 MAGEB5 MAGEB6 MAGEB6B MAGED4 MAGEE1 MAP3K7IP3 NRG3 PSMD7 RP11-104D21.1 RP11-104D21.2 RP11-104D21.3 RP11-121C22.1 RP11-156J23.1 RP11-1A15.2 RP11-357C3.2 RP11-357C3.3 RP11-363G10.2 RP1-137H15.2 RP1-138A5.1 RP11-38O23.3 RP11-38O23.4 RP11-38O23.5 RP11-38O23.7 RP11-3D23.1 RP11-434J24.2 RP11-467P22.4 RP11-479I1.4 RP11-517D11.3 RP11-54I5.1 RP11-552E4.2 RP11-617O8.1 RP11-637B23.1 RP11-637B23.3 RP11-702C7.1 RP11-702C7.2 RP11-761E20.1 RP11-81C12.1 RP11-93B10.3 RP1-20J23.1 RP1-267M5.1 RP1-267M5.2 RP1-290C9.2 RP13-188A5.1 RP13-346H10.2 RP13-348B13.1 RP13-348B13.2 RP13-34C21.1 RP13-60P5.2 RP1-54B20.7 RP3-433G13.1 RP4-551E13.2 RP5-1145L23.2 RP5-849L7.1 RP6-1O2.1 SHROOM4 SLITRK4 SNORA11 SNORA68 snoU13 SPACA5B SPANXN3 SPIN4 SSX5 SSX6 U40455.1 U6 VENTXP1 WWOX Y_RNA Z98304.1 ZFP112 ZFRP1 ZFX ZIC3 ZNF180 ZNF229 ZNF285

PANTHER analysis: 42 mapped ids are found, 106 mapped ids are not found.

5.8.4.6 Total Loss in Oestrogen Receptor Positive Pure DCIS Compared to Oestrogen Receptor Positive DCIS Associated with Invasive Breast Disease

There were total losses present in ER positive pure DCIS (n=5/8) not observed in ER positive DCIS associated with invasive breast disease (n=0/9).

1. p-values < 0.05;
2. A gene list is mapped from 13 genomic regions found on chromosomes 9, 11, 13, 15, 19;
3. These regions encompass 25 genes altered in for ER positive pure DCIS;

Genes:

7SK AC025678.1 AC027139.2 AC027139.3 AP000720.1 AP001482.1 AP003072.1 CCDC67 CTSC GOLGA8B GRM5 hsa-mir-1233 KDM4C LPAR6 NOX4 OR10V1 OSBP PATL1 RB1 RP11-657K20.1 SLC36A4 TYR U7 ZNF208 ZNF257

PANTHER analysis: 15 mapped ids are found, 10 mapped ids are not found.

There were total losses present in ER positive DCIS associated with invasive breast disease (n= 9/9) not observed in ER positive pure DCIS (n=0/8).

1. p-values < 0.05;
2. A gene list is mapped from 91 genomic regions found on chromosomes 11, 13, 16, 17, X;

3. These regions encompass genes altered in ER positive DCIS associated with invasive breast disease;

Genes:

5S_rRNA 7SK ABCC12 ABR AC000003.1 AC002347.1 AC002347.2 AC002366.3 AC003658.1 AC004070.1
AC004478.2 AC005277.1 AC005284.1 AC005323.1 AC005358.1 AC005358.3 AC005548.1 AC005548.2 AC005696.2 AC005696.3
AC005725.1 AC006435.1 AC007225.1 AC007339.1 AC009053.1 AC009110.1 AC009120.1 AC009120.3 AC009161.1 AC010546.1
AC015799.1 AC015799.2 AC015908.2 AC016292.1 AC016292.3 AC025287.1 AC025287.2 AC025287.3 AC025287.4 AC025518.1
AC027045.1 AC027763.1 AC027763.2 AC032044.1 AC055839.2 AC073493.1 AC073493.2 AC073493.3 AC087498.1 AC087501.1
AC087742.1 AC087742.2 AC090282.1 AC090617.1 AC091153.4 AC097370.1 AC099508.1 AC099684.1 AC100748.2 AC104581.1
AC109599.1 AC116914.1 AC118754.2 AC118754.4 AC127521.1 AC130343.2 AC130689.5 AC135178.7 ACA64 ADAT1
AIPL1 AL136160.1 AL355852.1 AL390738.2 AL450226.1 AL450226.2 AL589987.1 ALOX12 ALOX15 AMAC1L3
AMELX ANKFY1 ANKRD26P1 AP001970.1 ARHGAP6 ARHGEF15 ARHGEF9 ARRB2 ASB12 ASGR1 ASGR2
ASMT ASPA ATP2A3 ATP5EP2 BCAR1 BCL6B BHLHA9 BMP15 BRWD3 BX004827.1 BX649443.1
C13orf36 C16orf78 C16orf87 C17orf100 C17orf44 C17orf48 C17orf49 C17orf68 C17orf85 C17orf91
CAMKK1 CBLN1 CCDC42 CDH13 CDH8 CFDP1 CHD3 CHRNB1 CHST5 CHST6
CLEC10A CLEC18B CRK CRLF2 CTD-2503H21.1 CTD-2545G14.1 CTNS CTRB1 -CTRB2
CYB5D1 CYB5D2 DDX26B DHRS7C DHRSX DLG4 DNAH2 DNAH9 DNAJA2 DPH1 EEF1AL1
EIF4A1P10 ERN2 FA2H FAM123B FAM46D FAM64A FANCB FBXO39 FRMPD4 GABARAPL2 GAPDHP34
GAS7 GGT6 GLG1 GLP2R GLRA2 GPT2 GS1-466O4.2 GS1-466O4.3 GS1-466O4.5
GS1-541M1.1 GS1-541M1.2 GSG2 GTPBP6 HCCS HDHD1A HIC1 HK2P1
HMGA1L1 hsa-mir-1253 hsa-mir-132 hsa-mir-1468 hsa-mir-195 hsa-mir-212 hsa-mir-22 hsa-mir-497 INPP5K ITGAE KARS
KDM6B KIAA0664 KIAA0753 KRBA2 LDHD LL0YNC03-3F3.1 LSMD1 MAGEB18 MAGEB5 MAGEB6
MAGEB6B MAGED1 MAGED4 MAGED4B MAGEE1 MAP2K4 MED31 METT10D MFSD6L MLKL MNT
MTMR8 MTUS2 MYBBP1A MYH1 MYH10 MYH13 MYH2 MYH3 MYH4 MYH8
MYLK3 MYO1C MYOCD NCRNA00086 NCRNA00107 NCRNA00108 NDEL1 NETO2
NPIPL2 NTN1 NXN ODF4 OR1A1 OR1A2 OR1D2 OR1D5 OR1E1 OR1E2 OR1G1
OR3A1 OR3A2 OR3A3 OR3A4 ORC6L OVCA2 P2RX1 P2RX5 P2RY8 PAFAH1B1 PAN3
PCDH11X PDX1 PELP1 PFAS PHKB PIK3R5 PIK3R6 PIRT PITPNA PITPNM3
PLCXD1 PLK1 POLR2A PPP2R3B PRPF8 PRPSAP2 PSMD7 RAB43P1 RANGRF RAP1GAP2
RCVRN RFWD3 RILP RNASEK RNF222 RP1-107N3.1 RP1-107N3.2 RP11-114H20.1
RP11-120D5.1 RP11-145B3.2 RP11-151A2.2 RP11-16L6.3 RP11-197L7.2 RP11-217H19.1
RP11-234P3.2 RP11-234P3.3 RP11-234P3.4 RP11-234P3.5 RP11-265D19.5 RP11-265D19.6
RP11-284B18.3 RP11-2N21.2 RP11-309M23.1 RP11-309M23.2 RP11-311P8.1 RP11-311P8.2
RP11-314A20.1 RP11-314A20.2 RP11-325E14.1 RP11-325E14.2 RP11-325E14.5 RP11-331F4.1
RP11-331F4.4 RP11-33N11.1 RP11-342C20.3 RP11-344N17.11 RP11-344N17.2 RP11-344N17.3
RP11-344N17.6 RP11-344N17.7 RP11-344N17.8 RP11-357C3.2 RP11-357C3.3
RP11-360A9.1 RP11-363G10.2 RP11-364B14.1 RP11-364B14.2 RP11-364B14.3
RP11-403E24.1 RP11-432N13.2 RP11-432N13.3 RP11-459A10.1 RP11-459A10.2
RP11-459A10.3 RP11-462C21.1 RP11-471M2.1 RP11-471M2.2 RP11-481F23.1
RP11-483M24.2 RP11-48B14.1 RP11-51C14.1 RP11-51C14.2 RP11-520F9.2
RP11-552E4.3 RP11-552E4.4 RP11-552E4.5 RP11-565F19.1 RP11-572F4.1 RP11-609D21.1
RP11-617O8.1 RP11-637B23.1 RP11-637B23.3 RP11-647I17.1 RP11-702C7.1
RP11-702C7.2 RP11-713H12.1 RP11-93B10.3 RP11-963H4.1 RP11-963H4.2 RP1-279N11.1 RP13-210D15.1 RP13-210D15.4 RP13-210D15.6 RP13-297E16.3 RP13-297E16.4
RP13-297E16.5 RP13-34C21.1 RP13-465B17.2 RP13-465B17.3 RP13-565O16.2
RP13-60P5.2 RP13-858C7.1 RP13-926M18.1 RP3-428A13.1 RP4-710L4.1 RPA1
RPL26 RTN4RL1 SCARF1 SCARNA21 SCO1 SERPINF1 SERPINF2 SFRS17A SGSM2 SHCBP1

SHISA6 SHOX SHPK SHROOM4 SLC13A5 SLC16A11 SLC16A13 SLC25A35 SLC43A2 SLITRK5 SMG6 SMTNL2 SMYD4 SNORA11 SNORA69 SNORA76 SNORD91 snoU13 SOX3 SPATA22 SPDYE4 SPIN4 SPNS2 SPNS3 SRR SSX1 SSX3 SSX9 STX8 TAX1BP3 TBX22 TEKT1 TERF2IP TIMM22 TLCD2 TMEM170A TMEM220 TMEM231 TMEM88 TMEM93 TNFSF12 TNFSF12-TNFSF13 TNFSF13 TRPV1 TRPV3 TSR1 TUSC5 TXNDC17 U1 U6 U7 U70984.1 U8 UBE2G1 UPRT USP43 VAT1L VENTXP1 VPS35 WDR16 WDR59 WDR81 WSCD1 XAF1 Y_RNA YWHAE ZBTB4 ZDHHC15 ZFP1 ZNF423 ZNF449 ZNF75D ZNRF1 ZZEF1

PANTHER analysis: 219 mapped ids are found, 223 mapped ids are not found.

5.8.4.7 CdLOH in Oestrogen Receptor Positive Pure DCIS Compared to Oestrogen Receptor Positive DCIS Associated with Invasive Breast Disease

There is CdLOH present in ER positive pure DCIS (n=6/8) not observed in any ER positive DCIS associated with invasive breast disease (n=0/9).

1. p-values < 0.05;
2. A gene list is mapped from 54 genomic regions found on chromosomes 3, 9, 11;
3. These regions encompass 333 genes altered in ER positive pure DCIS;

Genes:

5S_rRNA ABCG4 AC015689.1 AC025029.1 AC087441.1 AC090587.2 AC090587.4 AC090587.5 AC090804.1 AC108448.2 AC108448.3 AC109309.4 AC132217.4 AC133041.1 ACAD8 AMOTL1 ANKRD42 ANKRD49 AP000438.1 AP000560.1 AP000619.1 AP000620.1 AP000620.2 AP000642.1 AP000654.1 AP000654.2 AP000767.1 AP000769.1 AP000787.1 AP000873.1 AP000911.1 AP000944.1 AP001267.1 AP001267.2 AP001528.1 AP001767.1 AP001922.1 AP001972.1 AP001979.1 AP001992.2 AP001999.1 AP002364.1 AP002364.2 AP002380.1 AP002380.2 AP002754.1 AP002783.1 AP002783.2 AP002783.3 AP002783.4 AP002783.5 AP002783.6 AP002802.1 AP002956.4 AP002991.1 AP003122.1 AP003175.1 AP003304.2 AP003392.1 AP003392.3 AP003461.1 AP003461.10 AP003461.11 AP003461.4 AP003461.5 AP003461.7 AP003499.3 AP003774.4 AP003774.5 AP003774.7 AP003780.2 AP003781.1 AP003971.1 AP004242.1 AP004242.2 AP004607.1 AP004607.2 AP004607.3 AP004609.2 AP004609.4 AP005273.1 AP005435.1 AP005718.1 AP005814.1 AP006288.1 ARCN1 ARHGAP42 ARHGEF12 ARHGEF17 ARRB1 ATM ATP5L B3GAT1 BCL9L BEST1 BIRC2 BIRC3 C11orf10 C11orf2 C11orf30 C11orf36 C11orf54 C11orf65 C11orf66 C11orf75 C11orf82 C11orf84 C11orf9 C11orf90 CADM1 CAPN1 CARS CBL CCDC153 CCDC67 CCDC82 CCDC83 CCDC84 CCDC89 CCDC90B CD3G CDC42EP2 CEP57 CHORDC1 CHRM1 CNTN5 CREBZF CTD-2026G6.1 CTD-2026G6.2 CWC15 CXCR5 DAGLA DCUN1D5 DDI1 DDX6 DGAT2 DLG2 DPF2 DYNC2H1 EIF3F ENDOD1 EXPH5 FADS1 FADS2 FADS3 FAM168A FAM181B FAM76B FAM86D FAU FCHSD2 FEN1 FOLH1B FOLR4 FOXR1 FRMD8 FTH1 FUT4 FZD4 GBE1 GLB1L2 GLB1L3 GPR83 GUCY1A2 HRASLS5 hsa-mir-1304 hsa-mir-1324 hsa-mir-1908 hsa-mir-483 hsa-mir-548l hsa-mir-611 hsa-mir-612 IFT46 IGF2 IGF2AS IGSF9B INS JAM3 JRKL KDELC2 KDM4D KDM4DL KIAA1731 LRRC10B MALAT1 MAML2 MAP6 MARK2 ME3 MED17 MLL MMP1 MMP10 MMP12 MMP13 MMP20 MMP27 MMP3 MMP7 MMP8 MOGAT2 MRE11A MRGPRE MRGPRG MRPL49 MTMR2 MYLKP1 NAALAD2 NCAPD3 NEU3 NLRX1 NOX4 NPAT NUP98 OR2AT2P OR2AT4 OR55B1P OSBPL5 P2RY2 P2RY6 PCF11 PDGFD PDZD3 PGAP2 PGR PHLDB1 PICALM PIWIL4 POLA2 PRCP PTPRD RAB30 RAB38 RAB3IL1 RELT RHOG RNF169 RP11-142L1.1 RP11-142L1.2 RP11-142L1.3 RP11-147I3.1 RP11-160H12.1 RP11-241K7.1 RP11-241K7.2 RP11-358N4.2 RP11-359D24.1 RP11-399J13.1 RP11-413E6.1 RP11-413E6.2

RP11-413E6.3 RP11-438N5.1 RP11-447G14.1 RP11-642N14.3 RP11-659G9.1
RP11-690D19.1 RP11-727A23.1 RP11-742N3.1 RP11-803B1.1 RP11-803B1.2
RP11-803B1.3 RP11-803B1.4 RP11-803B1.5 RP11-803B1.7 RP11-810P12.1
RP11-861M13.1 RP11-864G5.1 RP11-959F10.1 RPL23AP64 RPLP0P2 RRM1 SESN3
SFRS2B SLC22A10 SLC22A20 SLC22A24 SLC22A25 SLC22A6 SLC22A8 SLC22A9 SLC25A45 SLCO2B1
SNORA1 SNORA18 SNORA25 SNORA32 SNORA40 SNORA7 SNORA70 SNORA8 SNORD112 SNORD5
SNORD56 snoU13 snoU2_19 snoU2-30 snoZ40 SPATA19 SPCS2 SPDYC STIM1 SYT7 SYTL2 SYVN1
TAF1D THYN1 TIGD3 TM7SF2 TMEM123 TMEM126A TMEM126B TMEM135 TMEM136 TMEM25 TREH
TRIM49 TRIM49L TRIM53 TRIM53B TRIM64 TRIM64 TRIM77 TTC36 U2 U6 UBE4A UBTFL2
UBTFL3 UPK2 UVRAG VPS26B XRRA1 Y_RNA ZNHIT2

PANTHER analysis: 167 mapped ids are found, 166 mapped ids are not found.

There is CdLOH found in ER positive DCIS associated with invasive breast disease. (n=8/9) with some overlap in ER positive pure DCIS (n=1/8).

1. p-values < 0.05;
2. A gene list is mapped from 36 genomic regions found on chromosomes 5, 7, 10, 12, 16, 19, X;
3. These regions encompass 61 genes, 2 and 59 genes altered in ER positive DCIS associated with invasive breast disease;

Genes:

AC002519.2 AC005774.2 AC009055.1 AC009120.1 AC018558.1 AC022164.1 AC023824.2 AC025287.2 AC069278.1 AC073057.5
AC135776.1 ARHGEF9 ASPDH BX649443.1 C16orf67 C5orf50 CCNYL3 CDH11 DHRSX EFHC2 EIF2S3
FAM48B2 FDPSL5 FRMPD4 GPR64 JOSD2 LRRC4B MAGED4 NRG3 RP11-114G11.2 RP11-1217F2.15
RP11-133M24.1 RP11-357C3.2 RP11-357C3.3 RP11-363G10.2 RP11-479I1.4
RP11-617O8.1 RP11-93B10.3 RP1-290C9.2 RP13-297E16.4 RP13-297E16.5 RP13-34C21.1
RP13-858C7.1 RP4-551E13.2 SNORA11 SNORA68 SORCS3 SPIN4 U7 VN1R66P Y_RNA
ZFP112 ZFX ZNF180 ZNF229 ZNF285 ZNF716 ZNF720 ZNF720P1

PANTHER analysis: 41 mapped ids are found, 28 mapped ids are not found.

5.8.4.8 CnLOH in Oestrogen Receptor Positive Pure DCIS Compared to Oestrogen Receptor Positive DCIS Associated with Invasive Breast Disease

There is CnLOH present in ER positive pure DCIS (n=8/8) not observed in ER positive DCIS associated with invasive breast disease (n=0/9).

1. p-values < 0.05;

2. A gene list is mapped from 98 genomic regions found on chromosomes 1, 2, 3, 4, 6, 10, 11, 12, 16, 19, 20, 21;
3. These regions encompass 627 genes altered in ER positive pure DCIS;

Genes:

5S_rRNA 7SK ABI3BP ABT1 AC000032.1 AC002485.1 AC004699.1 AC012154.1 AC018809.6 AC021749.1
AC021749.2 AC021749.3 AC022007.1 AC022007.2 AC022007.4 AC022007.5 AC023085.1 AC025423.2 AC027288.1 AC027288.2
AC034102.1 AC034193.5 AC034193.7 AC063962.1 AC073366.1 AC078917.1 AC079598.1 AC079598.2 AC087521.1 AC087521.2
AC087521.3 AC087521.4 AC087521.5 AC093028.1 AC096649.1 AC096649.2 AC096649.3 AC124890.1 AC131263.1 AC131263.2
AC137628.1 AC137834.2 ACCS ACCSL ADAM30 ADAMTS14 ADH5P4 AF254982.1 AF254982.2 AF254982.3
AGAP10 AGAP6 AGAP7 AGAP8 AHCYL1 AL021807.2 AL021808.1 AL021808.2 AL021808.3 AL023913.1
AL031178.1 AL035045.1 AL035456.1 AL035467.1 AL035661.3 AL050321.1 AL050321.2 AL050322.1 AL050335.1 AL050335.2
AL109754.1 AL109922.1 AL118509.1 AL133255.1 AL136164.1 AL138850.1 AL139429.1 AL354680.1 AL354933.1 AL355344.1
AL359752.1 AL391137.2 AL442003.2 AL442003.3 AL450342.1 AL450342.2 AL512288.1 AL512503.1 AL590062.1 AL591034.2
AL591044.1 AL591044.2 AL591044.3 AL591044.4 AL672187.3 AL672187.4 AL713998.1 ALKBH3 ALX3 AMBRA1 ANKRD5
ANKRD52 ANO3 ANXA8L1 AP000302.58 AP000303.1 AP000304.12 AP000304.2 AP001992.2 APOF
ARHGAP1 ARHGAP9 ASAH2 ATF2 ATP5G3 B3GAT2 BANF2 BDNF BDNFOS BMS1P2 BTBD3
BYSL C10orf53 C11orf91 C1orf127 C1orf167 C1orf216 C20orf12 C20orf187 C20orf3 C20orf61
C20orf72 C20orf78 C20orf79 C20orf94 C22orf30 C3orf10 C3orf24 C6orf155 C6orf205 C6orf57
CASP14 CCDC34 CCT2 CD59 CD82 CDK2 CFLP6 CHRM4 CHST1 CIDECP
CLCN6 CLSPN CNPY2 COMTD1 COQ10A CR381653.1 CR381653.2 CR381653.3 CR381670.1 CR381670.2
CR382285.2 CR382287.1 CR392039.1 CR392039.2 CR392039.3 CREB3L1 CRELD1 CRYZL1 CS CSF1
CSRP2BP CST1 CST2 CST3 CST4 CST5 CST7 CSTF3 CSTP1 CSTP2 CTA-215D11.3
CTA-215D11.4 CTSLL7 CYCSP41 DEFB110 DEFB112 DEFB113 DEFB114 DEFB133 DEK DEPDC7
DGKZ DIP2C DNAJC28 DONSON DPCR1 DTNBP1 DUPD1 DUSP13 ELOVL5 ENO1
EPHA6 EPS8L3 ERBB3 ERRFI1 ESYT1 EXT2 EYA3 EYS F2 FAM135A
FAM21A FAM21D FAM25B FAM25D FAM35B2 FAM40A FAM72B FANCD2 FAT1P1 FBXO3
FBXO9 FCGR1B FRS2 FRS3 GART GCLC GCM1 GGTLA4 GLI1 GLUDP8 GMPR
GPR182 GSTM2 GSTM3 GSTM3P GSTM5 GUSBL1 HARBI1 HCG21 HIPK3 HIST1H2AH
HIST1H2BJ HIST1H2BK HIST1H4I HIST2H2BA HIST2H2BB HMGA1L5 HNRNPM hsa-mir-1228 hsa-mir-1252 hsa-mir-129-2
hsa-mir-30a hsa-mir-30c-2 hsa-mir-670 hsa-mir-933 HSD17B12 ICK IFNGR2 IGHV1OR15-5 IKZF4 IL17RC
IL23A INHBC INHBE IRAK2 ITSN1 JAG1 JARID2 KDM1B KHDRBS2 KIAA0319L
KIAA0652 KIAA1274 KIF16B LGR4 LIN28AP3 LIN7C LRP1 LRRC10 MACROD2 Mar02 MDK
MDM2 MED20 MKKS MRPS11P1 MTHFR MYCL1 MYL6 MYL6B MYLIP MYO1A MYST4
NAB2 NCDN NCOA4 NCRNA00240 NDUFA4L2 NEU3 NKX22 NKX2-4 NODAL NOTCH2 NTS
NXPH4 NXT1 OBFC2B OGDHL OGFRL1 OTOR OVOL2 PA2G4 PA2G4P2 PAK7 PAN2
PANK4 PARG PARK7 PGAM3P PGC PHACTR1 PHF21A PIP5K2A PISD PLCH2
PLK1S1 POM121L1P POM121L2 POM121L3P PPIAP13 PPIAP17 PPYR1 PRAM1 PRF1 PRICKLE4 PRPF19
PRRT3 PRSS16 PSMB2 PTMAP3 QSER1 R3HDM2 RAB5B RASSF9 RDH16 RERE
RFX4 RIC8B RIMS1 RNF144B RNF41 RP11-102J14.1 RP11-104F15.7 RP11-109G10.2
RP11-134K13.2 RP11-144G6.10 RP11-144G6.4 RP11-144G6.9 RP11-146I2.1
RP11-154D6.1 RP11-157E14.1 RP11-157E14.3 RP11-159H22.1 RP11-160A9.1 RP11-160A9.2
RP11-185B14.1 RP1-118J21.5 RP11-195M16.1 RP11-209A2.1 RP11-218C14.5 RP11-227D2.3
RP11-239L20.3 RP11-239L20.4 RP11-239L20.5 RP11-244C20.1 RP11-263F15.1
RP11-281P11.1 RP11-292F22.3 RP11-292F22.4 RP11-292F22.5 RP11-298J23.5
RP11-298J23.6 RP1-129L7.1 RP11-307F22.2 RP11-314P12.2 RP11-314P12.3 RP11-324H6.5
RP11-324H6.6 RP11-324H6.7 RP11-348A11.1 RP11-397G17.1 RP11-399K21.2

RP11-399K21.4 RP11-399K21.5 RP11-399K21.6 RP1-13D10.2 RP1-13D10.3 RP1-13D10.4 RP1-13D10.5 RP11-401E14.1 RP11-401E14.2 RP11-416N4.1 RP11-416N4.4 RP11-425L10.1 RP11-431K24.1 RP11-431K24.2 RP11-431K24.3 RP11-431K24.4 RP11-435D7.3 RP11-439A17.10 RP11-439A17.2 RP11-439A17.4 RP11-439A17.5 RP11-439A17.7 RP11-439A17.9 RP11-448N11.1 RP11-448N11.2 RP11-457M11.2 RP11-460I13.5 RP11-460I13.6 RP11-462G2.1 RP11-462G2.2 RP11-466G11.1 RP11-472I20.1 RP11-481A12.2 RP11-481A12.5 RP11-481A12.6 RP11-487I5.4 RP11-506E9.1 RP11-507K13.4 RP11-507K13.6 RP11-526K17.2 RP11-526K21.2 RP11-528A10.1 RP11-528A10.2 RP11-542F9.1 RP11-560J1.1 RP11-56A21.4 RP11-56N19.5 RP11-575L16.2 RP11-587D21.1 RP11-592B15.3 RP11-592B15.4 RP11-592B15.6 RP11-69I22.2 RP11-69I22.3 RP11-707M13.1 RP11-710A11.2 RP11-74E24.2 RP11-77G23.2 RP11-77G23.5 RP11-789A7.1 RP1-190J20.2 RP11-96J19.1 RP11-96J19.2 RP11-96J19.3 RP1-198K11.3 RP1-20N4.1 RP1-240B8.3 RP1-278O22.1 RP1-278O22.2 RP1-27K12.4 RP1-288M22.1 RP1-288M22.2 RP1-298M8.1 RP13-15M17.1 RP13-392I16.1 RP1-34L19.1 RP1-34L19.2 RP1-89D4.1 RP3-322G13.7 RP3-331H24.4 RP3-395M20.2 RP3-395M20.3 RP3-410C9.1 RP3-410C9.2 RP3-477M7.2 RP3-477M7.3 RP3-477M7.4 RP3-483K16.2 RP3-483K16.3 RP3-527G5.1 RP4-564O4.1 RP4-568F9.3 RP4-568F9.6 RP4-568F9.7 RP4-580G13.1 RP4-633I8.1 RP4-633I8.2 RP4-633I8.3 RP4-633I8.4 RP4-697P8.2 RP4-697P8.3 RP4-705D16.3 RP4-717M23.2 RP4-718D20.3 RP4-726N1.2 RP4-728D4.2 RP4-728D4.3 RP4-734C18.1 RP4-735C1.4 RP4-735C1.5 RP4-735C1.6 RP4-737E23.2 RP4-737E23.4 RP4-742J24.2 RP4-777D9.2 RP4-796I8.1 RP5-1018A4.3 RP5-1042I8.6 RP5-1053E7.1 RP5-1053E7.2 RP5-1068E13.3 RP5-1068F16.3 RP5-1069C8.1 RP5-1069C8.2 RP5-1099D15.1 RP5-1100I6.1 RP5-1100I6.2 RP5-1115A15.1 RP5-1177M21.1 RP5-1195D24.1 RP5-839B4.7 RP5-839B4.8 RP5-858B16.5 RP5-860P4.2 RP5-872K7.2 RP5-872K7.7 RP5-905G11.3 RP5-931K24.1 RP5-973N23.4 RP5-983H21.3 RP5-984P4.1 RP5-984P4.4 RPL15P1 RPL23AP6 RPL24P2 RPL41 RPL7AL3 RPLP0P1 RPS11P1 RPS15AP1 RPS26 RPS5L RRBP1 SAMD8 SDR9C7 SFTA2 SHMT2 SILV SLC15A3 SLC24A3 SLC25A33 SLC39A5 SLC45A1 SLC9A3P1 SLC9A3P3 SMAP1 SMARCC2 SMCHD1 SNAP25 SNORA48 SNORA70 SNORA74 SNORA77 SNORA8 SNORD17 snoU13 SNRPB2 SNX5 SON SPCS2 SPDEF SPTLC3 STAC3 STAT2 STAT6 SUOX SYT1 TAC3 TCP1 L1 TFAP2E TFEB TIMELESS TIMM23 TIMM23B TMEM109 TMEM111 TMEM132A TMEM132B TMEM194A TMEM50B TMEM90B TOMM6 TP53I11 TPMT TPTE TRIT1 TSPAN18 TTC17 U1 U2 U3 U4 U6 U7 USP49 VARSL VDAC2 VN1R11P VN1R12P VN1R13P VN1R14P XRN2 XRRA1 XXbac-BPG118E17.9 XXyac YR14BB7.1 XXyac-YX60D10.1 Y_RNA ZBTB39 ZC3H10 ZNF133 ZNF322A ZNF408 ZPLD1

PANTHER analysis: 248 mapped ids are found, 379 mapped ids are not found.

There is CnLOH in ER positive DCIS associated with invasive breast disease not observed in ER positive pure DCIS.

1. p-values < 0.05;
2. A gene list is mapped from 27 genomic regions found on chromosomes 5, 14, 15;

3. These regions encompass 149 genes altered in ER positive DCIS associated with invasive breast disease;

Genes:

7SK AB019439.2 AC008659.1 AC008659.2 AC009997.1 AC010674.2 AC010724.1 AC010724.2 AC010724.3 AC010724.4 AC010724.5
AC010724.6 AC010724.7 AC011295.1 AC011295.2 AC011295.3 AC011295.4 AC011295.5 AC011944.1 AC012050.1 AC018926.1
AC018926.2 AC022748.1 AC025580.2 AC025917.1 AC026624.1 AC026956.1 AC026956.2 AC039057.1 AC039057.3 AC044907.1
AC068870.1 AC069082.1 AC084882.1 AC087738.2 AC092373.1 AC104115.1 AC105339.1 AC105339.2 AC116903.1 AC116903.2
AC126339.1 AC126339.2 AC126339.3 AC126339.4 AC135995.1 AC135995.2 AC135995.3 AC135995.4 AC135995.5 AC136940.3
ADAMTS7 AGXT2L2 ANKRD34C AP3B2 ARPP19 BCL2L10 C15orf26 C15orf32 C15orf48 CCPG1
CHRNB4 CLK4 COL23A1 CPEB1 CTB-129O4.1 CTD-2184D3.1 CTD-2270N23.1 CTSH CYP19A1
DYX1C1 EFTUD1 F2RL1 FAM153C FAM154B FAM174B FSD2 GFPT2 GNB5 GOLGA6L10
GOLGA6L3 GOLGA6L5 GOLGA6L9 HNRNPAB HNRNPH1 HOMER2 hsa-mir-1266 hsa-mir-147b hsa-mir-184 hsa-mir-628 IGHD
IL16 KIAA1024 KIAA1199 KIAA1370 MAPK9 MAST4 MESDC1 MESDC2 MEX3B MORF4L1 MYO5A
MYO5C NEDD4 NHP2 ODZ2 PIGB PRTG PYGO1 RAB27A RASGEF1C RASGRF1 RFX7 RMND5B
RP11-1001M11.1 RP11-252I14.1 RP11-287J9.1 RP11-335K5.1 RP11-5P22.1 RP11-5P22.2
RP11-5P22.3 RP11-889L3.1 RP11-889L3.3 RP11-889L3.4 RP11-96J23.1 RP13-608F4.1
RP13-996F3.1 RPS17 S100Z SCARNA15 SEMA6D SH3GL3 SLC30A4 snoU109 snoU13
SPATA5L1 ST8SIA2 STARD5 TEX9 TMC3 TMED3 U1 U2 U7 UBE2Q2P2 UNC13C
WDR72 WHAMM

PANTHER analysis: 64 mapped ids are found, 84 mapped ids are not found.

5.8.5 Copy Number Aberrations for Oestrogen Receptor Positive Pure DCIS Compared to Oestrogen Positive Invasive Breast Disease

These series examines the difference between oestrogen receptor positive pure DCIS and oestrogen receptor positive invasive breast cancer.

Frequency plots showing copy number aberrations between oestrogen receptor positive pure DCIS and oestrogen receptor positive invasive breast disease were provided by Breakthrough Breast Cancer/Research Oncology, King's College London Bioinformatics Department (Figure 38).

Figure 38: Frequency plots showing copy number aberrations between oestrogen receptor positive pure DCIS and oestrogen positive invasive breast disease (amplifications, duplications, gains, Sc gains, losses, total losses CdLOH and CnLOH,) (pages 194-197).

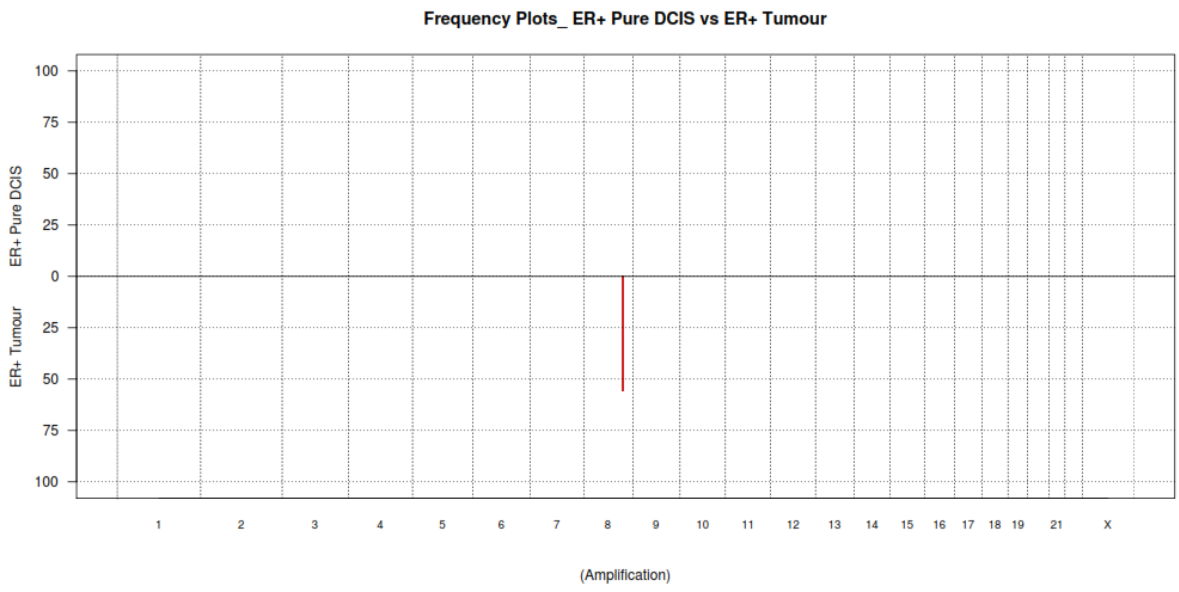
Frequency Plots_ ER+ Pure DCIS vs ER+ Tumour
ER+ Pure DCIS
ER+ Tumour
100
75
50
25
0
25
50
75
100
1
2
3
4
5
6
7
8
9
10
11
12
13
14
15
16
17
18
19
21
X
(Amplification)

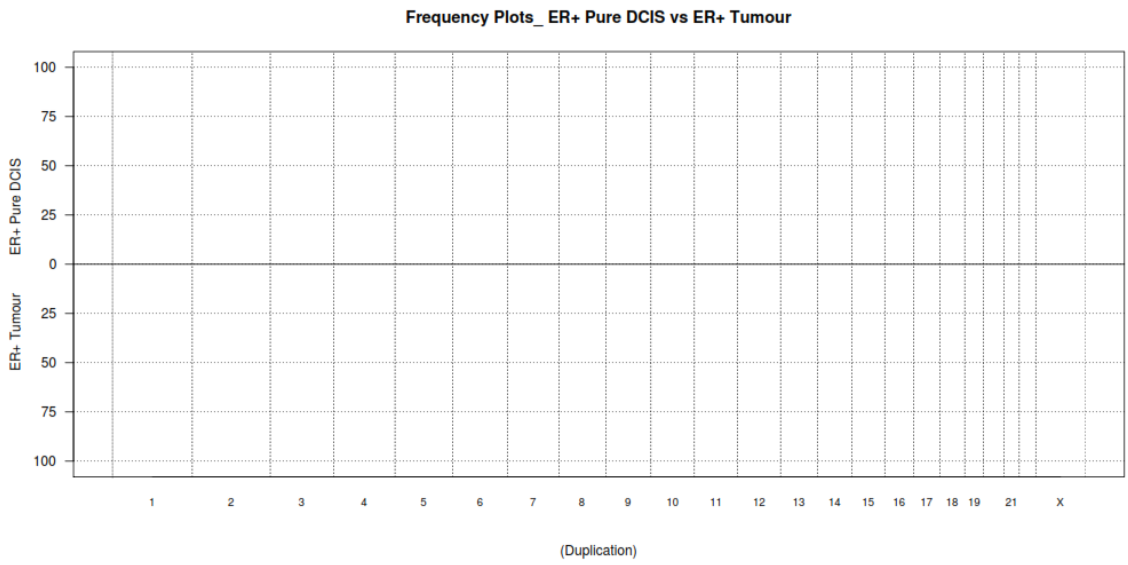
Frequency Plots_ ER+ Pure DCIS vs ER+ Tumour
ER+ Pure DCIS
ER+ Tumour
100
75
50
25
0
25
50
75
100
1 2 3 4 5 6 7 8 9 10 11 12 13 14 15 16 17 18 19 21 X
(Duplication)

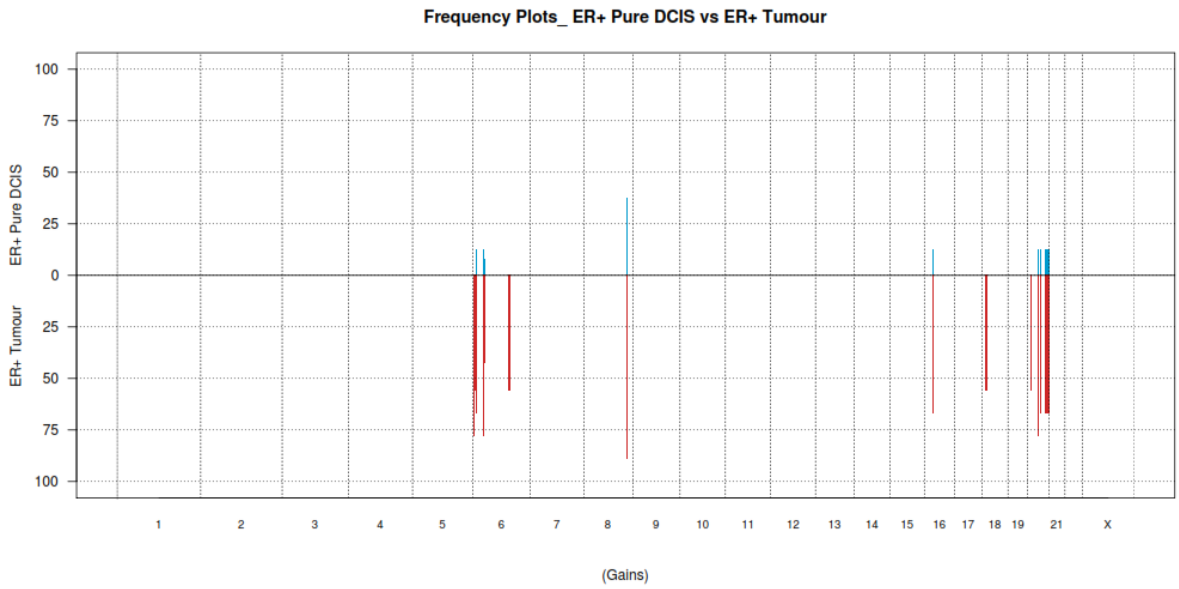
Frequency Plots_ ER+ Pure DCIS vs ER+ Tumour
ER+ Pure DCIS
ER+ Tumour
100
75
50
25
0
25
50
75
100
1 2 3 4 5 6 7 8 9 10 11 12 13 14 15 16 17 18 19 21 X
(Gains)

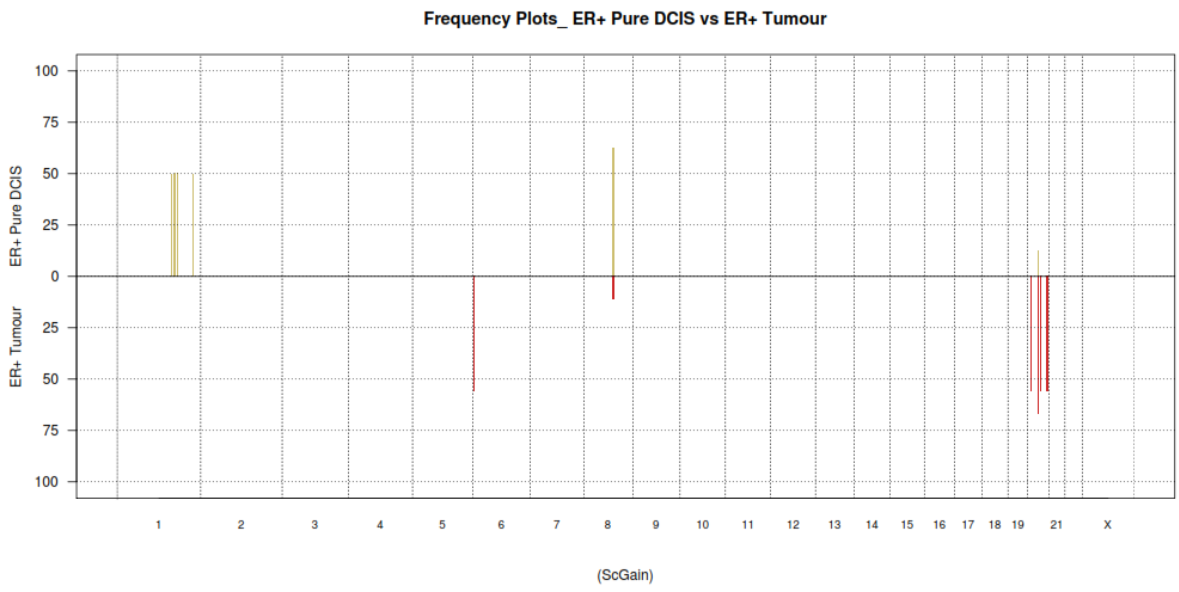
Frequency Plots_ ER+ Pure DCIS vs ER+ Tumour
ER+ Pure DCIS
ER+ Tumour
100
75
50
25
0
25
50
75
100
1
2
3
4
5
6
7
8
9
10
11
12
13
14
15
16
17
18
19
21
X
(ScGain)

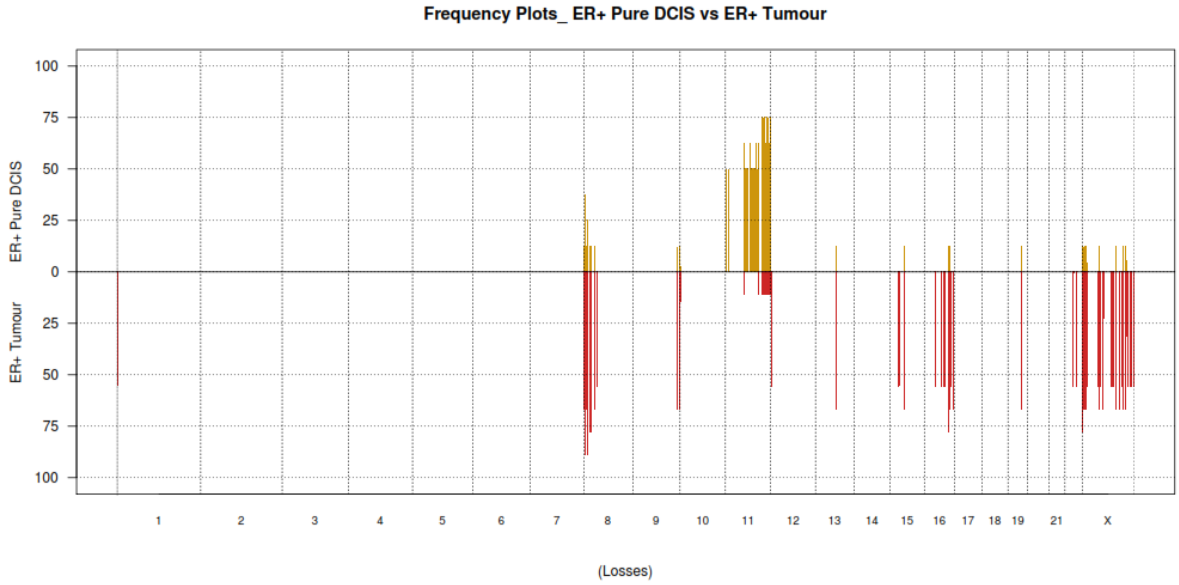
Frequency Plots_ ER+ Pure DCIS vs ER+ Tumour
ER+ Pure DCIS
ER+ Tumour
100
75
50
25
0
25
50
75
100
1
2
3
4
5
6
7
8
9
10
11
12
13
14
15
16
17
18
19
21
X
(Losses)

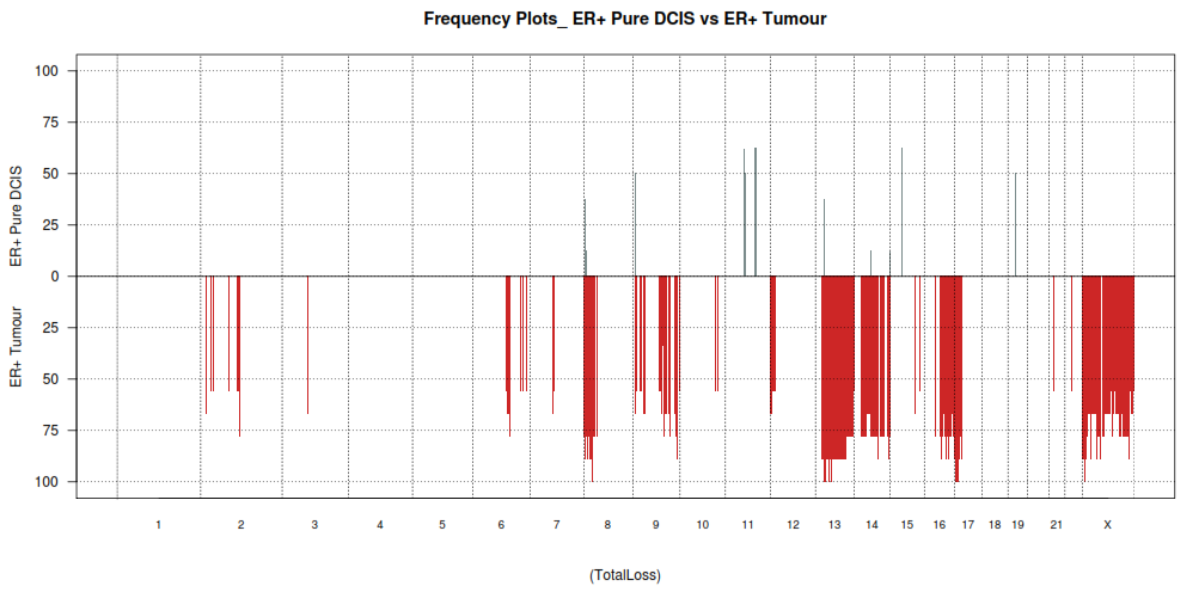
Frequency Plots_ ER+ Pure DCIS vs ER+ Tumour
ER+ Pure DCIS
ER+ Tumour
100
75
50
25
0
25
50
75
100
1
2
3
4
5
6
7
8
9
10
11
12
13
14
15
16
17
18
19
21
X
(TotalLoss)

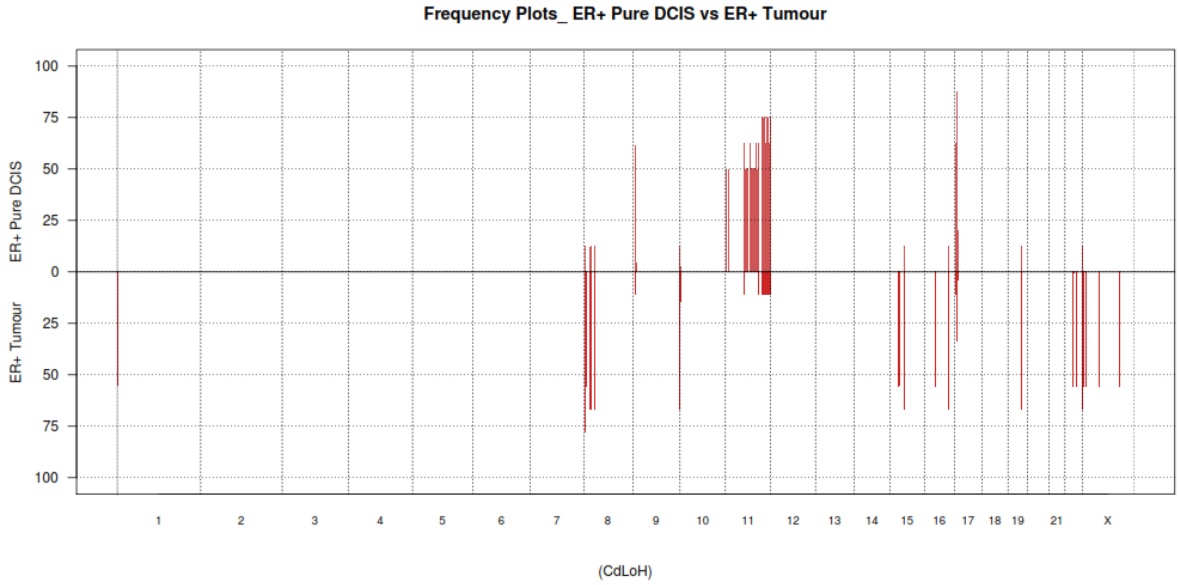
Frequency Plots_ ER+ Pure DCIS vs ER+ Tumour
ER+ Pure DCIS
ER+ Tumour
100
75
50
25
0
25
50
75
100
1
2
3
4
5
6
7
8
9
10
11
12
13
14
15
16
17
18
19
21
X
(CdLoH)

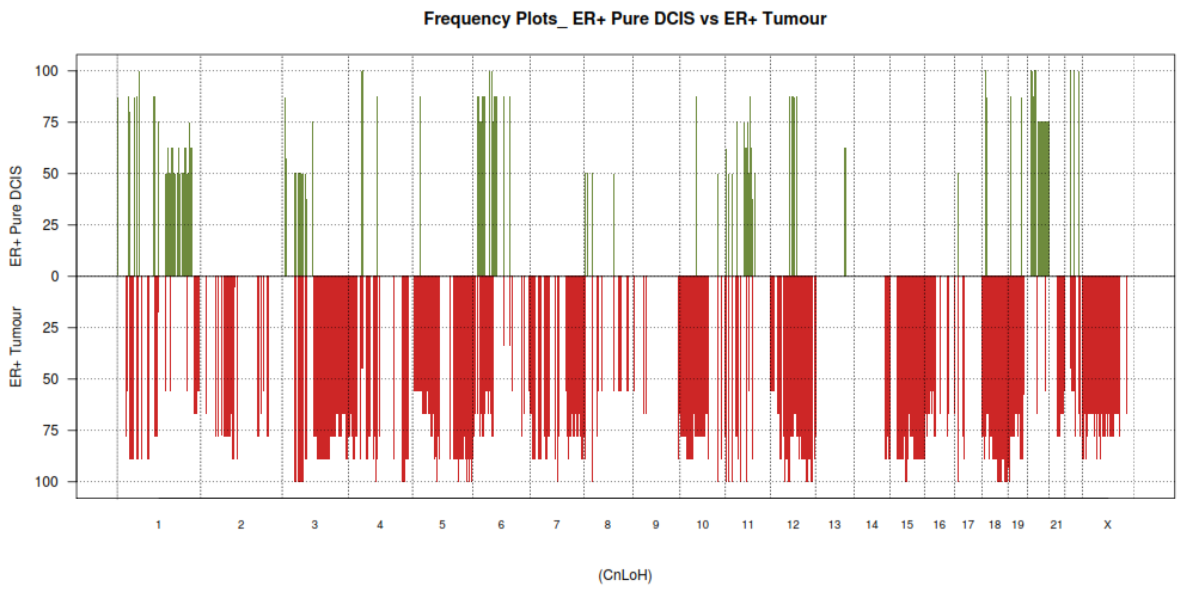

5.8.5.1 Amplification in Oestrogen Receptor Positive Pure DCIS Compared to Oestrogen Receptor Positive Invasive Breast Disease

There were no amplifications in ER positive pure DCIS (n=0/8) in this series. However, there were amplifications in ER positive invasive breast disease (n=5/9) not present in the ER positive pure DCIS.

1. p-values < 0.05;
2. A gene list is mapped from 2 genomic regions on chromosome 8;
3. These regions encompass 3 gene altered in ER positive invasive breast disease;

Genes:

AC103863.1 AF130342.1 EIF3H

PANTHER analysis: 1 mapped id is found, 2 mapped ids are not found.

Gene Information: ENSG00000147677 Protein ID: O15372

Gene Name: Eukaryotic translation initiation factor 3 subunit H Gene Symbol(s): EIF3H

Organism: Homo sapiens Alternate Ids: EIF3H_HUMAN (UniProtKB-ID) NP_003747 (refSeq)

ENSG00000147677 (Ensembl) 4503515(GI) IPI00977658 (IPI) EIF3H (Synonym) 603912(MIM) ENST00000521861(Ensembl_TRS) HGNC:3273(HGNC) ENSP00000429931(Ensembl_PRO)

5.8.5.2 Duplication in Oestrogen Receptor Positive Pure DCIS Compared to Oestrogen Receptor Positive Invasive Breast Disease

No duplications were found in either ER positive pure DCIS or ER positive invasive breast disease.

5.8.5.3 Genomic Gains in Oestrogen Receptor Positive Pure DCIS Compared to Oestrogen Receptor Positive Invasive Breast Disease

Gains present in ER positive pure DCIS (n=1/8) were present in gains found in ER positive invasive breast disease (n=7/9). This represents gains in both ER positive pure DCIS and ER positive invasive breast disease.

1. p-values < 0.05;
2. A gene list is mapped from 16 genomic regions found on chromosomes 6, 16, 20;
3. These regions encompass 91 genes altered in ER positive invasive breast disease and ER positive DCIS;

Genes:

AC006076.1 AC106739.1 AL109840.1 AL121583.1 AL121673.1 AL136532.1 ARF4P2 ASXL1 ATP5E C20orf11 C20orf112 C20orf166 C20orf195 C20orf20 C20orf200 C20orf90 C6orf48 COL9A3 CTD-3184A7.4 CTSZ DIDO1 DNMT3B DPH3B EEF1A2 GATA5 GCNT2 GMEB2 GNAS GNASAS HLA-DQA1 HLA-DQB1 HLA-DRB1 hsa-mir-1-1 hsa-mir-133a-2 HSPA1A HSPA1B HSPA1L IL4R JMJD5 KCNQ2 KIF3B LSM2 NSMCE1 NTSR1 OGFR PPDPF PTK6 RP11-11M20.2 RP11-358D14.2 RP11-360O19.1 RP11-360O19.4 RP11-93B14.4 RP11-93B14.5 RP11-93B14.6 RP1-1J6.2 RP1-290I10.3 RP1-290I10.4 RP1-290I10.5 RP1-290I10.6 RP1-290I10.7 RP1-290I10.8 RP1-309F20.2 RP1-309F20.3 RP13-30A9.1 RP13-30A9.2 RP4-543J19.8 RP4-697K14.12 RP4-697K14.3 RP4-697K14.7 RP4-724E16.2 RP5-1184F4.5 RP5-885L7.10 RP5-885L7.11 RPL7P3 RTEL1 SLC17A9 SLCO4A1 SLMO2 SNTA1 SRMS STMN3 TAF4 TCFL5 TFAP2A TH1L TOP1 TUBB1 VARS XXbac-BPG254F23.5 XXbac BPG254F23.6 ZNF217

PANTHER analysis: 43 mapped ids are found, 48 mapped ids are not found.

There were gains present in ER positive invasive breast disease (n=6/9) not observed in ER positive pure DCIS (n=0/8).

1. p-values < 0.05;
2. A gene list is mapped from 12 genomic regions found on chromosomes 6, 18, 20:
3. These regions encompass 91 genes altered in ER positive invasive breast disease;

Genes:

5S_rRNA 7SK AIM1 AL031963.1 AL031963.2 AL031963.3 AL031963.5 AL033383.2 AL033523.1 AL109754.1
AL133351.1 AL133509.1 AL138831.1 AL139092.1 AL160398.1 AL445309.1 AL445309.2 ANKRD5 AP005058.2 AP005482.1
AP006565.1 ATG5 BPHL C6orf145 C6orf146 C6orf195 C6orf201 CDYL CEP76 FAM136B
FAM50B FOXO3 LACE1 MYLK4 NQO2 PECI PRDM1 PRPF4B PSMG2 PSMG4
RIPK1 RP11-145H9.3 RP11-404H14.1 RP1-140K8.1 RP1-140K8.2 RP1-140K8.3
RP1-140K8.4 RP11-416N4.1 RP11-416N4.4 RP11-420G6.3 RP11-420G6.4
RP11-420L9.2 RP11-420L9.4 RP11-428J1.2 RP11-620A17.1 RP11-625P7.1
RP11-697G4.3 RP1-223B1.1 RP1-40E16.11 RP1-40E16.2 RP1-40E16.3 RP1-40E16.4
RP1-40E16.8 RP1-40E16.9 RP1-90J20.10 RP1-90J20.2 RP1-90J20.7 RP1-90J20.8 RP3-359N14.1
RP3-359N14.2 RP3-400B16.1 RP3-400B16.2 RP3-400B16.3 RP3-406P24.1 RP3-406P24.3
RP3-430A16.1 RP3-527G5.1 RP4-529N6.1 RP5-839B4.7 RP5-839B4.8 SERPINB1
SERPINB6 SERPINB9 SLC22A23 SNAP25 snoU13 SPIRE1 TUBB2A TUBB2B U6 WRNIP1 Y_RNA

PANTHER analysis: 26 mapped ids are found, 66 mapped ids are not found.

5.8.5.4 Genomic Sc Gains in Oestrogen Receptor Positive Pure DCIS Compared to Oestrogen Receptor Positive Invasive Breast Disease

Sc gains in ER positive pure DCIS (n=5/8) show some overlap with Sc gains in ER positive invasive breast disease (1/9).

1. p-values < 0.05;
2. A gene list is mapped from 6 genomic regions found on chromosomes 1, 8;
3. These regions encompass 28 genes altered in ER positive pure DCIS;

Genes:

ACBD6 AL359853.1 AL359853.3 AL390718.1 C1orf192 CEP350 FMO2 FMO3 FMO6P hsa-mir-1295 LHX4
QSOX1 RP11-122G18.5 RP11-12M5.4 RP11-145A3.1 RP11-145A3.2 RP11-216N21.1

RP1-127D3.4 RP11-502H18.2 RP11-52I18.1 RP11-533E19.2 RP11-533E19.3 RP1-45C12.1
RP5-1180C10.2 SDHC TOR1AIP1 TOR1AIP2 U6

PANTHER analysis: 11 mapped ids are found, 17 mapped ids are not found.

Sc gains in ER positive invasive breast disease (6/9) show some overlap with the Sc gains in ER positive pure DCIS (n=1/8).

1. p-values < 0.05;
2. A gene list is mapped from 10 genomic regions found on chromosomes 6, 20;
3. These regions encompass 67 genes altered in ER positive invasive breast disease;

Genes:

AL031963.1 AL031963.2 AL031963.5 AL109754.1 AL109840.1 AL121583.1 AL121673.1 AL133343.1 AL136532.1 ANKRD5
ARF4P2 ASXL1 ATP5E
BPHL C20orf11 C20orf112 C20orf166 C20orf20 C20orf200 C20orf90 COL9A3 CTSZ DIDO1 DNMT3B
DPH3B GATA5 GNAS GNASAS hsa-mir-1-1 hsa-mir-133a-2 KIF3B NTSR1 OGFR
RP11-11M20.2 RP11-410N8.1 RP11-410N8.3 RP11-410N8.4 RP11-416N4.1 RP11-416N4.4
RP11-93B14.4 RP11-93B14.5 RP11-93B14.6 RP1-1J6.2 RP1-309F20.2 RP1-309F20.3
RP13-30A9.1 RP13-30A9.2 RP1-40E16.11 RP1-40E16.8 RP1-40E16.9 RP4-543J19.8
RP5-1184F4.5 RP5-839B4.7 RP5-839B4.8 RP5-885L7.10 RP5-885L7.11 RPL7P3
SLC17A9 SLCO4A1 SLMO2 SNAP25 TAF4 TCFL5 TH1L TOP1 TUBB1 TUBB2A

PANTHER analysis: 23 mapped ids are found, 44 mapped ids are not found.

5.8.5.5 Losses in Oestrogen Receptor Positive Pure DCIS Compared to Oestrogen Receptor Positive Invasive Breast Disease

Genomic losses in ER positive pure DCIS (n=6/8) show some overlap with genomic losses in ER positive invasive breast disease (1/9).

1. p-values < 0.05;
2. A gene list is mapped from 32 genomic regions on chromosome 11;
3. These regions encompass 225 genes altered in ER positive pure DCIS;

Genes:

5S_rRNA 7SK AC009294.1 AC019227.1 AC019227.2 ACA59 ACAD8 ACRV1 ADAMTS15 ADAMTS8
AMICA1 ANKK1 AP000757.1 AP000770.1 AP000797.1 AP000797.2 AP000843.2 AP000844.1 AP000880.1 AP000892.4
AP000907.1 AP000907.2 AP000907.3 AP000908.1 AP000911.1 AP000925.2 AP000926.1 AP000936.1 AP000936.3 AP000936.4
AP000936.5 AP001122.1 AP001267.1 AP001267.2 AP001582.1 AP001781.1 AP001891.1 AP001979.1 AP001992.2 AP001998.1

AP002451.1 AP002806.1 AP002806.2 AP002856.4 AP002856.5 AP002856.6 AP002856.7 AP002884.4 AP002886.2 AP002962.1 AP002986.1 AP002991.1 AP003025.2 AP003039.3 AP003039.4 AP003040.1 AP003040.2 AP003041.1 AP003070.1 AP003402.1 AP003402.2 AP003500.1 AP003730.1 AP003730.2 AP004248.4 AP004372.1 AP005597.1 AP005638.1 AP005638.3 AP005639.1 AP006216.10 AP006216.11 AP006216.12 AP006216.5 APLP2 APOA1 APOA4 APOA5 APOC3 ARHGAP20 ARHGAP32 ARHGEF17 ATP5L B3GAT1 BACE1 BAK1P2 BARX2 BCO2 BSX BTG4 BUD13 C11orf1 C11orf44 C11orf45 C11orf52 C11orf57 C11orf63 C11orf71 C11orf88 CADM1 CD3D CD3E CD3G CEP164 CHEK1 CLDN25 CRTAM CRYAB CUL5 DDX10 DDX25 DDX6 DIXDC1 DLAT DRD2 DSCAML1 EI24 ETS1 FAM168A FAM55A FAM55B FAM55D FDX1 FDXACB1 FLI1 FXYD2 FXYD6 GLB1L2 GLB1L3 hsa-mir-34b hsa-mir-34c HSPA8 HSPB2 HTR3A HTR3B HYLS1 IGSF9B IL10RA IL18 JAM3 KCNJ1 KCNJ5 LAYN MLL MPZL2 MPZL3 NCAM1 NCAPD3 NCRNA00167 NEU3 NFRKB NNMT OPCML OR4A15 OR4A16 PAFAH1B2 PATE1 PATE2 PATE3 PATE4 PCSK7 PIH1D2 POU2AF1 PPIHP1 PPP2R1B PRDM10 PUS3 RAB39 RBM7 RDX RELT REXO2 RNF214 RP11-237N19.1 RP11-567M21.1 RP11-667M19.1 RP11-762B21.1 RP11-762B21.2 RP11-762B21.3 RP11-801G16.1 RP11-832N8.1 RPL37AP8 SCARNA11 SCN2B SCN4B SDHD SIDT2 SIK2 SIK3 SLC35F2 SNORD14 snoU13 SNX19 SPATA19 SPCS2 ST14 STT3A TAGLN TEX12 THYN1 TIMM8B TMEM225 TMEM45B TMPRSS13 TMPRSS4 TMPRSS5 TP53AIP1 TRIM48 TTC12 U2 U4 U4atac U6 U6atac UBASH3B UBE4A USP28 VPS26B XRRA1 Y_RNA ZBTB16 ZBTB44 ZC3H12C ZNF259 ZW10

PANTHER analysis: 129 mapped ids are found, 96 mapped ids are not found.

There is a degree of overlap of the genomic losses in ER positive invasive breast disease (n=8/9) compared to ER positive pure DCIS (n=3/8).

1. p-values < 0.05;
2. A gene list is mapped from 51 genomic regions found on chromosomes 8, 9, 13, 15, 16, 19, X;
3. These regions encompass 84 genes altered in both ER positive invasive breast disease and ER positive pure DCIS;

Genes:

5S_rRNA 7SK AC009707.1 AC011445.1 AC019176.2 AC022559.1 AC022716.1 AC073493.1 AC073493.2 AC073493.3 AC090204.1 AC090204.10 AC090204.2 AC090204.3 AC090204.4 AC090204.5 AC090204.6 AC090204.7 AC090204.8 AC090204.9 AC090420.1 AC100800.1 AC129915.1 AF238378.1 AL135784.1 AL590131.1 AL611925.1 ARHGEF10 BX649443.1 C8orf68 CACNA1B CLN8 CSMD1 DEFA5 DHRSX DLC1 DLGAP2 EHMT1 FREQ FRMPD4 GANC GFRA2 hsa-mir-596 hsa-mir-627 IGSF1 IL28A IL28B IL29 JPH3 KBTBD11 MAGED1 MAGED4B MRRFP MYOM2 NCCRP1 NLGN4X OR11N1P OR1AA1P OR5BH1P PCDH19 PLA2G4F PSD3 RP11-114H20.1 RP11-133M24.1 RP11-234P3.2 RP11-234P3.3 RP11-234P3.4 RP11-2N21.2 RP11-346L6.1 RP1-154J13.2 RP1-154J13.3 RP11-647I17.1 RP13-858C7.1 RP5-1168A5.1 RP5-1170D6.1 RP5-964N17.1 SNORA11 SNORA70 SYCN TMEM87A U3 U6 VPS39 Y_RNA

PANTHER analysis: 25 mapped ids are found, 59 mapped ids are not found.

5.8.5.6 Total Loss in Oestrogen Receptor Positive Pure DCIS Compared to Oestrogen Receptor Positive Invasive Breast Disease

There are total losses for ER positive pure DCIS (n=5/8) not observed in ER positive invasive breast disease (n=0/9).

1. p-values < 0.05;
2. A gene list is mapped from 12 genomic regions found on chromosomes 9, 11, 15, 19;
3. These regions encompass 22 genes altered in ER positive pure DCIS;

Genes:

7SK AC025678.1 AC027139.2 AC027139.3 AP000720.1 AP001482.1 AP003072.1 CCDC67 CTSC GOLGA8B GRM5 hsa-mir-1233 KDM4C NOX4 OR10V1 OSBP PATL1 RP11-657K20.1 SLC36A4 TYR U7 ZNF208 ZNF257

PANTHER analysis: 13 mapped ids are found, 10 mapped ids are not found.

There were total losses present for ER positive invasive breast disease (n=9/9) not observed in ER positive pure DCIS (n=0/8).

1. p-values < 0.05;
2. A gene list is mapped from 84 genomic regions found on chromosomes 8, 13, 14, 16, 17, X;
3. These regions encompass 443 genes altered in ER positive invasive breast disease;

Genes:

5S_rRNA 7SK AC000003.1 AC001226.2 AC002347.1 AC002366.3 AC002504.1 AC005284.1 AC005323.1 AC005410.2 AC005548.1 AC005548.2 AC005696.2 AC005696.3 AC005725.1 AC007333.1 AC007333.2 AC015799.1 AC015799.2 AC015908.2 AC016292.3 AC022716.1 AC025518.1 AC026462.1 AC027045.1 AC027763.1 AC027763.2 AC073493.1 AC073493.2 AC073493.3 AC074035.1 AC087498.1 AC090282.1 AC097370.1 AC099684.1 AC112778.1 AC112778.2 AC144838.1 AIPL1 AL136001.1 AL136160.1 AL136219.1 AL136359.1 AL138690.1 AL138815.1 AL138815.3 AL139002.1 AL139034.1 AL139082.1 AL158032.2 AL162377.1 AL162377.2 AL163544.1 AL355611.1 AL355611.2 AL355611.3 AL356863.1 AL359180.1 AL391384.1 AL442203.2 AL445989.1 AL450423.1 AL450447.1 AL512362.1 AL512652.1 AL589987.1 AL590007.2 AL596092.1 ALOX12 AMAC1L3 ARHGAP6 ARX ASGR1 ASGR2 ASPA ASPG ASS1P4 ATP7B ATP8A2 ATXN8OS B3GALTL BCL6B BTF3L1 BX649443.1 BX890604.1 BX890604.2 C13orf23 C13orf34 C13orf36 C13orf37 C14orf180 C17orf100 C17orf49 C17orf51 C17orf61 C17orf74 C17orf91 CCDC42 CCDC70 CCNA1 CDK8 CHRNB1 CLEC10A CLN5 CRYL1 CTD-2545G14.1 CTNS DACH1 DGKH DHRS7C DHRSX DHX9P1 DIAPH3 DIS3 DLC1 DLG4 DNAH9 DPH1 DUSP21 EBF2 EDNRB EFHA1 EIF4A1P6 FAM123A FAM64A FBXL3 FBXO39 FGF11 FGF9 FLT1 FOXO1 FREM2 FREQ

GAPDHP34 GAS7 GFRA2 GJA3 GJB2 GJB6 GLP2R GPR12 HDHD1A HMCN2 HNF4GP1 hsa-mir-1253 hsa-mir-195 hsa-mir-203 hsa-mir-22 hsa-mir-497 hsa-mir-744 hsa-mir-759 IFT88 IL17D IRG1 KCNJ12

KDM6A KIAA0564 KIAA0664 KIAA0753 KIF26A KLF12 KLF5 KLHL1 LHFPLIN28AP2 MAP2K3

MAP2K4 MED31 METT10D MFSD6L MTUS2 MXRA5 MYH1 MYH10 MYH13 MYH2 MYH3 MYH4

MYH8 N6AMT2 NDEL1 NEFL NEFM NEK3 NEK5 NFYAP1 NHLRC3 NLGN2

NLGN4X NTN1 NXN OLFM4 OR1A1 OR1A2 OR1D2 OR1D5 OR1E1 OR1E2 OR1G1

OR3A1 OR3A2 OR3A3 OR3A4 OVCA2 PABPC3 PAFAH1B1 PARP4 PCDH8 PIBF1 PIK3R5

PIK3R6 PIRT PITPNM3 PLSCR3 POLA1 POLR2A POU4F1 PRKX PSPC1 RAP1GAP2 RCVRN

RFXAP RNASEK RNF17 RNF219 RNF6 RP11-101P17.10 RP11-101P17.11 RP11-101P17.5 RP11-101P17.6 RP11-101P17.7 RP11-101P17.8 RP11-101P17.9 RP11-107B1.1 RP11-110K18.2 RP11-110K8.1

RP11-117N4.1 RP11-11C5.1 RP11-12I24.2 RP11-12I24.3 RP11-133M24.1 RP11-137M6.2 RP11-149B7.1 RP11-149B7.3 RP11-149B7.4 RP11-149B7.5 RP11-165I9.3 RP11-165I9.4 RP11-165I9.6 RP11-165I9.8 RP11-169O17.1 RP11-169O17.5 RP11-16D22.1 RP11-16L6.3 RP11-172E9.2

RP11-172H24.3 RP11-181D10.2 RP11-187A9.2 RP11-187A9.3 RP11-196I2.1 RP11-196P2.1

RP11-197L7.2 RP11-1M18.1 RP11-203P2.1 RP11-203P2.2 RP11-206H15.2 RP11-206L1.2

RP11-209P2.1 RP11-214O11.1 RP11-214O11.2 RP11-218I21.1 RP11-248G5.3

RP11-24H2.1 RP11-24H2.2 RP11-252B20.1 RP11-261P13.3 RP11-264J4.4 RP11-264J4.5

RP11-264J4.6 RP11-266E6.2 RP11-267I18.1 RP11-271B5.1 RP11-279N8.1 RP11-304M3.2

RP11-30C8.1 RP11-30C8.2 RP11-318G21.2 RP11-318G21.3 RP11-318G21.4 RP11-323P14.2 RP11-325D5.3 RP11-327P2.3 RP11-335N6.1 RP11-342C20.2 RP11-342C20.3

RP11-349O10.1 RP11-350A18.1 RP11-351N4.3 RP11-360A9.1 RP11-364B14.1

RP11-364B14.2 RP11-364B14.3 RP11-367C11.2 RP11-380N8.1 RP11-380N8.3 RP11-380N8.4

RP11-381L18.2 RP11-388E20.1 RP11-393H6.2 RP11-393H6.3 RP11-394A14.1

RP11-394A14.2 RP11-394A14.3 RP11-398O19.3 RP11-408O13.2 RP11-408O13.3 RP11-421P11.5 RP11-430I3.2 RP11-430K22.1 RP11-430K22.2 RP11-431O22.2 RP11-442F12.2

RP11-459A10.1 RP11-459A10.2 RP11-459A10.3 RP11-459J23.1 RP11-459J23.2

RP11-462C21.1 RP11-463M3.1 RP11-467D10.2 RP11-471M2.1 RP11-471M2.2 RP11-473M10.1

RP11-473M10.2 RP11-473M10.3 RP11-474L7.4 RP11-483M24.2 RP11-501G6.1 RP11-505F3.2

RP11-505F3.4 RP11-518D7.1 RP11-51B13.2 RP11-520F24.1 RP11-520F24.2 RP11-520F24.3

RP11-520F9.2 RP11-521H3.1 RP11-523H24.5 RP11-527F15.1 RP11-52L5.4 RP11-534K14.1

RP11-534K14.2 RP11-545M8.1 RP11-545M8.2 RP11-545M8.3 RP11-556N21.4 RP11-56M2.1 RP11-570F6.1

RP11-571G1.1 RP11-571G1.2 RP11-609D21.1 RP11-61K9.2 RP11-629E24.2 RP11-629O4.1 RP11-706O15.1 RP11-706O15.3 RP11-706O15.5 RP11-706O15.7 RP11-706O15.8 RP11-707P20.1

RP11-713H12.1 RP11-76N11.2 RP11-77P3.1 RP11-7B3.2 RP11-7B3.3 RP11-7B3.4 RP11-822E23.1

RP11-88G17.6 RP11-90M5.1 RP11-963H4.1 RP1-258N20.3 RP13-858C7.1 RP13-926M18.1 RPA1 RTN4RL1 SCEL SCO1 SERPINF1 SERPINF2 SHISA6 SHPK SLAIN1 SLC13A5 SLC16A11

SLC16A13 SLITRK5 SMAD9 SMYD4 SNORA25 SNORA48 SNORA68 SNORA9 SNORD116 SNORD37 snoU13 SPATA22 SPDYE4 SPEM1 STOML3 STX8 TCEB1P23 TDRD3 TDRD9 TEKT1 TLCD2

TMEM102 TMEM179 TMEM46 TNK1 TOX3 TRPC4 TRPV1 TRPV3 TXNDC17 U2 U3 U4 U6 U7 UFM1 UTP14C VCX3A WASF3 WDR81 WSCD1 XAF1 XPO4 Y_RNA ZBED1

ZBTB4 ZDHHC20 ZMYM2 ZMYM5

PANTHER analysis: 167 mapped ids are found, 276 mapped ids are not found.

5.8.5.7 CdLOH in Oestrogen Receptor Positive Pure DCIS Compared to Oestrogen Receptor Positive Invasive Breast Disease

There are similarities between CdLOH in ER positive pure DCIS (n=7/8) and CdLOH in ER positive invasive breast disease (n=3/9).

1. p-values < 0.05;
2. A gene list is mapped from 38 genomic regions found on chromosomes 9, 11, 17;
3. These regions encompass 281 genes altered in ER positive invasive breast disease and ER positive pure DCIS;

Genes:

5S_rRNA 7SK AC004148.1 AC006435.1 AC009294.1 AC019227.1 AC019227.2 AC055839.2 AC087500.1 AC087742.1 AC116914.1 AC129492.6 ACA59 ACAD8 ACRV1 ADAMTS15 ADAMTS8 ALOX12B ALOX15B ALOXE3 AMICA1 ANKFY1 ANKK1 AP000757.1 AP000770.1 AP000797.1 AP000797.2 AP000843.2 AP000844.1 AP000880.1 AP000892.4 AP000907.1 AP000907.2 AP000907.3 AP000908.1 AP000911.1 AP000925.2 AP000926.1 AP000936.1 AP000936.3 AP000936.4 AP000936.5 AP001122.1 AP001267.1 AP001267.2 AP001582.1 AP001781.1 AP001891.1 AP001979.1 AP001992.2 AP001998.1 AP002451.1 AP002806.1 AP002806.2 AP002856.4 AP002856.5 AP002856.6 AP002856.7 AP002884.4 AP002886.2 AP002962.1 AP002986.1 AP002991.1 AP003025.2 AP003039.3 AP003039.4 AP003040.1 AP003040.2 AP003041.1 AP003070.1 AP003402.1 AP003402.2 AP003500.1 AP003730.1 AP003730.2 AP004248.4 AP004372.1 AP005597.1 AP005638.1 AP005638.3 AP005639.1 AP006216.10 AP006216.11 AP006216.12 AP006216.5 APLP2 APOA1 APOA4 APOA5 APOC3 ARHGAP20 ARHGAP32 ARHGEF17 ATP2A3 ATP5L AURKB B3GAT1 BACE1 BAK1P2 BARX2 BCO2 BSX BTG4 BUD13 C11orf1 C11orf44 C11orf45 C11orf52 C11orf57 C11orf63 C11orf71 C11orf88 C17orf44 C17orf59 C17orf68 C17orf85 C17orf87 C1QBP CADM1 CAMKK1 CD3D CD3E CD3G CEP164 CHEK1 CLDN25 CNTROB CRTAM CRYAB CTNS CUL5 CYB5D2 DDX10 DDX25 DDX6 DERL2 DHX33 DIXDC1 DLAT DRD2 DSCAML1 EI24 ETS1 FAM168A FAM55A FAM55B FAM55D FDX1 FDXACB1 FLI1 FXYD2 FXYD6 GLB1L2 GLB1L3 GSG2 GUCY2D HES7 HIC1 hsa-mir-132 hsa-mir-212 hsa-mir-34b hsa-mir-34c HSPA8 HSPB2 HTR3A HTR3B HYLS1 IGSF9B IL10RA IL18 ITGAE JAM3 KCNJ1 KCNJ5 LAYN METT10D MIS12 MLL MPZL2 MPZL3 NCAM1 NCAPD3 NCRNA00167 NEU3 NFRKB NLRP1 NNMT NUP88 OPCML OR4A15 OR4A16 P2RX1 P2RX5 PAFAH1B2 PATE1 PATE2 PATE3 PATE4 PCSK7 PER1 PFAS PIH1D2 POU2AF1 PPIHP1 PPP2R1B PRDM10 PTPRD PUS3 RAB39 RABEP1 RANGRF RBM7 RDX RELT REXO2 RNF214 RP11-237N19.1 RP11-48B14.1 RP11-567M21.1 RP11-667M19.1 RP11-762B21.1 RP11-762B21.2 RP11-762B21.3 RP11-801G16.1 RP11-832N8.1 RPAIN RPL37AP8 SCARNA11 SCN2B SCN4B SDHD SIDT2 SIK2 SIK3 SLC25A35 SLC35F2 SMG6 SNORD14 snoU13 SNX19 SPATA19 SPCS2 ST14 STT3A TAGLN TAX1BP3 TEX12 THYN1 TIMM8B TMEM107 TMEM225 TMEM45B TMEM93 TMPRSS13 TMPRSS4 TMPRSS5 TP53AIP1 TRIM48 TTC12 U2 U4 U4atac U6 U6atac U7 U8 UBASH3B UBE4A USP28 USP6 VAMP2 VPS26B XRRA1 Y_RNA ZBTB16 ZBTB44 ZC3H12C ZNF259 ZNF594 ZW10 ZZEF1

PANTHER analysis: 168 mapped ids are found, 113 mapped ids are not found.

There are some similarities between CdLOH in ER positive invasive breast disease (n=7/9) and CdLOH in ER positive pure DCIS (n=1/8).

1. p-values < 0.05;
2. A gene list is mapped from 34 genomic regions found on chromosomes 1, 8, 9, 15, 16, 19, 22, X;
3. These regions encompass 51 genes altered in ER positive invasive breast disease and ER positive pure DCIS;

Genes:

5S_rRNA 7SK AC011445.1 AC018558.1 AC019176.2 AC022716.1 AC023824.2 AC073493.1 AC073493.2 AC073493.3
AF238378.1 AL611925.1 AP000351.4 BMP15 BX649443.1 CACNA1B CSMD1 DDT DEFA5 DHRSX
EHMT1 FRMPD4 GABRB3 GANC GFRA2 GSTT2 GSTTP1 hsa-mir-627 IL28A IL28B IL29
LARGE MAGED1 NCCRP1 PLA2G4F PRKCZ RP11-104D21.1 RP11-104D21.2 RP11-104D21.3
RP11-637B23.1 RP11-637B23.3 RP13-346H10.2 RP13-858C7.1 RP5-1168A5.1 RP5-1170D6.1 RP5-964N17.1 SNORA70 SYCN TMEM87A U3 VPS39

PANTHER analysis: 20 mapped ids are found, 31 mapped ids are not found.

5.8.5.8 CnLOH in Oestrogen Receptor Positive Pure DCIS Compared to Oestrogen Receptor Positive Invasive Breast Disease

There are similarities between ER positive pure DCIS (n=8/8) and ER positive invasive breast disease (n=4/9).

1. p-values < 0.05;
2. A gene list is mapped from 67 genomic regions found on chromosomes 1, 3, 4, 5, 6, 10, 11, 12, 18, 19, 20, 22;
3. These regions encompass 357 genes altered in ER positive pure DCIS;

Genes:

5S_rRNA 7SK ABT1 AC000032.1 AC002485.1 AC005399.1 AC025423.2 AC034193.1 AC099680.1 AC124890.1
RP11-209A2.1 ADH5P4 AGAP10 AHCYL1 AK3L1 AKD1 AL021807.2 AL021808.1 AL021808.2 AL021808.3
AL023913.1 AL035045.1 AL035661.3 AL050321.1 AL050321.2 AL050322.1 AL050335.1 AL050335.2 AL109754.1 AL109922.1
AL109947.1 AL109947.2 AL118509.1 AL121584.1 AL121988.1 AL132996.1 AL133255.1 AL133472.1 AL138850.1 AL139429.1
AL354680.1 AL391137.2 AL391559.1 AL589723.1 AL590062.1 AL591044.1 AL591044.2 AL591044.3 AL591044.4 AL691432.2
AL713998.1 ANKRD5 ANXA8L1 AP001029.1 AP001992.2 AP005482.1 APBB2 ASPHD2 BACH2 BANF2
BEND6 BMS1P2 BTBD3 BX255972.1 C1orf212 C20orf12 C20orf187 C20orf3 C20orf61 C20orf72
C20orf78 C20orf79 C20orf82 C20orf94 C3orf10 C6orf1 C6orf140 C6orf184 CD164 CDH12 CDK11A
CECR2 CECR9 CENPM CEP76 CRYBB2P1 CSF1 CSRP2BP CST1 CST2 CST3 CST4

CST5 CST7 CSTP1 CSTP2 CTA-221G9.9 CTA-246H3.11 CTA-246H3.7
CTA-246H3.8 CTA-250D10.15 CTA-250D10.19 CTB-1048E9.7 CTSLL7 CYP2S1 DEK
DHFRP2 DLGAP3 DTNBP1 ELAVL4 ENSAP1 EPS8L3 EYS FAM25B FAM35B2 FAM40A
FAT1P1 FGFR3P FIG4 FLOT1 GAPDP2 GGTLA4 GJA4 GJB3 GJB4 GJB5 GLS2 GLUDP8
GMPR GSTM2 GSTM3 GSTM3P GSTM5 GUSBL1 HCP5 HIST1H2AH HIST1H2BJ HIST1H2BK HIST1H4I HLA-B
HLA-S HMGA1 HNRNPM HPS4 hsa-mir-33a IRAK2 JARID2 KDM1B KHDRBS2 KIF13A KIF16B LGSN
LIN28AP3 LRP5L MACROD2 MAP3K7 MAR02 MDC1 MDM2 MICA MICAL1 MKKS
MMP23A MRPS11P1 MYLIP MYO1F N4BP2 NAV3 NCRNA00227 NCRNA00240 NEU3 NHLRC1
NKX2-2 NKX2-4 NUDT3 NXT1 OTOR OVOL2 PA2G4P2 PACSIN1 PAK7 PGAM3P PHACTR1
PLK1S1 POM121L1P POM121L2 POM121L3P PPIAP17 PPIL6 PPYR1 PRAM1 PRSS16 PSMG2
PTMAP3 PTPN2 RBMS2 RNF11B RNF144B RP11-102J14.1 RP11-124A7.2 RP11-129K24.4
RP11-144G6.10 RP11-144G6.4 RP11-144G6.9 RP11-146I2.1 RP11-157E14.1
RP11-157E14.3 RP11-195M16.1 RP11-218C14.5 RP11-227D2.3 RP11-239L20.3 RP11-239L20.4 RP11-239L20.5
RP11-292F22.3 RP11-292F22.4 RP11-292F22.5 RP1-129L7.1 RP11-307F22.2 RP11-314P12.2
RP11-314P12.3 RP11-388K2.1 RP1-13D10.2 RP1-13D10.3 RP1-13D10.4 RP1-13D10.5
RP11-401E14.1 RP11-401E14.2 RP11-416N4.1 RP11-416N4.4 RP11-457M11.2 RP11-492I2.1
RP11-513I15.3 RP11-513I15.5 RP11-513I15.6 RP11-526K17.2 RP11-528A10.1 RP11-528A10.2
RP11-542F9.1 RP11-560J1.1 RP11-575L16.2 RP11-69I22.2 RP11-69I22.3 RP11-707M13.1
RP11-74E24.2 RP1-187N21.2 RP1-190J20.2 RP1-198K11.3 RP1-240B8.3 RP1-298M8.1
RP3-322G13.7 RP3-453I5.2 RP3-462D8.2 RP3-525L6.2 RP4-564O4.1 RP4-568F9.3 RP4-568F9.6 RP4-
568F9.7 RP4-580G13.1 RP4-697P8.2 RP4-697P8.3 RP4-705D16.3 RP4-717M23.2 RP4-718D20.3
RP4-726N1.2 RP4-734C18.1 RP4-735C1.4 RP4-735C1.5 RP4-735C1.6 RP4-
737E23.2 RP4-737E23.4 RP4-742J24.2 RP4-777D9.2 RP4-794H19.4 RP4-796I8.1 RP5-1018A4.3 RP5-
1068E13.3 RP5-1068F16.3 RP5-1069C8.1 RP5-1069C8.2 RP5-1077I2.3 RP5-1077I2.4 RP5-1100I6.1
RP5-1100I6.2 RP5-1177M21.1 RP5-1195D24.1 RP5-839B4.7 RP5-839B4.8 RP5-860P4.2
RP5-872K7.2 RP5-872K7.7 RP5-905G11.3 RP5-919F19.5 RP5-931K24.1 RP5-984P4.1 RP5-
984P4.4 RP5-997D16.2 RPL13P RPL15P1 RPL23AP6 RPL24P2 RPL7AL3 RPLP0P1 RPS10
RPS10P2 RPS11P1 RPS15AP1 RRBP1 SEP03 SEZ6L SHISA8 SLC24A3 SMCHD1 SMPD2 SNAP25
SNORD17 SNORD83 snoU13 SNRPB2 SNX5 SPCS2 SPDEF SPIRE1 SPRYD4 SPTLC3
SREBF2 TASP1 TMEM90B TNFRSF13C TPMT TUBB U1 U2 U3 U6 U7 VHL
VN1R11P VN1R12P VN1R13P VN1R14P XRN2 XRRA1 XXbac-BPG181B23.4 XXbac-BPG181B23.6 XXbac-
BPG248L24.11 XXbac-BPG248L24.12 XXbac-BPG27H4.7 XXbac-BPG308K3.6 XXyac-YR14BB7.1 XXyac-
YX60D10.1 Y_RNA Z99716.2 ZBTB24 ZDHHC20P2 ZNF133 ZNF322A ZNF414

PANTHER analysis: 120 mapped ids are found, 237 mapped ids are not found.

There are similarities between ER positive invasive breast disease (n=4/9) and ER positive pure DCIS (n=8/8).

1. p-values < 0.05;
2. A gene list is mapped from 34 genomic regions found on chromosomes 3, 4, 5, 7, 8, 10, 11, 12, 15, 17, 18, 19;
3. These regions encompass 470 genes altered in ER positive invasive breast disease;

Genes:

5S_rRNA AAAS ABHD14A ABHD14B AC002347.1 AC002481.5 AC005323.1 AC008021.1 AC008590.1 AC009271.1
AC009704.1 AC009779.1 AC010297.1 AC011260.2 AC011385.1 AC011385.3 AC012379.1 AC012379.2 AC013558.1 AC015689.1
AC021066.1 AC022031.1 AC023055.2 AC023509.1 AC025165.2 AC025165.7 AC025165.8 AC026689.1 AC040963.1 AC044839.1
AC044839.2 AC055715.1 AC068473.1 AC068888.1 AC068987.1 AC068988.1 AC069209.1 AC073573.1 AC078778.1 AC078864.1
AC079600.1 AC087893.3 AC090398.1 AC090666.1 AC091103.1 AC091551.1 AC091934.1 AC091934.2 AC097359.1 AC097359.2
AC097359.3 AC099557.1 AC100783.1 AC103681.1 AC103681.2 AC104186.1 AC104448.1 AC104850.1 AC105105.1 AC105316.1
AC107016.1 AC107016.2 AC112205.1 AC112215.2 AC112215.4 AC116904.1 AC116917.2 AC126118.1 AC126118.2 AC132217.4
AC156455.1 AC190387.1 ACACB ACVR1B ACVRL1 ACY1 ALAS1 ALDOAP1 ALKBH2 ALPK2 AMHR2
ANAPC5 ANKRD33 AP005273.1 AP006288.1 ARHGEF3 ATCAY ATF7 ATP5G2 ATP9B ATRIP
ATXN2 ATXN7 B4G ALNT1 BAP1 BCL7A BIN2 BLOC1S1 BMP3 C11orf94 C12orf10 C12orf44
C18orf26 C18orf54 C18orf55 C3orf45 C3orf49 C3orf63 C3orf78 C4orf22 C4orf39 CACNA2D2 CACNA2D3
CAMKK2 CAMP CBX5 CCDC51 CCDC66 CCDC72 CCDC99 CCNG1 CCR8 CD63
CDC25A CELA1 CHST11 CNDP1 CNDP2 COPZ1 CPE CRY2 CSAD CSRNP1
CSRNP2 CTB-164L20.1 CTB-95B16.1 CTD-3211M3.1 CTDP1 CTNNA1 CUX2 CX3CR1
CYB561D2 CYB5A DAO DAPK3 DAZAP2 DCD DCTN2 DNAH1 DNAJC14 DOCK2 DTX3
DUSP7 DYM EEF1A1P24 EEF2 EIF1B EIF4B EIF4E1B ENTPD3 ESPL1 ETF1
FAF2 FAM109A FAM196B FAM69C FBLL1 FBXW12 FGFR4 FHIT GABRG2 GALNT6
GAS7 GDF11 GK3P GLP2R GLYCAM1 GLYCTK GNAI2 GOLGA4 GPR84 GPRIN1
GRASP GRP GTSF1 GYLTL1B HIGD1C HIGD1DP HMMR HNRNPA1 hsa-let-7g hsa-mir-103-1
hsa-mir-122 hsa-mir-135a-1 hsa-mir-148b hsa-mir-1979 hsa-mir-2115 hsa-mir-218-2 hsa-mir-483 hsa-mir-578 hsa-mir-637
HSPA9 HYAL1 HYAL2 HYAL3 IFRD2 IGF2 IGF2AS IGFBP6 IL31 INS
ITGA5 ITGA7 ITGB1BP3 ITGB7 KDM2B KIF5A KLHL2 KRT1 KRT2 KRT3 KRT4
KRT5 KRT6A KRT6B KRT6C KRT7 KRT71 KRT72 KRT73 KRT74 KRT75 KRT76 KRT77
KRT78 KRT79 KRT8 KRT80 KRT81 KRT82 KRT83 KRT84 KRT85 KRT86
LACRT LETMD1 LMO1 LRRC43 LRRFIP2 MAP2K2 MAP3K12 MAPK8IP1 MAT2B MBD2
METTL7B MEX3C MFSD5 MIP MLH1 MLXIP MMP19 MXI1 MYH1 MYH13 MYH2 MYH4
MYH8 MYRIP NACA3P NAT6 NCKAP1L NDUFB1P1 NEDD4L NEFL NEFM NFATC1 NFE2
NISCH NME6 NPFF NR4A1 NSD1 NT5DC2 NUDCD2 OR10P1 ORMDL2 P2RX4
P2RX7 PANK3 PBRM1 PCBP2 PCBP4 PCDH24 PDE1B PDZRN4 PEX16 PFDN5 PHF21A PHF7
PIAS4 PLXNB1 POLI POU6F1 PPM1M PPP1R1A PPTC7 PRDM11 PRICKLE1 PRKG2
PRR13 PSMD9 RAD9B RAPGEF2 RARG RARS RASSF1 RCVRN RDH5 RNF34
RNF44 RP11-100N20.1 RP11-1029M24.1 RP11-1029M24.2 RP11-138A23.1 RP11-138A23.2
RP11-153F5.1 RP11-155D18.11 RP11-168J18.4 RP11-168J18.6 RP11-219C20.1
RP11-241K18.1 RP11-241K18.2 RP11-24C3.2 RP11-25I15.1 RP11-285B24.1 RP11-294O2.2
RP11-330H6.5 RP11-331G2.4 RP11-366M4.1 RP11-366M4.11 RP11-366M4.12 RP11-366M4.13
RP11-366M4.14 RP11-366M4.15 RP11-366M4.17 RP11-366M4.2 RP11-366M4.3
RP11-366M4.4 RP11-366M4.5 RP11-366M4.6 RP11-366M4.8 RP11-391M1.2
RP11-391M1.3 RP11-416A17.1 RP11-438N5.1 RP11-462C21.1 RP11-469O11.2
RP11-502L5.2 RP11-504H5.1 RP11-50F24.3 RP11-51O17.1 RP11-528N21.2 RP11-528N21.3
RP11-541P9.3 RP11-554O1.1 RP11-644A7.1 RP11-727C1.1 RP11-834C11.3
RP11-834C11.4 RP11-834C11.5 RP11-834C11.6 RP11-834C11.7 RP11-834C11.8
RP11-972K6.1 RP5-1157M23.2 RPL14 RPL29 RPSA RRM1 SARNP SC4MOL
SCN8A SEC11C SEMA3B SEMA3E SEMA3G SH2B3 SHC4 SIL1 SLC11A2 SLC25A38
SLC26A10 SLC35C1 SLC38A3 SLC4A8 SLIT3 SMAD4 SMAGP SMNDC1 SMUG1 SNCB
SNORA30 SNORA62 SNORA64 SNORD28 SNORD37 SNORD63 snoU13 SOAT2 SOCS6 SP1 SP7
SPATA12 SPINK8 SPRYD3 STAB1 STARD6 STIM1 SVOP SYT13 TARBP2 TCF4
TCTN1 TENC1 TFCP2 THOC7 TIMELESS TLR9 TMEM115 TMEM192 TNNC1 TP53I11
TRIM60 TRIM61 TRIM75 TSPAN18 TTC21A TUSC2 TUSC4 TWF2 TXNL1 U1 U4 U5

U6 U6atac U7 U73166.1 U73166.2 U73167.7 U73169.1 UNG USP30 WDR51A
WDR66 WDR7 WDR82 WWC1 XIRP1 Y_RNA ZBTB7A ZMYND10 ZNF346 ZNF385A ZNF407
ZNF589 ZNF619 ZNF620 ZNF621 ZNF740

PANTHER analysis: 285 mapped ids are found, 185 mapped ids are not found.

5.8.6 Copy Number Aberrations for All Oestrogen Receptor Positive DCIS Compared to Oestrogen Receptor Positive Invasive Breast Disease

These series examines the difference between all oestrogen receptor positive DCIS (i.e. both pure and that associated with invasion) and oestrogen receptor positive invasive breast disease.

Frequency plots showing copy number aberrations between oestrogen receptor positive DCIS and oestrogen receptor positive invasive breast disease were provided by Breakthrough Breast Cancer/Research Oncology, King's College London Bioinformatics Department (Figure 39).

Figure 39: Frequency plots showing copy number aberrations between oestrogen positive DCIS and oestrogen positive invasive breast disease (amplifications, duplications, gains, Sc gains, losses, total losses CdLOH and CnLOH,) (pages 209-212).

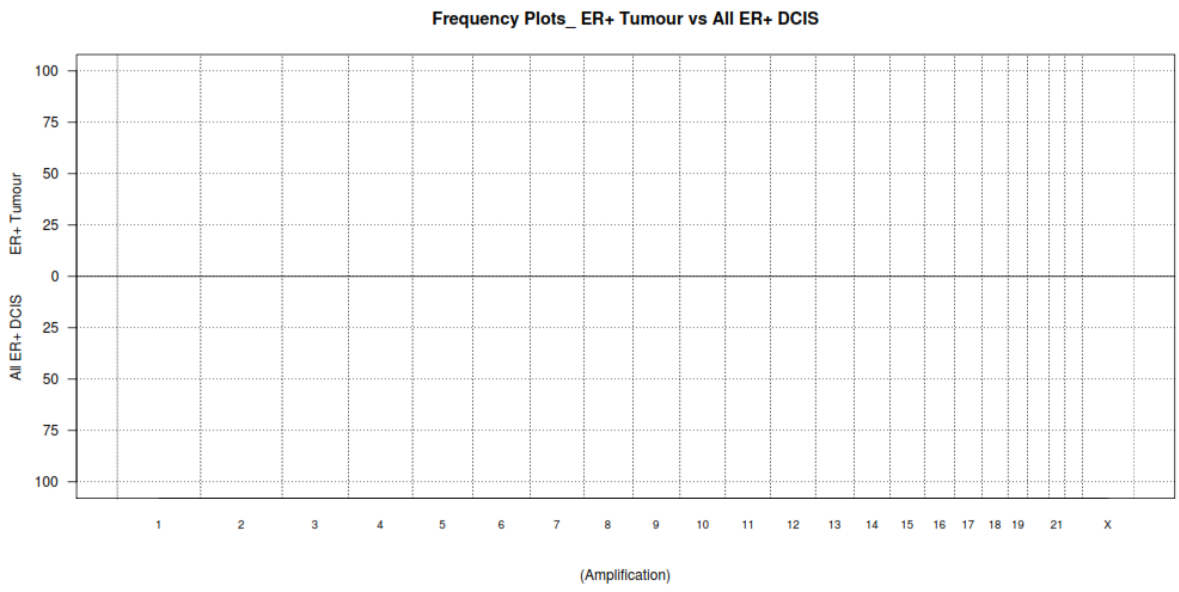
Frequency Plots_ ER+ Tumour vs All ER+ DCIS
ER+ Tumour
All ER+ DCIS
100
75
50
25
0
25
50
75
100
1
2
3
4
5
6
7
8
9
10
11
12
13
14
15
16
17
18
19
21
X
(Amplification)

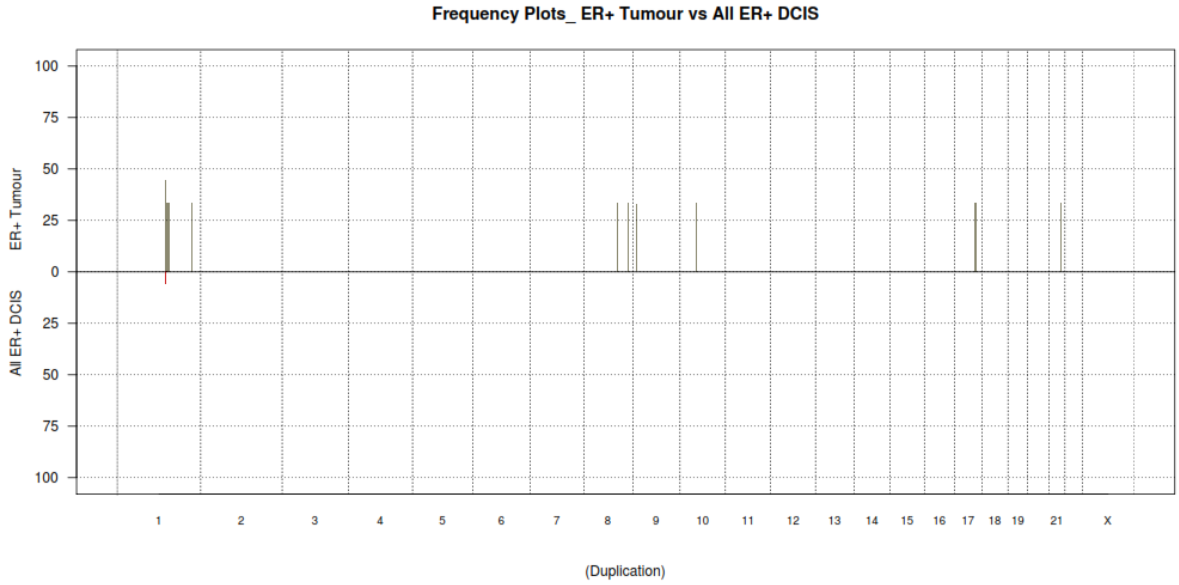
Frequency Plots_ ER+ Tumour vs All ER+ DCIS
ER+ Tumour
All ER+ DCIS
100
75
50
25
0
25
50
75
100
1
2
3
4
5
6
7
8
9
10
11
12
13
14
15
16
17
18
19
21
X
(Duplication)

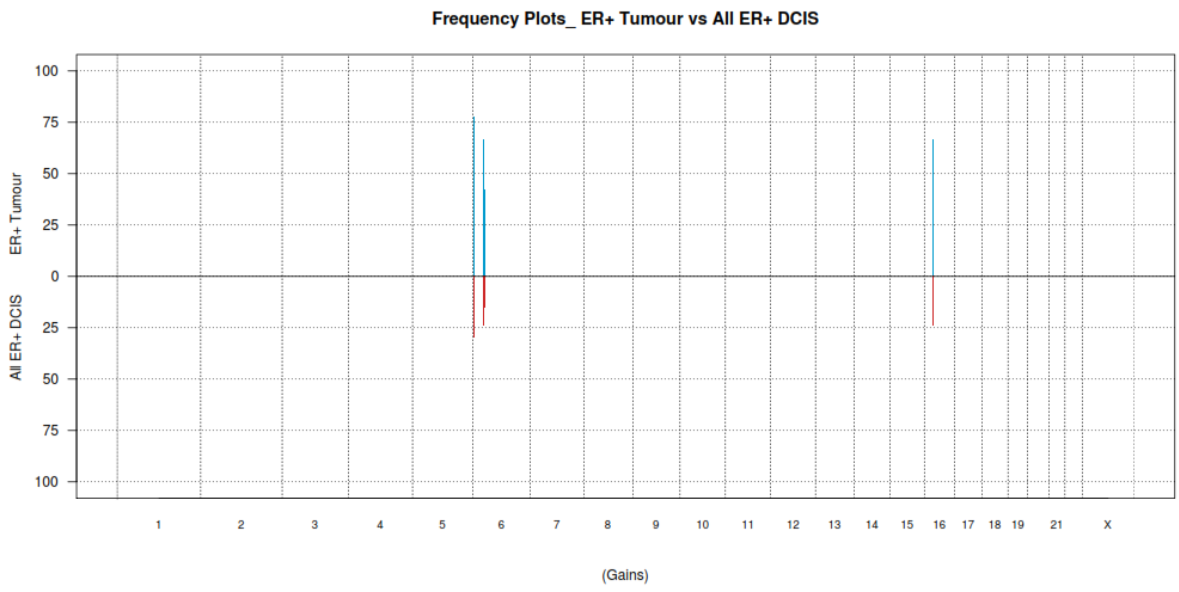
Frequency Plots_ ER+ Tumour vs All ER+ DCIS
ER+ Tumour
All ER+ DCIS
100
75
50
25
0
25
50
75
100
1
2
3
4
5
6
7
8
9
10
11
12
13
14
15
16
17
18
19
21
X
(Gains)

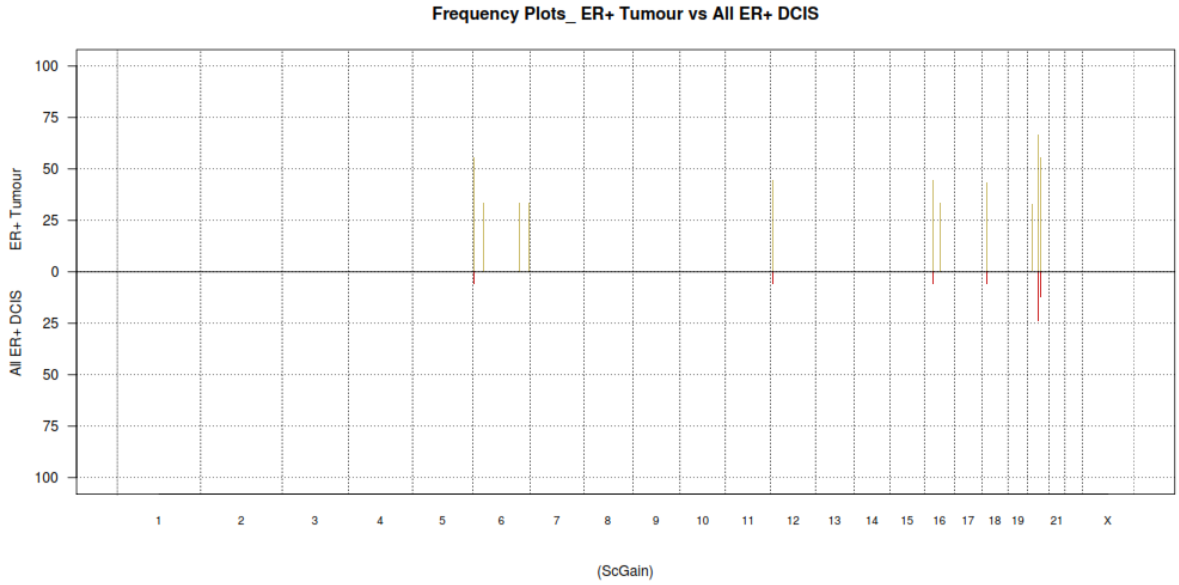
Frequency Plots_ ER+ Tumour vs All ER+ DCIS
ER+ Tumour
All ER+ DCIS
100
75
50
25
0
25
50
75
100
1
2
3
4
5
6
7
8
9
10
11
12
13
14
15
16
17
18
19
21
X
(ScGain)

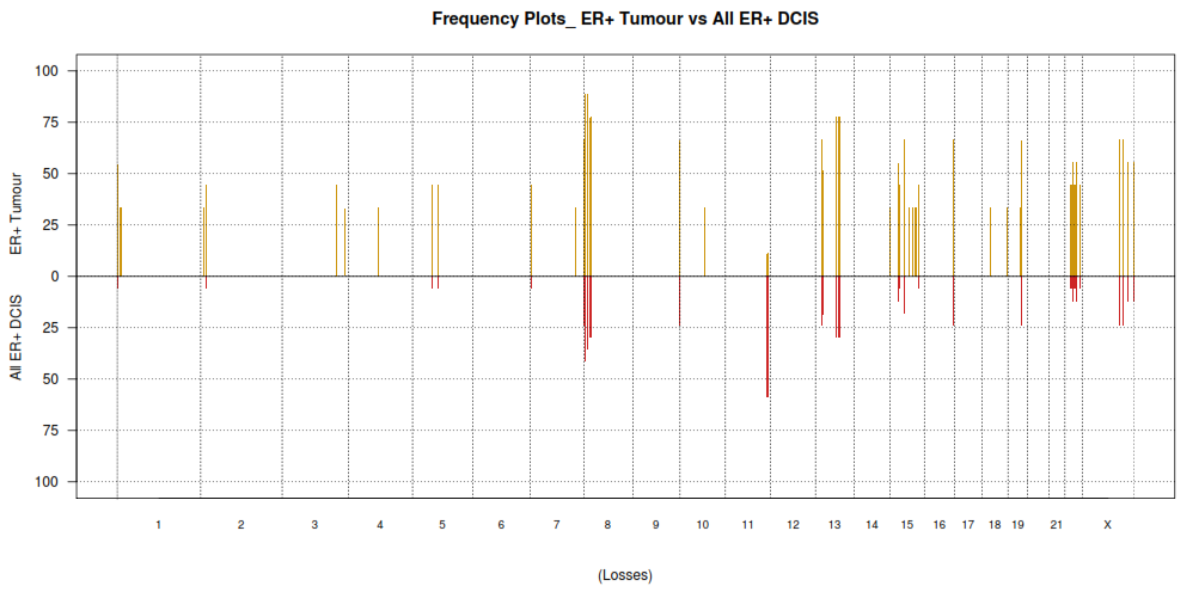
Frequency Plots_ ER+ Tumour vs All ER+ DCIS
ER+ Tumour
All ER+ DCIS
100
75
50
25
0
25
50
75
100
1
2
3
4
5
6
7
8
9
10
11
12
13
14
15
16
17
18
19
21
X
(Losses)

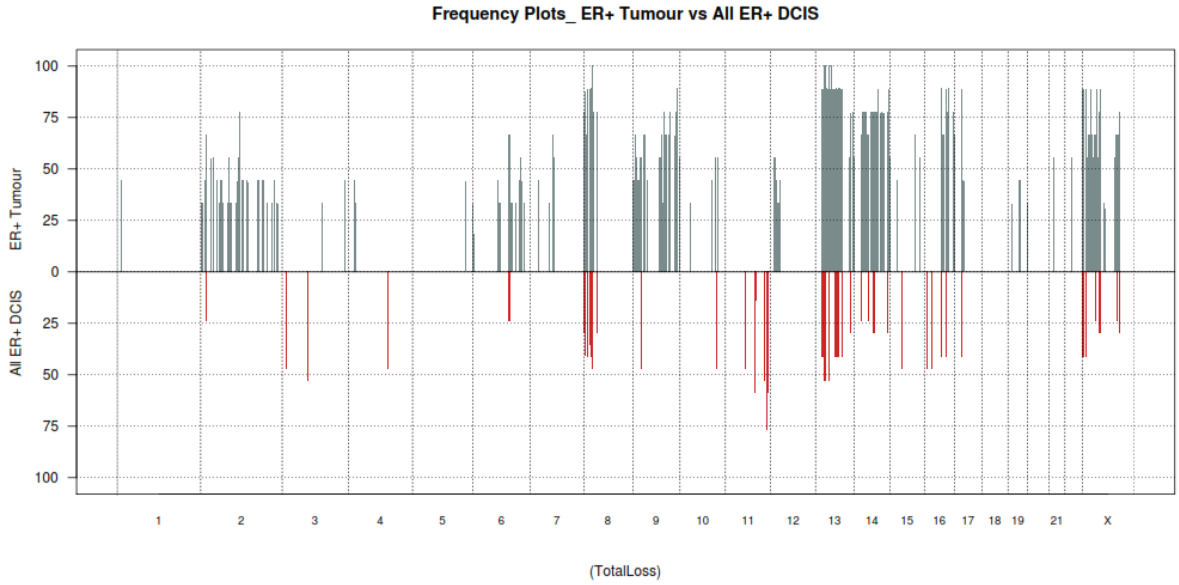
Frequency Plots_ ER+ Tumour vs All ER+ DCIS
ER+ Tumour
All ER+ DCIS
100
75
50
25
0
25
50
75
100
1
2
3
4
5
6
7
8
9
10
11
12
13
14
15
16
17
18
19
21
X
(TotalLoss)

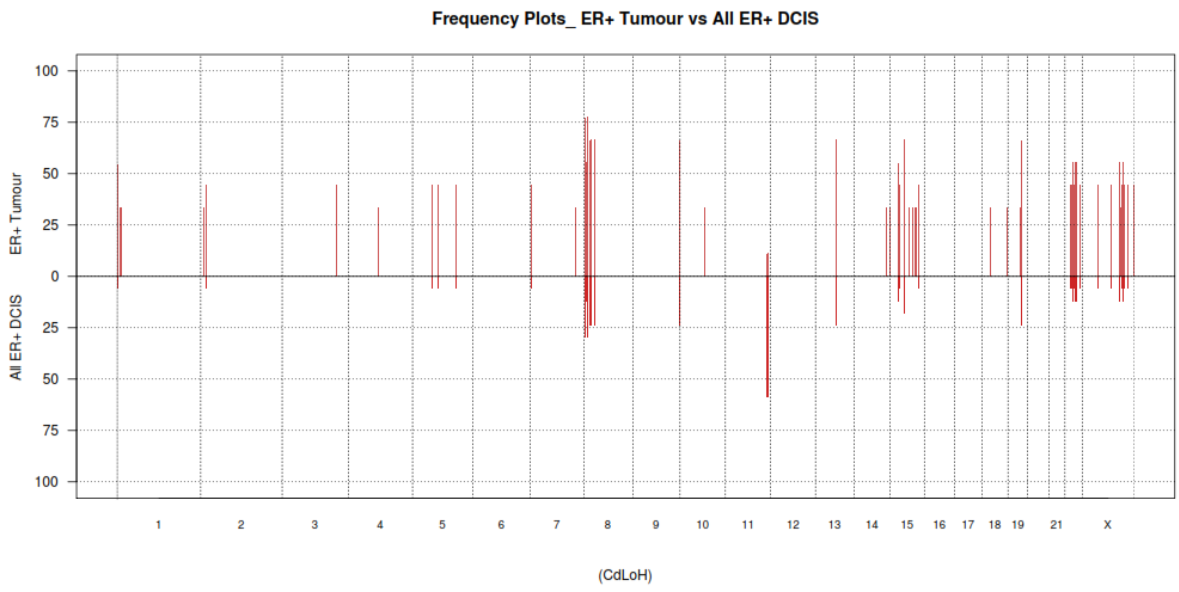

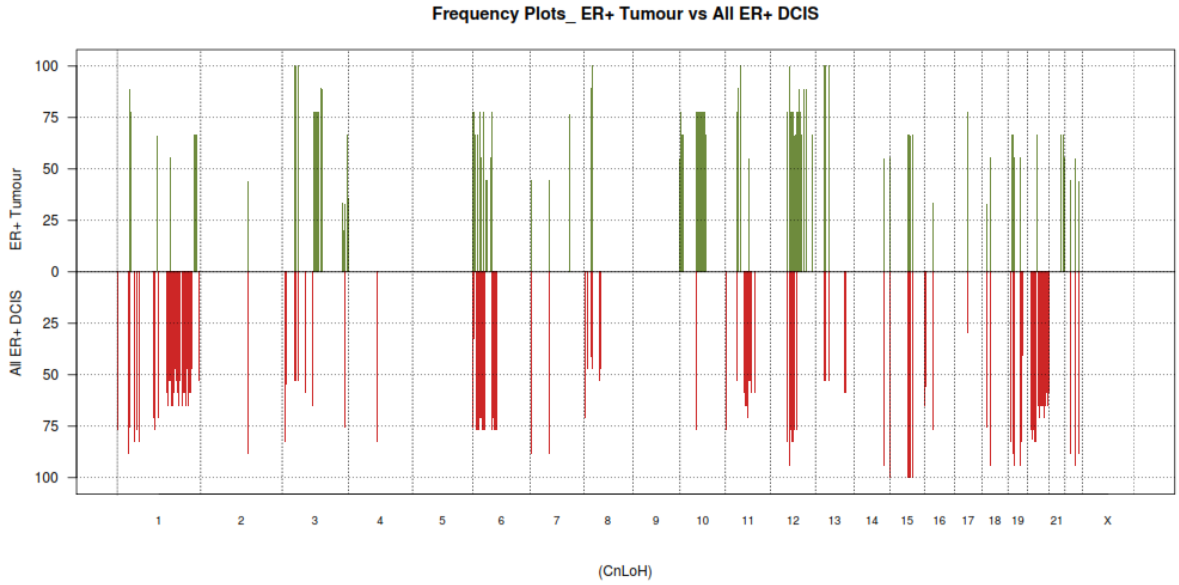

5.8.6.1 Amplification in Oestrogen Receptor Positive DCIS Compared to Oestrogen Receptor Positive Invasive Breast Disease

No amplifications in either ER positive DCIS or ER positive invasive breast disease are found in this series.

5.8.6.2 Duplication in Oestrogen Receptor Positive DCIS Compared to Oestrogen Receptor Positive Invasive Breast Disease

There are some overlaps in the duplications present in ER positive DCIS (n=4/17) and in ER positive invasive breast disease (n=1/9).

1. p-values < 0.05;
2. A gene list is mapped from 2 genomic regions on chromosome 1;
3. These regions encompass 18 genes altered in ER positive DCIS and some ER positive invasive breast disease;

Genes:

AL592307.2 HFE2 TXNIP POLR3GL ANKRD34A LIX1L RBM8A GNRHR2 PEX11B ITGA10 ANKRD35 PIAS3 RP11-458D21.2 RP11-458D21.1 RP11-315I20.1 RP11-315I20.3 U1 PDE4DIP

PANTHER analysis: 12 mapped ids are found, 6 mapped ids are not found.

There are duplications found in ER positive invasive disease (n=4/9) not present in ER positive DCIS (n=0/17).

1. p-values < 0.05;
2. A gene list is mapped from 17 genomic regions found on chromosomes 1, 8, 9, 10, 17, 21;
3. These regions encompass 255 genes altered in ER positive invasive breast disease;

Genes:

ADAM15 5S_rRNA 7SK AC046185.1 AC046185.2 AC110921.1 ADAR AF216667.1 AL359758.1 AL589764.2 AL589765.1 AL589986.2 AL590431.1 AL590431.2 AL590431.3 AL590666.2 AL591893.1 AL591893.2 AL591893.3 AL592307.1 AL592492.2 AL606500.1 AL713999.1 ANTXRL AP000304.12 AP000313.1 AP000313.2 AP000569.2 AP000569.8 APOA1BP AQP10 ASH1L ATP5O ATP8B2 BCAN BCL9 C1orf104 C1orf189 C1orf230 C1orf43 C1orf46 C1orf61 C1orf68 CAPN2 CCDC47 CCT3 CGN CHD1L CHRNB2 CKS1B CLK2 CRABP2 CRCT1 CRNN DAP3 DCST1 DCST2 DDX42 DPM3 EFNA1 EFNA3 EFNA4 FAM189B FDPS FLAD1 FLG FLG2 FTSJ3 GABPB2 GBA GBAP GPATCH4 HAPLN2 HAX1 HCN3 HDHD1CP HELZ HRNR hsa-mir-190b hsa-mir-548d-2 hsa-mir-554 hsa-mir-555 hsa-mir-9-1 hsa-mir-92b IL6R IQGAP3 ITSN1 KCNH6 KCNN3 KPRP KRTCAP2 LCE1D LCE1E LCE1F LCE2A LCE2B LCE2C LCE2D LCE3A LCE3B LCE3C LCE3D LCE3E LCE4A LCE5A LELP1 LENEP LIMD2 LINGO4 LOR LRRC6 LYSMD1 MAP3K3 MEF2D MLLT11 MRPL9 MSTO1 MTX1 MTX1P1 MUC1 NBPF10 NBPF15 NBPF16 NES NOTCH2NL NUP210L OAZ3 OR13Z1P

PBXIP1 PGLYRP3 PGLYRP4 PI4KB PIP5K1A PITPNC1 PKLR PMVK POGZ PRR9
PSMB4 PSMC5 PSMD12 PSMD4 PTPRD PYGO2 RAG1AP1 RFX5 RHBG RP11-107M16.2 RP11-126K1.2
RP11-126K1.6 RP11-126K1.8 RP11-139I14.2 RP11-201K10.1 RP11-21N7.2 RP11-21N7.6
RP11-21N7.7 RP11-243J18.2 RP11-263K19.4 RP11-263K19.6 RP11-274N19.2
RP11-284F21.5 RP11-284F21.7 RP11-289I10.1 RP11-289I10.2 RP11-292F22.2
RP11-292F22.3 RP11-29H23.1 RP11-29H23.2 RP11-29H23.4 RP11-29H23.5
RP11-29H23.6 RP11-307C12.11 RP11-316M1.11 RP11-337C18.4 RP11-350G8.3
RP11-350G8.4 RP11-350G8.5 RP11-350G8.7 RP11-404E16.1 RP1-140J1.1 RP1-140J1.4
RP11-441L11.1 RP1-14N1.2 RP11-540D14.6 RP11-540D14.8 RP11-61L14.2 RP11-61L14.6
RP11-666A1.1 RP11-666A1.2 RP11-666A1.3 RP11-666A1.4 RP11-666A1.5
RP11-66D17.3 RP11-66D17.5 RP11-68I18.2 RP11-74C1.2 RP11-74C1.4 RP11-763B22.2
RP11-763B22.3 RP11-763B22.4 RP11-89F3.2 RP11-89F3.3 RP11-98D18.1 RP11-98D18.2
RP11-98D18.3 RP11-98D18.7 RP11-98D18.9 RP11-98G7.1 RP1-43O17.1 RP1-43O17.2
RP1-52J10.9 RP1-91G5.1 RP1-91G5.3 RPTN RUSC1 SCAMP3 SCNM1 SEC22B SELENBP1 SEMA6C
SHC1 SHE SMARCD2 SNORA44 SNORA58 SNORA8 SNORD59 snoU13 SNX27 STRADA
TACO1 TCAM1 TCHH TCHHL1 TDRD10 TDRKH THBS3 TMEM71 TMOD4 TNFAIP8L2
TNRC4 TPM3 TRIM46 TTC24 TUFT1 U2 U6 U7 UBAP2L UBE2Q1 VPS72
Y_RNA YY1AP1 ZBTB7B ZNF687

PANTHER analysis: 137 mapped ids are found, 118 mapped ids are not found.

5.8.6.3 Genomic Gains in Oestrogen Receptor Positive DCIS Compared to Oestrogen Receptor Positive Invasive Breast Disease

There were gains present in both ER positive DCIS (n=5/17) and ER positive invasive breast disease (n=7/9) with considerable overlap in this series.

1. p-values < 0.05;
2. A gene list is mapped from 3 genomic regions found on chromosomes 6, 16;
3. These regions encompass 16 genes altered in both ER positive DCIS and ER positive invasive breast disease;

Genes:

AC106739.1 AL031963.1 AL031963.2 AL031963.5 BPHL HLA-DQA1 HLA-DQB1 IL4R JMJD5 NSMCE1 RP1-40E16.11 RP1-40E16.8 RP1-40E16.9

PANTHER analysis: 10 mapped ids are found, 6 mapped ids are not found.

5.8.6.4 Genomic Sc Gains in Oestrogen Receptor Positive DCIS Compared to Oestrogen Receptor Positive Invasive Breast Disease

There are similar Sc gains in both ER positive DCIS (n=4/17) and ER positive invasive breast disease (n=6/9) in this series.

1. p-values < 0.05;
2. A gene list is mapped from 16 genomic regions found on chromosomes 6, 12, 16, 18, 20;
3. These regions encompass 63 genes altered in both ER positive invasive breast disease and ER positive DCIS;

Genes:

ASXL1 5S_rRNA ABCC11 AC106739.1 AC125494.2 AL031963.1 AL031963.2 AL031963.3 AL031963.5 AL121935.1 AL133343.1 ATN1 BPHL C12orf57 C20orf112 CD4 COPS7A EMG1 ENO2 FAM136B GNB3 GPR162 HLA-DQA2 HLA-DQB2 HLA-DQB3 hsa-mir-141 hsa-mir-200c IL4R JMJD5 LAG3 LEPREL2 LONP2 LRRC23 MACROD2 MLF2 NQO2 NSMCE1 PHB2 PTMS PTPN6 RIPK1 RP11-356I2.2 RP11-356I2.4 RP11-410N8.1 RP11-410N8.3 RP11-410N8.4 RP11-568A7.1 RP1-1J6.2 RP1-40E16.11 RP1-40E16.2 RP1-40E16.3 RP1-40E16.4 RP1-40E16.8 RP1-40E16.9 RP1-90J20.8 RP5-1184F4.5 snoU89 TCP10L2 TNFAIP3 TOP1 TUBB2A U47924.1 U7

PANTHER analysis: 30 mapped ids are found, 33 mapped ids are not found.

5.8.6.5 Losses in Oestrogen Receptor Positive DCIS Compared to Oestrogen Receptor Positive Invasive Breast Disease

There are similar losses in both ER positive DCIS (n=7/17) and ER positive invasive breast disease (n=8/9) in this series.

1. p-values < 0.05;
2. A gene list is mapped from 29 genomic regions found on chromosomes 1, 8, 13, 15, 16, 22, X;
3. These regions encompass 114 genes altered in both ER positive invasive breast disease and ER positive DCIS;

Genes:

5S_rRNA AC022716.1 AC039056.1 AP000351.4 AP000553.1 AP000555.1 ARHGEF10 ATXN8OS CCDC116 CLN8 CSMD1 CT45A1 CT45A2 CT45A3 CT45A4 DDT DLC1 EHMT1 EIF4A1P6 F8A3 GANC GFRA2 GSTT1 GSTT2 GSTTP1 H2AFB3 hsa-mir-1184 hsa-mir-130b hsa-mir-301b hsa-mir-596 hsa-mir-627 JPH3 KB-1027C11.4 KLHL1 LARGE MAPK1 MRRFP PAK3 PLA2G4D PLA2G4E PLA2G4F PPIL2 PRKCZ RP11-110K18.2 RP11-206H15.2 RP11-218L14.4 RP11-264J4.5 RP11-264J4.6 RP11-520F24.1 RP11-520F24.2 RP11-520F24.3 RP11-521H3.1 RP11-77P3.1 RP11-954J6.3 RP13-36C9.4 RP13-36C9.5 RP5-1168A5.1 RP5-1170D6.1 RP5-964N17.1 SDF2L1 TDRD3 TMEM87A TMLHE TOP3B U3 U6 UBE2L3 VPS39 Y_RNA YDJC YPEL1 ZMYM2

PANTHER analysis: 35 mapped ids are found, 37 mapped ids are not found.

5.8.6.6 Total Loss in Oestrogen Receptor Positive DCIS Compared to Oestrogen Receptor Positive Invasive Breast Disease

There were total losses present in ER positive DCIS (n=13/17) not observed in ER positive invasive breast disease (n=0/9).

1. p-values < 0.05;
2. A gene list is mapped from 29 genomic regions found on chromosomes 3, 4, 8, 9, 10, 11, 13, 15, 16;
3. These regions encompass 60 genes altered in ER positive DCIS;

Genes:

7SK AC025678.1 AC090947.1 AC108056.1 AC133041.1 AL596092.1 AP000720.1 AP001482.1 AP001970.1 ATP8A2 CEP164 CTD-2026G6.1 CTD-2026G6.2 DSCAML1 ERN2 GRM5 hsa-mir-1324 LHFP MTUS2 NEFL NEFM NOX4 NUPL1 OR10D1P OR10D3P OR10V1 OR8B1P OR8B2 OR8B3 OR8B4 OR8C1P OR8D1 OR8D2 OR8F1P OR8G2P OR8G5 OSBP PATL1 PLK1 PPARG RP11-206I15.2 RP11-241K7.1 RP11-241K7.2 RP11-351N4.3 RP11-413E6.1 RP11-413E6.2 RP11-413E6.3 RP11-468L18.1 RP11-527F15.1 RP11-642N14.3 RP11-803B1.1 RP11-803B1.2 RP11-803B1.3 RP11-803B1.4 SNORA31 TYR U6 U7 U8 VWA5A

PANTHER analysis: 22 mapped ids are found, 38 mapped ids are not found.

There were total losses present in ER positive invasive breast disease (n=9/9) not observed in ER positive DCIS (n=0/17).

1. p-values < 0.05;
2. A gene list is mapped from 23 genomic regions found on chromosomes 9, 13, 14, 16, X;
3. These regions encompass 120 genes altered in ER positive invasive breast disease;

Genes: 5S_rRNA AC002504.1 AC112778.1 AC112778.2 AL136001.1 AL136359.1 AL138690.1 AL139082.1 AL162377.1 AL162377.2 AL163544.1 AL355611.1 AL355611.2 AL355611.3 AL356863.1 AL359180.1 AL391384.1 AL442203.2 AL450423.1 AL512362.1 AL590007.2 ARX ASPG ATP7B ATXN8OS C13orf23 C13orf34 C13orf36 C13orf37 C14orf180 CCDC70 CCNA1 DACH1 DGKH DIS3 DUSP21 FOXO1 FREM2 FREQ HMCN2 hsa-mir-203 hsa-mir-759 KDM6A KIAA0564 KIF26A KLF12 KLF5 KLHL1 NEK3 NEK5 NHLRC3 OLFM4 PCDH8 PIBF1 POLA1 RP11-117N4.1 RP11-11C5.1 RP11-12I24.2 RP11-12I24.3 RP11-133M24.1 RP11-16D22.1 RP11-187A9.2 RP11-187A9.3 RP11-196I2.1 RP11-206H15.2 RP11-206L1.2 RP11-209P2.1 RP11-214O11.1 RP11-214O11.2 RP11-218I21.1 RP11-248G5.3 RP11-24H2.1 RP11-24H2.2 RP11-266E6.2 RP11-279N8.1 RP11-30C8.1 RP11-30C8.2

RP11-327P2.3 RP11-335N6.1 RP11-349O10.1 RP11-381L18.2 RP11-393H6.2 RP11-393H6.3 RP11-430K22.1 RP11-430K22.2 RP11-431O22.2 RP11-459J23.1 RP11-459J23.2 RP11-474L7.4 RP11-501G6.1 RP11-505F3.2 RP11-505F3.4 RP11-520F24.1 RP11-520F24.2 RP11-520F24.3 RP11-56M2.1 RP11-571G1.1 RP11-571G1.2 RP11-629O4.1 RP11-76N11.2 RP11-77P3.1 RP11-7B3.2 RP11-7B3.3 RP11-7B3.4 RP11-88G17.6 RP1-258N20.3 SNORA25 SNORA68 SNORA9 SNORD37 STOML3 TDRD9 TMEM179 TRPC4 U4 U6 U7 UFM1 UTP14C Y_RNA

PANTHER analysis: 31 mapped ids are found, 89 mapped ids are not found.

5.8.6.7 CdLOH in Oestrogen Receptor Positive DCIS Compared to Oestrogen Receptor Positive Invasive Breast Disease

There is similar CdLOH present in both ER positive DCIS (n=10/17) and ER positive invasive breast disease (n=7/9).

1. p-values < 0.05;
2. A gene list is mapped from 67 genomic regions found on chromosomes 1, 2, 5, 7, 8, 9, 11, 13, 15, 19, 22, X;
3. These regions encompass 215 genes altered in both ER positive DCIS and ER positive invasive breast disease;

Genes:

5S_rRNA 7SK AC000035.3 AC000041.8 AC002472.8 AC002472.9 AC004019.10 AC004019.16 AC004019.17 AC005300.5 AC006946.12 AC006946.15 AC008162.1 AC011890.1 AC019176.2 AC022613.1 AC022716.1 AC027807.1 AC039056.1 AC068286.1 AC074389.1 AC074389.6 AC074389.7 AC074389.9 AC090510.1 AC102941.1 AC103965.1 AC110781.3 AC110781.5 ACRV1 ADAMTSL3 ADRBK2 AIFM3 AL022323.1 AL121825.1 AL451005.1 AP000347.2 AP000350.10 AP000350.6 AP000350.7 AP000350.8 AP000351.3 AP000351.4 AP000553.1 AP000555.1 AP1B1 AP3B1 ATP1B4 BPIL2 C1GALT1C1 C22orf28 C22orf30 CCDC116 CDAN1 CECR1 CECR2 CECR3 CECR4 CECR5 CECR6 CFP CHEK1 CPXCR1 CSMD1 CT45A1 CT45A2 CT45A3 CT45A4 CT47B1 CTA-211A9.5 CTA-221G9.11 CTA-256D12.11 CTA-256D12.12 CTA-292E10.6 CTA-292E10.7 CTA-407F11.6 CTA-407F11.7 CTA-407F11.8 CTA-85E5.7 CTA-984G1.5 CTD-2037K23.1 CTD-2037K23.2 CTD-2254N19.1 CUL4B CXorf25 CXorf64 DDT DDTL DLC1 EFCAB6 EHMT1 EIF4A1P6 ELFN1 ELK1 EMID1 FAM189A1 FAM32B FAM70A FBXO7 GANC GFRA2 GRIA3 GSTT1 GSTT2 GSTT2B GSTTP1 HAUS2 HMGN2L9 HORMAD2 hsa-mir-130b hsa-mir-301b hsa-mir-627 IGLV10-67 IGLV1-62 IGLVI-63 IGLVIV-64 IGLVIV-65 IGLVIV-66-1 IGLVV-66 IL17RA KB-1027C11.4 KIAA1671 LAMP2 LARGE LL22NC03-23C6.15 LL22NC03-28H9.5 LRRC57 LZTR1 MAD1L1 MAPK1 MCTS1 MRRFP MTMR3 NEFH NF2 NIPSNAP1 PA2G4P1 PAK3 PATE1 PATE2 PDE4D PLA2G4D PLA2G4E PLA2G4F PNPLA5 PPIL2 PRAMEL PRKCZ RFPL1 RFPL1S RFPL3 RFPL3S RGL4 RHBDD3 RP11-137D19.1 RP11-442I12.1 RP11-45J1.1 RP1-149A16.12 RP1-149A16.15 RP1-149A16.16 RP1-149A16.17 RP1-149A16.3 RP11-521H3.1 RP1-212G6.4 RP1-222H5.1 RP1-302D9.2 RP1-302D9.3 RP1-302D9.4 RP1-302D9.5 RP1-30E17.1 RP1-30E17.2

RP13-36C9.4 RP13-36C9.5 RP3-388M5.8 RP3-393P12.1 RP4-655L22.2 RP4-655L22.4
RP5-1168A5.1 RP5-1170D6.1 RP5-964N17.1 SC22CB-1D7.1 SCAMP1 SDF2L1
SGSM1 SLC27A6 SNAP23 SNORA70 SNORD56 snoU13 STARD9 SULT4A1 SYN1 SYN3
TDRD3 THAP7 THOC5 TJP1 TMEM211 TMEM87A TOP3B TTBK2 TTC28 U3 U6
UBE2L3 UBR1 UXT VPS39 XXbac-B135H6.15 Y_RNA YDJC YPEL1 Z71183.1 ZBTB33
ZNRF3

PANTHER analysis: 96 mapped ids are found, 115 mapped ids are not found.

5.8.6.8 CnLOH in Oestrogen Receptor Positive DCIS Compared to Oestrogen Receptor Positive Invasive Breast Disease

There is CnLOH in ER positive DCIS (n 16/17) not observed in ER positive invasive breast disease (n=0/9).

1. p-values < 0.05;
2. A gene list is mapped from 36 genomic regions found on chromosomes 1, 3, 4, 12, 19, 20;
3. These regions encompass 85 genes altered in ER positive;

Genes:

Mar-02 5S_rRNA 7SK AC003111.1 AC003111.2 AC006128.1 AC008764.1 AC022506.2 AC024075.1 AC027667.1 AC027667.2
AC034193.1 AC099680.1 AGAP2 AK3L1 AKAP8 AKAP8L AL121988.1 BRD4 C19orf42 C19orf44
C1orf212 C3orf10 CALR3 CHERP CST1 CST2 CST4 CST5 CSTP1 CSTP2 CTD-2356P16.1
CYP2A13 CYP2F1 CYP2S1 DLGAP3 ELAVL4 EPHX3 GJA4 GJB3 GJB4 GJB5 GSTM3P
HNRNPM hsa-mir-1470 IRAK2 KIF5A MACROD2 MED26 NKX2-2 NKX2-4 NOTCH3 OS9 PGLYRP2
PIP4K2C PLK1S1 PRAM1 RASAL3 RP11-227D2.3 RP11-415I12.1 RP11-492I2.1 RP11-766N7.1
RP1-198K11.3 RP4-777D9.2 RP5-1177M21.1 RP5-872K7.2 RP5-872K7.7 RP5-984P4.1 RP5-984P4.4 RP5-997D16.2 RPL24P2 RPS15AP1 SLC35E1 snoU13 TBC1D30 TMEM38A U1
U6 U6atac VHL WIBG WIF1 WIZ XRN2 XXyac-YX60D10.1

PANTHER analysis: 42 mapped ids are found, 43 mapped ids are not found.

There is CnLOH present in ER positive invasive breast disease (n=9/9) not observed in ER positive DCIS (n=0/17).

1. p-values < 0.05;
2. A gene list is mapped from 16 genomic regions found on chromosomes 1, 3, 11, 12;
3. These regions encompass 60 genes altered in ER positive DCISv

Genes:

5S_rRNA AC012598.1 AC044839.1 AC044839.2 AC061999.1 AC092910.1 AC092910.2 AC103681.1 AC103681.2 AC117377.1
AC119795.1 ADPRHL2 ALX4 ANKS1B C11orf74 C11orf94 C3orf15 COL8A2 COX17 CRY1 CRY2 DCTN2
DDIT3 EIF2C3 EXT2 GAP43 GSK3B GYLTL1B hsa-mir-616 KIF5A LSAMP MAPK8IP1
MARS MBD6 MGAT4C MIP NR1I2 PEX16 PHF21A POPDC2 PRDM11 RAG1 RAG2
RP11-169N13.1 RP11-169N13.4 RP11-18H7.1 RP11-190C22.1 RP11-326J18.1 RP11-767L7.1
RP11-767L7.2 RP4-665N4.4 RP4-665N4.5 SLC35C1 SYT13 TEKT2 TIMELESS TP53I11
TRAF6 TSPAN18 U6

PANTHER analysis: 37 mapped ids are found, 23 mapped ids are not found

5.8.7 Copy Number Aberrations for Triple Negative DCIS Compared to Non Triple negative DCIS

This series examines the differences between pure triple negative DCIS and all other types of DCIS (e.g. ER+, HER2+) (pure and in the presence of invasive disease). Frequency plots showing copy number aberrations between TN DCIS and non TN DCIS are given in Figure 40.

Figure 40: Frequency plots for copy number aberrations for triple negative DCIS versus non triple negative DCIS (amplifications, duplications, gains, Sc gains, losses, total losses CdLOH and CnLOH, pages 220-223).

Frequency plots below show the relative copy number gains and losses for an entire sample set compared to its counterpart e.g. the first plot in Figure 36 shows amplification for all triple negative DCIS and invasive breast disease compared to all non triple negative DCIS and invasive breast disease in this series. The number on the y axis refers to the number of cases showing a genomic difference. The x axis refers to the chromosome number. The lower half of the y axis represents the non triple negative and the upper half the triple negative. Amplification on chromosome 8 is apparent on several regions for non triple negative DCIS and invasive breast disease and is also present at a lower frequency on fewer loci for triple negative DCIS

and invasive breast disease. Amplification is present on chromosomes 6 (n=24), 11(n=25) and 17 (n=26) for non triple negative DCIS and invasive breast disease but absent in triple negative DCIS and invasive breast disease.

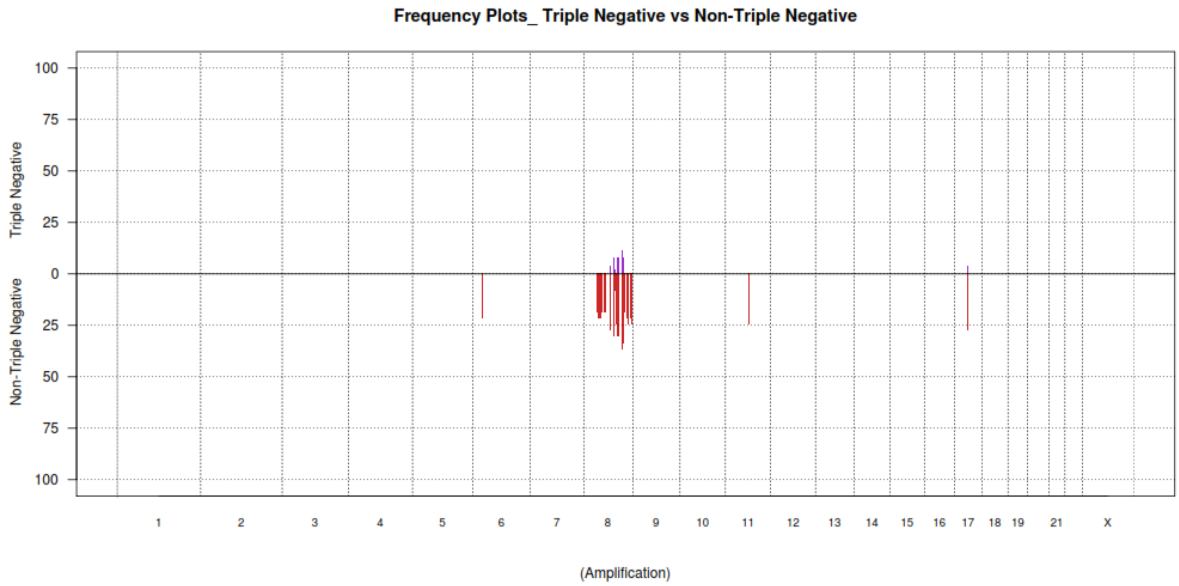

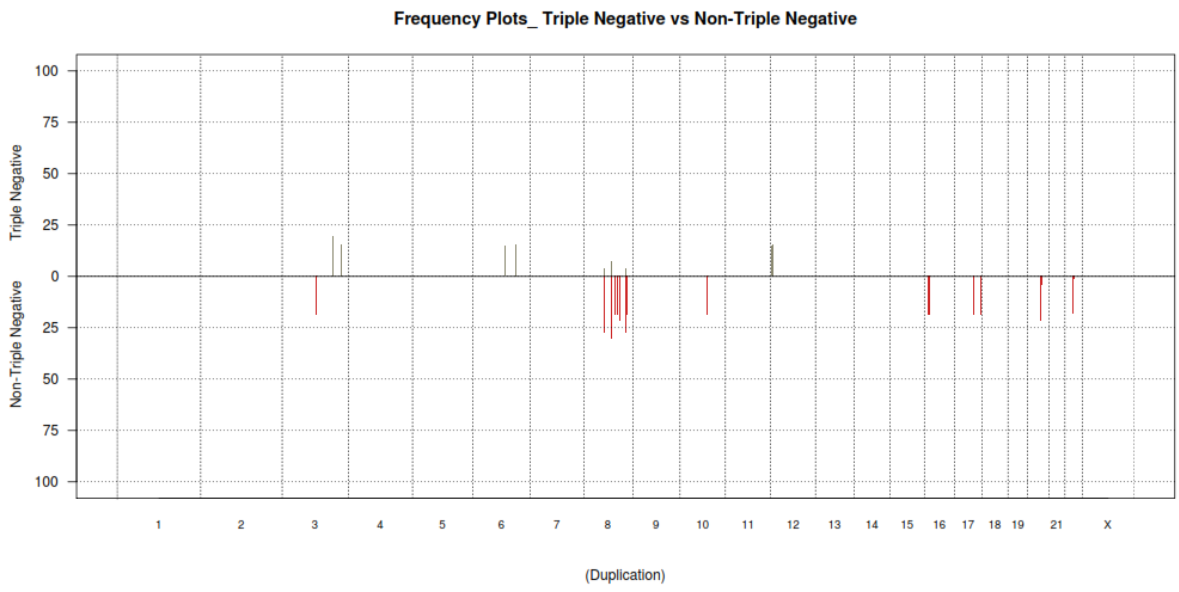
Frequency Plots_ Triple Negative vs Non-Triple Negative
Triple Negative
Non-Triple Negative
100
75
50
25
0
25
50
75
100
1
2
3
4
5
6
7
8
9
10
11
12
13
14
15
16
17
18
19
21
X
(Duplication)

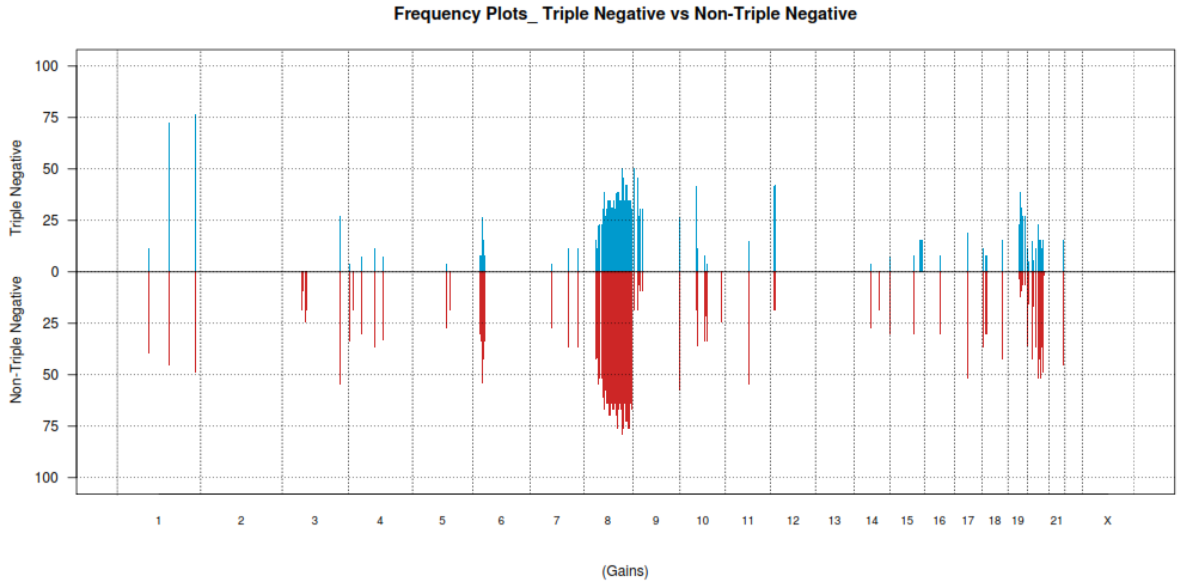
Frequency Plots_ Triple Negative vs Non-Triple Negative
Triple Negative
Non-Triple Negative
100
75
50
25
0
25
50
75
100
1
2
3
4
5
6
7
8
9
10
11
12
13
14
15
16
17
18
19
21
X
(Gains)

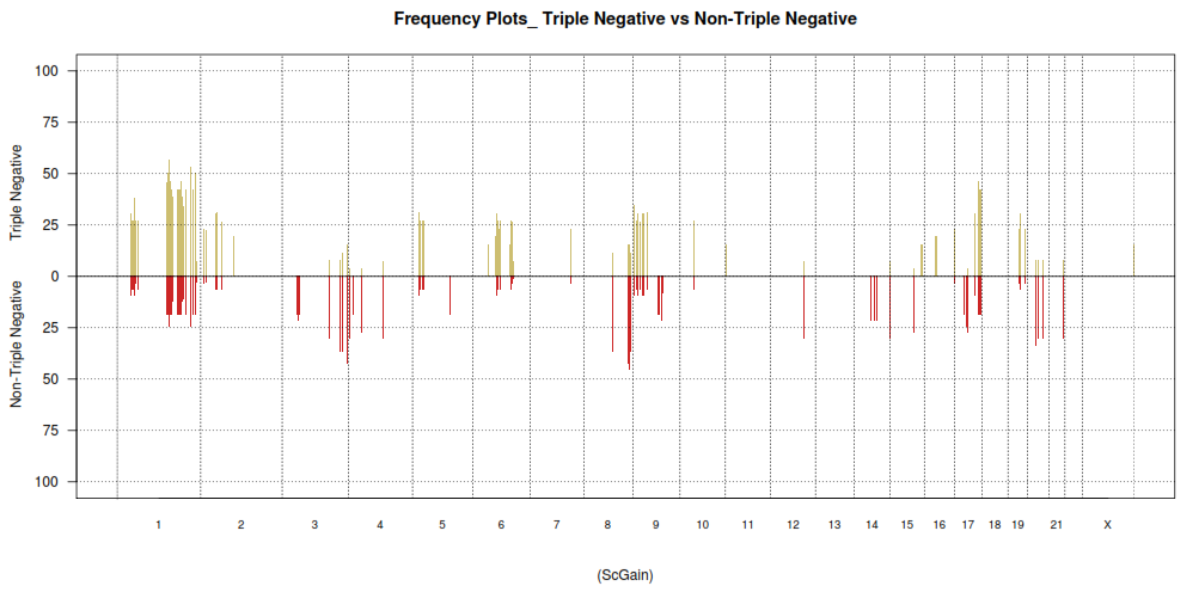
Frequency Plots_ Triple Negative vs Non-Triple Negative
Triple Negative
Non-Triple Negative
100
75
50
25
0
25
50
75
100
1
2
3
4
5
6
7
8
9
10
11
12
13
14
15
16
17
18
19
21
X
(ScGain)

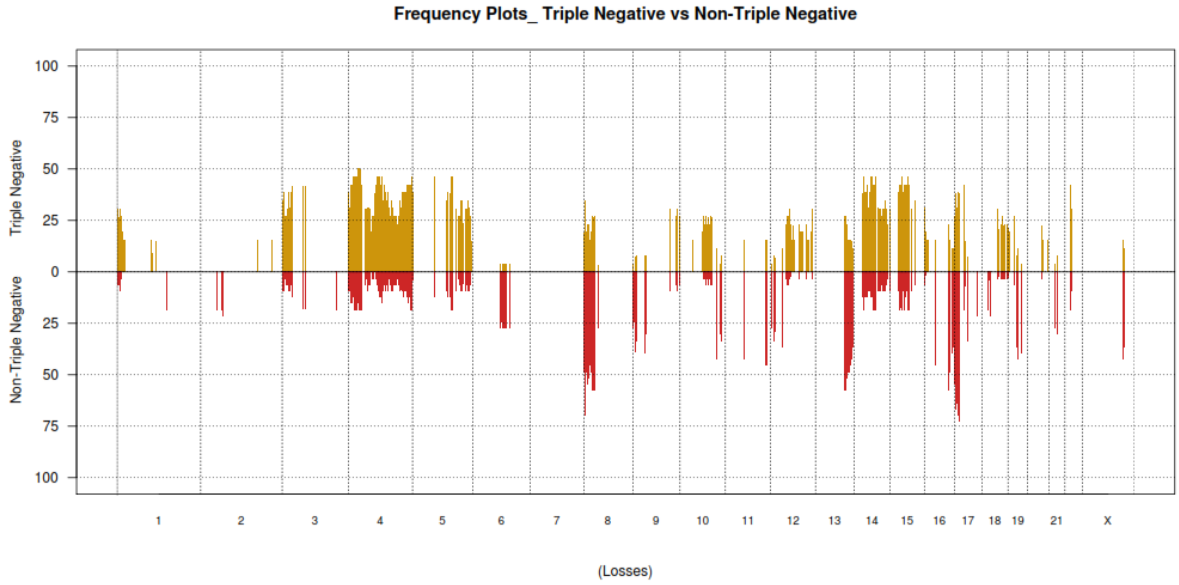
Frequency Plots_ Triple Negative vs Non-Triple Negative
Triple Negative
Non-Triple Negative
100
75
50
25
0
25
50
75
100
1
2
3
4
5
6
7
8
9
10
11
12
13
14
15
16
17
18
19
21
X
(Losses)

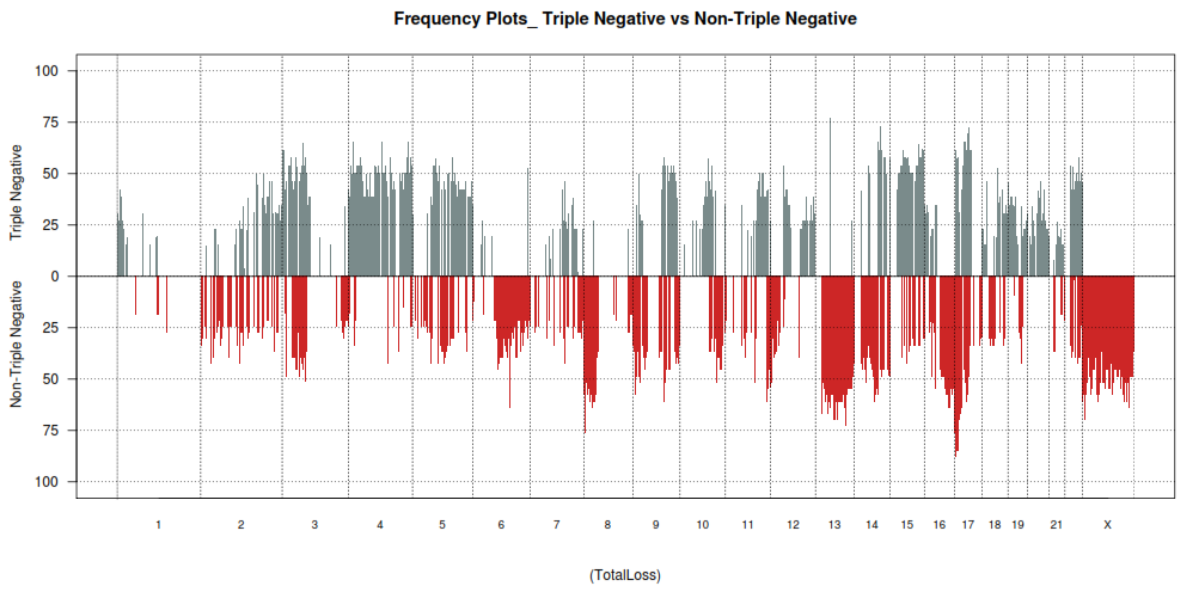
Frequency Plots_ Triple Negative vs Non-Triple Negative
Triple Negative
Non-Triple Negative
100
75
50
25
0
25
50
75
100
1
2
3
4
5
6
7
8
9
10
11
12
13
14
15
16
17
18
19
21
X
(TotalLoss)

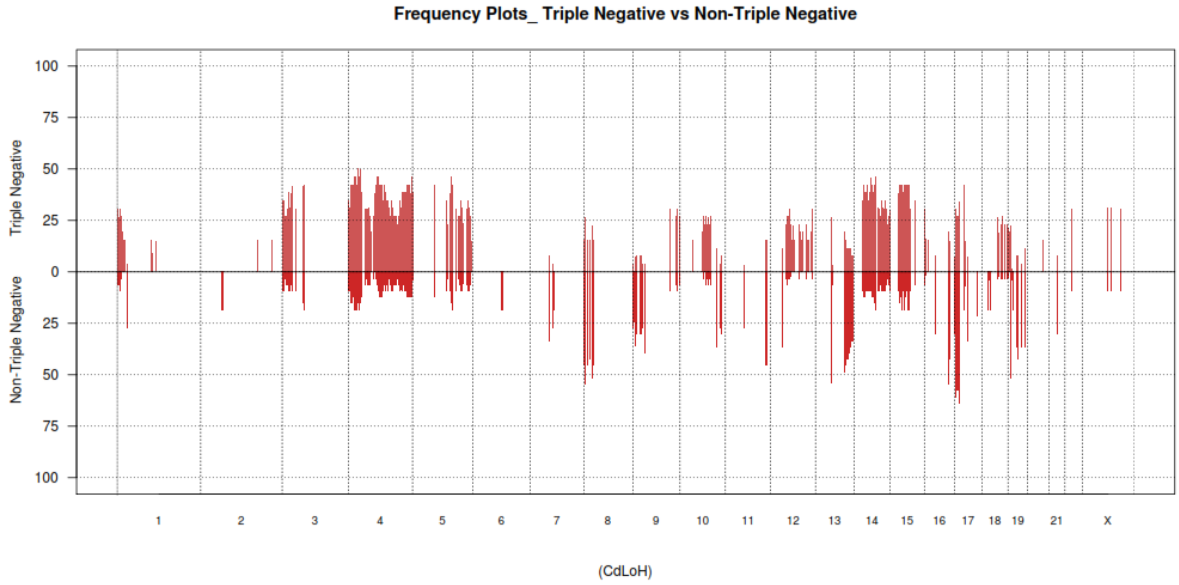
Frequency Plots_ Triple Negative vs Non-Triple Negative
Triple Negative
Non-Triple Negative
100
75
50
25
0
25
50
75
100
1
2
3
4
5
6
7
8
9
10
11
12
13
14
15
16
17
18
19
21
X
(CdLoH)

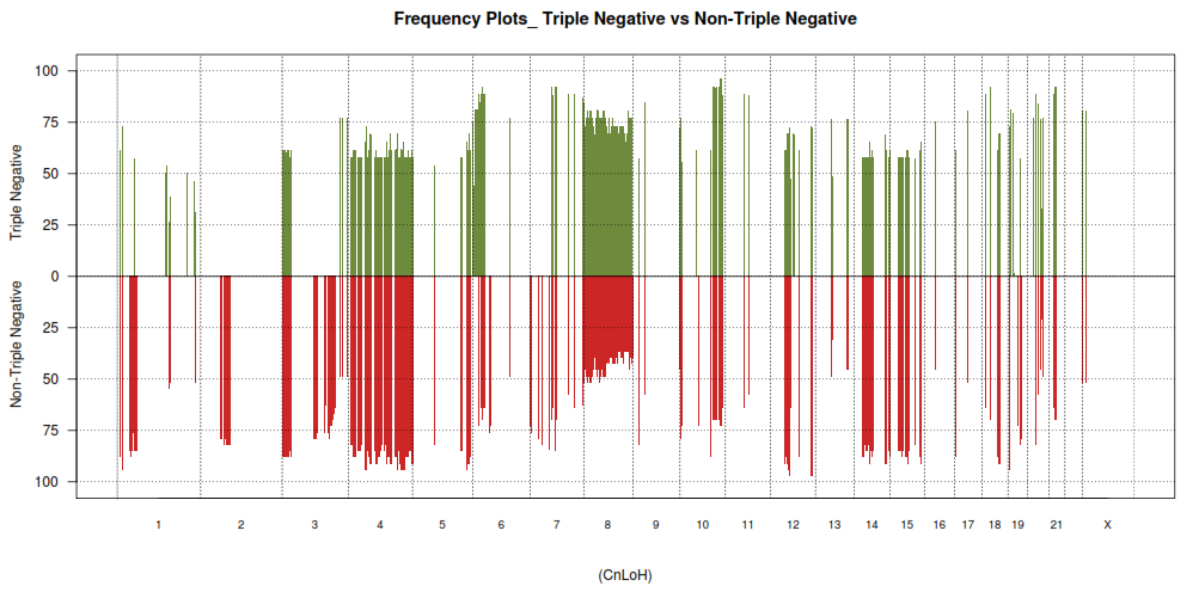

PANTHER Analysis is used to provide the following information the above copy number scenarios for all groups listed in sections 5.3.3 to 5.3.8

1. p-values- a significant p-value showing the genomic aberrations are not defined by chance and that the null hypothesis is correct, as an example – duplications found in triple negative DCIS compared to triple negative DCIS- a p-value of 0.5 showing that the there is a 5% chance that these duplication differences and found by random chance alone within our series.
2. The gene list mapped from different genomic regions on each chromosome. Each chromosome has been divided into overlapping genomic regions which are assessed for amplifications, duplications etc. Genes are identified in each region from different chromosomes. For each analysis the number of gene regions and chromosomes is given.

3. A list of genes is created from an online database (ESEMBL) and these genes are listed in the results section as gene ids.
4. The gene list (ids) are uploaded to the PANTHER analysis software, homo sapiens is the species genome selected and a functional analysis is requested. The Software provides a list of mapped genes with known biological, molecular and protein functions. Those genes entered into the software with established functions are returned as “mapped ids found” and those without are returned as “mapped ids not found”. The mapped ids are used to create pie charts showing biological processes, molecular functions and radar graphs for protein classes (representative charts and graphs are found in 5.3.7 the majority are stored on the accompanying disc.

Genomic data and subsequent PANTHER analysis for TN negative DCIS and non triple negative DCIS is given below.

5.8.7.1 Amplification in Triple Negative DCIS Compared to Amplification in Non Triple Negative DCIS

The comparison of amplifications in TN DCIS (n=3/26) compared to non TN DCIS (n=12/33) shows considerable overlap between those amplifications found in TN DCIS also found in non TN DCIS.

1. p-values < 0.05;
2. A gene list is mapped from 19 genomic regions found on chromosomes 6, 8, 11, 17;
3. These regions encompass 39 genes altered in TN DCIS and non TN DCIS; Genes:

AC107374.1 ADCY8 AF216667.1 CCND1 CEBPD CRKRS CSMD3 DENN DENND3 HIST1H2AB HIST1H3A HIST1H3B HIST1H4A HIST1H4B hsa-mir-151 IKBKB KIAA0146 KIAA1429 LRRC6 MYEOV ORAOV1 POLB PRKDC PTK2 PTK2 PTK2 PXDNL RP11-231D20.1 RP11697N18.1 SLC45A4 SNORA7 U6 U6

PANTHER analysis: 19 mapped ids found, 10 mapped ids are not found.

Amplifications are found in non TN DCIS (n=8/33) that are not observed in TN DCIS (n=0/26)

1. p-values < 0.05;
2. A gene list is mapped from 18 genomic regions found on chromosomes 8, 11, 17;
3. These regions encompass 39 genes altered in non TN DCIS;

   Genes:

   7SK AC013300.1 AC022973.1 AC103833.1 AC109322.1 ADCY8 C8orf4 CRKRS CSMD3 CYC1 DEPDC6 EFR3A EXOSC4 FAM49B FGF19 FGF3 FGF4 GPAA1 GPR20 GRINA GSDMC KCNQ3 KIAA1875 LRRC6 MAF1 OC90 OPLAH PARP10 PLEC PTK2 RP11-1023P17.1 RP11274M4.1 RP11473O4.1 SHARPIN SLC45A4 SNORA25 SPATC1 ST18 TMEM71

PANTHER analysis: 27 genes mapped, 1 id is not found.

5.4.1.1 Duplication of Triple Negative DCIS Compared to Duplication in Non Triple Negative DCIS

Duplications are found in TN DCIS (n=5/26) that are not observed in non TN DCIS (n=0/33)

1. p-values < 0.05;
2. A gene list is mapped from 18 genomic regions found on chromosomes 3, 6, 12;
3. These regions encompass 17 genes altered in TN DCIS;

   Genes:

   5S_rRNA AC004671.1 AC106722.1 AL096711.1 C6orf174 ECHDC1 MBNL1 NTF3 RNF146 RP11362A9.3 RP1-177A13.1 RP3-351K20.3 RP3-351K20.4 RP3-403A15.1 RSPO3 TMEM14E Y_RNA

PANTHER analysis: 6 mapped ids found, 11 mapped ids are not found.

Duplications are found in non TN DCIS (n=0/33) that are not observed in TN DCIS (n=7/26).

1. p-values < 0.05;

2. A gene list is mapped from 20 genomic regions found on chromosomes 3, 8, 10, 16, 17, 20, 22;
3. These regions encompass 54 genes altered in non TN DCIS;

Genes: AC015813.2AC020688.1 AC090922.1 AC092291.1 AC124319.3 AC136443.1 AC138932.2 AL031661.1 AL391421.1 AL391421.2 AL391421.3 AL391421.4 AP003355.2 ATG3P1 BFAR CTD-2561B21.1 CUEDC1 DLG5 FAM18A GSTTP2 H2AFZP5 hsamir-1972 HSPEP1 KCNS2 MAFB MRPS23 NIT2 NOMO1 NPIP NUBP1 OXR1 PARN PDXDC1 PLA2G10 POLR3A RALGAPB RP11-101E14.2 RP11-101E14.3 RP11126H7.3 RP1-191L6.2 RP4-564F22.2 RP4 564F22.5 RP5-1031J8.1 RPS24 SNHG11 SNORA71 SNORA71A SNORA71B SNORD112 TBC1D23 U6 U7 VEZF1 Y_RNA

PANTHER analysis: 19 mapped ids are found, 35 mapped ids are not found.

5.8.7.2 Genomic Gains in Triple Negative DCIS Compared to Genomic Gains in Non Triple Negative DCIS

Gains found in TN DCIS (n=10/26) have some overlap with gains found in non TN DCIS (n=3/33).

1. p-values < 0.05;
2. A gene list is mapped from 17 genomic regions found on chromosomes 3, 4, 5, 10, 10;
3. These regions encompass 77 genes altered in non TN DCIS;

Genes:

5S_rRNA AC006296.3 AC022400.3 AC096971.2 AC103560.1 ACADSB AGAP5APC BMS1P4 BUB3 C10orf55 CAMK2G CHCHD1 COQ6CTC-459M5.1 CTC-459M5.2 CTC-493D22.1 CTD2077I5.1 CTD 2192A1.1CTD-2201G3.1 ENTPD5 EPB41L4A FAM161B FHIT FOXP1 FTHL23 FUT11 GLT8D4 GLUDP3 HMX2 HMX3 IKZF5 KIAA0913 MCC MYOZ1 NCRNA00219 NDST2 PLAU PPP4R2 PSTK PTGR2 RNase_MRP RP11-162A23.5 RP11-282I1.1 RP11-417O11.5 RP11430J3.1 RP11-430J3.2 RP11-458B24.2 RP11-464F9.1 RP11-464F9.19 RP11-464F9.9 RP11526F3.1 RP11-574K11.12 RP11-574K11.16 RP11-574K11.18 RP11-574K11.20 RP11-574K11.5 RP11-574K11.8 RP11-624D20.1 RP11-654C22.1 RP11-728B21.2 RP11-905F6.1 SEC24C SHQ1 SNORA13 snoU13 SYNPO2L TSSK1B U1 U4atac U6 U7 USP54 VCL Y_RNA YTHDC2 ZNF410

There were gains found in non TN DCIS (n=8/33) that are not observed in TN DCIS (n=0/26).

1. p-values < 0.05;

2. A gene list is mapped from 36 genomic regions found on chromosomes 2, 6, 7, 9, 10, 17, 18, 19;
3. These regions encompass 99 genes altered in non TN DCIS;

   Genes:

AC004603.4 AC005176.1 AC005205.2 AC005205.3 AC005205.4 AC005239.1 AC006133.3 AC007842.1 AC008555.5 AC008655.1 AC009711.1 AC011443.1 AC011445.1 AC011455.1 AC011496.1 AC011500.1 AC011500.2 AC012309.4 AC012309.5 AC080032.1 AC091078.1 AC091078.2 AC092296.1 AC092296.3 AC093063.1 AC103996.1 ACAN ASPDH C19orf63 CDKN2BAS CEACAMP7 CLC DENND4C DLL3 DYRK1B EID2 EID2B FAM71E1 FBL FBXO27 FCGBP GMFG IL28A IL28B IL29 JOSD2 KCNC3 KCTD15 LEUTX LGALS13 LGALS14 LRFN1 LRRC4B MED29 MLLT3 MRPS12 MTAP MYBPC2 MYH14 NAPSA NAPSB NCCRP1 NFKBIB NR1H2 PAF1 PAK4 PLEKHG2 POLD1 PSG1 PSG10 PSG11 PSG6 PSG7 PSMC4 RINL RP11513M16.5 RPS16 RPS6 SAMD4BSARS2 SIRT2 snoU13 SPIB SUPT5H SYCN SYT3 TIMM50 VN1R96P Y_RNA ZFP14 ZFP36 ZFP82 ZNF146 ZNF30 ZNF383 ZNF546 ZNF565 ZNF780A ZNF780B

PANTHER analysis: 59 mapped ids found, 40 mapped ids are not found.

5.8.7.3 Genomic Sc Gains in Triple Negative DCIS Compared to Genomic Sc Gains in Non Triple Negative DCIS

There are Sc Gains found in TN DCIS (n=7/26) that are not observed from non TN DCIS (n=0/33).

1. p-values < 0.05;
2. A gene list is mapped from 21 genomic regions on 6 chromosomes 1, 2, 6, 9, 16, 19;
3. These regions encompass 86 genes altered in TN DCIS;

   Genes:

5S_rRNA AC016699.1 AC017099.3 AC018892.1 AC018892.3 AC018892.4 AC018892.5 AC018892.6 AC018892.7 AC018892.8 AC018892.9 AC079337.1 AC079395.1 AC092683.1 AC092683.2 AC092683.3 AC106785.1 AC106785.10 AC106785.14 AC106785.18 AC106785.20 AC106785.22 AC106785.25 AC106785.27 AC106785.28 AC106785.6 AC116553.1 AC137932.1 AC137932.3 AC159540.1 AC159540.14 AC159540.2 AC159540.3 ACTR1B AL391807.1 AL445568.1 AL590785.1 ANKRD11 ANKRD36 ANKRD36B B3GAT2 BAI3 CDKN2BAS CEBPG CHST8 COX5B CTD-2329C7.1 DBIP1 ELOVL4 FAHD2B FAM178B IRAK1BP1 KCNQ5 KCTD15 MTAP PEPD PHIP RIMS1 RP11-135M8__A.1 RP11-173D14.3 RP11-321C1.1 RP11-35J1.1 RP11-361F19.1 RP11-380M3.1 RP11-406O16.1 RP11-789A7.1 RP1-20N4.1 RP1-232L24.3 RP3-357D13.1 RP3-357D13.3 RP3-390M24.1 RP3-474G15.1 RP3-474G15.2 RP3-485C17.1 RP3-485C17.2 RP3-525N10.2 SNORD112 snoU13 TMEM131 U3 U4 U6 U7 UBTFL6 VWA3B ZAP70

PANTHER analysis: 21 mapped ids are found, 65 mapped ids are not found.

There are Sc Gains in non TN (n=8/33) not observed in TN DCIS (n=0/26).

1. p-values < 0.05;
2. A gene list is mapped from 36 genomic regions found on chromosomes 3, 4, 5, 9, 14, 17;
3. These regions encompass 93 genes altered in TN DCIS;

Genes:

7SK AC006296.3 AC068400.1 AC098869.1 AC099668.5 AC104996.1 AC105935.1 AC121252.2 AC126327.1 AC126327.4 AL117692.1 AL117692.2 AL136294.1 AL161626.1 AMIGO3 APC APEH ATP6V0A1 BLMH C14orf135 C14orf182 C14orf183 C3orf54 C9orf40 C9orf41 C9orf95 CAMKV CCDC55 CDCP1 CDH29 COASY CPD CTB-75G16.1 CTC-459M5.1 CTC-459M5.2 CTD-2184C24.1 CTD-2192A1.1 DDX52 DHRS11 DHRS7 DUSP14 EFCAB5 EPB41L4A FAM134C GCNT1 GGNBP2 GMPPB hsa-mir-423 HSD17B1 HSD17B1P1 IP6K1 LRRC9 MLX MRM1 MST1 MYO19 NAGLU NCRNA00219 NTRK2 OSTF1 PIGW PLEKHH3 PPM1A PRKAR2A PRUNE2 PSMC3IP RAD51L1 RBM47 RNF123 RP11-197P3.1 RP11-197P3.4 RP11-197P3.5 RP11-214N16.2 RP11-422N19.3 RP11-458B24.2 RP11-526F3.1 RP11-58E21.1 RP11-66C24.1 RP13-1056D16.2 RP13-480C15.1 SLC6A4 SNORA13 SNORD63 SYNRG TADA2A TMIGD1 TRAIP TRPM6 TUBG1 TUBG2 U6 UBA7 Y_RNA

PANTHER analysis: 50 mapped ids are found, 43 mapped ids are not found.

5.8.7.4 Losses in in Triple Negative DCIS Compared to Genomic Total Loss in Non Triple Negative DCIS

There are losses found in TN DCIS (n=11/26) that are not observed in non TN DCIS (n=0/33).

1. p-values <0.0001;
2. A gene list is mapped from 23 genomic regions on chromosome 4;
3. These regions encompass 94 altered genes in TN DCIS;

   Genes:

MAR01 7SK AC079349.1 AC095046.1 AC095047.1 AC096766.1 AC097534.1 AC097534.2 AC104082.1 AC104082.2 AC105285.2 AGPAT9 ANXA3 ARHGAP24 C4orf12 C4orf39 C4orf43 CDS1 CPE FAM175A FGF5 FRAS1 GALNT7 GALNTL6 GK2 GK3P HMGB2 hsa-mir-1979 hsa-mir-578 KLHL2 NACA3P NKX6-1 NPY5R OR7E94P RP11-10K16.1 RP11112L18.1 RP11-147K21.1 RP11-218C23.1 RP11-219C20.1 RP11-234K19.1 RP11-234K19.2 RP11-274J2.1 RP11-294O2.1 RP11-294O2.2 RP11-366M4.1 RP11-366M4.11 RP11-366M4.12 RP11-366M4.13 RP11-366M4.14 RP11-366M4.15 RP11-366M4.17 RP11-366M4.2 RP11-366M4.3 RP11-366M4.4 RP11-366M4.5 RP11-366M4.6 RP11-366M4.8 RP11-42A4.1 RP11-436A7.1 RP11-443J23.1 RP11-452C8.1 RP11-469O11.1 RP11-469O11.2 RP11-485C11.1 RP11-489G11.1 RP11-502M1.1 RP11-502M1.2 RP11-51G24.1 RP11-606P2.1 RP11-610O8.1 RP11-689K5.2 RP11-689K5.3 RP11-722P15.1 RP11-75A5.1 RP11-767N15.1 RP11-798M19.3 RP11-8L2.1 RPL35AP12 SAP30 SC4MOL SCRG1 SNORA31 SNORA75 SPOCK3 TKTL2 TMEM192 TRIM60 TRIM61 TRIM75 U4 U5 U6 WDFY3 Y_RNA

PANTHER analysis: 23 mapped ids are found, 71 mapped ids are not found.

There are losses in non TN DCIS (n=10/33) that are not observed in TN DCIS (n=0/26) represents losses for non TN DCIS (N=10/24).

1. P values < 0.05;
2. A gene list is mapped from 35 genomic regions found on chromosomes 1, 2, 3, 6, 9, 10, 17, 18, 19;
3. These regions encompass 127 altered genes in TN DCIS;

   Genes:

5S_rRNA AC002539.1 AC003051.1 AC004562.1 AC005176.1 AC005205.2 AC005205.3 AC005205.4 AC005208.1 AC005239.1 AC005307.1 AC005616.1 AC006133.3 AC007392.3 AC007392.4 AC007403.1 AC007403.2 AC007403.3 AC009474.1 AC009474.2 AC011443.1 AC011500.1 AC011500.2 AC023115.3 AC078941.1 AC091038.2 AC092155.1 AC092155.2 AC092155.4 AC093063.1 AL162419.2 AL356957.10 AL356957.2 AL356957.3 AL356957.4 AL356957.6 AL356957.7 AL356957.9 AL359836.1 AL732363.1 C9orf68 CAPN12 CDH2 CLCDLL3 DYRK1B EHBP1 EID2 EID2B EMX2OS FAM98C FBL FBXO27 FCGBP FSHR GLIS3 GMFG hsa-mir-1-2 hsa-mir-133a-1 KCNJ16 KCNJ2 KCNK18 KIAA1598 LEUTX LGALS13 LGALS14 LGALS7 LRFN1 MAP4K1 MED29 MEIS1 MIB1 NT5E PAF1 PAK4 PDZD8 PLEKHG2 RASGRP4 RP11-14N7.1 RP11-14N7.2 RP11-268I9.1 RP11321N4.3 RP11-33E24.1 RP11-33E24.3 RP11-358M14.2 RP11-403I13.1 RP11403I13.2 RP11-403I13.4 RP11-403I13.5 RP11-403I13.6 RP11-403I13.7 RP11403I13.8 RP11-501J20.2 RP11-501J20.3 RP11-501J20.5 RP11-5G18.2 RP11-70J12.1 RP11-744H18.1 RP11-744H18.2 RP11-763B22.5 RP11-763B22.6 RP11-763B22.7 RP11-763B22.8 RP11-763B22.9 RP1-3J17.3 RPS16 RSL24D1P2 RYR1 SAMD4B SARS2 SLC18A2 SLC1A1 SNHG5 SNORA73 SNORA81 SNORD50 snoU13 SNX14 SPRED3 SUPT5H SYNCRIP TIMM50 U1 U6 VAX1 Y_RNA ZFP36

PANTHER analysis: 41 mapped ids are found, 86 mapped ids are not found.

5.8.7.5 Total Loss in Triple Negative DCIS Compared to Genomic Total Loss in Non Triple Negative DCIS

There are total losses found in TN DCIS (n=17/26) that are not observed in non TN DCIS (n=0/33).

1. p-values = 0.05;
2. A gene list is mapped from 58 genomic regions found on chromosomes 3, 4,14,15,17;
3. These regions encompass 223 genes altered in Non TN DCIS;

   Genes:

5S_rRNA 7SK ABCD4 AC002117.1 AC003043.1 AC003043.2 AC003102.3 AC003963.2 AC004222.1 AC004596.1 AC004968.1 AC004968.2 AC006349.1 AC007056.1 AC007686.1 AC007722.1 AC008045.1 AC008105.1 AC012409.1

AC015936.1 AC015936.3 AC016251.1 AC019131.2 AC020704.1 AC026202.1 AC026202.5 AC026882.1 AC027708.1
AC027807.1 AC036222.1 AC055813.1 AC055873.1 AC068400.1 AC079915.1 AC084809.2 AC084809.3 AC090043.1
AC090283.1 AC090283.3 AC091199.1 AC096750.1 AC102948.1 AC102948.2 AC103702.1 AC103965.1 AC104260.1
AC113211.1 AC124789.1 AC134669.1 AC135724.1 AC138150.3 AC138150.4 AC183087.1 AC183087.2 ACBD4
ACCN1 ADAM11 ADAMTSL3 ADCK1 ADH1A ADH1B ADH1C ADH4 ADH5
ADH6 AF111168.1 AF111168.3 AHSA1 ALKBH1 ARHGAP23 ARRDC4 ASB16 ATXN7L3
C14orf148 C14orf156 C14orf174 C14orf178 C17orf104 C17orf105 C17orf46 C17orf53 C17orf65
C17orf93 C1QL1 C4orf37 CA10 CCDC103 CCDC43 CD300LG CDC6 CNTN4
CNTN6 COX6B1P2 CTD-2175M1.1 CTD-2377D24.1 CTD-2377D24.2 CTD-2377D24.4
CTD-2377D24.6 DBF4B DCAKD DDX52 DHX8 DUSP3 DYNLL1P1 EFTUD2
EIF4E ETV4 EVI2A EVI2B FAM149B2 FAM169B FAM171A2 FAM177A2 FAM187A
FMNL1 FZD2 G6PC3 GFAP GJC1 GPATCH8 GPR179 GRN GSTZ1
HDAC5 HEXIM1 HEXIM2 HIGD1B HNF1B HOXB13 HOXB7 HOXB9 hsa-mir-1260 hsa-mir-1469 hsa-mir-196a-1 hsa-mir-2117 ISM2 ITGA2B KIAA1737 KIF18B KRT222 KRT24
KRT25 LIN52 LSM12 MAP3K14 MCTP2 MEOX1 METAP1 MPP2 MPP3
MRPL45 MYO1D NAGS NF1 NGB NMT1 NR2F2 NRXN3 OMG
PCNAP1 PLCD3 POMT2 PPY PRAC PYY RAB11FIP4 RGS6 RP11-1072C15.1
RP11-15B17.1 RP11-176P14.1 RP11-187O7.1 RP11-204C23.1 RP11-299L17.1
RP11-332E19.1 RP11-352E6.1 RP11-352E6.2 RP11-357H14.4 RP11-369I16.1
RP11-428B4.2 RP11-522B15.1 RP11-522B15.2 RP11-571L19.2 RP11-571L19.4
RP11-624A4.1 RP11-696N14.1 RP11-765K14.1 RP11-799A12.1 RP11-799A12.2
RUNDC3A SIPA1L1 SLC25A39 SLC4A1 SMARCE1 SNORA32 SNORA46 SNORD56 snoZ178
SNW1 SOCS7 SOST SPACA3 SPATA8 SPRED1 SPTLC2 SRCIN1 STON2
SYNRG TBC1D3 TMED8 TMEM101 TMEM63C TMEM98 TMUB2 U3 U6 U7
UBTF VEGFC VIPAR VSX2 WIPF2 Y_RNA ZDHHC22

PANTHER analysis: 115 mapped ids are found, 108 mapped ids are not found.

There are total losses found in non TN DCIS (n=27/33) that are not observed in TN DCIS (n=0/26).

1. p-values <0.0001;
2. A gene list is mapped from 18 genomic regions on 1 chromosome (17) ;
3. These regions encompass 46 genes altered in TN DCIS;

Genes:

AC000003.1 AC027763.1 AC027763.2 AIPL1 ALOX12 AMAC1L3 ASGR1 ASGR2 BCL6B C17orf49 C17orf61 C17orf74 CCDC42 CHRNB1 CLEC10A CTD-2545G14.1 DLG4 DPH1 FBXO39 FGF11 GAS7 hsa-mir-195 hsa-mir-497 MFSD6L NLGN2 OVCA2 PIK3R5 PIK3R6 PLSCR3 POLR2A RNASEK RNF222 RP11-609D21.1 SLC16A11 SLC16A13 SPDYE4 SPEM1 TEKT1 TMEM102 TNFSF12 TNFSF12-TNFSF13 TNFSF13 TNK1 U6 Y_RNA ZBTB4

PANTHER analysis: 33 mapped ids are found, 13 mapped ids are not found.

5.8.7.6 CdLOH in Triple Negative DCIS Compared to with CdLOH in Non Triple Negative DCIS

There is CdLOH found in TN DCIS (n=11/26) that are not present in non TN DCIS (n=0/33).

1. p-values <0.0001;
2. A gene list is mapped from 24 genomic regions on 2 chromosomes (4 and 5);
3. These regions encompass 91 genes altered in TN DCIS;

Genes: Mar01 7SK AC023355.1 AC023355.3 AC079349.1 AC095047.1 AC096766.1 AC097534.1 AC097534.2 AC104082.1 AC104082.2 AC105285.2 AGPAT9 ANXA3 ARHGAP24 C4orf39 C4orf43 CDS1 CPE DUT FBN1 FGF5 FRAS1 GALNT7 GALNTL6 GK2 GK3P HMGB2 hsa-mir-1979 hsa-mir-578 KLHL2 NACA3P NKX6-1 NPY5R OR7E94P RP11-10K16.1RP11-112L18.1 RP11-218C23.1 RP11-219C20.1 RP11-234K19.1 RP11-234K19.2 RP11-274J2.1 RP11294O2.1 RP11-294O2.2 RP11-366M4.1 RP11-366M4.11 RP11-366M4.12 RP11-366M4.13 RP11-366M4.14 RP11-366M4.15 RP11-366M4.17 RP11-366M4.2 RP11-366M4.3 RP11-366M4.4 RP11-366M4.5 RP11-366M4.6 RP11-366M4.8 RP11-42A4.1 RP11-436A7.1 RP11-443J23.1 RP11-469O11.1 RP11-469O11.2 RP11-485C11.1 RP11-489G11.1 RP11-502M1.1 RP11-502M1.2 RP11-51G24.1 RP11-606P2.1 RP11-689K5.2 RP11-689K5.3 RP11-75A5.1 RP11-767N15.1 RP11-798M19.3 RP11-8L2.1 RPL35AP12 SAP30 SC4MOL SCRG1 SLC12A1 SNORA31 SPOCK3 TKTL2 TMEM192 TRIM60 TRIM61 TRIM75 U4 U5 U6 WDFY3 Y_RNA

PANTHER analysis: 25 mapped ids are found, 66 mapped ids are not found.

There is CdLOH found in non TN DCIS (n=10/26) that are not observed in TN DCIS (0/26)

1. p-values < 0.05;
2. A gene list is mapped from 36 genomic regions found on chromosomes 2, 6, 7, 9, 10, 17, 18, 19;
3. These regions encompass 107 genes altered in TN DCIS;

Genes: 5S_rRNA AC002539.1 AC003051.1 AC004562.1 AC005176.1 AC005205.2 AC005205.3 AC005205.4 AC005208.1 AC005239.1 AC005307.1 AC005616.1 AC006133.3 AC007392.3 AC007392.4 AC007403.1 AC007403.2 AC009474.1 AC009474.2 AC011443.1 AC011500.1 AC011500.2 AC091038.2 AC092155.4 AC093063.1 AL133476.1 AL359836.1 ATP8B5P C6orf161 CAPN12 CDH2 CLC DLL3 DYRK1B EHBP1 EID2 EID2B EMX2OS FAM98C FBL FBXO27 FCGBP GLIS3 GMFG hsa-mir-1-2 hsa-mir-133a-1 KCNJ16 KCNJ2 KCNK18 KIAA1598 LEUTX LGALS13 LGALS14 LGALS7 LRFN1 MAP4K1 MED29 MEIS1 MIB1 NT5E PAF1 PAK4 PDZD8 PLEKHG2 RASGRP4 RP11-207F8.1 RP11-268I9.1 RP11-30P6.1 RP11-30P6.2 RP11-30P6.3 RP11-30P6.4 RP11-30P6.6 RP11-321N4.3 RP11-33E24.1 RP11-33E24.3 RP11-424A16.1 RP11-501J20.2 RP11 501J20.3 RP11-501J20.5 RP11-5G18.2 RP1-161C16.1 RP11-70J12.1 RP1-263J7.1 RP1263J7.2 RP1-3J17.3 RP3-455E7.1 RYR1 SAMD4B SARS2 SLC18A2 SNHG5 SNORA73 SNORA81 SNORD50 snoU13 SNX14 SPRED3 SUPT5H SYNCRIP TEK TIMM50 U4 U6 UNC13B VAX1 Y_RNA ZFP36

PANTHER analysis: 51 mapped ids are found, 104 mapped ids are not found.

5.8.7.7 CnLOH in Non Triple Negative DCIS Compared with CnLOH in Triple Negative DCIS

There is CnLOH found in TN DCIS (23/26) that are not observed in non TN DCIS (0/33).

1. p-values < 0.05;
2. A gene list is mapped from 31 genomic regions found on chromosomes 6,10,19, 20;
3. These regions encompass 145 genes altered in TN DCIS;

Genes:

Mar02	5S_rRNA	7SK	AC010323.1	AC114273.1	AL023583.1	AL024498.1	AL031123.1	AL031123.2	AL033539.1
AL033539.2	AL136305.1	AL136307.1	AL136307.2	AL139807.1	AL158198.1	AL158817.1	AL357054.1	AL357497.1	AL662797.1
ANGPTL4	ATP5GP1	BMP6	C6orf134	C6orf136	C6orf52	CAGE1	CAP2	CCDC90A	CD320
CD83	DHX16	DSP	DTD1	EDN1	EEF1A1P34	EEF1E1	ELOVL2	F13A1	FARS2
GCM2	GCNT2	GCNT6	HDGFL1	HIVEP1	KANK3	KIAA1949	KLF6	LASS4	LPCAT3
LY86	MAK	MRPS18B	MUTED	NDUFA7	NEDD9	NOL7	NRM	NRN1	OFCC1
PAK1IP1	PIP5K1P1	PPP1R10	PRL	PTMAP1	RAB11B	RANBP9	RBM24	RIOK1	RNF182
RP11-125M16.1	RP11-127P7.2	RP11-146I2.1	RP11-184A2.2	RP11-239H6.2					
RP11-239H6.3	RP11-288G3.2	RP11-288G3.3	RP11-288G3.4	RP11-320C15.1					
RP11-339A7.1	RP11-359N11.1	RP11-359N11.2	RP11-360O19.1	RP11-360O19.4					
RP11-360O19.5	RP11-379J5.4	RP11-379J5.5	RP11-405O10.2	RP11-456H18.1					
RP11-456H18.2	RP11-464C19.2	RP11-464C19.3	RP11-556O15.1	RP11-637O19.2					
RP11-69L16.4	RP11-69L16.5	RP11-69L16.6	RP11-716O23.1	RP11-716O23.2	RP1-182O16.1	RP1-182O16.2	RP1-23O21.1	RP1-273P12.1	RP1-290I10.2
RP1-290I10.3	RP1-290I10.4	RP1-290I10.5	RP1-290I10.6	RP1-290I10.7	RP1-290I10.8	RP1-303A1.1	RP1-309H15.2	RP1-62D2.3	RP1-80N2.2
RP3-336K20__B.2	RP3-380B8.1	RP3-380B8.3	RP3-380B8.4	RP3-380E11.2	RP3-398D13.2	RP3-398D13.3	RP3-429O6.1	RP3-451B15.3	RP3-470L22.1
RP3-486D24.1	RP3-510L9.1	RP4-761I2.2	RP4-761I2.4	RP5-1068E13.3					
RPL15P3	RPS28	RREB1	snoU13	SNRNP48	SSR1	SYCP2L	TFAP2A	TMEM14B	TMEM14C
TXNDC5	U1	U6atac	U7	Y_RNA					

PANTHER analysis: 51 mapped ids are found, 104 mapped ids are not found.

There is CnLOH found in non TN DCIS (29/33) that are not observed in TN DCIS (0/26).

1. p-values < 0.05;
2. A gene list is mapped from 70 genomic regions on chromosomes 1, 2, 3, 7, 10, 19, 20;

3. These regions encompass 244 genes altered in non TN DCIS;

Genes:

5S_rRNA AC005034.2 AC006039.1 AC007040.5 AC007099.1 AC007099.2 AC007878.1 AC010733.2 AC010733.4 AC010733.7
AC010744.1 AC010975.1 AC011245.1 AC011455.1 AC012494.1 AC012671.1 AC012671.2 AC016747.3 AC023881.1
AC062029.1 AC064872.1 AC073628.1 AC078841.5 AC083864.3 AC083864.4 AC084149.1 AC084149.2 AC092660.1
AC093616.1 AC096540.1 AC098581.1 AC104134.2 AC104135.2 AC104135.3 AC104135.4 AC104170.1 AC108479.1
AC108479.2 AC110491.1 AC117444.2 AC117444.3 ACOT11 ACPL2 ADARB2 AHSA2 AKIRIN1
AL031289.1 AL031985.1 AL110502.1 AL161740.1 AL592166.1 AL929472.1 AL929472.3 ARL6 ATP1B3P1
ATP6V1B1 BAZ1B BEST4 BMP8B BTBD19 C1orf122 C1orf168 C1orf175 C1orf228
C2orf51 C2orf74 C8A C8B CCDC163P CITED4 CRYBG3 CST1 CST4
CSTP2 CTNNA2 CTPS DAB1 DEM1 DYSF EBNA1BP2 EDN2 EEPD1
EGFR EIF2AK3 EIF2B3 EPHA10 EPHA6 EPS15 FABP1 FAM126A FAM151A
FAM176A FAM183A FHL3 FOXI3 FOXJ3 FOXO6 GABRR3 GRIK3 GUCA2A
GUCA2B HEYL HIVEP3 HK2 HPCAL4 hsa-mir-30c-1 hsa-mir-30e INPP5B
KCNQ4 KIAA1841 KIF2C KRCC1 LRRTM4 MANEAL MINA MMACHC MRPS12 MT-
ATP8 MTF1 MYCL1 NDUFA4P2 NDUFS5 NFKBIB NFYC NT5C1A OMA1 OR5AC1
OR5AC1P OR5AC2 OR5AC4P OR5H1 OR5H14 OR5H15 OR5H2 OR5H3P OR5H4P
OR5H5P OR5H6 OR5H7P OR5H8P OR5K3 OR5K4 OSBPL9 OXCT2 PABPC4
PAIP2B PAPOLG PEX13 PLK3 POLE4 POU5F1P7 PPAP2B PPIE PRKAA2
PTCH2 PUS10 RASA2 RGPD2 RIMS3 RINL RNF220 RP11-109P14.1
RP11-109P14.10 RP11-109P14.2 RP11-109P14.8 RP11-109P14.9 RP11-124D9.1
RP11-15J6.1 RP1-118J21.24 RP1-118J21.5 RP11-191G24.1 RP11-191G24.2
RP11-213P13.1 RP11-215L17.1 RP11-223A3.1 RP11-231L11.1 RP11-231L11.3
RP11-240D10.2 RP11-240D10.4 RP11-253A20.1 RP11-269F19.2 RP11-269F19.4
RP11-275F13.1 RP11-275F13.3 RP11-282K6.3 RP11-316C10.1 RP11-319C21.1
RP11-325B23.2 RP11-343D2.11 RP11-346M10.1 RP11-346M10.2 RP11-348A7.1
RP11-348A7.2 RP11-377K22.2 RP11-377K22.3 RP11-378I13.1 RP11-399E6.1
RP11-399E6.2 RP11-399E6.4 RP11-416L21.1 RP11-438D8.2 RP11-438D8.3
RP11-438D8.4 RP1-144F13.3 RP1-144F13.4 RP11-486B10.3 RP11-486B10.4
RP11-4H14.1 RP11-526K17.2 RP1-158P9.1 RP11-656D10.3 RP11-656D10.5
RP11-656D10.6 RP11-764I5.1 RP11-781D11.1 RP11-789L4.1 RP1-21K4.1 RP1-
63P18.2 RP4-564O4.1 RP4-580G13.1 RP4-614N24.1 RP4-635E8.1 RP4-657D16.4
RP4-657D16.5 RP4-678E16.4 RP4-705F19.1 RP4-705F19.2 RP4-710M16.1
RP4-710M16.2 RP4-739H11.1 RP4-739H11.3 RP4-783C10.3 RP5-1066H13.4
RP5-1090E8.1 RP5-1103B4.3 RP5-1180C18.1 RP5-860P4.2 RP5-866L20.1
RP5-866L20.2 RP5-866L20.3 RP5-882O7.1 RP5-882O7.3 RP5-882O7.4
RP6-239D12.1 RPIA RPL38 RPS8 SARS2 SCMH1 SF3A3 SIRT2
SLC25A36 SLFNL1 SMYD1 SNORA26 SNORA63 SNORD112 SNORD38 SNORD46 snosnR61
snoU109 snoU13 SPSB4 SSBP3 TACR1 TCTEX1D4 TESK2 THNSL2 TMEM53
TMEM90B TRIT1 TTC39A U2 U5 U6 U7 USP34 UTP11L
VAX2 WDR65 Y_RNA YRDC ZBTB38 ZNF638 ZNF642 ZNF643 ZNF684
ZPLD1

PANTHER analysis: 118 mapped ids are found, 170 mapped ids are not found.

5.8.8 Copy Number Aberrations for Pure Triple Negative DCIS Compared to Triple Negative DCIS Associated with Invasive Breast Disease

These series examines the differences between pure triple negative DCIS and triple negative DCIS associated with invasive breast disease, i.e. the DCIS component not the invasive breast disease.

Frequency plots showing copy number aberrations between Pure TN DCIS and TN DCIS associated with invasive breast disease were provided by Breakthrough Breast Cancer/Research Oncology, King's College London Bioinformatics Department (Figure 41).

Figure 41: frequency plots showing copy number aberrations between pure triple negative dcis and triple negative DCIS associated with invasive breast disease (amplifications, duplications, gains, Sc gains, losses, total losses CdLOH and CnLOH,) (pages 236-238).

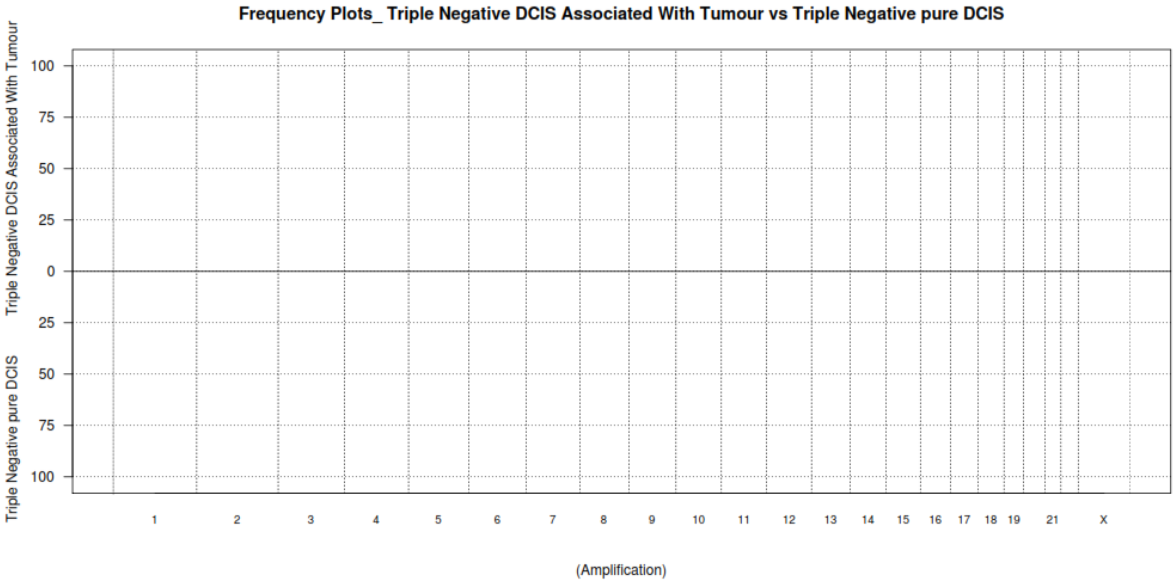
Frequency Plots_ Triple Negative DCIS Associated With Tumour vs Triple Negative pure DCIS
Triple Negative DCIS Associated With Tumour
Triple Negative pure DCIS
100
75
50
25
0
25
50
75
100
1
2
3
4
5
6
7
8
9
10
11
12
13
14
15
16
17
18
19
21
X
(Amplification)

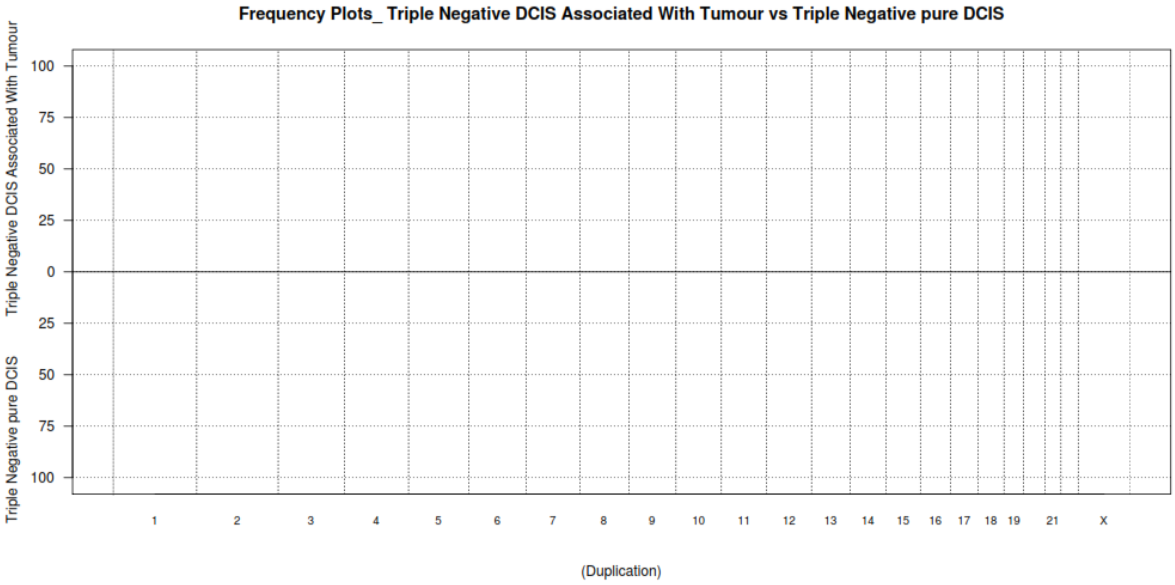
Frequency Plots_ Triple Negative DCIS Associated With Tumour vs Triple Negative pure DCIS
Triple Negative DCIS Associated With Tumour
Triple Negative pure DCIS
100
75
50
25
0
25
50
75
100
1
2
3
4
5
6
7
8
9
10
11
12
13
14
15
16
17
18
19
21
X
(Duplication)

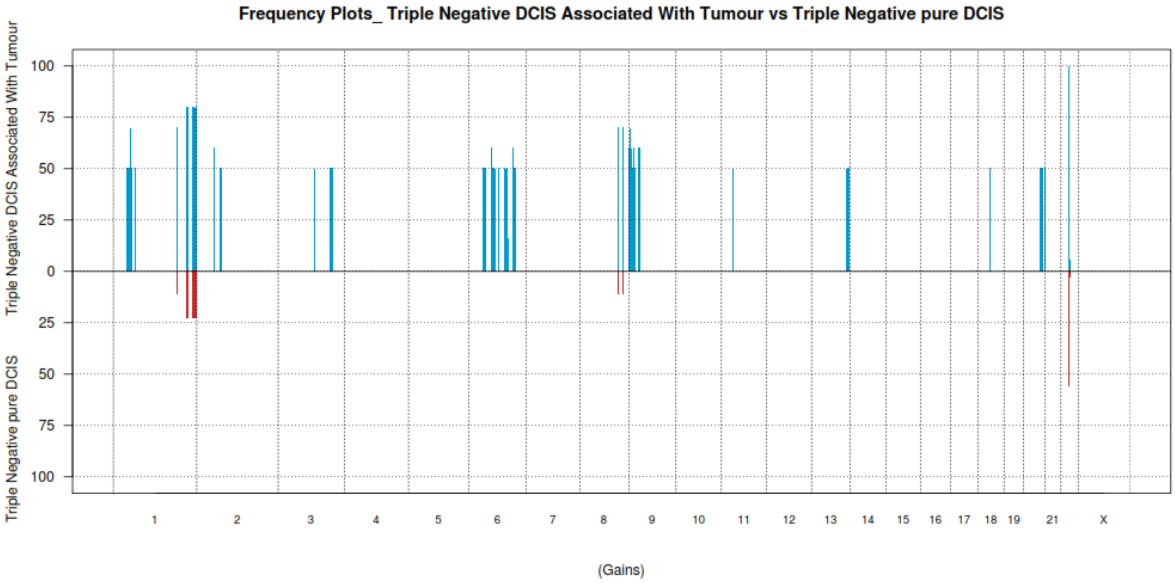
Frequency Plots_ Triple Negative DCIS Associated With Tumour vs Triple Negative pure DCIS
Triple Negative DCIS Associated With Tumour
Triple Negative pure DCIS
100
75
50
25
0
25
50
75
100
1
2
3
4
5
6
7
8
9
10
11
12
13
14
15
16
17
18
19
21
X
(Gains)

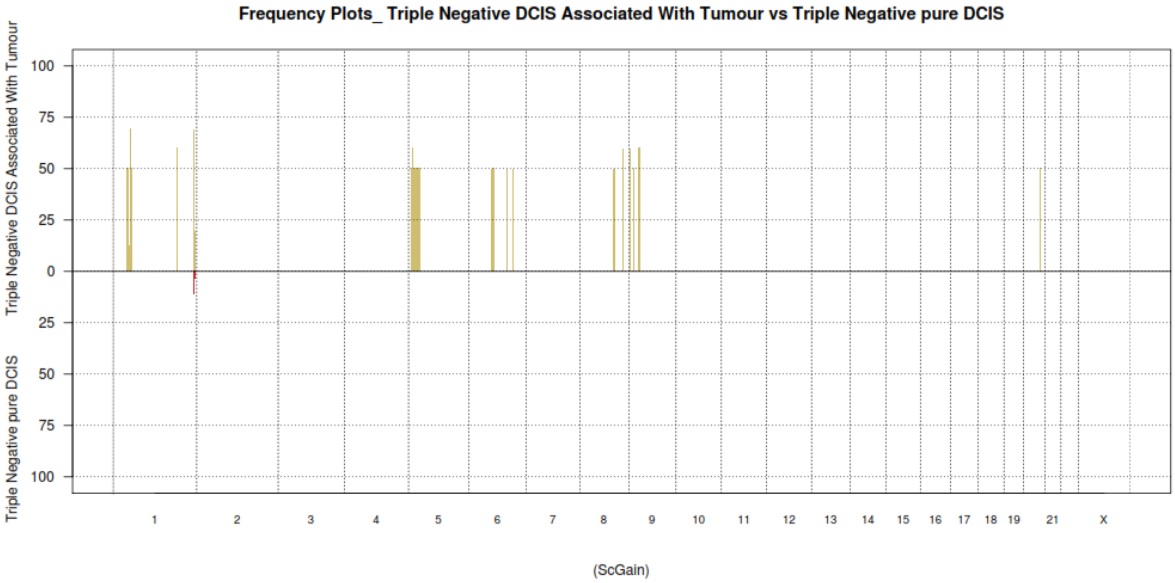
Frequency Plots_ Triple Negative DCIS Associated With Tumour vs Triple Negative pure DCIS
Triple Negative DCIS Associated With Tumour
Triple Negative pure DCIS
100
75
50
25
0
25
50
75
100
1
2
3
4
5
6
7
8
9
10
11
12
13
14
15
16
17
18
19
21
X
(ScGain)

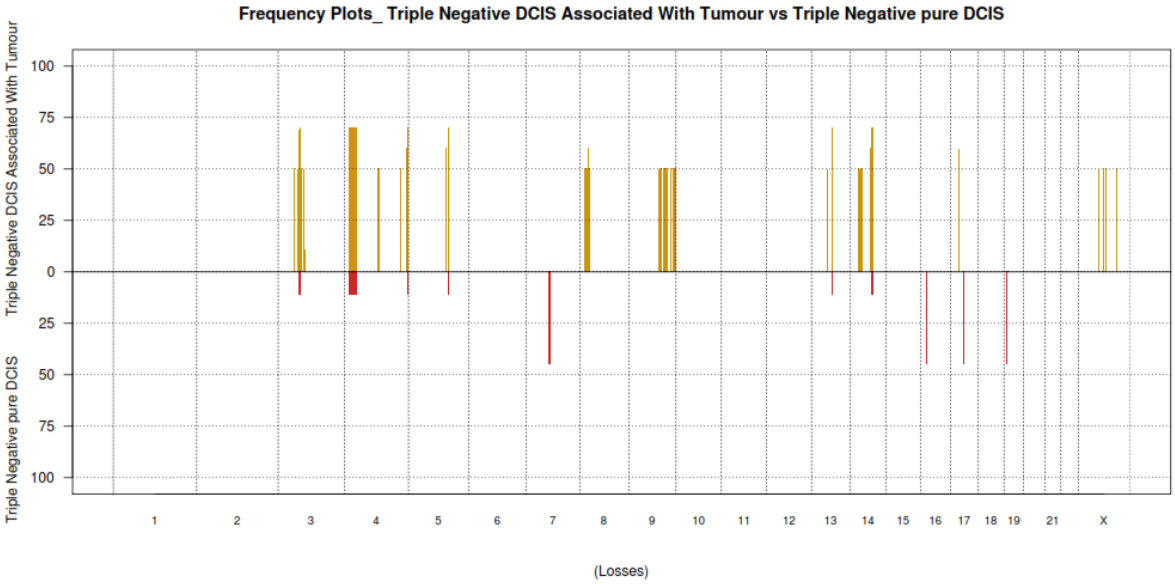
Frequency Plots_ Triple Negative DCIS Associated With Tumour vs Triple Negative pure DCIS
Triple Negative DCIS Associated With Tumour
Triple Negative pure DCIS
100
75
50
25
0
25
50
75
100
1
2
3
4
5
6
7
8
9
10
11
12
13
14
15
16
17
18
19
21
X
(Losses)

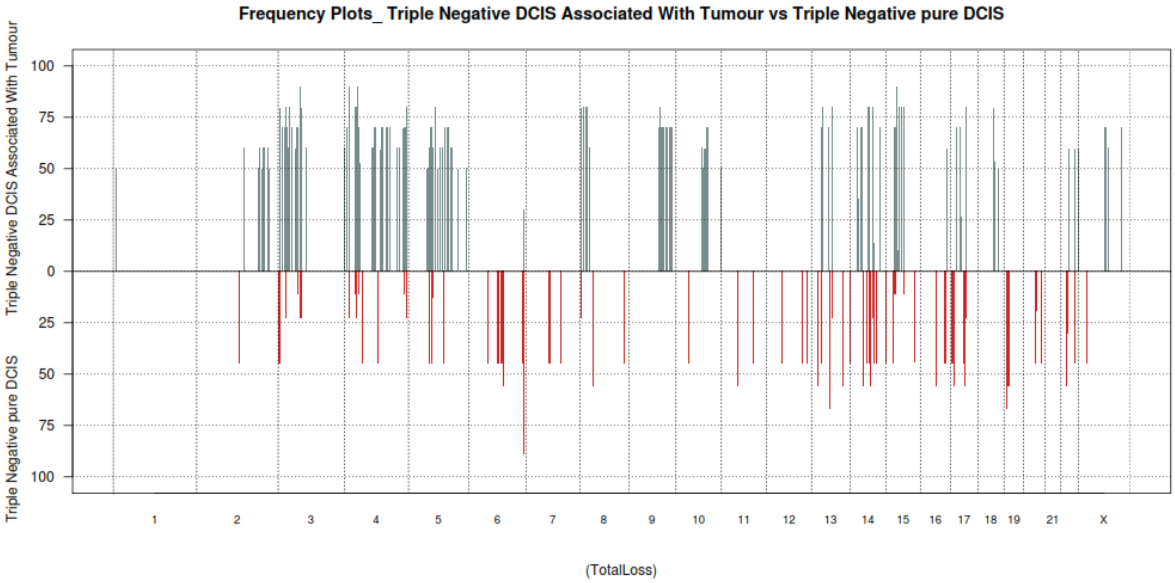
Frequency Plots_ Triple Negative DCIS Associated With Tumour vs Triple Negative pure DCIS
Triple Negative DCIS Associated With Tumour
Triple Negative pure DCIS
100
75
50
25
0
25
50
75
100
1
2
3
4
5
6
7
8
9
10
11
12
13
14
15
16
17
18
19
21
X
(TotalLoss)

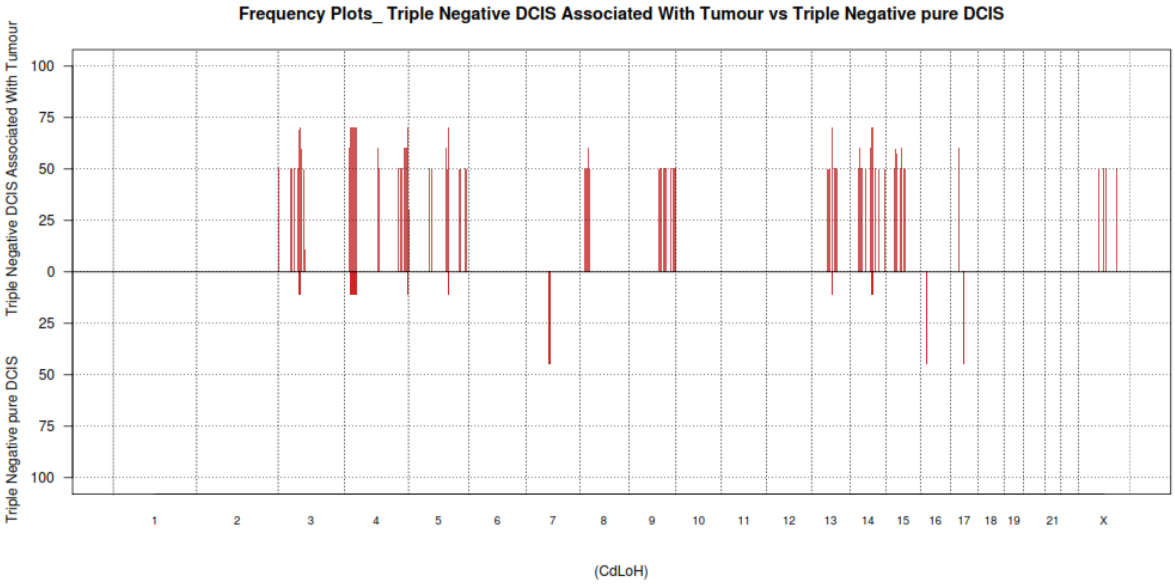
Frequency Plots_ Triple Negative DCIS Associated With Tumour vs Triple Negative pure DCIS
Triple Negative DCIS Associated With Tumour
Triple Negative pure DCIS
100
75
50
25
0
25
50
75
100
1
2
3
4
5
6
7
8
9
10
11
12
13
14
15
16
17
18
19
21
X
(CdLoH)

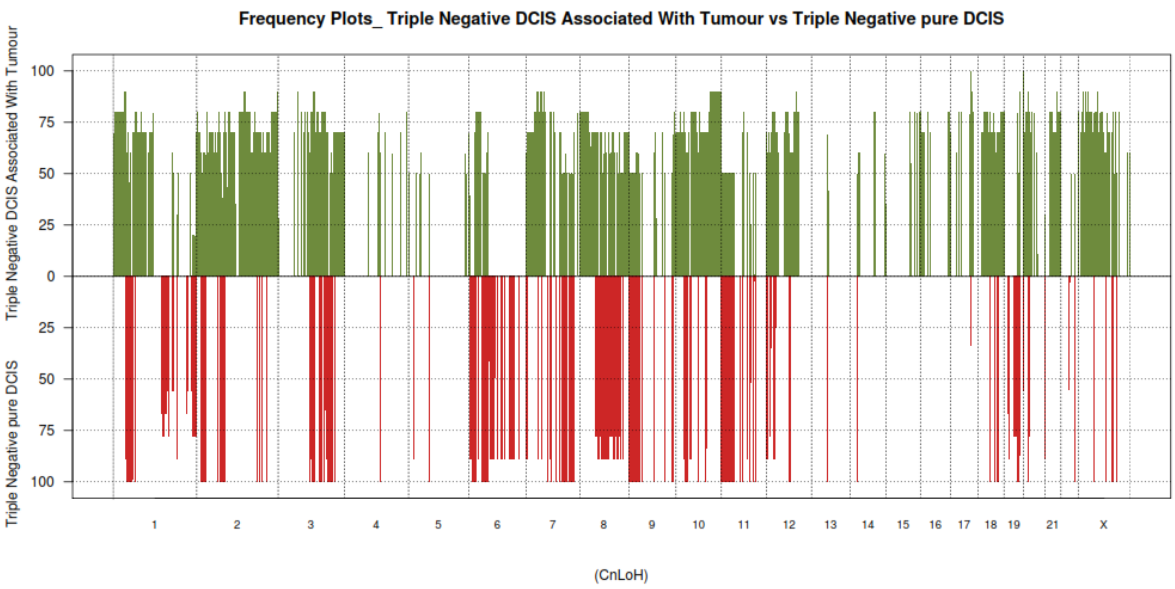

5.8.8.1 Amplification of Pure Triple Negative DCIS and Triple Negative DCIS Associated with Invasive Breast Disease

No amplifications in TN pure DCIS or TN DCIS associated with invasive breast disease were found in this series.

5.8.8.2 Duplication of TN pure DCIS and TN DCIS Associated with Invasive Breast Disease

No Duplications in TN pure DCIS or TN DCIS associated with invasive breast disease found in this series.

5.8.8.3 Genomic Gains of TN pure DCIS and TN DCIS Associated with Invasive breast disease

There is considerable overlap between the genomic gains seen in TN pure DCIS (n=5/9) and TN DCIS associated with invasive breast disease (n=10/10).

1. p-values < 0.05;
2. A gene list is mapped from 13 genomic regions found on chromosomes 1, 8, 22;

3. These regions encompass 67 genes altered in TN pure DCIS and TN DCIS associated with invasive breast disease;

   Genes:

5S_rRNA	7SK	AC108925.1	ACTN2	AL513363.1	AP000351.1	AP000351.10	AP000351.2	AP000351.6
	AP000351.7	AP000351.8	AP000351.9	CFLP4	CHML	CHRM3	CSMD3	EDARADD
	ENO1P1	EXO1	FH	GSTT1	GSTTP1	GSTTP2	HEATR1	hsa-mir-1204
	KMO	KRT18P32	LGALS8	MAP1LC3C	MTR	NCRNA00210	OPN3	PLD5
	PVT1	RP11-149J18.1	RP11-152L7.1	RP11-152L7.2	RP11-177F15.1	RP11-182B22.2	RP11-307O1.1	RP11-323D18.1
	RP11-323D18.4	RP11-323D18.5	RP11-362H12.1	RP11-371I1.2	RP11-385F5.2	RP11-385F5.4	RP11-397A15.4	RP11-400N13.1
	RP11-439E19.3	RP11-439E19.5	RP11-439E19.6	RP11-439E19.8	RP11-463J7.2	RP11-488L18.1	RP11-488L18.8	RP11-544D21.1
	RP11-553N16.1	RP11-561I11.2	RP11-561I11.3	SCCPDH	SNORD112	SPATA17	U6	VN1R17P
	VN1R5	WDR64						

PANTHER analysis: 18 mapped ids are found, 49 mapped ids are not found.

There were gains present in TN DCIS associated with invasive breast disease (n=7/7) not observed in pure DCIS (n=0/9).

1. p-values < 0.05;
2. A gene list is mapped from 13 genomic regions found on chromosomes 1, 2, 6, 9;
3. These regions encompass 69 genes altered in TN DCIS associated with invasive breast disease;

   Genes:

AC002485.1	AC096583.1	AC139712.2	AL158147.1	AL161450.1	AL161450.10	AL161450.11	AL161450.13	AL161450.16	
AL161450.2	AL161450.3	AL161450.4	AL161450.8	AL161450.9	C9orf146	C9orf46	C9orf66	CBWD1	CD274
DMRTA2	DOCK8	ELAVL4	FAF1	FAM138C	FOXD4	hsa-mir-101-2	hsa-mir-1302-2	JAK2	
LAMA2	NFIB	PDCD1LG2	PTPRD	RCL1	RLN1	RP11-125K10.2	RP11-125K10.4	RP11-125K10.5	
RP11-12D24.6	RP11-12D24.7	RP11-143M1.2	RP11-143M1.3	RP11-143M1.4	RP11-143M1.7	RP11-183G22.1	RP11-183G22.2	RP11-183G22.3	
RP11-25O10.1	RP11-280O24.1	RP11-284P20.2	RP11-284P20.3	RP11-284P20.4	RP11-32F11.2	RP11-39K24.11	RP11-39K24.14	RP11-39K24.2	
RP11-39K24.4	RP11-39K24.5	RP11-39K24.9	RP11-492I2.1	RP11-560D2.2	RP11-567C20.2	RP11-567C20.3	RP11-572H4.1	RP11-59O6.3	
U6	XXyac-YRM2039.1	XXyac-YRM2039.2	XXyac-YRM2039.3	ZCCHC11					

PANTHER analysis: 16 mapped ids are found, 53 mapped ids are not found.

5.8.8.4 Genomic Sc Gains of TN pure DCIS and TN DCIS Associated with Invasive Breast Disease

There are no significant Sc gains found in pure DCIS in this series. There are Sc gain found in TN DCIS associated with invasive breast disease (n=7/10) that mapped ids in TN pure DCIS (n=0/9).

1. p-values< 0.05;
2. A gene list is mapped from 49 genomic regions found on chromosomes 1, 5, 6, 8, 9, 20;
3. These regions encompass 350 genes altered in TN DCIS associated with invasive breast disease;

   Genes:

5S_rRNA 7SK AC008949.1 AC010455.1 AC010491.1 AC010627.1 AC012640.3 AC016553.1 AC016575.1 AC024589.2
AC025181.1 AC025472.1 AC025647.3 AC034229.1 AC091878.1 AC099784.2 AC106774.1 AC108925.1 AC112200.1
AC114981.1 AC138409.1 AC138409.2 AC138951.3 AC139783.1 ADAMTS12 AGBL4 AL034429.1 AL035467.1 AL133230.2
AL136164.1 AL136310.1 AL354933.1 AL357519.1 AL390776.1 AL592166.1 AL596225.1 AL645730.1 AL645730.2
AMACR ANKH ANKRD33B ANKRD46 BASP1 BEST4 BTBD19 C1orf123 C1orf163 C1orf185
C1orf228 C1QTNF3 C5orf17 C5orf22 C5orf23 C6orf155 CC2D1B CCT5 CDH12 CDH18
CDH6 CDH9 CDKN2C CFLP2 CMBL COX6CP2 CPT2 CTB-40H15.1
CTB-40H15.2 CTB-40H15.3 CTB-55B8.1 CTC-305H11.1 CTC-461F20.1
CTD-2001E22.1 CTD-2001E22.2 CTD-2004A9.1 CTD-2008E3.1 CTD-2010I22.1
CTD-2010I22.2 CTD-2011G10.1 CTD-2011G17.1 CTD-2017D15.1 CTD-2023M8.1
CTD-2057J6.1 CTD-2057J6.2 CTD-2061E9.1 CTD-2066L21.1 CTD-2066L21.2
CTD-2066L21.3 CTD-2134P3.1 CTD-2138O14.1 CTD-2139B15.1 CTD-2139B15.2 CTD-2139B15.4
CTD-2139B15.5 CTD-2143L24.1 CTD-2151L9.1 CTD-2151L9.2 CTD-2154B17.1
CTD-2165H16.1 CTD-2165H16.2 CTD-2165H16.3 CTD-2194F12.1 CTD-2197O4.1
CTD-2199O4.1 CTD-2201E9.1 CTD-2201E9.2 CTD-2201E9.3 CTD-2201E9.4
CTD-2203K17.1 CTD-2206G10.1 CTD-2206G10.2 CTD-2215L10.1 CTD-2218G20.1
CTD-2218G20.2 CTD-2233C11.2 CTD-2233C11.3 CTD-2256P15.1 CTD-2269E23.1
CTD-2269E23.2 CTD-2290C23.1 CTD-2290C23.2 CTD-2290C23.3 CTD-2290P7.1
CTD-2313D3.1 CTD-2351A8.1 CTD-2533K21.1 CTD-2533K21.2 CTD-2533K21.3
CTD-2533K21.4 CTD-3007L5.1 CTD-3065A13.1 CTNND2 DAP DMRTA2
DMRTB1 ECHDC2 EIF2B3 ELAVL4 ERI3 FAF1 FAM105A FAM105B FAM134B FAM159A
FAM173B FBXL7 FBXO43 FTHL10 GPX7 GRHL2 GUCA2A GUCA2B HIVEP3 hsa-
mir-30a hsa-mir-30c-2 hsa-mir-579 KB-1615E4.1 KIF2C LAMA2 LRP8 MAGOH Mar11 Mar6
MTMR12 MYCL1 MYO10 NCALD NPR3 OGFRL1 ORC1L PDZD2 PLK3
PMCHL1 PRDM9 PRPF38A PTCH2 PTPN1 REV3L RGS22 RIMS1 RNASEN
RNF19A RNF220 ROPN1L RP11-1023L17.1 RP11-1023L17.2 RP11-1084J3.1 RP11-1084J3.2
RP11-1084J3.3 RP11-113I22.1 RP11-117D22.1 RP11-117D22.2 RP11-124N3.1
RP11-124N3.2 RP11-124N3.3 RP11-1250I15.1 RP11-1250I15.2 RP11-1325J9.1
RP11-154D6.1 RP11-155O18.3 RP11-159C21.3 RP11-159C21.4 RP11-183G22.1

RP11-183G22.2 RP11-183G22.3 RP1-118J21.5 RP11-197O8.1 RP11-19O2.1
RP11-19O2.2 RP11-19O2.4 RP11-1C1.1 RP11-1C1.3 RP11-1C1.4 RP11-1C1.5 RP11-1C1.6
RP11-1C1.7 RP11-215G15.2 RP11-215G15.3 RP11-215G15.4 RP11-25O10.1 RP11-260E18.1
RP11-263F15.1 RP11-269F19.2 RP11-269F19.4 RP11-275B7.1 RP11-291J9.1
RP11-291J9.2 RP11-308B16.1 RP11-308B16.2 RP11-319C21.1 RP11-321E2.10
RP11-321E2.11 RP11-321E2.12 RP11-321E2.13 RP11-321E2.2 RP11-321E2.3
RP11-321E2.4 RP11-321E2.5 RP11-321E2.6 RP11-321E2.7 RP11-321E2.8
RP11-321E2.9 RP11-32F11.2 RP11-36C20.1 RP1-137K24.1 RP11-419C19.1
RP11-419C19.2 RP11-419C19.3 RP11-42L13.1 RP11-42L13.2 RP11-432M8.1
RP11-432M8.10 RP11-432M8.11 RP11-432M8.12 RP11-432M8.13 RP11-432M8.14
RP11-432M8.15 RP11-432M8.16 RP11-432M8.17 RP11-432M8.18 RP11-432M8.19
RP11-432M8.2 RP11-432M8.3 RP11-432M8.4 RP11-432M8.5 RP11-432M8.6
RP11-432M8.7 RP11-432M8.8 RP11-432M8.9 RP11-447B18.1 RP11-454P21.1
RP11-463J7.1 RP11-463J7.2 RP11-463J7.3 RP11-46C20.1 RP11-478A7.1
RP11-492I2.1 RP11-54F2.1 RP11-560A7.1 RP11-560D2.2 RP11-567C20.2 RP11-567C20.3
RP11-572H4.1 RP11-572H4.2 RP11-5N11.1 RP11-5N11.2 RP11-5N11.3
RP11-5N11.4 RP11-5N11.5 RP11-5N11.6 RP11-5N11.7 RP1-167G20.1 RP1-
167G20.2 RP11-81B23.1 RP11-823P9.1 RP11-823P9.3 RP11-93G23.1 RP11-93N19.1 RP11-93N19.2
RP11-93N19.3 RP1-21K4.1 RP1-251I12.1 RP1-288M22.1 RP1-288M22.2 RP3-331H24.4
RP3-415N12.1 RP3-487J7.2 RP4-631H13.2 RP4-784A16.1 RP4-784A16.2 RP4-784A16.3
RP4-784A16.4 RP4-784A16.5 RP4-795A5.1 RP4-796B4.1 RP5-1024G6.2 RP5-
1024G6.5 RP5-850O15.3 RP5-882O7.1 RP5-926E3.1 RPS8 RXFP3 SEMA5A SLC45A2
SNORA18 SNORA40 SNORD123 SNORD38 SNORD46 snosnR61 snoU13 SPAG1 SUB1 TARS TAS2R1
TCTEX1D4 TMEM53 TRIO TRIT1 U2 U4 U5 U6 U8 Y_RNA
ZCCHC11 ZFR ZNF622 ZNF859P ZYG11A ZYG11B

PANTHER analysis: 84 mapped ids are found, 266 mapped ids are not found.

5.8.8.5 Losses in TN pure DCIS and TN DCIS Associated with Invasive Breast Disease

There are genomic losses in TN pure DCIS (n=4/9) which were not observed in TN DCIS associated with invasive breast disease (n=0/10).

1. p-values < 0.05;
2. A gene list is mapped from 7 genomic regions found on chromosomes 7, 16, 17, 19;
3. These regions encompass 29 genes altered in TN pure DCIS;

   Genes:

AC006013.1 AC006480.2 AC008734.1 AC067941.1 AC099758.1 AC131384.1 CALN1 KRT14 KRT16 KRT17
KRT42P PMS2L4 RP11-166O4.1 RP11-166O4.4 RP11-166O4.5 RP11-166O4.6
RP11-358M3.1 RP11-421N10.1 RP4-635O5.1 RP4-736H5.1 RP4-736H5.2
RP4-736H5.3 RP5-945F2.1 RP5-945F2.2 RP5-945F2.3 STAG3L4 TYW1 WBSCR17
Y_RNA

PANTHER analysis: 6 mapped ids are found, 23 mapped ids are not found.

There are some similarities in genomic losses in TN DCIS associated with invasive breast disease (n=7/10) compared to TN pure DCIS (n=1/9).

1. p-values < 0.05;
2. A gene list is mapped from 19 genomic regions found on chromosomes 3, 4, 5, 13, 14;
3. These regions encompass 49 genes altered in TN DCIS associated with invasive breast disease;

   Genes:

AC006427.1 AC006427.2 AC006427.3 AC093848.1 AC106868.1 AC107394.1 AC109351.1 AC110766.1 AL590102.1 AL596329.1 CCKAR CTC-507E12.1 FHIT GPHB5 GPHN KCNH5 KCNIP4 LDB2 MAGI1 PACRGL PCDH7 PPP2R5E RHOJ RP11-120A1.1 RP11-141E13.1 RP11-174E22.1 RP11-174E22.2 RP11-293A21.1 RP11-293A21.2 RP11-308K2.1 RP11-315A17.1 RP11-390C19.1 RP11-415C15.1 RP11-417M17.1 RP11-429G17.1 RP11-495L18.2 RP11-543A18.1 RP11-617I14.1 RP11-619J20.1 RP11-93M12.1 SCARNA20 SLIT2 SNORD74 snoU13 STIM2 SYNE2 TAPT1 TBC1D19 U6

PANTHER analysis: 16 mapped ids are found, 33 mapped ids are not found.

5.8.8.6 TN DCIS Associated with Invasive breast disease

There were total losses present in TN pure DCIS (n=8/9) which were not observed in TN DCIS associated with invasive breast disease (n=0/10).

1. p-value<0.05;
2. A gene list is mapped from 25 genomic regions found on chromosomes 6, 8, 11, 13, 14, 16, 17, 19, 22;
3. These regions encompass 72 genes altered in TN pure DCIS;

Genes:

AARSD1 ABCC12 ABCC4 AC004019.10 AC004019.17 AC004659.1 AC005513.1 AC008734.1 AC008734.2 AC087650.1 AC087650.8 AC090427.1 AC100793.2 ADAM5P AL136359.1 AL137001.1 AOC2 AOC3 ARL4D BRCA1 CACNA1A CCDC105 CECR2 CTD-3199J23.2 DNAH9 EMR2 EMR3 FBXO33 G6PC GPC5 hsa-mir-2117 IFI35 MBD3L1 MUC16 OLFM4 OR4C3 OR4C45 OR4C5 OR4S1 OR4X1 OR4X2 OR7A10 OR7A11P OR7A17 OR7A2P OR7A5 OR7C1 OR7C2 PARK2 PSME3 RND2 RP11-24H2.1 RP11-24H2.2 RP11-301J16.2 RP11-301J16.3 RP11-301J16.5

RP11-301J16.7 RP11-442J17.4 RPL27 RTN1 RUNDC1 SLC1A6 SNORA40 U2 U6 VAT1 Y_RNA ZNF333 ZNF558

PANTHER analysis: 40 mapped ids are found, 29 mapped ids are not found.

There were total losses present in TN DCIS associated with invasive breast disease (n=8/10) which were not observed in TN pure DCIS (n=0/9).

1. p-values < 0.05;
2. A gene list is mapped from 32 genomic regions found on chromosomes 3, 4, 5, 8, 9, 13, 14, 15, 17, 18;
3. These regions encompass 56 genes altered in TN DCIS associated with invasive breast disease;

   Genes:

7SK AC021860.1 AC022559.1 AC023385.1 AC034111.1 AC084882.1 AC091133.1 AC096750.1 AC103702.1 AC114477.1 AC139426.1 AC139426.3 AC139426.4 ACTR10 AL079307.3 AL079307.4 AL079307.5 AL121579.1 AL132989.2 AL138995.1 AL139021.2 AL163952.2 ARAP2 ARID4A ASPN B4GALNT2 C14orf166 C14orf181 CENPP CSMD1 CTD-2015H6.1 CTD-2015H6.2 CTD-2015H6.3 CTD-2244F11.2 CTD-2325P2.2 DTHD1 ECM2 FAM151B FAM7A1 FMN1 FRMD6 GIP GNG2 GREM1 HMGB1L14 HOXB7 HOXB9 IGF2BP1 KIAA0586 KLB KLF3 KLHL5 LIAS MITF MSRA MTUS1 OMD PDCD6IP PDS5B PELI2 PRSS55 PSMA3 RAD51L1 RFC1 RP11-1000B6.2 RP11-212F11.1 RP11-213G21.1 RP11-213G21.2 RP11-22A3.2 RP11-360F5.1 RP11-360F5.2 RP11-360F5.3 RP11-380B4.2 RP11-431M7.2 RP11-431M7.3 RP11-501C14.5 RP11-501C14.6 RP11-501C14.7 RP11-617D20.1 RP11-708H21.1 RP11-83C7.1 RP11-83C7.2 RP13-395E19.1 RP1L1 RPL9 SCG5 SNF8 SNORA18 snoU13 SPRED1 TIMM9 TMEM156 TOMM20L U1 U3 U6 U8 UBE2Z WDR19 Y_RNA ZFP36L1 ZFYVE16

5.8.8.7 CdLOH of TN pure DCIS and TN DCIS Associated with Invasive breast disease

There is CdLOH present in TN pure DCIS (n=4/9) which were not observed in TN DCIS associated with invasive breast disease (n=0/10)

1. p-values < 0.05;
2. A gene list is mapped from 4 genomic regions found on chromosomes 7, 16, 17;

3. These regions encompass 12 genes altered in TN pure DCIS;

   Genes:

   AC006013.1 AC131384.1 CALN1 KRT14 KRT16 KRT17 KRT42P RP11-358M3.1 RP4-635O5.1 RP5-945F2.1RP5-945F2.2 RP5-945F2.3

PANTHER analysis: 4 mapped ids are found, 8 mapped ids are not found.

There is CdLOH present in TN DCIS associated with invasive disease (n=7/10) not observed in TN pure DCIS (n=0/9).

1. p-values < 0.05;
2. A gene list is mapped from 37 genomic regions found on chromosomes 3, 4, 5, 8, 13, 14, 15, 17;
3. These regions encompass 96 genes altered in TN DCIS associated with invasive breast disease;

   Genes:

   7SK AC006160.1 AC006160.2 AC006160.4 AC006160.5 AC006445.6 AC006445.7 AC007126.1 AC015688.1 AC020698.1
   AC093848.1 AC098830.1 AC106868.1 AC107394.1 AC110766.1 AC111152.1 ADH1A ADH1B ADH1C
   AL110292.1 BOD1L C14orf53 C4orf47 C5orf13 CCDC110 CDCA2 CLRN2 CTC-459M5.1 CTC-459M5.2
   CTD-2022H16.1 CTD-2192A1.1 EPB41L4A FAM184B FAM189A1 FAM19A4 GBA3 GPM6A
   GPR125 KCNH5 KCNIP4 KSR1 LAP3 LDB2 LGALS9 MED28 MTNR1A
   NCRNA00219 PCDH7 PDLIM3 PPARGC1A PTPRG QDPR RP11-103J17.1 RP11-10G12.1
   RP11-10G12.2 RP11-120A1.1 RP11-141E13.1 RP11-17E2.2 RP11-196P2.1
   RP11-215A19.1 RP11-24D11.1 RP11-279O9.4 RP11-301L8.2 RP11-315A17.1
   RP11-333E5.1 RP11-333E5.2 RP11-341G5.1 RP11-380P13.1 RP11-380P13.2
   RP11-495L18.2 RP11-540E16.2 RP11-556G22.1 RP11-556G22.2 RP11-556G22.3
   RP11-576E20.1 RP11-598O12.1 RP11-598O12.2 RP11-617I14.1 RP11-619J20.1
   RP11-626E13.1 RP11-665I14.1 RP11-696N14.1 RP11-722M1.1 RP11-806K15.1
   RP11-93M12.1 RP13-497K6.1 RPL10AP6 SNORA13 SNORA51 SNORA75 snoU13 SORBS2
   TJP1 U6 WDR17 Y_RNA

PANTHER analysis: 28 mapped ids are found, 68 mapped ids are not found.

5.8.8.8 CnLOH of TN pure DCIS and TN DCIS Associated with Invasive Breast Disease

There is CnLOH present in TN pure DCIS (n=9/9) which were not observed in TN DCIS associated with invasive breast disease (n=0/10).

1. p-values < 0.05;
2. A gene list is mapped from 74 genomic regions found on chromosomes 1, 2, 3, 6, 7, 10, 11, 19;
3. These regions encompass 574 genes altered in TN pure DCIS;

   Genes:

5S_rRNA 7SK AC002066.1 AC005487.2 AC005779.1 AC010087.1 AC010087.4 AC010087.5 AC011489.2 AC011489.3
AC013251.1 AC013251.2 AC017083.1 AC017083.2 AC017083.3 AC022210.2 AC023165.1 AC067950.1 AC073130.3
AC073210.1 AC079112.1 AC084193.1 AC092958.1 AC099680.1 AC104073.1 AC105342.1 AC108697.1 AC117508.1 ACTG2
ADAM22 ADCY5 AGTR1 AKR1A1 AL008729.1 AL023583.1 AL023807.1 AL023807.2 AL024498.1 AL031785.1
AL031905.1 AL034372.1 AL035464.1 AL035555.2 AL035670.1 AL049710.1 AL049710.2 AL049710.4 AL050335.1
AL050335.2 AL079341.1 AL109918.1 AL117340.2 AL117340.3 AL121946.1 AL135912.1 AL136230.1 AL136305.1
AL137003.1 AL138724.3 AL157773.1 AL162579.1 AL354680.1 AL357079.1 AL357079.2 AL357497.1 AL359316.1
AL391839.1 AL391839.3 AL445669.2 AL590068.1 AL603888.1 AL604028.1 AL604028.2 ALG1L AP003774.4
AP003774.5 AP003774.6 AP003774.7 APBB1IP APLNR ARTN ATP5LP5 ATP6V0B ATXN1 B4GALT2
BCL7B BLOC1S3 BMP5 BPESC1 BRAF BTBD9 BTF3L4 C10orf68 C1D
C1orf210 C1orf50 C2orf89 C3orf16 C3orf72 C6orf114 C6orf142 C6orf52 C6orf64 CAP2
CAV2 CCDC14 CCDC17 CCDC23 CCDC24 CCDC30 CCDC88B CCDC90A CCT6P3 CD2AP
CD83 CEP70 CLDN19 CNRIP1 COL21A1 COL9A2 COMMD2 CTB-54D4.1 CYP26B1
CYP39A1 DAAM2 DEFB110 DEFB112 DEFB113 DEFB114 DEFB133 DEK DNAH6 DNAH8
DNAJB9 DNAJC30 DPH2 EBNA1BP2 EDN1 EEF1A1P25 EFHC1 ELOVL2 EPC1
ERMAP ERV3 ESYT3 EXOC3L2 FAIM FAM8A1 FOXL2 GAPDHP39 GCLC
GCM2 GCNT2 GCNT6 GEMIN7 GFOD1 GFRAL GJA9 GLO1 GLP1R
GMPR GPBP1L1 GPR110 GPR111 GPR115 GPR116 GSTA1 GSTA2 GSTA3 GSTA5
GSTA6P HCRTR2 HIVEP1 HMGCLL1 hsa-mir-1237 hsa-mir-133b hsa-mir-206 hsa-mir-548a-1 hsa-mir-761
IL17A IL17F INTS4L1 IPO13 IPP IQCJ ITGB1 JAK1 KCNK16 KCNK17
KCNK5 KDM1B KDM4A KIF13A KIF6 KLHL31 KTI12 LEPRE1 LRFN2
LRRC1 LRRC55 LRRC68 LTBP4 LYZL2 MAK MAST2 MCM3 MEP1A
MLXIPL MME MRAS MRPS22 MYCBP MYLIP MYLK NASP NEDD9 NKPD1 NOL7
NRCAM NRD1 NRP1 NUP153 OFCC1 OSBPL9 P2RY1 PABPC1P10 PAK1IP1 PAQR8
PDIA5 PFN2 PHACTR1 PIK3CB PIK3R3 PKHD1 PLA2G7 PNO1 PNPLA8 PPCS
PPIH PPP3R1 PRIM2 PRR23A PRR23B PRR23C PTPLB PTPRF RAB3B
RAB7A RANBP9 RARRES1 RAVER2 RBM24 RCAN2 RELB RHBDL2 RIMKLA
RNF13 RNF144B RNF182 RP11-10O22.2 RP11-117F22.1 RP11-121P10.1 RP11-125M16.1
RP11-127P7.2 RP11-135A24.2 RP11-135A24.4 RP11-146I2.1 RP11-146I2.2
RP11-14C22.5 RP11-14H3.3 RP11-157D18.2 RP11-163G10.2 RP11-163G10.3
RP11-163G10.4 RP11-166N17.1 RP11-166N17.3 RP11-167H9.3 RP11-167H9.4
RP11-184I16.2 RP11-184I16.3 RP11-184I16.4 RP11-192K2.3 RP11-192P3.1
RP11-192P3.3 RP11-202D20.1 RP11-203H2.1 RP11-203H2.2 RP11-204E9.1
RP11-221E20.3 RP11-221E20.4 RP11-221E20.5 RP11-228O6.2 RP11-232M24.1
RP11-253D19.1 RP11-253D19.2 RP11-255N4.2 RP11-255N4.3 RP11-268F1.2
RP11-268F1.3 RP11-282K6.3 RP11-306L14.1 RP11-322N21.2 RP11-323I14__A.1 RP11-
328P23.2 RP11-330A16.1 RP11-330O11.2 RP11-342D11.3 RP11-342M1.2 RP11-342M1.3
RP11-342M1.4 RP11-345L23.1 RP11-354I10.1 RP11-359N11.1 RP11-359N11.2
RP11-360O19.1 RP11-360O19.4 RP11-360O19.5 RP11-379B18.4 RP11-379B18.5
RP1-137F1.3 RP11-385F7.2 RP11-38P22.2 RP11-392A23.4 RP11-392A23.5 RP11-

397G17.1 RP1-13D10.2 RP1-13D10.3 RP1-13D10.4 RP1-13D10.5 RP11-401E14.1
RP11-401E14.2 RP11-411K7.1 RP11-411K7.2 RP11-411K7.4 RP11-411K7.5
RP11-418B12.1 RP11-420A21.1 RP1-142O9.2 RP11-430C17.1 RP11-446F17.3
RP11-451G4.2 RP11-451G4.3 RP11-460H18.1 RP11-460H18.2 RP11-460N20.3
RP11-460N20.4 RP11-460N20.5 RP11-462L8.1 RP11-462L8.2 RP11-466L17.1
RP11-470H9.1 RP11-472N13.2 RP11-479G22.3 RP11-479G22.5 RP11-479G22.6
RP11-479G22.7 RP11-501I19.3 RP11-501I19.4 RP11-501O2.1 RP11-501O2.2
RP11-501O2.3 RP11-501O2.4 RP11-501O2.5 RP11-505J9.1 RP1-151F17.1
RP11-529G21.4 RP1-152L7.1 RP1-152L7.3 RP1-152L7.5 RP1-152L7.6 RP11-548O1.1 RP11-548O1.3
RP11-550C4.6 RP11-590C23.1 RP11-598F17.1 RP11-630I5.1 RP11-635I10.1 RP11-637O19.2
RP11-639B1.1 RP11-63E16.1 RP11-649A16.1 RP11-649A16.5 RP11-651P23.2
RP11-651P23.3 RP11-651P23.4 RP11-651P23.5 RP11-651P23.6 RP11-666A20.1
RP11-666A20.3 RP11-666A20.4 RP11-689D3.4 RP11-71N10.1 RP11-722C17.1
RP11-723O4.2 RP11-735A5.1 RP11-746P2.5 RP11-767N6.2 RP11-767N6.7
RP11-771D21.2 RP11-788A4.1 RP11-788A4.2 RP11-793K1.1 RP11-795J1.1
RP11-795J1.2 RP11-797H7.1 RP11-797H7.2 RP11-797H7.3 RP11-797H7.5
RP11-79N23.1 RP11-7O11.3 RP1-180E22.3 RP11-812I20.2 RP11-90C4.1
RP11-90C4.2 RP11-90C4.3 RP11-90C4.4 RP1-190J20.2 RP11-91A18.1
RP11-91A18.4 RP11-91A18.5 RP11-9N20.1 RP1-202I21.3 RP1-202I21.5
RP1-207H1.2 RP1-207H1.3 RP1-217P22.2 RP1-228H13.1 RP1-228H13.2 RP1-
257A7.4 RP1-273P12.1 RP1-273P12.3 RP1-27K12.2 RP1-27K12.4 RP1-290I10.4 RP1-
290I10.5 RP1-290I10.7 RP1-295F6.2 RP1-304B14.3 RP1-319M7.2 RP13-469O16.1
RP13-476E20.1 RP1-62D2.3 RP1-71H19.2 RP3-322I12.2 RP3-322L4.2 RP3-335N17.2
RP3-347E1.2 RP3-365O12.2 RP3-380E11.2 RP3-437C15.1 RP3-445N2.1 RP3-
448I9.1 RP3-448I9.2 RP3-451B15.3 RP3-462C17.1 RP3-486B10.1 RP3-486D24.1 RP3-503A6.2
RP3-510L9.1 RP4-533D7.3 RP4-533D7.4 RP4-533D7.5 RP4-633H17.2 RP4-
657D16.3 RP4-724P12.1 RP4-753D5.3 RP4-753D5.4 RP4-761I2.2 RP4-761I2.4 RP5-1043E3.1
RP5-864K19.4 RP5-994D16.3 RP5-994D16.7 RP5-994D16.9 RPL15P3 RPN1
RPS15AP10 RPS15AP16 RPS17P5 RPS6KA4 RRAGC SEC22A SFRS16 SHKBP1 SHMT1P1
SIRT5 SLC25A20P1 SLC25A27 SLC35B3 SLC6A9 SMAP2 SNORA15 SNORA22
SNORA24 SNORA5 SNORA8 SNORD45 SNORD66 snoU13 SOX4 SPTBN4 ST3GAL3 STX1A
SUCLA2P2 SYCP2L TBC1D7 TBL2 TDRD6 TFAP2B TFAP2D TFEC THAP5 TMEM125
TMEM14A TMEM14B TMEM14C TMEM69 TMSB10 TNFRSF21 TPMT TRAM2 TRAPPC6A
TSPAN1 TXNDC12 U1 U3 U6 U7 USP34 VPS37D WBSCR22 WDR92
WWTR1 Y_RNA YBX1 ZEB1 ZFAND3 ZIC1 ZIC4 ZMYND12 ZNF117
ZNF138 ZNF273 ZNF296 ZNF438 ZNF643 ZNF691

PANTHER analysis: 126 mapped ids are found, 331 mapped ids are not found.

There is some overlap in CnLOH in TN DCIS associated with invasive breast cancer (n=10/10) and CnLOH in TN pure DCIS (n=5/9).

This represents CnLOH for TN DCIS associated with invasive breast disease.

1. p-values < 0.05;

2. A gene list is mapped from 49 genomic regions found on chromosomes 1, 2, 3, 7,10,12,17, 19, 20, 21, X;
3. These regions encompass 309 genes altered in TN DCIS associated with invasive breast disease;

   Genes:

5S_rRNA	AC004455.1	AC004691.5	AC005189.6	AC005537.2	AC005879.1	AC006466.5	AC006960.7	AC006978.1	AC010789.1	
	AC015923.1	AC016706.1	AC063927.2	AC063927.3	AC063927.4	AC063927.5	AC063927.6	AC063927.7	AC063927.8	
	AC063927.9	AC063944.1	AC068765.1	AC073585.1	AC087069.2	AC113554.1	AC114788.1	AC114788.2	AC138128.1	
	ACADSB	ACE	ACE2	ADCYAP1R1	ADRB1	AF015262.1	AF015262.2	AF015720.3	AF015726.1	
	AF020802.1	AF020802.2	AF020802.3	AF020802.4	AL133215.1	AL133387.2	AL135794.1	AL157788.1	AL158014.1	
	AL162407.1	AL353664.1	AL355598.1	AL355861.1	AL359747.1	AL359836.1	AL591845.1	AL603764.1	AL731543.1	
	ANLN	AOAH	AP000688.8	AQP1	ARMS2	ATE1	BBX	BLVRA	BMX	
	BRIP1	BTBD16	BTRC	BUB3	C10orf118	C10orf119	C10orf120	C10orf2	C10orf46	
	C10orf76	C10orf84	C10orf88	C10orf90	C1orf113	C7orf44	CA5B	CA5BP	CASC2	
	CCDC54	CD3EAP	CSF3R	CUZD1	CYB561	DCAF7	DCLRE1A	DLGAP3	DMBT1	
	DNMBP	DOCK1	DPCD	EIF3A	ELOVL3	EMX2	EMX2OS	ERCC1	FAM176B	
	FAM178A	FAM188B	FAM24A	FAM24B	FAM45A	FBXW4	FGF8	FGFR2	FOSB	
	FTLP18	GBF1	GHRHR	GLI3	GPAM	GRK5	GS1-594A7.3		GS1-594A7.5	
	HDAC4	HECW1	HMX2	HMX3	HPS6	hsa-mir-608	hsa-mir-802	HTRA1	IKZF5	
	INMT	INPP5F	INTS2	JAKMIP3	KAZALD1	KCNH6	KCNIP2	KCNK18	KIAA1598	
	LBX1	LDB1	LSM10	LZTS2	MGEA5	MRPL43	MRPS15	MRPS24	MT-ATP6	MT-
CO1	MT-CO3	MT-ND1	MT-ND2	MT-ND3	MT-ND4	MT-ND4L	MT-ND5	MT-ND6	NANOS1	
	NCRNA00093		NHLRC2	NKX2-3	NOLC1	NPM3	NSMCE4A	OSCP1	PDZD7	
	PDZD8	PITX3	PLEKHA1	POLL	PPM1N	PPP1R13L	PPP1R2P2	PPRC1	PRDX3	
	PRLHR	PSTK	RAB11FIP2	RGS9	RP11-107C16.2		RP11-107I14.1		RP11-107I14.2	
	RP11-107I14.4		RP11-107I14.5		RP11-108L7.4		RP11-108L7.7		RP11-129J12.1	
	RP11-153N17.1		RP11-162A23.5		RP11-179H18.8		RP11-181E22.1		RP11-190J1.10	
	RP11-190J1.3		RP11-190J1.7		RP11-198M6.2		RP11-198M6.5		RP11-214N15.5	
	RP11-215A21.2		RP11-223P11.2		RP11-223P11.3		RP11-244H3.1		RP11-244H3.2	
	RP11-245J24.1		RP11-248I9.2		RP11-25C19.1		RP11-25C19.3		RP11-280F2.1	
	RP11-280F2.2		RP11-282I1.1		RP11-298H24.1		RP11-302K17.3		RP11-302K17.4	
	RP11-302K17.7		RP11-309P22.1		RP11-319I23.2		RP11-319I23.3		RP11-31L23.3	
	RP11-324L3.1		RP11-328K15.1		RP11-338O1.2		RP11-354M20.3		RP11-36N22.1	
	RP11-36N22.3		RP11-381K7.1		RP11-381K7.2		RP11-411P18.2		RP11-446H18.1	
	RP11-446H18.3		RP11-446H18.5		RP11-45P22.1		RP11-45P22.2		RP11-462G8.2	
	RP11-462G8.3		RP11-498J9.1		RP11-498J9.2		RP11-498J9.4		RP11-500G22.2	
	RP11-501J20.2		RP11-501J20.3		RP11-501J20.5		RP11-561O4.1		RP11-564D11.3	
	RP11-567J24.4		RP11-56I23.1		RP11-57H14.3		RP11-5G18.2		RP11-781P14.3	
	RP11-78C6.1		RP11-79M19.2		RP11-93B21.1		RP13-314C10.5		RP5-1158B12.1	
	RP5-877J2.1	RPL23AP3	RPL34P3	RPS20P1	RTN2	RUNX1	SAT1	SCN4A	SEC23IP	
	SEMA4G	SETD4	SFPQ	SFXN3	SFXN4	SLC18A2	SNORA19	SNORA63	SNORD112	
	SNORD60	snoU13	SORCS3	STK40	TACC2	TANC2	TCERG1L	THRAP3	TLX1	
	TLX1NB	TMEM27	TWIST2	U2	U3	U4	U6	URGCP	USP29	
	VASP	VAX1	VTI1A	Y_RNA	ZIM3	ZMYM1	ZMYM6			

PANTHER analysis: 134 mapped ids are found, 157 mapped ids are not found.

5.8.9 Copy Number Aberrations for Triple Negative Pure DCIS Compared to Triple Negative Invasive Breast Disease

These series examines the difference between pure triple negative DCIS only and TN invasive breast disease.

Frequency plots showing copy number aberrations between Pure TN DCIS and TN invasive breast disease were provided by Breakthrough Breast Cancer/Research Oncology, King's College London Bioinformatics Department (Figure 42).

Figure 42: Frequency plots showing copy number aberrations between pure triple negative DCIS and triple negative invasive breast disease (amplifications, duplications, gains, Sc gains, losses, total losses CdLOH and CnLOH,) (pages 249-251).

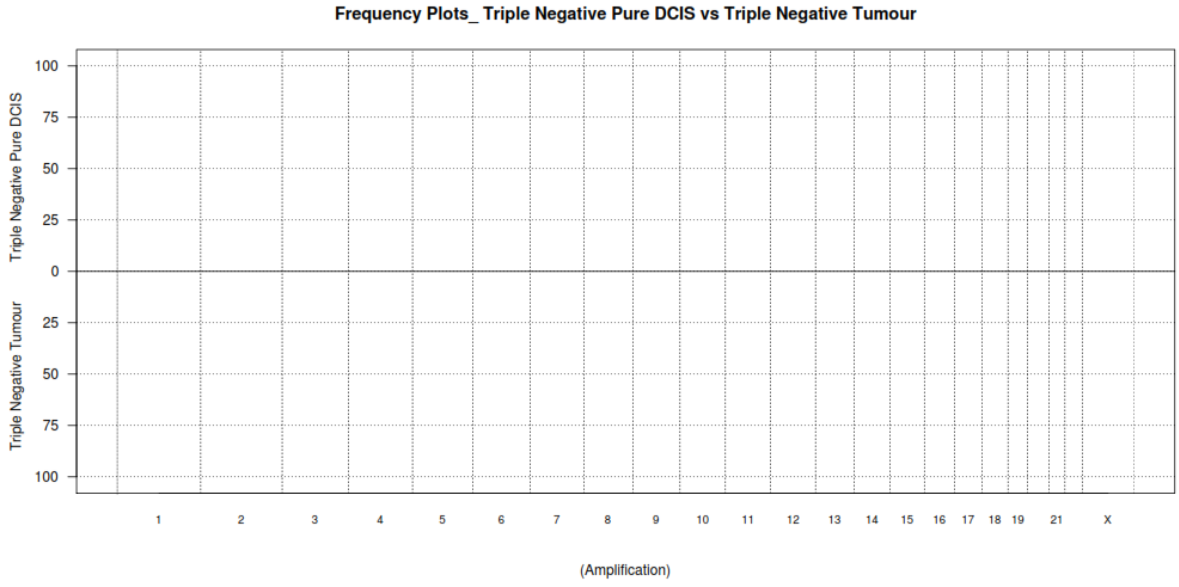
Frequency Plots_ Triple Negative Pure DCIS vs Triple Negative Tumour
Triple Negative Pure DCIS
Triple Negative Tumour
100
75
50
25
0
25
50
75
100
1
2
3
4
5
6
7
8
9
10
11
12
13
14
15
16
17
18
19
21
X
(Amplification)

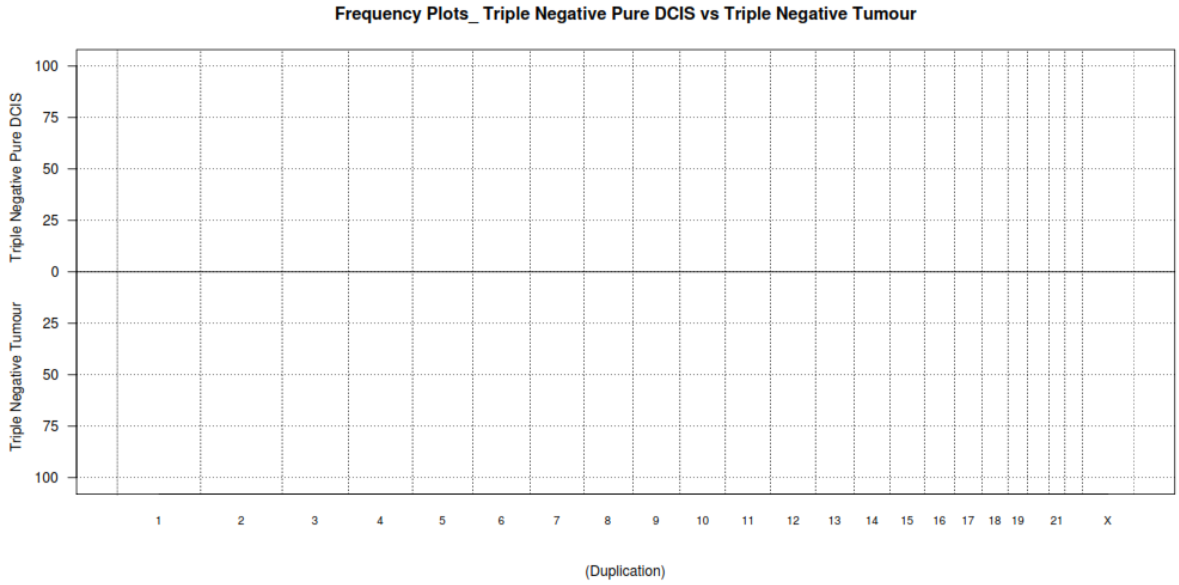
Frequency Plots_ Triple Negative Pure DCIS vs Triple Negative Tumour
Triple Negative Pure DCIS
Triple Negative Tumour
100
75
50
25
0
25
50
75
100
1
2
3
4
5
6
7
8
9
10
11
12
13
14
15
16
17
18
19
21
X
(Duplication)

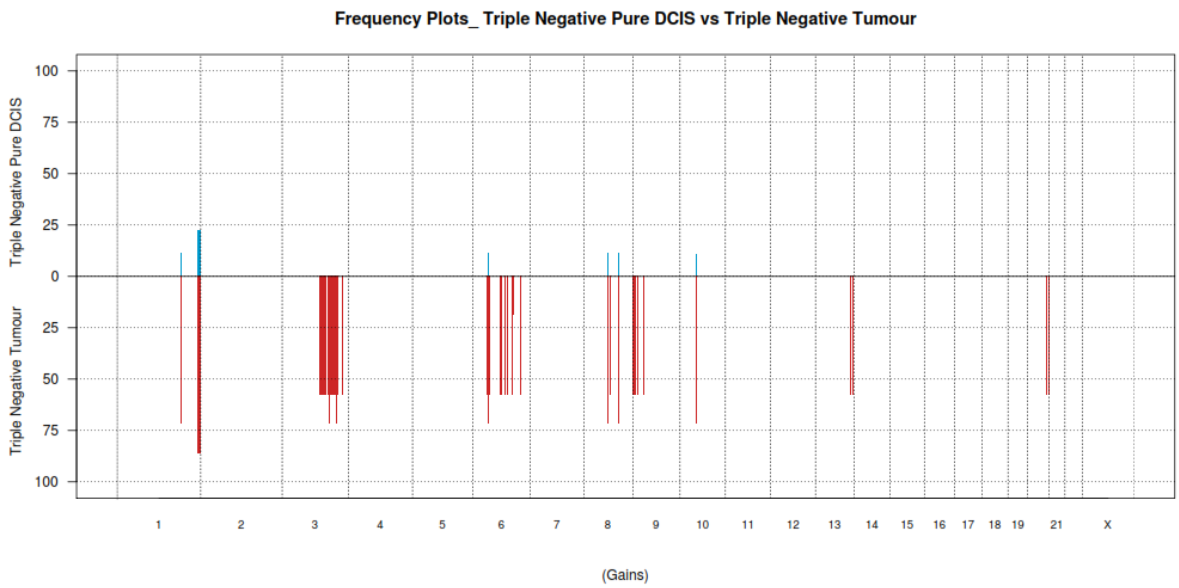
Frequency Plots_ Triple Negative Pure DCIS vs Triple Negative Tumour
Triple Negative Pure DCIS
Triple Negative Tumour
100
75
50
25
0
25
50
75
100
1
2
3
4
5
6
7
8
9
10
11
12
13
14
15
16
17
18
19
21
X
(Gains)

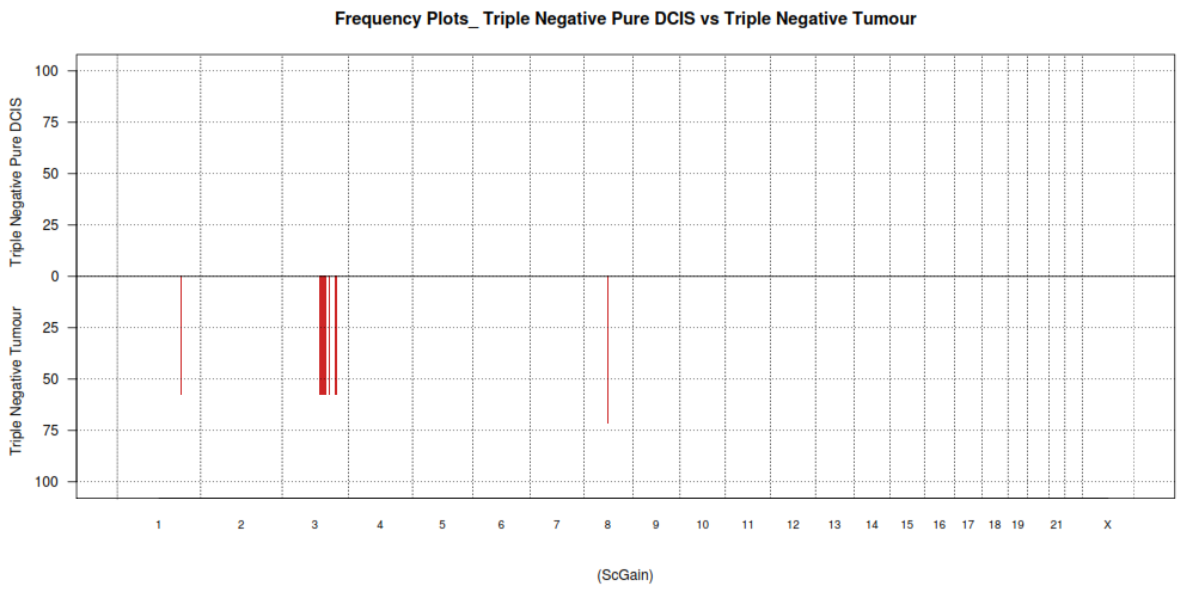
Frequency Plots_ Triple Negative Pure DCIS vs Triple Negative Tumour
Triple Negative Pure DCIS
Triple Negative Tumour
100
75
50
25
0
25
50
75
100
1
2
3
4
5
6
7
8
9
10
11
12
13
14
15
16
17
18
19
21
X
(ScGain)

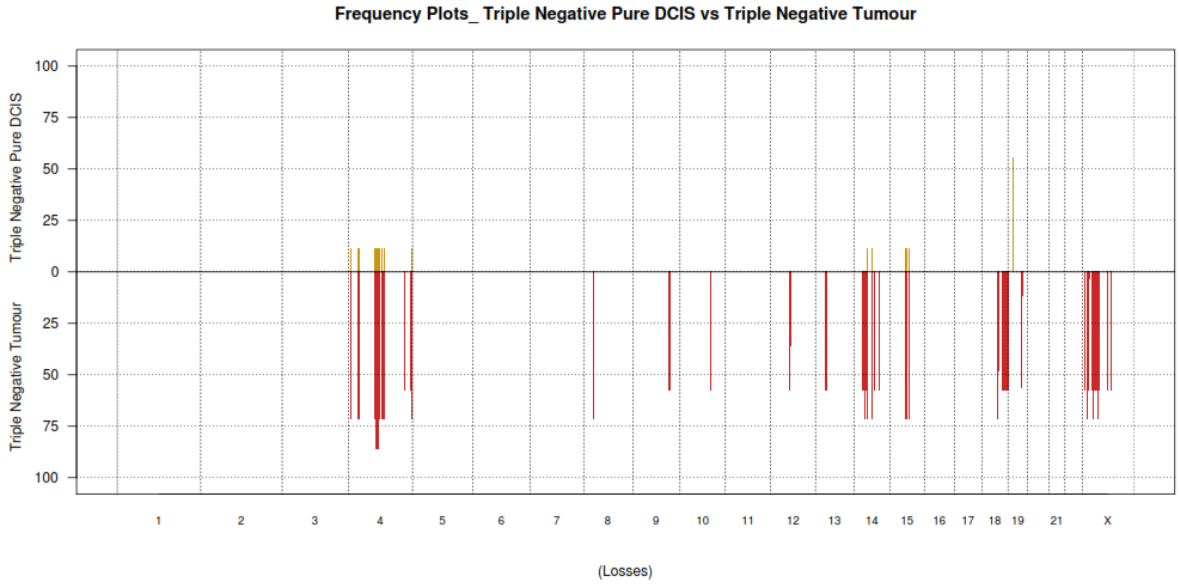
Frequency Plots_ Triple Negative Pure DCIS vs Triple Negative Tumour
Triple Negative Pure DCIS
Triple Negative Tumour
100
75
50
25
0
25
50
75
100
1
2
3
4
5
6
7
8
9
10
11
12
13
14
15
16
17
18
19
21
X
(Losses)

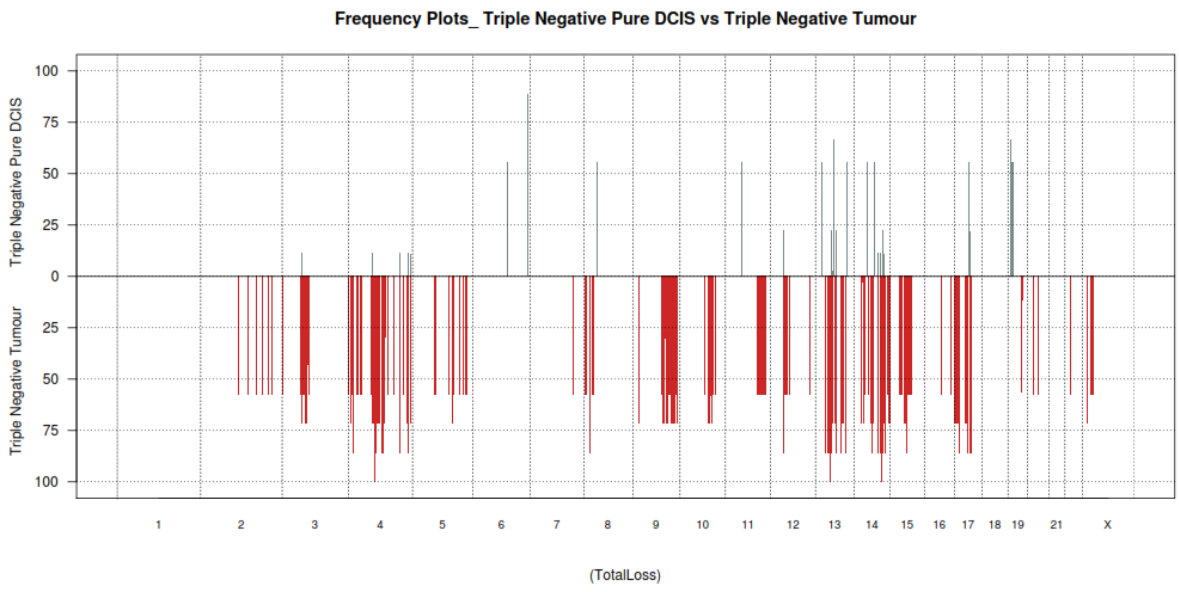
Frequency Plots_ Triple Negative Pure DCIS vs Triple Negative Tumour
Triple Negative Pure DCIS
Triple Negative Tumour
100
75
50
25
0
25
50
75
100
1
2
3
4
5
6
7
8
9
10
11
12
13
14
15
16
17
18
19
21
X
(TotalLoss)

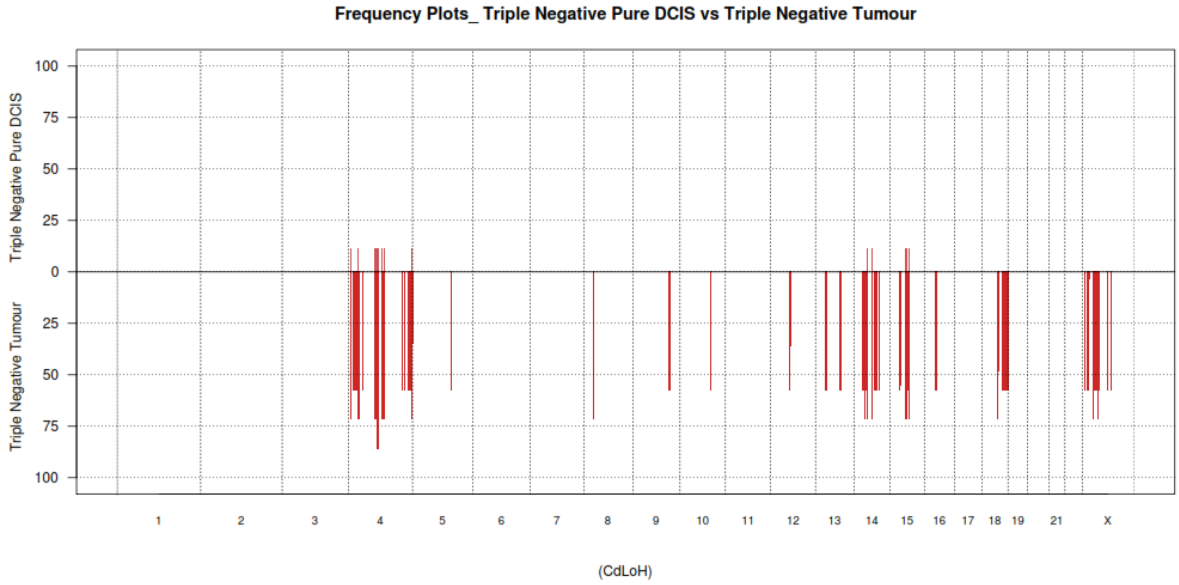
Frequency Plots_ Triple Negative Pure DCIS vs Triple Negative Tumour
Triple Negative Pure DCIS
Triple Negative Tumour
100
75
50
25
0
25
50
75
100
1
2
3
4
5
6
7
8
9
10
11
12
13
14
15
16
17
18
19
21
X
(CdLoH)

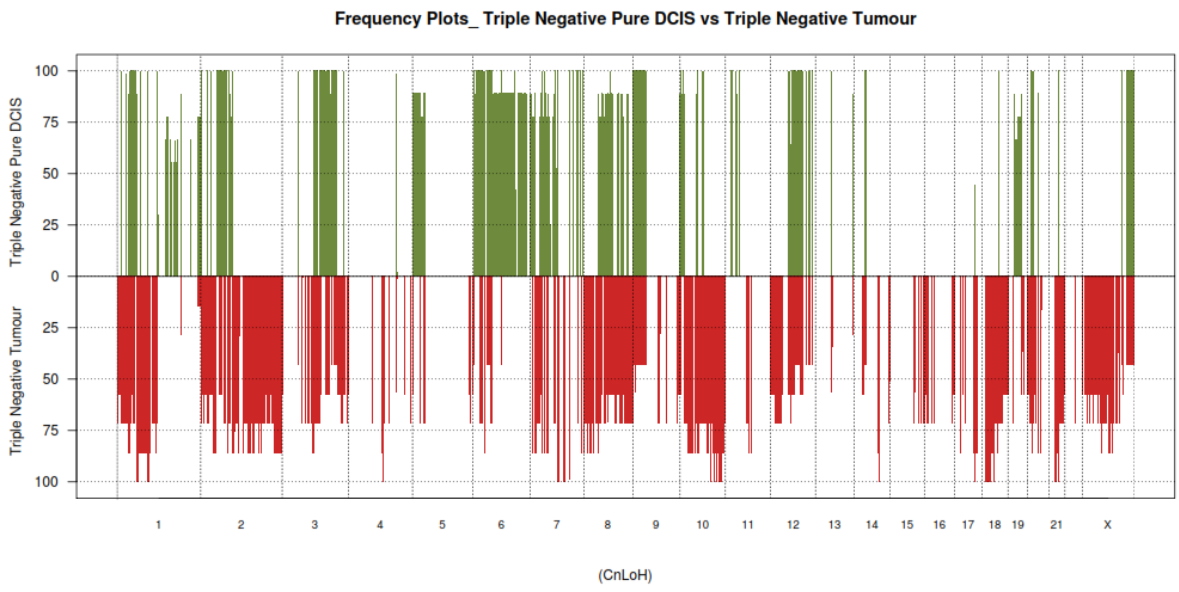

5.8.9.1 Amplification of Pure Triple Negative DCIS and Triple Negative Invasive Breast Disease

No amplifications are found in TN pure DCIS or TN invasive breast disease in this series.

5.8.9.2 Duplication in Pure Triple Negative DCIS and Triple Negative Invasive Breast Disease

There are duplications are found in TN pure DCIS (n=1/9) and TN invasive breast disease (n=3/7).

1. p-values < 0.05;
2. A gene list is mapped from 13 genomic regions found on chromosomes 2, 6, 8, 12;
3. These regions encompass 181 genes altered in TN pure DCIS and TN invasive breast disease;

Genes:

5S_rRNA	7SK	ABCC10	AC012494.1	AC079600.1	AL080315.3	AL096711.1	AL121959.1	AL136304.1	AL136304.2
AL136304.3	AL451073.1	AL583834.1	ARG1	BMP5	BYSL	C6orf108	C6orf132	C6orf15_2	C6orf154
C6orf174	C6orf192	C6orf226	C6orf58	C8orf85	CCND3	CENPW	CLIC5	CNPY3	COL21A1
CRIP3	CTAGE9	CTGF	CUL7	CUL9	DLK2	ECHDC1	EEF1A1P36	EEF1DP5	ENPP1
ENPP3									

ENPP4 ENPP5 EYA4 FRS3 GFRAL GNMT GUCA1A GUCA1B HCRTR2 HEY2 HINT3 HMGB1L13 HMGCLL1 hsa-mir-588 KIAA0240 KLC4 KLHDC3 LAMA2 LRFN2 MEA1 MED20 MED23 MOXD1 MRPL2 MRPS10 NCOA7 OR2A4 PEX6 PGC POLR1C PPP2R5D PRB2 PRICKLE1 PRICKLE4 PTCRA PTK7 PTPRK RNF146 RP11-103C16.2 RP11-121P10.1 RP11-123H21.1 RP11-151M7.1 RP11-162L10.1 RP11-203B4.1 RP11-213N20.1 RP11-228O6.2 RP11-25I15.1 RP11-295F4.4 RP11-298J23.5 RP11-298J23.6 RP11-314E23.1 RP1-131F15.2 RP11-325O24.1 RP11-325O24.2 RP11-357P24.2 RP1-139D8.6 RP11-480N24.3 RP11-480N24.4 RP11-480N24.6 RP11-527F13.1 RP11-527F13.2 RP11-533O20.2 RP11-570K4.1 RP11-624M8.1 RP11-69I8.2 RP11-69I8.3 RP11-753G20.1 RP11-775I22.2 RP1-177A13.1 RP1-179E13.1 RP1-283K11.3 RP1-293L8.2 RP1-293L8.5 RP13-469O16.1 RP1-55C23.4 RP1-55C23.5 RP1-55C23.7 RP1-6P5.2 RP1-78N10.2 RP1-86D1.2 RP1-86D1.3 RP1-86D1.4 RP1-86D1.5 RP1-8B1.4 RP3-323K23.3 RP3-330M21.5 RP3-337H4.6 RP3-351K20.3 RP3-351K20.4 RP3-403A15.1 RP3-416F10.1 RP3-447E21.3 RP3-462C17.1 RP3-475N16.1 RP3-523C21.1 RP3-523C21.2 RP5-973N23.4 RP5-988G15.1 RPL24P4 RPL7L1 RPS12 RSPO3 SCARNA15 SLC22A7 SLC30A8 SNORA33 SNORA8 SNORD100 SNORD101 snoU13 SRF STX7 TAAR1 TAAR2 TAAR3 TAAR4P TAAR5 TAAR6 TAAR7P TAAR8 TAAR9 TAF8 TFEB THEMIS TJAP1 TOMM6 TRERF1 TRMT11 TTBK1 U4 U6 U7 USP49 VNN1 VNN2 VNN3 XPO5 Y_RNA YIPF3 ZNF318

PANTHER analysis: 83 mapped ids are found, 98 mapped ids are not found.

5.8.9.3 Genomic Gains of Pure Triple Negative DCIS and Triple Negative Invasive Breast Disease

There is overlap in the genomic gains present in TN pure DCIS (n=2/9) and TN Invasive breast disease (n=6/7).

1. p-values < 0.05;
2. A gene list is mapped from 11 genomic regions found on chromosomes 1, 6, 8, 10;
3. These regions encompass 133 genes altered in TN pure DCIS and TN invasive breast disease;

Genes:

5S_rRNA 7SK AC099805.1 AL139392.1 AL359983.1 AP001207.1 C1orf150 CAPN11 CFLP4 CHML EXO1 EYA1 FH FMN2 GREM2 GRHL2 HSD17B7P1 KIF26B KMO MAP1LC3C MRPL14 NCALD NLRP3 OPN3 OR11L1 OR13G1 OR14A16 OR14A2 OR14C36 OR14K1 OR14L1P OR1C1 OR2AJ1 OR2AK2 OR2B11 OR2C3 OR2G2 OR2G3 OR2G6 OR2L13 OR2L1P OR2L2 OR2L3 OR2L5 OR2L8 OR2M1P OR2M2 OR2M3 OR2M4 OR2M5 OR2M7 OR2T1 OR2T10 OR2T11 OR2T12 OR2T2 OR2T29 OR2T3 OR2T33 OR2T34 OR2T35 OR2T4 OR2T5 OR2T6 OR2T8 OR2W3 OR2W5 OR6F1 OR9H1P PLD5 RGS7 RP11-132G10.2 RP11-177F11.1 RP11-314P12.2 RP11-323D18.1 RP11-323D18.4 RP11-323D18.5 RP11-331N16.1 RP11-397A15.4 RP11-407H12.4 RP11-407H12.8 RP11-430I15.2 RP11-430I15.4 RP11-435F13.1 RP11-435F13.2 RP11-438F14.1 RP11-438F14.3

RP11-438H8.3 RP11-438H8.8 RP11-438H8.9 RP11-439E19.3 RP11-439E19.5
RP11-439E19.6 RP11-439E19.8 RP11-463J7.1 RP11-463J7.2 RP11-463J7.3
RP11-467I20.2 RP11-467I20.3 RP11-467I20.4 RP11-467I20.5 RP11-467I20.6 RP11-488L18.1
RP11-488L18.8 RP11-513D4.1 RP11-513D4.2 RP11-513D4.3 RP11-553N16.1
RP11-561I11.2 RP11-561I11.3 RP11-634B7.1 RP11-634B7.4 RP11-634B7.5
RP11-80B9.1 RP11-80B9.2 RP11-80B9.4 RP11-80B9.5 RP11-978I15.10
RP11-978I15.9 RSL24D1P4 SCCPDH SLC29A1 SNORD112 snoU13 TMEM63B TRIM58 U5 U6
VN1R17P VN1R5 WDR64 XXyac-YR14BB7.1 Y_RNA

PANTHER analysis: 62 mapped ids are found, 71 mapped ids are not found.

There are genomic gains present in some samples of TN invasive breast disease (n=2/9), none of which are observed in TN pure DCIS (n=0/9).

1. p-values < 0.005;
2. A gene list is mapped from 2 genomic regions on chromosome 3;
3. These regions encompass 17 genes altered in TN invasive breast disease;

Genes:

AC133435.2 AC112504.2 RNF7 GRK7 ATP1B3 TFDP2 AC128648.1 GK5 RP11-340E6.1 RP11-340E6.2
RP11-144C9.1 RP11-271K21.2 RP11-271K21.4 RP11-271K21.7 RP11-343B5.1 AC133435.1 U6

PANTHER analysis: Number of mapped IDs found 5, 12 mapped ids are not found.

Genomic Sc Gains in TN pure DCIS and TN Invasive Breast Disease

There are no Sc gains in TN pure DCIS in this series (n=0/9). Sc gains are, however, present in TN invasive breast disease (n=4/7).

1. p-values < 0.05;
2. A gene list is mapped from 14 genomic regions found on chromosomes 1, 3, 8;
3. These regions encompass 143 genes altered in TN invasive breast disease;

Genes:

5S_rRNA AC023165.1 AC092898.1 AC092902.1 AC099805.1 AC112484.1 AC112504.2 AC117401.1 AC117508.1 AC128648.1
AC133435.1 AC133435.2 ACAD9 ADCY5 ALDH1L1 ALG1L ATP1B3 C3orf15 C3orf22 C3orf37
CCDC14 CCDC48 CHCHD6 CHST13 CNBP COPG COX17 ENO1P3 EYA1 GK5 GP9
GRAMD1C GRK7 GS1-388B5.1 GS1-388B5.2 GS1-388B5.3 GS1-388B5.4 GS1-388B5.5
GS1-388B5.6 GS1-388B5.7 GS1-388B5.8 GSK3B H1FX HEG1 hsa-mir-548i-1 ISY1
ITGB5 KALRN KIAA1257 KIAA1407 MUC13 MYLK NR1I2 OSBPL11 PLXNA1 POPDC2 PTPLB
QTRTD1 RAB43 RAB7A RNF7 ROPN1 ROPN1B RP11-124N2.1 RP11-124N2.2 RP11-124N2.3
RP11-144C9.1 RP11-158I23.1 RP11-169N13.1 RP11-169N13.4 RP11-18H7.1 RP11-190C22.1

RP11-197K3.1 RP11-202D20.1 RP11-221E20.3 RP11-221E20.4 RP11-221E20.5 RP11-255E6.1
RP11-271K21.2 RP11-271K21.4 RP11-271K21.7 RP11-290K4.2 RP11-340E6.1
RP11-340E6.2 RP11-343B5.1 RP11-379B18.1 RP11-379B18.2 RP11-379B18.3
RP11-379B18.4 RP11-379B18.5 RP11-390G14.1 RP11-434H6.2 RP11-435F17.1
RP11-435F17.3 RP11-463J7.1 RP11-463J7.2 RP11-463J7.3 RP11-521J5.1
RP11-529F4.1 RP11-605F14.1 RP11-605F14.2 RP11-605F14.3 RP11-666A20.1 RP11-666A20.3
RP11-666A20.4 RP11-689D3.4 RP11-71H17.1 RP11-71H17.6 RP11-722C17.1
RP11-723O4.2 RP11-723O4.3 RP11-723O4.6 RP11-723O4.7 RP11-723O4.8
RP11-767L7.1 RP11-767L7.2 RP11-775J23.1 RP11-775J23.2 RP11-9N20.1 RP13-685P2.4
RP13-685P2.5 RPS15AP16 RPS27P12 RSRC1 SHOX2 SLC12A8 SLC41A3 SNORA24 SNORA5
snoU13 SNX4 TFDP2 TXNRD3 TXNRD3IT1 U1 U6 UMPS UROC1 Y_RNA
ZBTB20 ZDHHC23 ZNF148 ZXDC

PANTHER analysis: 51 mapped ids are found, 92 mapped ids are not found.

5.8.9.4 Genomic Losses in TN pure DCIS and TN Invasive Breast Disease

There are genomic losses found in TN pure DCIS (n=1/9) also present in TN invasive breast disease (n=5/7).

1. p-values >0.05;
2. A gene list is mapped from 28 genomic regions found on chromosomes 4, 14, 15, 19;
3. These regions encompass 165 genes altered in TN pure DCIS and TN invasive breast disease;

Genes:

Y_RNA 5S_rRNA 7SK ABLIM2 AC011912.1 AC012379.1 AC012379.2 AC013452.1 AC013452.2 AC018926.1
AC084882.1 AC090427.1 AC093680.1 AC093827.1 AC093848.1 AC097381.1 AC104059.1 AC104650.2 AC106868.1 AC107394.1
AC108516.1 AC109351.1 AC110766.1 ACOX3 ADH1A ADH1B ADH1C ADH7 AF146191.4 AF250324.2
AFAP1 AFF1 AGPAT9 AIMP1 AL133444.1 AL160471.2 AL160471.3 ANXA3 AP001962.3 ARD1B
ARHGAP24 ARHGEF38 C15orf33 C4orf12 C4orf17 C4orf23 C4orf36 C4orf6 CCPG1 CEP152
CGRRF1 COPS2 CPZ CRMP1 DAPP1 DNAJB14 DTWD1 EMR2 EVC EVC2
FAM175A FAM190A FBN1 FGF5 FGF7 FOXA1 FRAS1 FRG1 FRMD6 GALK2
GCH1 GK2 GMPSP GPR78 GSTCD H2AFZ hsa-mir-95 HSD17B11 HSD17B13 HTRA3
INTS12 KLHL8 MAPK10 MAPKSP1 MIPOL1 MTTP NID2 NPNT NUDT9 OR7E94P
PCDH7 PIGB PRDM8 PTPN13 RAB27A RASGEF1B RG9MTD2 RP11-112L18.1 RP11-11N6.1
RP11-1258F18.1 RP11-15B17.1 RP11-15B17.4 RP11-162K6.1 RP11-174E22.1
RP11-174E22.2 RP11-218C23.1 RP11-234K19.1 RP11-234K19.2 RP11-274J2.1
RP11-311D14.1 RP11-311D14.2 RP11-377G16.2 RP11-390C19.1 RP11-397E7.1
RP11-397E7.2 RP11-397E7.3 RP11-397E7.4 RP11-417M17.1 RP11-42A4.1
RP11-438E5.1 RP11-452C8.1 RP11-45L9.1 RP11-463J17.1 RP11-476C8.1 RP11-476C8.2
RP11-476C8.3 RP11-529H2.1 RP11-610O8.1 RP11-617I14.1 RP11-656C2.1
RP11-689K5.3 RP11-689P11.2 RP11-689P11.3 RP11-696N14.1 RP11-696N14.3
RP11-710E1.1 RP11-710F7.2 RP11-710F7.3 RP11-722P15.1 RP11-766F14.1

RP11-766F14.2 RP11-767N15.1 RP11-774O3.1 RP11-774O3.2 RP11-774O3.3
RP11-778J15.1 RP11-792D21.1 RP11-792D21.2 RP11-8L2.1 RP11-93M12.1 RP13-612N21.1
RSL24D1 SAMD4A SH3TC1 SHC4 SLC10A6 SNORA75 snoU13 SPARCL1 STK32B TBCK U5
U6 U6atac WDFY3

PANTHER analysis: 67 mapped ids are found, 98 mapped ids are not found.

There are genomic losses found in TN invasive breast disease (5/7) not observed in TN pure DCIS (0/9).

1. p-values < 0.05;
2. A gene list is mapped from 8 genomic regions found on chromosomes 4, 8,14, 18, X;
3. These regions encompass 33 genes altered in TN invasive breast disease;

Genes:

AC018797.3 AF196969.5 AF196972.1 AF196972.9 AF213884.1 AF224669.3 AKAP6 AL592043.1 BMX EBP
FAM47A FTSJ1 MANBA NFKB1 PIR PORCN RBM3 RP11-10L12.1 RP11-10L12.2
RP11-10L12.4 RP11-10L12.5 RP11-10L12.6 RP11-1148L6.5 RP11-1148L6.6
RP11-281B1.2 RP11-305F18.1 RP11-545D19.1 RP13-202B6.2 SMAD4 snoU13
TBC1D25 UBE2D3 WDR13

PANTHER analysis: 14 mapped ids are found, 19 mapped ids are not found.

5.8.9.5 Total Loss in TN pure DCIS and TN Invasive Breast Disease

There are total genomic losses present in TN pure DCIS (n=8/9) not observed in TN invasive breast disease (n=0/7).

1. p-values < 0.05;
2. A gene list is mapped from 23 genomic regions found on chromosomes 6, 8, 11, 13, 14, 17, 19;
3. These regions encompass 69 genes altered in TN pure DCIS;

Genes:

AARSD1 ABCC4 AC004659.1 AC005513.1 AC008734.1 AC008734.2 AC087650.1 AC087650.8 AC090427.1 AC100793.2
ACTL9 ADAM5P ADAMTS10 AL136359.1 AL137001.1 AOC2 AOC3 ARL4D BRCA1
CACNA1A CCDC105 CTD-2557P19.1 CTD-3199J23.2 EMR2 EMR3 FBXO33
G6PC GPC5 hsa-mir-2117 IFI35 MBD3L1 MUC16 MYO1F OLFM4 OR2Z1

OR4C3 OR4C45 OR4C5 OR4S1 OR4X1 OR4X2 OR7A10 OR7A11P OR7A17
OR7A2P OR7A5 OR7C1 OR7C2 PARK2 PSME3 RND2 RP11-24H2.1 RP11-24H2.2
RP11-301J16.2 RP11-301J16.3 RP11-301J16.5 RP11-301J16.7 RP11-442J17.4
RPL27 RTN1 RUNDC1 SLC1A6 SNORA40 U2 U6 VAT1 Y_RNA
ZNF333 ZNF558

PANTHER analysis: 41 mapped ids are found, 28 mapped ids are not found.

There are total genomic losses present in TN invasive breast disease (n=7/7) not observed in TN pure DCIS (n=0/9).

1. p-values < 0.05;
2. A gene list is mapped from 30 genomic regions found on chromosomes 4, 8, 13, 14, 15, 17;
3. These regions encompass 112 genes altered in TN invasive breast disease;

Genes:

5S_rRNA AC005324.1 AC005324.2 AC005324.4 AC005324.6 AC005324.7 AC007686.1 AC015922.1 AC015922.2 AC015922.7
AC090283.1 AC090283.3 AC096750.1 AC098487.1 ADCK1 AF111168.1 AF111168.3 AHSA1 AL049775.1 AL136160.1
AL357172.1 AL359180.1 ALKBH1 ARD1B ATP5C1P1 C13orf23 C13orf36 C14orf148 C14orf156 C14orf174
C14orf178 C14orf184 CACNA1G CATSPERB CNOT6L CTD-2175M1.1 DDIT4L DYNLL1P1 FLRT2
GAPDHP34 GK2 GNG5P5 GSTZ1 hsa-mir-1260 IL6STP1 ISM2 KIAA1737 KRT222 KRT24
KRT25 LHFP LMO7 MEIS3P1 MTUS1 NGB NHLRC3 NRXN3 OR7E94P POMT2 RASGEF1B
RFXAP RP11-15B17.1 RP11-16L6.3 RP11-197L7.2 RP11-226P1.1 RP11-234K19.1 RP11-234K19.2
RP11-299L17.1 RP11-352E6.1 RP11-352E6.2 RP11-421P11.5 RP11-438E5.1 RP11-452C8.1
RP11-478K15.1 RP11-478K15.2 RP11-478K15.3 RP11-478K15.4 RP11-478K15.5
RP11-499E18.1 RP11-527F15.1 RP11-588P8.1 RP11-610O8.1 RP11-624A4.1
RP11-689K5.3 RP11-765K14.1 RP11-94C24.10 RP11-94C24.11 SLC39A8 SMAD9
SMARCE1 SNORA32 SNORA46 SNORA75 snoU13 SNW1 SPTLC2 STOML3 STON2 TBC1D26 TMED8
TMEM63C TRIM16 U3 U7 UBE2Z VEGFC VIPAR Y_RNA ZDHHC22 ZNF286
ZNF29P

PANTHER analysis: 39 mapped ids are found, 72 mapped ids are not found.

5.8.9.6 CdLOH of TN pure DCIS and TN Invasive Breast Disease

There is CdLOH present in TN pure DCIS (n=1/9) also present in TN invasive breast disease (n=5/7).

1. p-values>0.05;
2. A gene list is mapped from 23 genomic regions found on chromosomes 4, 14, 15;

3. These regions encompass 128 genes altered in TN pure DCIS and TN invasive breast disease;

Genes:

5S_rRNA	7SK	ABLIM2	AC011912.1	AC012379.1	AC012379.2	AC013452.1	AC013452.2	AC018926.1	AC084882.1	
AC093680.1	AC093827.1	AC093848.1	AC097381.1	AC104059.1	AC106868.1	AC108516.1	AC109351.1	ACOX3	AF146191.4	
AF250324.2	AFAP1	AFF1	AGPAT9	AIMP1	AL133444.1	AL160471.2	AL160471.3	ANXA3	AP001962.3	
ARHGAP24	ARHGEF38	C15orf33	C4orf23	C4orf36	C4orf6	CCPG1	CEP152	CGRRF1	COPS2	CPZ
CRMP1	DAPP1	DNAJB14	DTWD1	EVC	EVC2	FBN1	FGF5	FGF7	FOXA1	
FRAS1	FRG1	FRMD6	GALK2	GCH1	GPR78	GSTCD	H2AFZ	HSD17B11	HSD17B13	
HTRA3	INTS12	KLHL8	MAPK10	MAPKSP1	MIPOL1	NID2	NPNT	NUDT9	PIGB	
PRDM8	PTPN13	RAB27A	RASGEF1B	RP11-112L18.1		RP11-15B17.1		RP11-15B17.4		
RP11-162K6.1		RP11-174E22.1		RP11-174E22.2		RP11-218C23.1		RP11-274J2.1		
RP11-311D14.1		RP11-311D14.2		RP11-377G16.2		RP11-390C19.1		RP11-397E7.1		
RP11-397E7.2		RP11-397E7.3		RP11-397E7.4		RP11-417M17.1		RP11-42A4.1		
RP11-45L9.1	RP11-463J17.1		RP11-476C8.1		RP11-476C8.2		RP11-476C8.3		RP11-529H2.1	
RP11-656C2.1		RP11-689K5.3		RP11-689P11.2		RP11-689P11.3		RP11-710E1.1		
RP11-710F7.2		RP11-710F7.3		RP11-766F14.2		RP11-767N15.1		RP11-774O3.1		
RP11-774O3.2		RP11-774O3.3		RP11-778J15.1		RP11-792D21.1		RP11-792D21.2		
RP11-8L2.1	RP13-612N21.1		RSL24D1	SAMD4A	SHC4	SLC10A6	snoU13	SPARCL1	STK32B	
TBCK	U5	U6	U6atac	Y_RNA+AA1:A128						

PANTHER analysis: 56 mapped ids are found, 72 mapped ids are not found.

There is CdLOH present in TN invasive breast disease (n=4/7) not observed in TN pure DCIS (0/9).

1. p-values < 0.05;
2. A gene list is mapped from 103 genomic regions found on chromosomes 4, 5, 8, 9, 10, 12, 13, 14, 15, 16, 18, X;
3. These regions encompass 433 genes altered in TN invasive breast disease;

Genes:

5S_rRNA	AC003658.1	AC004053.1	AC006160.1	AC006160.2	AC006160.4	AC006160.5	AC006445.1	AC006445.6	AC006445.7
AC006445.8	AC007126.1	AC007956.2	AC008245.1	AC010296.1	AC013558.1	AC018413.1	AC018558.1	AC019131.2	AC020698.1
AC023824.2	AC034110.1	AC034110.2	AC068473.1	AC090360.1	AC091551.1	AC091602.1	AC091646.1	AC092621.1	AC092846.1
AC093628.1	AC093848.1	AC096742.1	AC098830.1	AC105423.1	AC106785.1	AC106785.10		AC106785.14	
AC106785.18		AC106785.20		AC106785.22		AC106785.25		AC106785.27	
AC106785.28		AC106785.6	AC106868.1	AC111152.1	AC114688.1	AC116553.1	AC134978.1	AC139100.1	ACTBP1
ACYP1	ADH1A	ADH1B	ADH1C	ADH4	ADH5	ADH7	ADNP2	AF196970.3	AF196972.3
AF196972.4	AF213884.1	AF241726.2	AF241726.4	AF241726.6	AKAP6	AL096700.1	AL096700.2	AL121578.2	AL132716.1
AL132716.2	AL132777.1	AL132777.2	AL132988.1	AL132988.2	AL132988.3	AL132988.4	AL359219.1	AL445487.1	AL591394.1
AL929101.1	ANXA10	AP002075.1	ARAF	ASB5	ATP8A1	ATP9B	B3GALTL	BANK1	BCL2
BDH2	BOD1L	C13orf26	C13orf33	C14orf149	C14orf38	C14orf53	C15orf43	C18orf22	C4orf37

C8orf75 CDH7 CENPE CENPVL1 CFP CHST7 CISD2 CLRN2 COMMD10 CTB-118N6.3
CTC-339F2.2 CTD-2022H16.1 CTD-2522E6.4 CTDP1 CXorf24 CXorf25 CXorf31
CXXC4 CYP4V2 DCTN2 DDIT3 DDX60 DDX60L DLST DUOX1 DUOX2 DUOXA1
DUOXA2 DUSP4 EEF1DP3 EGLN3 EIF2B2 EIF4E ELK1 EMCN FAM149A FAM164C
FAM177A2 FAM184B FANCB FCF1 FRY FTLP16 FTSJ1 GALR1 GBA3 GLRA2
GPR125 GPR64 GSPT2 hsa-mir-1255a hsa-mir-221 hsa-mir-222 hsa-mir-616 HSBP1L1 HSP90AB2P
HSPH1 INE1 JKAMP KCNG2 KCNH5 KCNIP4 KIAA0317 KIF5A KLF12 KLHL4
KLKB1 KRT8P14 LAP3 LDB2 LRRC9 LTBP2 MAGED1 MAGED4 MAGED4B MAP3K15
MARS MBD6 MBP MED28 METAP1 MEX3C MLH3 MNAT1 MOSPD2 MTNR1A
NDUFB11 NEK9 NFATC1 NFKB1 NHEDC1 NHEDC2 NKX3-2 NOVA1 NPAS3 NUS1P1 OTC
PARD6G PCDH7 PCTK1 PDHA1 PGF PHF16 PHKA2 PPARGC1A PPEF1 PPP3CA
PQLC1 PROX2 QDPR RAB28 RAD23B RBM10 RGN RP11-109E24.1 RP11-10G12.1
RP11-10G12.2 RP11-10L12.4 RP11-1148L6.6 RP11-114H20.1 RP11-120A1.1
RP11-123O22.1 RP11-1299A16.1 RP11-1299A16.2 RP11-141E13.1 RP11-159J2.1
RP11-159J2.2 RP11-162A12.1 RP11-167N19.1 RP11-167N19.2 RP11-173M11.1
RP11-173M11.2 RP11-173P16.2 RP11-17E2.2 RP11-196I18.2 RP11-196I18.3
RP11-196I18.4 RP11-198M15.1 RP11-200A24.1 RP11-207N4.2 RP11-207N4.3
RP11-215A19.1 RP11-22B10.3 RP11-234P3.2 RP11-234P3.3 RP11-234P3.4
RP11-234P3.5 RP11-245M24.1 RP11-24D11.1 RP11-252M21.1 RP11-252M21.3
RP11-252M21.4 RP11-252M21.6 RP11-252M21.7 RP11-289C17.1 RP11-289C17.2
RP11-292B1.1 RP11-292B1.2 RP11-297P16.1 RP11-297P16.3 RP11-297P16.4
RP11-305F18.1 RP11-30C8.1 RP11-30C8.2 RP11-310I9.1 RP11-311P8.1
RP11-311P8.2 RP11-315A17.1 RP11-324B6.1 RP11-328K4.1 RP11-333E5.1
RP11-333E5.2 RP11-341G5.1 RP11-367C11.2 RP11-380P13.1 RP11-380P13.2 RP1-
138A5.1 RP11-38O23.3 RP11-38O23.4 RP11-38O23.5 RP11-38O23.7 RP11-417L14.1
RP11-428B4.2 RP11-433O3.1 RP11-451L9.2 RP11-451L9.3 RP11-45F23.1
RP11-462G22.1 RP11-473D24.1 RP11-474L7.4 RP11-495L18.2 RP11-498M5.2
RP11-499E18.1 RP11-49F1.1 RP11-508N12.2 RP11-508N12.3 RP11-508N12.4 RP11-552E4.2
RP11-552E4.3 RP11-552E4.4 RP11-556G22.1 RP11-556G22.2 RP11-556G22.3
RP11-56H2.1 RP11-571E6.1 RP11-571E6.3 RP11-571E6.4 RP11-571L19.2
RP11-571L19.4 RP11-576E20.1 RP11-617I14.1 RP11-619J20.1 RP11-644A7.1
RP11-655M19.1 RP11-665C14.1 RP11-665C14.2 RP11-665I14.1 RP11-692P14.1
RP11-696N14.1 RP11-696N14.3 RP11-6C14.1 RP11-703G6.1 RP11-729M20.1
RP11-75A9.1 RP11-75A9.2 RP11-75A9.3 RP11-769N22.1 RP11-799A12.1
RP11-799A12.2 RP11-87F15.2 RP1-212G6.4 RP1-30G7.2 RP13-43E11.1 RP13-479F17.2
RP13-497K6.1 RP13-928P6.3 RP1-54B20.7 RP1-71L16.1 RP1-71L16.2 RP1-71L16.3 RP1-71L16.6 RP2
RP3-393P12.1 RP3-393P12.2 RP3-393P12.3 RP3-436M11.3 RP3-499B10.3 RP3-
499B10.4 RP3-499B10.5 RP4-733D15.1 RP4-774G10.1 RP5-1158E12.1 RP5-1158E12.2
RP5-1158E12.3 RP5-972B16.2 RP6-227L5.1 RP6-227L5.2 RP6-99M1.1 RPGR RPS6KL1 RTN1
RXFP2 SALL3 SEMA6A SLC25A21 SLC38A5 SLC38A6 SLC7A1 SLC9A7 SMAD4 SNORA11
SNORA25 SNORA31 SNORA7 SNORA75 SNORD37 snosnR60_Z15 snoU13 SOCS6 SORD
SPACA5 SPACA5B SPCS3 SRPX SSX5 SSX6 STAMBPL1 SUV39H1 SYN1 SYTL5
TACR3 TIMP1 TJP1 TLR3 TMED10 TRMT5 TSHZ1 TSPAN5 TSPAN7 TXNL4A U1
U12 U2 U3 U4atac U6 U7 U70984.1 UBA1 UBE2D3 UNC13C
UPRT USP11 UXT WAS WDR72 Y_RNA YLPM1 Z98304.1 ZADH2 ZDHHC15
ZNF157 ZNF182 ZNF236 ZNF41 ZNF462 ZNF516 ZNF630 ZNF673 ZNF674 ZNF81

PANTHER analysis: 163 mapped ids are found, 270 mapped ids are not found.

5.8.9.7 CnLOH of TN pure DCIS and TN Invasive Breast Disease

There is CnLOH present in TN pure DCIS (n=9/9) not observed in TN invasive breast disease (n=0/7).

1. p-values < 0.05;
2. A gene list is mapped from 110 genomic regions found on chromosomes 1, 2, 3, 6, 7, 10, 11, 12, 20, 21;
3. These regions encompass 891 genes altered in TN pure DCIS;

Genes:

5S_rRNA 7SK ABHD11 AC004975.1 AC004979.1 AC004979.2 AC004979.3 AC004979.4 AC004979.5 AC004979.6 AC004979.7 AC005537.2 AC005586.2 AC006021.1 AC007092.1 AC007238.1 AC007560.1 AC007680.2 AC007682.1 AC007682.2 AC008173.1 AC010087.1 AC010087.4 AC010087.5 AC012361.1 AC012368.1 AC012368.2 AC013251.1 AC013251.2 AC016727.3 AC016894.1 AC017083.1 AC017083.2 AC017083.3 AC018462.2 AC018462.3 AC022210.2 AC023115.1 AC023115.3 AC023165.1 AC025594.1 AC025594.2 AC064868.1 AC067950.1 AC069304.1 AC073422.1 AC073464.11 AC073464.9 AC073846.1 AC073846.2 AC073846.3 AC074289.1 AC078811.1 AC078941.1 AC079112.1 AC079807.4 AC083868.1 AC083883.1 AC092898.1 AC092902.1 AC092910.1 AC092910.2 AC092958.1 AC093087.1 AC093168.1 AC097463.1 AC097463.2 AC106874.1 AC106874.3 AC107081.1 AC107081.2 AC107081.5 AC108039.1 AC108039.2 AC108039.3 AC108462.1 AC108697.1 AC108729.1 AC108739.1 AC112484.1 - AC112694.1 AC114752.1 AC114808.2 AC114808.3 AC117401.1 AC117472.1 AC117472.2 AC117508.1 AC126182.1 AC131571.1 AC131571.2 AC138655.4 AC144441.1 ACAD9 ACTG2 ACTGP9 ACTR3C ADCY5 AF131217.1 AF227510.7 AGK AGTR1 AKR1A1 AL008729.1 AL022170.1 AL023583.1 AL023807.1 AL023807.2 AL024498.1 AL034372.1 AL035670.1 AL049635.1 AL049635.2 AL049710.1 AL049710.2 AL049710.4 AL050335.1 AL050335.2 AL109918.1 AL121946.1 AL133268.1 AL136230.1 AL136305.1 AL137003.1 AL138724.3 AL139044.2 AL157773.1 AL160037.2 AL160400.1 AL160400.2 AL162579.1 AL354680.1 AL357079.1 AL357079.2 AL357497.1 AL359316.1 AL445669.2 AL589723.1 AL590062.1 AL603888.1 AL604028.1 AL604028.2 AL645811.1 ALG1L ALK ANKRD20B APOB ARGFX ARTN ASB3 ASS1P1 ATP5LP2 ATP5LP5 ATP6V0B ATP6V1F ATXN1 B3GNT1 B4GALT2 BAK1 BBS9 BCL7B BMP5 BPESC1 BTF3L4 C1D C1orf210 C1orf50 C1orf84 C2orf43 C2orf89 C3orf16 C3orf22 C3orf33 C3orf37 C3orf72 C6orf114 C6orf142 C6orf227 C6orf52 C7orf29 C7orf55 CAP1 CAP2 CCDC136 CCDC14 CCDC17 CCDC23 CCDC24 CCDC30 CCDC48 CCDC90A CCT4 CD2AP CD83 CD96 CEP70 CHCHD6 CHST13 CLDN19 CLDN3 CLDN4 CLEC5A CMAH CNBP COL21A1 COL9A2 COMMD1 COMMD2 COPG COX6B1P1 CTD-2021J15.1 CTD-2021J15.2 CYP26B1 CYP39A1 DEFB110 DEFB112 DEFB113 DEFB114 DEFB133 DEK DNAH6 DNAJB6 DNAJC30 DPH2 EBNA1BP2 EDN1 EEF1A1P25 EFHC1 ELOVL2 ELP4 ENO1P3 EPCAM ERBB3 ERMAP ESYT3 FABP7 FAIM FAM161A FAM65B FAM8A1 FBXO40 FLNC FOXL2 FOXN2 FSTL1 GAPDHP39 GCLC GCM2 GCNT2 GCNT6 GFOD1 GFRAL GGNBP1 GIMAP2 GIMAP4 GIMAP6 GIMAP7 GIMAP8 GJA9 GMNN GMPR GMPS GP9 GPBP1L1 GPR110 GPR111 GPR115 GPR116 GPR156 GRM8 GS1-388B5.1 GS1-388B5.2 GS1-388B5.3 GS1-388B5.4 GS1-388B5.5 GS1-388B5.6 GS1-388B5.7 GS1-388B5.8 GSK3B GSTA1 GSTA2 GSTA3 GSTA5 GSTA6P GTF2E1 GTF2H1 H1FX HCRTR2 HEG1 HGD HIPK2 HIVEP1 HLA-DQA1 HLA-DQB1 HMGCLL1 HMGCS2 hsa-mir-133b hsa-mir-206 hsa-mir-548a-1 hsa-mir-548i-1 hsa-mir-559 hsa-mir-761 HSPDP7 HYI IGSF22 IL17A IL17F IMMP1L IPO13 IPP IQCJ IRF5 ISY1 ITGB5 ITPR3 JARID2 JHDM1D KALRN KCNK12 KCP KDM1B KDM4A KIAA0319L KIAA0467 KIAA1147 KIAA1257 KIF13A KLHL31 KLRAQ1 KLRG2 KTI12 LDHA LDHAL6A LDHC LEPRE1 LRFN2 LRRC1 LRRC16A LRRC4C LRRC58 LRRC61 LUC7L2 MAK MAST2 MCM3 MED8 MEP1A MFSD2A MGAM MKRN1 MLXIPL MME MRAS MRPL32

MRPS22 MSH2 MTCO3P1 MUC13 MUTYH MYCBP MYL6P4 MYLIP MYLK N6AMT1
NAP1L1P3 NASP NCDN NCRNA00240 NEDD9 NHLRC1 NOL7 NRD1 NRXN1 NUP153 OFCC1
OR5AK2 OR9A1P OR9A3P OR9A4 OSBPL11 OSBPL9 P2RY1 PABPC1P10 PAK1IP1 PAQR8
PARP12 PAX6 PDIA4 PDIA5 PELI1 PFN2 PHACTR1 PHGDH PIK3CB PIK3R3 PKHD1 PKIB
PLA2G7 PLCH1 PLCXD2 PLXNA1 PNO1 PPCS PPIH PPP3R1 PPT1 PRIM2 PRR23A
PRR23B PRR23C PRSS37 PSMB2 PTPLB PTPN5 PTPRF RAB19 RAB3B RAB43
RAB7A RABL3 RANBP9 RARRES1 RARRES2 RBM24 RCAN2 REPIN1 RHBDL2 RIMKLA RLF
RNF13 RNF144B RNF160 RNF182 ROPN1 RP11-100F22.1 RP11-10O22.2 RP11-115D7.3
RP11-117F22.1 RP11-117L15.1 RP11-117L15.3 RP11-121P10.1 RP11-1220K2.2 RP11-125M16.1
RP11-127P7.2 RP11-128A6.2 RP11-128A6.3 RP11-138N21.1 RP11-146I2.1 RP11-146I2.2 RP11-14H3.3
RP11-157D18.2 RP11-163G10.2 RP11-163G10.3 RP11-163G10.4 RP11-167H9.3 RP11-167H9.4
RP11-174O3.1 RP11-174O3.3 RP11-174O3.4 RP11-184I16.2 RP11-184I16.3 RP11-184I16.4
RP11-18H7.1 RP11-191A15.1 RP11-191A15.2 RP11-191A15.3 RP11-191A15.4 RP11-192K2.3
RP11-197K3.1 RP11-202D20.1 RP11-219E24.1 RP11-221E20.3 RP11-221E20.4 RP11-221E20.5
RP11-228O6.2 RP11-232M24.1 RP11-255N4.2 RP11-255N4.3 RP11-268F1.2
RP11-268F1.3 RP11-280H21.1 RP11-282K6.3 RP11-290K4.1 RP11-290K4.2 RP11-291L19.1
RP11-306L14.1 RP11-309L24.2 RP11-309L24.4 RP11-309L24.6 RP11-310F12.1
RP11-311B18.1 RP11-321G3.1 RP11-322N21.2 RP11-330A16.1 RP11-33K5.1
RP11-342M1.2 RP11-342M1.3 RP11-342M1.4 RP11-345L23.1 RP11-359H3.1 RP11-359H3.4
RP11-359N11.1 RP11-359N11.2 RP11-360O19.1 RP11-360O19.4 RP11-360O19.5 RP11-365F18.1
RP11-365F18.3 RP11-367G6.1 RP11-379B18.1 RP11-379B18.2 RP11-379B18.3
RP11-379B18.4 RP11-379B18.5 RP11-383F6.1 RP11-384F7.1 RP11-384F7.2
RP11-385F7.2 RP11-38P22.2 RP11-390G14.1 RP11-392A23.4 RP11-392A23.5 RP11-397G17.1
RP1-13D10.2 RP1-13D10.3 RP1-13D10.4 RP1-13D10.5 RP11-401E14.1 RP11-401E14.2
RP11-402J7.2 RP11-402J7.3 RP11-40M23.1 RP11-411K7.1 RP11-411K7.2 RP11-411K7.4
RP11-411K7.5 RP11-418B12.1 RP11-428L9.1 RP1-142O9.1 RP1-142O9.2
RP11-434H6.2 RP11-446F17.3 RP11-446F3.2 RP11-451G4.2 RP11-451G4.3 RP11-466L17.1
RP11-470H9.1 RP11-500K19.1 RP11-501I19.3 RP11-501I19.4 RP11-501O2.1
RP11-501O2.2 RP11-501O2.3 RP11-501O2.4 RP11-501O2.5 RP11-505J9.1
RP11-506B15.4 RP11-506B15.6 RP11-511P7.2 RP1-151F17.1 RP11-521J5.1 RP11-526P5.1
RP11-526P5.2 RP11-529F4.1 RP11-529G21.4 RP1-152L7.1 RP1-152L7.3 RP1-152L7.5 RP1-152L7.6 RP11-543F8.1
RP11-543F8.2 RP11-548O1.1 RP11-548O1.3 RP11-550C4.6 RP11-560J1.1 RP11-567P17.1
RP11-567P17.2 RP11-585F20.1 RP11-598F17.1 RP11-605F14.1 RP11-605F14.2
RP11-605F14.3 RP11-622P13.2 RP11-630I5.1 RP11-632K21.1 RP11-632K21.3
RP11-635I10.1 RP11-637O19.2 RP11-639B1.1 RP11-639F1.1 RP11-639F1.2 RP11-639F1.3
RP11-63E16.1 RP11-649A16.1 RP11-649A16.5 RP11-651P23.2 RP11-651P23.3 RP11-651P23.4
RP11-651P23.5 RP11-651P23.6 RP11-666A20.1 RP11-666A20.3 RP11-666A20.4
RP11-674E16.1 RP11-681L4.1 RP11-689D3.4 RP11-69C17.3 RP11-69C17.4
RP11-71H17.1 RP11-71H17.6 RP11-71N10.1 RP11-722C17.1 RP11-723C11.2
RP11-723O4.2 RP11-723O4.3 RP11-723O4.6 RP11-723O4.7 RP11-723O4.8
RP11-735A5.1 RP11-767N6.2 RP11-767N6.7 RP11-771D21.2 RP11-775J23.1
RP11-775J23.2 RP11-779P15.1 RP11-779P15.2 RP11-785H2.1 RP11-788A4.1
RP11-788A4.2 RP11-793K1.1 RP11-795J1.1 RP11-795J1.2 RP11-79N23.1 RP11-7O11.3
RP1-180E22.3 RP11-812I20.2 RP11-90C4.1 RP11-90C4.2 RP11-90C4.3 RP11-90C4.4
RP1-190J20.2 RP11-91A18.1 RP11-91A18.4 RP11-91A18.5 RP11-9N20.1 RP1-228H13.1
RP1-228H13.2 RP1-245M18.2 RP1-257A7.4 RP1-273P12.1 RP1-273P12.3 RP1-27K12.2
RP1-27K12.4 RP1-290I10.4 RP1-290I10.5 RP1-290I10.7 RP1-304B14.3 RP13-476E20.1
RP13-685P2.4 RP13-685P2.5 RP1-39G22.4 RP1-39G22.5 RP1-62D2.3 RP1-71H19.2 RP1-
92O14.6 RP3-335N17.2 RP3-342P20.2 RP3-347E1.2 RP3-365O12.2 RP3-380E11.2 RP3-
425P12.1 RP3-425P12.2 RP3-425P12.4 RP3-425P12.5 RP3-437C15.1 RP3-448I9.1 RP3-448I9.2 RP3-

451B15.3 RP3-462C17.1 RP3-486B10.1 RP3-486D24.1 RP3-501N12.3 RP3-510L9.1 RP3-522P13.1 RP3-522P13.2 RP3-522P13.3 RP3-525L6.2 RP4-533D7.3 RP4-533D7.4 RP4-533D7.5 RP4-584D14.5 RP4-584D14.6 RP4-633H17.2 RP4-657D16.3 RP4-724P12.1 RP4-728D4.2 RP4-728D4.3 RP4-753D5.3 RP4-753D5.4 RP4-761I2.2 RP4-761I2.4 RP4-765A10.1 RP4-765A10.2 RP5-1142J19.1 RP5-1142J19.2 RP5-1154E9.5 RP5-1154E9.6 RP5-1154E9.7 RP5-864K19.4 RP5-894A10.2 RP5-894A10.5 RP5-983H21.3 RP5-994D16.3 RP5-994D16.7 RP5-994D16.9 RPL15P3 RPN1 RPS15AP10 RPS15AP16 RPS17P5 RPS27P12 RRAGC SCGN SEC22A SEMA5B SHMT1P1 SIRT5 SLC12A8 SLC25A20P1 SLC25A27 SLC33A1 SLC37A3 SLC6A9 SMAP2 SMPDL3A SNORA24 SNORA5 SNORA70 SNORD66 SNORD78 snoU13 SNTG2 SNX4 SOX6 SPTY2D1 SSBP1 ST3GAL3 STX1A SUCLA2P2 SUCLG1 SYCP2L TAS2R3 TAS2R38 TAS2R4 TAS2R5 TBC1D7 TBL2 TBXAS1 TDRD6 TESK2 TFAP2B TFAP2D TFAP2E TGFBR3 TIE1 TMCO2 TMEM125 TMEM14A TMEM14B TMEM14C TMEM69 TMEM86A TMSB10 TNFRSF21 TNPO3 TOE1 TPI1P2 TPMT TPO TRAM2 TRIM38 TSG101 TSPAN1 TTC26 TXNDC12 TXNRD3 TXNRD3IT1 U1 U3 U4 U6 U7 UBE3C UBN2 UEVLD UMPS UROC1 USP34 VN1R11P VN1R12P VN1R13P VPS37D WBSCR22 WBSCR26 WBSCR27 WBSCR28 WDR92 WEE2 WWTR1 XPO1 XXbac-BPG254F23.5 XXbac-BPG254F23.6 XXbac-BPG254F23.7 Y_RNA YBX1 Z83001.1 Z93017.1 ZBTB20 ZC3HAV1 ZC3HAV1L ZIC1 ZIC4 ZMPSTE24 ZMYM4 ZMYND12 ZNF148 ZNF398 ZNF425 ZNF643 ZNF691 ZNF775 ZNF786

PANTHER analysis: 335 mapped ids are found, 497 mapped ids are not found.

There is CnLOH present in TN invasive breast disease (n=7/7) not observed in TN pure DCIS (n=0/9).

1. p-values < 0.05;
2. A gene list is mapped from 30 genomic regions found on chromosomes 1, 4, 7, 10, 14, 18, 21;
3. These regions encompass 379 genes altered in TN invasive breast disease;

Genes:

5S_rRNA 7SK ABCA4 ABCD3 ABLIM1 AC005071.1 AC005071.2 AC005071.3 AC005879.1 AC006557.1 AC007922.2 AC007956.2 AC016839.1 AC018797.3 AC022884.1 AC023983.1 AC069281.1 AC069281.2 AC073585.1 AC073588.1 AC073842.18 AC073842.19 AC090363.1 AC091588.1 AC093577.3 AC093577.5 AC093577.7 AC093577.8 AC096947.1 AC104961.1 AC105247.1 ACADSB ACTL6B AFAP1L2 AFG3L2 AGFG2 AL109761.3 AL109761.5 AL117351.1 AL117351.2 AL117351.3 AL117351.4 AL117351.5 AL117351.6 AL117351.7 AL133384.1 AL157788.1 AL158014.1 AL353664.1 AL355598.1 AL355861.1 AL359747.1 AL359836.1 AL603764.1 AL731543.1 ALG14 AMAC1L1 ANKRD62 AP000431.1 AP000431.2 AP000432.2 AP000457.1 AP000568.2 AP000745.1 AP000855.4 AP000946.2 AP000963.2 AP000963.3 AP000998.1 AP000998.2 AP001029.1 AP001120.1 AP001171.1 AP001439.2 AP001441.1 AP001442.2 AP001525.1 AP001525.2 AP001604.3 AP001605.4 AP001605.6 AP001607.1 AP002414.1 AP002414.2 AP005264.2 AP4M1 APP ARHGAP29 ARMS2 ATE1 BAG3 BCAR3 BTBD16 BTG3 BUB3 C10orf119 C10orf120 C10orf46 C10orf82 C10orf84 C10orf88 C10orf96 C18orf1 C18orf19 C18orf45 C1orf87 C1QBPP C21orf131 C21orf37 C21orf91 C7orf43 C7orf47 C7orf51 C7orf59 C7orf61 CABLES1 CACNA2D1 CASC2 CCDC18 CDH2 CELF4 CHODL CHST9 CIDEA CNN3 CNPY4 COPS6 CTA-109P11.1 CTAGE1 CTB-161A2.2 CTB-161A2.3 CTB-161A2.4 CUZD1 CXADR CYP2J2 DLST DMBT1 DNMBP DNTTIP2 DR1 EIF3A EIF4A1P EMX2 EMX2OS ENO4 F3 FAM24A FAM24B FAM45A FAM69A FBXO24 FCF1 FDPSP FGFR2

FGGY FNBP1L GAL3ST4 GAPDHP29 GATA6 GATS GCLM GFRA1 GIGYF1 GNAL GNB2
GPC2 GRK5 HMX2 HMX3 HOOK1 HRH4 hsa-mir-106b hsa-mir-1-2 hsa-mir-133a-1 hsa-mir-25 hsa-mir-320c-2 hsa-mir-760 hsa-mir-93 HSPA12A HTR7 HTRA1 IKZF5 IMPA2 IMPACT INADL
INPP5F KCNK18 KCTD1 KIAA0317 KIAA1598 KRT18P2 LRCH4 LTBP2 MANBA MBLAC1
MC2R MC5R MCM7 MEPCE MIB1 MIR1255B1 MOSPD3 MPPE1 MTF2 NANOS1 NCAM2
NCRNA00093 NCRNA00113 NCRNA00157 NFIA NFKB1 NSMCE4A ORC5L OSBPL1A PCOLCE
PDZD8 PILRA PILRB PLEKHA1 PMS2L1 PNLIP PNLIPRP1 PNLIPRP2 PNLIPRP3 PPIAP
PRDX3 PRLHR PROX2 PRSS7 PSMA8 PSTK PVRIG RAB11FIP2 RELN RGS10
RNMT RP11-107C16.2 RP11-10L12.1 RP11-10L12.2 RP11-10L12.4 RP11-10L12.5
RP11-10L12.6 RP11-145M4.2 RP11-145M4.3 RP11-148B18.1 RP11-148B18.3 RP11-148B18.4
RP11-162A23.5 RP11-179H18.2 RP11-179H18.4 RP11-179H18.5 RP11-179H18.7 RP11-179H18.8
RP11-198M6.2 RP11-198M6.5 RP11-215A21.2 RP11-245J24.1 RP11-268I9.1
RP11-26N15.1 RP11-282I1.1 RP11-295O23.2 RP11-295O23.4 RP11-313A24.1 RP11-317F20.2
RP11-319I23.2 RP11-319I23.3 RP11-328K15.1 RP11-33D13.2 RP11-354M20.3 RP11-366L18.1
RP11-36N22.1 RP11-36N22.3 RP11-430G17.1 RP11-436K8.1 RP11-44M6.1
RP11-44M6.3 RP11-465K1.2 RP11-470E16.1 RP11-488P3.1 RP11-498B4.2 RP11-498B4.5
RP11-498B4.7 RP11-498J9.1 RP11-498J9.2 RP11-498J9.4 RP11-500G22.2
RP11-501J20.2 RP11-501J20.3 RP11-501J20.5 RP11-506M12.1 RP11-539I5.1
RP11-539I5.2 RP11-564D11.3 RP11-567J24.4 RP11-575B7.2 RP11-575B7.3 RP11-57H12.2
RP11-5G18.2 RP11-62L18.3 RP11-681N23.1 RP11-758P17.2 RP11-758P17.3 RP11-781P14.3
RP11-786F14.1 RP11-78A18.2 RP11-78O9.1 RP11-79M19.2 RP11-86H7.1 RP11-86H7.2
RP11-86H7.3 RP11-86H7.6 RP11-86H7.7 RP13-530H6.2 RP4-612C19.1 RP4-612C19.2 RP4-639F20.1 RP4-639F20.3 RP4-668G5.1 RP4-713B5.2 RP4-717I23.2
RP4-717I23.3 RP4-782L23.1 RP4-782L23.2 RP5-1033H22.2 RP5-833A20.1 RP5-837O21.1 RP5-837O21.2 RP5-837O21.3 RP5-837O21.4 RP5-837O21.5 RP5-837O21.6 RP5-837O21.7
RP5-837O21.8 RP5-837O21.9 RPL10P1 RPL37P3 RPL37P4 RPS15AP5 RPS3AP1 RPS6KL1
SEC23IP SFXN4 SLC18A2 SLC44A3 SLC6A6P SLMO1 SNORA19 SNORA7 SNORA73 snoU13
SPDYE3 SPIRE1 SS18 STAG3 TACC2 TAF4B TAF6 TFR2 TGFBR3 TIAL1 TM2D1 TMED5
TMEM56 TSC22D4 TUBB6 U1 U3 U6 U6atac U7 UBE2D3 VAX1 Y_RNA
YLPM1 ZCWPW1 ZNF3 ZNF519 ZNF521 ZSCAN21

PANTHER analysis: 152 mapped ids are found, 227 mapped ids are not found.

5.8.10 Copy Number Aberrations in All Triple Negative DCIS compared to Triple Negative Invasive breast disease

This series examines the difference between TN DCIS and TN invasive breast disease.

Frequency plots showing copy number aberrations between TN DCIS and TN invasive breast disease were provided by King's College London Bioinformatics department; Figure 43.

Figure 43: Frequency plots showing copy number aberrations between triple negative DCIS and triple negative invasive disease (amplifications, duplications, gains, Sc gains, losses, total losses CdLOH and CnLOH,) (pages 264-266).

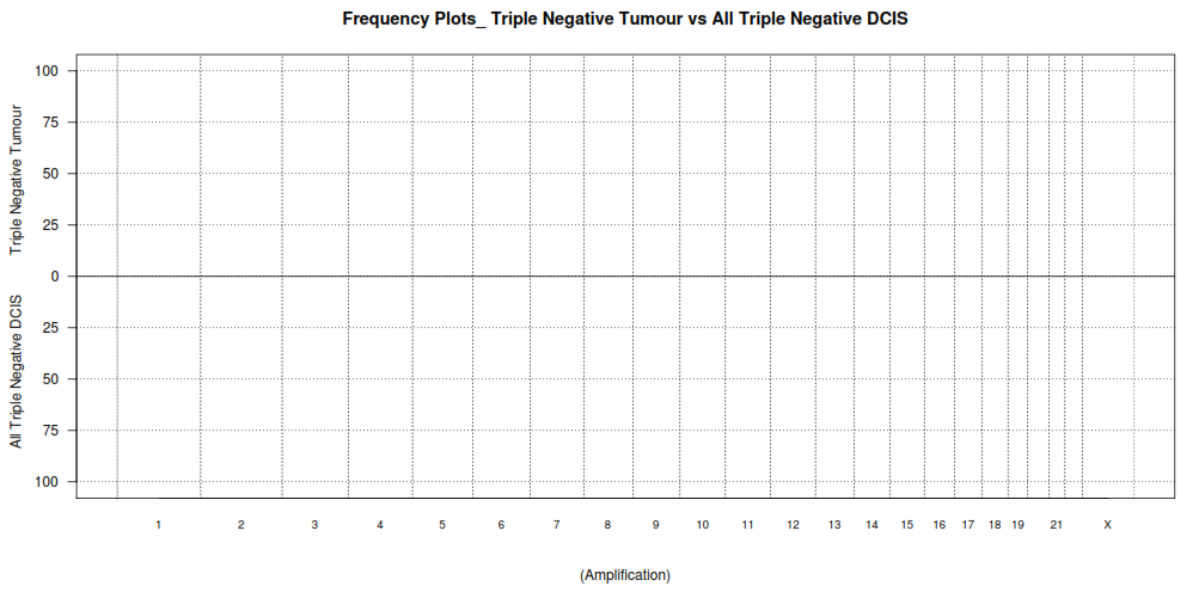
Frequency Plots_ Triple Negative Tumour vs All Triple Negative DCIS
Triple Negative Tumour
All Triple Negative DCIS
100
75
50
25
0
25
50
75
100
1
2
3
4
5
6
7
8
9
10
11
12
13
14
15
16
17
18
19
21
X
(Amplification)

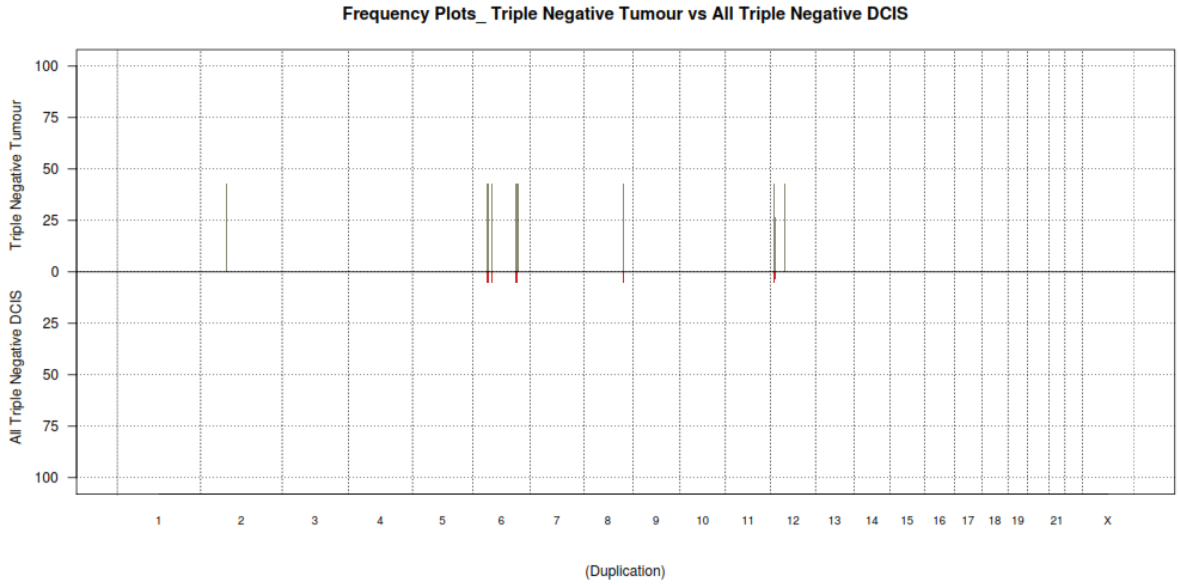
Frequency Plots_ Triple Negative Tumour vs All Triple Negative DCIS
Triple Negative Tumour
All Triple Negative DCIS
100
75
50
25
0
25
50
75
100
1
2
3
4
5
6
7
8
9
10
11
12
13
14
15
16
17
18
19
21
X
(Duplication)

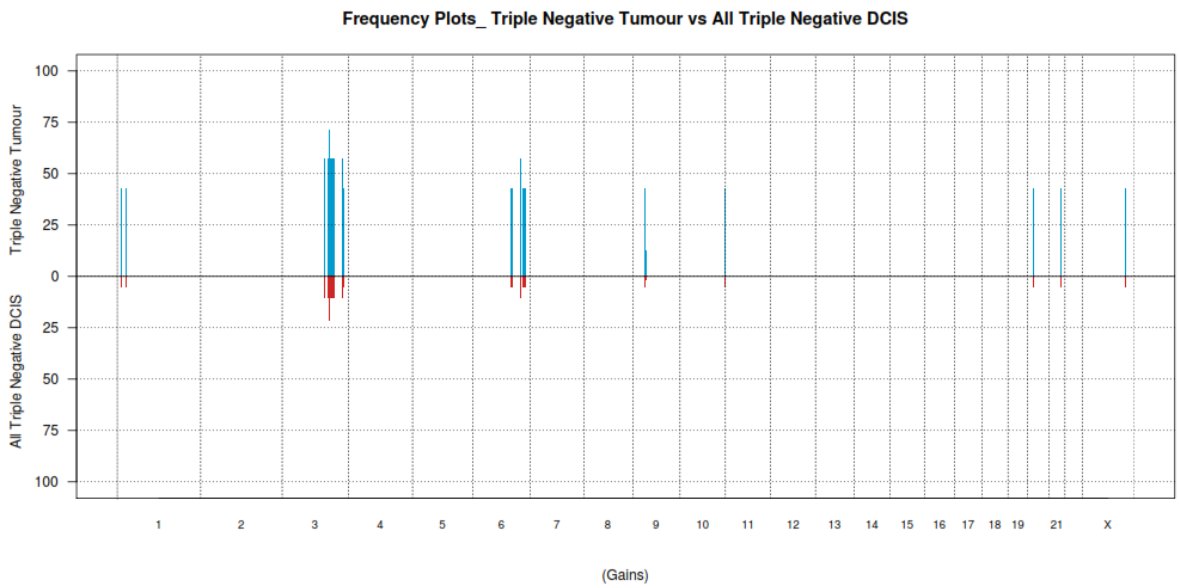
Frequency Plots_ Triple Negative Tumour vs All Triple Negative DCIS
Triple Negative Tumour
All Triple Negative DCIS
100
75
50
25
0
25
50
75
100
1
2
3
4
5
6
7
8
9
10
11
12
13
14
15
16
17
18
19
21
X
(Gains)

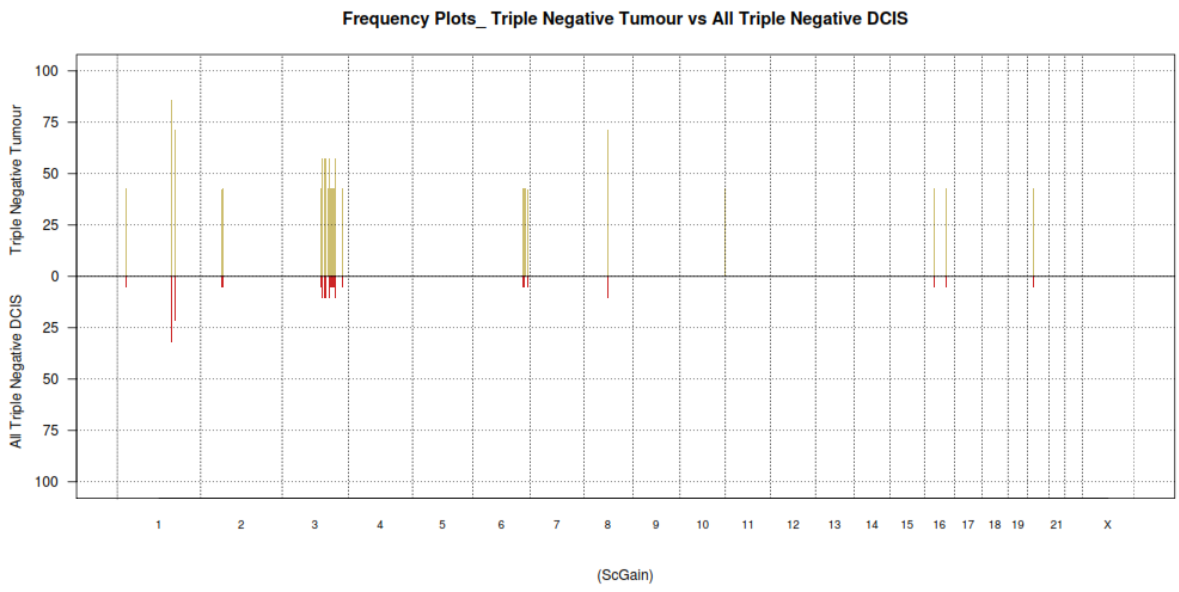
Frequency Plots_ Triple Negative Tumour vs All Triple Negative DCIS
Triple Negative Tumour
All Triple Negative DCIS
100
75
50
25
0
25
50
75
100
1
2
3
4
5
6
7
8
9
10
11
12
13
14
15
16
17
18
19
21
X
(ScGain)

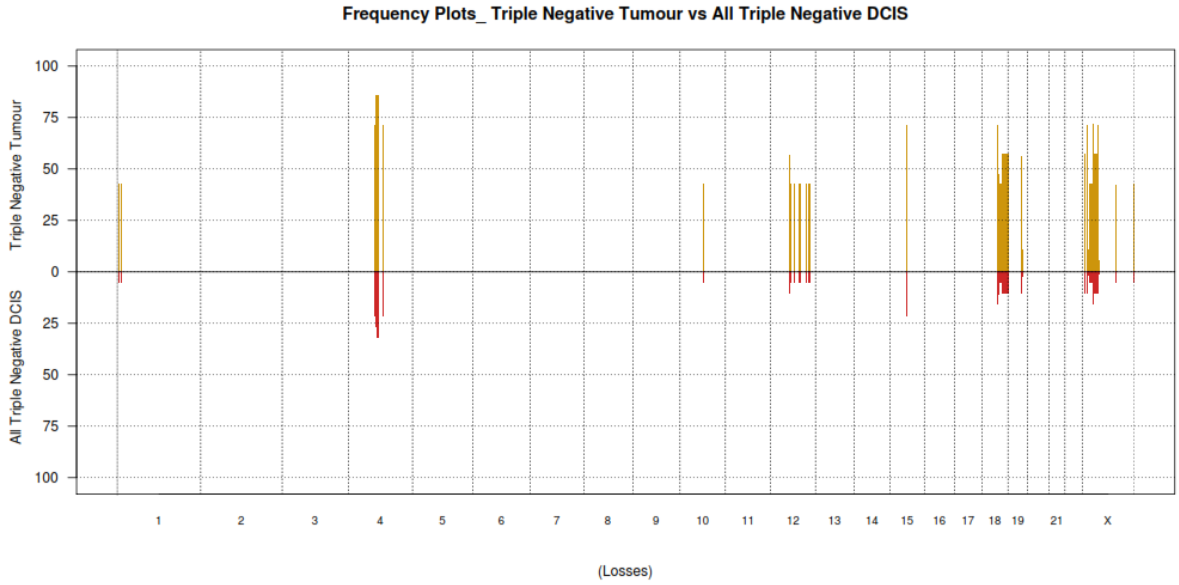
Frequency Plots_ Triple Negative Tumour vs All Triple Negative DCIS
Triple Negative Tumour
All Triple Negative DCIS
100
75
50
25
0
25
50
75
100
1
2
3
4
5
6
7
8
9
10
11
12
13
14
15
16
17
18
19
21
X
(Losses)

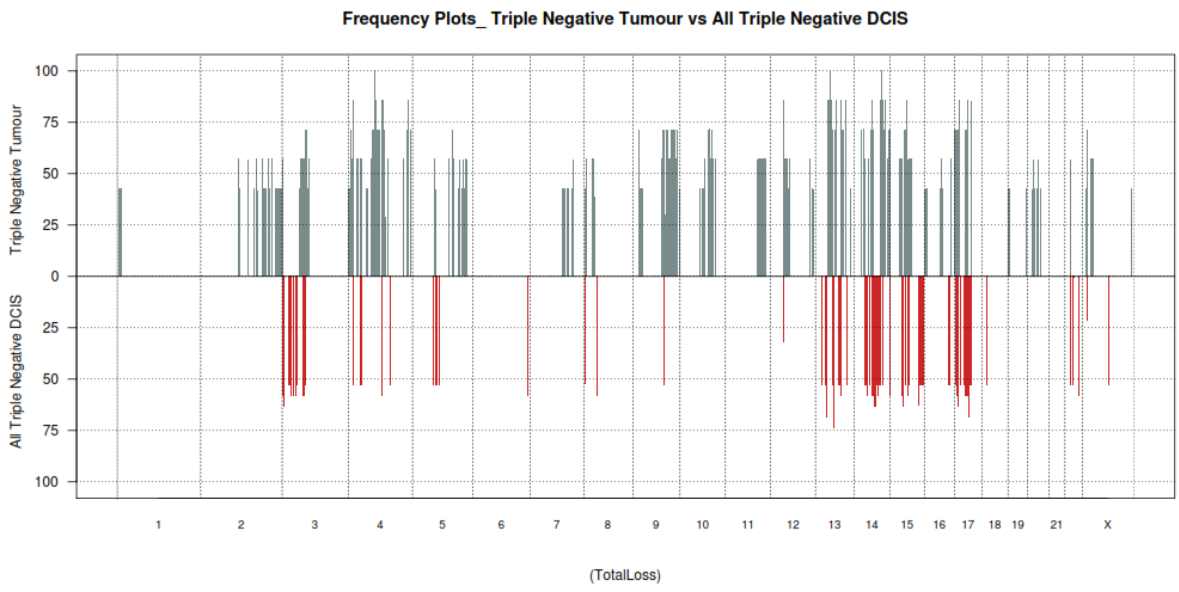
Frequency Plots_ Triple Negative Tumour vs All Triple Negative DCIS
Triple Negative Tumour
All Triple Negative DCIS
100
75
50
25
0
25
50
75
100
1
2
3
4
5
6
7
8
9
10
11
12
13
14
15
16
17
18
19
21
X
(TotalLoss)

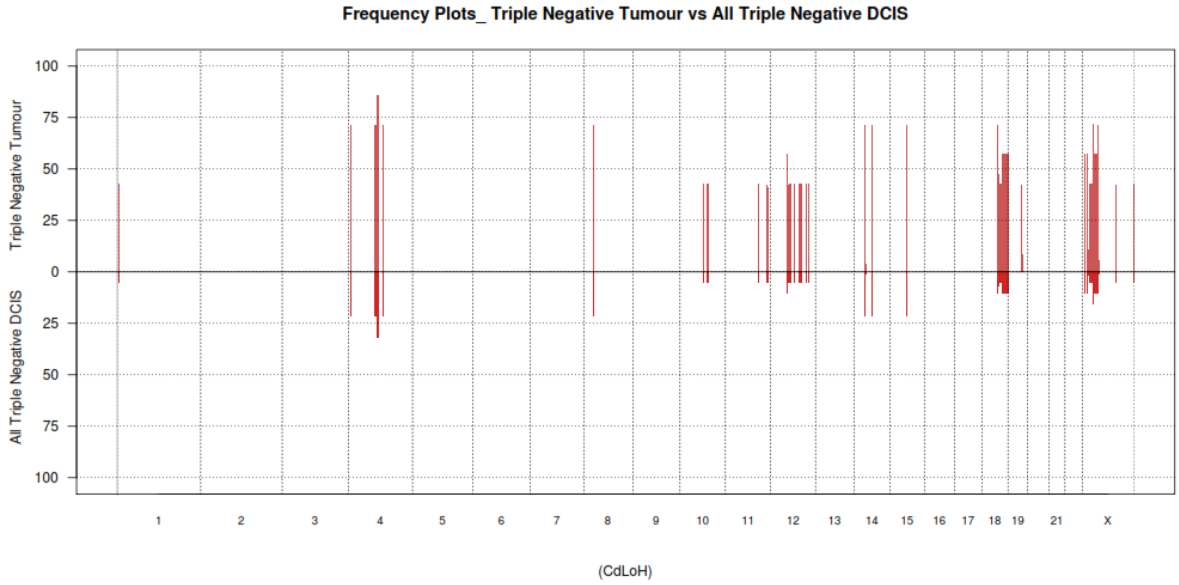
Frequency Plots_ Triple Negative Tumour vs All Triple Negative DCIS
Triple Negative Tumour
All Triple Negative DCIS
100
75
50
25
0
25
50
75
100
1
2
3
4
5
6
7
8
9
10
11
12
13
14
15
16
17
18
19
21
X
(CdLoH)

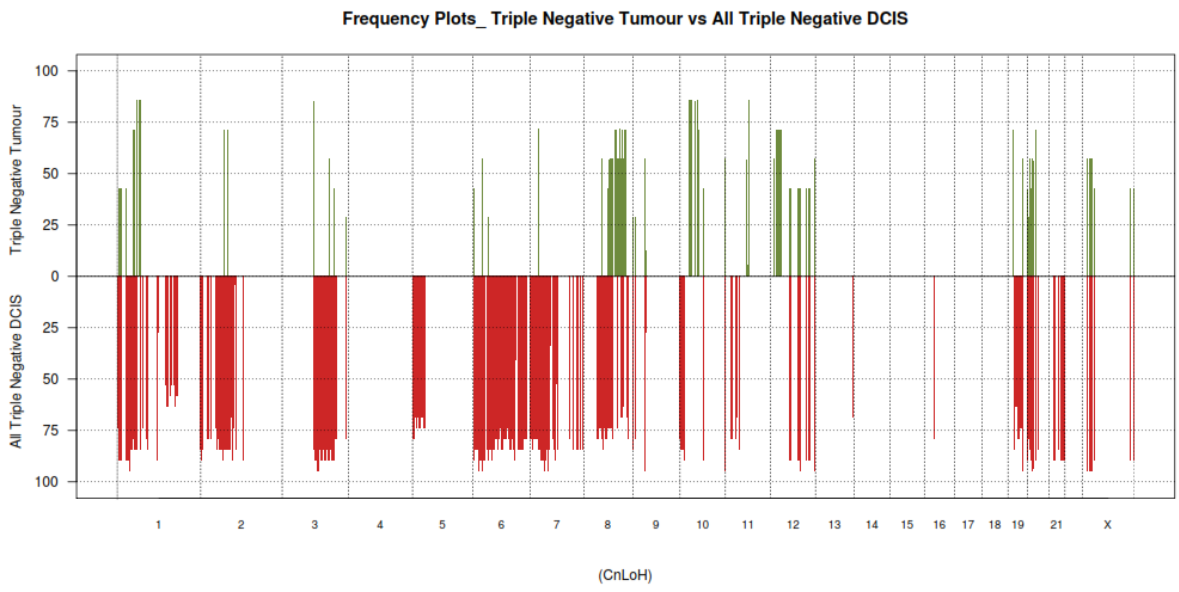

5.8.10.1 Amplification of Triple Negative DCIS and Triple negative Invasive Breast Disease

No amplifications were present in triple negative DCIS (n=0/19) or triple negative invasive breast disease (n=0/7).

5.8.10.2 Duplication of Triple Negative DCIS Compared to Duplication in Triple Negative Invasive Breast Disease

Duplicated genes found in TN DCIS (1/19) were also present in TN invasive breast disease (n=3/7).

1. p-values < 0.05;
2. The gene list is created from 5 genomic regions found on chromosomes 2, 6, 12;
3. These regions encompass 57 genes altered in TN DCIS;

Genes:

7SK AC012494.1 AC079600.1 AL121959.1 ARG1 C6orf192 CTAGE9 CTGF EEF1A1P36 ENPP1 ENPP3 EYA4 HCRTR2 HMGB1L13 LRFN2 MED23 MOXD1 OR2A4 PRICKLE1 RP11-121P10.1 RP11-123H21.1 RP11-203B4.1 RP11-25I15.1 RP11-295F4.4 RP11-314E23.1 RP1-131F15.2 RP11-69I8.2 RP11-69I8.3 RP1-283K11.3 RP1-55C23.4 RP1-55C23.5 RP1-55C23.7 RP1-78N10.2 RP3-

323K23.3 RP3-416F10.1 RP3-462C17.1 RP3-523C21.1 RP3-523C21.2 RP5-988G15.1 RPS12 SNORA33 SNORD100 SNORD101 STX7 TAAR1 TAAR2 TAAR3 TAAR4P TAAR5 TAAR6 TAAR7P TAAR8 TAAR9 U4 VNN1 VNN2 VNN3

PANTHER analysis: 22 mapped ids are found, 35 mapped ids are not found.

Duplication of genes found in TN invasive breast disease (n=3/7) which are not observed in TN DCIS (n=0/19):

1. p-values < 0.05;
2. The gene list is created from 8 genomic regions found on chromosomes 6, 8, 12;
3. These regions encompass 126 genes altered in TN invasive breast disease;

Genes:

5S_rRNA 7SK ABCC10 AL080315.3 AL096711.1 AL136304.1 AL136304.2 AL136304.3 AL451073.1 AL583834.1 BMP5 BYSL C6orf108 C6orf132 C6orf15_2 C6orf154 C6orf174 C6orf226 C6orf58 C8orf85 CCND3 CENPW CLIC5 CNPY3 COL21A1 CRIP3 CUL7 CUL9 DLK2 ECHDC1 EEF1DP5 ENPP4 ENPP5 FRS3 GFRAL GNMT GUCA1A GUCA1B HCRTR2 HEY2 HINT3 HMGCLL1 hsa-mir-588 KIAA0240 KLC4 KLHDC3 LAMA2 MEA1 MED20 MRPL2 MRPS10 NCOA7 PEX6 PGC POLR1C PPP2R5D PRB2 PRICKLE4 PTCRA PTK7 PTPRK RNF146 RP11-103C16.2 RP11-151M7.1 RP11-162L10.1 RP11-213N20.1 RP11-228O6.2 RP11-298J23.5 RP11-298J23.6 RP11-325O24.1 RP11-325O24.2 RP11-357P24.2 RP1-139D8.6 RP11480N24.3 RP11-480N24.4 RP11-480N24.6 RP11-527F13.1 RP11-527F13.2 RP11-533O20.2 RP11-570K4.1 RP11-624M8.1 RP11-753G20.1 RP11-775I22.2 RP1-177A13.1 RP1-179E13.1 RP1-293L8.2 RP1-293L8.5 RP13-469O16.1 RP1-6P5.2 RP1-86D1.2 RP1-86D1.3 RP1-86D1.4 RP1-86D1.5 RP1-8B1.4 RP3-330M21.5 RP3-337H4.6 RP3-351K20.3 RP3-351K20.4 RP3-403A15.1 RP3-447E21.3 RP3-475N16.1 RP5-973N23.4 RPL24P4 RPL7L1 RSPO3 SCARNA15 SLC22A7 SLC30A8 SNORA8 snoU13 SRF TAF8 TFEB THEMIS TJAP1 TOMM6 TRERF1 TRMT11 TTBK1 U6 U7 USP49 XPO5 Y_RNA YIPF3 ZNF318

PANTHER analysis: 62 mapped ids are found, 64 mapped ids are not found.

5.8.10.3 Genomic Gains of Triple Negative DCIS Compared to Genomic Gains in Non Triple Negative DCIS

Gene gains for TN DCIS (n= 4/19) and TN invasive breast disease (n=5/7) show considerable overlap, i.e. genes are present in both groups.

1. p-values < 0.05;
2. A gene list is mapped from 25 genomic regions found on chromosomes 1, 3, 6, 9, 10, 20, 21, X;

3. These regions encompass 232 genes altered in TN DCIS and TN invasive breast disease;

   Genes:

5S_rRNA 7SK AC055758.1 AC072028.2 AC092898.1 AC107021.1 AC108729.1 AC112504.2 AC128648.1 AC133435.1 AC133435.2 AKAP12 AL096840.2 AL133260.1 AL158155.2 AL356137.1 AL357514.2 AL357561.2 AL365214.2 AL450307.1 AL583849.1 ATP1B3 ATR BNIP3 C1orf135 C3orf16 C3orf58 C3orf70 CCDC39 CCIN CHCHD6 CLIC6 CLTA COMMD2 CTD-2501O3.1 CTD-2501O3.2 CTD-2501O3.3 DCAF10 DHX36 EEF1A1P25 EHHADH EIF2S2P2 ESR1 EXOSC3 EXTL1 FAM54B FBXO10 FLYWCH1P1 FRMPD1 FXR1 GK5 GLIPR2 GM2AP1 GNE GPR149 GRHPR GRK7 HRCT1 IPCEF1 IYD JAKMIP3 MACROD2 MAN1C1 MAP3K13 MELK MFN2 MIIP MME MTHFD1L NCRNA00160 OPRM1 OR2S2 PABPC1P10 PAFAH2 PAQR7 PAX5 PCOLCE2 PDIK1L PFN2 PIK3CB PLCH1 PLEKHG1 PLOD2 PLS1 PLSCR1 PLSCR2 PLSCR4 PLSCR5 PLXNA1 POLR1E PPP1R14C PPP2R2D RAB1C RECK RFPL4B RG9MTD3 RNF13 RNF38 RNF7 RP1-105O18.1 RP11-110C15.4 RP11-113A10.1 RP11-113A10.2 RP11-113A10.3 RP11-113A10.5 RP11-117F22.1 RP11-117L15.1 RP11-136K14.1 RP11-136K14.2 RP11-136K14.3 RP11-144C9.1 RP11-167H9.2 RP11-167H9.3 RP11-167H9.4 RP11-167H9.5 RP11-167H9.6 RP11-190C21.3 RP11-190C21.4 RP11-217E22.1 RP11-217E22.2 RP11-217E22.5 RP11-21M4.2 RP11-220I1.1 RP11-220I1.2 RP11-220I1.4 RP11-232M24.1 RP1123D24.1 RP11-23D24.2 RP11-255N4.2 RP11-255N4.3 RP11-259P15.1 RP11-259P15.3 RP1-125I3.2 RP1-125I3.3 RP1-125I3.4 RP1-125I3.7 RP11-270G15.2 RP11271K21.2 RP11-271K21.4 RP11-271K21.7 RP11-274H2.2 RP11-274H2.3 RP11-291C6.1 RP11-297B17.2 RP11-29A1.3 RP11-317B3.2 RP11-327L3.1 RP11-327L3.3 RP11-327L3.4 RP11-327L3.5 RP11-340E6.1 RP11-340E6.2 RP11-343B5.1 RP11-383G6.3 RP11-383G6.4 RP11-397D12.4 RP11-397D12.6 RP11-397D12.7 RP11-405L18.1 RP11-405L18.2 RP11-405L18.4 RP11427D1.1 RP11-439C8.1 RP11-439C8.2 RP11-451G4.1 RP11-451G4.2 RP11-451G4.3 RP11-465M18.1 RP11-471B18.1 RP11-483E7.1 RP11-506B6.1 RP11-506B6.2 RP11-506B6.3 RP11-548O1.1 RP1-159M24.1 RP11-605F14.3 RP11-613F7.1 RP11-613M10.6 RP11-622L21.1 RP11639F1.1 RP11-639F1.2 RP11-639F1.3 RP11-63E16.1 RP11-649A16.1 RP11-651P23.2 RP11651P23.3 RP11-651P23.4 RP11-651P23.5 RP11-651P23.6 RP11-656A15.1 RP11-65C6.1 RP11-758I14.2 RP11-758I14.3 RP11-785G3.1 RP11-84P7.1 RP11-84P7.2 RP11-84P7.3 RP11-88H10.1 RP1188H10.2 RP11-88H10.3 RP1-197O17.3 RP1-292B18.1 RP1-292B18.3 RP1-292B18.4 RP1-297M16.2 RP1-317E23.3 RP1-44A20.4 RP1-99E18.2 RP3-422F24.2 RP3-460G2.2 SCARNA17 SCARNA18 SEPN1 SLC30A2 SLC35F1 snoU13 STMN1 TFDP2 TOMM5 TRIM63 TRPC1 U1 U3 U4 U6 U7 U8 WWTR1 XRN1 Y_RNA ZBTB5 ZCCHC7

PANTHER analysis: 77 mapped ids are found, 155 mapped ids are not found.

5.8.10.4 Sc Gains of Triple Negative DCIS Compared to Sc Gains in Triple Negative Invasive Breast Disease

The comparison of values for Sc gains in TN invasive breast disease (n=3/7) and TN DCIS (n=0/19)

1. p-values <0.05;
2. A gene list is mapped from 32 genomic regions found on chromosomes 1, 2, 3, 6, 10, 16, 20. This represents Sc gains for TN Invasive breast disease;

3. These regions encompass 209 genes altered in TN invasive breast disease;

   Genes:

5S_rRNA 7SK AADAC AADACL2 AC007392.3 AC007403.1 AC007403.2 AC009086.1 AC009086.3 AC009086.4 AC009474.1 AC009474.2 AC025279.1 AC055758.1 AC072028.2 AC078784.1 AC107021.1 AC107027.2 AC108729.1 AC121332.1 AC128648.1 AC133435.1 AC133435.2 AC133555.1 AC133555.2 AC133555.3 AC133555.4 AC133555.6 AC133555.7 ACPL2 AL357561.2 AL450307.1 ARHGAP31 ASTE1 ATP2C1 ATP5LP5 ATR B4GALT4 BNIP3 BOLA2 C1orf135 C2orf86 C3orf16 C3orf30 C3orf58 CCDC39 COMMD2 CPNE4 CTD-2501O3.1 CTD-2501O3.2 CTD-2501O3.3 DHX36 EEF1A1P25 EXTL1 FAM54B GIYD1 GK5 GM2AP1 GPR149 GSTO3P IGSF11 IYD JAKMIP3 LSAMP MACROD2 MAN1C1 MME MRPL3 NEK11 NUDT16 NUDT16P OPRM1 P2RY1 PABPC1P10 PAFAH2 PAQR7 PARK2 PCOLCE2 PDIK1L PFN2 PIK3CB PLCH1 PLOD2 PLS1 PLSCR1 PLSCR2 PLSCR4 PLSCR5 PPP1R14C PPP2R2D QPRT RASA2 RNF13 RP11-117F22.1 RP11-117L15.1 RP11-167H9.2 RP11-167H9.3 RP11167H9.4 RP11-167H9.5 RP11-167H9.6 RP11-190C21.3 RP11-190C21.4 RP11-217E22.1 RP11217E22.2 RP11-217E22.5 RP11-21M4.2 RP11-232M24.1 RP11-23D24.1 RP11-23D24.2 RP11255N4.2 RP11-255N4.3 RP1-125I3.2 RP1-125I3.3 RP1-125I3.4 RP1-125I3.7 RP11265F19.1 RP11-270G15.2 RP11-274H2.2 RP11-274H2.3 RP11-291C6.1 RP11-305I9.1 RP11-316C10.1 RP11-340E6.1 RP11-343B5.1 RP11-383G6.3 RP11-383G6.4 RP11-38P22.2 RP11-39E3.3 RP11-39E3.4 RP11-39E3.5 RP11-39E3.6 RP11-402E20.1 RP11-420J11.2 RP11-427D1.1 RP11-438D8.2 RP11-438D8.3 RP11-438D8.4 RP11-439C8.1 RP11-439C8.2 RP11-451G4.1 RP11-451G4.2 RP11-451G4.3 RP11-454C18.2 RP11-483E7.1 RP11-484M3.4 RP11-484M3.5 RP11-496B10.1 RP11-496B10.3 RP11-496B10.5 RP11-517B11.2 RP11-517B11.4 RP11-517B11.6 RP11-548O1.1 RP11-622L21.1 RP11-639F1.1 RP11-639F1.2 RP11-639F1.3 RP11-63E16.1 RP11-63L4.1 RP11-649A16.1 RP11-64D22.1 RP11-64D22.2 RP11-64D22.5 RP11-651P23.2 RP11-651P23.3 RP11-651P23.4 RP11-651P23.5 RP11-651P23.6 RP11-656A15.1 RP11-758I14.2 RP11-758I14.3 RP11-785G3.1 RP11-788A4.1 RP11-788A4.2 RP11-789L4.1 RP11-88H10.1 RP11-88H10.2 RP11-88H10.3 RP11-933H2.4 RP1-317E23.3 RP3-422F24.2 RP4-635B5.1 RUNDC2B SCARNA17 SCARNA18 SEPN1 SLC30A2 SNORA58 snoU13 SPN STMN1 SUCNR1 SULT1A4 TFDP2 TM4SF4 TRIM63 TRPC1 TTC14 U1 U3 U4 U6 U7 U8 UPK1B WWTR1 XRN1 Y_RNA ZBTB38

PANTHER analysis: 64 mapped ids are found, 145 mapped ids are not found.

5.8.10.5 Losses in Triple Negative DCIS Compared to Losses in Triple Negative Invasive Breast Disease

Losses in TN DCIS (n=1/19) show similarities with losses in TN invasive breast disease (n=3/7). This represents losses for TN DCIS and TN invasive breast disease.

1. p-values <0.05;
2. The gene list is created from 31 genomic regions found on chromosomes 1, 2, 3, 6, 10, 16, 20;
3. These regions encompass 203 genes altered in TN DCIS;

   Genes:

5S_rRNA 7SK AADAC AADACL2 AC007392.3 AC007403.1 AC007403.2 AC009086.1 AC009086.3 AC009086.4
AC009474.1 AC009474.2 AC025279.1 AC055758.1 AC072028.2 AC078784.1 AC107021.1 AC107027.2 AC108729.1 AC121332.1
AC133555.1 AC133555.2 AC133555.3 AC133555.4 AC133555.6 AC133555.7 ACPL2 AL357561.2 AL450307.1 ARHGAP31
ASTE1 ATP2C1 ATP5LP5 ATR B4GALT4 BNIP3 BOLA2 C1orf135 C2orf86 C3orf16 C3orf30
C3orf58 CCDC39 COMMD2 CPNE4 CTD-2501O3.1 CTD-2501O3.2 CTD-2501O3.3 DHX36
EEF1A1P25 EXTL1 FAM54B GIYD1 GM2AP1 GPR149 GSTO3P IGSF11 IYD JAKMIP3 LSAMP
MACROD2 MAN1C1 MME MRPL3 NEK11 NUDT16 NUDT16P OPRM1 P2RY1 PABPC1P10
PAFAH2 PAQR7 PARK2 PCOLCE2 PDIK1L PFN2 PIK3CB PLCH1 PLOD2 PLS1
PLSCR1 PLSCR2 PLSCR4 PLSCR5 PPP1R14C PPP2R2D QPRT RASA2 RNF13 RP11-117F22.1
RP11-117L15.1 RP11-167H9.2 RP11-167H9.3 RP11-167H9.4 RP11-167H9.5 RP11-167H9.6
RP11-190C21.3 RP11-190C21.4 RP11-217E22.1 RP11-217E22.2 RP11-217E22.5
RP11-21M4.2 RP11-232M24.1 RP11-23D24.1 RP11-23D24.2 RP11-255N4.2
RP11-255N4.3 RP1-125I3.2 RP1-125I3.3 RP1-125I3.4 RP1-125I3.7 RP11-265F19.1 RP11-270G15.2
RP11-274H2.2 RP11-274H2.3 RP11-291C6.1 RP11-305I9.1 RP11-316C10.1
RP11-340E6.1 RP11-383G6.3 RP11-383G6.4 RP11-38P22.2 RP11-39E3.3 RP11-39E3.4
RP11-39E3.5 RP11-39E3.6 RP11-402E20.1 RP11-420J11.2 RP11-427D1.1
RP11-438D8.2 RP11-438D8.3 RP11-438D8.4 RP11-439C8.1 RP11-439C8.2
RP11-451G4.1 RP11-451G4.2 RP11-451G4.3 RP11-454C18.2 RP11-483E7.1
RP11-484M3.4 RP11-484M3.5 RP11-496B10.1 RP11-496B10.3 RP11-496B10.5
RP11-517B11.2 RP11-517B11.4 RP11-517B11.6 RP11-548O1.1 RP11-622L21.1
RP11-639F1.1 RP11-639F1.2 RP11-639F1.3 RP11-63E16.1 RP11-63L4.1 RP11-649A16.1
RP11-64D22.1 RP11-64D22.2 RP11-64D22.5 RP11-651P23.2 RP11-651P23.3 RP11-651P23.4
RP11-651P23.5 RP11-651P23.6 RP11-656A15.1 RP11-758I14.2 RP11-758I14.3 RP11-785G3.1
RP11-788A4.1 RP11-788A4.2 RP11-789L4.1 RP11-88H10.1 RP11-88H10.2 RP11-88H10.3
RP11-933H2.4 RP1-317E23.3 RP3-422F24.2 RP4-635B5.1 RUNDC2B SCARNA17 SCARNA18
SEPN1 SLC30A2 SNORA58 snoU13 SPN STMN1 SUCNR1 SULT1A4 TM4SF4 TRIM63
TRPC1 TTC14 U1 U3 U4 U6 U7 U8 UPK1B WWTR1
XRN1 Y_RNA ZBTB38

PANTHER analysis: 62 mapped ids are found, 141 mapped ids are not found.

The comparison of losses represents losses in TN DCIS and TN invasive breast disease

1. p-values < 0.05;
2. A gene list is mapped from 98 genomic regions found on chromosomes 1, 4, 10, 12, 15, 18, 19, X;
3. These regions encompass 317 genes altered in TN DCIS and TN invasive breast disease;

   Genes:

5S_rRNA AC005184.1 AC008245.1 AC009731.1 AC012379.1 AC012379.2 AC013452.1 AC013452.2 AC013558.1 AC018413.1
AC018797.3 AC022046.2 AC025263.1 AC034110.1 AC034110.2 AC036176.2 AC064801.1 AC068473.1 AC083805.1
AC083805.2 AC090360.1 AC090393.1 AC090669.1 AC091551.1 AC091643.1 AC091646.1 AC093827.1 AC100783.1
AC100843.1 AC104059.1 AC114688.1 AC134978.1 AC139100.1 AC139100.2 ACE2 ADNP2 AF196969.5
AF196972.1 AF196972.10 AF196972.2 AF196972.3 AF196972.4 AF196972.9 AF213884.1 AF224669.3 AF241726.2

AF241726.4 AF241726.6 AFF1 AL031311.1 AL136137.1 AL353691.1 AL356741.1 AL591378.1 AL591394.1
AL592043.1 AL627402.1 ALPK2 ANXA3 APOF ARAF ARD1B ARHGAP24 ARHGEF16 ATP9B
AVIL BCL2 BEST3 BMX C18orf22 C4orf36 CA5B CA5BP CASK CBLN2
CDH19 CDH7 CDK4 CEP152 CHST7 CHTF8P COPS2 CTD-2522E6.4 CTDP1
CTDSP2 CXorf24 CXorf36 CXorf58 CYP27B1 CYP2A6 DNAJC12 DUSP21 EBP
EIF2S3 ELAC1 FAM47A FGF5 FIGF FRAS1 FTLP16 FTSJ1 GALK2
GALR1 GPR34 GPR82 GRPR GS1-541M1.1 GS1-541M1.2 GS1-594A7.3
GS1-594A7.5 HERC4 HMGA1L1 hsa-mir-221 hsa-mir-222 hsa-mir-26a-2 hsa-mir-551a
HSBP1L1 IL1RAPL1 INE1 KAL1 KCNG2 KDM6A KDSR KIAA1468 KLHL15 KLHL8
KRT8P14 L1CAM MALT1 MANBA MAOA MAOB MAPK10 March9 MBP ME2
MEGF6 MEX3C NDP NDUFB11 NFATC1 NFKB1 NTS NUAK1 NUS1P1 OTC
PARD6G PCTK1 PIGN PIR PORCN PPP1R2P9 PQLC1 PRDM8 PTCHD2
PTPN13 RAB3IP RASGEF1B RASSF9 RBM10 RBM19 RBM3 RNF152 RP11-10L12.1
RP11-10L12.2 RP11-10L12.4 RP11-10L12.5 RP11-10L12.6 RP11-1148L6.5
RP11-1148L6.6 RP11-126O1.1 RP11-149B9.2 RP11-162A12.1 RP11-162K6.1 RP11-204C16.4
RP11-245M24.1 RP11-281B1.2 RP11-305F18.1 RP11-342D14.1 RP11-344N17.11
RP11-344N17.12 RP11-344N17.13 RP11-344N17.2 RP11-344N17.3 RP11-344N17.6
RP11-344N17.7 RP11-344N17.8 RP11-344N17.9 RP11-377B2.2 RP11-377G16.2
RP11-38O23.3 RP11-38O23.4 RP11-38O23.5 RP11-38O23.7 RP11-397E7.1
RP11-397E7.2 RP11-397E7.3 RP11-397E7.4 RP11-438E5.1 RP11-474D14.2
RP11-476C8.2 RP11-479I1.4 RP11-524P6.1 RP11-540L11.2 RP11-545D19.1
RP1-154K9.2 RP11-552E4.2 RP11-552E4.3 RP11-552E4.4 RP11-552E4.5
RP11-571E6.1 RP11-571E6.3 RP11-571E6.4 RP11-57G10.6 RP11-617O8.1
RP11-640A1.1 RP11-644A7.1 RP11-652N17.1 RP11-689K5.3 RP11-692P14.1
RP11-702C7.1 RP11-702C7.2 RP11-75A9.2 RP11-75A9.3 RP11-778J15.1
RP11-792D21.1 RP11-792D21.2 RP11-9H16.1 RP1-22N22.1 RP1-290C9.2
RP13-202B6.2 RP13-479F17.2 RP13-928P6.3 RP1-50A13.1 RP1-50A13.2
RP1-54B20.7 RP1-69M21.2 RP1-71L16.1 RP1-71L16.2 RP1-71L16.6 RP3-326I13.1 RP3-393P12.2 RP3-393P12.3 RP4-733D15.1 RP5-1174J21.1 RP5-1174J21.2 RP5-972B16.2 RP6-105D16.1
RP6-218J18.3 RP6-99M1.1 RPGR RPL12P8 RTTN SALL3 SERPINB5 SHC4 SIRT1
SLC10A6 SLC38A5 SLC9A7 SMAD4 SNORA11 SNORA25 SNORA31 SNORA68 SNORD56
snoU13 SOCS6 SPACA5 SPACA5B SSX1 SSX3 SSX4 SSX4B SSX5 SSX6
SSX9 STAT2 SYN1 TBC1D25 TIMP1 TMEM27 TNFRSF11A TSHZ1 TSPAN7
TXNL1 TXNL4A U1 U2 U52112.12 U6 U7 U8 UBA1
UBE2D3 USP11 VCX3B VENTXP1 WAS WDR13 WDR7 Y_RNA Z98304.1 ZADH2 ZCCHC2
ZFX ZNF157 ZNF182 ZNF236 ZNF407 ZNF41 ZNF516 ZNF532 ZNF630
ZNF673 ZNF674 ZNF81

PANTHER analysis: 138 mapped ids are found, 179 mapped ids are not found.

5.8.10.6 Total Loss of Triple Negative DCIS Compared to Total Loss in Triple Negative Invasive Breast Disease

There were total losses present in TN DCIS (n=13/19) that are not observed from TN invasive breast disease (n=0/7).

1. p-values < 0.05;

2. A gene list is mapped from 150 genomic regions found on chromosomes 3, 4, 5, 6, 8, 9, 13, 14, 15, 17, 18, 22 & X;
3. These regions encompass 419 genes altered in TN DCIS;

Genes:

5S_rRNA 7SK AARSD1 AB019438.55 AB019438.63 AB019438.66 AB019439.3 ABCD4 AC002117.1 AC003043.1 AC003043.2 AC003102.3 AC003963.2 AC004222.1 AC004596.1 AC004968.1 AC004968.2 AC005399.1 AC006059.1 AC006349.1 AC006445.1 AC006445.6 AC006445.7 AC006445.8 AC007126.1 AC007722.1 AC008105.1 AC011193.1 AC012409.1 AC015936.1 AC015936.3 AC016251.1 AC019131.2 AC020704.1 AC021205.1 AC025287.1 AC025287.2 AC025287.3 AC025287.4 AC026202.1 AC026202.5 AC027139.2 AC027139.3 AC027139.4 AC027708.1 AC027807.1 AC027807.2 AC036222.1 AC044797.1 AC044797.2 AC044797.3 AC055813.1 AC055873.1 AC068400.1 AC079915.1 AC084809.2 AC084809.3 AC084882.1 AC087650.1 AC087742.1 AC092047.1 AC092048.1 AC092421.1 AC098830.1 AC100793.2 AC102948.1 AC102948.2 AC103702.1 AC103965.1 AC104260.1 AC105750.1 AC107982.4 AC109357.1 AC112693.1 AC113171.1 AC114477.1 AC121253.1 AC124789.1 AC134669.1 AC138150.3 AC138150.4 AC183087.1 AC183087.2 ACBD4 ACTR10 ADAM11 ADAM3A ADAM5P ADAMTSL3 ADH4 ADH5 AGBL1 AKAP6 AL008582.1 AL035659.2 AL035659.4 AL035659.6 AL079307.3 AL079307.4 AL079307.5 AL132989.2 AL135978.1 AL136359.1 AL139021.2 AL139089.1 AL162377.1 AL162377.2 AOC2 AOC3 AP000351.4 ARAP2 ARHGAP23 ARID4A ARL4D ARRDC4 ASB16 ASPN ATXN7L3 AY269186.1 AY269186.2 AZI2 BBS12 BOD1L BRCA1 BTF3 C14orf149 C14orf166 C14orf38 C14orf54 C17orf102 C17orf104 C17orf105 C17orf46 C17orf53 C17orf65 C1QL1 C4orf37 CA10 CARTPT CCDC103 CCDC43 CD300LG CDC6 CECR2 CECR9 CENPP CETN4P CHADL CMC1 CSMD1 CTD-2015H6.1 CTD-2015H6.2 CTD-2015H6.3CTNS CWC25 DBF4B DCAKD DDT DDX52 DHRS11 DHX8 DTHD1 DUSP3 ECM2 EDEM1 EFTUD2 EIF4BP4 EIF4E EP300 ETV4 EVI2A EVI2B FAM149B2 FAM151B FAM169B FAM171A2 FAM177A2 FAM187A FAM18B FAM19A1 FBXL2 FBXO33 FBXW10 FGF2 FLT3 FMNL1 FOXD1 FRMD6 FZD2 G6PC G6PC3 GFAP GJC1 GNG2 GOLGA8B GPATCH8 GPC5 GPHN GPR179 GRN GSTT2 HDAC5 HEXIM1 HEXIM2 HIGD1B HMGB1L14 HOXB7 HOXB9 hsa-mir-1233hsa-mir-1281hsa-mir-1469hsa-mir-196a-1 hsa-mir-2117hsa-mir-759 HSP90AB2P IFI35 IGHV1-45 IGHV1-46 IGHV3-33-2 IGHV3-35 IGHV3-36 IGHV3-37 IGHV3-38 IGHV3-41 IGHV3-42 IGHV3-43 IGHV3-47 IGHV4-34 IGHV4-39 IGHV7-34-1 IGHV7-40 IGHVII-33-1 IGHVII-40-1 IGHVII-43-1 IGHVII-44-2 IGHVII-46-1 IGHVIII-38-1 IGHVIII-44 IGHVIV-44-1 IKZF3 IPO11 ITGA2B ITGAE JKAMP KCNH5 KIAA0586 KIF18B KIF2A KLHL5 L3MBTL2 LECT1 LIN52 LPAR4 LRRC70 LSM12 LYZL4 MAP3K14 MCTP2 MEOX1METAP1 MITF MPP2 MPP3 MPP5 MRM1 MRPL45 MYO1D NAGS NF1 NID2 NKTR NKX3-2 NMT1 NR2F2 NUDT6 OCLN_2 OLFM4 OMD OMG P2RX5 PARK2 PCDH8 PDCD6IP PDS5B PIP5K2B PLCD3 PPY PRPSAP2 PSMA3 PSMB3 PSME3 PYY RAB28 RAD51L1 RANGAP1 RGS6 RHCGRNF180 RP11-1072C15.1 RP11-1280N14.3 RP11-1280N14.4 RP11-1299A16.1 RP11-1299A16.2 RP11-12M9.4 RP11-159J2.1 RP11-159J2.2 RP11-170N16.1 RP11-170N16.2 RP11-187O7.1 RP11-209K10.1 RP11-219I21.1 RP11-223D18.1 RP11-241P3.2 RP11-248N6.1 RP11-248N6.2 RP11-24H2.1 RP11-24H2.2 RP11-301J16.5 RP11-30C8.1 RP11-30C8.2 RP11-327P2.5 RP11-341G5.1 RP11-357H14.4 RP11-360F5.1 RP11-360F5.2 RP11-360F5.3 RP11-369I16.1 RP11-380B4.2 RP11-428B4.2 RP11-431M7.2 RP11-431M7.3 RP11-431O22.2 RP11-442J17.4 RP11-474L7.4 RP11-475D8.1 RP11-48B14.1 RP11-520F24.1 RP11-520F24.2 RP11-520F24.3 RP11-522B15.1 RP11-522B15.2 RP11-571L19.2 RP11-571L19.4 RP11-696N14.1 RP11-799A12.1 RP11-799A12.2 RP11-79P5.2 RP11-79P5.3 RP11-79P5.5 RP11-79P5.6 RP11-79P5.7 RP11-79P5.8 RP11-81N13.1 RP11-85I21.1 RP11-880O3.1 RP11-95I19.1 RP11-95I19.2 RP1-85F18.4 RP1-85F18.5RP1-85F18.6RP4-613B23.1 RP4-756G23.5 RPL27 RTN1 RUNDC1 RUNDC3A SEC22C SHISA6 SHPK SIPA1L1 SLC25A21 SLC25A39 SLC4A1 SMN1 SMOC1 SNORA18 SNORA40 SNORD56 SNORD74 snoU13 snoZ178 SOCS7 SOST SPATA5 SPATA8 SPRED1 SRCIN1 SS18L2 SUCLG2 SYNRG SYT16 TAX1BP3 TBC1D3 TEF TIMM9 TMEM101 TMEM132E TMEM93

TMEM98 TMUB2 TOMM20L TRPV1 TRPV3 TSPAN5 U3 U6 U7 UBP1 UBTF VAT1 VSX2
WIPF2 WSCD1 Y_RNA ZBTB47 ZC3H7B ZCCHC5 ZCWPW2 ZFYVE16

PANTHER analysis: 194 mapped ids are found, 225 mapped ids are not found.

There were total losses present in TN invasive breast (n=7/7) disease that are not observed in TN DCIS (n=0/19).

1. p-values < 0.05;
2. A gene list is mapped from 98 genomic regions found on chromosomes 3, 4, 5, 9, 10, 12, 13, 14, 15, 17;
3. These regions encompass 479 genes altered in TN invasive breast disease;

Genes:

5S_rRNA 7SK AATF AB019437.56 ABHD12B ABLIM2 ABR AC003664.1 AC005277.1 AC005304.1
AC005304.2 AC005304.3 AC005324.1 AC005324.2 AC005324.4 AC005324.6 AC005324.7 AC005358.1 AC005358.3 AC005517.1
AC005517.2 AC005517.3 AC005703.2 AC005703.3 AC005772.2 AC005773.1 AC005838.2 AC005863.1 AC005863.2 AC007686.1
AC013248.1 AC013248.2 AC015842.1 AC015922.1 AC015922.2 AC015922.7 AC024610.1 AC027045.1 AC073940.1 AC087742.1
AC087742.2 AC090283.1 AC090283.3 AC090516.1 AC090516.2 AC090519.1 AC090519.10 AC090519.11
AC090519.2 AC090519.3 AC090519.4 AC090519.5 AC090519.6 AC090519.7 AC090519.8 AC090519.9 AC091487.1 AC093819.1
AC093824.1 AC098487.1 AC103560.1 AC104650.2 AC108477.2 AC123769.1 ACCN1 ADCK1 AE000658.6 AE000659.1
AE000659.10 AE000659.12 AE000659.13 AE000659.14 AE000659.15 AE000659.16
AE000659.17 AE000659.18 AE000659.19 AE000659.23 AE000659.6 AE000659.8 AE000659.9
AF111168.1 AF111168.3 AGPAT9 AHSA1 AL049775.1 AL121768.1 AL133223.1 AL133413.1 AL136160.1 AL137024.1
AL139041.1 AL157702.1 AL158058.1 AL162727.1 AL353141.1 AL353782.1 AL353805.1 AL354751.2 AL354751.3 AL354896.1
AL356214.2 AL357172.1 AL358334.1 AL358334.2 AL359180.1 AL359392.1 AL360004.1 AL365364.1 AL732479.1 ALDOB
ALKBH1 AMBP ANKFY1 ANKRD40 ANKS6 ARD1B ASTN2 ATAD1 ATP5C1P1 BAAT
C10orf4 C13orf23 C13orf36 C14orf148 C14orf156 C14orf174 C14orf178 C14orf184 C14orf23 C4orf41 C9orf107
C9orf109 C9orf110 C9orf125 C9orf147 C9orf170 C9orf30 C9orf44 C9orf80 CACNA1G CASC4 CATSPERB
CDC20P CDKN2AIP CDRT1 CDRT4 CDRT7 CEP55 CNOT6L COL27A1 CTC-448D22.1
CTC-507E12.1 CTD-2158P22.1 CTD-2158P22.2 CTD-2158P22.4 CTD-2175M1.1
CTDSPL2 CYB5D2 CYP26A1 CYP26C1 DAB2IP DBC1 DDIT4L DHRS7C DKK2 DLEU1
DLEU2 DTWD2 DYNLL1P1 ELAC2 EML5 EXOC6 FAM154A FAM170A FAM175A FAM18B2
FAM190 FAM190A FAM33B FKBP15 FLRT2 FOXG1 FRMD5 FYTTD1P1 GABBR2 GALNT12
GALNTL6 GAPDHP34 GAS1 GAS7 GK2 GLP2R GMPSP GNG5P5 GPM6A GPR107 GPR120 GRID1
GRIN3A GSTZ1 HELT HS3ST3A1 hsa-mir-1260 hsa-mir-15a hsa-mir-16-1 hsa-mir-346 hsa-mir-455 hsa-mir-548h-3
hsa-mir-95 HSD17B4 HSDL2 HTRA3 IGHV1-67 IGHV1-68 IGHV1-69 IGHV2-70 IGHV3-62 IGHV3-63 IGHV3-64
IGHV3-65 IGHV3-66 IGHV3-71 IGHV3-72 IGHV3-73 IGHV4-61 IGHVII-60-1 IGHVII-62-1 IGHVII-65-1 IGHVII-67-1
IGHVIII-67-2 IGHVIII-67-3 IGHVIII-67-4 IL6STP1 ING2 ISM2 KIAA1737 KIAA1958 KIF12 KRT222 KRT24
KRT25 KTN1 LGI1 LHFP LHX6 LMO7 MEIS3P1 MITF MMRN1 MORN5
MRPL50 MRRF MURC MYOCD MYOF NDUFA8 NGB NHLRC3 NRXN3 NTN1 NXN
OR1B1 OR1H1P OR1J2 OR1J4 OR1L1 OR1L3 OR1L4 OR1L6 OR1L8 OR1N1
OR1N2 OR1Q1 OR7E94P PAPPA PAPSS1 PAPSS2 PDE6C PDZRN3 PMP22 POMT2 PPP3R2 PYGL
RASGEF1B RBM18 RBP4 RCVRN RFXAP RGS3 RNF20 ROR2 RP11-100G15.10 RP11-100G15.2
RP11-100G15.3 RP11-100G15.4 RP11-100G15.5 RP11-100G15.6 RP11-100G15.7
RP11-115D19.1 RP11-115G5.1 RP11-118F2.2 RP11-118F2.3 RP11-122F14.4 RP11-1258F18.1 RP11-127L21.1 RP11-127L21.2 RP11-15B17.1 RP11-162D16.4 RP11-168K11.2

RP11-168K11.3 RP11-16L6.3 RP11-181F12.1 RP11-18B16.1 RP11-18B16.2 RP11-197L7.2
RP11-20O12.1 RP11-226P1.1 RP11-234K19.1 RP11-234K19.2 RP11-24E1.1
RP11-264C15.2 RP11-276E15.4 RP11-276H19.1 RP11-276H19.2 RP11-276H19.4 RP11-280G19.1
RP11-280G19.2 RP11-296L20.1 RP11-299L17.1 RP11-32M23.4 RP11-332E3.2
RP11-348J12.2 RP11-349E4.1 RP11-34F20.4 RP11-34F20.5 RP11-352E6.1
RP11-352E6.2 RP11-35N6.1 RP11-35N6.3 RP11-35N6.4 RP11-35N6.6 RP11-367N14.1
RP11-367N14.2 RP11-385D13.1 RP11-386B13.1 RP11-386B13.3 RP11-386B13.4 RP11-388N2.1
RP11-394D2.1 RP11-395D3.1 RP11-397J18.1 RP11-408O19.3 RP11-421P11.5
RP11-438E5.1 RP11-44F21.4 RP11-452B18.1 RP11-452B18.2 RP11-45A16.3 RP11-45A16.4
RP11-45I20.1 RP11-462C21.1 RP11-477L16.2 RP11-478K15.1 RP11-478K15.2
RP11-478K15.3 RP11-478K15.4 RP11-478K15.5 RP11-480P3.1 RP11-490D19.6
RP11-490D19.8 RP11-499E18.1 RP11-51N22.1 RP11-51N22.2 RP11-521H3.1
RP11-524G24.2 RP11-527F15.1 RP11-534I8.1 RP11-542G1.1 RP11-542G1.2
RP11-542G1.3 RP11-545P6.1 RP11-545P6.2 RP11-54K22.1 RP11-565F19.1
RP11-567N4.2 RP11-567N4.3 RP11-576C12.1 RP11-588P8.1 RP11-58C3.2
RP11-598G2.1 RP11-610O8.1 RP11-616K22.1 RP11-61P7.3 RP11-624A4.1 RP11-624L12.1
RP11-626E13.1 RP11-64P14.7 RP11-67K19.3 RP11-67M1.1 RP11-689K5.3 RP11-692E14.1
RP11-701P16.3 RP11-701P16.4 RP11-713M6.1 RP11-713M6.2 RP11-722P15.1 RP11-765K14.1
RP11-806K15.1 RP11-84H6.1 RP11-88G17.2 RP11-92C4.3 RP11-94C24.10 RP11-94C24.11
RPL10P3 RPS3AP5 RWDD4A SEPT7P7 SH3TC1 SLC31A2 SLC39A8 SLC46A2 SLC4A4 SMAD9 SMARCE1
SNCA SNORA26 SNORA31 SNORA32 SNORA46 SNORA70 SNORA74 SNORD112 SNORD65 snoU13
snoU83B SNW1 SNX30 SORBS2 SPRY2 SPTLC1 SPTLC2 STOML3 STON2 STOX2 STX8
TBC1D26 TEKT3 TIMM22 TLK1P1 TMED8 TMEFF1 TMEM20 TMEM63C TRIM16 TRIM32
TTC8 TTLL11 U1 U3 U4 U6 U7 UBE2G1 USP43 VEGFC VIPAR
WDR16 WDR20 Y_RNA ZDHHC22 ZFP37 ZNF189 ZNF286 ZNF29P ZNF618 ZNF883
ZYG11AP1 ZZEF1

PANTHER analysis: 160 mapped ids are found, 319 mapped ids are not found.

5.8.10.7 CdLOH of Triple Negative DCIS Compared to CdLOH in Triple Negative Invasive Breast Disease.

There is considerable overlap between CdLOH in TN DCIS (n=1/19) and CdLOH in TN invasive breast disease (n=3/7).

1. p-values < 0.05;
2. A gene list is mapped from 55 genomic regions found on chromosomes 1, 10, 11, 12, 18, 19, X;
3. These regions encompass 133 genes altered in TN DCIS and TN invasive breast disease;

   Genes:

Mar09 AC005184.1 AC009731.1 AC011260.2 AC022046.2 AC025263.1 AC036176.2 AC064801.1 AC083805.1 AC083805.2
AC090666.1 AC090669.1 AC100783.1 AC100843.1 AC139100.1 AC139100.2 AL031311.1 AL136137.1 AL353691.1

AL356741.1 AL627402.1 ALPK2 ARHGEF16 AVIL BCL2 BEST3 C10orf100 CASK CBLN2 CD226
CDK4 CHEK1 CHTF8P CTDSP2 CXorf36 CXorf58 CYP27B1 CYP2A6 DNAJC12 DOK6
DUSP21 EIF2S3 ELAC1 GPR34 GPR82 GRPR GS1-541M1.1 GS1-541M1.2
HERC4 HMGA1L1 hsa-mir-26a-2 hsa-mir-551a IL1RAPL1 KAL1 KDM6A KDSR KIAA1468
KLHL15 L1CAM MALT1 MAOA MAOB MBD2 ME2 MEGF6 NDP NEDD4L
NRG3 NTS NUAK1 OS9 PARD6G PHLPP1 PIGN PPP1R2P9 RAB3IP RASSF9 RBM19
RNF152 RP11-126O1.1 RP11-149B9.2 RP11-202D18.2 RP11-204C16.4 RP11-20E23.1
RP11-342D14.1 RP11-377B2.2 RP11-472N6.1 RP11-474D14.2 RP11-479I1.4
RP11-514F8.2 RP11-524P6.1 RP11-540L11.2 RP1-154K9.2 RP11-57G10.6 RP11-617O8.1 RP11-640A1.1
RP11-652N17.1 RP11-702C7.1 RP11-702C7.2 RP11-9H16.1 RP1-22N22.1 RP1-
290C9.2 RP1-50A13.1 RP1-50A13.2 RP3-326I13.1 RP5-1174J21.1 RP5-1174J21.2 RP6-
105D16.1 RP6-218J18.3 RPL12P8 RTTN SCN8A SERPINB5 SH2D4B SIRT1 SNORA68 snoU13
TNFRSF11A TXNL1 U1 U2 U52112.12 U6 U8 VCX3B VENTXP1 VPS4B WDR7 Y_RNA
ZCCHC2 ZFX ZNF407 ZNF532

PANTHER analysis: 65 mapped ids are found, 68 mapped ids are not found.

There are some similarities between CdLOH in TN invasive breast disease (n=4/7) and CdLOH in TN DCIS (n=1/19).

1 p-values < 0.05;

2 A gene list is mapped from 71 genomic regions found on chromosomes 1, 10, 11, 12, 18, 19, X;

3 These regions encompass 167 genes altered in TN DCIS and TN invasive breast disease;

Genes:

Mar09 5S_rRNA AC005184.1 AC008245.1 AC009731.1 AC011260.2 AC022046.2 AC025263.1 AC036176.2 AC064801.1 AC083805.1
AC083805.2 AC090360.1 AC090393.1 AC090666.1 AC090669.1 AC091551.1 AC091643.1 AC100783.1 AC100843.1 AC114688.1
AC139100.1 AC139100.2 ADNP2 AF196972.3 AF196972.4 AL031311.1 AL136137.1 AL353691.1 AL356741.1 AL627402.1
ALPK2 ARHGEF16 ATP9B AVIL BCL2 BEST3 C10orf100 C18orf22 CASK CBLN2
CD226 CDH19 CDH7 CDK4 CHEK1 CHTF8P CTDSP2 CXorf36 CXorf58 CYP27B1
CYP2A6 DNAJC12 DOK6 DUSP21 EIF2S3 ELAC1 FTSJ1 GPR34 GPR82 GRPR GS1-541M1.1
GS1-541M1.2 HERC4 HMGA1L1 hsa-mir-26a-2 hsa-mir-551a HSBP1L1 IL1RAPL1 KAL1 KDM6A KDSR
KIAA1468 KLHL15 L1CAM MALT1 MAOA MAOB MBD2 MBP ME2 MEGF6 MEX3C NDP
NEDD4L NFATC1 NRG3 NTS NUAK1 OS9 PARD6G PHLPP1 PIGN PPP1R2P9 PQLC1
RAB3IP RASSF9 RBM19 RNF152 RP11-126O1.1 RP11-149B9.2 RP11-162A12.1 RP11-202D18.2 RP11-
204C16.4 RP11-20E23.1 RP11-342D14.1 RP11-377B2.2 RP11-38O23.5 RP11-38O23.7 RP11-472N6.1
RP11-474D14.2 RP11-479I1.4 RP11-514F8.2 RP11-524P6.1 RP11-540L11.2 RP1-154K9.2
RP11-552E4.2 RP11-552E4.3 RP11-57G10.6 RP11-617O8.1 RP11-640A1.1 RP11-652N17.1 RP11-702C7.1
RP11-702C7.2 RP11-9H16.1 RP1-22N22.1 RP1-290C9.2 RP1-50A13.1 RP1-
50A13.2 RP3-326I13.1 RP5-1174J21.1 RP5-1174J21.2 RP6-105D16.1 RP6-218J18.3
RPL12P8 RTTN SALL3 SCN8A SERPINB5 SH2D4B SIRT1 SLC38A5 SNORA68 snoU13

SOCS6 SSX5 TNFRSF11A TSHZ1 TXNL1 TXNL4A U1 U2 U52112.12 U6 U7 U8 VCX3B VENTXP1 VPS4B WDR7 Y_RNA ZADH2 ZCCHC2 ZFX ZNF236 ZNF407 ZNF532

PANTHER analysis: 83 mapped ids are found, 84 mapped ids are not found.

5.8.10.8 CnLOH of Triple Negative DCIS Compared to CnLOH in Triple Negative Invasive Breast Disease

There is CnLOH present in TN DCIS (n=18/19) that are not observed in TN invasive breast disease (n=0/7). This represents CnLOH for TN DCIS.

1. P-values <0.0001;
2. A gene list is mapped from 78 genomic regions found on chromosomes 1, 2, 3, 6, 7, 10, 20, 21;
3. These regions encompass 529 genes altered in TN DCIS;

   Genes:

sept7 5S_rRNA 7SK ABHD11 AC004455.1 AC004691.5 AC005154.5 AC005189.6 AC005537.2 AC005582.1 AC006022.4 AC006466.5 AC006478.1 AC006960.7 AC006978.1 AC007392.3 AC007403.1 AC007403.2 AC009474.1 AC009474.2 AC010132.10 AC010132.11 AC010132.9 AC011738.4 AC018685.2 AC027269.2 AC063927.2 AC063927.3 AC063927.4 AC063927.5 AC063927.6 AC063927.7 AC063927.8 AC063927.9 AC073464.11 AC073464.9 AC073846.1 AC073846.2 AC073846.3 AC078784.1 AC078811.1 AC087069.2 AC092265.1 AC092898.1 AC093168.1 AC107027.2 AC108729.1 AC117477.1 AC121332.1 ADCYAP1R1 ADPRHL2 AF064859.2 AF127577.10 AF127577.11 AF127577.12 AF127577.8 AF127936.3 AF127936.5 AF127936.6 AF127936.7 AF127936.8 AF130358.5 AF165138.6 AF165138.7 AIF1 AIM1L AJ006998.2 AJ009632.3 AL022170.1 AL023807.1 AL031655.1 AL031655.2 AL034372.1 AL034449.2 AL035670.1 AL049570.1 AL050322.1 AL121988.1 AL133268.1 AL136230.1 AL138724.3 AL138889.1 AL139044.1 AL139044.2 AL139286.1 AL160037.2 AL160400.1 AL160400.2 AL162579.1 AL355877.1 AL589723.1 AL590062.1 AL591845.1 AL645811.1 ANKRD20B ANLN AOAH AP000304.12 AP000313.1 AP000313.2 AP000318.2 AP000569.2 AP000569.8 AP001347.1 AP001347.5 AP001347.6 AP001466.1 AP001466.7 AP001634.5 APOM AQP1 ARHGAP31 ASS1P1 ASTE1 ATP2C1 ATP5LP2 ATP5O ATP6V1G2 B4GALT4 BAK1 BAT1 BAT2 BAT3 BAT4 BAT5 BCL7B BIN1 BLVRA BPESC1 BRWD1 BZW1L1 C1orf113 C1orf212 C1orf216 C20orf187 C21orf81 C3orf16 C3orf30 C3orf72 C6orf125 C6orf15 C6orf227 C6orf25 C6orf26 C6orf27 C6orf47 C7orf25 C7orf44 CAMK1D CAP2 CATSPER4 CCDC21 CCHCR1 CD52 CDSN CEP70 CHCHD6 CLDN3 CLDN4 CLIC1 CLSPN CMAH CNKSR1 COL21A1 COL6A6 COL8A2 COMMD2 CPNE4 CRHR2 CSF3R CSNK2B CST2 CST5 CSTP1 CTD-2021J15.1 CTD-2021J15.2 CYCSP42 CYP39A1 DDAH2 DHFRP2 DLGAP3 DNAJC30 EEF1A1P25 EIF2C1 EIF2C3 EIF2C4 ENTPD6 EPDR1 ERLEC1P1 ESYT3 EXTL1 FABP7 FAIM FAM176B FAM188B FAM65B FAM8A1 FAT1P1 FGFR3P FOXL2 FTLP18 GAPDHP39 GARS GGNBP1 GGTLA4 GHRHR GJA4 GJB3 GJB4 GJB5 GLI3 GMNN GPR116 GRRP1 GS1-179L18.1 GS1-278J22.1 GS1-278J22.2 GSTO3P HCG27 HCP5 HECW1 HIST1H1A HIST1H1PS2 HLA-B HLA-C HLA-DQA1 HLA-DQB1 HLA-S HMGCS2 hsa-mir-548a-1 HSF2BP IGSF11 INMT IP6K3

ITPR3 ITSN1 KDM1B KIAA0319L KIF13A LEMD2 LIPI LRRC16A LSAMP LSM10
LST1 LTA LTB LY6G5B LY6G5C LY6G6C LY6G6D LY6G6E LY6G6F
MAP7D1 MCCD1 MEP1A MICA MICB MLN MLXIPL MME MRAS MRPL3
MRPL32 MRPS15 MRPS22 MRPS24 MRPS6 MSH5 MT-ATP6 MT-CO1 MT-CO3
MTCO3P1 MT-ND1 MT-ND2 MT-ND3 MT-ND4 MT-ND4L MT-ND5 MT-ND6 NCDN NCR3
NCRNA00240 NEK11 NF1L1 NFKBIL1 NHLRC1 NRIP1 NUDT16 NUDT16P NUP153
OR2AD1P OR2W1 OSCP1 PA2G4P2 PABPC1P10 PAFAH2 PCBP2P1 PCCB PDIK1L
PFN2 PHGDH PIK3CB PIK3R4 PKIB PLA2G7 PLCB1 PLCH1 PLXNA1
POLR2CP POLR2LP POM121L3P POU5F1 PPIAP9 PRIM2 PRR23A PRR23B PRR23C PSMA2
PSMB2 PSMG1 PSORS1C1 PSORS1C2 PSORS1C3 RAD23BLP RBM11 RBM24 RBPMSLP
RCAN2 RHOT1P2 RNF13 RNF144B RP11-102J14.1 RP11-115O13.1 RP11-117F22.1 RP11-117L15.1
RP11-14H3.3 RP11-153N17.1 RP11-167H9.3 RP11-167H9.4 RP11-191A15.1
RP11-191A15.2 RP11-191A15.3 RP11-191A15.4 RP11-201E8.1 RP11-221J22.1
RP11-221J22.2 RP11-231P20.2 RP11-231P20.3 RP11-232M24.1 RP11-238O13.1
RP11-255N4.2 RP11-255N4.3 RP11-263A24.1 RP11-265F19.1 RP11-268F1.2
RP11-268F1.3 RP11-280F2.1 RP11-280F2.2 RP11-280H21.1 RP11-305I9.1
RP11-306L14.1 RP11-324H4.1 RP11-367G6.1 RP11-384F7.1 RP11-384F7.2
RP11-394D14.1 RP11-39E3.3 RP11-39E3.4 RP11-39E3.5 RP11-39E3.6
RP11-40M23.1 RP11-435D7.3 RP11-446F17.3 RP11-446H18.3 RP11-451G4.2
RP11-451G4.3 RP11-463H24.1 RP11-484M3.4 RP11-484M3.5 RP11-517B11.2
RP11-517B11.4 RP11-517B11.6 RP11-548O1.1 RP11-548O1.3 RP11-561O4.1
RP11-569G9.7 RP11-605F14.3 RP11-622P13.2 RP11-631B21.1 RP11-631B21.2
RP11-639F1.1 RP11-639F1.2 RP11-639F1.3 RP11-63E16.1 RP11-649A16.1
RP11-651P23.2 RP11-651P23.3 RP11-651P23.4 RP11-651P23.5 RP11-651P23.6
RP11-768G7.1 RP11-768G7.2 RP11-768G7.3 RP11-779P15.1 RP11-779P15.2
RP11-795J1.1 RP11-795J1.2 RP11-810H18.1 RP11-933H2.4 RP11-93B21.1
RP11-96L14.7 RP1-245M18.2 RP1-273P12.1 RP1-273P12.3 RP1-278O22.2
RP1-71H19.2 RP3-347E1.2 RP3-425P12.1 RP3-425P12.2 RP3-425P12.4
RP3-425P12.5 RP3-437I16.1 RP3-468B3.2 RP3-501N12.3 RP3-522P13.1 RP3-522P13.2
RP3-522P13.3 RP3-525L6.2 RP4-564O4.1 RP4-635B5.1 RP4-665N4.4 RP4-665N4.5
RP4-697P8.2 RP4-697P8.3 RP4-718N17.1 RP4-718N17.2 RP4-728D4.2
RP4-728D4.3 RP4-738P15.1 RP4-738P15.4 RP4-765A10.1 RP4-765A10.2 RP4-
796I8.1 RP5-1100I6.1 RP5-1100I6.2 RP5-877J2.1 RP5-983H21.3 RP5-997D16.2
RPL15P4 RPL3P2 RRP1B SAMSN1 SCARNA17 SCARNA18 SCGN SEPT7P3 SFRP4 SH3BGRL3
SLC25A27 SLC30A2 SLC5A3 SMPDL3A SNORA38 SNORA58 SNORA63 SNORA73 SNORD45 SNORD83
snoU13 STAG1 STK40 STX1A TBL2 TCF19 TDRD6 TEKT2 TFAP2E THRAP3
TMEM45A TNF TPMT TRAPPC3 TRIM38 TRIM63 TXNDC3 U1 U3 U4 U5
U6 U7 UBXN11 UPK1B UQCRHP1 URGCP USP25 USP8P VARS VN1R11P
VN1R13P VPS37D WASF5P WBSCR22 WBSCR26 WBSCR27 WBSCR28 WWTR1 XXbac-
BPG181B23.4 XXbac-BPG181B23.6 XXbac-BPG248L24.10 XXbac-BPG248L24.11 XXbac-BPG248L24.12 XXbac-
BPG254F23.5 XXbac-BPG254F23.6 XXbac-BPG254F23.7 XXbac-BPG296P20.14 XXbac-BPG296P20.15
XXbac-BPG299F13.14 XXbac-BPG32J3.18 XXbac-BPG3 J3.19 XXyac-YX60D10.1 Y_RNA
Z93017.1 ZDHHC20P2 ZMYM4 ZNF593 ZNF683 ZPLD1

PANTHER analysis: 208 mapped ids are found, 321 mapped ids are not found.

There is CnLOH present in TN invasive breast disease (n=6/7) that are not observed in TN DCIS (n=0/19).

1. p-values < 0.05;
2. A gene list is mapped from 40 genomic regions found on chromosomes 1, 2, 3, 10, 11, 12, 19, 20;
3. These regions encompass 291 genes altered in TN invasive breast disease;

Genes:

ZSWIM4 5S _rRNA 7SK ABRA AC004016.1 AC004016.2 AC005082.1 AC005082.12 AC005082.2 AC006039.1 AC006039.4 AC006039.5 AC008686.2 AC009908.1 AC011118.2 AC011626.1 AC016405.1 AC017084.1 AC017084.6 AC021876.3 AC021876.4 AC022021.2 AC022201.4 AC023590.1 AC023632.1 AC025370.1 AC025370.2 AC025647.3 AC027238.1 AC027419.1 AC048346.1 AC064807.1 AC068228.4 AC068228.5 AC084083.1 AC084083.2 AC084114.1 AC090192.1 AC090192.2 AC090193.2 AC090802.1 AC090811.1 AC090921. AC090922.1 AC099680.1 AC103816.1 AC104212.2 AC120053.1 ADD2 AL049651.1 AL136985.2 AL160287.2 AL161932.2 AL451107.1 AL512654.1 ANGPT1 ANKRD46 ANXA13 AP000428.1 AP002852.1 AP002907.1 AP003550.10 APBB1IP ARHGAP12 ATAD2 ATP6V1G1P4 BAALC BRD7P6 C10orf50 C7orf30 C7orf31 C8orf37 C8orf39 C8orf54 C8orf56 C8orf76 C8orf85 CACHD1 CCND1 CCNY CDH17 CLSTN2 COLEC10 CREM CSDA CSGALNACT2 CSTF2T CTC-788C1.1 CTHRC1 CUL2 CYB5P4 CYCS DCAF13 DEPDC1 DERL1 DFNA5 EXT1 EYA1 FABP5 FAM159A FAM83A FAM91A1 FAM92A1 FBXO32 FBXO43 FER1L6 FGF19 FXYD4 FZD6 GAPDP2 GEM GLUDP5 GPNMB GPX7 HAS2 HAS2AS HNRNPF hsa-mir-1273hsa-mir-23a hsa-mir-24-2 hsa-mir-27a hsa-mir-548d-1 IAPP IGF2BP3 KB-1137H10.1 KB-1247B1.1KB-1554H10.1 KB-1615E4.1KB-1980E6.1KIAA0196 KIF5B KLF10 KLHL38 KLHL7 KRT18P3 MACROD1 MAL2 MED30 MPP7 MTSS1 MYSM1 NCALD NDUFB9 NIPAL2 NOV NRP1 NSMCE2 NUPL2 ODF1 ORAOV1 OSBPL3 OVCH1 OXR1 PABPC1 PCDH15 PCMTD1 PDP1 PDSS1 PDZK1IP1 PIK3C2G POP1 PRB3 PRH1 PRH2 PRKG1 PRR4 RAD54B RASGEF1A RAVER2 RBM12B RET RGS22 RNF139 RNF19A RP11-1082L8.1 RP11-1110J8.1RP11-128B16.3 RP11-13L2.1 RP11-13L2.2RP11-14C22.3 RP11-14C22.4 RP11-14C22.6 RP11-152P17.1 RP11-167O6.2 RP11-168L22.2 RP11-168O22.1 RP11-189G24.2 RP11-200A13.1 RP11-200A13.2RP11-241I20.1 RP11-241I20.3 RP11-241I20.4 RP11-241I20.5 RP11-273P3.1 RP11-297A16.2 RP11-30P9.1 RP11-318G8.1 RP11-324I22.2 RP11-342D11.2 RP11-351M16.1 RP11-351M16.2 RP11-351M16.3 RP11-359G22.2 RP11-414D17.1 RP11-472N13.3 RP11-484J3.1 RP11-51B10.3 RP11-51B10.4 RP11-539E17.1 RP11-668N23.1 RP11-68L1.1RP11-68L1.2RP11-778D12.1 RP1-18D14.2 RP1-18D14.3 RP1-18D14.4 RP11-941H19.1 RP11-941H19.2 RP11-959I15.1 RP13-16H11.1 RP13-16H11.2 RP13-16H11.5 RP13-16H11.6 RP13-16H11.7 RP3-388N13.1 RP4-694A7.2 RP4-694A7.3 RP4-694A7.4 RP4-753D10.3 RP4-753D10.5 RP4-794H19.2 RP5-1033K19.2 RPE65 RRM2B RSPO2 SAMD12 SLC25A32 SLC30A8 SLCO1A2 SLCO1B1 SNORA20 SNORA31 SNORA32 SNORD77 snoU13 SNX31 SPAG1 SQLE SSTR4 STYK1 TAS2R10 TAS2R13 TAS2R14 TAS2R19 TAS2R20 TAS2R31 TAS2R42 TAS2R50 TAS2R7 TAS2R8 TAS2R9 TASP1 TATDN1 TCEB1P18 TGFA THBD TMEM65 TMEM67 TMEM74 TMTC1 TNFRSF11B TPD52 TRHR TRIB1 TRIM42 TRMT12 TRPS1 U3 U4 U6 U6atac U7 UBR5 WAC WDR67 WDYHV1 Y_RNA ZFPM2 ZHX1 ZHX2 ZNF572

PANTHER analysis: 140 mapped ids are found, 151 mapped ids are not found.

5.8.11 Copy Number Aberrations for HER2 Positive DCIS Compared to Oestrogen Receptor Positive DCIS and Triple Negative DCIS.

These series examines the difference between Her2 positive pure DCIS and oestrogen receptor positive DCIS and triple negative positive DCIS

Frequency plots showing copy number aberrations between HER2 positive DCIS compared to oestrogen receptor positive DCIS and triple negative DCIS were provided by Breakthrough Breast Cancer/Research Oncology, King's College London Bioinformatics Department (Figure 44).

Figure 44: Frequency plots showing copy number aberrations between HER2 positive pure DCIS compared to oestrogen positive dcis and triple negative DCIS (amplifications, duplications, gains, Sc gains, losses, total losses CdLOH and CnLOH,) (pages 279-282).

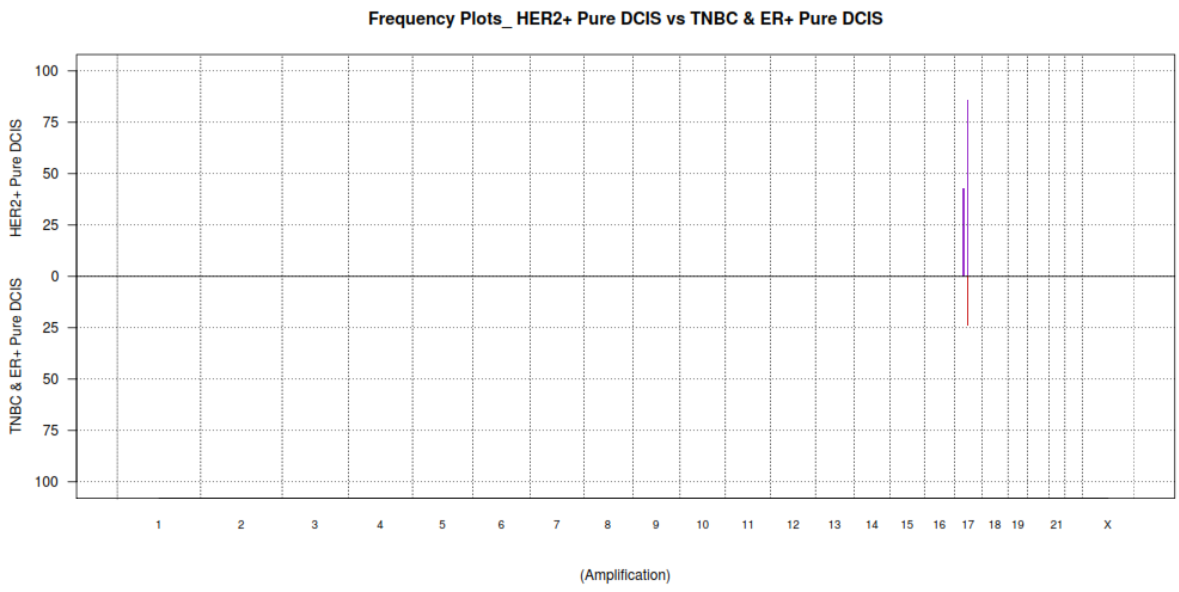
Frequency Plots_ HER2+ Pure DCIS vs TNBC & ER+ Pure DCIS
HER2+ Pure DCIS
TNBC & ER+ Pure DCIS
100
75
50
25
0
25
50
75
100
1
2
3
4
5
6
7
8
9
10
11
12
13
14
15
16
17
18
19
21
X
(Amplification)

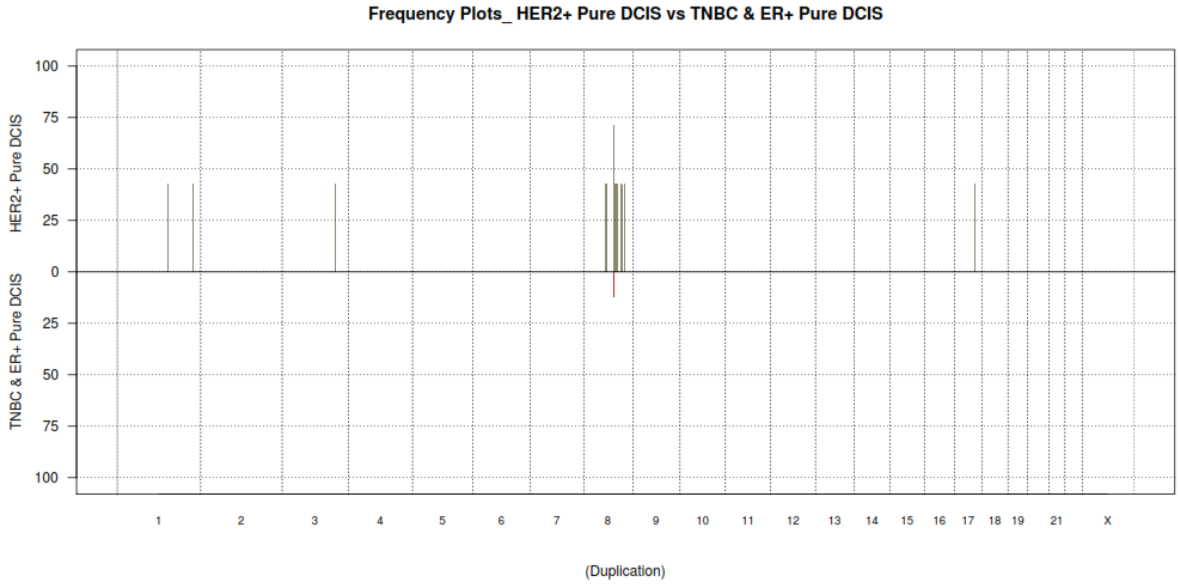
Frequency Plots_ HER2+ Pure DCIS vs TNBC & ER+ Pure DCIS
HER2+ Pure DCIS
TNBC & ER+ Pure DCIS
100
75
50
25
0
25
50
75
100
1
2
3
4
5
6
7
8
9
10
11
12
13
14
15
16
17
18
19
21
X
(Duplication)

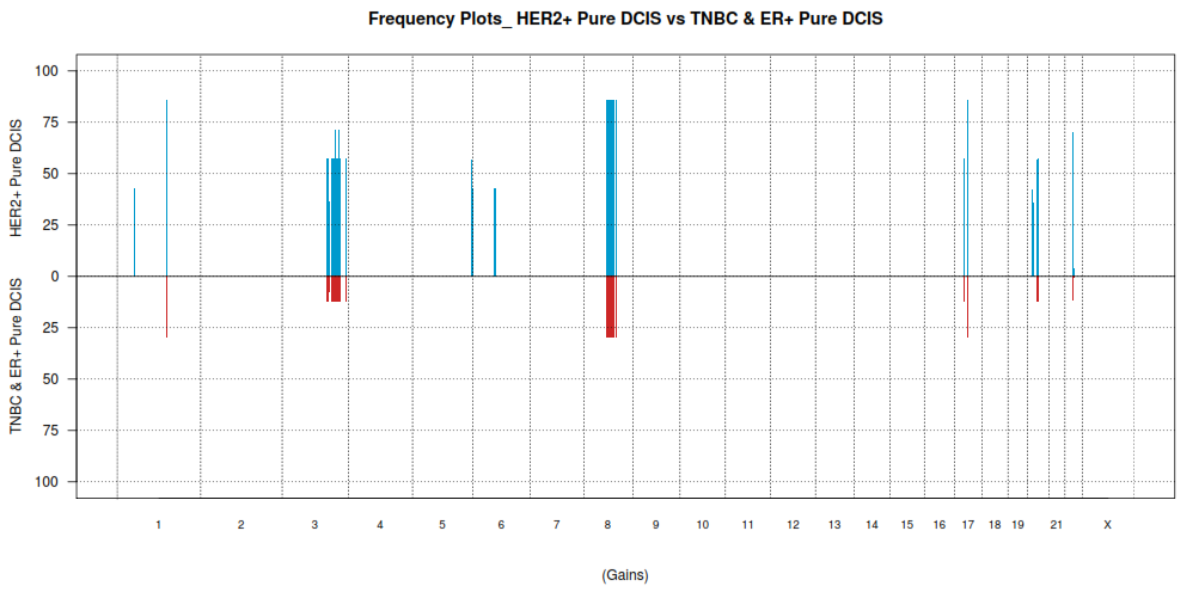
Frequency Plots_ HER2+ Pure DCIS vs TNBC & ER+ Pure DCIS
HER2+ Pure DCIS
TNBC & ER+ Pure DCIS
100
75
50
25
0
25
50
75
100
1
2
3
4
5
6
7
8
9
10
11
12
13
14
15
16
17
18
19
21
X
(Gains)

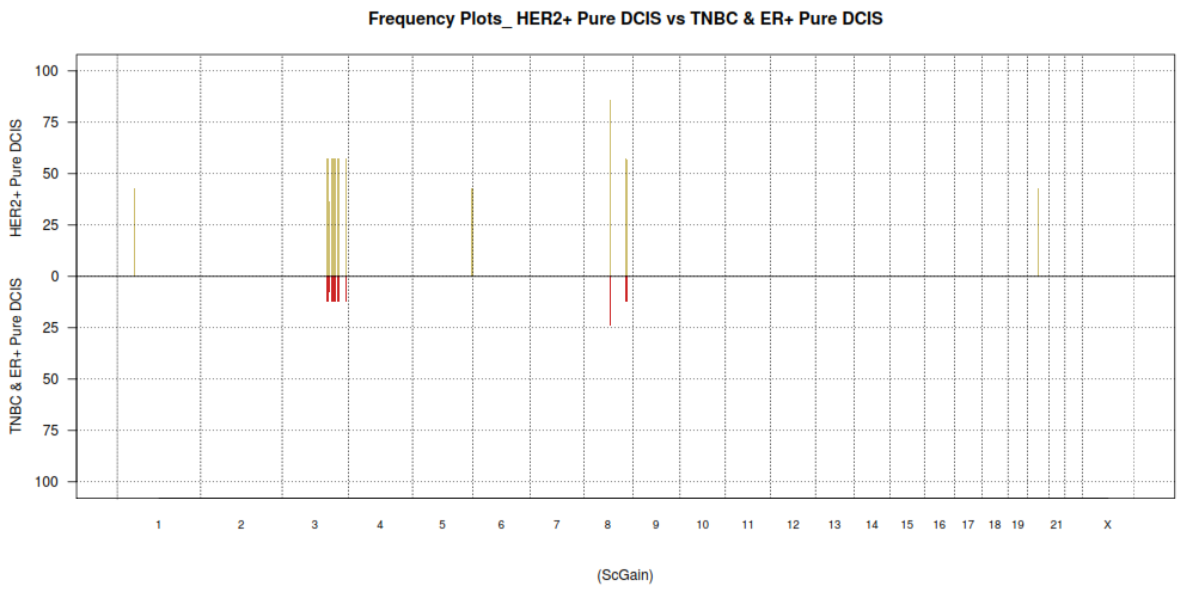
Frequency Plots_ HER2+ Pure DCIS vs TNBC & ER+ Pure DCIS
HER2+ Pure DCIS
TNBC & ER+ Pure DCIS
100
75
50
25
0
25
50
75
100
1
2
3
4
5
6
7
8
9
10
11
12
13
14
15
16
17
18
19
21
X
(ScGain)

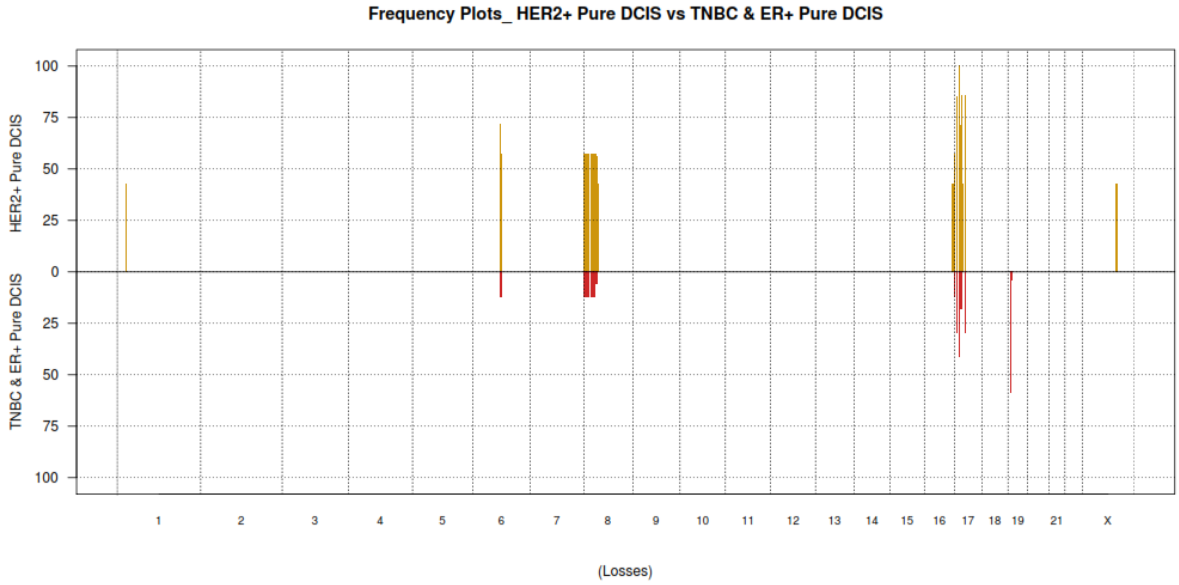
Frequency Plots_ HER2+ Pure DCIS vs TNBC & ER+ Pure DCIS
HER2+ Pure DCIS
TNBC & ER+ Pure DCIS
100
75
50
25
0
25
50
75
100
1
2
3
4
5
6
7
8
9
10
11
12
13
14
15
16
17
18
19
21
X
(Losses)

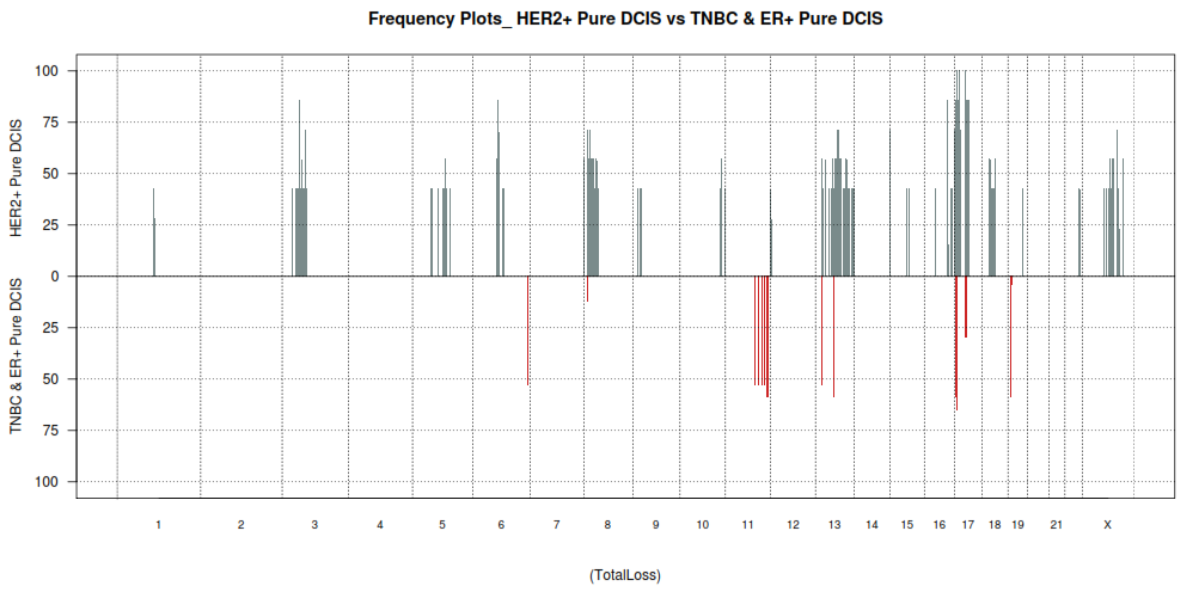
Frequency Plots_ HER2+ Pure DCIS vs TNBC & ER+ Pure DCIS
HER2+ Pure DCIS
TNBC & ER+ Pure DCIS
100
75
50
25
0
25
50
75
100
1
2
3
4
5
6
7
8
9
10
11
12
13
14
15
16
17
18
19
21
X
(TotalLoss)

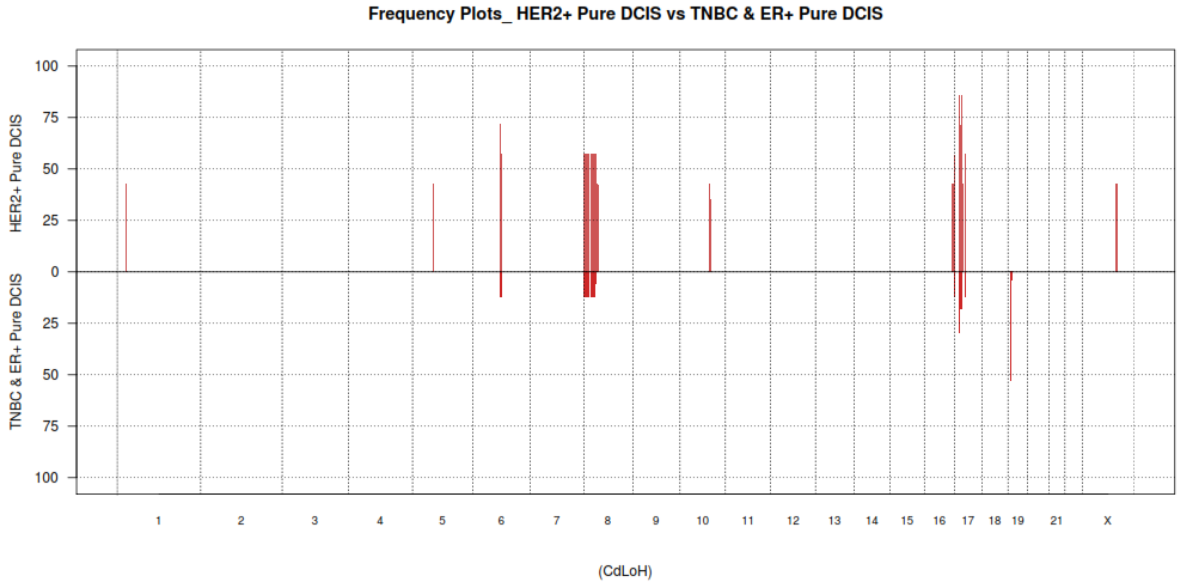
Frequency Plots_ HER2+ Pure DCIS vs TNBC & ER+ Pure DCIS
HER2+ Pure DCIS
TNBC & ER+ Pure DCIS
100
75
50
25
0
25
50
75
100
1
2
3
4
5
6
7
8
9
10
11
12
13
14
15
16
17
18
19
21
X
(CdLoH)

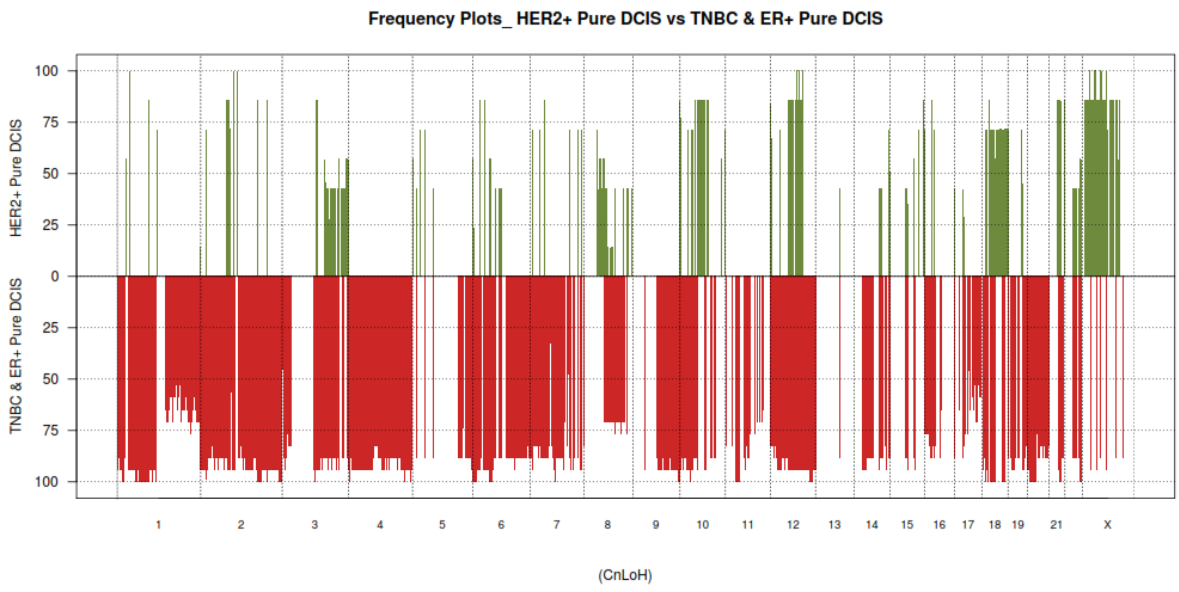

5.8.11.1 Amplification in HER2 Positive DCIS Compared to ER Positive DCIS and Triple Negative DCIS.

There are overlaps between the amplifications found in HER2 positive pure DCIS (n=6/7) and all other pure DCIS (TN and ER n=4/17).

1. p-values < 0.05;
2. A gene list is mapped from 7 regions on chromosome 17;
3. These regions encompass 45 genes altered in HER2 positive DCIS;

Genes:

AC002094.1	AC002094.2	AC002094.3	AC002094.4	AC002094.5	AC015917.1	AC015917.2	AC015917.3	AC061975.1	AC061975.2
AC061975.3	AC061975.4	AC061975.5	AC061975.6	AC079199.1	AC079199.2	AC087491.2	C17orf37	CRKRS	EFCAB5
ERBB2	GRB7	IFT20	IKZF3	NEUROD2	PGAP3	PNMT	POLDIP2	PPP1R1B	PPY2
PY2	RP11-338L22.1	SARM1	SLC13A2	SLC46A1	snoU13	SSH2	STARD3	TCAP	TMEM199
TMEM97	TNFAIP1	U6	VTN	ZPBP2					

PANTHER analysis: 20 mapped ids are found, 25 mapped ids are not found.

5.8.11.2 Duplication of HER2 Positive DCIS Compared to Oestrogen Positive DCIS and Triple Negative DCIS.

There were duplications present in HER2 positive DCIS (n=3/7) not observed in ER and TN pure DCIS (n=0/17).

1. p-values < 0.05;
2. A gene list is mapped from 14 regions found on chromosomes 1, 3, 8, 17;
3. These regions encompass 91 genes altered in HER2 positive DCIS;

Genes:

5S_rRNA AC005746.1 AC005901.1 AC011118.2 AC083928.1 AC092811.1 AC104958.1 AC120042.2 AC120053.1 AP003357.3
ARFGEF1 ARL14 BCAS3 C17orf82 C1orf46 C1orf68 C8orf39 C8orf44 C8orf46 COL14A1 COPS5
CSMD3 CSPP1 CTC-820M8.1 DEPDC6 DNAH14 ENAH FAM92A1 GGH IVL KB-1589B1.1KB-1683C8.1 KPRP LAPTM4B LBR LCE1A LCE1B LCE1C LCE1D LCE1E LCE1F LCE2A
LCE2B LCE2C LCE2D LCE3A LCE3B LCE3C LCE3D LCE3E LCE4A LCE6A
LRRC67 MATN2 MRPL13 MTBP MTDH MYBL1 PDP1 RBM12B RP11-145A3.1
RP11-145A3.2 RP11-145A3.4 RP1-13P20.6 RP11-453N18.1 RP11-496N12.6 RP1-20N18.4
RP1-43O17.1 RP1-43O17.2 RP1-52J10.9 RP3-388N13.1 SMCP SNORA31 SNTB1
SPRR1A SPRR1B SPRR2A SPRR2B SPRR2D SPRR2E SPRR3 SPRR4 SRP9 TBX2
TBX4 TMEM67 TTPA U6 U7 VCPIP1 Y_R

PANTHER analysis: 58 mapped ids are found, 33 mapped ids are not found.

5.8.11.3 Genomic Gains in HER2 Positive DCIS Compared to Oestrogen Positive DCIS and Triple Negative DCIS.

There are genomic gains in HER2 positive pure DCIS (n=4/7) not present in ER and TN pure DCIS (n=0/17).

1. p-values < 0.05;
2. A gene list is mapped from 10 genomic regions found on chromosomes 1, 5, 6, 20;
3. These regions encompass 92 genes altered in HER2 positive pure DCIS;

Genes:

AACSL AC022096.2 AC027317.2 AC027317.2 AC091934.1 AC104115.1 AC104117.1 AC104117.2 AC136940.3 AC145098.1
AC145098.2 AC145098.3 AC146507.1 ADAMTS2 AGXT2L2 AL050329.1 AL589736.1 CNOT6 COL23A1 CTB-129O4.1
CTC-573N18.1 CTD-2301A4.1 CTD-2301A4.3 DBN1 DDX41 DMRTA2 DOK3
EIF4E1B EYS F12 FAF1 FAM193B FGFR4 FGFR4 FKBP1C FLT4 GCNT1P4
GFPT2 GRK6 GRM6 HNRNPAB LGSN LMAN2 MACROD2 MAPK9 MXD3 NSD1

OR2AI1P OR2Y1 PDLIM7 PFN3 PHF3 PRELID1 PRR7 PTP4A1 RAB24 RASGEF1C
RGS14 RP11-1334A24.4 RP11-1334A24.5 RP11-1334A24.6 RP11-164N20.1 RP11-183G22.1
RP11-183G22.2 RP11-183G22.3 RP11-184C23.1 RP11-184C23.3 RP11-184C23.4
RP11-252I14.1 RP11-349P19.1 RP11-442B12.1 RP11-448N11.2 RP11-451H23.1
RP11-451H23.2 RP11-451H23.3 RP11-59D5__B.2 RP11-59D5__B.3 RP3-407E4.2 RP3-
407E4.3 RP3-407E4.4 RP5-1148A21.1 SCGB3A1 SLC34A1 SNCB TSPAN17 U1 U1
U6 ZFP2 ZNF346 ZNF346 ZNF354A ZNF354B ZNF354C ZNF454 ZNF879

PANTHER analysis: 47 mapped ids are found, 45 mapped ids are not found.

There are genomic gains in TN and ER pure DCIS (n=5/17) with associated genomic gains in HER2 positive pure DCIS (n=6/7).

1. p-values < 0.05;
2. A gene list is mapped from 14 genomic regions found on chromosomes 1,8,17.
3. These regions encompass 129 genes altered in TN v DCIS, ER pure DCIS and HER2 positive pure DCIS.

Genes:

5S_rRNA AC012533.1 AC016057.1 AC016240.1 AC022598.1 AC022861.1 AC022861.2 AC022861.3 AC022861.4 AC022861.5
AC022861.6 AC022861.7 AC023644.1 AC024367.1 AC027006.1 AC037450.1 AC083928.1 AC087491.2 AC091175.1 AC099805.1
AC103816.1 AC104012.1 AC104212.2 AC110998.1 AC132219.1 AC132219.2 AF121898.1 AL592492.2 ARFGEF1 C8orf44
C8orf45 C8orf46 CHMP4C CNBD1 COPS5 CPA6 CSPP1 DCAF4L2 E2F5 ERBB2
EYA1 FABP12 FABP4 FABP5 FABP9 FAM164A HEY1 IKZF3 IL7 IMPA1
JPH1 LRRC67 LRRCC1 LY96 MMP16 MRPS28 MSC MYBL1 NBPF10 NBPF14
NBPF15 NBPF16 NEUROD2 PAG1 PGAP3 PKIA PMP2 PNMT PPIAL4A PPP1R1B
PTTG3P RALYL RP11-289I10.1 RP11-289I10.2 RP11-34M16.1 RP11-34M16.2
RP11-367C12.1 RP11-367E12.1 RP11-453N18.1 RP11-48B3.1 RP11-495P10.1
RP11-495P10.2 RP11-508K19.1 RP11-656G20.1 RP11-666A1.1 RP11-666A1.2
RP11-666A1.3 RP11-666A1.4 RP11-666A1.5 RP11-69I13.1 RP11-6I2.1 RP11-763B22.2
RP11-763B22.3 RP11-763B22.4 RP11-7F18.1 RP11-89F3.2 RP11-89F3.3 RP11-91G11.1 RP11-941H19.1
RP11-941H19.2 RP11-98H4.1 RP6-74O6.1 SGK3 SLC10A5 SNHG6 SNORA20 SNORD87
snoU13 SNX16 STARD3 STMN2 TCAP TCEB1 TMEM70 TPD52 TRPA1 U1 U11
U2 U6 U7 U8 VCPIP1 WWP1 Y_RNA ZBTB10 ZFAND1 ZFHX4
ZNF704

PANTHER analysis: 56 mapped ids are found, 73 mapped ids are not found.

5.8.11.4 Genomic Sc Gains in HER2 Positive DCIS Compared to Oestrogen Positive DCIS and Triple Negative DCIS.

There were Sc gains present in HER2 positive pure DCIS (n=6/7) and ER and TN pure DCIS (n=4/17).

1. p-values < 0.05;
2. A gene list is mapped from 10 regions found on chromosomes 1, 3, 5, 8, 20;
3. These regions encompass 188 genes altered in HER2 positive pure DCIS and ER and TN pure DCIS;

Genes:

5S_rRNA 7SK A4GNT AACSL AADAC AADACL2 AC022096.2 AC026320.2 AC027317.2 AC087667.1
AC091934.1 AC092965.1 AC104117.1 AC104117.2 AC104629.1 AC104629.2 AC104629.3 AC104629.4 ADAMTS2 ARMC8
C3orf36 C3orf55 C3orf72 CCDC50 CCRL1 CDV3 CEP63 CEP70 CLDN18 DBR1 DEFB121
DEFB122 DEFB123 DEFB124 DHX36 DMRTA2 DNAJC13 DZIP1L EEF1A1P25 EIF4E1B EPHB1
ESYT3 FAF1 FAIM FGF12 FGFR4 FOXL2 GAPDHP39 GFM1 GPR149 GPR79 GRM6
HM13 IL20RB IQCJ KY LXN MFSD1 MLF1 MRAS MSL2 NCK1
NCRNA00028 NPHP3 OSTN OTTHUMG00000159780 PCCB PDCD10 PHC3 PIK3CB PPP2R3A
PRKCI PYDC2 RAB6B RARRES1 REM1 RP11-102M11.1 RP11-113A11.1 RP11-117F22.1
RP11-12N13.1 RP11-12N13.2 RP11-12N13.3 RP11-12N13.4 RP11-12N13.5 RP11-12N13.6
RP11-167H9.1 RP11-183G22.1 RP11-183G22.2 RP11-183G22.3 RP11-192K2.3
RP11-197K6.1 RP11-202A13.1 RP11-202A13.2 RP11-206M11.4 RP11-206M11.7 RP11-217E22.1 RP11-217E22.2 RP11-217E22.5 RP11-237P21.1 RP11-23D24.1 RP11-23D24.2
RP11-278L15.1 RP11-278L15.2 RP11-290K4.1 RP11-290K4.2 RP11-293N1.1
RP11-2A4.1 RP11-2A4.3 RP11-2G17.1 RP11-305O4.1 RP11-305O4.2 RP11-333H9.6 RP11-379F4.1
RP11-379F4.4 RP11-404G16.1 RP11-404G16.2 RP11-413G22.2 RP11-440K22.1
RP11-450H5.1 RP11-452B4.1 RP11-454C18.1 RP11-454C18.2 RP11-463H24.1 RP11-463H24.4
RP11-468F18.2 RP11-538P18.1 RP11-538P18.2 RP11-548O1.1 RP11-548O1.3
RP11-575C1.1 RP11-576M8.2 RP11-598P12.1 RP11-642L11.1 RP11-64D22.1
RP11-64D22.2 RP11-64D22.5 RP11-655G22.1 RP11-655G22.2 RP11-656G9.3 RP11-657O9.1
RP11-65E22.3 RP11-731C17.1 RP11-785G3.1 RP11-79L9.2 RP11-79M21.2 RP11-79M21.3
RP11-85F14.1 RP11-85F14.5 RP11-85F14.6 RP11-91K8.2 RP13-81O8.1 RP3-324O17.4 RSRC1 RYK SERPINI1 SERPINI2 SHOX2 SLCO2A1 SNCB SNORA33 snoU13 SOX14
SRPRB STAG1 SUCNR1 TF TM4SF1 TM4SF18 TMEM22 TOPBP1 TSPAN17 TXNDC6 U1
U6 U7 U8 UBA5 UTS2D VEPH1 WDR49 Y_RNA ZBBX ZFP2 ZNF346
ZNF354B ZNF354C ZNF454 ZNF879

PANTHER analysis: 82 mapped ids are found, 106 mapped ids are not found.

5.8.11.5 Losses in HER2 Positive DCIS Compared to Oestrogen Positive DCIS and Triple Negative DCIS.

There were losses present in HER2 positive pure DCIS (n=3/7) not observed in ER and TN positive pure DCIS (n=0/17).

1. p-values < 0.05;
2. A gene list is mapped from 9 regions found on chromosomes 1, 8, 15, 16, X;
3. These regions encompass 87 genes altered in HER2 positive pure DCIS;

Genes:

AC009113.1	AC009113.2	AC009113.3	AC010531.1	AC010531.2	AC027702.2	AC092139.1	AC092139.2	AC092384.1	AC092384.2
AC099524.1	AC116552.1	AC136285.1	AC138028.1	AC138028.2	AC138028.3	ACSF3	AGPAT6	AHDC1	AL049610.1
ANK1	AP3M2	APRT	C16orf81	C16orf85	CBFA2T3	CD164L2	CDH15	CDT1	CTU2
CYBA	FAM38A	FBXO31	FCN3	GALNS	GAN	GINS4GLRA4	GOLGA7	GPR3	hsa-mir-486
IKBKB	IL17C	LL0XNC01-250H12.2		LL0XNC01-250H12.3		MAP1LC3B	MAP3K6	MORF4L2	MVD MYST3
NGFRAP1	NKX6-3	PABPN1L	PLAT	PLCG2	PLP1	RAB40A	RAB9B	RNF166	RP11-173M1.1
RP11-178L8.1		RP1-144C9.2		RP11-589C21.1		RP1-159A19.4		RP4-752I6.1	RP5-1055C14.4
RP5 1055C14.6		RP5-1055C14.7		RP5-1142A6.2		SLC20A2	SNAI3	SNORD112	snoU13
snoU13	SYTL1	TCEAL1	TCEAL3	TCEAL4	TMEM31	TRAPPC2L	WASF2	Y_RNA	Z73964.1
ZC3H18	ZCCHC14	ZFPM1	ZNF469	ZNF778					

PANTHER analysis: 50 mapped ids are found, 37 mapped ids are not found.

There were losses present in ER and TN pure DCIS (n=10/17) not observed in any HER2 positive pure DCIS (n=0/24).

1. P-values < 0.05;
2. A gene list is mapped from 3 genomic regions from chromosome 19;
3. These regions encompass 3 genes altered in non HER2 DCIS;

Genes:

MUC16	AC008734.1	AC008734.2

PANTHER analysis: 1 mapped ID found, 2 mapped ids are not found.

5.8.11.6 Total Loss in HER2 Positive DCIS Compared to Oestrogen Positive DCIS and Triple Negative DCIS.

There were total losses present in HER2 positive pure DCIS (n= 7/7) also present in some ER and TN pure DCIS (n=4 /17).

1. p-values < 0.05;
2. A gene list is mapped from 28 regions found on chromosomes 3, 6, 16, 17;
3. These regions encompass 293 genes altered in HER2 positive pure DCIS and ER and TN pure;

Genes:

5S_rRNA	7SK	AARS	AC000003.1	AC003664.1	AC003958.1	AC003958.2	AC003958.5	AC003958.6	AC004223.2
AC004675.1	AC005224.2	AC005277.1	AC005304.1	AC005304.2	AC005304.3	AC005358.1	AC005358.3	AC005410.2	AC006070.11
AC006070.12		AC006070.13		AC006070.7	AC009060.1	AC009060.2	AC009060.3	AC011193.1	AC012184.1
AC015842.1	AC015849.1	AC015849.4	AC019349.4	AC024610.1	AC025335.1	AC025518.1	AC026468.1	AC026954.6	AC027045.1
AC069363.1	AC087742.1	AC091178.1	AC100793.1	AC100808.10		AC100808.7	AC104581.1	AC107993.1	AC113189.5
AC123769.1	AC126327.1	AC126327.4	AC129492.6	AC131056.1	AC135178.7	ACADVL	ACAP1	ACCN1	ALOX12B
ALOX15B	ALOXE3	AMAC1L3	ANKFY1	ARHGEF15	ARL5C	ATP6V0A1	AURKB	BECN1	C17orf102
C17orf44	C17orf59	C17orf61	C17orf68	C17orf74	C17orf81	C17orf96	C17orf98	CACNB1	CCDC56
CCL1	CCL11	CCL13	CCL14	CCL15	CCL16	CCL18	CCL2	CCL23	CCL3
CCL3L1	CCL4	CCL4L1	CCL4L2	CCL7	CCL8	CCR10	CCT6B	CD68	CDRT15
CDRT15P	CHD3	CHRNB1	CISD3	CLDN7	CLEC18A	CLEC18C	CNTD1	CNTNAP1	CNTROB
COASY	COG4	COX10	CTB-75G16.1		CTD-2303K11.1		CTD-3193K9.1		CWC25
CYB5D1	CYB5D2	DDX19A	DDX19B	DHRS11	DHRS7C	DLG4	DNAH2	DNAH9	DULLARD
DUSP7	DVL2	EFNB3	EIF4A1	EIF5A	ELAC2	EXOSC6	EZH1	FAM134C	FBXO47
FGF11	FNDC8	FUK	FXR2	GABARAP	GAS7	GGNBP2	GPS2	GUCY2D	HES7
HS3ST3A1	hsa-mir-140	hsa-mir-1972	hsa-mir-324	hsa-mir-548h-3		hsa-mir-744	HSD17B1	HSD17B1P1	KCNAB3
KCTD11	KDM6B	KRBA2	KRT31	KRT33A	KRT33B	KRT34	KRT37	KRT38	KRTAP16-1
KRTAP17-1	KRTAP2-1	KRTAP2-4	KRTAP29-1	KRTAP4-1	KRTAP4-12	KRTAP4-14	KRTAP4-2	KRTAP4-3	KRTAP4-4
KRTAP4-5	KRTAP4-6	KRTAP4-7	KRTAP4-8	KRTAP4-9	KRTAP9-1	KRTAP9-2	KRTAP9-3	KRTAP9-4	KRTAP9-6
KRTAP9-7	KRTAP9-8	KRTAP9-9	LASP1	LIG3	LSMD1	LYZL6	MAP2K4	MLLT6	MLX
MPDU1	MRM1	MYH10	MYO19	MYOCD	NAGLU	NDEL1	NEURL4	NLE1	NLGN2
ODF4	PCGF2	PDXDC2	PER1	PFAS	PHF23	PIGW	PIP5K2B	PLEKHH3	PLSCR3
PLXDC1	POLR2A	PSMB3	PSMC3IP	PSME3	PTRF	RAD51L3	RAMP2	RANGRF	RDM1
RFFL	RNF222	RP11-106J23.1		RP11-1096G20.1		RP11-462C21.1		RP11-554D15.1	
RP11-554D15.3		RP11-554D15.4		RP11-565F19.1		RP11-713H12.1		RP5-837J1.1	RPL19
RPL23	RPL26	RPS27P26	SCARNA21	SENP3	SLC25A35	SLC2A4	SNORA21	SNORA48	SNORA67
SNORA69	SNORA74	snoU13	snoU6-77	SOX15	SPEM1	ST3GAL2	STAC2	STAT3	STX8
TBC1D3B	TBC1D3C	TBC1D3G	TBC1D3H	TMEM102	TMEM107	TMEM132E	TMEM88	TMEM95	TNFSF12
TNFSF12-TNFSF13		TNFSF13	TNK1	TP53	TRAPPC1	TUBG1	TUBG2	U11	U6
U7									
U8	UBE2G1	USP43	VAMP2	Vault	VPS25	WDR16	WDR51A	WNK4	WRAP53
WWP2	Y_RNA	YBX2	ZBTB4	ZNF18	ZNF830	ZNHIT3	ZZEF1		

PANTHER analysis: 192 mapped ids are found, 101 mapped ids are not found.

There were total losses present in more than half of the ER pure DCIS and TN pure DCIS (n=11/17) not present in any of the HER2 positive pure DCIS cases (n=0/7)

1. p-values < 0.05;
2. A gene list is mapped from 42 genomic regions found on chromosomes 6,11,13,17, 19.
3. These regions encompass 67 genes altered in ER pure DCIS and TN pure DCIS.

Genes:

5S_rRNA AC008734.1 AC008734.2 AC087498.1 AC090282.1 AC097370.1 ACRV1 ACTL9 ADAMTS10 AL136359.1
AL137001.1 AP001482.1 AP003027.2 ASPA C11orf87 CEP164 CHEK1 CTD-2557P19.1 DDX25
GRAMD1B GRM5 hsa-mir-1253 HYLS1 MUC16 OLFM4 OR10D1P OR10D3P OR1A1 OR1A2
OR1D2 OR1D5 OR1E1 OR1E2 OR1G1 OR2Z1 OR3A1 OR3A2 OR3A3 OR3A4 OR6X1
OR8D1 OR8D2 OR8F1P OR8G2P OR8G5 PARK2 PATE1 PATE2 PATE3 PATE4 PUS3
RAP1GAP2 RP11-24H2.1 RP11-24H2.2 RP11-301J16.2 RP11-301J16.3 RP11-301J16.5
RP11-301J16.7 RP11-442J17.4 SCN3B SPATA22 TRPV3 U1 U6 VWA5A WSCD1
ZNF202

Genes PANTHER analysis: 39 mapped ids are found, 28 mapped ids are not found.

5.8.11.7 CdLOH in HER2 Positive DCIS Compared to Oestrogen Positive DCIS and Triple Negative DCIS.

There is CdLOH present in HER2 positive pure DCIS (n= 4/7) not observed in any of the ER and TN pure DCIS (n= 0/17).

1. p-values < 0.05;
2. A gene list is mapped from 13 regions found on chromosomes 1, 5, 8, 10, 16, 17, X;
3. These regions encompass 83 genes altered in HER2 positive pure DCIS;

Genes:

AC009113.1 AC009113.2 AC009113.3 AC010531.1 AC010531.2 AC092139.1 AC092139.2 AC092384.1 AC092384.2 AC099524.1
AC116552.1 AC136285.1 AC138028.1 AC138028.2 AC138028.3 ACSF3 AGPAT6 AHDC1 AL049610.1 ANK1
APRT ATAD1 C16orf81 C16orf85 CBFA2T3 CD164L2 CDH15 CDT1 CFLP1 CTU2
CYBA FAM38A FBXO31 FCN3 GALNS GAN GINS4 GLRA4 GOLGA7 GPR3 hsa-mir-486
IKBKB IL17C LL0XNC01-250H12.2 LL0XNC01-250H12.3 MAP1LC3B MAP3K6 MORF4L2 MVD NGFRAP1
NKX6-3 PABPN1L PAPSS2 PLAT PLCG2 PLP1 RAB40A RAB9B RNF166 RP11-173M1.1
RP11-178L8.1 RP1-144C9.2 RP1-159A19.4 RP4-752I6.1 RP5-1055C14.4 RP5-1055C14.6

RP5-1055C14.7 RP5-1142A6.2 SLC20A2 SNAI3 snoU13 SYTL1 TCEAL1 TCEAL3 TCEAL4 TMEM31 TRAPPC2L WASF2 Z73964.1 ZC3H18 ZCCHC14 ZFPM1 ZNF469

PANTHER analysis: 50 mapped ids are found, 33 mapped ids are not found.

There is CdLOH present in ER pure DCIS (n= 9/17) not observed in HER2 Positive pure DCIS (n=0/7)

1. p-values < 0.05;
2. A gene list is mapped from 1 genomic regions found on chromosomes 19;
3. These regions encompass 1 gene altered in ER pure DCIS;

Gene: Muc16

PANTHER analysis: 1 mapped id is found.

5.8.11.8 CnLOH in HER2 Positive DCIS Compared to Oestrogen Positive DCIS and Triple Negative DCIS.

There is CnLOH present in HER2 positive pure DCIS (n=7/7) not observed in ER and TN pure DCIS (n=0/17)

1. p-values < 0.05;
2. A gene list is mapped from 14 regions found on chromosomes 1, 2, 12, X;
3. These regions encompass 104 genes altered in HER2 positive pure DCIS;
4. Genes: AC117494.15S_rRNA AC004074.1 AC004074.3 AC004074.4 AC004673.1 AC092198.1 AC117517.1 AF241726.2 AF241726.4 AF241726.6 AL031115.1 AL121578.2 AL161779.1 AL591845.1 AL627402.1 ATP6AP2 BCOR C1orf113 C2orf55 CASK CTD-2324A24.1 CXorf38 CYBB DDX3X DDX53 DYNLT3 FAM176B FAM3C2 FTLP16 GS1-433O24.1 GS1-590J15.1 hsa-let-7f-2 hsa-mir-492 hsa-mir-98 HSD17B10 HUWE1 IQSEC2 LSM10 MED14 MID1IP1 MKRNP5 NAP1L2 NAV3 NYX OSCP1 OTC PTCHD1 PTCHD1 RIBC1 RP11-126D17.1 RP11-126D17.4 RP11-157D23.1 RP11-157D23.2 RP11-169L17.2 RP11-169L17.3 RP11-169L17.5 RP11-185O17.3 RP11-204C16.4 RP11-265P11.1 RP11-265P11.2 RP11-272G22.1 RP11-272G22.2 RP11-272G22.3 RP11-320G24.1 RP11-40F8.2 RP11-469E19.1 RP11-478I12.1 RP11-494I9.1 RP11-494I9.2 RP11-540L11.2 RP11-654E17.2 RP1-169I5.4 RP11-77G22.2 RP11-77G22.3 RP13-126P21.1 RP13-13A3.1 RP13-444K19.1 RP3-339A18.3 RP3-339A18.6 RP4-646N3.1 RP4-646N3.3 RP5-1172N10.2 RP5-972B16.2 RP5-972B16.2 RP6-186E3.1 RP6-29D12.2 RP6-29D12.3 RP6-29D12.4 RPGR SLC6A15 SMC1A SNORA31 SNORA63 snoU13 snoU13 STK40 SYT1 THRAP3 TSPAN7 U4 U6 U6 U6 U7 USP9X Vault Y_RNA Y_RNA ZXDB

PANTHER analysis: 30 mapped ids are found, 74 mapped ids are not found.

There is CnLOH present in ER and TN pure DCIS (n=017/17) not observed in HER2 positive pure DCIS (n=0/7).

1. p-values < 0.05;
2. A gene list is mapped from 84 genomic regions found on chromosomes 1, 2, 3, 4, 6, 7, 9, 10, 11, 12, 18, 20, 21;
3. These regions encompass 630 genes altered in ER pure DCIS and TN pure DCIS;

Genes:

7SK	AACS	ABCB11	ABHD11	ABTB2	AC007556.3	AC009336.1	AC009336.21		AC009336.23	
	AC009336.24		AC009475.2	AC010145.2	AC010145.3	AC010148.1	AC011998.2	AC011998.4	AC011998.5	AC016739.1
	AC016739.2	AC016757.1	AC017048.1	AC017048.2	AC017048.3	AC017048.4	AC026366.1	AC026366.2	AC055713.1	AC064874.1
	AC068706.1	AC068799.1	AC069209.1	AC069214.1	AC069234.1	AC073069.2	AC073846.1	AC073846.2	AC073846.3	AC078875.1
	AC090670.1	AC091609.1	AC091611.1	AC092162.1	AC092576.1	AC095030.1	AC096536.1	AC097713.2	AC097713.3	AC097713.4
	AC099680.1	AC104169.1	AC104387.1	AC104837.1	AC114486.1	AC114814.2	AC114814.3	AC114814.4	AC117503.2	AC122688.1
	AC125603.1	AC126309.2	AC127164.1	AC131263.2	AC132216.1	ACADS	ACOT11	ACTL8	ADAMTSL2	ADH5P2
	AFG3L2	AGAP1	AK3L1	AK5	AL031427.1	AL033381.1	AL033381.2	AL034344.1	AL035400.1	AL035706.1
	AL049710.1	AL049710.2	AL049710.4	AL049745.2	AL109843.1	AL136324.1	AL137855.1	AL138781.1	AL139244.1	AL157773.1
	AL158068.1	AL158167.1	AL160060.2	AL161452.1	AL161740.1	AL161915.1	AL162579.1	AL353771.1	AL353898.1	AL353898.2
	AL353898.3	AL353898.4	AL354946.1	AL355574.1	AL357054.1	AL358512.1	AL390994.1	AL391728.1	AL512329.1	AL512329.2
	AL512329.3	ALDH4A1	ANAPC5	ANKRD13C	ANXA10	AP000302.58		AP005264.2	ARHGEF10L	ARHGEF19
	ARL4C	ATP5GP1	ATP6V0A2	BAG2	BBS5	BCAS2	BEND6	BMP6	BRDT	BRI3BP
	BSND	BTBD8	C11orf74	C12orf43	C12orf49	C1orf134	C1orf141	C1orf168	C1orf175	C1orf177
	C1orf191	C1orf224	C1orf64	C1orf83	C1orf89	C2orf19	C6orf142	C6orf195	C8A	C8B
	C9orf116	C9orf62	C9orf69	CABP1	CAGE1	CAMKK2	CAMSAP1	CAPN10	CAPRIN1	CCDC73
	CCDC92	CDC7	CDCP2	CIDEA	CLCNKA	CLCNKB	CLDN3	CLDN4	COL5A1	COX6B1P7
	CR392000.1	CR392000.2	CRISP1	CRYZ	CST1	CST2	CST4	CST5	CSTP1	CSTP2	CTH
	CYB5RL	DAB1	DBH	DCLRE1B	DDI2	DDX55	DDX60	DEFB110	DEFB112	DEFB113
	DEFB114	DEFB133	DENND2C	DEPDC1	DEPDC7	DHCR24	DHRS9	DHX37	DIO1	DIRAS3
	DNAH10	DNAJC30	DOK7	DSP	DST	EEF1E1	EIF2B1	EIF2S2P5	EIF3M	ELTD1
	ENTPD8	EPHX4	ESPNL	EVX2	EXD3	EXOC2	FAM101A	FAM131C	FAM132B	FAM151A
	FAM163B	FAM83B	FASTKD1	FBLIM1	FBXO21	FBXO3	FBXO42	FBXW8	FCN1	FCN2
	FOXC1	FOXF2	FOXQ1	FTLP17	G6PC2	GDI2P2	GFRAL	GLIS1	GLT6D1	GMDS
	GOT2L1	GPR177	GPR35	GREB1L	GTF2H3	HCRTR2	HECW2	HHLA3	HIPK1	HNF1A
	HOXD1	HOXD10	HOXD11	HOXD12	HOXD13	HOXD3	HOXD4	HOXD8	HOXD9	HRK	hsa-mir-10b
	hsa-mir-1262	hsa-mir-1290	hsa-mir-604	hsa-mir-938	HSP90B3P	HSPB11	HSPB7	HUS1B	IFFO2	IFI44
	IFI44L	IFNGR2	IGSF21	IL12RB2	IL17A	IL23R	ILKAP	IRF4	KBTBD10	KCNT1
	KDM2B	KIAA0649	KIAA1586	KLHL30	KLHL31	KSR2	LASS6	LCN1	LCN9	LDLRAD1
	LHX3	LIN28AP3	LMO2	LPAR3	LPCAT2BP	LPHN2	LRP2	LRPAP1	LRRC1	LRRC40
	LRRC42	LRRC7	LYZL1	MACROD2	MAP1LC3B2	MCOLN2	MCOLN3	MIER1	MLEC	MRPL37

MRPS11P1 MRPS2 MTL1 MTX2 MUTED MYCN MYCNOS MYLK4 NACC2 NAT10
NCOR2 NCRNA00118 NCRNA00159 NCRNA00173 NEGR1 NELF NOS1
NOSTRIN NOXA1 NRARP OASL OBP2A OFCC1 OLFM1 OMA1 ORAI1 OSBPL6
P2RX4 P2RX7 PADI2 PAEP PARS2 PAX7 PCSK9 PDE11A PEBP1 PGAM3P
PGK2 PIGK PIN1L PIP5K1P1 PKHD1 PLEKHM2 PNPLA7 PPAP2B PRIM2 PRKAA2
PRPF31 PRRG4 PTGFR QSER1 QSOX2 RAB23 RAMP1 RAPGEF4 RBM45 RFC5
RILPL1 RIOK1 RNF34 RNFT2 RP11-101C11.1 RP11-109I2.3 RP11-124G5.1
RP11-124I4.2 RP11-129K24.3 RP11-129K24.4 RP11-12C17.2 RP11-139O18.1
RP11-145H9.3 RP11-157J24.1 RP11-159J16.1 RP11-169K16.4 RP11-169K16.6
RP11-169K16.7 RP11-169K16.8 RP11-169K16.9 RP11-175G14.1 RP11-17E13.3
RP11-180O5.2 RP11-181B18.1 RP11-192N10.2 RP11-203B9.4 RP11-203H2.1
RP11-203H2.2 RP11-213P13.1 RP11-218C14.5 RP11-240D10.2 RP11-240D10.4
RP11-240G22.1 RP11-243M12.1 RP11-263F14.3 RP11-288G3.2 RP11-288G3.3
RP11-288G3.4 RP11-288I21.1 RP11-292O17.1 RP11-2B19.1 RP11-310I9.1
RP11-320E2.1 RP11-324K6.1 RP11-335E14.1 RP11-338K17.1 RP11-339A11.1
RP11-343L14.2 RP11-363H12.1 RP11-375A5.1 RP11-377K22.2 RP11-377K22.3
RP11-378I13.1 RP11-380J14.1 RP11-380L11.1 RP11-393N21.1 RP11-397G17.1
RP11-399H11.2 RP11-399H11.3 RP11-407P2.1 RP11-411K7.1 RP11-411K7.2
RP11-411K7.4 RP11-411K7.5 RP11-426A6.5 RP11-426A6.7 RP11-426A6.8
RP11-426A6.9 RP11-42O15.2 RP11-432J22.2 RP11-447M12.2 RP11-473A10.2
RP11-475O6.1 RP11-478C1.6 RP11-478C1.7 RP11-478C1.8 RP11-47K11.2
RP11-47K11.3 RP11-518D3.1 RP11-518D3.3 RP11-518D3.4 RP11-524H19.1
RP11-524H19.2 RP11-524K22.1 RP11-529E10.8 RP11-532F6.2 RP11-534G20.3
RP11-548C21.1 RP11-549I9.1 RP11-550H2.1 RP11-550H2.2 RP11-555H7.2
RP11-5P18.1 RP11-5P18.10 RP11-5P18.2 RP11-5P18.3 RP11-5P18.5
RP11-614L17.1 RP11-622P13.2 RP1-167A19.5 RP11-67L3.2 RP11-67L3.4 RP11-67L3.5 RP11-67L3.6
RP11-69L16.4 RP11-69L16.5 RP11-69L16.6 RP11-719J20.1 RP11-724O16.1
RP11-779P15.1 RP11-779P15.2 RP11-79N23.1 RP1-181J22.1 RP11-82L20.1
RP11-91I11.1 RP11-98L5.2 RP11-98L5.4 RP11-98L5.5 RP1-20B11.2 RP1-28O17.1 RP1-303A1.1
RP13-476E20.1 RP1-71H19.2 RP3-334F4.1 RP3-334F4.2 RP3-335N17.2 RP3-336K20__B.2 RP3-368B9.1 RP3-380B4.1 RP3-417L20.3 RP3-417L20.4 RP3-445O10.1 RP3-510B21.1
RP4-552O12.2 RP4-591B8.2 RP4-609E1.2 RP4-609E1.3 RP4-621B10.3 RP4-633H17.2 RP4-641G12.3 RP4-641G12.4 RP4-654H19.2 RP4-660H19.1 RP4-677H15.2
RP4-677H15.4 RP4-694A7.2 RP4-694A7.3 RP4-694A7.4 RP4-705F19.1 RP4-705F19.2 RP4-706A16.2 RP4-706A16.3 RP4-710M16.2 RP4-726F1.1 RP4-733M16.2 RP4-734C18.1 RP4-753D5.3 RP4-753D5.4 RP4-758J24.4 RP4-763G1.1 RP4-763G1.2
RP5-1033K19.2 RP5-1073O3.7 RP5-1077H22.1 RP5-1103B4.3 RP5-1177M21.1 RP5-827O9.1 RP5-831K15.1 RP5-836J3.1 RP5-837I24.1 RP5-837I24.2 RP5-837I24.3 RP5-837I24.4 RP5-837I24.5 RP5-837I24.6 RP5-866L20.1 RP5-866L20.2 RP5-866L20.3
RP5-997D24.3 RP5-997D24.5 RP6-102O10.1 RP6-239D12.1 RPE65 RPS11P1
RPS17P5 RPS5L RSC1A1 SARDH SCARB1 SCLY SERBP1 SFRS11 SH3BP4 SLC25A34
SLC35D1 SNORA31 SNORA58 SNORA70 SNORA9 SNORD112 SNORD115 snoU13 SNRNP48 SOHLH1
SORBS2 SPC25 SPEN SSBP3 SSR1 SSX2IP ST6GALNAC3 ST6GALNAC5
STX1A SUDS3 SVIL TAOK3 TAS1R2 TCEB1P18 TCP11L1 TCTN2 TESC TFAP2B
TFAP2D TGFBR3 TINAG TMED2 TMEM48 TMEM50B TMEM59 TMEM61 TMEM82 TRIM33
TTC22 TTC4 TTLL7 TUBB6 TXNDC5 TYW3 U4atac U5 U6 U6atac U7
UBAC1 UBC UBE2F UNC119B USP24 VPS37D VSIG10 WBSCR22 WBSCR26 WDR63
WDR78 WSB2 XXyac-YX60D10.1 Y_RNA YIPF1 ZBTB17 ZFYVE28 ZNF326 ZNF385B
ZNF451 ZNF664

PANTHER analysis: 292 mapped ids are found, 338 mapped ids are not found;

5.9 Summary and Discussion of Genomic Differences between Pure DCIS and DCIS Associated with Invasive Breast Disease

This section addresses point 2 of the study aims (page 67): “To undertake an analysis of archival DCIS samples to identify genomic variation, abnormalities and changes between different pure DCIS lesions and DCIS lesions associated with invasion” and refers to pure ER positive DCIS compared to ER positive DCIS associated with invasive tumour (5.8.4) and pure TN DCIS compared to TN DCIS associated with invasive tumour (5.8.8)

Comparisons of copy number aberrations were used to produce charts highlighting molecular functions, biological processes and protein classes were generated. Examples are given within this chapter; however the majority of charts are saved to the accompanying disc.

In this initial analysis of the genomic data, only regions showing complete differences are examined. Caution should be taken in this series when looking at CnLOH in the samples analysed here due to the lack on corresponding normal tissues. Samples were normalised against a standard via Affymetrix, but not against associated normal tissues from the same sample.

5.9.1 Genomic Differences found in Oestrogen Receptor Positive Pure DCIS Versus Oestrogen Receptor Positive DCIS Associated with Invasive Breast Disease

(See section 5.8.4)

The frequency plots for ER pure DCIS and ER positive DCIS associated with invasion show a high degree of heterogeneity with ER pure DICS having some homologous regions but mainly distinct and separate CNAs compared to ER positive DCIS associated with invasive breast disease. There are no amplifications present in ER positive pure DCIS whereas ER positive DCIS associated with invasive breast disease shows amplification found on chromosomes 6 and 8. CdLOH are varied, with ER pure DCIS showing loss of heterozygosity found on chromosomes 3, 5, 7, 9, 10, 11, 12, 11, 16, 17 and X. CdLOH is present on chromosome 5, 7, 10, 11, 12, 16, 17, 19, X in ER positive DCIS associated with tumour. ER positive pure DCIS shows duplication on chromosome 8 although this is not seen in the ER positive DCIS associated with invasive breast disease.

There are a large number of gains seen in ER positive DCIS associated with invasive breast disease across all chromosomes (except 13, X) whilst ER positive pure DCIS show gains less frequently on all, except certain regions found on chromosomes 1, 2, 4, 5, 6, 9, 11, 12, 16, 17, 18, 19 and 20. There are no gains on 12, 14 or 20.

As with pure TN DCIS versus TN DCIS associated with invasive breast disease, it may be that for ER positive lesions further genomic changes maybe either required or assist in the pathway to invasive disease.

There are amplifications identified in ER positive DCIS associated with invasive breast disease which we did not observe in ER positive pure DCIS. PANTHER analysis reveals 29 mapped genes. Of these, 13 are histones with epigenetic post translational modifications of histones being described as hallmarks of cancer (226). Elsheikh et al have correlated global histone modifications with breast tumour phenotypes, prognostic factors and patient outcome in invasive breast cancer. Utilising IHC on TMAs they identified; “Variations in bulk histone modifications in

different grades, morphologic types, and phenotype classes of invasive breast tumors. Furthermore, we have identified hypomodified and hypermodified tumor clusters, which correlate with known prognostic factors and clinical outcome" (227).

In this series there are duplications in the ER positive pure DCIS but not in ER positive DCIS associated with invasive breast disease. PANTHER analysis reveals a single gene, ASPH, which has been shown to be amplified in breast tumours in one previous study (228). Kadota et al (228) describe ASPH as one of four potentially novel oncogenes although they did not investigate ASPH further.

For gains in ER positive pure DCIS and ER positive DCIS associated with invasive breast disease there is considerable overlap in the gene patterns with no specific gains identified, and therefore these have not been further examined in this initial analysis.

Sc gains were found in ER positive pure DCIS not present in ER positive DCIS associated with invasive breast disease. PANTHER analysis reveals 8 mapped genes. Of these 2 are tyrosine kinases, one of these, tyrosine kinases (PTK2), has been previously shown to be up-regulated in DCIS (229). Also known as FAC Lightfoot et al (234) describe this kinase as a mediator of several functions including proliferation adhesion and survival. They found overexpression in DCIS in 66% of cases (n=34/51) and 33% of invasive lesion (n=6/18) but no expression in fibrocystic disease. They suggest that FAK has an active role in DCIS and survival in tumourigeneis. Other Sc gains were found in ER positive DCIS associated with invasive breast disease not observed in ER positive pure DCIS. PANTHER analysis reveals 62 know genes with a variety of molecular, biological and protein classes (see

PANTHER analysis) is used to create pie charts and radar map for molecular functions, biological processes and protein class (Figures 45-47).

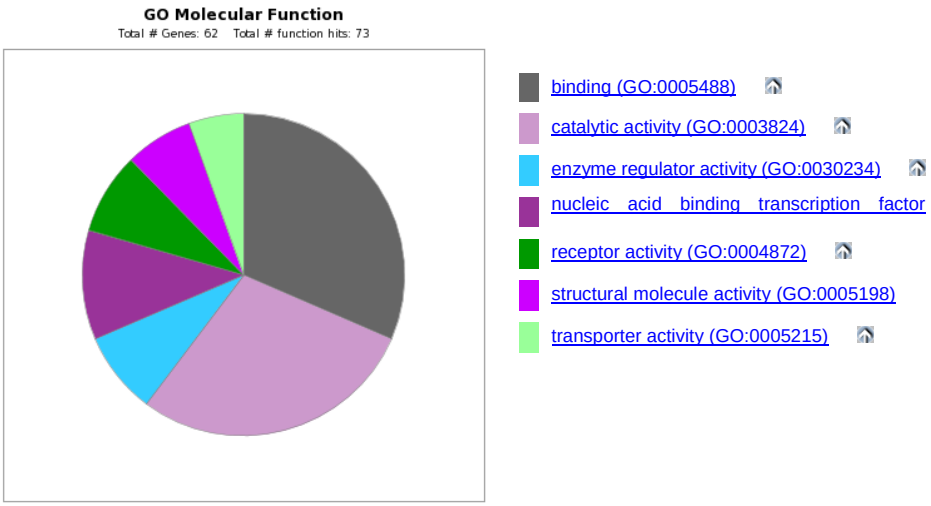

Figure 45: Molecular functions associated with Sc gains in ER positive DCIS associated with invasive breast diseases and ER positive pure DCIS.

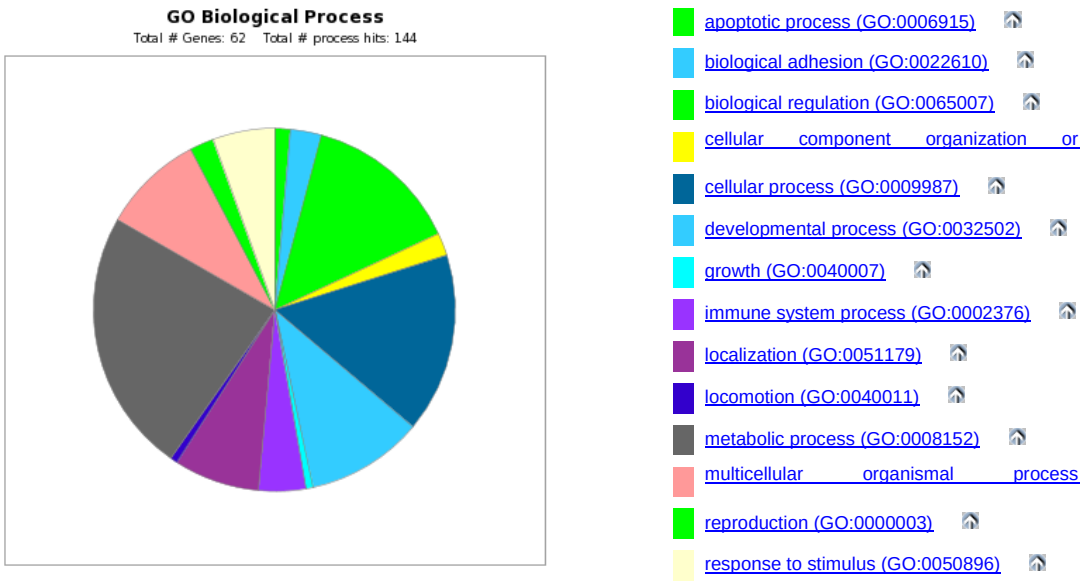

Figure 46: Biological processes associated with Sc gains in ER positive DCIS associated with invasive breast disease and ER positive pure DCIS

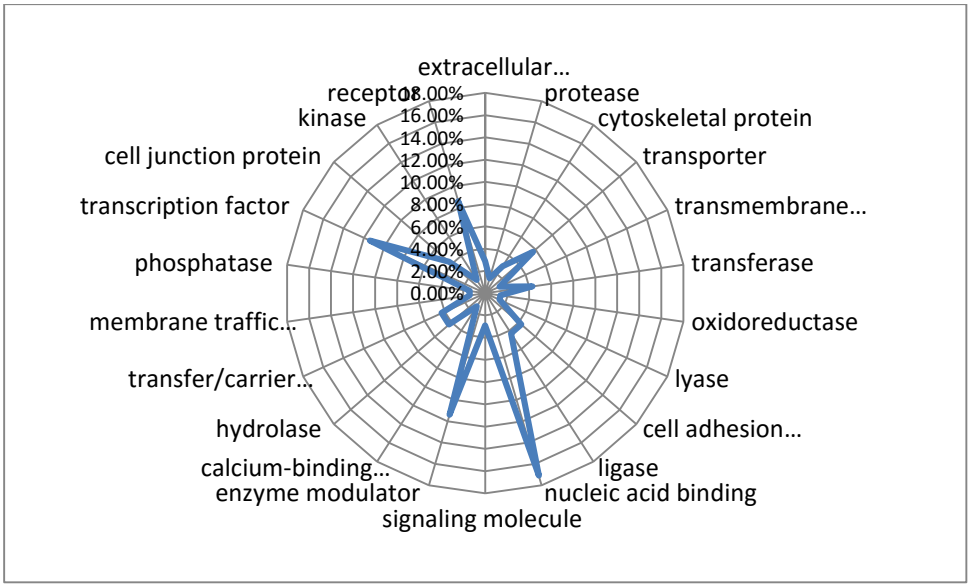

Figure 47: Protein classes associated with ER positive DCIS associated with invasive breast disease and ER positive pure DCIS.

Oh the 62 genes, TNFRSF4 (a tumour necrosis factor) has been previously described in both invasive disease and DCIS (230). Also known by the alias OX40, this membrane-bound member of the tumour-necrosis-factor-receptor (TNFR) superfamily, plays an important role in proliferation, survival and infiltration of activated T cells via binding to OX40L (230). Xie et al suggest that high OX40 expression may be associated with malignant transformation, progression, invasion and metastasis in breast cancer biology (230).

There are losses in ER positive DCIS associated with invasive breast disease not observed in ER positive pure DCIS. PANTHER analysis reveals 42 mapped genes, of which 6 are zinc finger proteins. Losses include NRG3 which encodes for the EGF containing ligands that mediate binding to ERBB receptor tyrosine kinases (231). NRG is reported to regulate mammary phenotype (232).

Total losses in pure ER positive DCIS include RB1 (retinoblastoma gene) that has tumour suppressor function. It has been shown to be frequently altered in breast carcinomas leading to loss of expression (233). Total Losses seen in DCIS associated with invasive breast disease but not in pure DCIS are far more common (Figures 49-51). PANTHER analysis reveals 219 mapped genes. There is a wide variation in the genes and the molecular functions with total loss. Of these MAP2K4 (mitogen activated protein kinase) whose deletion has been suggested as one of a set of putative cancer genes (234).

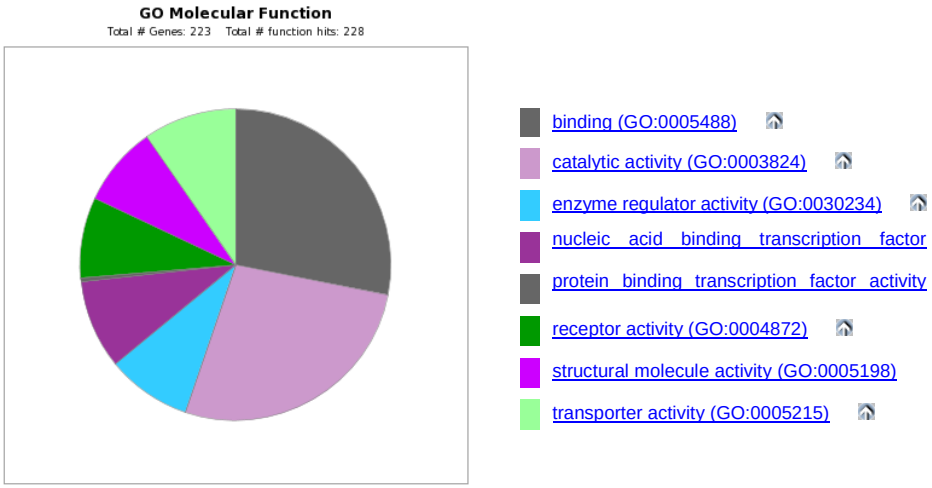

Figure 48: Molecular functions associated with total loss in ER positive DCIS associated with invasive breast disease.

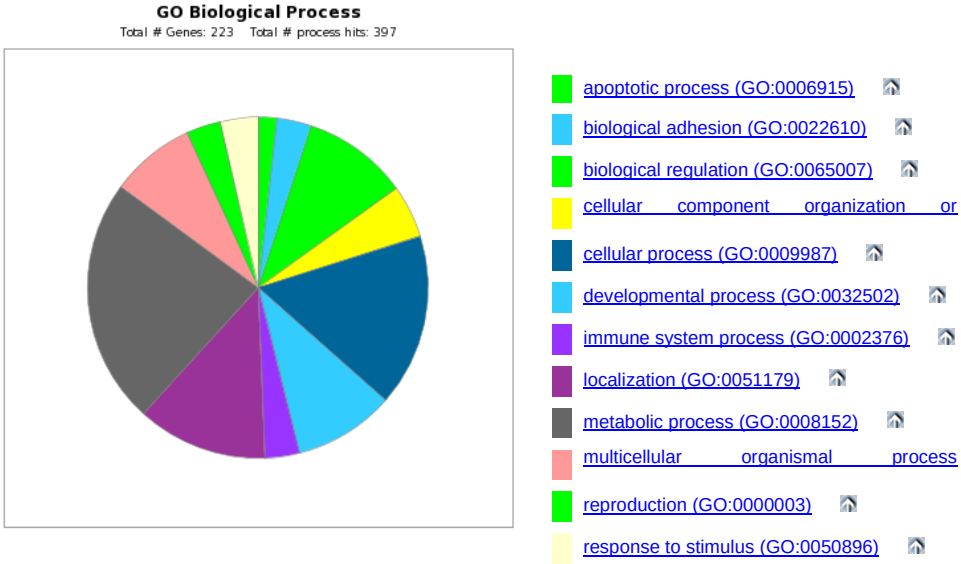

Figure 49: Biological processes associated with total loss in ER positive DCIS associated with invasive breast disease

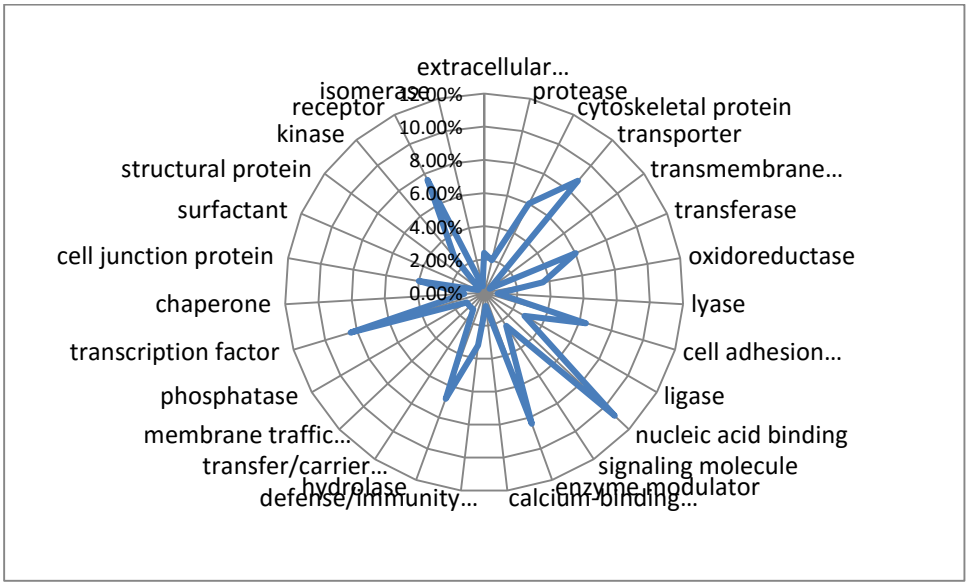

Figure 50: Protein classes associated with ER positive DCIS associated with invasive breast disease.

There is CdLOH present in ER positive pure DCIS not observed in ER positive DCIS associated with invasive breast disease. PANTHER analysis reveals 176 mapped

genes with a variety of molecular functions and protein classes. A number matrix metalloproteases or MMPs (MMP1, MMP3, MMP 7, MMP8, MMP10, MMP13, MMP20, MMP27, PTGFD) have CdLOH ER positive pure DCIS. Loss of Matrix metalloproteases (MMPs) activity may result in a wide range of diseases including cancer (235).

CdLOH present in ER positive DCIS associated with invasive breast disease has similarities to the ER pure DCIS with no speicifc changes identified and is not examined further in this initial analysis.

There is CnLOH present in ER positive pure DCIS not observed in ER positive DCIS associated with invasive breast disease. PANTHER analysis reveals 248 mapped genes

representing a wide variety of molecular functions (Figures 51-53). ERBB 2, MDM2 (a regulator of p53) and Notch2 have CnLOH. MDM2 (236) and Notch2 (237) have been suggested as candidate genes in breast cancer progression.

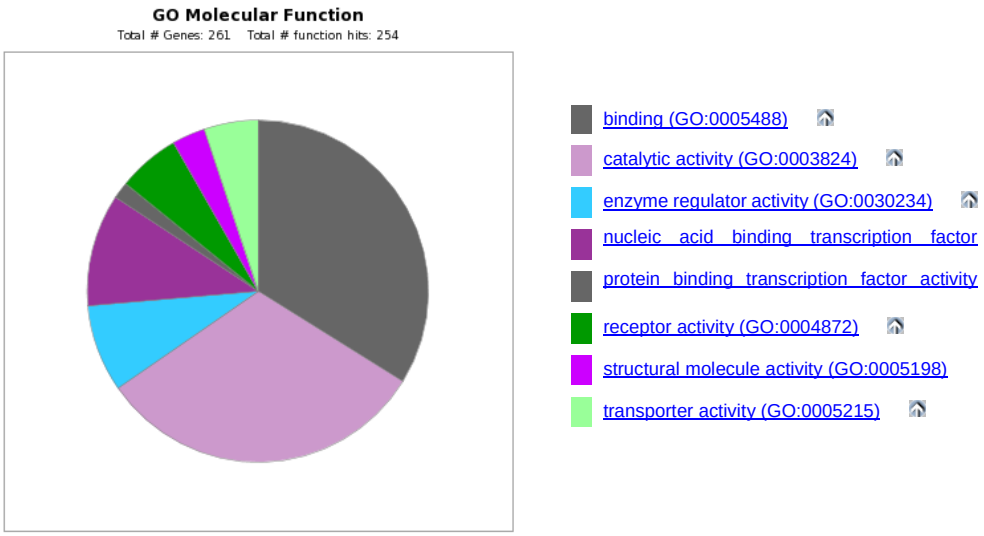

Figure 51: Molecular functions associated with CnLOH in ER positive pure DCIS

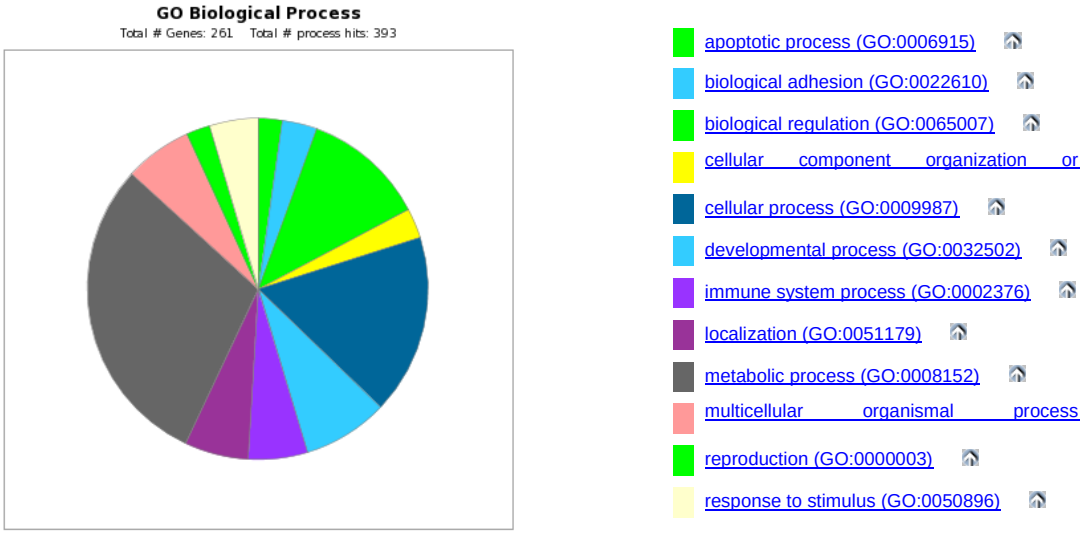

Figure 52: Biological processes associated with CnLOH in ER positive pure DCIS

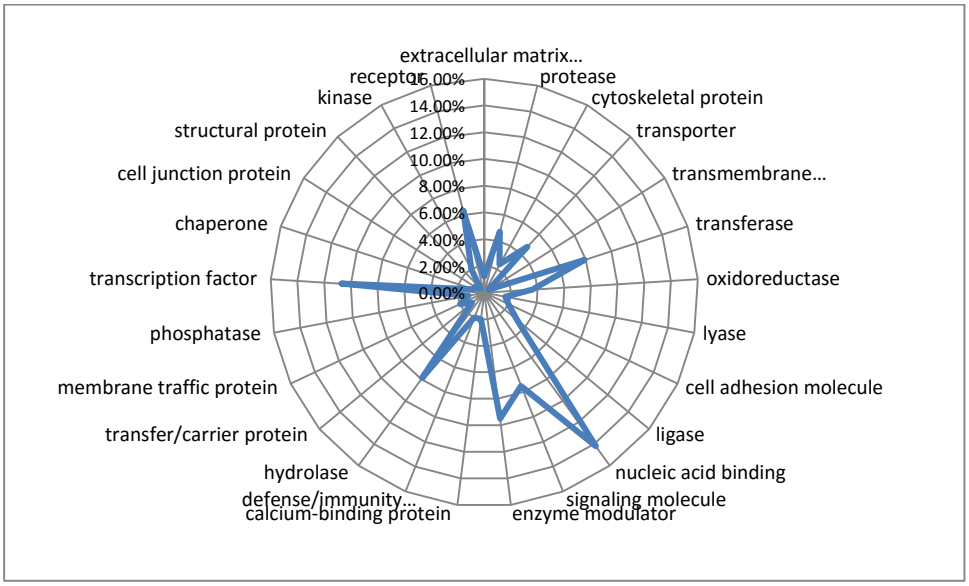

Figure 53: Protein classes associated with CnLOH in ER positive pure DCIS

There is CnLOH in ER positive DCIS associated with invasive breast disease which is not observed in ER positive pure DCIS. PANTHER analysis reveals 64 mapped

genes. In this series the gene S100z shows CnLOH whereas in one previous study it was reported to be up-regulated (238).

5.9.2 Genomic Differences found in Triple Negative Pure DCIS Versus Triple Negative DCIS Associated with Invasive Breast Disease

The frequency plots for CNAs show that samples of triple negative DCIS associated with invasion in this series exhibit many more genomic aberrations at the chromosomal level than pure triple negative DCIS. CdLOH, gains, losses and Sc gains all show a higher frequency of aberrations for the DCIS associated with invasive breast disease than pure DCIS which has not progressed. There are some homology present with CnLOH (see below) and total losses in TN pure DCIS and TN DCIS associated with breast disease. CdLOH are also located on distinctly separate chromosomal and loci for pure TN DCIS (chromosome 7, 16) compared to CdLOH on chromosome 3, 4, 5, 8, 9, 13, 14, 15, X for TN DCIS associated with invasive disease. Aberrations in both are located on chromosome 17 but in different regions. Gains are present found on chromosomes 1 and 8 for both types of lesion, but at a lower frequency for TN pure DCIS. Gains are found only on chromosome 3, 6, 11, 13, 18, 21 for TN DCIS associated with invasive breast disease. Losses show a similar pattern, with pure TN DCIS having distinct losses on chromosome 7, 16, and 19 compared to distinct losses on 4, 5, 8, 9, 14, X in TN DCIS associated with invasive breast disease. Sc gains on chromosome 1, 2, 5, 6, 8, 9 are more abundant in TN DCIS associated with invasive breast disease with pure DCIS only showing Sc gains on chromosome 1.

These differences in TN pure DCIS and TN DCIS associated with invasive breast disease may indicate that although a cancerous phenotype exists within pure TN DCIS several further copy number aberrations may be necessary to switch to an

invasive TN phenotype. Both gains and losses are present in TN DCIS associated with invasion which are not seen in pure TN DCIS in this series. There is a degree of homology in some chromosomal changes such as gains on chromosome 1 and losses on chromosome 4 in both pure TN DCIS and TN DCIS associated with invasive breast disease. However, there are few gains and losses present found in pure DCIS alone.

Comparison of TN pure DCIS and TN DCIS associated with invasive breast disease shows no amplifications or duplications found in either process.

Comparing the chromosomal gains in TN pure DCIS and in TN DCIS associated with invasion there is some homology present, with pure TN DCIS cases having gains comparable to those seen in the TN DCIS associated with invasion in 5/9 cases. However, the TN DCIS associated with invasion shows additional gains not present in the TN pure DCIS. PANTHER analysis of the genes identifies 16 known genes with a range of biological functions associated with several protein classes (Figure 54-56). Of these, one - NFIB has been previously identified as associated with ER negative invasive breast cancer (239) and proposed as a genomically distinct TN subgroup mainly composed of adenoid cystic carcinomas (240).

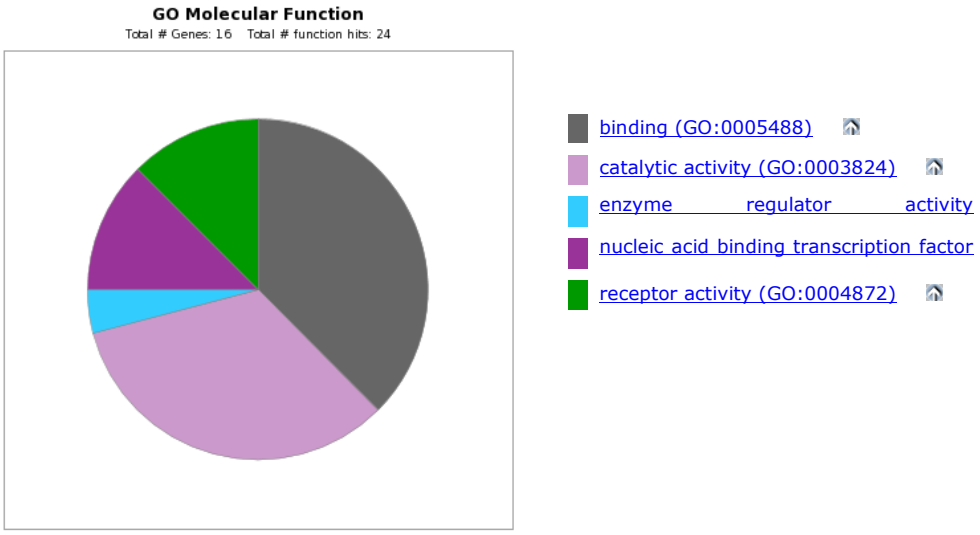

Figure 54: Molecular functions associated with the genomic gains identified in TN DCIS associated with invasive breast cancer.

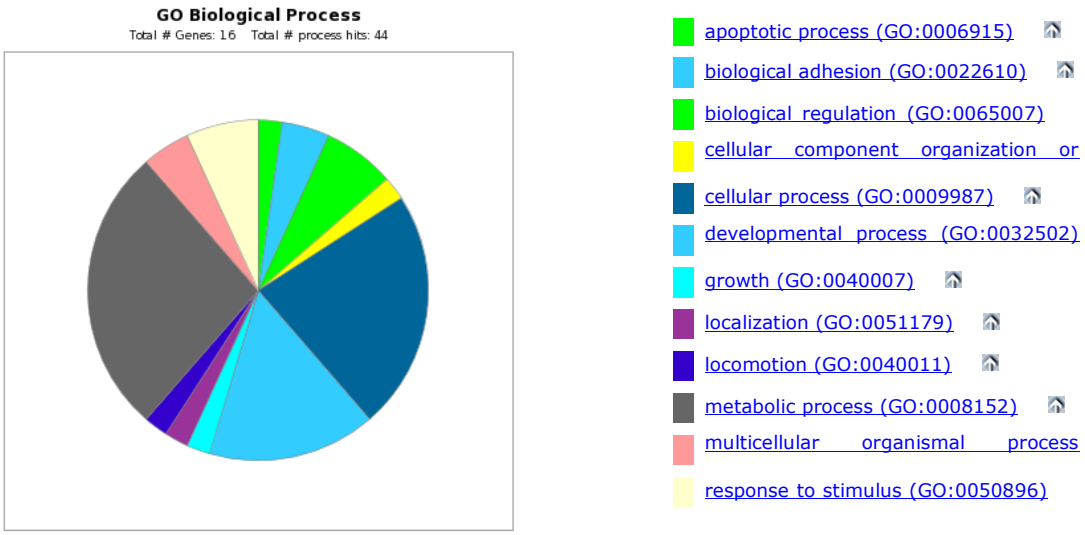

Figure 55: Biological processes associated with the gains identified in TN DCIS associated with invasive breast cancer.

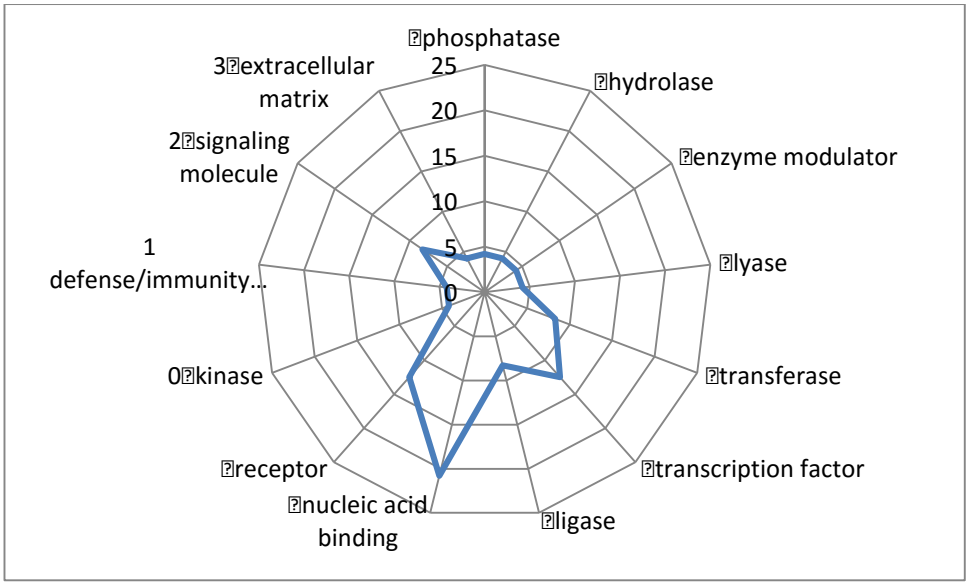

Figure 56: Protein classes associated with the genomic gains identified in TN DCIS associated with invasive breast cancer.

Sc gains were present in TN DCIS associated with invasive breast disease but not in TN pure DCIS. PANTHER analysis maps 86 of the 350 genes giving a range of molecular and biological functions associated with several protein classes (Figure 57-59)

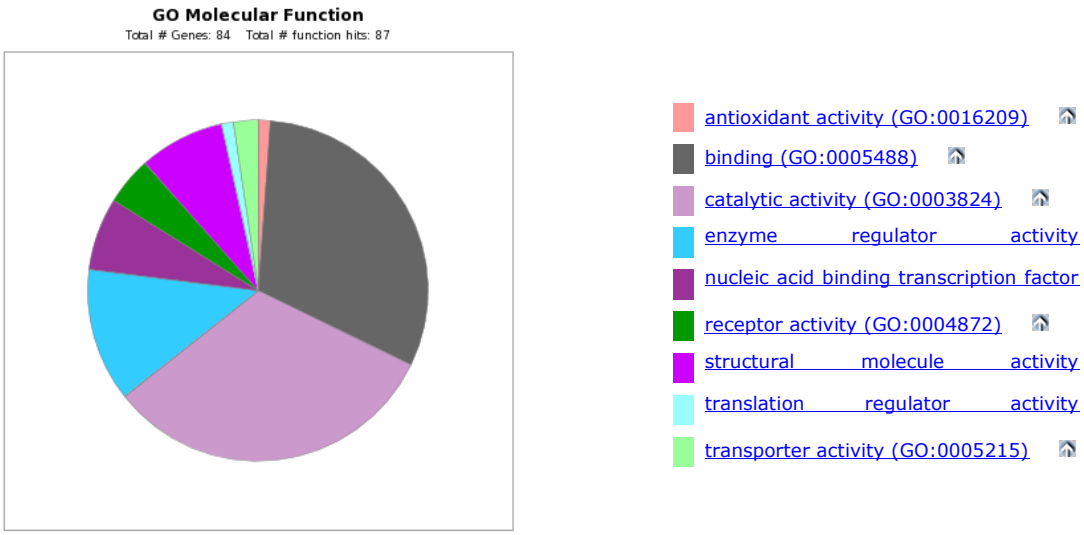

Figure 57: Molecular functions associated with Sc gains for TN DCIS associated with invasive breast disease.

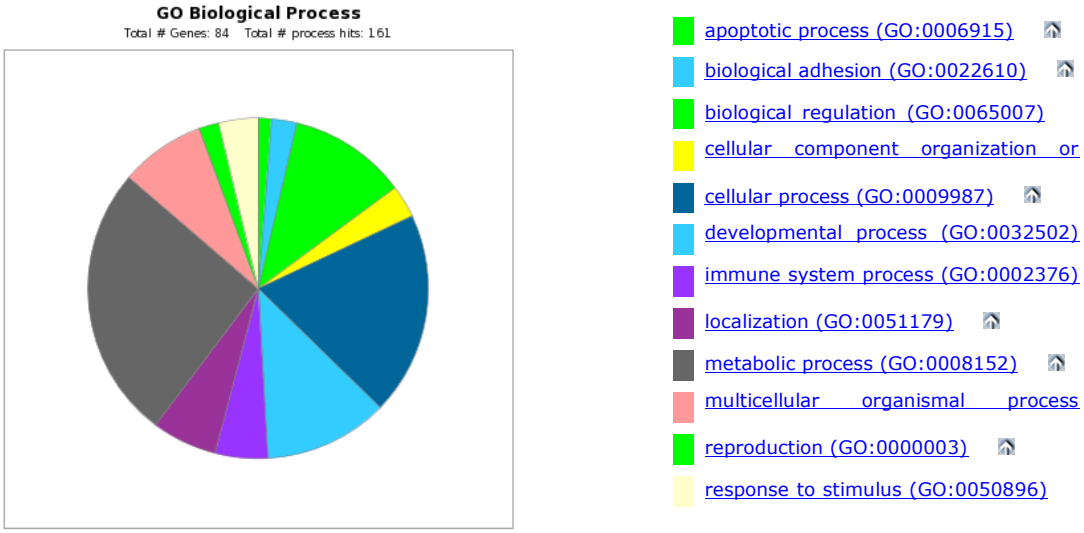

Figure 58: Biological processes associated with Sc gains for TN DCIS associated with invasive breast disease.

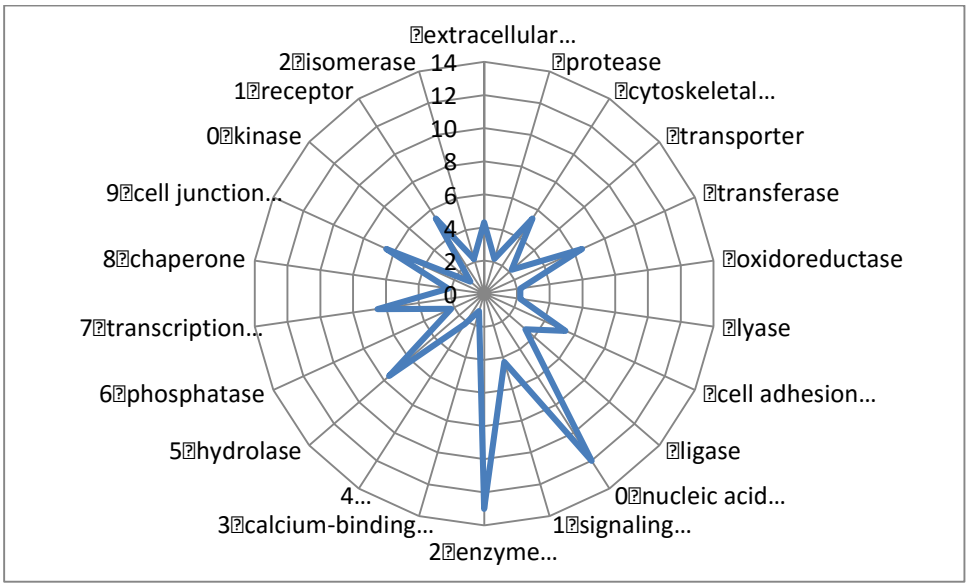

Figure 59: Protein classes associated with Sc gains in TN DCIS associated with invasive breast disease.

The genes showing Sc gains in TN DCIS associated with invasive breast disease but not observed in TN pure DCIS include PTP1B (Protein tyrosine phosphatase 1B) which has been reported to have both tumour suppressor and tumour promoting roles (241). Similarly ADAMTS-12, a secreted metalloprotease, shows both oncogenic and

tumour-suppressive effects has Sc gains in this series (242). PLK3 also shows Sc gain; this is a member of the pololike kinases and whilst is involved in cell cycle regulation its expression remains steady throughout the cell cycle. It has been shown to be widely expressed in cancer cell lines (243). Some cadherin's (CDNH) 6 (K-cadherin), 9 (T1 cadherin) 12 (n-cadherin), 18 (ungrouped) show Sc gains in this series.

As opposed to the Sc gains seen in the TN DCIS associated with invasive compared to the pure form of TN DCIS, losses in TN pure DCIS not observed in TN DCIS associated with invasive disease are noted, with six genes mapped by PANTHER analysis. Three of these are in the type 1 keratins (14, 16, 17) which are structural components of the cytoskeleton.
Conversely, 7 gene losses are mapped by PANTHER analysis in TN DCIS associated with invasive breast disease showing a variety of molecular functions.

Total losses for pure DCIS not observed in TN DCIS associated with invasive disease reveal 40 genes mapped by PANTHER analysis. These include BRCA1, zinc finger like proteins (333 and 558) and olfactory receptor (OR) gene. Previous studies have shown up-regulation of ten OR genes in breast cancer cell lines clustered in 11q12.1 (244).

Total losses for TN DCIS associated with invasive breast but not observed in TN pure DCIS associated with invasive disease reveal 46 genes mapped by PANTHER analysis. These include metalloproteases, protease zinc finger protein, and extra cellular matrix protein. In this series there is total loss of the apoptotic marker PDCD6IP (3p23) in some cases of TN DCIS. Previously copy number analysis has reported that amplification of this gene is associated with an increased risk of

recurrence in invasive breast disease when considered as part of a trio of markers (*CYP24/PDCD6IP/BIRC)* for ER/PR-positive cancers. Individually PDCD6IP is reported to have no significant correlation in invasive breast cancer prognosis but does when associated with CYP24 and BIRC (245) highlighting the complex interactions of different genomic markers.

CdLOH for TN DCIS associated with invasive disease not observed in TN pure DCIS revealed 12 genes mapped by PANTHER analysis. These include a kinase suppressor of Ras1 (KSR1) which has been identified as a potential tumour suppressor in BRCA1 tumours (246). CnLOH for TN DCIS associated with invasive disease show similarities in 5/9 cases with the CnLOH in pure DCIS. However, there are 10/10 cases showing CdLOH observed in TN pure DCIS not observed in TN DCIS associated with invasive disease. PANTHER analysis reveals genes mapped by PANTHER analysis. Conversely, CdLOH for TN pure DCIS not observed in TN DCIS associated with invasive disease revealed 4 altered genes mapped by PANTHER analysis of which 3 are keratins -14, 16,17.

5.7.3 Observations on Genomic Analysis of Pure DCIS Compared to DCIS Associated with Invasive Breast Disease.

In this series the following observations can be made regarding analyses:

Amplifications and duplications between pure DCIS and DCIS associated with invasive disease show no similarity regardless of subtype.

Gains and losses show similarity for all types of DCIS with regard to chromosomal region, however the number of genomic gains or losses in DCIS associated with tumours is greater than those found in pure DCIS. In addition there are gains present in tumour associated DCIS not seen in pure DCIS lesions. This would fit with a hypothesis that further downstream genetic mutations occur post DCIS and lead certain credence to the possibility that not all pure DCIS is not wholly committed to an

invasive phenotype. Downstream events post establishment of pure DCIS may be required to for the initiation of invasive potential. SC gains show no overall pattern between these two cohorts.

Total losses between pure DCIS and DCIS associated with tumour show few matching genetic aberrations. As with amplifications and duplications and Sc gains these differences may indicate drivers in pure DCIS that inhibit the progression to invasive disease or in DCIS associated with invasion they may indicate invasive promoting genes. An alternative approach is that these differences could indicate increased heterogeneity giving rise to unidentified subtypes.

Copy neutral and copy deletion loss of hetereozygosity is marked in both sets of data regardless of tumour subtype. The use of MIP arrays used control tissue of normal human breast as a reference point to give a baseline for the samples analysed. Ideally the control reference would have been taken from normal tissue from the same patient. The lack of normal tissue availability prevented this approach so it is acknowledged that there may be a certain amount of background “noise” which gives a higher number of comparative genomic differences than expected as there would be a disparity between the normal tissue of different individuals.

5.10 Summary of Genomic Differences between DCIS and Invasive Breast Disease

This section addresses point 4 in the study aims: “To identify any protein and/or genomic changes in all DCIS (pure and that associated with invasion) compared to invasive breast disease to determine potential biomarkers responsible for progression to an invasive state”.

In this series only those copy number aberrations seen in one series and absent in the second set, i.e. present in pure DCIS but not in invasive carcinoma, and vice versa, are addressed in this initial analysis.

5.10.1 Genomic Difference between ER Positive DCIS and ER Positive Invasive Breast Disease. (See section 5.8.4).

The frequency plots for CNAs in all ER positive DCIS compared to ER positive invasive disease show a mixed pattern, with some homology and a degree of heterogeneity. CdLOH shows similar aberrations on regions of chromosomes 8, 10, 11, 13, 15, 19, 20 X for both sample sets although ER positive DCIS has a lower frequencies. However, there are exclusive CnLOH regions found on chromosomes 1, 3, 4, 7, 10, 14, 15, 18, X in ER positive invasive breast cancer not seen in ER positive DCIS. There are duplications seen only in ER positive invasive disease, found on chromosomes 1, 8, 9, 10, 17, 21 not present in ER positive DCIS. The gains found show homology on chromosome 6 and 16 with a lower frequency in DCIS. There are losses on chromosomes 1, 2, 5, 7, 8, 11, 13, 15, 16, 19, 21 X found in both sample sets with a lower frequency found in ER positive DCIS. The exception is chromosome 11 where ER positive DCIS samples have greater losses than ER positive tumours. Sc gains are seen at similar frequencies but, as with other CNAs, the frequency in DCIS is lower. For total loss there are many more aberrations in ER positive invasive breast disease than ER positive DCIS. Again, there are some homologous regions (chromosomes 2, 6, 8, 8, 10, 13, 14, 16, 17, x) and regions of exclusive total loss for ER breast disease (chromosomes 2, 3, 4, 5, 7, 8, 9, 10, 12, 13, 14, 15, 16, 19, 20, 21, X). These data all indicate that further genomic differences are present in invasive breast disease not present in DCIS.

There are no amplifications in the comparison of ER positive DCIS versus ER positive invasive breast disease.

Duplications found in ER DCIS are also present in ER positive invasive breast disease and are not addressed in this initial analysis. Conversely, there are duplications in ER positive invasive disease not present in ER positive DCIS. PANTHER analysis reveals 137 mapped genes. In this series the gene loss or CnLOH of PTPRD is found in both pure ER positive DCIS and ER DCIS associated with invasion. In this series Muc1 is also duplicated; this has previously been shown to be elevated in ER positive invasive breast disease (247) but having less frequent expression (i.e. fewer cases) in ER positive DCIS (248). Notch2 also show duplications (236).

There are genomic similarities in the pattern of gains, Sc gains and losses in ER positive DCIS and ER positive invasive breast disease which have not been analysed in this preliminary study.

There are total losses of genes present in ER positive DCIS that are not present in ER positive invasive breast disease. PANTHER analysis reveals 40 genes showing total loss. Total loss in this series includes BRCA1 and several olfactory receptor genes.

CdLOH found in ER DCIS are also present in duplications for ER positive invasive breast disease and are not examined in this thesis.

There is CnLOH present in ER positive DCIS not observed in ER positive invasive breast disease. PANTHER analysis reveals 42 mapped genes. Of these genes MACROD2 has been suggested as a possible cause of Tamoxifen resistance when

overexpressed in metastatic tumours (249). PANTHER analysis of the converse, CnLOH present in ER positive invasive breast disease not observed in ER positive DCIS, reveals 37 mapped genes. Of these genes TIMELESS, one of the core circadian genes, has been proposed as an epigenetic risk factor by possibly regulating hormone functions. Its overexpression is reported to influence breast carcinogenesis (250) and warrants

5.10.2 Genomic Difference between Triple Negative DCIS and Triple Negative Invasive Breast Disease.

The frequency plots for CNAs show that there is a high degree of homology between TN DCIS and TN invasive tumours. DCIS lesions show similar but less complex copy number aberrations to the invasive disease. This concurs with the findings by Johnson et al who performed a similar MIP analysis on 21 cases of invasive ductal carcinoma with synchronous DCIS although with no phenotypic subgrouping (251). In the present series, a high degree of total loss is apparent found on chromosomes 3, 13, 14, 15 and 17. Gains found on chromosomes 3 and 6 are also identified in both TN DCIS and in TN invasive carcinoma, whilst gains in TN invasive breast cancer are seen in chromosome 11 although this is not apparent in TN DCIS. CdLOH is seen in both TN DCIS and TN invasive breast disease found on chromosomes 4, 12, 18 and X. However, for CnLOH TN DCIS shows a higher degree of complexity than TN invasive disease. CnLOH for TN DCIS are present more frequently found on chromosomes 1, 2, 3, 6, 7, 8, 9, 10,11, 12, 19 20, and X. CNLOH is present in TN DCIS found on chromosomes 5, 13, 16 and 21, where no CnLOH is found in TN invasive breast disease.

Gains and (and Sc gains) show very similar patterns between DCIS and invasive breast disease with regard to chromosome number. The level of complexity is raised in the invasive samples.

There are no amplifications in the comparison of TN DCIS versus TN invasive breast disease.

There are duplications found in TN invasive breast cancer not present in TN DCIS. PANTHER analysis reveals 62 mapped genes. Of these, protein tyrosine kinases PTPRK and PTK7 show duplications. PTPRK has been reported as a potential tumour suppressor (252) whilst positive immunohistochemical expression of antibodies raised against PTK7 has been shown in anthracycline-resistant invasive breast disease (253).

Gains, Sc gains and losses in TN DCIS and TN invasive disease show overlap of genes and are not examined in this initial analysis.

There are total gene losses found in some cases of TN DCIS not observed in some cases of TN invasive disease. PANTHER analysis reveals 205 mapped genes with a variety of molecular functions, biological processes and protein classes (Figures 60-62).

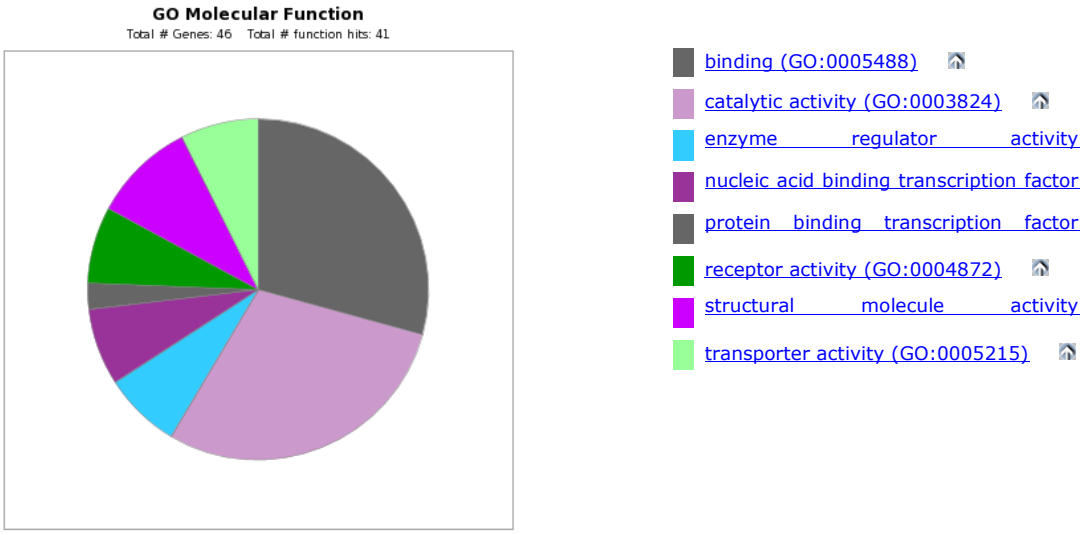

Figure 60: Molecular functions associated with total loss in TN DCIS

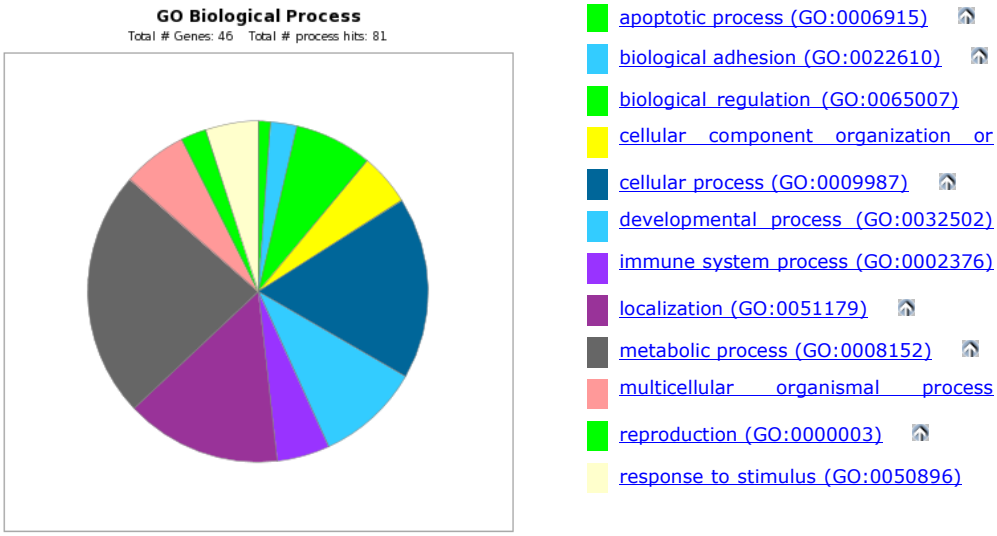

Figure 61: Biological processes associated with total loss in TN DCIS

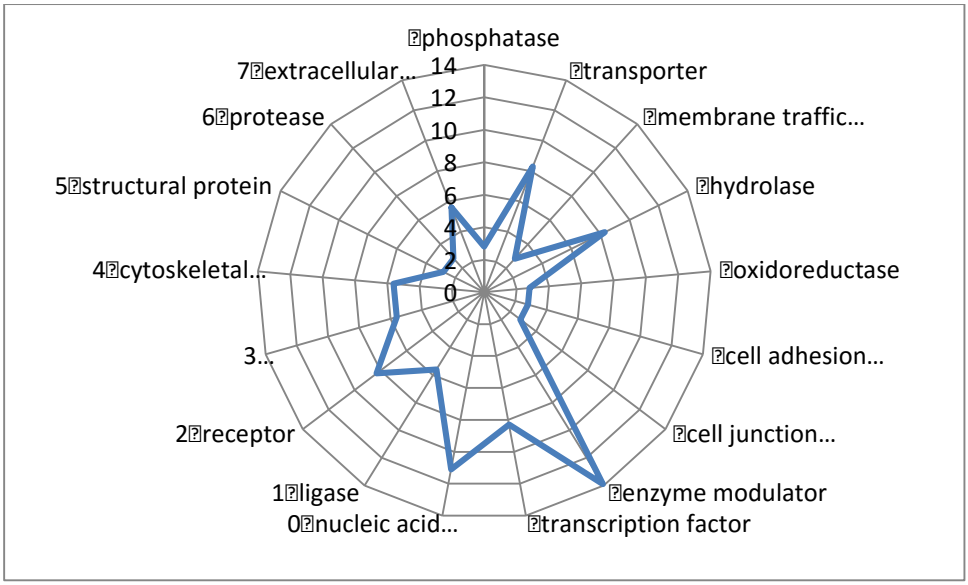

Figure 62: Protein classes associated with total loss in TN DCIS

In this series, FOXD1 shows total genomic loss in some cases of TN DCIS whilst it has been suggested as an upregulated oncogene in breast cancer (254).

There are total losses found in some cases of TN invasive breast disease not seen in some cases of TN pure DCIS. PANTHER analysis reveals 160 mapped genes. Olfactory receptor genes are predominant with 11 showing total loss (OR1B1, OR1J2, OR1J4, OR1L1, OR1L3, OR1L4, OR1L6, OR1L8, OR1N1, OR1N2, OR1Q1). Fonseca-Sanchez et al identify 55 olfactory receptor genes up-regulated in breast cancer cell lines (244). However, the olfactory receptor gene family is the largest in the genome.

There is CnLOH present in TN DCIS that are not observed in TN invasive breast disease. PANTHER analysis reveals 205 mapped genes. Genes showing high levels of CNLOH in invasive breast cancer include, CSNK2B and HLA-DQA1. CSNK2B is a casein kinase a ubiquitous protein kinase which regulates metabolic pathways, signal transduction, transcription, translation, and replication. Kren et al (255) suggest that

down-regulation of casein 2 induces loss of breast cancer cell viability and may be a potential target for triple negative breast cancer therapy. HLA-DQA1 (major histocompatibility complex, class II, DQ alpha 1) is one of the HLA (human leucocyte antigen complex). It encodes for a protein of the major histocompatibility complex (MHC II) which is involved in antigen presentation within the immune system. A variant of HLA-DQA1 has been implicated in increased risk of breast cancer (256).

There is CnLOH present in TN invasive breast disease not observed in TN DCIS. PANTHER analysis reveals 140 mapped genes. Of these, there is CnLOH of a number of taste receptor genes (TAS2R10, TAS2R13, TAS2R14, TAS2R19, TAS2R20, TAS2R31, TAS2R42, TAS2R50, TAS2R7, TAS2R8, TAS2R9). There is no current literature on the significance of these in breast cancer.

5.10.3 Observations on Genomic Analysis of DCIS Compared to DCIS Invasive Breast Disease.

In this series the following observations can be made which are true for all DCIS compared to invasive tumour regardless of subtype (see 5.8.6. and 5.6.10) No amplifications are present for DCIS compared to invasive breast disease. Duplications are more prevalent in invasive breast disease indicating more genomic instability. Invasive breast disease exhibits a greater number of gains and SC gains compared to DCIS further illustrating more complex genetic aberrations. There are also greater losses in invasive breast disease. There is a similar pattern observed in the chromosomal regions of duplications, gains, losses which could in turn be explained as a sampling bias. DCIS and invasive samples from the same patient were included in this cohort and not matched against each other in this analysis. This would result in similar chromosomal regions of instability if the DCIS had similar genetic

aberrations to the associated invasive tumour analysed. The discrepancy in lower signal could be due in part to the pure DCIS samples not showing the same genomic changes as DCIS associated with invasive breast disease. Interestingly cnLOH (unlike cdLOH) shows greater genomic variation in DCIS than invasive breast disease. It may be that these multiple minor variations reduce as clonal expansion takes place of tumour cells with a proliferative advantage. Further research on this dataset is required to illicit the key drivers of these results.

5.11 Summary of Genomic Differences between Pure DCIS versus Invasive Breast Disease

5.11.1 Pure ER Positive DCIS compared to ER Positive Invasive Breast Disease

The frequency plots for CNAs between ER positive pure DCIS and ER positive invasive breast disease exhibit some homologous regions for both gains and losses when compared to invasive breast disease, albeit with much higher frequencies seen in ER positive invasive breast cancers. Gains on chromosome 6, 8 16, 20 and 21 are mirrored between both sets. Similarly losses on regions of chromosomes 8, 9, 11 12, 15, 16, 19, X are also present in both types of sample in this series. There are a greater number of losses on several regions of chromosome 11 in ER positive pure DCIS. Sc gains in this series show little homology, with Sc gains found on chromosomes 1 and 8 in ER pure DCIS and Sc gains found on chromosomes 6 and 20 in ER positive invasive breast disease. There are Sc gains on chromosome 8 for ER pure DCIS also seen in ER positive invasive breast disease. There are many more CNAs showing total loss in ER positive invasive breast disease than ER positive pure DCIS.

These finding somewhat contradict the findings seen in the comparison of ER positive pure DCIS and ER positive DCIS associated with invasive breast cancer. ER positive invasive breast cancer samples compared to ER positive pure DCIS seem to have

more in common than pure DCIS and DCIS associated with invasive breast disease. It must be acknowledged that this is a small cohort (ER positive pure DCIS n=8, ER positive invasive breast disease n=9) and this may contribute. However, it may be that combinations of genomic changes are required in the progression from DCIS to an invasive phenotype. There may be genomic changes already present in pure DCIS that are required for tumour survival that are uninvolved in progression to an invasive state. These may be conserved in an invasive tumour but play no role in invasion. Conversely these genomic changes may be required to trigger downstream mutations in order for invasion to occur and be conserved as either drivers of invasion or redundant post DCIS mutations.

There are no amplifications in ER positive pure DCIS in this series. There are amplifications in ER positive invasive breast disease. PANTHER analysis reveals 1 gene (*EIF3H)* which has previously been significantly associated with risk of low-grade breast cancer (257). Located on chromosome 8q23 the exact role of E1F3H in cell cycle regulation is unknown(258). The EIF3H gene encodes the eukaryotic translation initiation factor 3 (EIF-3) complex, associated in several steps in protein synthesis initiation and mRNA recruitment. Translational control is a crucial component of cancer development and progression (259), and EIF3H in particular is frequently amplified in breast and prostate cancers (260).

No duplications are found in either ER positive pure DCIS or ER positive invasive breast disease.

There were gains present in both ER positive pure DCIS and ER positive invasive breast cancer and, without significant differences, these are not addressed in this thesis. However, there were gains found in ER positive invasive breast disease not found in ER positive pure DCIS. PANTHER analysis reveals 26 mapped genes. Of

these 26 genes, SPIRE1 has been proposed as a possible driver of invasion as under- or over-expression can result in increased or decreased extra cellular matrix degradation (261).

There were Sc gains present in both ER positive pure DCIS and ER positive invasive breast disease which are not analysed in this preliminary assessment.

There are losses present in ER positive pure DCIS and ER positive invasive breast disease not addressed in this initial analysis.

There are total losses of genes which are present in ER positive pure DCIS but not seen in ER positive invasive breast disease. PANTHER analysis reveals 13 mapped genes. Of these, NOX4 is proposed as a contributory gene in the epithelial to mesenchymal transition (EMT) process involved in cancer invasion (262).

There are genes showing total loss in ER positive invasive breast disease not found in ER positive pure DCIS. PANTHER analysis reveals 172 mapped genes. GBJ2 is a gene responsible for cellular adhesion and has also been shown to be present in invasive disease and proposed as a possible cause for invasion, although this is contradicted by the present findings (263).

There is CdLOH present in both ER positive pure DCIS and ER positive invasive breast disease not analysed in this thesis. Similarly there are CnLOH present in both ER positive pure DCIS and ER positive invasive breast disease which are omitted from this preliminary work.

5.11.2 Pure Triple Negative DCIS versus Triple Negative Invasive Breast Disease (See section 5.8.9).

The frequency plots for pure TN DCIS compared to TN invasive breast disease exhibit many more CNAs in the invasive breast disease compared to DCIS although some homology is present the majority of changes exist in TN invasive breast disease

alone. The genomic frequencies also show a higher complexity of genomic aberrations across multiple chromosome regions compared to corresponding ER positive DCIS and invasive breast disease. This reveals a much more complex phenotype, which may possibly contain sub-groups within this series. CdLOH is found exclusively on regions of chromosomes 4, 5, 8, 9, 10, 12, 13, 14, 15, 16, 18, X for TN invasive breast cancer. Shared regions, although at much lower frequency, are found on chromosomes 4, 5, 14 and 15. Exclusive regions of gain are seen on chromosomes 1, 3, 6, 8, 9, 10, 13 and 20. Sc gains are seen exclusively in TN invasive breast carcinomas in this series found on chromosomes 1, 3 and 8.

These findings are similar to those seen in TN pure DCIS versus TN DCIS associated with invasive breast disease indicating that genomic changes found in invasive breast disease are much more complex than those seen in DCIS.

There are no amplifications in TN pure DCIS or TN invasive breast cancer in this series.

There are similarities in duplication of gene which are seen in both TN pure DCIS and TN invasive breast disease and these are not further addressed in this initial analysis.

There are similarities in gains found in both TN pure DCIS and TN invasive breast disease so these are not specifically addressed in this initial analysis. However, there are genomic gains present in some samples of TN invasive breast disease not observed in TN pure DCIS. PANTHER analysis reveals 5 mapped genes. None of these genes have been linked in previous studies to tumourigenesis or breast cancer.

There are no Sc gains in TN pure DCIS in this series. Sc gains are, however, present in TN invasive breast disease. PANTHER analysis reveals 51 mapped genes. This includes the gene ALDH1L1, loss of function or expression of this gene is associated

with decreased apoptosis, increased cell motility, and cancer progression. ALDH1L1 may contribute to ALDH1 activity in breast cancer as high expression of ALDH1A1 mRNA was found to be significantly correlated with poor overall survival in some breast cancer patients (264).

There are similarities found in genomic losses found in TN pure DCIS also present in TN invasive breast disease, these are not examined in this thesis. However, there are genomic losses found in TN invasive breast disease not observed in TN pure DCIS. PANTHER analysis reveals 13 mapped genes. Of these SMAD4 has been suggested as a mediator in the TGF beta pathway acting as a tumour suppressor gene supressing carcinogenesis (265).

There are total genomic losses present in TN pure DCIS not observed in TN invasive breast disease. PANTHER analysis reveals 41 mapped genes. In this group are 13 olfactory related genes (OLFM4, OR2Z1, OR2Z1, OR4C3, OR4C5, OR4S1, OR4X1, OR4X2, OR7A10, OR7A17, OR7A5, OR7C1, OR7C2). The total loss of OLFM4 in this series is contradictory to previous studies where OLFM4 gene product (Olfactomedin-4) is cited as a candidate biomarker for detection or progression for a variety of solid tumours including breast cancer (266, 267).

There are total genomic losses present in TN invasive breast disease not observed in TN pure DCIS. PANTHER analysis reveals 39 mapped genes. These include the loss of 3 genes encoding for keratins (KRT222, KRT24, KRT25). Loss of keratins has been suggested as one of the possible key components in invasion, although it is acknowledged that loss alone of keratins is not sufficient to cause invasion and/or metastasis (268).

CdLOH found in TN pure DCIS are also present in TN invasive breast disease and have not been analysed in this thesis. There is CdLOH present in TN invasive breast cancer not observed in TN pure DCIS. PANTHER analysis reveals 165 mapped genes. Genes include BCL2, SMAD4, MLH3, alcohol dehydrogenases (ADH1A, ADH1B, ADH4, ADH5, ADH7, ADNP2) and NFKB1. NFKB1 is one of the down regulated genes proposed as part of a seven-gene signature a panel for predicting distant recurrence in patients with triple-negative breast cancers receiving adjuvant chemotherapy following surgery (269).

PANTHER analysis of the CnLOH seen in TN pure DCIS not observed in TN invasive breast disease reveals 335 mapped genes. These include NEDD9 (270) NRD1(271) TGFBR3(272) which have all been associated with invasion in breast cancer. There is CnLOH present in TN invasive breast disease not observed in TN pure DCIS. PANTHER analysis reveals 152 mapped genes. These include BUB3 (273) MCM7 (274) SPIRE1 (261) TGFBR3 (272) which have all been associated with invasion in breast cancer.

5.11.3 Observations of Genomic Analysis of Pure DCIS Compared to Invasive Breast Disease.

See sections 5.8.5 and 5.8.9. As with other series the genomic aberrations for amplifications, duplications, gains, losses, Sc gains and total loss for invasive ER positive breast disease are more pronounced than compared to pure ER positive DCIS. For TN pure DCIS and TN invasive breast disease this is similar without any amplifications or duplications. However, there is greater variation in the chromosomal regions affected for all the pure DCIS compared to the invasive breast disease. This is partially accounted for by the unmatched samples being excluded in this part of the

analysis. However there may be potential genomic regions of interest that identify markers only found in pure DCIS i.e. lesions that are unlikely to progress. Further work is required to elucidate these potential markers.

5.12 Summary of HER2 positive DCIS versus ER positive DCIS and triple negative DCIS

(See section 5.8.11)

Frequency plots for HER2 positive pure DCIS compared to ER positive pure DCIS and TN positive pure DCIS show a surprising similarity. As expected, amplification on chromosome 17 has a much higher frequency than in TN or ER positive pure DCIS as this is the locus of the ERBB2 gene which encodes for the HER2 protein and thus the definition of HER2 positivity in the series. However, CdLOH found on chromosomes 8 and 17, duplication on 8, gains on 3, 8, 17, 20, 21, losses on 6, 8, 17 Sc gains on 3, 8 and total losses on 13, 17 all have similarities between the two groups, albeit at different frequencies.

These findings may indicate that, whilst there are specific genomic changes that are present in immunohistochemical phenotypes that may be suitable targets for therapeutic decisions, these may be independent of genes that are responsible for either the tumourigenesis of DCIS or its progression to an invasive phenotype.

There are differences, as expected, between the two sets particularly with total losses in HER2 positive DCIS found on chromosomes 1, 3, 5, 6, 8, 9, 10, 13, 18, 19, 21 and X seen in the HER2 cohort.

There are similarities between amplifications found in HER2 positive DCIS, ER positive DCIS and TN DCIS. These are not addressed in this initial analysis.

There were duplications present in HER2 positive DCIS not observed in ER and TN DCIS. PANTHER analysis reveals 58 mapped genes. Of these 17 are genes related to the LCE (late cornified envelope) gene cluster within the epidermal differentiation complex on chromosome 1. These have previously been reported in a mouse model of triple negative breast cancer as potential novel driver mutations (275). They have not been previously linked to HER2 positive DCIS.

There are genomic gains in HER2 positive pure DCIS not observed in ER positive and TN pure DCIS. PANTHER analysis reveals 47 mapped genes. Of these genes MACROD2 is has been suggested as a possible cause of Tamoxifen resistance when overexpressed in metastatic tumours (249) but has not been described in association with DCIS.

Genomic gains and Sc gains found in ER positive DCIS, TN DCIS associated with genomic gains in HER2 Pure DCIS demonstrate similar genetic profiles and are not discussed in this work.

There are losses of genes present in HER2 positive DCIS which were not observed in ER and TN positive DCIS. PANTHER analysis reveals 48 mapped genes. One of these CDT1 is an integral part of the pre-replication complex associated with geminin and minichromosome maintenance proteins involved in cellular proliferation (276). Loss of CDT1 expression would be expected to inhibit cellular proliferation and thus may be of importance in preventing further progression of DCIS.

Conversely, there were losses present in ER and TN pure DCIS not observed in HER2 positive pure DCIS. PANTHER analysis identifies 1 gene (MUC16). Increased

serum levels of Ca125 (Muc16) have been shown to correlate with increased pathological grade of breast carcinoma (277).

Total losses in HER2 positive pure DCIS observed in ER and TN pure DCIS show similarity and are not examined in this preliminary research.

There were total losses present in ER pure DCIS and TN pure DCIS not observed in HER2 positive pure DCIS. PANTHER analysis identifies 39 mapped genes. As previously noted (section 5.4.3.2) there are several olfactory genes (OLFM4, OR1A1, OR1A2, OR1D2, OR1E1, OR1E2, OR1G1, OR2Z1, OR2Z1, OR3A1, OR3A2, OR3A3, OR6X1, OR8D1, OR8D2) showing total loss within TN DCIS.

There is CdLOH present in HER2 positive pure DCIS not observed in ER and TN pure DCIS. PANTHER analysis reveals 50 mapped genes. Of these one, IKBKB, was used in a panel of 21 breast cancer related genes compared in DCIS and associated invasive breast disease. The authors state there “were no significant differences in copy number DCIS and adjacent IDC, indicating that DCIS is genetically as advanced as its invasive counterpart” (278).

In the CdLOH analysis comparing ER positive and TN pure DCIS with HER2 positive pure DCIS, one gene (Muc6) is been identified (see total loss in this paragraph).

.

There is CnLOH present in HER2 DCIS not observed in ER positive and TN DCIS. PANTHER analysis identifies 30 mapped genes. DDX3 is an RNA helicase that has antiapoptotic properties, and promotes proliferation and transformation (279). It has been suggested that the protein product could be a potential therapeutic target as overexpression demonstrated by IHC may indicate an oncogenic role (279).

There is CnLOH present in ER and TN pure DCIS not observed in HER2 positive pure DCIS. PANTHER analysis identifies 292 mapped genes. There are several interleukin genes identified (IL12RB2, IL17A, IL23R, ILKAP). Interleukins are key regulators of immune response which may influence increased risk of developing breast cancer (280).

5.12.1 Observations of Genomic Analysis of Pure Her2 DCIS compared to Pure ER positive DCIS and Pure TN DCIS

The frequency plots for pure Her2 DCIS show, unsurprisingly, amplification on chromosome 17 not present in ER positive or TN pure DCIS. However, with the exception of cnLOH the severity of genomic changes (amplification, duplication, gains, Sc gains, losses, total losses and cdLOH) is more marked in HER2 pure DCIS than in either pure ER positive or pure TN DCIS. There is a significant degree of homology in chromosomal regions. This homology could indicate that regardless of subtype that all pure DCIS has common genomic aberrations that either initiate and/or maintain the formation of DCIS. Common gains and losses on the same area e.g. chromosomes 3 and 8 would therefore be candidates for further study. One area of large variation within this series is the number of total losses found in pure Her2 DCIS when compared to other types of pure DCIS. The reason for this comparatively high genomic instability remains elusive.

Chapter 6. Conclusions

6.1 Tissue Microarrays

Tissue microarrays have become an established method for analysing tissue samples from archival formalin fixed paraffin wax embedded samples. In this series using traditional tinctorial staining, immunohistochemistry and in situ hybridisation we have shown the versatility of such a technique. TMAs have increased the number of samples that can be analysed using a variety of biomarkers with a relatively little cost. We have demonstrated that some morphology can be retained with larger cores. However, it is also shown that care and planning is required in using TMAs analysis. Design and planning of TMAs should reflect the scientific question being asked but also enable subsequent further studies on the precious tissue resource. Problems associated with scoring methods for immunohistochemistry and the need for standardisation of TMA research have been highlighted in a publication related to this theses (281). In this series of DCIS samples we have analysed a selection of biomarkers with varying success. This DCIS cohort remains as a TMA resource for further studies.

5.13 6.2 Immunohistochemical Studies of DCIS

The first aim of this thesis was “To determine the expression of a range of immunohistochemical markers in DCIS lesions and determine if these markers can identify molecular subtypes similar to those found in invasive breast cancer.”

These immunohistochemical studies of DCIS have demonstrated that DCIS can be classified into different phenotypic subgroups which are essentially similar to those found in invasive breast cancer. The frequencies within the groups differ slightly from those seen in the literature regarding invasive breast cancer. This could be due to several factors: the cohort used in this study was obtained from a central London hospital. Compared to other regions in the United Kingdom, at least, there may be differences in the patient demographic as London is a particularly ethnically diverse population. The choice of antibodies to define the phenotypic subgroups and the methods used to score markers also varies from some of those used in other studies of invasive breast cancer. The need to standardise immunohistochemical reporting and staining methods needs further work.

In this study we found that although immunohistochemical assessment may be used to define subgroups this was not related to the propensity for a DCIS lesion to progress to an invasive phenotype or to remain in a pure DCIS form in this series, i.e. in terms of recurrence of the disease. This does not necessarily exclude the possibility that panels of IHC biomarkers could be used to determine either invasive potential or risk of recurrence of DCIS. The choice of IHC markers in this study was based upon those already established in invasive breast cancer and either used to predict treatment options in some instances (ER and HER2) or with some evidence of prognostic significance in the literature. It is possible that there is an immunohistochemical marker, or panel of markers, yet to be discovered that could identify the potential to switch from DCIS to an invasive phenotype. It is also possible that there may not be such a marker or panel and the heterogeneity of DCIS prevents such prediction with this ‘routine’ technique.

6.3 Genomic Studies of DCIS

The second aim of this study was to create a database of significant size providing information on DCIS samples with genomic, immunohistochemical and demographic data. In this respect the aim has been fulfilled. Chapter 5 contains only a small fraction of the data that is available to be analysed and even in this small subset of the available data there is scope for greater analysis. The entire database has great potential for a number of research questions. Should a researcher wish to examine the role of a single gene of interest and its expression in pure DCIS, DCIS associated with invasion or even its absence then a search of the files can be carried out. Alternatively comparison of groups either currently acknowledged such as the basal-like group or groups not yet identified could be elucidated from this data. This study has produced one of the largest genomic data sets on DCIS created to date. It is hoped that this valuable resource will help define the molecular diversity found in both precursor and invasive breast disease to enable improved treatment options for patients.

One advantage of this dataset is the nature of the information provided. This data is not simply a list of genes that may or may not have potential as biomarkers for therapeutic intervention but also contains demographic data on patients, protein expression, immunohistochemical profiles and a number of genomic identifiers. This includes information on copy neutral loss of heterozygosity which is not produced through previous genomic studies. However, the advent of whole genome profiling at reduced costs does indicate that such data sets for comparison will be available in the future building upon the work produced here. The data is currently being analysed by the King's College bioinformatics team and further insights of how this information can be used are expected.

The third aim of this thesis was to undertake an analysis of archival DCIS samples to identify genomic variation, abnormalities and changes between different pure DCIS

lesions and DCIS lesions associated with invasion. This aim has only been partially fulfilled.

Given the vast amount of data available it is not possible within the realm of this thesis to address each of the possible genes that may, or may not, be involved in progression to an invasive state. The copy number aberrations discussed here are a small subset of all the potential markers identified in this heterogeneous disease. The author also acknowledges that the selection of candidate genes here is based upon a combination of selection based upon literature review of breast cancer pathways and personal choice (see 6.4 Limitations of the Study).

There are few studies have examined the genomic diversity of DCIS in a large number of samples. This is one of the largest to date utilising the relatively new molecular inversion probe array platform. Given the known heterogeneity of DCIS, we focussed upon comparing smaller defined sub-groups of DCIS identified using a surrogate immunopanel for the molecular phenotypes as described in invasive cancer by Perou et al (76). Pure DCIS, DCIS associated with invasive disease and invasive disease have all been compared. Whilst chromosomal changes have been shown across all types of DCIS there with similar frequencies, differences have been identified between DCIS subtypes (triple negative, HER2 positive and oestrogen positive). Some of these are expected (i.e. *HER2* gene amplification on chromosome 17) but many others have yet to be fully analysed. Additionally there are also similarities between pure DCIS, DCIS associated with invasion and invasive breast disease. The overall similarity of copy number aberrations in both DCIS and invasive breast cancer indicates that DCIS already has a significant genetic heterogeneity compared to normal mammary epithelium. It may be that the transition from normal tissue to DCIS is where key drivers of tumourigenesis are found. However, further analysis of DCIS at the genomic level has may be required to identify if all key drivers of the invasive phenotype are in place are at the DCIS stage or if further CNVs are required.

Differences in different types of DCIS and their associated invasive tumours have demonstrated a vast array of copy number changes and identified a host of genes some of which may be involved in the transition to an invasive state.

The use of this MIP arrays to analyse over 80 DCIS and associated invasive breast disease samples has resulted in a vast amount of genomic data. It has to be acknowledged that this thesis cannot hope to give a robust and systematic analysis of all of this data. This work has outlined a few of the genes that may be of significance in the transition state from DCIS to invasion. Whilst there are possible flaws in the selection criteria for the genes highlighted (see limitations of the study), this work has provided a significant amount of genomic data previously unavailable in such a large series which will prove invaluable for further studies on DCIS. In addition to the large amount of information available this series of samples can be analysed further within distinctive subgroups; analysis of high grade versus low grade DCIS, pure DCIS versus DCIS associated with invasion and invasive breast disease are available for further study. Unlike many previous studies, the DCIS samples studied here are fully classified in terms of histopathological features, immunoprofiling and a large amount of detailed genomic data and therefore can be segregated into a variety of subgroups to help elucidate the changes that give rise to such heterogeneity in DCIS. It is hoped that further work upon this series of genomic data will continue to help further our understanding of DCIS and its subsequent progression to invasive disease thus facilitating the development of better clinical treatments and decisions.

The final aim of this study was to identify any protein and/or genomic changes in all DCIS (pure and that associated with invasion) compared to invasive breast disease to determine potential biomarkers responsible for progression to an invasive state. In this respect the study has fallen short of the stated aim. Identification of specific

proteins and genes still remains elusive. However, this body of work has produced a dataset that could potentially be used in conjunction with other research to help determine such candidates in the future. The author acknowledges that this is a challenging proposition given the diversity shown at the molecular level of both precursor lesions and invasive forms of breast neoplasms.

6.4 Limitations of the Study

In this study, samples of DCIS and associated invasive tissues were examined. Due to the natural progression of breast cancers, the timeframe for collection of these samples had to, by necessity, particularly for the DCIS cases, be over a significant period. The analysis of a large cohort of samples over an extended time period is fraught with certain problems. These include, but may not be exclusive of, the following:

6.4.1 Availability of clinical data

Clinical data over a time period may be lost due to changes in saving such data and changes in the fine details and definitions of the dataset collated. The time period for the samples in this study encompassed the switch from a paper-based system and through different computer-based systems and data from one system may have been incompatible with newer or alternative systems. The King's College Breast Cancer Tissue and Data Bank provided a most thorough examination and upgrade of the clinical data available. However, it has to be acknowledged that the data provided to the bank did have omissions. These gaps could be for a variety of reasons; patients moving to different localities, poor data storage, and lack of details in original patient files. The latter is the most likely cause of missing data; as our understanding of the

complexities of breast cancer have improved the information required and subsequent data collection have become increasingly complicated.

As our understanding of breast cancer has improved, so have treatment options. The introduction of new drugs (new chemotherapy agents such as the taxanes and anthracyclines, trastuzumab, tamoxifen and the aromatase inhibitors) and radiotherapy options have varied over time. Additionally, surgical considerations such as the historical use of mastectomy over wide local excision have reduced the number of cases with follow-up samples.

6.4.2 Technical Considerations

Alongside therapeutic and surgical advances, there have been significant changes in the technical and laboratory treatment of samples. Improved fixation, reduced cold ischaemic times, slicing of large samples, better processing and advances in microscopy have all improved the quality of tissue being analysed. This has led to more accurate and better reporting of disease states.

Immunohistochemistry is widely used as a diagnostic tool in histology. Improvements in antibody clones, immunohistochemical detection methods, antigen retrieval and automation have improved the somewhat capricious nature of this science. Accordingly the introduction of external quality assurance schemes to ensure reproducibly and correct laboratory procedures are followed has improved standardisation of this technique. This does however introduce disparities to samples taken over a long time period. Original reporting and scoring of markers, for example, oestrogen receptor have changed as clones have improved and clinical cut-offs have changed. Historically negative ER cases may now be considered ER positive due to enhanced detection. Re-evaluation may not be entirely accurate as changes in the use of fixatives and processing may produce false negative or even false positive

results. Assessment of historical tissue samples should therefore be judged with caution with known positives and negatives from the same time period assessed in the modern setting.

6.4.3 Genomics

The science of genomics has moved at an astonishing pace since the release of the first human genome in 2000 AD. Whole genome analysis is now both available within a relatively short timeframe at much reduced costs. This has huge benefits for research. However this has raised issues regarding the interpretation of such vast amounts of data. This study has undertaken one of the larger genomic studies of DCIS to date using MIP array analysis of over eighty samples. This created a vast amount of bioinformatics data giving almost whole genome wide information on all of these samples. It is beyond the scope of a single PhD thesis to analyse such data, so a compromise on the best approach had to be taken. In this study comparison of different types of DCIS was first undertaken. This created gene lists of often of thousands of possible genes to analyse for each particular genomic aberration (amplification, duplication, CdLOH, CnLOH, gains, losses, total losses, Sc gains). It was after discussion with the bioinformatics team decided appropriate to concentrate on those samples that showed the greatest variation between each other i.e. where copy number differences occurred in one set of samples (e.g. ER positive pure DCIS) but not another (e.g. TN pure DCIS). This gave a slightly more manageable subset ranging from an estimated 1% to 10% of data to be analysed, dependent upon the particular CNA comparison. Even with this reduction, there were still hundreds of possible genes to analyse. Those suggested here have no basis in selection other than they have been cited previously in the literature. This does raise the possibility of exclusion based upon literary bias. In defence of the selection criteria is the understanding at the outset that that this work was never destined to be a stand-alone

study and that further analysis would be essential. This thesis may therefore be regarded as an initial analysis.

6.5 Further Work

As mentioned to in the previous sections, there is a significant amount of further work that may be undertaken beyond this study. For the immunohistochemical analysis there are many antibody markers that could be assessed in the remaining TMA series. In the selection for this study, certain markers of interest in apoptosis (BCL2, TUNEL, survivin), stem cell markers (ALDH1, CD44, CD24), proliferation markers (geminin) were all omitted based solely on considerations of time and cost. These are just a few of the hundreds of markers already available, not including those in development. One of the advantages of the TMA construction in this series is that there is a reserve of tissue that has already has pathological and genomic analysis performed. This will hopefully help define the suitability of this cohort for use with a particular marker of interest.

The genomic component of this thesis has yielded a comprehensive resource for over eighty samples of DCIS lesions. The analysis of these data sets has only just begun. In the present study only a fraction of the data has been examined with a limited number of genes identified. The data mining methods here will be evaluated for their suitability in determining progression from pure DCIS to an invasive phenotype as well as differences between various forms of DCIS lesion. Different methods of analysis can be explored and further extraction of DNA from samples will provide an additional resource for future studies. As molecular techniques become further enhanced these data could be used as a comparative set to validate further methods.

References

1. F.P. OM, S.E. P, A.M M. Breast Pathology. 2nd ed. R GJ, editor: Elsevier Saunders; 2011.
2. Kuhl CK, Schrading S, Bieling HB, Wardelmann E, Leutner CC, Koenig R, et al. MRI for diagnosis of pure ductal carcinoma in situ: a prospective observational study. Lancet. 2007;370(9586):485-92.
3. Evans.A, Pinder.S.E, Puroshotham.A, Bundred.N. Uncertainties in the management of screen-detected ductal carcinoma in situ. In: Programs NCS, editor. 1st ed. Sheffield: NHSBSP; July 2008. p. 28.
4. Boughey JC, Gonzalez RJ, Bonner E, Kuerer HM. Current treatment and clinical trial developments for ductal carcinoma in situ of the breast. Oncologist. 2007;12(11):1276-87.
5. Kumar V, Abbas K. MBBS N, Nelson F, J A, K. KVA. Robbins & Contran Pathological Basis of Disease: Saunders; 2010. 1464 p.
6. Program NHSBS. NHS Breast Screening Programme Review 2012. NHSBHP: http://www.cancerscreening.nhs.uk/breastscreen/publications/nhsbsp-annualreview2012.pdf; 2012.
7. Breast Cancer Statistics http://www.cancerresearchuk.org/cancer-info/cancerstats/types/breast/2014 [
8. **NIH Consensus and State-of-the-Science Statements**. September 22-24 ed2009.
9. SEER Report Cancer Statistics. In: (NPCR) NPoCR, editor. National Program of Cancer Registries (NPCR)2010.
10. Joslyn SA. Ductal carcinoma in situ: trends in geographic, temporal, and demographic patterns of care and survival. Breast J. 2006;12(1):20-7.
11. Pappo I, Wasserman I, Halevy A. Ductal carcinoma in situ of the breast in men: a review. Clin Breast Cancer. 2005;6(4):310-4.
12. Smith KL, Adank M, Kauff N, Lafaro K, Boyd J, Lee JB, et al. BRCA mutations in women with ductal carcinoma in situ. Clin Cancer Res. 2007;13(14):4306-10.
13. Hwang ES, McLennan JL, Moore DH, Crawford BB, Esserman LJ, Ziegler JL. Ductal carcinoma in situ in BRCA mutation carriers. J Clin Oncol. 2007;25(6):642-7.
14. Kerlikowske K, Barclay J, Grady D, Sickles EA, Ernster V. Comparison of risk factors for ductal carcinoma in situ and invasive breast cancer. Journal of the National Cancer Institute. 1997;89(1):76-82.
15. Claus EB, Stowe M, Carter D. Breast carcinoma in situ: risk factors and screening patterns. J Natl Cancer Inst. 2001;93(23):1811-7.
16. Kabat GC, Kim M, Shikany JM, Rodgers AK, Wactawski-Wende J, Lane D, et al. Alcohol consumption and risk of ductal carcinoma in situ of the breast in a cohort of postmenopausal women. Cancer Epidemiol Biomarkers Prev. 2010;19(8):2066-72.
17. Kabat GC, Kim M, Kakani C, Tindle H, Wactawski-Wende J, Ockene JK, et al. Cigarette smoking in relation to risk of ductal carcinoma in situ of the breast in a cohort of postmenopausal women. Am J Epidemiol. 2010;172(5):591-9.
18. Claus EB, Stowe M, Carter D. Oral contraceptives and the risk of ductal breast carcinoma in situ. Breast Cancer Res Treat. 2003;81(2):129-36.
19. Phillips LS, Millikan RC, Schroeder JC, Barnholtz-Sloan JS, Levine BJ. Reproductive and hormonal risk factors for ductal carcinoma in situ of the breast. Cancer Epidemiol Biomarkers Prev. 2009;18(5):1507-14.
20. The Nurses Health Study http://www.channing.harvard.edu/nhs/?page_id=70 [

21. Collins LC, Tamimi RM, Baer HJ, Connolly JL, Colditz GA, Schnitt SJ. Outcome of patients with ductal carcinoma in situ untreated after diagnostic biopsy: results from the Nurses' Health Study. Cancer. 2005;103(9):1778-84.
22. Betsill WL, Rosen PP, Lieberman PH, Robbins GF. Intraductal carcinoma. Long-term follow-up after treatment by biopsy alone. JAMA. 1978;239(18):1863-7.
23. Evans A. The diagnosis and management of pre-invasive breast disease: radiological diagnosis. Breast Cancer Res. 2003;5(5):250-3.
24. Yamada T, Mori N, Watanabe M, Kimijima I, Okumoto T, Seiji K, et al. Radiologic-pathologic correlation of ductal carcinoma in situ. Radiographics. 2010;30(5):1183-98.
25. Cho KR, Seo BK, Kim CH, Whang KW, Kim YH, Kim BH, et al. Non-calcified ductal carcinoma in situ: ultrasound and mammographic findings correlated with histological findings. Yonsei Med J. 2008;49(1):103-10.
26. Breast Pathology. 2nd ed. Philadelphia: Elsevier Saunders; 2011.
27. Boetes C, Mann RM. Ductal carcinoma in situ and breast MRI. Lancet. 2007;370(9586):459-60.
28. Schnitt SJ. The diagnosis and management of pre-invasive breast disease: flat epithelial atypia--classification, pathologic features and clinical significance. Breast Cancer Res. 2003;5(5):263-8.
29. O'Malley FP, Mohsin SK, Badve S, Bose S, Collins LC, Ennis M, et al. Interobserver reproducibility in the diagnosis of flat epithelial atypia of the breast. Mod Pathol. 2006;19(2):172-9.
30. Bombonati A, Sgroi DC. The molecular pathology of breast cancer progression. J Pathol. 2011;223(2):307-17.
31. Lopez-Garcia MA, Geyer FC, Lacroix-Triki M, Marchió C, Reis-Filho JS. Breast cancer precursors revisited: molecular features and progression pathways. Histopathology. 2010;57(2):171-92.
32. Pathology Reporting Of Breast Disease. NHSBSP Publication Number 58 January 2005. NHS Cancer Screening Proammes. Report No.: Contract No.
33. Quinn CM, Ostrowski JL. Cytological and architectural heterogeneity in ductal carcinoma in situ of the breast. J Clin Pathol. 1997;50(7):596-9.
34. C FR. Pre-Invasive Disease: Pathogenesis and Clinical Management. 1st ed: Springer; 2011. 520 p.
35. Holland R, Hendriks JH, Vebeek AL, Mravunac M, Schuurmans Stekhoven JH. Extent, distribution, and mammographic/histological correlations of breast ductal carcinoma in situ. Lancet. 1990;335(8688):519-22.
36. Mai KT, Yazdi HM, Burns BF, Perkins DG. Pattern of distribution of intraductal and infiltrating ductal carcinoma: a three-dimensional study using serial coronal giant sections of the breast. Hum Pathol. 2000;31(4):464-74.
37. Thomson JZ, Evans AJ, Pinder SE, Burrell HC, Wilson AR, Ellis IO. Growth pattern of ductal carcinoma in situ (DCIS): a retrospective analysis based on mammographic findings. Br J Cancer. 2001;85(2):225-7.
38. Silverstein MJ, Poller DN, Waisman JR, Colburn WJ, Barth A, Gierson ED, et al. Prognostic classification of breast ductal carcinoma-in-situ. Lancet. 1995;345(8958):1154-7.
39. Silverstein MJ, Lagios MD, Craig PH, Waisman JR, Lewinsky BS, Colburn WJ, et al. A prognostic index for ductal carcinoma in situ of the breast. Cancer. 1996;77(11):2267-74.
40. Tavassoli FA. Ductal carcinoma in situ: introduction of the concept of ductal intraepithelial neoplasia. Mod Pathol. 1998;11(2):140-54.
41. Holland R, Peterse JL, Millis RR, Eusebi V, Faverly D, van de Vijver MJ, et al. Ductal carcinoma in situ: a proposal for a new classification. Semin Diagn Pathol. 1994;11(3):167-80.

42. Sloane JP, Amendoeira I, Apostolikas N, Bellocq JP, Bianchi S, Boecker W, et al. Consistency achieved by 23 European pathologists in categorizing ductal carcinoma in situ of the breast using five classifications. European Commission Working Group on Breast Screening Pathology. Hum Pathol. 1998;29(10):1056-62.
43. Poller DN, Silverstein MJ, Galea M, Locker AP, Elston CW, Blamey RW, et al. Ideas in pathology. Ductal carcinoma in situ of the breast: a proposal for a new simplified histological classification association between cellular proliferation and c-erbB-2 protein expression. Mod Pathol. 1994;7(2):257-62.
44. Silverstein MJ. The University of Southern California/Van Nuys prognostic index for ductal carcinoma in situ of the breast. Am J Surg. 2003;186(4):337-43.
45. Shoker BS, Sloane JP. DCIS grading schemes and clinical implications. Histopathology. 1999;35(5):393-400.
46. Pinder SE, Duggan C, Ellis IO, Cuzick J, Forbes JF, Bishop H, et al. A new pathological system for grading DCIS with improved prediction of local recurrence: results from the UKCCCR/ANZ DCIS trial. Br J Cancer. 2010;103(1):94-100.
47. Moran MS, Bai HX, Harris EE, Arthur DW, Bailey L, Bellon JR, et al. ACR Appropriateness Criteria(®) Ductal Carcinoma in Situ. Breast J. 2012;18(1):8-15.
48. Donker M, Litière S, Werutsky G, Julien JP, Fentiman IS, Agresti R, et al. Breast-Conserving Treatment With or Without Radiotherapy in Ductal Carcinoma In Situ: 15-Year Recurrence Rates and Outcome After a Recurrence, From the EORTC 10853 Randomized Phase III Trial. J Clin Oncol. 2013;31(32):4054-9.
49. Holmberg L, Garmo H, Granstrand B, Ringberg A, Arnesson LG, Sandelin K, et al. Absolute risk reductions for local recurrence after postoperative radiotherapy after sector resection for ductal carcinoma in situ of the breast. J Clin Oncol. 2008;26(8):1247-52.
50. Cuzick J, Sestak I, Pinder SE, Ellis IO, Forsyth S, Bundred NJ, et al. Effect of tamoxifen and radiotherapy in women with locally excised ductal carcinoma in situ: long-term results from the UK/ANZ DCIS trial. Lancet Oncol. 2011;12(1):21-9.
51. Julien JP, Bijker N, Fentiman IS, Peterse JL, Delledonne V, Rouanet P, et al. Radiotherapy in breast-conserving treatment for ductal carcinoma in situ: first results of the EORTC randomised phase III trial 10853. EORTC Breast Cancer Cooperative Group and EORTC Radiotherapy Group. Lancet. 2000;355(9203):528-33.
52. Bijker N, Meijnen P, Peterse JL, Bogaerts J, Van Hoorebeeck I, Julien JP, et al. Breast-conserving treatment with or without radiotherapy in ductal carcinoma-in-situ: ten-year results of European Organisation for Research and Treatment of Cancer randomized phase III trial 10853--a study by the EORTC Breast Cancer Cooperative Group and EORTC Radiotherapy Group. J Clin Oncol. 2006;24(21):3381-7.
53. Francis A, Thomas J, Fallowfield L, Wallis M, Bartlett JM, Brookes C, et al. Addressing overtreatment of screen detected DCIS; the LORIS trial. Eur J Cancer. 2015;51(16):2296-303.
54. Staley H, McCallum I, Bruce J. Postoperative tamoxifen for ductal carcinoma in situ. Cochrane Database Syst Rev. 2012;10:CD007847.
55. Fisher B, Dignam J, Wolmark N, Wickerham DL, Fisher ER, Mamounas E, et al. Tamoxifen in treatment of intraductal breast cancer: National Surgical Adjuvant Breast and Bowel Project B-24 randomised controlled trial. Lancet. 1999;353(9169):1993-2000.
56. Nath ME, Robinson TM, Tobon H, Chough DM, Sumkin JH. Automated large-core needle biopsy of surgically removed breast lesions: comparison of samples obtained with 14-, 16-, and 18-gauge needles. Radiology. 1995;197(3):739-42.
57. Helbich TH, Rudas M, Haitel A, Kohlberger PD, Thurnher M, Gnant M, et al. Evaluation of needle size for breast biopsy: comparison of 14-, 16-, and 18-gauge biopsy needles. AJR Am J Roentgenol. 1998;171(1):59-63.

58. Houssami N, Ciatto S, Ellis I, Ambrogetti D. Underestimation of malignancy of breast core-needle biopsy: concepts and precise overall and category-specific estimates. Cancer. 2007;109(3):487-95.
59. Shah VI, Raju U, Chitale D, Deshpande V, Gregory N, Strand V. False-negative core needle biopsies of the breast: an analysis of clinical, radiologic, and pathologic findings in 27 concecutive cases of missed breast cancer. Cancer. 2003;97(8):1824-31.
60. Londero V, Zuiani C, Furlan A, Nori J, Bazzocchi M. Role of ultrasound and sonographically guided core biopsy in the diagnostic evaluation of ductal carcinoma in situ (DCIS) of the breast. Radiol Med. 2007;112(6):863-76.
61. Rutstein LA, Johnson RR, Poller WR, Dabbs D, Groblewski J, Rakitt T, et al. Predictors of residual invasive disease after core needle biopsy diagnosis of ductal carcinoma in situ. Breast J. 2007;13(3):251-7.
62. Chan MY, Lim S. Predictors of invasive breast cancer in ductal carcinoma in situ initially diagnosed by core biopsy. Asian J Surg. 2010;33(2):76-82.
63. Hahn M, Kagan KO, Siegmann KC, Krainick-Strobel U, Kraemer B, Fehm T, et al. Mammotome versus ATEC: a comparison of two breast vacuum biopsy techniques under sonographic guidance. Arch Gynecol Obstet. 2010;281(2):287-92.
64. Philpotts LE, Shaheen NA, Carter D, Lange RC, Lee CH. Comparison of rebiopsy rates after stereotactic core needle biopsy of the breast with 11-gauge vacuum suction probe versus 14-gauge needle and automatic gun. AJR Am J Roentgenol. 1999;172(3):683-7.
65. Shi SR, Cote RJ, Taylor CR. Antigen retrieval techniques: current perspectives. J Histochem Cytochem. 2001;49(8):931-7.
66. Park K, Han S, Kim HJ, Kim J, Shin E. HER2 status in pure ductal carcinoma in situ and in the intraductal and invasive components of invasive ductal carcinoma determined by fluorescence in situ hybridization and immunohistochemistry. Histopathology. 2006;48(6):702-7.
67. Borgquist S, Zhou W, Jirström K, Amini RM, Sollie T, Sørlie T, et al. The prognostic role of HER2 expression in ductal breast carcinoma in situ (DCIS); a population-based cohort study. BMC Cancer. 2015;15:468.
68. Kononen J, Bubendorf L, Kallioniemi A, Bärlund M, Schraml P, Leighton S, et al. Tissue microarrays for high-throughput molecular profiling of tumor specimens. Nat Med. 1998;4(7):844-7.
69. Lander ES, Linton LM, Birren B, Nusbaum C, Zody MC, Baldwin J, et al. Initial sequencing and analysis of the human genome. Nature. 2001;409(6822):860-921.
70. Venter JC, Adams MD, Myers EW, Li PW, Mural RJ, Sutton GG, et al. The sequence of the human genome. Science. 2001;291(5507):1304-51.
71. Tuna M, Knuutila S, Mills GB. Uniparental disomy in cancer. Trends Mol Med. 2009;15(3):120-8.
72. Maciejewski JP, Tiu RV, O'Keefe C. Application of array-based whole genome scanning technologies as a cytogenetic tool in haematological malignancies. Br J Haematol. 2009;146(5):479-88.
73. Stankiewicz P, Lupski JR. Structural variation in the human genome and its role in disease. Annu Rev Med. 2010;61:437-55.
74. Mardis ER. A decade's perspective on DNA sequencing technology. Nature. 2011;470(7333):198-203.
75. Hardenbol P, Banér J, Jain M, Nilsson M, Namsaraev EA, Karlin-Neumann GA, et al. Multiplexed genotyping with sequence-tagged molecular inversion probes. Nat Biotechnol. 2003;21(6):673-8.
76. Perou CM, Sørlie T, Eisen MB, van de Rijn M, Jeffrey SS, Rees CA, et al. Molecular portraits of human breast tumours. Nature. 2000;406(6797):747-52.

77. Sørlie T, Perou CM, Tibshirani R, Aas T, Geisler S, Johnsen H, et al. Gene expression patterns of breast carcinomas distinguish tumor subclasses with clinical implications. Proc Natl Acad Sci U S A. 2001;98(19):10869-74.
78. Zhao H, Langerød A, Ji Y, Nowels KW, Nesland JM, Tibshirani R, et al. Different gene expression patterns in invasive lobular and ductal carcinomas of the breast. Mol Biol Cell. 2004;15(6):2523-36.
79. Cheang MC, van de Rijn M, Nielsen TO. Gene expression profiling of breast cancer. Annu Rev Pathol. 2008;3:67-97.
80. Cheang MC, Voduc D, Bajdik C, Leung S, McKinney S, Chia SK, et al. Basal-like breast cancer defined by five biomarkers has superior prognostic value than triple-negative phenotype. Clin Cancer Res. 2008;14(5):1368-76.
81. Livasy CA, Karaca G, Nanda R, Tretiakova MS, Olopade OI, Moore DT, et al. Phenotypic evaluation of the basal-like subtype of invasive breast carcinoma. Mod Pathol. 2006;19(2):264-71.
82. Nielsen TO, Hsu FD, Jensen K, Cheang M, Karaca G, Hu Z, et al. Immunohistochemical and clinical characterization of the basal-like subtype of invasive breast carcinoma. Clin Cancer Res. 2004;10(16):5367-74.
83. Zhao X, Rødland EA, Sørlie T, Naume B, Langerød A, Frigessi A, et al. Combining gene signatures improves prediction of breast cancer survival. PLoS One. 2011;6(3):e17845.
84. Rakha E, Reis-Filho JS. Basal-like breast carcinoma: from expression profiling to routine practice. Arch Pathol Lab Med. 2009;133(6):860-8.
85. Livasy CA, Perou CM, Karaca G, Cowan DW, Maia D, Jackson S, et al. Identification of a basal-like subtype of breast ductal carcinoma in situ. Hum Pathol. 2007;38(2):197-204.
86. Dabbs DJ, Chivukula M, Carter G, Bhargava R. Basal phenotype of ductal carcinoma in situ: recognition and immunohistologic profile. Mod Pathol. 2006;19(11):1506-11.
87. Bryan BB, Schnitt SJ, Collins LC. Ductal carcinoma in situ with basal-like phenotype: a possible precursor to invasive basal-like breast cancer. Mod Pathol. 2006;19(5):617-21.
88. Norum JH, Andersen K, Sørlie T. Lessons learned from the intrinsic subtypes of breast cancer in the quest for precision therapy. Br J Surg. 2014;101(8):925-38.
89. Xu J, Wu X, Zhou WH, Liu AW, Wu JB, Deng JY, et al. Aurora-A identifies early recurrence and poor prognosis and promises a potential therapeutic target in triple negative breast cancer. PLoS One. 2013;8(2):e56919.
90. Yamamoto S, Yamamoto-Ibusuki M, Yamamoto Y, Fujiwara S, Iwase H. A comprehensive analysis of Aurora A; transcript levels are the most reliable in association with proliferation and prognosis in breast cancer. BMC Cancer. 2013;13:217.
91. Ali HR, Dawson SJ, Blows FM, Provenzano E, Leung S, Nielsen T, et al. A Ki67/BCL2 index based on immunohistochemistry is highly prognostic in ER-positive breast cancer. J Pathol. 2012;226(1):97-107.
92. Callagy GM, Webber MJ, Pharoah PD, Caldas C. Meta-analysis confirms BCL2 is an independent prognostic marker in breast cancer. BMC Cancer. 2008;8:153.
93. Dawson SJ, Makretsov N, Blows FM, Driver KE, Provenzano E, Le Quesne J, et al. BCL2 in breast cancer: a favourable prognostic marker across molecular subtypes and independent of adjuvant therapy received. Br J Cancer. 2010;103(5):668-75.
94. Pinder SE, Ellis IO. The diagnosis and management of pre-invasive breast disease: ductal carcinoma in situ (DCIS) and atypical ductal hyperplasia (ADH)--current definitions and classification. Breast Cancer Res. 2003;5(5):254-7.

95. Buerger H, Simon R, Schäfer KL, Diallo R, Littmann R, Poremba C, et al. Genetic relation of lobular carcinoma in situ, ductal carcinoma in situ, and associated invasive carcinoma of the breast. Mol Pathol. 2000;53(3):118-21.
96. Abd El-Rehim DM, Ball G, Pinder SE, Rakha E, Paish C, Robertson JF, et al. High-throughput protein expression analysis using tissue microarray technology of a large well-characterised series identifies biologically distinct classes of breast cancer confirming recent cDNA expression analyses. Int J Cancer. 2005;116(3):340-50.
97. Goldhirsch A, Wood WC, Coates AS, Gelber RD, Thürlimann B, Senn HJ, et al. Strategies for subtypes--dealing with the diversity of breast cancer: highlights of the St. Gallen International Expert Consensus on the Primary Therapy of Early Breast Cancer 2011. Ann Oncol. 2011;22(8):1736-47.
98. Zhou W, Jirström K, Amini RM, Fjällskog ML, Sollie T, Lindman H, et al. Molecular subtypes in ductal carcinoma in situ of the breast and their relation to prognosis: a population-based cohort study. BMC Cancer. 2013;13:512.
99. Camp RL, Neumeister V, Rimm DL. A decade of tissue microarrays: progress in the discovery and validation of cancer biomarkers. J Clin Oncol. 2008;26(34):5630-7.
100. Kyndi M, Sørensen FB, Knudsen H, Overgaard M, Nielsen HM, Andersen J, et al. Tissue microarrays compared with whole sections and biochemical analyses. A subgroup analysis of DBCG 82 b&c. Acta Oncol. 2008;47(4):591-9.
101. Zhang D, Salto-Tellez M, Putti TC, Do E, Koay ES. Reliability of tissue microarrays in detecting protein expression and gene amplification in breast cancer. Mod Pathol. 2003;16(1):79-84.
102. Ruiz C, Seibt S, Al Kuraya K, Siraj AK, Mirlacher M, Schraml P, et al. Tissue microarrays for comparing molecular features with proliferation activity in breast cancer. Int J Cancer. 2006;118(9):2190-4.
103. Graham AD, Faratian D, Rae F, Thomas JS. Tissue microarray technology in the routine assessment of HER-2 status in invasive breast cancer: a prospective study of the use of immunohistochemistry and fluorescence in situ hybridization. Histopathology. 2008;52(7):847-55.
104. Bhargava R, Lal P, Chen B. Feasibility of using tissue microarrays for the assessment of HER-2 gene amplification by fluorescence in situ hybridization in breast carcinoma. Diagn Mol Pathol. 2004;13(4):213-6.
105. Sapino A, Marchiò C, Senetta R, Castellano I, Macrì L, Cassoni P, et al. Routine assessment of prognostic factors in breast cancer using a multicore tissue microarray procedure. Virchows Arch. 2006;449(3):288-96.
106. Hunter S, Jones P, Mitchell A, Apweiler R, Attwood TK, Bateman A, et al. InterPro in 2011: new developments in the family and domain prediction database. Nucleic Acids Res. 2012;40(Database issue):D306-12.
107. McDowall J. Estrogen Receptors https://www.ebi.ac.uk/interpro/potm/2003_4/Page_1.htm2011 [
108. Jones P, Binns D, McMenamin C, McAnulla C, Hunter S. The InterPro BioMart: federated query and web service access to the InterPro Resource. Database (Oxford). 2011;2011:bar033.
109. Kumar R, Thompson EB. The structure of the nuclear hormone receptors. Steroids. 1999;64(5):310-9.
110. Kumar R, Zakharov MN, Khan SH, Miki R, Jang H, Toraldo G, et al. The dynamic structure of the estrogen receptor. J Amino Acids. 2011;2011:812540.
111. Enmark E, Gustafsson JA. Oestrogen receptors - an overview. J Intern Med. 1999;246(2):133-8.
112. Mangelsdorf DJ, Thummel C, Beato M, Herrlich P, Schütz G, Umesono K, et al. The nuclear receptor superfamily: the second decade. Cell. 1995;83(6):835-9.

113. Pike AC, Brzozowski AM, Hubbard RE, Bonn T, Thorsell AG, Engström O, et al. Structure of the ligand-binding domain of oestrogen receptor beta in the presence of a partial agonist and a full antagonist. EMBO J. 1999;18(17):4608-18.
114. Segars JH, Driggers PH. Estrogen action and cytoplasmic signaling cascades. Part I: membrane-associated signaling complexes. Trends Endocrinol Metab. 2002;13(8):349-54.
115. McDevitt MA, Glidewell-Kenney C, Jimenez MA, Ahearn PC, Weiss J, Jameson JL, et al. New insights into the classical and non-classical actions of estrogen: evidence from estrogen receptor knock-out and knock-in mice. Mol Cell Endocrinol. 2008;290(1-2):24-30.
116. Anderson E. The role of oestrogen and progesterone receptors in human mammary development and tumorigenesis. Breast Cancer Res. 2002;4(5):197-201.
117. Gown AM. Current issues in ER and HER2 testing by IHC in breast cancer. Mod Pathol. 2008;21 Suppl 2:S8-S15.
118. Payne SJ, Bowen RL, Jones JL, Wells CA. Predictive markers in breast cancer--the present. Histopathology. 2008;52(1):82-90.
119. Pike MC, Spicer DV, Dahmoush L, Press MF. Estrogens, progestogens, normal breast cell proliferation, and breast cancer risk. Epidemiol Rev. 1993;15(1):17-35.
120. Kerlikowske K, Molinaro AM, Gauthier ML, Berman HK, Waldman F, Bennington J, et al. Biomarker expression and risk of subsequent tumors after initial ductal carcinoma in situ diagnosis. J Natl Cancer Inst. 2010;102(9):627-37.
121. Provenzano E, Hopper JL, Giles GG, Marr G, Venter DJ, Armes JE. Biological markers that predict clinical recurrence in ductal carcinoma in situ of the breast. Eur J Cancer. 2003;39(5):622-30.
122. Zhou W, Johansson C, Jirström K, Ringberg A, Blomqvist C, Amini RM, et al. A Comparison of Tumor Biology in Primary Ductal Carcinoma In Situ Recurring as Invasive Carcinoma versus a New In Situ. Int J Breast Cancer. 2013;2013:582134.
123. Pritchard KI. Breast cancer prevention with selective estrogen receptor modulators: a perspective. Ann N Y Acad Sci. 2001;949:89-98.
124. Arpino G, Weiss H, Lee AV, Schiff R, De Placido S, Osborne CK, et al. Estrogen receptor-positive, progesterone receptor-negative breast cancer: association with growth factor receptor expression and tamoxifen resistance. J Natl Cancer Inst. 2005;97(17):1254-61.
125. Howell A, Cuzick J, Baum M, Buzdar A, Dowsett M, Forbes JF, et al. Results of the ATAC (Arimidex, Tamoxifen, Alone or in Combination) trial after completion of 5 years' adjuvant treatment for breast cancer. Lancet. 2005;365(9453):60-2.
126. Cuzick J, Sestak I, Baum M, Buzdar A, Howell A, Dowsett M, et al. Effect of anastrozole and tamoxifen as adjuvant treatment for early-stage breast cancer: 10-year analysis of the ATAC trial. Lancet Oncol. 2010;11(12):1135-41.
127. Salomon DS, Brandt R, Ciardiello F, Normanno N. Epidermal growth factor-related peptides and their receptors in human malignancies. Crit Rev Oncol Hematol. 1995;19(3):183-232.
128. Moasser MM. The oncogene HER2: its signaling and transforming functions and its role in human cancer pathogenesis. Oncogene. 2007;26(45):6469-87.
129. Burgess AW, Cho HS, Eigenbrot C, Ferguson KM, Garrett TP, Leahy DJ, et al. An open-and-shut case? Recent insights into the activation of EGF/ErbB receptors. Mol Cell. 2003;12(3):541-52.
130. Zhang X, Gureasko J, Shen K, Cole PA, Kuriyan J. An allosteric mechanism for activation of the kinase domain of epidermal growth factor receptor. Cell. 2006;125(6):1137-49.
131. Hubbard SR, Miller WT. Receptor tyrosine kinases: mechanisms of activation and signaling. Curr Opin Cell Biol. 2007;19(2):117-23.

132. Arkhipov A, Shan Y, Kim ET, Dror RO, Shaw DE. Her2 activation mechanism reflects evolutionary preservation of asymmetric ectodomain dimers in the human EGFR family. Elife. 2013;2:e00708.
133. Eccles SA, Modjtahedi H, Box G, Court W, Sandle J, Dean CJ. Significance of the c-erbB family of receptor tyrosine kinases in metastatic cancer and their potential as targets for immunotherapy. Invasion Metastasis. 1994;14(1-6):337-48.
134. Woodburn JR. The epidermal growth factor receptor and its inhibition in cancer therapy. Pharmacol Ther. 1999;82(2-3):241-50.
135. Kamath S, Buolamwini JK. Targeting EGFR and HER-2 receptor tyrosine kinases for cancer drug discovery and development. Med Res Rev. 2006;26(5):569-94.
136. Flynn JF, Wong C, Wu JM. Anti-EGFR Therapy: Mechanism and Advances in Clinical Efficacy in Breast Cancer. J Oncol. 2009;2009:526963.
137. Walker RA, Bartlett JM, Dowsett M, Ellis IO, Hanby AM, Jasani B, et al. HER2 testing in the UK: further update to recommendations. J Clin Pathol. 2008;61(7):818-24.
138. Hanahan D, Weinberg RA. The hallmarks of cancer. Cell. 2000;100(1):57-70.
139. Scholzen T, Gerdes J. The Ki-67 protein: from the known and the unknown. J Cell Physiol. 2000;182(3):311-22.
140. Gerdes J, Schwab U, Lemke H, Stein H. Production of a mouse monoclonal antibody reactive with a human nuclear antigen associated with cell proliferation. Int J Cancer. 1983;31(1):13-20.
141. Brown DC, Gatter KC. Ki67 protein: the immaculate deception? Histopathology. 2002;40(1):2-11.
142. Rahmanzadeh R, Hüttmann G, Gerdes J, Scholzen T. Chromophore-assisted light inactivation of pKi-67 leads to inhibition of ribosomal RNA synthesis. Cell Prolif. 2007;40(3):422-30.
143. Endl E, Gerdes J. The Ki-67 protein: fascinating forms and an unknown function. Exp Cell Res. 2000;257(2):231-7.
144. Schlüter C, Duchrow M, Wohlenberg C, Becker MH, Key G, Flad HD, et al. The cell proliferation-associated antigen of antibody Ki-67: a very large, ubiquitous nuclear protein with numerous repeated elements, representing a new kind of cell cycle-maintaining proteins. J Cell Biol. 1993;123(3):513-22.
145. Hofmann K, Bucher P. The FHA domain: a putative nuclear signalling domain found in protein kinases and transcription factors. Trends Biochem Sci. 1995;20(9):347-9.
146. Chelsky D, Ralph R, Jonak G. Sequence requirements for synthetic peptide-mediated translocation to the nucleus. Mol Cell Biol. 1989;9(6):2487-92.
147. Dingwall C, Laskey RA. Nuclear targeting sequences--a consensus? Trends Biochem Sci. 1991;16(12):478-81.
148. Silver PA. How proteins enter the nucleus. Cell. 1991;64(3):489-97.
149. Bullwinkel J, Baron-Lühr B, Lüdemann A, Wohlenberg C, Gerdes J, Scholzen T. Ki-67 protein is associated with ribosomal RNA transcription in quiescent and proliferating cells. J Cell Physiol. 2006;206(3):624-35.
150. Darb-Esfahani S, Loibl S, Müller BM, Roller M, Denkert C, Komor M, et al. Identification of biology-based breast cancer types with distinct predictive and prognostic features: role of steroid hormone and HER2 receptor expression in patients treated with neoadjuvant anthracycline/taxane-based chemotherapy. Breast Cancer Res. 2009;11(5):R69.
151. Jones RL, Salter J, A'Hern R, Nerurkar A, Parton M, Reis-Filho JS, et al. The prognostic significance of Ki67 before and after neoadjuvant chemotherapy in breast cancer. Breast Cancer Res Treat. 2009;116(1):53-68.

152. Cheang MC, Chia SK, Voduc D, Gao D, Leung S, Snider J, et al. Ki67 index, HER2 status, and prognosis of patients with luminal B breast cancer. J Natl Cancer Inst. 2009;101(10):736-50.
153. Altintas S, Lambein K, Huizing MT, Braems G, Asjoe FT, Hellemans H, et al. Prognostic significance of oncogenic markers in ductal carcinoma in situ of the breast: a clinicopathologic study. Breast J. 2009;15(2):120-32.
154. Ruiz Martín J, Pérez Sánchez C, de las Heras Camino A. Three molecular classifications surrogate to four immunohistochemical markers in 374 invasive breast carcinomas with long follow-up: which is better? Pathol Res Pract. 2013;209(6):337-44.
155. Bochman ML, Schwacha A. The Mcm complex: unwinding the mechanism of a replicative helicase. Microbiol Mol Biol Rev. 2009;73(4):652-83.
156. Madine MA, Swietlik M, Pelizon C, Romanowski P, Mills AD, Laskey RA. The roles of the MCM, ORC, and Cdc6 proteins in determining the replication competence of chromatin in quiescent cells. J Struct Biol. 2000;129(2-3):198-210.
157. Maine GT, Sinha P, Tye BK. Mutants of S. cerevisiae defective in the maintenance of minichromosomes. Genetics. 1984;106(3):365-85.
158. Takahashi K, Yamada H, Yanagida M. Fission yeast minichromosome loss mutants mis cause lethal aneuploidy and replication abnormality. Mol Biol Cell. 1994;5(10):1145-58.
159. Chong JP, Blow JJ. DNA replication licensing factor. Prog Cell Cycle Res. 1996;2:83-90.
160. Bochman ML, Schwacha A. The Mcm2-7 complex has in vitro helicase activity. Mol Cell. 2008;31(2):287-93.
161. Lei M, Tye BK. Initiating DNA synthesis: from recruiting to activating the MCM complex. J Cell Sci. 2001;114(Pt 8):1447-54.
162. Bell SP, Mitchell J, Leber J, Kobayashi R, Stillman B. The multidomain structure of Orc1p reveals similarity to regulators of DNA replication and transcriptional silencing. Cell. 1995;83(4):563-8.
163. Nishitani H, Lygerou Z, Nishimoto T, Nurse P. The Cdt1 protein is required to license DNA for replication in fission yeast. Nature. 2000;404(6778):625-8.
164. Bochman ML, Bell SP, Schwacha A. Subunit organization of Mcm2-7 and the unequal role of active sites in ATP hydrolysis and viability. Mol Cell Biol. 2008;28(19):5865-73.
165. Gonzalez MA, Pinder SE, Callagy G, Vowler SL, Morris LS, Bird K, et al. Minichromosome maintenance protein 2 is a strong independent prognostic marker in breast cancer. J Clin Oncol. 2003;21(23):4306-13.
166. Sanchez-Berrondo J, Mesa P, Ibarra A, Martínez-Jiménez MI, Blanco L, Méndez J, et al. Molecular architecture of a multifunctional MCM complex. Nucleic Acids Res. 2012;40(3):1366-80.
167. Freeman A, Morris LS, Mills AD, Stoeber K, Laskey RA, Williams GH, et al. Minichromosome maintenance proteins as biological markers of dysplasia and malignancy. Clin Cancer Res. 1999;5(8):2121-32.
168. Sirieix PS, O'Donovan M, Brown J, Save V, Coleman N, Fitzgerald RC. Surface expression of minichromosome maintenance proteins provides a novel method for detecting patients at risk for developing adenocarcinoma in Barrett's esophagus. Clin Cancer Res. 2003;9(7):2560-6.
169. Scott IS, Morris LS, Bird K, Davies RJ, Vowler SL, Rushbrook SM, et al. A novel immunohistochemical method to estimate cell-cycle phase distribution in archival tissue: implications for the prediction of outcome in colorectal cancer. J Pathol. 2003;201(2):187-97.
170. Shetty A, Loddo M, Fanshawe T, Prevost AT, Sainsbury R, Williams GH, et al. DNA replication licensing and cell cycle kinetics of normal and neoplastic breast. Br J Cancer. 2005;93(11):1295-300.

171. Gonzalez MA, Pinder SE, Callagy G, Vowler SL, Morris LS, Bird K, et al. Minichromosome maintenance protein 2 is a strong independent prognostic marker in breast cancer. J Clin Oncol. 2003;21(23):4306-13.
172. Gonzalez MA, Tachibana KE, Chin SF, Callagy G, Madine MA, Vowler SL, et al. Geminin predicts adverse clinical outcome in breast cancer by reflecting cell-cycle progression. J Pathol. 2004;204(2):121-30.
173. Wojnar A, Kobierzycki C, Krolicka A, Pula B, Podhorska-Okolow M, Dziegiel P. Correlation of Ki-67 and MCM-2 proliferative marker expression with grade of histological malignancy (G) in ductal breast cancers. Folia Histochem Cytobiol. 2010;48(3):442-6.
174. Saydam O, Senol O, Schaaij-Visser TB, Pham TV, Piersma SR, Stemmer-Rachamimov AO, et al. Comparative protein profiling reveals minichromosome maintenance (MCM) proteins as novel potential tumor markers for meningiomas. J Proteome Res. 2010;9(1):485-94.
175. Honeycutt KA, Chen Z, Koster MI, Miers M, Nuchtern J, Hicks J, et al. Deregulated minichromosomal maintenance protein MCM7 contributes to oncogene driven tumorigenesis. Oncogene. 2006;25(29):4027-32.
176. Williams GH, Swinn R, Prevost AT, De Clive-Lowe P, Halsall I, Going JJ, et al. Diagnosis of oesophageal cancer by detection of minichromosome maintenance 5 protein in gastric aspirates. Br J Cancer. 2004;91(4):714-9.
177. Wharton SB, Chan KK, Anderson JR, Stoeber K, Williams GH. Replicative Mcm2 protein as a novel proliferation marker in oligodendrogliomas and its relationship to Ki67 labelling index, histological grade and prognosis. Neuropathol Appl Neurobiol. 2001;27(4):305-13.
178. Meng MV, Grossfeld GD, Williams GH, Dilworth S, Stoeber K, Mulley TW, et al. Minichromosome maintenance protein 2 expression in prostate: characterization and association with outcome after therapy for cancer. Clin Cancer Res. 2001;7(9):2712-8.
179. Reena RM, Mastura M, Siti-Aishah MA, Munirah MA, Norlia A, Naqiyah I, et al. Minichromosome maintenance protein 2 is a reliable proliferative marker in breast carcinoma. Ann Diagn Pathol. 2008;12(5):340-3.
180. Nasir A, Chen DT, Gruidl M, Henderson-Jackson EB, Venkataramu C, McCarthy SM, et al. Novel molecular markers of malignancy in histologically normal and benign breast. Patholog Res Int. 2011;2011:489064.
181. Taylor-Papadimitriou J, Stampfer M, Bartek J, Lewis A, Boshell M, Lane EB, et al. Keratin expression in human mammary epithelial cells cultured from normal and malignant tissue: relation to in vivo phenotypes and influence of medium. J Cell Sci. 1989;94 (Pt 3):403-13.
182. Moll R, Franke WW, Schiller DL, Geiger B, Krepler R. The catalog of human cytokeratins: patterns of expression in normal epithelia, tumors and cultured cells. Cell. 1982;31(1):11-24.
183. Jarasch ED, Nagle RB, Kaufmann M, Maurer C, Böcker WJ. Differential diagnosis of benign epithelial proliferations and carcinomas of the breast using antibodies to cytokeratins. Hum Pathol. 1988;19(3):276-89.
184. Cleator S, Heller W, Coombes RC. Triple-negative breast cancer: therapeutic options. Lancet Oncol. 2007;8(3):235-44.
185. Ross JS, Fletcher JA. The HER-2/neu Oncogene in Breast Cancer: Prognostic Factor, Predictive Factor, and Target for Therapy. Oncologist. 1998;3(4):237-52.
186. Zhao J, Wu R, Au A, Marquez A, Yu Y, Shi Z. Determination of HER2 gene amplification by chromogenic in situ hybridization (CISH) in archival breast carcinoma. Mod Pathol. 2002;15(6):657-65.

187. Dowsett M, Nielsen TO, A'Hern R, Bartlett J, Coombes RC, Cuzick J, et al. Assessment of Ki67 in breast cancer: recommendations from the International Ki67 in Breast Cancer working group. J Natl Cancer Inst. 2011;103(22):1656-64.
188. Walker RA, Hanby A, Pinder SE, Thomas J, Ellis IO, Subgroup NCCfBPR. Current issues in diagnostic breast pathology. J Clin Pathol. 2012;65(9):771-85.
189. Poller DN, Snead DR, Roberts EC, Galea M, Bell JA, Gilmour A, et al. Oestrogen receptor expression in ductal carcinoma in situ of the breast: relationship to flow cytometric analysis of DNA and expression of the c-erbB-2 oncoprotein. Br J Cancer. 1993;68(1):156-61.
190. Thomas J, Hanby A, Pinder S, Ellis I, Macartney J, Clements K, et al. Implications of inconsistent measurement of ER status in non-invasive breast cancer: a study of 1,684 cases from the Sloane Project. Breast J. 2008;14(1):33-8.
191. Karayiannakis AJ, Bastounis EA, Chatzigianni EB, Makri GG, Alexiou D, Karamanakos P. Immunohistochemical detection of oestrogen receptors in ductal carcinoma in situ of the breast. Eur J Surg Oncol. 1996;22(6):578-82.
192. Hannemann J, Velds A, Halfwerk JB, Kreike B, Peterse JL, van de Vijver MJ. Classification of ductal carcinoma in situ by gene expression profiling. Breast Cancer Res. 2006;8(5):R61.
193. Thomas J, Evans A, Macartney J, Pinder SE, Hanby A, Ellis I, et al. Radiological and pathological size estimations of pure ductal carcinoma in situ of the breast, specimen handling and the influence on the success of breast conservation surgery: a review of 2564 cases from the Sloane Project. Br J Cancer. 2010;102(2):285-93.
194. Hu Z, Fan C, Oh DS, Marron JS, He X, Qaqish BF, et al. The molecular portraits of breast tumors are conserved across microarray platforms. BMC Genomics. 2006;7:96.
195. Sørlie T. Molecular portraits of breast cancer: tumour subtypes as distinct disease entities. Eur J Cancer. 2004;40(18):2667-75.
196. Meijnen P, Peterse JL, Antonini N, Rutgers EJ, van de Vijver MJ. Immunohistochemical categorisation of ductal carcinoma in situ of the breast. Br J Cancer. 2008;98(1):137-42.
197. Clark SE, Warwick J, Carpenter R, Bowen RL, Duffy SW, Jones JL. Molecular subtyping of DCIS: heterogeneity of breast cancer reflected in pre-invasive disease. Br J Cancer. 2011;104(1):120-7.
198. Zhou W, Jirström K, Johansson C, Amini RM, Blomqvist C, Agbaje O, et al. Long-term survival of women with basal-like ductal carcinoma in situ of the breast: a population-based cohort study. BMC Cancer. 2010;10:653.
199. Steinman S, Wang J, Bourne P, Yang Q, Tang P. Expression of cytokeratin markers, ER-alpha, PR, HER-2/neu, and EGFR in pure ductal carcinoma in situ (DCIS) and DCIS with co-existing invasive ductal carcinoma (IDC) of the breast. Ann Clin Lab Sci. 2007;37(2):127-34.
200. Tamimi RM, Baer HJ, Marotti J, Galan M, Galaburda L, Fu Y, et al. Comparison of molecular phenotypes of ductal carcinoma in situ and invasive breast cancer. Breast Cancer Res. 2008;10(4):R67.
201. Tang P, Skinner KA, Hicks DG. Molecular classification of breast carcinomas by immunohistochemical analysis: are we ready? Diagn Mol Pathol. 2009;18(3):125-32.
202. Hernandez L, Wilkerson PM, Lambros MB, Campion-Flora A, Rodrigues DN, Gauthier A, et al. Genomic and mutational profiling of ductal carcinomas in situ and matched adjacent invasive breast cancers reveals intra-tumour genetic heterogeneity and clonal selection. J Pathol. 2012;227(1):42-52.
203. Ma XJ, Salunga R, Tuggle JT, Gaudet J, Enright E, McQuary P, et al. Gene expression profiles of human breast cancer progression. Proc Natl Acad Sci U S A. 2003;100(10):5974-9.

204. Buerger H, Otterbach F, Simon R, Poremba C, Diallo R, Decker T, et al. Comparative genomic hybridization of ductal carcinoma in situ of the breast-evidence of multiple genetic pathways. J Pathol. 1999;187(4):396-402.
205. Rydén L, Landberg G, Stål O, Nordenskjöld B, Fernö M, Bendahl PO. HER2 status in hormone receptor positive premenopausal primary breast cancer adds prognostic, but not tamoxifen treatment predictive, information. Breast Cancer Res Treat. 2008;109(2):351-7.
206. Alqaisi A, Chen L, Romond E, Chambers M, Stevens M, Pasley G, et al. Impact of estrogen receptor (ER) and human epidermal growth factor receptor-2 (HER2) co-expression on breast cancer disease characteristics: implications for tumor biology and research. Breast Cancer Res Treat. 2014;148(2):437-44.
207. Vincent-Salomon A, Lucchesi C, Gruel N, Raynal V, Pierron G, Goudefroye R, et al. Integrated genomic and transcriptomic analysis of ductal carcinoma in situ of the breast. Clin Cancer Res. 2008;14(7):1956-65.
208. Yao J, Weremowicz S, Feng B, Gentleman RC, Marks JR, Gelman R, et al. Combined cDNA array comparative genomic hybridization and serial analysis of gene expression analysis of breast tumor progression. Cancer Res. 2006;66(8):4065-78.
209. Gao Y, Niu Y, Wang X, Wei L, Lu S. Genetic changes at specific stages of breast cancer progression detected by comparative genomic hybridization. J Mol Med (Berl). 2009;87(2):145-52.
210. Liao S, Desouki MM, Gaile DP, Shepherd L, Nowak NJ, Conroy J, et al. Differential copy number aberrations in novel candidate genes associated with progression from in situ to invasive ductal carcinoma of the breast. Genes Chromosomes Cancer. 2012;51(12):1067-78.
211. Cowell CF, Weigelt B, Sakr RA, Ng CK, Hicks J, King TA, et al. Progression from ductal carcinoma in situ to invasive breast cancer: revisited. Mol Oncol. 2013;7(5):859-69.
212. Iafrate AJ, Feuk L, Rivera MN, Listewnik ML, Donahoe PK, Qi Y, et al. Detection of large-scale variation in the human genome. Nat Genet. 2004;36(9):949-51.
213. Shlien A, Malkin D. Copy number variations and cancer. Genome Med. 2009;1(6):62.
214. R ZN. Copy Number Profiling in Normal and Tumour Genomes2012.
215. Ueno T, Emi M, Sato H, Ito N, Muta M, Kuroi K, et al. Genome-wide copy number analysis in primary breast cancer. Expert Opin Ther Targets. 2012;16 Suppl 1:S31-5.
216. Byler S, Goldgar S, Heerboth S, Leary M, Housman G, Moulton K, et al. Genetic and epigenetic aspects of breast cancer progression and therapy. Anticancer Res. 2014;34(3):1071-7.
217. Xu H, Eirew P, Mullaly SC, Aparicio S. The omics of triple-negative breast cancers. Clin Chem. 2014;60(1):122-33.
218. Reis-Filho JS, Simpson PT, Gale T, Lakhani SR. The molecular genetics of breast cancer: the contribution of comparative genomic hybridization. Pathol Res Pract. 2005;201(11):713-25.
219. Martin V, Botta F, Zanellato E, Molinari F, Crippa S, Mazzucchelli L, et al. Molecular characterization of EGFR and EGFR-downstream pathways in triple negative breast carcinomas with basal like features. Histol Histopathol. 2012;27(6):785-92.
220. Ando Y, Iwase H, Ichihara S, Toyoshima S, Nakamura T, Yamashita H, et al. Loss of heterozygosity and microsatellite instability in ductal carcinoma in situ of the breast. Cancer Lett. 2000;156(2):207-14.
221. Johnson CE, Gorringe KL, Thompson ER, Opeskin K, Boyle SE, Wang Y, et al. Identification of copy number alterations associated with the progression of DCIS to invasive ductal carcinoma. Breast Cancer Res Treat. 2011.

222. Lee S, Stewart S, Nagtegaal I, Luo J, Wu Y, Colditz G, et al. Differentially Expressed Genes Regulating the Progression of Ductal Carcinoma in Situ to Invasive Breast Cancer. Cancer Res. 2012.
223. Carraro DM, Elias EV, Andrade VP. Ductal carcinoma in situ of the breast: morphological and molecular features implicated in progression. Biosci Rep. 2013.
224. Vargas AC, Reed AE, Waddell N, Lane A, Reid LE, Smart CE, et al. Gene expression profiling of tumour epithelial and stromal compartments during breast cancer progression. Breast Cancer Res Treat. 2012.
225. Mi H, Muruganujan A, Casagrande JT, Thomas PD. Large-scale gene function analysis with the PANTHER classification system. Nat Protoc. 2013;8(8):1551-66.
226. Seligson DB, Horvath S, Shi T, Yu H, Tze S, Grunstein M, et al. Global histone modification patterns predict risk of prostate cancer recurrence. Nature. 2005;435(7046):1262-6.
227. Elsheikh SE, Green AR, Rakha EA, Powe DG, Ahmed RA, Collins HM, et al. Global histone modifications in breast cancer correlate with tumor phenotypes, prognostic factors, and patient outcome. Cancer Res. 2009;69(9):3802-9.
228. Kadota M, Sato M, Duncan B, Ooshima A, Yang HH, Diaz-Meyer N, et al. Identification of novel gene amplifications in breast cancer and coexistence of gene amplification with an activating mutation of PIK3CA. Cancer Res. 2009;69(18):7357-65.
229. Lightfoot HM, Lark A, Livasy CA, Moore DT, Cowan D, Dressler L, et al. Upregulation of focal adhesion kinase (FAK) expression in ductal carcinoma in situ (DCIS) is an early event in breast tumorigenesis. Breast Cancer Res Treat. 2004;88(2):109-16.
230. Xie F, Wang Q, Chen Y, Gu Y, Mao H, Zeng W, et al. Costimulatory molecule OX40/OX40L expression in ductal carcinoma in situ and invasive ductal carcinoma of breast: an immunohistochemistry-based pilot study. Pathol Res Pract. 2010;206(11):735-9.
231. Howard BA. The role of NRG3 in mammary development. J Mammary Gland Biol Neoplasia. 2008;13(2):195-203.
232. Kogata N, Oliemuller E, Wansbury O, Howard BA. Neuregulin-3 regulates epithelial progenitor cell positioning and specifies mammary phenotype. Stem Cells Dev. 2014;23(22):2758-70.
233. Varley JM, Armour J, Swallow JE, Jeffreys AJ, Ponder BA, T'Ang A, et al. The retinoblastoma gene is frequently altered leading to loss of expression in primary breast tumours. Oncogene. 1989;4(6):725-9.
234. Curtis C, Shah SP, Chin SF, Turashvili G, Rueda OM, Dunning MJ, et al. The genomic and transcriptomic architecture of 2,000 breast tumours reveals novel subgroups. Nature. 2012;486(7403):346-52.
235. Visse R, Nagase H. Matrix metalloproteinases and tissue inhibitors of metalloproteinases: structure, function, and biochemistry. Circ Res. 2003;92(8):827-39.
236. Cao YW, Wan GX, Zhao CX, Hu JM, Li L, Liang WH, et al. Notch1 single nucleotide polymorphism rs3124591 is associated with the risk of development of invasive ductal breast carcinoma in a Chinese population. Int J Clin Exp Pathol. 2014;7(7):4286-94.
237. Yu Q, Li Y, Mu K, Li Z, Meng Q, Wu X, et al. Amplification of Mdmx and overexpression of MDM2 contribute to mammary carcinogenesis by substituting for p53 mutations. Diagn Pathol. 2014;9:71.
238. Carlsson H, Petersson S, Enerbäck C. Cluster analysis of S100 gene expression and genes correlating to psoriasin (S100A7) expression at different stages of breast cancer development. Int J Oncol. 2005;27(6):1473-81.

239. Moon HG, Hwang KT, Kim JA, Kim HS, Lee MJ, Jung EM, et al. NFIB is a potential target for estrogen receptor-negative breast cancers. Mol Oncol. 2011;5(6):538-44.
240. Wetterskog D, Lopez-Garcia MA, Lambros MB, A'Hern R, Geyer FC, Milanezi F, et al. Adenoid cystic carcinomas constitute a genomically distinct subgroup of triple-negative and basal-like breast cancers. J Pathol. 2012;226(1):84-96.
241. Soysal S, Obermann EC, Gao F, Oertli D, Gillanders WE, Viehl CT, et al. PTP1B expression is an independent positive prognostic factor in human breast cancer. Breast Cancer Res Treat. 2013;137(2):637-44.
242. Fontanil T, Rúa S, Llamazares M, Moncada-Pazos A, Quirós PM, García-Suárez O, et al. Interaction between the ADAMTS-12 metalloprotease and fibulin-2 induces tumor-suppressive effects in breast cancer cells. Oncotarget. 2014;5(5):1253-64.
243. Naik MU, Pham NT, Beebe K, Dai W, Naik UP. Calcium-dependent inhibition of polo-like kinase 3 activity by CIB1 in breast cancer cells. Int J Cancer. 2011;128(3):587-96.
244. Fonseca-Sanchéz MA, Pérez-Plasencia C, Fernández-Retana J, Arechaga-Ocampo E, Marchat LA, Rodríguez-Cuevas S, et al. microRNA-18b is upregulated in breast cancer and modulates genes involved in cell migration. Oncol Rep. 2013;30(5):2399-410.
245. Davis LM, Harris C, Tang L, Doherty P, Hraber P, Sakai Y, et al. Amplification patterns of three genomic regions predict distant recurrence in breast carcinoma. J Mol Diagn. 2007;9(3):327-36.
246. Stebbing J, Zhang H, Xu Y, Lit LC, Green AR, Grothey A, et al. KSR1 regulates BRCA1 degradation and inhibits breast cancer growth. Oncogene. 2014;0.
247. Rakha EA, Boyce RW, Abd El-Rehim D, Kurien T, Green AR, Paish EC, et al. Expression of mucins (MUC1, MUC2, MUC3, MUC4, MUC5AC and MUC6) and their prognostic significance in human breast cancer. Mod Pathol. 2005;18(10):1295-304.
248. Do SI, Kim K, Kim DH, Chae SW, Park YL, Park CH, et al. Associations between the Expression of Mucins (MUC1, MUC2, MUC5AC, and MUC6) and Clinicopathologic Parameters of Human Breast Ductal Carcinomas. J Breast Cancer. 2013;16(2):152-8.
249. Mohseni M, Cidado J, Croessmann S, Cravero K, Cimino-Mathews A, Wong HY, et al. MACROD2 overexpression mediates estrogen independent growth and tamoxifen resistance in breast cancers. Proc Natl Acad Sci U S A. 2014;111(49):17606-11.
250. Fu A, Leaderer D, Zheng T, Hoffman AE, Stevens RG, Zhu Y. Genetic and epigenetic associations of circadian gene TIMELESS and breast cancer risk. Mol Carcinog. 2012;51(12):923-9.
251. Johnson CE, Gorringe KL, Thompson ER, Opeskin K, Boyle SE, Wang Y, et al. Identification of copy number alterations associated with the progression of DCIS to invasive ductal carcinoma. Breast Cancer Res Treat. 2012;133(3):889-98.
252. Sun PH, Ye L, Mason MD, Jiang WG. Protein tyrosine phosphatase kappa (PTPRK) is a negative regulator of adhesion and invasion of breast cancer cells, and associates with poor prognosis of breast cancer. J Cancer Res Clin Oncol. 2013;139(7):1129-39.
253. Ataseven B, Gunesch A, Eiermann W, Kates RE, Högel B, Knyazev P, et al. PTK7 as a potential prognostic and predictive marker of response to adjuvant chemotherapy in breast cancer patients, and resistance to anthracycline drugs. Onco Targets Ther. 2014;7:1723-31.
254. Zhao YF, Zhao JY, Yue H, Hu KS, Shen H, Guo ZG, et al. FOXD1 promotes breast cancer proliferation and chemotherapeutic drug resistance by targeting p27. Biochem Biophys Res Commun. 2015;456(1):232-7.

255. Kren BT, Unger GM, Abedin MJ, Vogel RI, Henzler CM, Ahmed K, et al. Preclinical evaluation of cyclin dependent kinase 11 and casein kinase 2 survival kinases as RNA interference targets for triple negative breast cancer therapy. Breast Cancer Res. 2015;17(1):19.
256. Mahmoodi M, Nahvi H, Mahmoudi M, Kasaian A, Mohagheghi MA, Divsalar K, et al. HLA-DRB1,-DQA1 and -DQB1 allele and haplotype frequencies in female patients with early onset breast cancer. Pathol Oncol Res. 2012;18(1):49-55.
257. Purrington KS, Slettedahl S, Bolla MK, Michailidou K, Czene K, Nevanlinna H, et al. Genetic variation in mitotic regulatory pathway genes is associated with breast tumor grade. Hum Mol Genet. 2014;23(22):6034-46.
258. Marchione R, Leibovitch SA, Lenormand JL. The translational factor eIF3f: the ambivalent eIF3 subunit. Cell Mol Life Sci. 2013;70(19):3603-16.
259. Silvera D, Formenti SC, Schneider RJ. Translational control in cancer. Nat Rev Cancer. 2010;10(4):254-66.
260. Nupponen NN, Porkka K, Kakkola L, Tanner M, Persson K, Borg A, et al. Amplification and overexpression of p40 subunit of eukaryotic translation initiation factor 3 in breast and prostate cancer. Am J Pathol. 1999;154(6):1777-83.
261. Lagal V, Abrivard M, Gonzalez V, Perazzi A, Popli S, Verzeroli E, et al. Spire-1 contributes to the invadosome and its associated invasive properties. J Cell Sci. 2014;127(Pt 2):328-40.
262. Boudreau HE, Casterline BW, Rada B, Korzeniowska A, Leto TL. Nox4 involvement in TGF-beta and SMAD3-driven induction of the epithelial-to-mesenchymal transition and migration of breast epithelial cells. Free Radic Biol Med. 2012;53(7):1489-99.
263. Castellana B, Escuin D, Peiró G, Garcia-Valdecasas B, Vázquez T, Pons C, et al. ASPN and GJB2 Are Implicated in the Mechanisms of Invasion of Ductal Breast Carcinomas. J Cancer. 2012;3:175-83.
264. Wu S, Xue W, Huang X, Yu X, Luo M, Huang Y, et al. Distinct prognostic values of ALDH1 isoenzymes in breast cancer. Tumour Biol. 2015.
265. Yang G, Yang X. Smad4-mediated TGF-beta signaling in tumorigenesis. Int J Biol Sci. 2010;6(1):1-8.
266. Guette C, Valo I, Vétillard A, Coqueret O. Olfactomedin-4 is a candidate biomarker of solid gastric, colorectal, pancreatic, head and neck, and prostate cancers. Proteomics Clin Appl. 2015;9(1-2):58-63.
267. Koshida S, Kobayashi D, Moriai R, Tsuji N, Watanabe N. Specific overexpression of OLFM4(GW112/HGC-1) mRNA in colon, breast and lung cancer tissues detected using quantitative analysis. Cancer Sci. 2007;98(3):315-20.
268. Loschke F, Seltmann K, Bouameur JE, Magin TM. Regulation of keratin network organization. Curr Opin Cell Biol. 2015;32C:56-64.
269. Park YH, Jung HH, Do IG, Cho EY, Sohn I, Jung SH, et al. A seven-gene signature can predict distant recurrence in patients with triple-negative breast cancers who receive adjuvant chemotherapy following surgery. Int J Cancer. 2015;136(8):1976-84.
270. Iida J, Dorchak J, Clancy R, Slavik J, Ellsworth R, Katagiri Y, et al. Role for chondroitin sulfate glycosaminoglycan in NEDD9-mediated breast cancer cell growth. Exp Cell Res. 2015;330(2):358-70.
271. Choong LY, Lim SK, Chen Y, Loh MC, Toy W, Wong CY, et al. Elevated NRD1 metalloprotease expression plays a role in breast cancer growth and proliferation. Genes Chromosomes Cancer. 2011;50(10):837-47.
272. Elderbroom JL, Huang JJ, Gatza CE, Chen J, How T, Starr M, et al. Ectodomain shedding of TβRIII is required for TβRIII-mediated suppression of TGF-β signaling and breast cancer migration and invasion. Mol Biol Cell. 2014;25(16):2320-32.

273. Wang P, Wang Y, Yan H, Xie Q, Zhao L, Xu S, et al. Genetic variation in the major mitotic checkpoint genes and risk of breast cancer: a multigenic study on cancer susceptibility. Tumour Biol. 2014;35(7):6701-5.
274. Huang TH, Huo L, Wang YN, Xia W, Wei Y, Chang SS, et al. Epidermal growth factor receptor potentiates MCM7-mediated DNA replication through tyrosine phosphorylation of Lyn kinase in human cancers. Cancer Cell. 2013;23(6):796-810.
275. Johnson JP, Kumar P, Koulnis M, Patel M, Simin K. Crucial and novel cancer drivers in a mouse model of triple-negative breast cancer. Cancer Genomics Proteomics. 2014;11(3):115-26.
276. Gonzalez MA, Tachibana KE, Chin SF, Callagy G, Madine MA, Vowler SL, et al. Geminin predicts adverse clinical outcome in breast cancer by reflecting cell-cycle progression. J Pathol. 2004;204(2):121-30.
277. Zhang SJ, Hu Y, Qian HL, Jiao SC, Liu ZF, Tao HT, et al. Expression and significance of ER, PR, VEGF, CA15-3, CA125 and CEA in judging the prognosis of breast cancer. Asian Pac J Cancer Prev. 2013;14(6):3937-40.
278. Moelans CB, de Weger RA, Monsuur HN, Maes AH, van Diest PJ. Molecular differences between ductal carcinoma in situ and adjacent invasive breast carcinoma: a multiplex ligation-dependent probe amplification study. Anal Cell Pathol (Amst). 2010;33(3):165-73.
279. Bol GM, Raman V, van der Groep P, Vermeulen JF, Patel AH, van der Wall E, et al. Expression of the RNA helicase DDX3 and the hypoxia response in breast cancer. PLoS One. 2013;8(5):e63548.
280. Slattery ML, Herrick JS, Torres-Mejia G, John EM, Giuliano AR, Hines LM, et al. Genetic variants in interleukin genes are associated with breast cancer risk and survival in a genetically admixed population: the Breast Cancer Health Disparities Study. Carcinogenesis. 2014;35(8):1750-9.
281. Pinder SE, Brown JP, Gillett C, Purdie CA, Speirs V, Thompson AM, et al. The manufacture and assessment of tissue microarrays: suggestions and criteria for analysis, with breast cancer as an example. J Clin Pathol. 2012.

Appendices

Appendix 1: Copyright Permissions

JOHN WILEY AND SONS LICENSE
TERMS AND CONDITIONS

May 13, 2014

This is a License Agreement between John P Brown ("You") and John Wiley and Sons ("John Wiley and Sons") provided by Copyright Clearance Center ("CCC"). The license consists of your order details, the terms and conditions provided by John Wiley and Sons, and the payment terms and conditions.

All payments must be made in full to CCC. For payment instructions, please see information listed at the bottom of this form.

License Number	3386970712499
License date	May 13, 2014
Licensed content publisher	John Wiley and Sons
Licensed content publication	The EMBO Journal
Licensed content title	Cell cycle-dependent regulation of the association between origin recognition proteins and somatic cell chromatin
Licensed copyright line	Copyright Â© 2002 European Molecular Biology Organization
Licensed content author	Wei-Hsin Sun,Thomas R. Coleman,Melvin L. DePamphilis
Licensed content date	Mar 15, 2002
Start page	1437
End page	1446
Type of use	Dissertation/Thesis
Requestor type	University/Academic
Format	Electronic
Portion	Figure/table
Number of figures/tables	1
Original Wiley figure/table number(s)	Figure 8
Will you be translating?	No
Title of your thesis / dissertation	Classification of Ductal Carcinoma in Situ of the Human Breast
Expected completion date	Feb 2015
Expected size (number of pages)	250
Total	BP

5.15

5.16 Appendix 2: Excel TMA Maps and IHC Scores

TMA block number	DCIS TMA location	ER Average	PR	HER2	EGFR	CK5/6	CK14	KI67	MCM2
DCIS 15A	A1	0	0	0	0	0	1	1	0
DCIS 15A	A2	0	0	0	0	0	0	x	0
DCIS 15A	A4	2	0	0	0	x	10	1	0
DCIS 15A	A5	0	0	1	3	0	5	40	10
DCIS 15A	B1	x	x	x	0	x	x	x	x
DCIS 15A	B3	0	0	0	3	0	0	10	40
DCIS 15A	B4	0	0	0	0	0	0	30	x
DCIS 15A	B5	2	0	0	1	0	0	15	30
DCIS 15A	C2	5	0	0	0	0	0	5	5
DCIS 15A	C3	1	0	1	2	0	0	5	5
DCIS 15A	C4	5	7	2	0	0	0	1	1
DCIS 15A	C5	8	8	0	0	0	0	0	2
DCIS 15A	D1	x	x	x	x	x	x	x	x
DCIS 15A	D2	x	x	x	x	x	x	x	x
DCIS 15A	D3	0	x	x	x	x	x	x	x
DCIS 15A	D4	x	x	x	x	x	x	x	x
DCIS 15A	E1	2	x	x	x	x	x	x	x

DCIS 15A	E2	0	0	0	0	0	x	0	5
DCIS 15A	E3	5	x	x	x	x	x	x	x
DCIS 15A	E4	8	x	0	0	0	0	1	1
DCIS 16A	A1	0	x	x	x	x	x	x	x
TMA block number	INVASIVE TUMOUR location	ER (Allred)	PR (Allred)	HER2 (HER2)	EGFR (HER2)	CK5/6 (%)	CK14 (%)	KI67 (%)	MCM
DCIS 16A	A2	8	5	x	0	0	0	1	3
DCIS 16A	A4	7	0	3	0	0	0	1	5
DCIS 16A	A5	2	4	2	0	0	0	0	0
DCIS 16A	B1	3	x	x	x	x	x	x	x
DCIS 16A	B3	5	8	2	0	0	0	2	5
DCIS 16A	B4	1	x	x	x	0	0	x	x
DCIS 16A	B5	4	0	0	x	0	0	20	45
DCIS 16A	C2	5	8	2	x	0	0	10	25
DCIS 16A	C3	4	0	1	3	0	0	25	30
DCIS 16A	C4	2	0	0	1	0	0	10	25
DCIS 16A	C5	4	0	3	1	0	0	5	35
DCIS 16A	D1	0	0	0	0	0	0	15	40
DCIS 16A	D2	3	x	x	x	x	x	x	x
DCIS 16A	D3	5	x	x	x	x	x	x	x
DCIS 16A	D4	5	8	0	0	0	0	x	x
DCIS 16A	E1	5	0	x	x	0	0	10	10
DCIS 16A	E2	1	x	3	0	0	0	x	x

DCIS 16A	E3	4	0	3	0	0	0	10	30
DCIS 16A	E4	2	0	2	1	1	0	2	10
DCIS 16A	E5	x	0	x	2	0	0	3	35
INV T 15	A1	0	0	0	3	15	0	8	8
INV T 15	A2	0	0	0	3	0	0	5	2
INV T 15	A4	0	0	0	3	60	95	4	53
INV T 15	A5	0	0	1	3	0	0	50	17
TMA block number	INVASIVE TUMOUR location	ER (Allred)	PR (Allred)	HER2 (HER2)	EGFR (HER2)	CK5/6 (%)	CK14 (%)	KI67 (%)	MCM
INV T 15	A6	0	0	2	3	0	20	30	17
INV T 15	A7	0	0	0	3	0	100	10	37
INV T 15	B1	0	0	0	0	0	0	50	17
INV T 15	B3	4	0	x	2	0	25	20	15
INV T 15	B4	6	0	1	2	0	0	20	7
INV T 15	B5	8	6	0	0	0	0	3	1
INV T 15	B6	8	7	2	0	0	0	15	5
INV T 15	B7	8	8	0	0	0	0	0	0
INV T 15	C2	8	7	1	0	0	0	15	5
INV T 15	C3	8	8	1	0	0	0	4	1
INV T 15	C4	3	0	0	1	0	0	x	x
INV T 15	C5	8	0	3	1	0	0	5	2
INV T 15	C6	4	0	0	3	0	0	20	7
INV T 15	C7	6	0	0	3	0	0	5	2

INV T 15	D1	8	8	3	0	0	0	8	3
INV T 15	D2	8	7	0	0	0	0	5	2
INV T 15	D3	7	8	2	1	0	0	4	1
INV T 15	D4	8	6	0	1	0	0	3	1
INV T 15	D6	8	6	1	1	0	0	4	1
INV T 15	D7	8	0	3	0	0	0	4	1
INV T 15	E1	8	7	0	0	0	0	0	0
INV T 15	E2	8	8	0	0	0	0	4	1
INV T 15	E3	7	0	3	0	0	0	5	x
INV T 15	E4	6	0	0	1	0	80	30	37
TMA block number	INVASIVE TUMOUR location	ER (Allred)	PR (Allred)	HER2 (HER2)	EGFR (HER2)	CK5/6 (%)	CK14 (%)	KI67 (%)	MCM
INV T 15	E5	8	8	0	1	0	0	5	2
INV T 15	E6	4	0	0	2	0	0	35	12
INV T 15	E7	0	0	0	2	0	0	20	7
INV T 15	F1	3	0	3	0	0	0	x	x
INV T 15	F2	0	3	0	2	5	4	20	10
INV T 15	F3	8	8	3	0	0	0	8	3
INV T 15	F4	8	8	0	0	0	0	5	2
INV T 15	F5	8	4	0	1	0	0	4	1
INV T 15	F7	8	0	0	0	0	0	5	2
INV T 15	G1	4	0	3	1	0	0	15	5
INV T 15	G2	8	0	3	0	0	0	x	x

INV T 15	G3	3	0	0	2	20	0	25	15
INV T 15	G4	0	0	0	2	10	0	40	17
INV T 15	G6	8	0	2	0	0	0	5	2
INV T 15	G7	4	0	0	3	0	0	12	4

5.17 Appendix 3: Tissue Microarray Patient Demographics

Research id number	Surgery type	Side	Recurrence surgery type	Side	Time between specimens (days)	Size (mm)	Margins	Grade	Main architecture	Necrosis	Chronic inflammation	Recurrence y/n	Recurrence type	Size recoded at median of 15mm
100448	Excision biopsy	Left	Radical mastectomy	Left	5	7.0	Not available	High grade	Solid	Marked	Marked	Y	DCIS	Less than 15mm
100453	Excision biopsy	Left	Radical mastectomy	Left	5	16.0	Not available	High grade	Micropapillary	Moderate	Mild	Y	DCIS	15mm or more
100465	Excision biopsy	Right	Simple mastectomy	Right	0	13.0	Not available	High grade	Solid	Mild	Moderate	Y	DCIS	Less than 15mm
100466	Excision biopsy	Right	Simple mastectomy	Right	7	5.0	Not available	High grade	Cribriform	None	None	Y	DCIS	Less than 15mm
100491	Micdo	Right	Simple mastectomy	Right	14	16.0	Not available	High grade	Micropapillary	Moderate	Moderate	Y	DCIS	15mm or more
100494	Excision biopsy	Right	Radical mastectomy	Right	7	29.0	Not available	High grade	Solid	Marked	Marked	Y	DCIS	15mm or more
100508	Excision biopsy	Left	Simple mastectomy	Left	35			No DCIS				Y	DCIS	
100523	Excision biopsy	Right	Wide local excision	Right	62	21.0	Not available	High grade	Cribriform	Marked	None	Y	DCIS	15mm or more
100528	Micdo	Left	Simple mastectomy	Left	24	2.0	Not available	High grade	Papillary	None	None	Y	DCIS	Less than 15mm
100534	Excision biopsy	Left	Simple mastectomy	Left	0	15.0	Not available	High grade	Solid	Marked	Marked	Y	DCIS	15mm or more
100538	Biopsy	Left	Simple mastectomy	Left	9	21.0	Not available	Intermediate grade	Micropapillary	Moderate	Moderate	Y	DCIS	15mm or more
100541	Wide excision	Right	Simple mastectomy	Right	14	20.0	0.0	High grade	Solid	Marked	Moderate	Y	DCIS	15mm or more
100543	Excision biopsy	Right	Simple mastectomy	Right	19	25.0	0.0	High grade	Solid	Marked	Marked	Y	DCIS	15mm or more
100546	Biopsy	Right			0	19.0	0.0	High grade	Solid	Moderate	Mild	N	No	15mm or more
100547	Excision biopsy	Left	Radical mastectomy	Right	0	Na	Not available	Intermediate grade	Cribriform	None	Moderate	Y	DCIS	
100548	Excision biopsy	Right	Wide local excision	Right	21	31.0	0.0	Intermediate grade	Cribriform	Mild	Mild	Y	DCIS	15mm or more
Research id number	Surgery type	Side	Recurrence surgery type	Side	Time between specimens	Size	Margins	Grade	Main architecture	Necrosis	Ci	Recurrence y/n	DCIS	Less than 15mm
100555	Excision biopsy	Left	Wide local excision	Left	12	12.0	0.0	Intermediate grade	Cribriform	Mild	Mild	Y	DCIS	Less than 15mm
100561	Excision biopsy	Left	Simple mastectomy	Left	12	18.0	0.0	High grade	Solid	Marked	Marked	Y	DCIS	15mm or more
100562	Excision biopsy	Left	Excision biopsy	Left	2126							Y	DCIS	
100572	Excision biopsy	Left	Radical mastectomy	Left	29	26.0	0.0	High grade	Solid	Marked	Moderate	Y	DCIS	15mm or more
100580	Excision biopsy	Right	Wide local excision	Right	15	16.0	Not available	Intermediate grade	Cribriform	Moderate	None	Y	DCIS	15mm or more
100590	Excision biopsy	Right	Simple mastectomy	Right	26	21.0	Not available	Intermediate grade	Cribriform	Mild	None	Y	DCIS	15mm or more
100591	Biopsy	Left	Radical mastectomy	Left	19	25.0	0.0	Intermediate grade	Cribriform	Marked	Moderate	Y	DCIS	15mm or more

100597	Excision biopsy	Left	Wide local excision	Left	41	22.0	0	High grade	Micropapillary	Marked	Mild	Y	DCIS	Less than 15mm
100601	Excision biopsy	Right	Radical mastectomy	Right	40	8.0	0.0	High grade	Solid	Moderate	Marked	Y	DCIS	Less than 15mm
100602	Referral	Left	Excision biopsy, simple mastectomy	Left	46	3.0	1.0	High grade	Solid	Moderate	Mild	N	N	Less than 15mm
100607	Excision biopsy	Left	Radical mastectomy	Left	27	22.0	0.0	High grade	Cribriform	Moderate	None	Y	DCIS	15mm or more
100609	Excision biopsy	Left	Wide local excision	Left	33	12.0	0.0	High grade	Solid	Marked	Marked	Y	DCIS	Less than 15mm
100611	Excision biopsy	Left	Wide local excision	Left	34	18.0	0.0	Intermediate grade	Cribriform	Mild	Moderate	Y	DCIS	15mm or more
100613	Referral	Right	Excision biopsy	Right	0	11.0	0.0	High grade	Solid	Moderate	Mild	N	N	Less than 15mm
100615	Biopsy	Left	Excision biopsy	Left	33	16.0	0.0	High grade	Cribriform	Moderate	Mild	N	N	15mm or more
100617	Referral	Left	Simple mastectomy	Left	22	21.0	0.0	Intermediate grade	Cribriform	None	None	Y	DCIS	15mm or more
100618	Excision biopsy	Right	Wide local excision	Right	30	17.0	0.0	Intermediate grade	Cribriform	Moderate	Mild	Y	DCIS	15mm or more
100619	Referral	Left	Simple mastectomy	Left	33	21.0	Not available	High grade	Solid	Marked	Marked	N	N	15mm or more
100621	Excision biopsy	Left	Wide local excision	Left	21	10.0	Not available	Intermediate grade	Cribriform	None	Mild	Y	DCIS	Less than 15mm
100630	Referral	Left	Excision biopsy	Left	0	14.0	1.0	Low grade	Cribriform	None	Mild	N	N	Less than 15mm
Research id number	Surgery type	Side	Recurrence surgery type	Side	Time between specimens (days)	Size (mm)	Margins	Grade	Main architecture	Necrosis	Chronic inflammation	Recurrence y/n	Recurrence type	Size recoded at median of 15mm
100631	Referral		Simple mastectomy	Left	769	15.0	Not available	High grade	Cribriform	Moderate	Moderate	N	N	15mm or more
100633	Excision biopsy	Right	Wide local excision	Right	36	6.0	0.0	Intermediate grade	Cribriform	None	Na	No rid	DCIS	Less than 15mm
100639	Excision biopsy	Right	Wide local excision	Right	27	15.0	0.0	High grade	Solid	Marked	Marked	No research id number	DCIS	15mm or more

100643	Referral		Excision biopsy	Left	226	20.0	0.0	Intermediate grade	Cribriform	Moderate	Moderate	N	N	15mm or more
100644	Excision biopsy	Right	Wide local excision	Right	43	10.0	0.0	High grade	Cribriform	Mild	Moderate	Y	DCIS	Less than 15mm
100645	Micdo	Right	Simple mastectomy	Right	29	15.0	0.0	High grade	Micropapillary	Mild	Moderate	No research id number		15mm or more
100646	Referral	Left	Excision biopsy	Left	108							Y	DCIS	
100649	Referral	Right	Excision biopsy	Right	36	10.0	Not available	Intermediate grade	Cribriform	Mild	Mild	N	N	Less than 15mm
100650	Referral	Right	Excision biopsy	Right	36	5.0	1.5	High grade	Solid	Mild	Marked	N	N	Less than 15mm
100651	Excision biopsy	Left	Wide local excision	Left	126	16.0	0.0	High grade	Solid	Marked	Marked	No research id number		15mm or more
100658	Excision biopsy	Left	Wide local excision, simple mastectomy	Left	63	17.0	Not available	High grade	Cribriform	Marked	Moderate	Y	DCIS	15mm or more
100662	Excision biopsy	Right	Simple mastectomy	Right	54	14.0	0.0	High grade	Cribriform	Marked	Marked	Y	DCIS	Less than 15mm
100663	Referral	Right	Simple mastectomy	Right	80	7.0	Not available	Low grade	Cribriform	None	None	N	N	Less than 15mm
100667	Micdo	Right	Simple mastectomy	Right	49	23.0	0.0	High grade	Solid	Marked	Mild	Y	DCIS	15mm or more
100671	Excision biopsy	Left	Wide local excision, simple mastectomy	Left	34	14.0	0.0	Intermediate grade	Cribriform	Mild	Moderate	Y	DCIS	Less than 15mm
100674	Excision biopsy	Right	Wide local excision, simple mastectomy	Right left	50	9.0	0.0	High grade	Cribriform	Mild	Moderate	Y	DCIS	Less than 15mm

NOTE: All patient identifiers and dates have been removed.

Table 32: Patient Demographics: RID= Research Number

Research id number	Surgery type	Side	Recurrence surgery type	Side	Time between specimens (days)	Size (mm)	Margins	Grade	Main architecture	Necrosis	Chronic inflammation	Recurrence y/n	Recurrence type	Size recoded at median of 15mm
100676	Excision biopsy	Right	Wide local excision. Simple mastectomy	Right	36	15.0	Not available	High grade	Micropapillary	Moderate	Marked	Y	DCIS	15mm or more
100679	Excision biopsy	Right	Simple mastectomy	Right	43	27.0	0.0	High grade	Micropapillary	Marked	Marked	Y	DCIS	15mm or more
100696	Micdo	Left	Simple mastectomy	Left	55	8.0	Not available	High grade	Cribriform	None	Mild	N	N	Less than 15mm
100699	Excision biopsy	Left	Simple mastectomy	Left	63			No DCIS						
100701	Excision biopsy	Right	Simple mastectomy	Right left	34	1.0	Not available	High grade	Solid	None	None	N	N	Less than 15mm
100703	Excision biopsy	Right	Simple mastectomy	Right	28	20.0	Not available	High grade	Cribriform	Mild	Mild	No research id number		15mm or more
													N	
117057	Micdo	Right	Simple mastectomy	Right	27	19.0	0.0	High grade	Solid	None	Mild	Y	DCIS	15mm or more
117066			Wide local excision	Right	27	22.0	0.0	Intermediate grade	Cribriform	Mild	Mild	N	N	15mm or more
117079	Excision biopsy	Left	Simple mastectomy	Left	40	16.0	Not available	Intermediate grade	Micropapillary	None	Mild	Y	DCIS	15mm or more
117081	Excision biopsy	Left	Wide local excision	Left	21	20.0	Not available	Intermediate grade	Cribriform	Mild	Mild	Y	DCIS	15mm or more
117088	Excision biopsy	Right	Wide local excision	Right	21	24.0	0.0	High grade	Solid	Marked	Marked	Y	DCIS	15mm or more
117092	Excision biopsy	Left	Simple mastectomy	Left	22	18.0	Not available	Intermediate grade	Papillary	None	Mild	N	N	15mm or more
117098	Micdo	Left	Wide local excision & ancillary clearance	Left	61	Na	Not available	Intermediate grade	Papillary	None	None	Y	DCIS	
117105	Referral	Right	Excision biopsy	Right	?	11.0	Not available	Intermediate grade	Solid	Marked	None	N	N	Less than 15mm
117119	Excision biopsy	Right	Wide local excision	Right	21	12.0	0.0	Intermediate grade	Micropapillary	None	None	Y	DCIS	Less than 15mm
117122	Referral	Right	Simple mastectomy	Right	?	Na	Not available	Low grade	Cribriform	None	None	N	N	
117124	Referral	Left	Simple mastectomy	Left	14	29.0	Not available	High grade	Cribriform	Mod	Mild	N	N	15mm or more

Research id number	Surgery type	Side	Recurrence surgery type	Side	Time between specimens (days)	Size (mm)	Margins	Grade	Main architecture	Necrosis	Chronic inflammation	Recurrence y/n	Recurrence type	Size recoded at median of 15mm
117125	Excision biopsy	Right	Wide local excision	Right	58	13.0	0.0	Intermediate grade	Cribriform	None	Moderate	No id number	DCIS	Less than 15mm
117130	Referral		Excision biopsy& wide local excision	Left	?	6.0	3.0	High grade	Solid	Marked	Marked	N	N	Less than 15mm
117145	Referral	Right	Simple mastectomy	Right	?	16.0	Not available	High grade	Cribriform	Marked	Moderate	N	N	15mm or more
117147	Wle	Right	Simple mastectomy	Right	62	19.0	Not available	High grade	Solid	Marked	Marked	Y	DCIS	15mm or more
117148	Excision biopsy	Left	Referral	Left	0	9.0	Not available	Intermediate grade	Papillary	None	Mild	Y	DCIS	Less than 15mm
117152	Referral	Left	Simple mastectomy	Left	?	24.0	Not available	High grade	Solid	Mod	None	N	N	15mm or more
117155	Excision biopsy	Right	Wide local excision	Right	20	13.0	0.0	Intermediate grade	Solid	Mild	None	Y	DCIS	Less than 15mm
117159	Wle	Right	Radical mastectomy	Right	26	17.0	Not available	High grade	Solid	Mild	Marked	Y	DCIS	15mm or more
117163	Excision biopsy	Right	Simple mastectomy	Right	28	16.0	0.0	Intermediate grade	Cribriform	Mod	None	Y	DCIS	15mm or more
117174	Sm	Left	Referral	Left	0	21.0	Not available	High grade	Solid	Mod	Marked	Y	DCIS	15mm or more
117176	Referral	Left	Excision biopsy	Left	?	21.0	Not available	Intermediate grade	Solid	Mild	Mild	N	N	
117178	Excision biopsy	Left	Simple mastectomy	Left	14	19.0	0.0	Low grade	Cribriform	None	Mild	Y	DCIS	15mm or more
117181	Excision biopsy	Left	Referral & simple mastectomy	Left	14	20.0	0.0	High grade	Solid	Mod	Moderate	Y	DCIS	15mm or more
117183	Referral	Left	Excision biopsy	Left	?	8.0	Not available	High grade	Solid	None	Mild	N	N	Less than 15mm
117184	Excision biopsy	Right	Ref & wide local excision	Right	43	Na	Not available	High grade	Cribriform	None	Moderate	Y	DCIS	
117185	Referral	Left	Excision biopsy & simple mastectomy	Left	?	27.0	0.0	Intermediate grade	Cribriform	Mild	Mild	N	N	15mm or more
117195	Excision biopsy	Left	Wide local excision	Left	15	19.0	0.0	High grade	Solid	Mod	Marked	Y	DCIS	15mm or more
117204	Excision biopsy	Right	Wide local excision	Right	23	8.0	1.0	Low grade	Cribriform	None	None	No research id number		Less than 15mm
117208	Excision biopsy	Right	Wide local excision	Right	23	27.0	0.0	Intermediate grade	Papillary	Mild	Moderate	Y	DCIS	15mm or more

Table 33: *IHC* scores for TMA cases with associated patient data.

Research id number	Final HER2 status	Final egfr positive score (any)	Final average er score	Final er status	Final average pr scores	Final pr status	Final highest ck5 scores	Final positive ck5 s (more than 1%)	Final highest ck5/6 score	Ck 5/6 positive (more than 1%)	Final highest ck14 score	Ck14 positive (more than 1%)	Ki67 tma average	Ki67 positive more than 5% (median)	MCM2 tma average (%)	MCM2 Positive (median 27.5%)
100448	0	1	0	0	0	0	0.5	0	1.0	1	1.0	1	7	1	33	1
100453	0	0	5	1	1	0	0.0	0	5.0	1	0.5	0	13	1	40	1
100465	1	1	1	0	0	0	0.5	0	1.0	1	0.5	0	13	1	28	1
100466																
100491	1	0	0	0	0	0	0.0	0	0.0	0	0.0	0	17	1	40	1
100494	1	0	1	0	0	0	1.0	0	5.0	1	5.0	1	45	1	91	1
100508	0	0			2	0			1.0	1	5.0	1	40	1	35	1
100523	0	0	7	1	2	0	0.0	0	0.0	0	0.0	0	10	1	5	0
100528																
100534	1	0	0	0	0	0	0.5	0	2.0	1	20.0	1	13	1	88	1
100538	0	0	4	1	0	0	0.0	0	0.0	0	0.5	0	8	1	30	1
100541	1	0	3	0	0	0	2.0	1	0.0	0	5.0	1	28	1	85	1
100543	1	0	1	0	0	0	0.5	0	1.0	1	2.0	1	18	1	72	1
100546	0	0	8	1	6	1	0.0	0	0.0	0	1.0	1	0	0	4	0
100547	0	0	8	1	6	1	0.0	0	1.0	1	0.0	0	1	0	25	0
100548	1	0	8	1	0	0	0.5	0	0.0	0	0.5	0	2	0	13	0
100550	0	0	6	1	2	0	0.0	0	1.0	1	10.0	1	6	1	48	1
100555	0	0	8	1	7	1	0.5	0	0.0	0	1.0	1	5	1	25	0
100561	1	1	0	0	0	0	0.5	0	0.0	0	0.0	0	7	1	78	1
100562	0				0	0	0.0	0			0.0	0	5	1	5	0

100572	1	0	8	1	0	0	0.5	0	1.0	1	1.0	1	30	1	50	1
Research id number	Final HER2 status	Final egfr positive score (any)	Final average er score	Final er status	Final average pr scores	Final pr status	Final highest ck5 scores	Final positive ck5 s (more than 1%)	Final highest ck5/6 score	Ck 5/6 positive (more than 1%)	Final highest ck14 score	Ck14 positive (more than 1%)	Ki67 tma average	Ki67 positive more than 5% (median)	MCM2 tma average (%)	MCM2 Positive (median 27.5%)
100580	0	0	7	1	7	1	0.0	0	0.0	0	0.0	0	5	1	15	0
100590	0	0	7	1	2	0	0.0	0	0.0	0	0.0	0	6	1	0	0
100597	0	0	8	1	6	1	0.0	0	0.0	0	0.0	0	5	1	13	0
100601	1				0	0	0.0	0			0.0	0			0	0
100602	0	0	8	1	4	1	0.0	0	0.0	0	0.0	0	10	1	70	1
100606	0	0	6	1	6	1	1.0	0	0.5	0	0.5	0	5	1	23	0
100607	1	0	0	0	0	0	1.0	0	10.0	1	5.0	1	40	1	30	1
100609	0	1	0	0	0	0	60.0	1	50.0	1	0.0	0	15	1	18	0
100611	1	0	3	1	0	0	1.0	0	0.0	0	0.0	0	0	0	30	
100613	1	0	5	1	0	0	0.0	0			0.0	0	1	0	35	1
100615	0	0	4	1	0	0	0.0	0	0.0	0	0.0	0	1	0	9	0
100617	0	0	8	1	2	0	0.0	0	0.0	0	0.0	0	0	0	16	0
100618	0	0	8	1	8	1	0.0	0	1.0	1	0.0	0	2	0	15	0
100619	1	0	0	0	0	0	1.0	0	1.0	1	1.0	1	25	1	80	1
100621	0	0	7	1	8	1	1.0	0	0.0	0	0.0	0	7	1	20	0
100630	0	0	7	1	3	1	0.0	0	0.0	0	0.0	0	0	0	5	0
100631	0	1	5	1	1	0	5.0	1	0.0	0	0.0	0	0	0	63	1
100633	0	0	8	1	4	1	0.0	0	0.0	0	0.0	0	0	0	8	0
100637	0	0	6	1	0	0	0.0	0	2.0	1	0.0	0	4	0	53	1
100639	1	0	7	1	5	1	2.0	1	1.0	1	0.0	0	8	1	88	1

100643	0	0	8	1	7	1	0.0	0	0.0	0	0.0	0	0	0	43	1
100644	0	0	8	1	7	1	1.0	0	0.0	0	0.0	0	3	0	30	1
100645	1	0	0	0	0	0	0.0	0	0.0	0	0.0	0	5	1	27	0
100646	1	0	0	0	0	0	1.0	0	0.0	0	0.0	0	10	1	45	1

Research id number	Final HER2 status	Final egfr positive score (any)	Final average er score	Final er status	Final average pr scores	Final pr status	Final highest ck5 scores	Final positive ck5 s (more than 1%)	Final highest ck5/6 score	Ck 5/6 positive (more than 1%)	Final highest ck14 score	Ck14 positive (more than 1%)	Ki67 tma average	Ki67 positive more than 5% (median)	MCM2 tma average (%)	MCM2 Positive (median 27.5%)
100649	0	0	8	1	8	1	0.0	0	0.0	0	0.0	0	5	1	65	1
100650	1	0	0	0	0	0	0.0	0	0.0	0	0.0	0	10	1	70	1
100651	1	0	0	0	0	0	10.0	1	15.0	1	5.0	1	10	1	50	1
100662	1	0	0	0	0	0	0.0	0	1.0	1	0.0	0	7	1	47	1
100663	0	0	8	1	6	1	0.0	0	5.0	1	0.0	0	0	0	7	0
100667	0	0	6	1	6	1	0.0	0	0.0	0	0.0	0	18	1	32	1
100671	1	0	8	1	7	1	2.0	1	1.0	1	0.0	0	10	1	32	1
100674	0	0	6	1	3	1	2.0	1	10.0	1	5.0	1	8	1	23	0
100676	0	0	0	0	0	0	1.0	0	0.0	0	0.0	0	6	1	23	0
100679	1	0	8	1	1	0	1.0	0	1.0	1	0.0	0	5	1	42	1
100696	0	0			7	1	0.0	0	0.0	0	0.0	0	3	0	13	0
100699																
100701																
100703	0	0	8	1	7	1	0.0	0	0.0	0	0.0	0	3	0	29	1
117044	1	0	0	0	0	0	1.0	0	1.0	1	1.0	1	10	1	13	0
117057	0	0	8	1	8	1	5.0	1	2.0	1	2.0	1	0	0	20	0
117061	0	0	8	1	5	1	0.0	0	0.0	0	0.0	0	0	0	10	0
117066	0	0	6	1	0	0	0.0	0	0.0	0	0.0	0	8	1	10	0
117079	0	0	0	0	2	0	5.0	1	1.0	1	0.0	0	10	1	0	0
117081	0	0	7	1	0	0	0.0	0	1.0	1	0.0	0	5	1	27	0
117088	1	0	0	0	0	0	1.0	0	2.0	1	1.0	1	23	1	65	1

117092	0	0	8	1	7	1	1.0	0	0.5	0	0.5	0	3	0	11	0
117098	0	0	8	1	2	0	0.0	0	0.0	0	0.0	0	0	0	0	0

Research id number	Final HER2 status	Final egfr positive score (any)	Final average er score	Final er status	Final average pr scores	Final pr status	Final highest ck5 scores	Final positive ck5 s (more than 1%)	Final highest ck5/6 score	Ck 5/6 positive (more than 1%)	Final highest ck14 score	Ck14 positive (more than 1%)	Ki67 tma average	Ki67 positive more than 5% (median)	MCM2 tma average (%)	MCM2 Positive (median 27.5%)
117105	0	0	8	1	4	1	0.0	0	0.0	0	0.0	0	0	0	10	0
117119	0	0			0	0	0.0	0			0.0	0	1	0	1	0
117122	0				8	1							0	0	1	0
117124	0	0	8	1	4	1	1.0	0	0.0	0	0.0	0	2	0	40	1
117125	0	0	8	1		1	2.0	1	0.0	0	0.0	0	0	0	10	0
117145	0	0	8	1	6	1	0.0	0	0.0	0	0.0	0	2	0	28	1
117147	1	1	1	0	0	0	0.0	0	0.0	0	0.0	0	12	1	82	1
117148	0	0	8	1	8	1	0.0	0	0.0	0	0.0	0				
117152	0	0	8	1	4	1	0.0	0	0.0	0	0.0	0	2	0	10	0
117155	0	0			5	1			1.0	1	0.0	0	2	0	25	0
117159	0	0	0	0	0	0	0.0	0	0.0	0	0.0	0	3	0	35	1
117163	0	0	8	1	6	1	0.0	0	0.0	0	0.0	0	5	1	57	1
117164	0	0	8	1	1	0	5.0	1	5.0	1	5.0	1	20	1	87	1
117174	1	0	0	0	0	0	1.0	0	1.0	1	0.0	0	27	1	75	1
117176	0		8	1	8	1	0.0	0	0.0	0	0.0	0				
117178	0	0	8	1	8	1	0.0	0	1.0	1	0.0	0	5	1	43	1
117181	0	0	8	1	4	1	5.0	1	3.0	1	5.0	1	7	1	23	0
117183	0	0	5	1	5	1	0.0	0	0.0	0	0.0	0			40	1
117184	0	0	6	1	1	0	0.0	0	0.0	0	0.0	0	0	0	10	0
117185	0	0			6	1							0	0	10	0
117195	0	0	8	1	5	1	0.0	0	0.0	0	0.0	0	8	1	35	1
117204	0	0	8	1	7	1	0.0	0	0.5	0	0.0	0	1	0	29	1

117208	0	0	8	1	0	0	0.0	0	0.0	0	0.0	0	4	0	33	1

5.18 Appendix 4: Immunohistochemistry Protocols

i) Dewax slides in dewax solution followed by alcohol.
ii) Epitope retrieval solution according to antibody.
iii) Peroxidase block, 5 mins.
iv) Primary antibody incubation, 15 mins.
v) Post-primary, 8 mins.
vi) Polymer, 8 mins.
vii) DAB, 10 mins.
viii) DAB Enhancer, 10 mins.
ix) Haematoxylin counterstain, 5 mins.
x) Rinse in water, dehydrate, clear and mount manually.

Bond wash buffer rinses were carried out by the machine between each of these steps.

Antibodies were diluted using Bond Antibody Diluent. Bond epitope retrieval solutions 1, & 2 were used where stated at a temperature of 95ºC

Antibody	Dilution	Epitope retrieval soln	Epitope retrieval incubation (minutes)
ER 6F11	1/100	ER1	30
PR	1/400	ER1	30
CK5/6	1/100	ER1	30
CK5	1/100	ER1	30
CK14	1/100	ER1	30
EGFR	1/50	ER1	20

HER2 IHC was performed using the Bond “Oracle” HER2 kit as per manufacturers instructions.

5.19 Appendix 5: Frequency Tables and Non Parametric Statistical Analysis of DCIS IHC

Frequency Distribution for FINAL HER2 STATUS
Row exclusion: DCIS STATVIEW DATASET

	Count	Percent
0	191	77.016
1	57	22.984
Total	248	100.000

Frequency Distribution for FINAL EGFR STATUS
Row exclusion: DCIS STATVIEW DATASET

	Count	Percent
0	216	95.154
1	11	4.846
Total	227	100.000

Frequency Distribution for FINAL ER STATUS
Row exclusion: DCIS STATVIEW DATASET

	Count	Percent
0	59	26.339
1	165	73.661
Total	224	100.000

Frequency Distribution for FINAL PR STATUS
Row exclusion: DCIS STATVIEW DATASET

	Count	Percent
0	123	52.119
1	113	47.881
Total	236	100.000

Frequency Distribution for FINAL CK5 (AT 1%)
Row exclusion: DCIS STATVIEW DATASET

	Count	Percent
0	195	85.903
1	32	14.097
Total	227	100.000

Frequency Distribution for FINAL CK5/6 (AT 1%)
Row exclusion: DCIS STATVIEW DATASET

	Count	Percent
0	151	68.636
1	69	31.364
Total	220	100.000

Frequency Distribution for FINAL CK14 (AT 1%)
Row exclusion: DCIS STATVIEW DATASET

	Count	Percent
0	193	83.550
1	38	16.450
Total	231	100.000

Frequency Distribution for GRADE
Row exclusion: DCIS STATVIEW DATASET

	Count	Percent
HG	98	57.988
IG	58	34.320
LG	13	7.692
Total	169	100.000

Frequency Distribution for ARCH
Row exclusion: DCIS STATVIEW DATASET

	Count	Percent
CRIB	68	40.237
MICROPAP	18	10.651
PAP	13	7.692
SOLID	70	41.420
Total	169	100.000

Frequency Distribution for NECROSIS
Row exclusion: DCIS STATVIEW DATASET

	Count	Percent
MARKED	42	24.852
MILD	47	27.811
MOD	38	22.485
NONE	42	24.852
Total	169	100.000

Frequency Distribution for CI
Row exclusion: DCIS STATVIEW DATASET

	Count	Percent
MARKED	37	22.156
MILD	59	35.329
MOD	36	21.557
NONE	35	20.958
Total	167	100.000

Frequency Distribution for REC Y/N
Row exclusion: DCIS STATVIEW DATASET

	Count	Percent
N	140	85.366
Y	24	14.634
Total	164	100.000

Frequency Distribution for REC TYPE
Row exclusion: DCIS STATVIEW DATASET

	Count	Percent
BILATERAL INVASIVE CARCINOMA	1	.613
CONTRALATERAL INVASIVE CARCINOMA	3	1.840
IPSILATERAL DCIS	6	3.681
IPSILATERAL INVASIVE CA	7	4.294
NK	6	3.681
NONE	140	85.890
Total	163	100.000

Summary Table for FINAL KI67 (AT MEDIAN, 5%), FINAL HER2 STATUS
Row exclusion: DCIS STATVIEW DATASET

Num. Missing	43
DF	1
Chi Square	15.451
Chi Square P-Value	<.0001
G-Squared	16.560
G-Squared P-Value	<.0001
Contingency Coef.	.250
Phi	.258
Cty. Cor. Chi Square	14.255
Cty. Cor. P-Value	.0002
Fisher's Exact P-Value	<.0001

Observed Frequencies for FINAL KI67 (AT MEDIAN, 5%), FINAL HER2 STATUS
Row exclusion: DCIS STATVIEW DATASET

	0	1	Totals
0	87	11	98
1	89	45	134
Totals	176	56	232

Summary Table for FINAL EGFR STATUS, FINAL KI67 (AT MEDIAN, 5%)
Row exclusion: DCIS STATVIEW DATASET

Num. Missing	53
DF	1
Chi Square	4.869
Chi Square P-Value	.0273
G-Squared	5.872
G-Squared P-Value	.0154
Contingency Coef.	.146
Phi	.148
Cty. Cor. Chi Square	3.580
Cty. Cor. P-Value	.0585
Fisher's Exact P-Value	.0294

Observed Frequencies for FINAL EGFR STATUS, FINAL KI67 (AT MEDIAN, 5%)
Row exclusion: DCIS STATVIEW DATASET

	0	1	Totals
0	90	121	211
1	1	10	11
Totals	91	131	222

Summary Table for FINAL ER STATUS, FINAL KI67 (AT MEDIAN, 5%)
Row exclusion: DCIS STATVIEW DATASET

Num. Missing	59
DF	1
Chi Square	23.351
Chi Square P-Value	<.0001
G-Squared	25.940
G-Squared P-Value	<.0001
Contingency Coef.	.312
Phi	.329
Cty. Cor. Chi Square	21.868
Cty. Cor. P-Value	<.0001
Fisher's Exact P-Value	<.0001

Observed Frequencies for FINAL ER STATUS, FINAL KI67 (AT MEDIAN, 5%)
Row exclusion: DCIS STATVIEW DATASET

	0	1	Totals
0	8	51	59
1	78	79	157
Totals	86	130	216

Summary Table for FINAL PR STATUS, FINAL KI67 (AT MEDIAN, 5%)
Row exclusion: DCIS STATVIEW DATASET

Num. Missing	51
DF	1
Chi Square	15.527
Chi Square P-Value	<.0001
G-Squared	15.684
G-Squared P-Value	<.0001
Contingency Coef.	.255
Phi	.263
Cty. Cor. Chi Square	14.479
Cty. Cor. P-Value	.0001
Fisher's Exact P-Value	<.0001

Observed Frequencies for FINAL PR STATUS, FINAL KI67 (AT MEDIAN, 5%)
Row exclusion: DCIS STATVIEW DATASET

	0	1	Totals
0	36	82	118
1	60	46	106
Totals	96	128	224

Summary Table for FINAL CK5 (AT 1%), FINAL KI67 (AT MEDIAN, 5%)
Row exclusion: DCIS STATVIEW DATASET

Num. Missing	58
DF	1
Chi Square	1.222
Chi Square P-Value	.2690
G-Squared	1.254
G-Squared P-Value	.2629
Contingency Coef.	.075
Phi	.075
Cty. Cor. Chi Square	.830
Cty. Cor. P-Value	.3623
Fisher's Exact P-Value	.3305

Observed Frequencies for FINAL CK5 (AT 1%), FINAL KI67 (AT MEDIAN, 5%)
Row exclusion: DCIS STATVIEW DATASET

	0	1	Totals
0	77	108	185
1	10	22	32
Totals	87	130	217

Summary Table for FINAL CK5/6 (AT 1%), FINAL KI67 (AT MEDIAN, 5%)
Row exclusion: DCIS STATVIEW DATASET

Num. Missing	63
DF	1
Chi Square	1.733
Chi Square P-Value	.1881
G-Squared	1.756
G-Squared P-Value	.1851
Contingency Coef.	.090
Phi	.090
Cty. Cor. Chi Square	1.358
Cty. Cor. P-Value	.2439
Fisher's Exact P-Value	.2279

Observed Frequencies for FINAL CK5/6 (AT 1%), FINAL KI67 (AT MEDIAN, 5%)
Row exclusion: DCIS STATVIEW DATASET

	0	1	Totals
0	59	84	143
1	22	47	69
Totals	81	131	212

Summary Table for FINAL CK14 (AT 1%), FINAL KI67 (AT MEDIAN, 5%)
Row exclusion: DCIS STATVIEW DATASET

Num. Missing	54
DF	1
Chi Square	4.985
Chi Square P-Value	.0256
G-Squared	5.275
G-Squared P-Value	.0216
Contingency Coef.	.149
Phi	.150
Cty. Cor. Chi Square	4.209
Cty. Cor. P-Value	.0402
Fisher's Exact P-Value	.0290

Observed Frequencies for FINAL CK14 (AT 1%), FINAL KI67 (AT MEDIAN, 5%)
Row exclusion: DCIS STATVIEW DATASET

	0	1	Totals
0	79	104	183
1	9	29	38
Totals	88	133	221

Summary Table for FINAL MCM2 (AT MEDIAN, 27.5%), FINAL KI67 (AT MEDIAN, 5%)
Row exclusion: DCIS STATVIEW DATASET

Num. Missing	38
DF	1
Chi Square	41.483
Chi Square P-Value	<.0001
G-Squared	42.558
G-Squared P-Value	<.0001
Contingency Coef.	.386
Phi	.418
Cty. Cor. Chi Square	39.807
Cty. Cor. P-Value	<.0001
Fisher's Exact P-Value	<.0001

Observed Frequencies for FINAL MCM2 (AT MEDIAN, 27.5%), FINAL KI67 (AT MEDIAN, 5%)
Row exclusion: DCIS STATVIEW DATASET

	0	1	Totals
0	70	37	107
1	31	99	130
Totals	101	136	237

Summary Table for GRADE, FINAL KI67 (AT MEDIAN, 5%)
Row exclusion: DCIS STATVIEW DATASET

Num. Missing	121
DF	2
Chi Square	13.981
Chi Square P-Value	.0009
G-Squared	14.052
G-Squared P-Value	.0009
Contingency Coef.	.288
Cramer's V	.301

Observed Frequencies for GRADE, FINAL KI67 (AT MEDIAN, 5%)
Row exclusion: DCIS STATVIEW DATASET

	0	1	Totals
HG	26	65	91
IG	28	24	52
LG	8	3	11
Totals	62	92	154

Summary Table for ARCH, FINAL KI67 (AT MEDIAN, 5%)
Row exclusion: DCIS STATVIEW DATASET

Num. Missing	121
DF	3
Chi Square	12.020
Chi Square P-Value	.0073
G-Squared	12.697
G-Squared P-Value	.0053
Contingency Coef.	.269
Cramer's V	.279

Observed Frequencies for ARCH, FINAL KI67 (AT MEDIAN, 5%)
Row exclusion: DCIS STATVIEW DATASET

	0	1	Totals
CRIB	34	30	64
MICROPAP	2	13	15
PAP	6	5	11
SOLID	20	44	64
Totals	62	92	154

Summary Table for NECROSIS, FINAL KI67 (AT MEDIAN, 5%)
Row exclusion: DCIS STATVIEW DATASET

Num. Missing	121
DF	3
Chi Square	27.774
Chi Square P-Value	<.0001
G-Squared	28.911
G-Squared P-Value	<.0001
Contingency Coef.	.391
Cramer's V	.425

Observed Frequencies for NECROSIS, FINAL KI67 (AT MEDIAN, 5%)
Row exclusion: DCIS STATVIEW DATASET

	0	1	Totals
MARKED	7	35	42
MILD	18	25	43
MOD	12	24	36
NONE	25	8	33
Totals	62	92	154

Summary Table for CI, FINAL KI67 (AT MEDIAN, 5%)
Row exclusion: DCIS STATVIEW DATASET

Num. Missing	123
DF	3
Chi Square	21.210
Chi Square P-Value	<.0001
G-Squared	24.603
G-Squared P-Value	<.0001
Contingency Coef.	.350
Cramer's V	.374

Observed Frequencies for CI, FINAL KI67 (AT MEDIAN, 5%)
Row exclusion: DCIS STATVIEW DATASET

	0	1	Totals
MARKED	3	33	36
MILD	27	26	53
MOD	15	20	35
NONE	16	12	28
Totals	61	91	152

Summary Table for FINAL MCM2 (AT MEDIAN, 27.5%), FINAL HER2 STATUS
Row exclusion: DCIS STATVIEW DATASET

Num. Missing	39
DF	1
Chi Square	19.314
Chi Square P-Value	<.0001
G-Squared	20.682
G-Squared P-Value	<.0001
Contingency Coef.	.275
Phi	.286
Cty. Cor. Chi Square	17.992
Cty. Cor. P-Value	<.0001
Fisher's Exact P-Value	<.0001

Observed Frequencies for FINAL MCM2 (AT MEDIAN, 27.5%), FINAL HER2 STATUS
Row exclusion: DCIS STATVIEW DATASET

	0	1	Totals
0	94	11	105
1	85	46	131
Totals	179	57	236

Summary Table for FINAL EGFR STATUS, FINAL MCM2 (AT MEDIAN, 27.5%)
Row exclusion: DCIS STATVIEW DATASET

Num. Missing	50
DF	1
Chi Square	5.588
Chi Square P-Value	.0181
G-Squared	6.671
G-Squared P-Value	.0098
Contingency Coef.	.156
Phi	.158
Cty. Cor. Chi Square	4.217
Cty. Cor. P-Value	.0400
Fisher's Exact P-Value	.0254

Observed Frequencies for FINAL EGFR STATUS, FINAL MCM2 (AT MEDIAN, 27.5%)
Row exclusion: DCIS STATVIEW DATASET

	0	1	Totals
0	97	117	214
1	1	10	11
Totals	98	127	225

Summary Table for FINAL ER STATUS, FINAL MCM2 (AT MEDIAN, 27.5%)
Row exclusion: DCIS STATVIEW DATASET

Num. Missing	56
DF	1
Chi Square	9.119
Chi Square P-Value	.0025
G-Squared	9.500
G-Squared P-Value	.0021
Contingency Coef.	.200
Phi	.204
Cty. Cor. Chi Square	8.215
Cty. Cor. P-Value	.0042
Fisher's Exact P-Value	.0032

Observed Frequencies for FINAL ER STATUS, FINAL MCM2 (AT MEDIAN, 27.5%)
Row exclusion: DCIS STATVIEW DATASET

	0	1	Totals
0	15	44	59
1	77	83	160
Totals	92	127	219

Summary Table for FINAL PR STATUS, FINAL MCM2 (AT MEDIAN, 27.5%)
Row exclusion: DCIS STATVIEW DATASET

Num. Missing	47
DF	1
Chi Square	8.977
Chi Square P-Value	.0027
G-Squared	9.029
G-Squared P-Value	.0027
Contingency Coef.	.195
Phi	.198
Cty. Cor. Chi Square	8.196
Cty. Cor. P-Value	.0042
Fisher's Exact P-Value	.0033

Observed Frequencies for FINAL PR STATUS, FINAL MCM2 (AT MEDIAN, 27.5%)
Row exclusion: DCIS STATVIEW DATASET

	0	1	Totals
0	42	77	119
1	60	49	109
Totals	102	126	228

Summary Table for FINAL CK5 (AT 1%), FINAL MCM2 (AT MEDIAN, 27.5%)
Row exclusion: DCIS STATVIEW DATASET

Num. Missing	54
DF	1
Chi Square	.912
Chi Square P-Value	.3396
G-Squared	.928
G-Squared P-Value	.3353
Contingency Coef.	.064
Phi	.064
Cty. Cor. Chi Square	.581
Cty. Cor. P-Value	.4460
Fisher's Exact P-Value	.4392

Observed Frequencies for FINAL CK5 (AT 1%), FINAL MCM2 (AT MEDIAN, 27.5%)
Row exclusion: DCIS STATVIEW DATASET

	0	1	Totals
0	82	107	189
1	11	21	32
Totals	93	128	221

Summary Table for FINAL CK5/6 (AT 1%), FINAL MCM2 (AT MEDIAN, 27.5%)
Row exclusion: DCIS STATVIEW DATASET

Num. Missing	60
DF	1
Chi Square	.898
Chi Square P-Value	.3434
G-Squared	.904
G-Squared P-Value	.3418
Contingency Coef.	.064
Phi	.065
Cty. Cor. Chi Square	.641
Cty. Cor. P-Value	.4235
Fisher's Exact P-Value	.3772

Observed Frequencies for FINAL CK5/6 (AT 1%), FINAL MCM2 (AT MEDIAN, 27.5%)
Row exclusion: DCIS STATVIEW DATASET

	0	1	Totals
0	65	81	146
1	26	43	69
Totals	91	124	215

Summary Table for FINAL CK14 (AT 1%), FINAL MCM2 (AT MEDIAN, 27.5%)
Row exclusion: DCIS STATVIEW DATASET

Num. Missing	50
DF	1
Chi Square	1.624
Chi Square P-Value	.2025
G-Squared	1.655
G-Squared P-Value	.1983
Contingency Coef.	.085
Phi	.085
Cty. Cor. Chi Square	1.201
Cty. Cor. P-Value	.2732
Fisher's Exact P-Value	.2151

Observed Frequencies for FINAL CK14 (AT 1%), FINAL MCM2 (AT MEDIAN, 27.5%)
Row exclusion: DCIS STATVIEW DATASET

	0	1	Totals
0	85	102	187
1	13	25	38
Totals	98	127	225

Summary Table for FINAL KI67 (AT MEDIAN, 5%), FINAL MCM2 (AT MEDIAN, 27.5%)
Row exclusion: DCIS STATVIEW DATASET

Num. Missing	38
DF	1
Chi Square	41.483
Chi Square P-Value	<.0001
G-Squared	42.558
G-Squared P-Value	<.0001
Contingency Coef.	.386
Phi	.418
Cty. Cor. Chi Square	39.807
Cty. Cor. P-Value	<.0001
Fisher's Exact P-Value	<.0001

Observed Frequencies for FINAL KI67 (AT MEDIAN, 5%), FINAL MCM2 (AT MEDIAN, 27.5%)
Row exclusion: DCIS STATVIEW DATASET

	0	1	Totals
0	70	31	101
1	37	99	136
Totals	107	130	237

Summary Table for GRADE, FINAL MCM2 (AT MEDIAN, 27.5%)
Row exclusion: DCIS STATVIEW DATASET

Num. Missing	117
DF	2
Chi Square	21.592
Chi Square P-Value	<.0001
G-Squared	21.981
G-Squared P-Value	<.0001
Contingency Coef.	.347
Cramer's V	.370

Observed Frequencies for GRADE, FINAL MCM2 (AT MEDIAN, 27.5%)
Row exclusion: DCIS STATVIEW DATASET

	0	1	Totals
HG	28	66	94
IG	36	17	53
LG	7	4	11
Totals	71	87	158

Summary Table for ARCH, FINAL MCM2 (AT MEDIAN, 27.5%)
Row exclusion: DCIS STATVIEW DATASET

Num. Missing	117
DF	3
Chi Square	11.396
Chi Square P-Value	.0098
G-Squared	11.601
G-Squared P-Value	.0089
Contingency Coef.	.259
Cramer's V	.269

Observed Frequencies for ARCH, FINAL MCM2 (AT MEDIAN, 27.5%)
Row exclusion: DCIS STATVIEW DATASET

	0	1	Totals
CRIB	38	27	65
MICROPAP	7	8	15
PAP	6	5	11
SOLID	20	47	67
Totals	71	87	158

Summary Table for NECROSIS, FINAL MCM2 (AT MEDIAN, 27.5%)
Row exclusion: DCIS STATVIEW DATASET

Num. Missing	117
DF	3
Chi Square	26.520
Chi Square P-Value	<.0001
G-Squared	27.928
G-Squared P-Value	<.0001
Contingency Coef.	.379
Cramer's V	.410

Observed Frequencies for NECROSIS, FINAL MCM2 (AT MEDIAN, 27.5%)
Row exclusion: DCIS STATVIEW DATASET

	0	1	Totals
MARKED	9	33	42
MILD	21	24	45
MOD	14	23	37
NONE	27	7	34
Totals	71	87	158

Summary Table for CI, FINAL MCM2 (AT MEDIAN, 27.5%)
Row exclusion: DCIS STATVIEW DATASET

Num. Missing	119
DF	3
Chi Square	19.049
Chi Square P-Value	.0003
G-Squared	20.421
G-Squared P-Value	.0001
Contingency Coef.	.330
Cramer's V	.349

Observed Frequencies for CI, FINAL MCM2 (AT MEDIAN, 27.5%)
Row exclusion: DCIS STATVIEW DATASET

	0	1	Totals
MARKED	6	31	37
MILD	31	24	55
MOD	14	21	35
NONE	18	11	29
Totals	69	87	156

Section 2: Non Parametric Tests- Univariate Paired analysis:

Oestrogen receptor in DCIS, frequencies and paired univariate analysis.

ER and HER2 IHC

Fishers exact test p value < 0.0001

	ER -ve	ER +ve	Total
HER2 -ve	23	145	168
HER2 +ve	36	19	55
Total	59	164	223

ER and EGFR IHC

Fishers exact test p value < 0.0001.

	ER -ve	ER +ve	Total
EGFR -ve	45	159	204
EGFR +ve	10	1	11
Total	55	160	215

ER and PR IHC

Fishers exact test p value <0.0001.

	ER -ve	ER +ve	Total
PR -ve	56	55	111
PR +ve	0	102	102
Total	56	157	213

ER and CK5 IHC

Fishers exact test p value = 0.0033.

	ER -ve	ER +ve	Total
CK5 -ve	41	147	188
CK5 +ve	15	16	31
Total	56	163	219

ER and CK5/6 IHC

Fishers exact test p value = 0.298

	ER -ve	ER +ve	Total
CK5/6 -ve	33	114	147
CK5/6 +ve	25	41	66
Total	58	155	213

ER and CK14 IHC

Fishers exact test p value = 0.0018.

	ER -ve	ER +ve	Total
CK14 -ve	40	142	182
CK14 +ve	18	19	37
Total	58	161	219

ER and Ki67 (>5%) IHC

Fishers exact test p value <0.0001

	ER -ve	ER +ve	Total
Ki67 -ve	8	78	86
Ki67+ve	51	79	130
Total	59	157	216

ER and MCM2 (>5%) IHC

Fishers exact test p value = 0.0032

	ER -ve	ER +ve	Total
MCM2 -ve	15	77	92
MCM2+ve	44	83	127
Total	59	160	219

ER and Histological Grade

Chi Square p value <0.0001

	ER -ve	ER +ve	Total
HG	35	55	90
IG	4	46	50
LG	0	9	9
Total	39	110	149

ER and Histological Architecture

Chi square p Value < 0.0001

	ER -ve	ER +ve	Total
Crib	5	55	60
Micropap	7	6	13
Pap	1	11	12
Solid	26	38	64
Total	39	110	149

ER and Necrosis

	ER -ve	ER +ve	Total
Marked	23	18	41
Mild	6	37	43
Moderate	8	28	36
None	2	27	29
Total	39	110	149

ER and Chronic Inflammation

	ER -ve	ER +ve	Total
Marked	25	10	35
Mild	3	49	52
Moderate	9	25	34
None	1	25	26
Total	38	109	147

Progesterone Receptor in DCIS, frequencies and paired univariate analysis.

PR and HER2

Fishers exact test p value <0.0001

	HER2 -ve	HER2 +ve	Total
PR -ve	70	50	120
PR +ve	104	6	110
Total	174	56	230

PR and EGFR IHC

Fishers exact test p value = 0.0008

	PR -ve	PR +ve	Total
EGFR -ve	102	105	207
EGFR +ve	11	0	11
Total	113	105	218

PR and CK5/6 IHC

Fishers exact test p value = 0.0542

	PR -ve	PR +ve	Total
CK5/6 -ve	69	76	145
CK5/6 +ve	42	25	67
Total	111	101	212

PR and CK5 IHC

Fishers exact test p value = 0.2385

	PR -ve	PR +ve	Total
CK5 -ve	94	92	186
CK5 +ve	19	11	30
Total	113	103	216

PR and CK14 IHC

Fishers exact test p value = 0.2791

	PR -ve	PR +ve	Total
CK14 -ve	94	90	184
CK14 +ve	23	14	37
Total	117	104	221

PR and Ki67 (>5%) IHC

Fishers exact test p value <0.0001

	PR -ve	PR +ve	Total
Ki67 -ve	36	60	96
Ki67+ve	82	46	128
Total	118	106	224

PR and MCM2 (<5%) IHC

Chi squared p value = 0.0027

	PR -ve	PR +ve	Total
MCM2 -ve	42	60	102
MCM2+ve	77	49	126
Total	119	109	228

PR and Histological Grade

Chi Squared p value = 0.0006

	PR -ve	PR +ve	Total
HG	54	37	91
IG	23	33	56
LG	0	10	10
Total	77	80	157

PR and Histological Architecture

Chi squared p value = 0.0011

	PR -ve	PR +ve	Total
Crib	22	43	65
Micropap	12	3	15
Pap	4	8	12
Solid	39	26	65
Total	77	80	157

PR and Necrosis

Chi squared p value 0.0013

	PR -ve	PR +ve	Total
Marked	28	13	41
Mild	20	24	44
Moderate	21	17	38
None	8	26	34
Total	77	80	157

PR and Chronic Inflammation

Chi squared p value <0.0001

	PR -ve	PR +ve	Total
Marked	30	6	36
Mild	17	38	55
Moderate	17	17	34
None	12	18	30
Total	76	79	155

5.20 Appendix 6: DNA Extraction and Purification Protocols

PROTOCOL TO EXTRACT DNA FROM PARAFFIN EMBEDDED TISSUE

DAY 1 - SLIDE PREPARATION

8μm sections (number depending on size of specimen,) cut and mounted on slides.

Air dry overnight

DAY 2 -PARAFFIN REMOVAL & STAINING

Xylene 1 for 5’

Xylene 2 for 5’

100% ETOH 1 for 30’’

100% ETOH 2 for 30’’

70% ETOH for 30’’

Wash in autoclaved water for 2’

Repeat wash with fresh autoclaved water

Stain with nuclear fast red (NFR) 1% - 4’

Wash with autoclaved water for 2’

Repeat wash with fresh autoclaved water

DAY 2 -MICRODISSECTION

Use H&E sections previously prepared and marked by Consultant Pathologists as a guide

Examine NFR stained sections under light microscope and using 12G sterile needle/scalpel scrape away unwanted areas and blow off with air spray

Incubate slides in 1M Na Thiocyanate at 37°C overnight.

DAY 3 – COMPLETE MICRODISSECTION AND TISSUE LYSIS

Wash in PBS-A, 10min on shaker, replace PBS then another 10mins on shaker.

Air dry.

Label appropriately (top and side) as many 1.5 ml eppendorf tubes as the samples you have (N) and add 180 µl of DNeasy Buffer ATL to each tube

Pipette 2-5 µl of ATL buffer at the edge of each section to moisten the tissue and lift using pipette tip or needle

Transfer the tissue in the appropriately labelled tube containing the ATL buffer.

Repeat steps 3-5 for all sections

Once microdissection is completed, add 20 µl Proteinase K, vortex for 15 seconds and spin.

Seal tubes with parafilm and incubate @56-58°C in a rotisserie/or on shaker in oven overnight.

Day 4 - DNA EXTRACTION

Reagents from Qiagen DNeasy Blood and Tissue Kit

Protocol: Purification of Total DNA from Animal Tissues (Spin-Column Protocol)

At 12 hours check that tissue fully lysed. If so, vortex well for 15 seconds and continue with DNeasy protocol by adding 200ul Buffer AL etc.

If tissue not fully lysed, add extra 20ul of DNeasy Proteinase K, vortex for 15 seconds and return to oven for 1-4hours, until tissue fully lysed

Once fully lysed continue with DNeasy protocol.

NB – Once lysed, samples can remain in buffer at -20 C until extraction proceeds

- Store at -20C after extraction

DCIS DNA Extraction using Qiagen FFPE Kit.

This protocol is adapted from the “QIAamp DNA FFPE Tissue handbook” October 2007. The original protocol is “Isolation of Genomic DNA from FFPE tissue sections” on page 15. This protocol is required AFTER manual microdissection of tissue sections on uncoated slides and follows incubation in 1M sodium thiocyanate prior to proteinase k treatment. It starts at point 14 of the original protocol. The reagents are all (except ETOH) part of the FFPE DNA extraction kit.

Between six and twelve samples should be prepared prior to extracting and be placed in 1.5ml eppendorfs tubes. Place frozen tube on wet ice and proceed with protocol.

In an eppendorf holder set out one row of samples followed by 1 set of labelled eluting columns on collecting tubes. Next 2 sets of collecting tubes followed by 2 sets of eppendorfs with labels corresponding to the sample numbers. The final set should be identified in some way as a spare.

Vortex all samples for approx. 15seconds

Add 200μl of buffer AL to each sample, if sample had extra proteinase k then add an additional 10-20 μl. The solution is viscous so pipette slowly. Re-vortex samples.

Add 200μl of 100% alcohol (ETOH) to each sample vortexing each sample immediately. The solution may start to precipitate, if this occurs keep vortexing until an almost clear homogenate is seen.

NB AL and ETOH can be premixed for all samples before adding.

Transfer the entire sample into a corresponding eluting column.

Centrifuge at 8000rpm (6000g) for one minute.

Place each eluting column into a new collection tube and discard the old one and contents.

Add 500μl of AW1 (check solution is correctly made up and ensure there is no precipitate present) to each sample. Spin at 8000rpm (6000g) for one minute. Put eluting column into new collection tube and discard old collecting tube and contents.

Add 500μl of AW2 and spin for 3.5 minutes at 13,500 rpm. Remove eluting and collection tubes ensuring that no liquid touches eluting tube membrane. If this occurs then re-spin.

Place eluting column into first labelled eppendorfs (not spare) and discard collecting tube and contents ensuring eluting tube membranes stay dry.

Add 20μl of ATE to eluting column making sure it is placed directly onto the membrane. Do this for all samples and then spin at 8000rpm for 1 minute.

Repeat step twelve spinning into same eppendorf to give total volume of ATE/DNA to 35-40μl.

Place eluting column into second eppendorf (spare) making sure lid is closed on first samples. Add 50μl of AE and spin at 8000rpm for one minute. Remove from centrifuge and discard eluting column and close sample lids.

Test for DNA quality using nanodrop and MultiplexPCR. If yield sufficient proceed to pico green testing and then store samples at -20°C. NB Nandrop deemed to be poor for quality analysis proceed straight to PicoGreen if desired.

5.21 Appendix 7. Qubit DNA quantities Quality: DNA Quibit Readings for MIP Array Analysis

Affymetrix ID	Grid Reference	Specimen type	Sample 1 Volume (ul)	Qubit Reading (ug/µl)	Qubit stock conc	Total DNA per original sample (ng per 40µl)
DCISJPB1OK 001	A1	Triple Negative Pure DCIS	40	0.456	91.2	3648
DCISJPB1OK 002	A2	Triple Negative Pure DCIS	40	1.030	206.0	8240
DCISJPB1OK 003	A3	Triple Negative Pure DCIS	40	0.102	20.4	816
DCISJPB1OK 004	A4	Triple negative DCIS associated with tumour	40	0.0479	9.58	383.2
DCISJPB1OK 005	A5	Triple negative Tumour associated with DCIS	40	1.15	230	9200
DCISJPB1OK 006	A6	Triple Negative Pure DCIS	40	0.188	37.6	1504
DCISJPB1OK 007	A7	HER2 Positive	40	0.91	18.2	728
DCISJPB1OK 008	A8	HER2 Positive	40	1.39	27.8	1112
DCISJPB1OK 009	A9	Pure DCIS ER positive	40	1.600	320	12800
DCISJPB1OK 010	A10	Triple negative DCIS associated with tumour	40	0.668	134	5360
DCISJPB1OK 011	A11	Triple negative Tumour associated with DCIS	40	0.917	183	7320
DCISJPB1OK 012	B1	Matched Normal from Triple negative DCIS and Tumour	40	0.818	16.36	654.4
DCISJPB1OK 013	B2	Triple negative DCIS associated with tumour	40	0.858	172	6880

DCISJPB1OK 014	B3	Triple negative Tumour associated with DCIS	40	1.13	226	9040

Affymetrix ID	Grid Reference	Specimen type	Sample 1 Volume (ul)	Qubit Reading (ug/µl)	Qubit stock conc	Total DNA per original sample (ng per 40µl)
DCISJPB1OK 015	B4	Matched Normal from Triple negative DCIS and Tumour	40	1.69	33.8	1352
DCISJPB1OK 016	B5	HER2 Positive	40	0.778	15.56	622.4
DCISJPB1OK 017	B6	Pure DCIS ER positive	40	0.643	128.6	5144
DCISJPB1OK 018	B7	Triple negative DCIS associated with tumour	40	1.24	248	9920
DCISJPB1OK 019	B8	Triple negative Tumour associated with DCIS	40	0.831	166	6640
DCISJPB1OK 020	B9	Triple Negative Pure DCIS	40	0.222	44.4	1776
DCISJPB1OK 021	B10	Pure DCIS ER positive	40	2.510	502	20080
DCISJPB1OK 022	B11	Triple Negative Pure DCIS	40	0.078	15.7	627.2
DCISJPB1OK 023	B12	HER2 Positive	40	1.06	21.2	848
DCISJPB1OK 024	C1	Pure DCIS ER positive	40	1.670	334	13360
DCISJPB1OK 025	C2	HER2 Positive	40	1.46	29.2	1168

DCISJPB1OK 026	C3	Triple negative DCIS associated with tumour	40	0.782	156	6240
DCISJPB1OK 027	C4	Triple negative Tumour associated with DCIS	40	0.936	187	7480
DCISJPB1OK 028	C5	Matched Normal from Triple negative DCIS and Tumour	40	1.59	31.8	1272

Affymetrix ID	**Grid Reference**	**Specimen type**	**Sample 1 Volume (ul)**	**Qubit Reading (ug/µl)**	**Qubit stock conc**	**Total DNA per original sample (ng per 40µl)**
DCISJPB1OK 029	C6	Triple negative DCIS associated with tumour	40	1.59	318	12720
DCISJPB1OK 030	C7	Triple negative Tumour associated with DCIS	40	1.37	274	10960
DCISJPB1OK 031	C8	Matched Normal from Triple negative DCIS and Tumour	40	0.297	5.94	237.6
DCISJPB1OK 032	C9	Triple Negative Pure DCIS	40	0.153	30.6	1224
DCISJPB1OK 033	C10	Triple negative DCIS associated with tumour	40	1.68	336	13440
DCISJPB1OK 034	C11	Triple negative Tumour associated with DCIS	40	2.68	536	21440
DCISJPB1OK 035	D1	Matched Normal from Triple negative DCIS and Tumour	40	1.84	36.8	1472
DCISJPB1OK 036	D2	HER2 Positive	40	0.951	19.02	760.8
DCISJPB1OK 037	D3	HER2 Positive	40	1.75	35	1400

DCISJPB1OK 038	D4	Triple Negative Pure DCIS	40	0.049	9.7	389.6
DCISJPB1OK 039	D5	Matched Normal from Triple negative DCIS and Tumour	40	1.28	25.6	1024
DCISJPB1OK 040	D6	Pure DCIS ER positive	40	0.447	89.4	3576
DCISJPB1OK 041	D7	Triple negative DCIS associated with tumour	40	0.265	53	2120
DCISJPB1OK 042	D8	Triple negative Tumour associated with DCIS	40	1.86	372	14880

Affymetrix ID	**Grid Reference**	**Specimen type**	**Sample 1 Volume (ul)**	**Qubit Reading (ug/µl)**	**Qubit stock conc**	**Total DNA per original sample (ng per 40µl)**
DCISJPB1OK 043	D9	Triple negative DCIS associated with tumour	40	0.647	129	5160
DCISJPB1OK 044	D10	Triple negative Tumour associated with DCIS	40	1.23	246	9840
DCISJPB1OK 045	D11	Matched Normal from Triple negative DCIS and Tumour	40	1.86	372	14880
DCISJPB1OK 046	D12	Triple negative DCIS associated with tumour	40	1.13	226	9040
DCISJPB1OK 047	E1	Triple negative Tumour associated with DCIS	40	2.12	434	17360
DCISJPB1OK 048	E2	Matched Normal from Triple negative DCIS and Tumour	40	0.558	11.16	446.4
DCISJPB1OK 049	E3	Pure DCIS ER positive	40	2.330	466	18640

DCISJPB1OK 050	E4	Pure DCIS ER positive	40	1.150	230	9200
DCISJPB1OK 051	E5	DCIS ER positive associated with tumour	40	0.702	140.4	5616
DCISJPB1OK 052	E6	Tumour ER positive associated with DCIS	40	0.780	156	6240
DCISJPB1OK 053	E7	Matched Normal from ER positive DCIS and Tumour	40	0.582	11.64	465.6
DCISJPB1OK 054	E8	DCIS ER positive associated with tumour	40	0.105	21	840
DCISJPB1OK 055	E9	Tumour ER positive associated with DCIS	40	1.190	238	9520

Affymetrix ID	**Grid Reference**	**Specimen type**	**Sample 1 Volume (ul)**	**Qubit Reading (ug/µl)**	**Qubit stock conc**	**Total DNA per original sample (ng per 40µl)**
DCISJPB1OK 056	E10	Matched Normal from ER positive DCIS and Tumour	40	2.06	41.2	1648
DCISJPB1OK 057	E11	DCIS ER positive associated with tumour	40	0.611	122.2	4888
DCISJPB1OK 058	F1	Tumour ER positive associated with DCIS	40	0.788	157.6	6304
DCISJPB1OK 059	F2	Matched Normal from ER positive DCIS and Tumour	40	0.0883	1.766	70.64
DCISJPB1OK 060	F3	DCIS ER positive associated with tumour	40	0.367	73.4	2936

DCISJPB1OK 061	F4	Tumour ER positive associated with DCIS	40	1.760	352	14080
DCISJPB1OK 062	F5	Matched Normal from ER positive DCIS and Tumour	40	1.46	29.2	1168
DCISJPB1OK 063	F6	DCIS ER positive associated with tumour	40	1.150	230	9200
DCISJPB1OK 064	F7	Tumour ER positive associated with DCIS	40	1.350	270	10800
DCISJPB1OK 065	F8	Pure DCIS ER positive	40	0.277	55.4	2216
DCISJPB1OK 066	F9	Pure DCIS ER positive	40	1.560	312	12480
DCISJPB1OK 067	F10	DCIS ER positive associated with tumour	40	0.568	113.6	4544
DCISJPB1OK 068	F11	Tumour ER positive associated with DCIS	40	0.794	158.8	6352
DCISJPB1OK 070	G1	Matched Normal from ER positive DCIS and Tumour	40	1.29	25.8	1032

Affymetrix ID	**Grid Reference**	**Specimen type**	**Sample 1 Volume (ul)**	**Qubit Reading (ug/µl)**	**Qubit stock conc**	**Total DNA per original sample (ng per 40µl)**
DCISJPB1OK 069	F12	HER2 Positive	40	2.19	43.8	1752
DCISJPB1OK 071	G2	Pure DCIS ER positive	40	0.571	114.2	4568
DCISJPB1OK 072	G3	Triple Negative Pure DCIS	40	0.062	12.4	494.4

DCISJPB1OK 073	G4	Triple Negative Pure DCIS	40	0.400	80.0	3200
DCISJPB1OK 074	G5	Triple Negative Pure DCIS	40	0.835	167.0	6680
DCISJPB1OK 075	G6	Triple Negative Pure DCIS	40	0.085	17.0	680
DCISJPB1OK 076	G7	DCIS ER positive associated with tumour	40	0.628	125.6	5024
DCISJPB1OK 077	G8	Tumour ER positive associated with DCIS	40	0.234	46.8	1872
DCISJPB1OK 078	G9	DCIS ER positive associated with tumour	40	0.095	19.08	763.2
DCISJPB1OK 079	G10	Tumour ER positive associated with DCIS	40	0.189	37.8	1512
DCISJPB1OK 080	G11	Matched Normal from ER positive DCIS and Tumour	40	1.03	20.6	824
DCISJPB1OK 081	H1	DCIS ER positive associated with tumour	40	0.932	186.4	7456
DCISJPB1OK 082	H2	Tumour ER positive associated with DCIS	40	0.875	175	7000
DCISJPB1OK 083	H3	Matched Normal from ER positive DCIS and Tumour	40	2.79	55.8	2232

5.22 Appendix 8. MIP Array Analysis- DNA Samples sent to Affymetrix

List of specimens

UNIQUE IDENTIFER	PLATE REFERENCE	Specimen type
DCISJPB1OK 001	A1	Triple Negative Pure DCIS
DCISJPB1OK 002	A2	Triple Negative Pure DCIS
DCISJPB1OK 003	A3	Triple Negative Pure DCIS
DCISJPB1OK 004	A4	Triple negative DCIS
DCISJPB1OK 005	A5	Triple negative Tumour
DCISJPB1OK 006	A6	Triple Negative Pure DCIS
DCISJPB1OK 007	A7	HER2 Positive
DCISJPB1OK 008	A8	HER2 Positive
DCISJPB1OK 009	A9	Pure DCIS ER positive
DCISJPB1OK 010	A10	Triple negative DCIS
DCISJPB1OK 011	A11	Triple negative Tumour
DCISJPB1OK 012	B1	Matched Normal from Triple negative DCIS and Tumour
DCISJPB1OK 013	B2	Triple negative DCIS
DCISJPB1OK 014	B3	Triple negative Tumour
DCISJPB1OK 015	B4	Matched Normal from Triple negative DCIS and Tumour
DCISJPB1OK 016	B5	HER2 Positive
DCISJPB1OK 017	B6	Pure DCIS ER positive
DCISJPB1OK 018	B7	Triple negative DCIS
DCISJPB1OK 019	B8	Triple negative Tumour
DCISJPB1OK 020	B9	Triple Negative Pure DCIS
DCISJPB1OK 021	B10	Pure DCIS ER positive
DCISJPB1OK 022	B11	Triple Negative Pure DCIS
DCISJPB1OK 023	B12	HER2 Positive

DCISJPB1OK 024	C1	Pure DCIS ER positive
DCISJPB1OK 025	C2	HER2 Positive
DCISJPB1OK 026	C3	Triple negative DCIS
DCISJPB1OK 027	C4	Triple negative Tumour
DCISJPB1OK 028	C5	Matched Normal from Triple negative DCIS and Tumour
DCISJPB1OK 029	C6	Triple negative DCIS
DCISJPB1OK 030	C7	Triple negative Tumour
DCISJPB1OK 031	C8	Matched Normal from Triple negative DCIS and Tumour
DCISJPB1OK 032	C9	Triple Negative Pure DCIS
DCISJPB1OK 033	C10	Triple negative DCIS
DCISJPB1OK 034	C11	Triple negative Tumour
DCISJPB1OK 035	D1	Matched Normal from Triple negative DCIS and Tumour
DCISJPB1OK 036	D2	HER2 Positive
DCISJPB1OK 037	D3	HER2 Positive
DCISJPB1OK 038	D4	Triple Negative Pure DCIS
DCISJPB1OK 039	D5	Matched Normal from Triple negative DCIS and Tumour
DCISJPB1OK 040	D6	Pure DCIS ER positive
DCISJPB1OK 041	D7	Triple negative DCIS
DCISJPB1OK 042	D8	Triple negative Tumour
DCISJPB1OK 043	D9	Triple negative DCIS
DCISJPB1OK 044	D10	Triple negative Tumour
DCISJPB1OK 045	D11	Matched Normal from Triple negative DCIS and Tumour
DCISJPB1OK 046	D12	Triple negative DCIS
DCISJPB1OK 047	E1	Triple negative Tumour
DCISJPB1OK 048	E2	Matched Normal from Triple negative DCIS and Tumour

DCISJPB1OK 049	E3	Pure DCIS ER positive
DCISJPB1OK 050	E4	Pure DCIS ER positive
DCISJPB1OK 051	E5	Tumour ER positive (basal negative)
DCISJPB1OK 052	E6	DCIS ER positive (basal negative)
DCISJPB1OK 053	E7	Matched Normal from ER positive DCIS and Tumour
DCISJPB1OK 054	E8	Tumour ER positive (basal negative)
DCISJPB1OK 055	E9	DCIS ER positive (basal negative)
DCISJPB1OK 056	E10	Matched Normal from ER positive DCIS and Tumour
DCISJPB1OK 057	E11	Tumour ER positive (basal negative)
DCISJPB1OK 058	F1	DCIS ER positive (basal negative)
DCISJPB1OK 059	F2	Matched Normal from ER positive DCIS and Tumour
DCISJPB1OK 060	F3	Tumour ER positive (basal negative)
DCISJPB1OK 061	F4	DCIS ER positive (basal negative)
DCISJPB1OK 062	F5	Matched Normal from ER positive DCIS and Tumour
DCISJPB1OK 063	F6	Tumour ER positive (basal negative)
DCISJPB1OK 064	F7	DCIS ER positive (basal negative)
DCISJPB1OK 065	F8	Pure DCIS ER positive
DCISJPB1OK 066	F9	Pure DCIS ER positive
DCISJPB1OK 067	F10	Tumour ER positive (basal negative)
DCISJPB1OK 068	F11	DCIS ER positive (basal negative)
DCISJPB1OK 069	F12	Matched Normal from ER positive DCIS and Tumour
DCISJPB1OK 070	G1	HER2 Positive

DCISJPB1OK 071	G2	Triple Negative Pure DCIS
DCISJPB1OK 072	G3	Triple Negative Pure DCIS
DCISJPB1OK 073	G4	Triple Negative Pure DCIS
DCISJPB1OK 074	G5	Triple Negative Pure DCIS
DCISJPB1OK 075	G6	Pure DCIS ER positive
DCISJPB1OK 076	G7	Tumour ER positive (basal negative)
DCISJPB1OK 077	G8	DCIS ER positive (basal negative)
DCISJPB1OK 078	G9	Tumour ER positive (basal negative)
DCISJPB1OK 079	G10	DCIS ER positive (basal negative)
DCISJPB1OK 080	G11	Matched Normal from ER positive DCIS and Tumour
DCISJPB1OK 081	H1	Tumour ER positive (basal negative)
DCISJPB1OK 082	H2	DCIS ER positive (basal negative)
DCISJPB1OK 083	H3	Matched Normal from ER positive DCIS and Tumour

5.23 Appendix 9 MIP Array Charts

ER	DCISJPB10K 009 P238/1989	A09	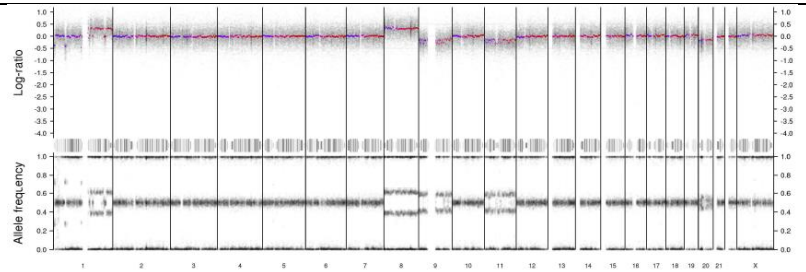
	DCISJPB10K P611/1989	B06	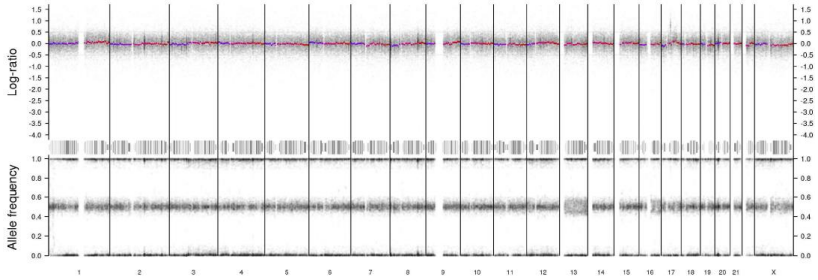

	DCISJPB10K P300/1991	B10	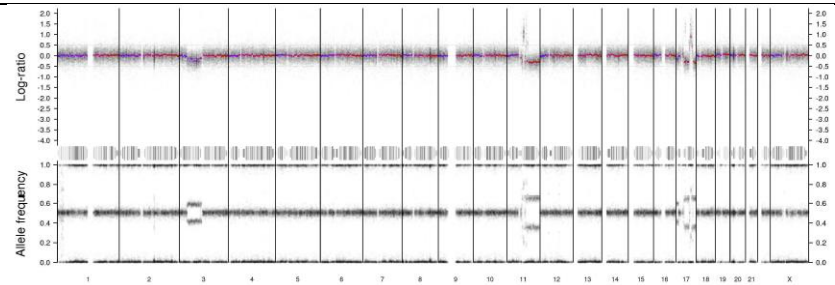
	DCISJPB10K P598/1992	C01	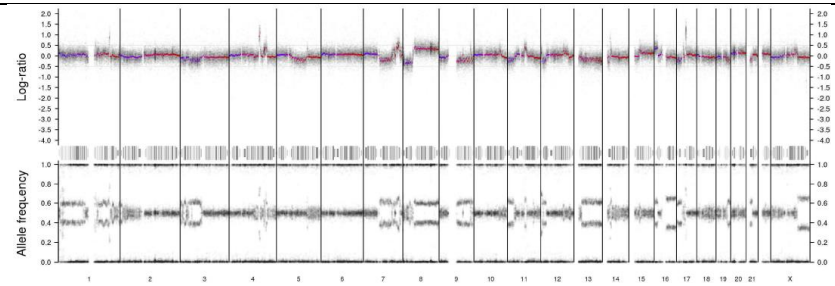
	DCISJPB10K P1072/1995	D06	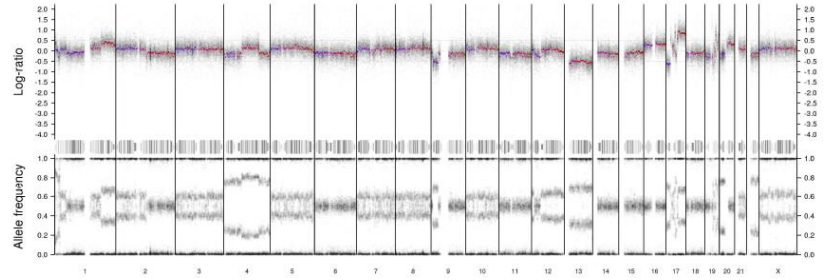

	DCISJPB10K P413/1997	E03	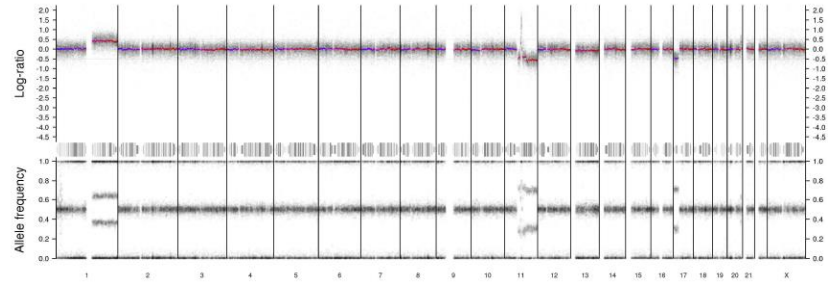
	DCISJPB10K P754/1997	E04	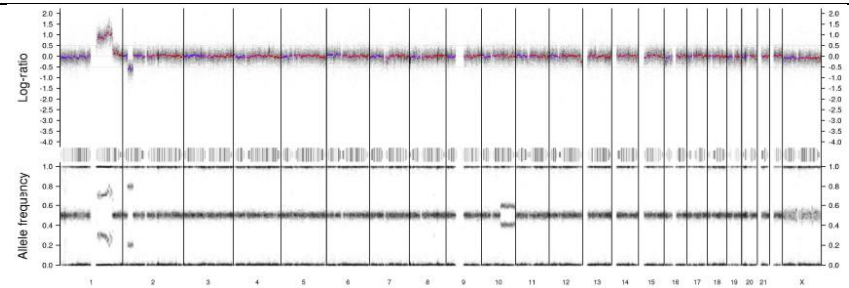
	P198/1999	F08	na
	DCISJPB10K 66 P1194/1999	F09	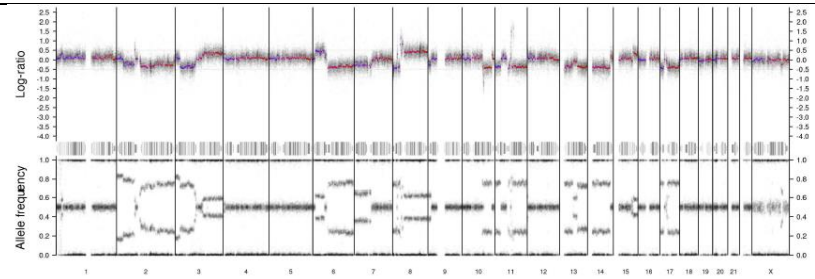

	DCISJPB10K P430/2000	G02	na
HER2	DCISJPB10K P914/1988	A07	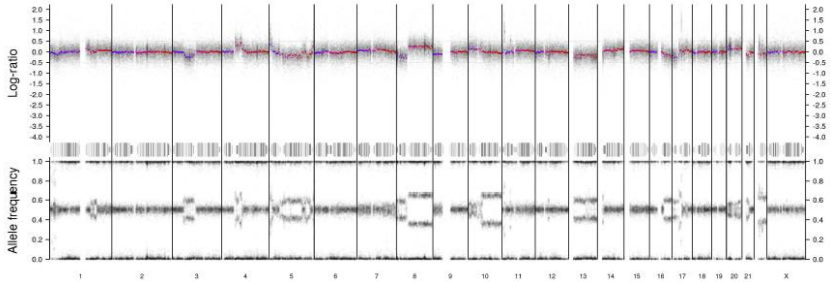
	DCISJPB10K P10/1989	A08	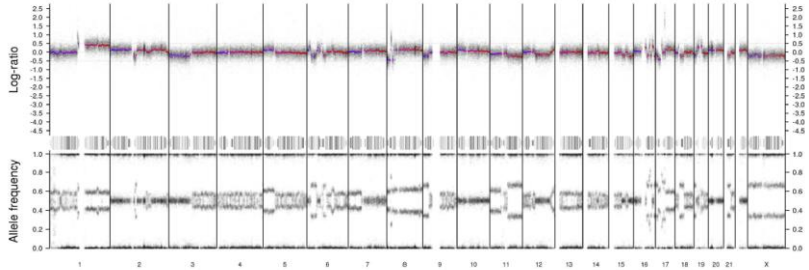

	DCISJPB10K P539/1989	B05	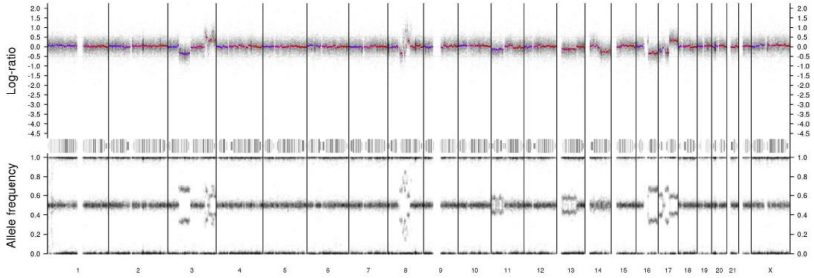
	DCISJPB10K P558/1991	B12	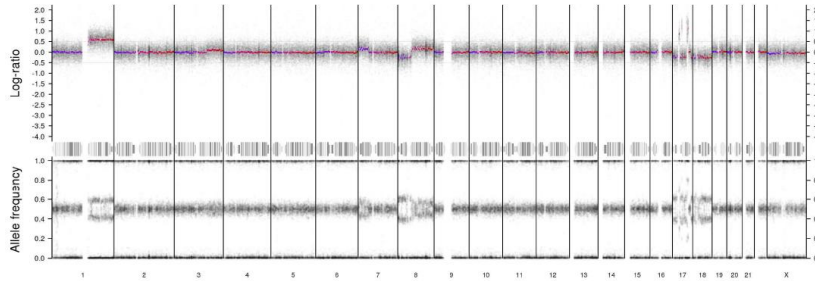
	DCISJPB10K P639/1992	C02	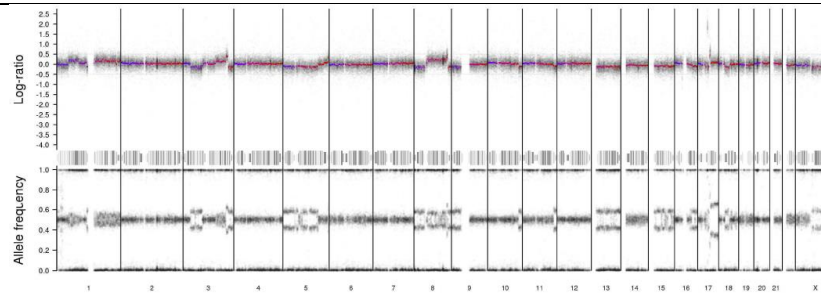

	DCISJPB10K P461/1994	D02	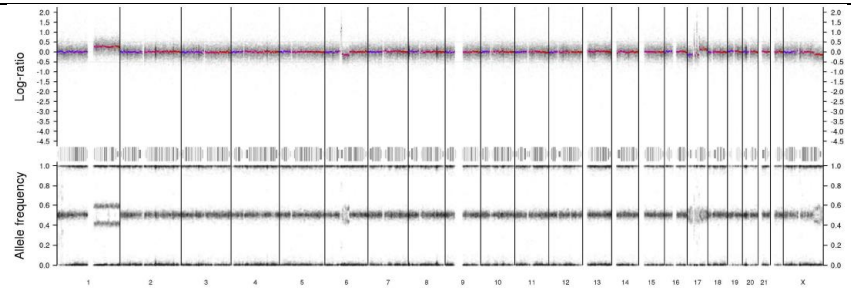
	P970/1995	D03	Na
	DCISJPB10K 070 P346/2000	G01	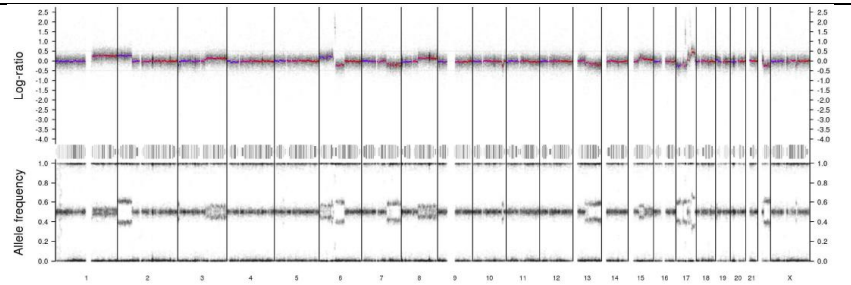
TN	DCISJPB10K P337/1978	A01	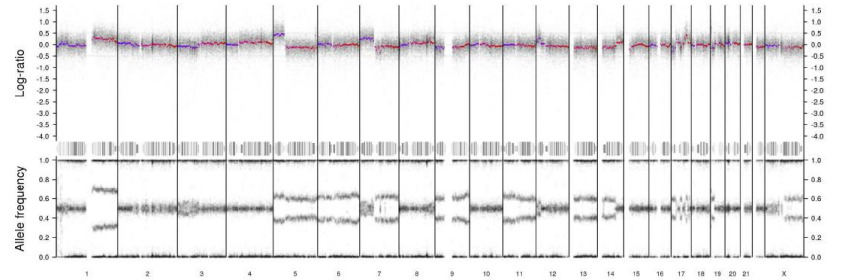

	DCISJPB10K P997/1982	A02	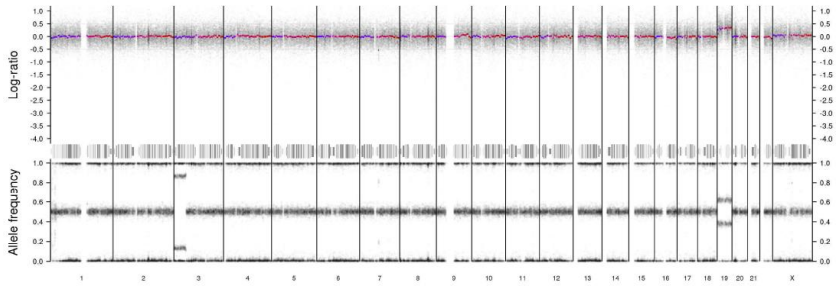
	DCISJPB10K P591/1984	A03	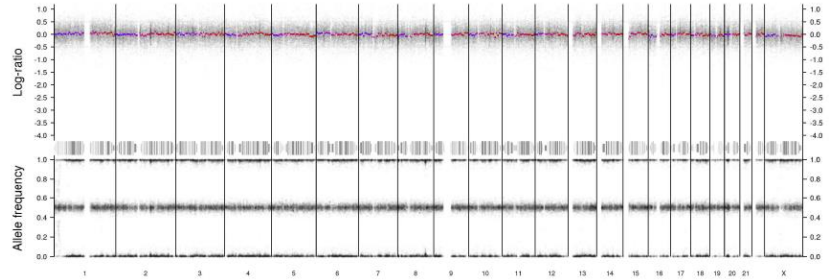
	DCISJPB10K P621/1988	A06	Na

	DCISJPB10K P267/1991	B09	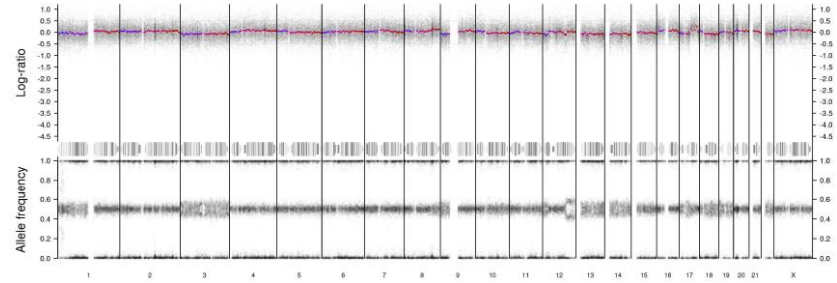
	DCISJPB10K P313/1991	B11	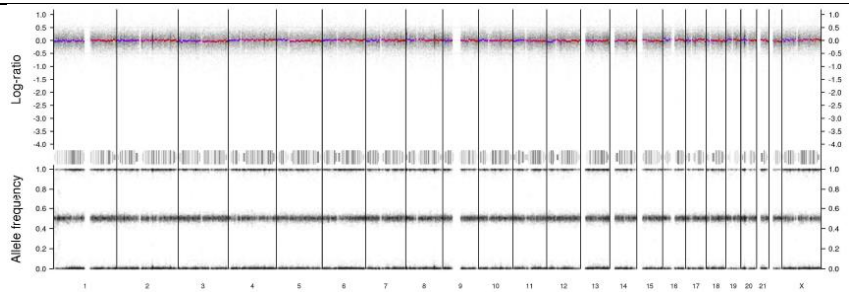
	DCISJPB10K P823/1993	C09	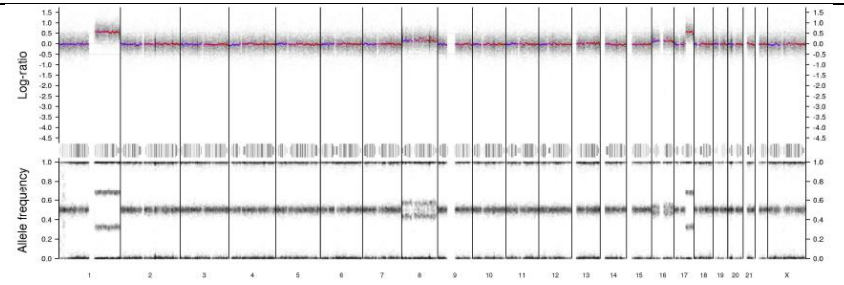

	DCISJPB10K P990/1995	D04	na
	DCISJPB10K P1074/2000	G03	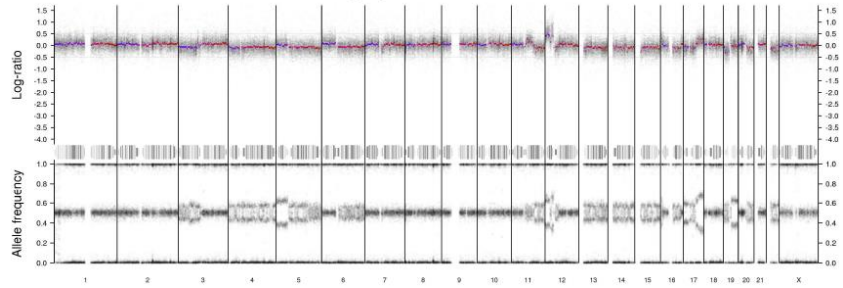
	DCISJPB10K P1093/2000	G04	na
	P701/2001	G05	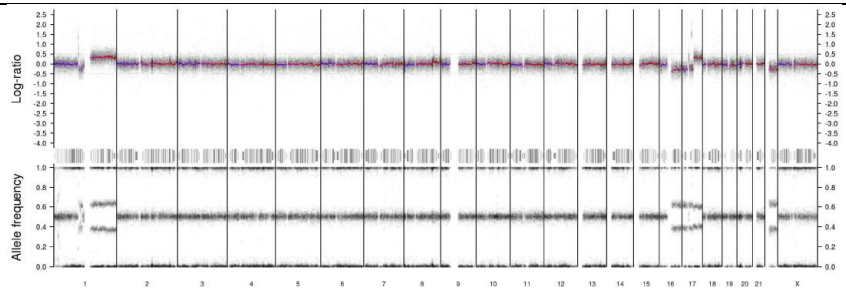

	P1002/2001	G06	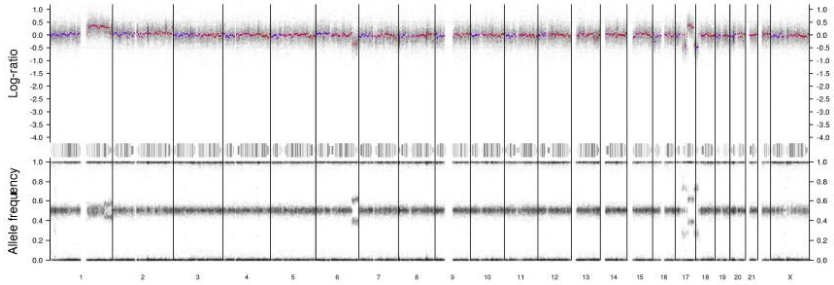

-

	case no	normal		DCIS		invasive breast disease	
ER	**P123/1998**	E07	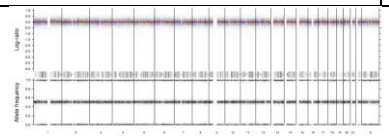	E06	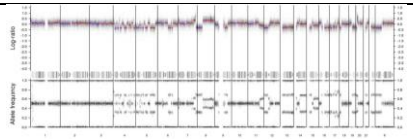	E05	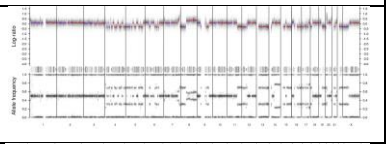
	P1310/2004	H03	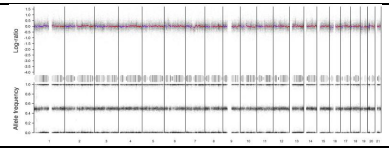	H02	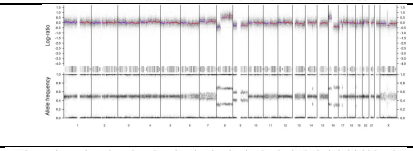	H01	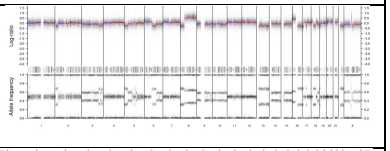
	P168/1999			F07	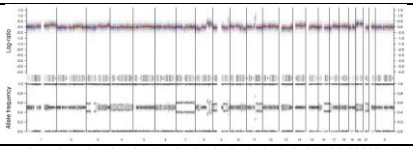	F06	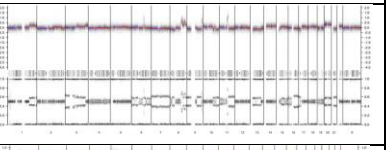
	P258/2004			G08	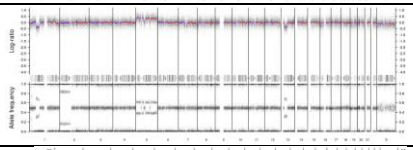	G07	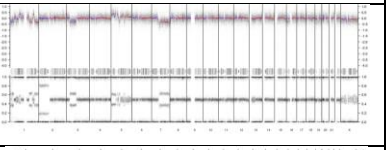
	P339/2000			F11	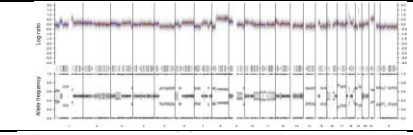	F10	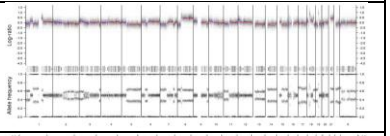
	P367/2004	G11	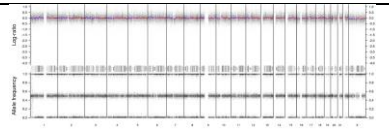	G10	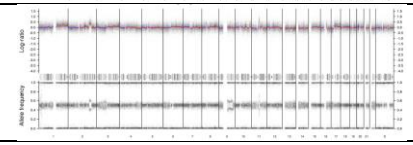	G09	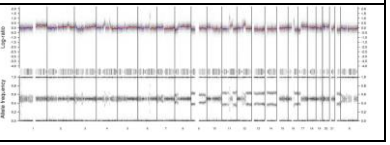

	P46/1999	F05	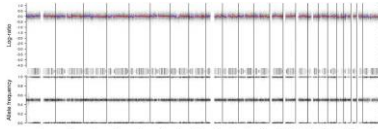	F04	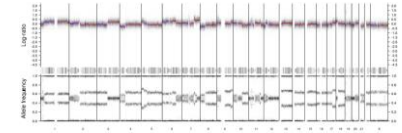	F03	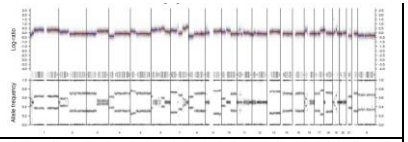
	P585/1998	E10	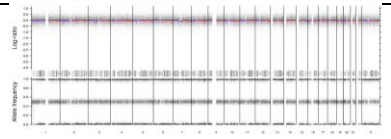	E09	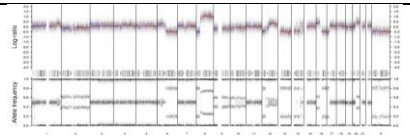	E08	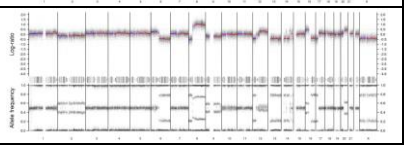
	P769/1998	F02	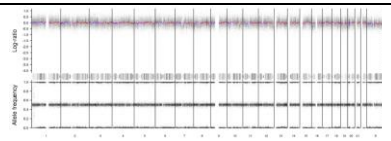	F01	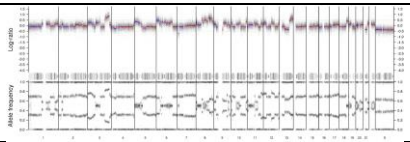	E11	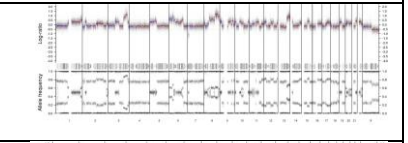
Triple Negative	**P110/1987**			A04	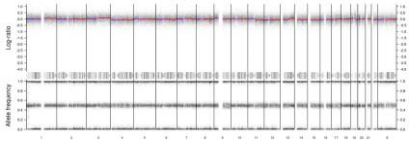	A05	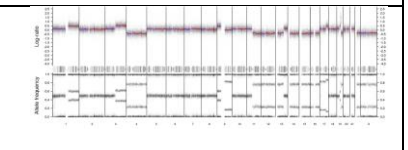
	P126/1997	D11	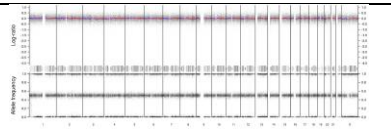	D09	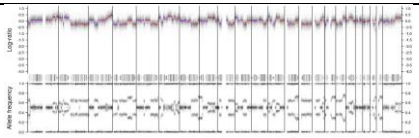	D10	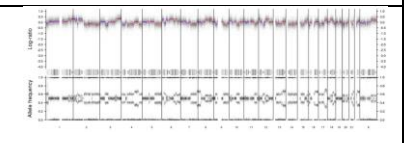
	P137/1997	E02	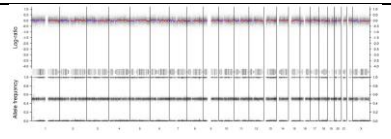	D12	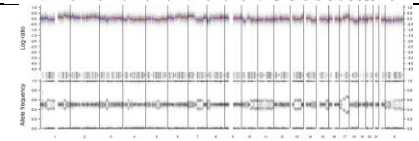	E01	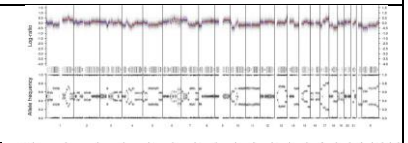
	P220/1990			B07	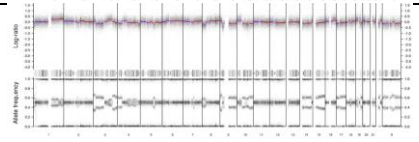	B08	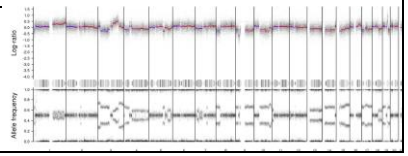

P456/1989	B01	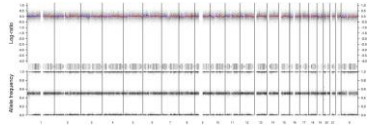	A10	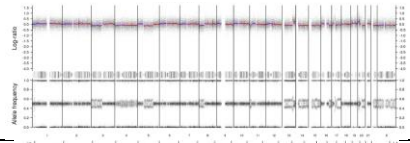	A11	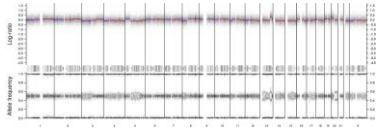
P497/1989			B02	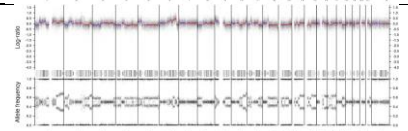	B03	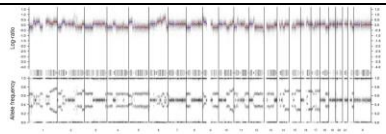
P9/1994	D01	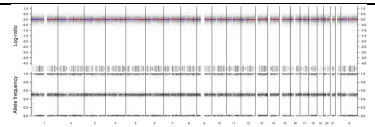	C10	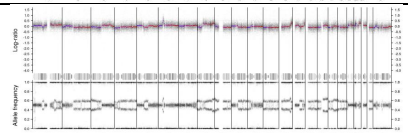	C11	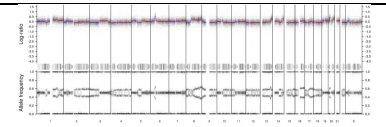
P540/1993	C08	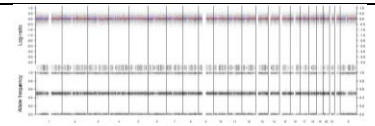	C06	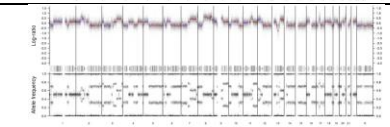		
P730/1992	C05	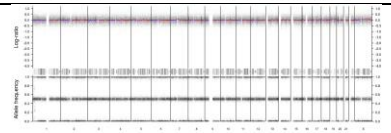	C03	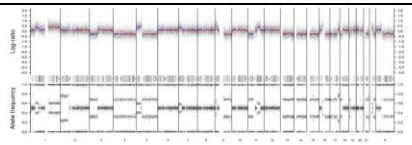		
P1012/1995	D05	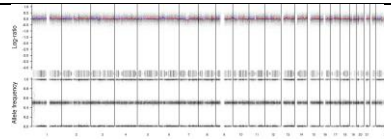				
P400/2000	F12	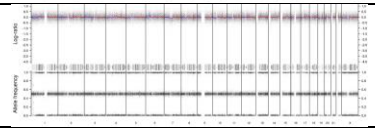				

	P536/1989	B04	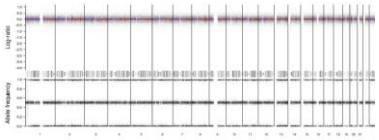		
	P1202/1995			D07